Université de Montréal

Indényles greffés d'un bras moléculaire fonctionnalisé comme ligands hémilabiles de nouveaux catalyseurs de nickel(II)

Par

Laurent F. Groux

Département de chimie

Faculté des arts et des sciences

Thèse présentée à la Faculté des études supérieures

en vue de l'obtention du grade de *Philosophiae Doctor* (Ph.D.)

en Chimie

Juin 2003

Université de Montréal

Faculté des arts et des sciences

Cette thèse intitulée :

Indényles greffés d'un bras moléculaire fonctionnalisé comme ligands hémilabiles de nouveaux catalyseurs de nickel(II)

Présentée par :

Laurent F. Groux

A été évaluée par un jury composé des personnes suivantes :

Prof. Garry Hanan_____Président-rapporteur

Prof. Davit Zargarian_____Directeur de recherche

Prof. Hélène Lebel_____Membre du jury

Prof. Josef Takats_____Examinateur externe

Department of Chemistry, University of Alberta

Prof. Danilo Klvana_____Représentant du doyen de la FES

Sommaire

De nouveaux ligands indényle fonctionnalisés de type Ind^NRR' (^ représente une chaîne aliphatique de 2 à 4 carbones; NRR' = NH_2, NMe_2, N-*i*Pr_2, 2-Py, NHBz, NH-*t*Bu, Pyrrolidine) ont été préparés et caractérisés par spectroscopie RMN (^1H et $^{13}C\{^1H\}$), analyse élémentaire et dans le cas de $Ind(CH_2)_3NHBz{\cdot}HCl$, par diffraction des rayons X.

A partir de ces ligands, trois types de composés de nickel ont été obtenus : les deux premiers, avec la fonction amine non-coordonnée au métal comprennent les composés neutres (η^3:η^0-Ind^N)Ni(PR_3)X (R = Ph, Cy, Me; X = Cl, I, Me, *n*-Bu, CCPh) et les composés cationiques $[(Ind^N)NiLL']^+$ (LL' = $(PPh_3)_2$, dppe, PPh_3/PMe_3, PPh_3/Pyridine). D'autre part, le troisième groupe est formé des composés cationiques ayant l'amine chélatée au nickel $[(\eta^3:\eta^1\text{-Ind}^N)Ni(PR_3)]^+$ (R = Ph, Cy, Me).

Ces composés ont été caractérisés par spectroscopie RMN (^1H, $^{13}C\{^1H\}$ et $^{31}P\{^1H\}$) et analyse élémentaire. La diffraction des rayons X a été utilisée pour résoudre la structure de plusieurs de ces nouveaux composés organométalliques tandis que les études électrochimiques (voltampérométrie cyclique) ont permis de déterminer la densité électronique des centres métalliques.

L'étude du comportement et de l'influence du bras moléculaire dans ce type de composés constitue le thème central de la thèse. Au niveau structural, il a été constaté que la chélation de l'amine apportait plusieurs contraintes géométriques et changeait partiellement le mode de coordination de l'indényle. De plus, en corrélation avec les études électrochimiques, un phénomène inattendu a pu être observé en variant les ligands X : plus le métal est dur (pauvre en électron, cationique) plus la coordination de l'indényle et de la phosphine était faible, à l'inverse, plus le métal est enrichi par le ligand X (le méthyle étant le meilleur donneur) plus l'indényle et la phosphine se lient fortement à ce dernier.

D'autre part, le comportement hémilabile de l'amine greffée sur l'indène a été observé en solution par spectroscopie RMN à température variable sur les composés neutres, dans lesquels on pouvait, dans certains cas, observer une coordination-

décoordination dynamique du bras. Dans le cas des composés cationiques chélatés, la décoordination du bras a été sondée par réaction avec différentes bases de Lewis (phosphine, amine, etc). Elles ont permis de montrer que le lien Ni-N était relativement fort et que pour le briser, il fallait de très bons ligands coordonnants et un excès de ligands monodentates ou un ligand bidentate.

Ce comportement hémilabile a permis de préparer des catalyseurs cationiques ne nécessitant pas d'activateur pour la polymérisation des oléfines (principalement le styrène, le norbornène, le vinylcarbazole, le vinyléthyléther). $(Ind(CH_2)_2NMe_2)Ni(PPh_3)Cl$ et $[\eta^3;\eta^1\text{-}(Ind(CH_2)_2NMe_2)Ni(PPh_3)]^+$ ont aussi été testés comme catalyseur pour la polymérisation de l'éthylène. Le composé neutre peut être activé par MAO (méthylaluminoxane) pour produire du polyéthylène linéaire alors que le complexe cationique ne peut que dimériser celui-ci de façon très efficace. Des études mécanistiques montrant la réaction des catalyseurs avec les activateurs en présence et en absence du monomère apportent des éclaircissements sur la réactivité observée.

On retrouve également quelques réactions d'oligomérisation des silanes, de polymérisation des alcènes (phénylacétylène), et d'hydrosilylation des oléfines.

Finalement, dans cette thèse sont présentées les difficultés à synthétiser des composés avec un ligand $Ind\text{^}PR_2$ et les débuts d'un projet montrant de très belles perspectives : la chimie du nickel avec des ligands indényles comportant une oléfine en bout de chaîne.

Mots clés : nickel, indényle, ligand hémilabile, polymérisation cationique, polystyrène, éthylène, diffraction des rayons X, voltampérométrie cyclique, RMN, GPC.

Summary

New functionalized indenyl ligands: Ind^NRR' (^ represents a side chain of 2 to 4 carbons; NRR' = NH_2, NMe_2, N-*i*Pr_2, 2-Py, NHBz, NH-*t*Bu, Pyrrolidine) have been prepared and characterized by NMR spectroscopy (^1H and $^{13}C\{^1H\}$), elemental analysis and, in the case of $Ind(CH_2)_3NHBz{\cdot}HCl$, by X-ray diffraction studies.

With these ligands, three types of nickel compounds have been obtained, as follows. The first two types of these complexes have the tether uncoordinated to the metal, including both the neutral compounds $(\eta^3{:}\eta^0\text{-Ind}^N)Ni(PR_3)X$ (R = Ph, Cy, Me; X = Cl, I, Me, *n*-Bu, CCPh) and the cationic compounds $[(Ind^N)NiLL']^+$ (LL' = $(PPh_3)_2$, dppe, PPh_3/PMe_3, PPh_3/Pyridine). On the other hand, the third group contains cationic complexes having the tether chelated to the nickel: $[(\eta^3{:}\eta^1\text{-Ind}^N)Ni(PR_3)]^+$ (R = Ph, Cy, Me).

The study of the structures of the complexes and the influence of the functionalized tether on the reactivities forms the core of this thesis. These compounds have been characterized by NMR specrtoscopy (^1H, $^{13}C\{^1H\}$ and $^{31}P\{^1H\}$) and elemental analysis. X-ray diffraction techniques have been used to solve many structures of these new organometallic complexes. Electrochemical measurements (cyclic voltammetry) allowed the determination of the electronic density on the metal centers.

In the structures, it has been observed that the chelation of the amine gives rise to a certain number of structural constraints and affected the coordination mode of the indenyl. Moreover, the structural, spectroscopic and electrochemical studies have revealed an interesting correlation between the nature of the X ligand and the Ni-P and Ni-Ind binding. When X = Cl (neutral complex) or N (cationic complex), the nickel appears to be bonded less strongly with both the phosphine and the indenyl, while when X = Me or CCPh, Ni-P and Ni-Ind bonds appear to be stronger.

Studying the solution behavior of the amino-tether in the neutral complexes using variation temperature NMR has shown a dynamic coordination-decoordination of the tether (hemilabile behavior). For the cationic species having the tether chelated to the nickel, the strength of the Ni-N binding has been probed by reacting them with different

Lewis bases (phosphine, amines, etc.). These studies showed that strongly donor ligands are required (either in excess or as bidentates ligands) for disrupting the Ni-tether interaction. This hemilabile behavior allowed the preparation of single component cationic catalysts for the polymerization of olefines (styrene, norbornene, vinylcarbazole, vinylethylether).

The complexes $(Ind(CH_2)_2NMe_2)Ni(PPh_3)Cl$ and $[\eta^3:\eta^1\text{-}(Ind(CH_2)_2NMe_2)Ni(PPh_3)]^+$ have also been tested as catalysts for the polymerization of ethylene. The neutral compound can be activated by MAO (methylaluminoxane) to produce linear polyethylene whereas the cationic complex only dimerizes it very effectively. Mechanistic studies of the reaction of the activators with the catalysts, in the presence and in the absence of monomers, gave useful information on the observed reactivity. Oligomerization of silanes, polymerization of alkynes, and hydrosilylation of olefins are also reported.

Finally, this thesis presents the difficulties encountered while trying to prepare nickel compounds with a ligand bearing a phosphino tether ($Ind\text{^}PR_2$) and the starting of a very promising project: the use of indenyl ligand bearing an olefin tether with nickel.

Key words: nickel, indenyl, hemilabile ligand, cationic polymerization, polystyrene, ethylene, X-Ray diffraction, cyclic voltammetry, NMR, GPC.

Table des matières

Liste des tableaux

Liste des figures

Liste des abréviations

br	*broad* (RMN)
Bu	butyle
n-Bu	$-CH_2CH_2CH_2CH_3$
t-Bu	$-C(CH_3)_2$
Bz	benzyle
cat.	catalyseur
ClBz	chlorobenzène
Cp	cyclopentadiényle $(C_5H_5)^-$
Cp*	pentaméthylecyclopentadiényle $(C_5Me_5)^-$
CP-MAS	*cross-polarization magic angle spinning*
CuKα	longueur d'onde Kα du cuivre (rayons X)
Cy	cyclohexyle
δ	déplacement chimique en RMN (ppm)
d	doublet (RMN)
D	deutériun
Da.	Dalton
DCE	dichloroéthane
Deg	degré
dme	diméthoxyéthane
DMSO	diméthylesulfoxyde
dppe	bis(diphénylphosphino)éthane
DSC	*differential scanning calorimetry*
Eq. ou Equiv	équivalent
E_{red}	potentiel de réduction
Et	éthyle
F	facteur de structure
FA	*fold angle*
GC	*gas chromatography*

GPC	*gel permeation chromatography*
HA	*hinge angle*
HDPE	*high-density polyethylene*
HRMS	*high resolution mass spectroscopy*
i-	ipso
Ind	indényle
J	constante de couplage (RMN)
L	ligand neutre donneur de deux électrons
LDPE	*low-density polyethylene*
LLDPE	*linear low-density polyethylene*
K_{eq}	constante d'équilibre
m-	méta
m	multiplet (RMN)
M	métal
M_w	poids moléculaire en masse
M_n	poids moléculaire en nombre
MAO	méthylaluminoxane
Me	méthyle
Mol wt	*molecular weight*
MS	*mass spectrometry*
MVK	*methykvinylketone*
NMR	*nuclear magnetic resonance*
o-	ortho
ORTEP	*oak ridge thermal ellipsoids plot*
Otf	ligand triflate
p-	para
PE	*polyethylene*
Ph	phényle
PPA	poly(phényleacétylène)
ppm	parties par million
Pr	propyle

i-Pr	$-CH(CH_3)_2$
Py	pyridine
R	groupement alkyle
RMN	résonance magnétique nucléaire
SCE	*standard calomel electrode*
t	triplet (RMN)
T_c	température de coalescence
Temp	température
THF	tétrahydrofurane
TOF	*turnover frequencies*
Tol	toluène
TON	*turnover numbers*
UV	ultraviolet
VEE	*vinylethylether*
VT	*variation temperature*
X	ligand anionique donneur de deux électrons

À Macarena, Alissa, Christine et Daniel

Ma famille tant aimée

Remerciements

Lorsque je regarde cette thèse, fruit de ces années de doctorat, je ne peux taire les noms de ceux qui m'ont aidé, soutenu, enseigné ou encore supporté :

Premièrement, mon directeur de recherche, le professeur Davit Zargarian mérite un gros MERCI. Il m'a enseigné, guidé et donné les moyens de devenir le chercheur que je suis. Son désir de faire connaître la chimie, m'a permis de vivre l'expérience de nombreux congrès mémorables, tout en améliorant mes capacités à communiquer. Son esprit vif et son imagination débordante sauront certainement motiver un bon nombre d'étudiants.

MERCI aux anciens et aux membres actuels de son groupe, ces dernières années ont été plus faciles, plus productives et plus agréables grâce à eux.

MERCI également aux professeurs André Beauchamp, Christian Reber et François Brisse à qui je dois beaucoup pour ma formation et pour leur soutien dans mes demandes de bourses et recherches d'emploi. Leurs étudiants ont été déterminants dans la bonne atmosphère qui règne parmi les inorganiciens.

Pour un certain nombre de résultats, j'ai eu le soutien d'une équipe efficace : Francine, Michel, Thierry et Christian m'ont formé à la cristallographie; Robert, Sylvie et Tan m'ont guidé pour mes expériences RMN; Willms, Ernesto et Héloïse du groupe du professeur Zhu ont toujours été prêts à analyser mes polymères alors que Fredéric m'a aidé pour mes études électrochimiques et Christine pour la correction du français dans cette thèse.

Certains résultats ont été produits dans d'autres laboratoires avec qui nous collaborions. Ainsi, j'ai eu le plaisir de travailler avec Leonardo Simon du groupe du professeur Joao Soares (University of Waterloo) et Russel Stapelton étudiant du professeur Scott Collins (University of Akron). Chaque fois, j'ai reçu une bonne formation et un accueil très chaleureux.

Finalement, le plus GROS MERCI est attribué, sans conteste, à ma femme Macarena et mes enfants à qui cette thèse est dédiée. Ma famille a toujours été ma plus grande source de joie et de motivation pour continuer sans abandonner. Je les aime énormément.

Chapitre 1 : Introduction

Au centre du tableau périodique se situent les métaux de transition. Ils représentent une partie importante des éléments disponibles aux chercheurs pour développer une chimie riche en couleur, en structure, en réactivité, en propriété optique, électrique ou magnétique, et bien d'autres propriétés interessantes. Les ligands, atomes ou molécules, constituent la garde-robe de ces métaux et n'ont que l'imagination pour limite. Ils habillent ce dernier et déterminent en grande partie les propriétés des composés, ce qui force le chimiste à choisir la bonne combinaison de ligands pour un métal afin de lui donner la réactivité désirée.

Cette thèse, rapportant les résultats de notre étude de l'utilisation des ligands amino-indényles hémilabiles avec le nickel, démontre une fois de plus le rôle essentiel de l'environnement autour du métal. Dans ce chapitre d'introduction, on présentera tout d'abord cette catégorie particulière de ligands ainsi que quelques unes de leurs applications. La chimie des composés nickel-indényle sera ensuite située par rapport à l'avancement actuel des connaissances et finalement, suivront les objectifs du projet et la description des travaux.

1.1 Les ligands hémilabiles

Un ligand hémilabile contient au moins deux sites de coordination disponibles pour se lier à un centre métallique (ligand bidentate ou multidentate). Comme présenté dans la Figure 1.1, les liens qu'il peut former avec le métal doivent être de deux types. Un des sites doit pouvoir se coordonner relativement fortement pour ancrer le ligand, ce qui nécessite une bonne compatibilité entre le métal et le ligand, tout en étant spectateur lors des réactions envisagées. La seconde fonctionnalité doit garder une grande labilité. Dans certains cas, la coordination entre ce deuxième ligand et le métal sera très défavorisée et ne se produira que grâce à l'effet chélate, car la proximité engendrée par la coordination de la première fonctionnalité favorisera entropiquement la coordination de la deuxième.

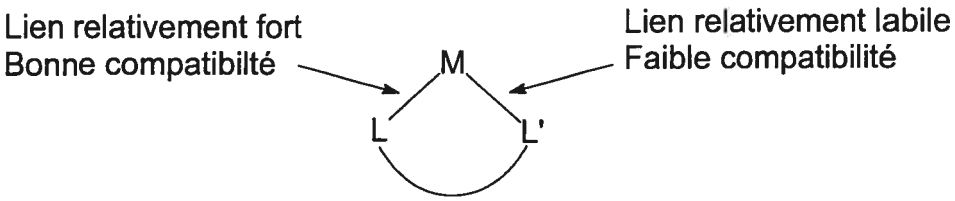

Figure 1.1. Les ligands hémilabiles

La théorie des acides et des bases durs et mous proposée par Pearson[1] qui se simplifie ainsi : « *les acides durs préfèrent se lier aux bases dures, et les acides mous préfèrent se lier aux bases molles.* » permet de guider le chercheur dans le choix des fonctions à utiliser dans la préparation de ligands hémilabiles pour un métal donné. Dans la littérature, une majorité de ces ligands utilisent une phosphine ou le ligand cyclopentadiényle (Cp) comme ancrage sur lequel est greffé un bras moléculaire fonctionnalisé (Figure 1.2). Le comportement hémilabile est obtenu grâce au choix intentionnel d'une « mauvaise » combinaison (dur-mou) entre la fonction en bout de chaîne et le métal.

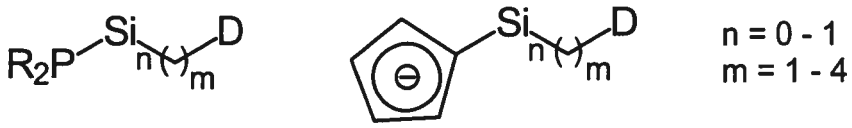

D = NRR', PRR', P(O)RR', AsRR', OR, SR, C=C

Figure 1.2. Ligands hémilabiles basés sur une phosphine ou le Cp

Dans les exemples présentés (Schéma 1.1-1.3), on constate déjà l'utilité de ce type de ligand. En présence d'un substrat, la partie labile du ligand se détache et libère un site de coordination sur le métal pour permettre une certaine réactivité, tel que des réactions de couplage, d'insertion ou de polymérisation. Cette stratégie permet l'isolation de composés stables mais réactifs, prêts à être utilisés sans avoir besoin d'activateur. De plus, comme la fonction labile reste à proximité du métal, elle peut revenir stabiliser le métal dès qu'il en a besoin.

D'un autre côté, Mirkin *et al.* a utilisé des ligands hémilabiles dans une approche relativement différente. En effet, à l'aide de ces derniers, il forme des structures macrocycliques possédant une cavité dans laquelle il envisage de la chimie hôte-invité.[2]

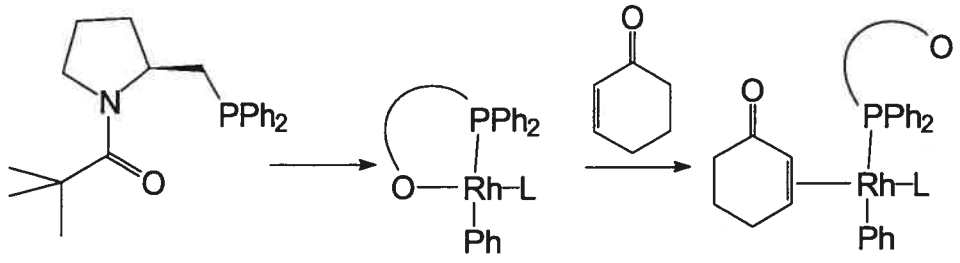

Schéma 1.1. Ligand hémilabile P-O chiral[3]

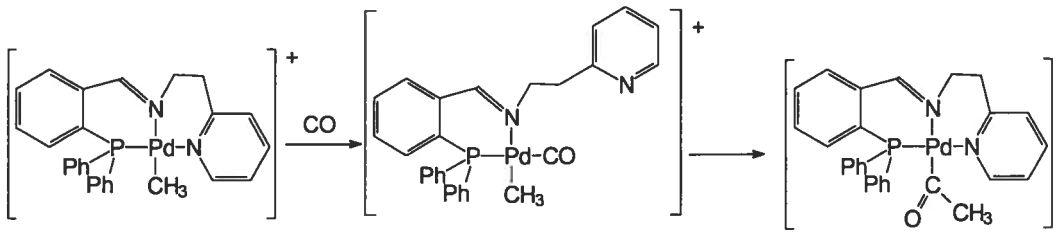

Schéma 1.2. Ligand hémilabile P-N-N tridentate[4]

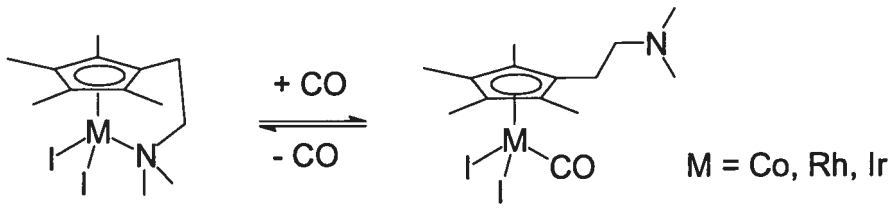

Schéma 1.3. Ligand hémilabile Cp^*-N[5]

Le groupe Cp présente l'avantage de stabiliser des fragments métalliques de degré d'oxydation élevé ou bas tout en étant relativement inerte. Il est devenu très populaire à la suite de la découverte du ferrocène et a permis le développement rapide de la chimie

organométallique des métaux de transition. Un de ses dérivés, l'indényle (Ind), qui comporte un cycle benzénique, a rapidement pris de l'importance en chimie organométallique comme alternative au Cp. On retrouve donc un certain nombre d'exemples de ligands utilisant l'indényle comme ancrage.[6] Ces ligands hémilabiles sont facilement préparés en ajoutant au Cp ou à l'Ind une chaîne aliphatique à l'extrémité de laquelle est accroché un groupement fonctionnel donneur tel qu'une amine,[7] une phosphine,[8] une arsine,[8] un thiol,[8] un alcool[9] ou une oléfine.[9]

Il faut cependant noter que ces ligands Cp ou Ind fonctionnalisés ne se limitent pas à leur comportement hémilabile. Ils peuvent également être des ligands spectateurs dont la fonction ajoutée n'a pas d'interaction avec le métal. Par contre, elle peut se coordonner à un autre métal, ce qui forme des composés hétéro-bimétalliques, ou se fixer sur un support solide, donnant accès à l'hétérogénéisation d'un catalyseur homogène. D'un autre côté, elle peut se coordonner fortement avec le métal pour former des composés chiraux dans certains cas. La Figure 1.3 présente un aperçu des applications rapportées à ce jour.[9]

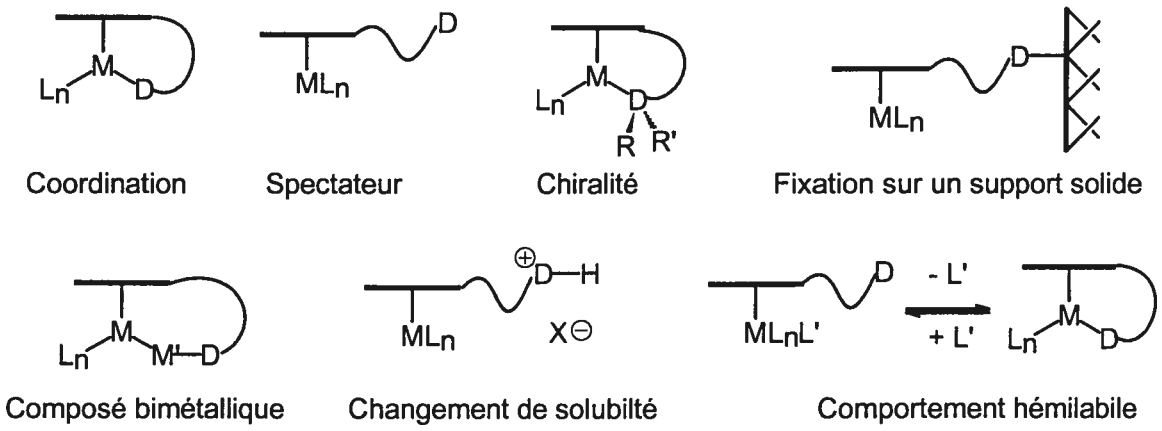

Figure 1.3. Applications des ligands Cp fonctionnalisés

1.2 Le nickel

La chimie organométallique du nickel a commencé par la découverte du $Ni(CO)_4$ par Ludwig Mond. Il a développé un procédé portant son nom permettant la purification du nickel.[10] De nombreuses applications ont été développées pour le nickel et ces complexes. Alors que le nickel métallique est largement utilisé dans des alliages, ses complexes sont reconnus pour leur utilité : on les retrouve comme catalyseurs en synthèse organique, principalement dans des réactions de couplage ainsi que dans la chimie macromoléculaire, comme catalyseur pour l'oligomérisation et la polymérisation d'oléfines.[11] Les catalyseurs découverts par Keim pour le procédé SHOP,[12] ceux de Brookhart[13] et de Grubbs[14] figurent parmi les plus connus. Au fil des ans, de nombreux composés comportant des liens σ Ni-C et π Ni-C ont été préparés et caractérisés.[15] Parmi ces derniers, deux grands groupes se démarquent : les composés nickel-allyle et les composés nickel-Cp, ainsi qu'un relativement petit nombre de composés nickel-Ind.

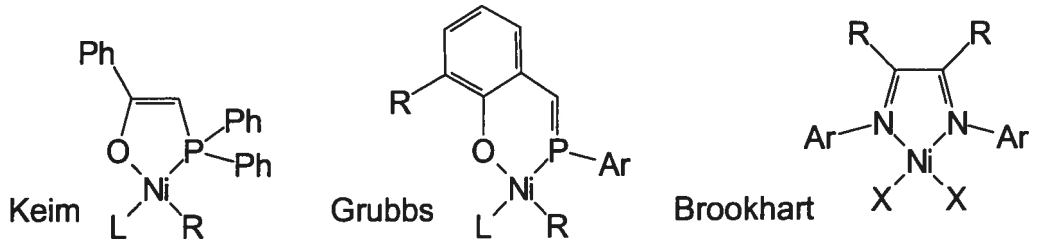

Figure 1.4. Catalyseurs de nickel pour la polymérisation ou l'oligomérisation de l'éthylène

1.2.1 Composés nickel-allyle[15]

De nombreux exemples de composés allyles sont rapportés dans la littérature, principalement sous les formes $Ni(\eta^3\text{-}C_3H_4R\text{-}2)LX$ neutres et $[Ni(\eta^3\text{-}C_3H_4R\text{-}2)L_2]^+X^-$ cationiques (L = ligand donneur de deux électrons et X = halogénure, etc) avec un certain nombre de composés dimères. Ces composés stables de nickel(II) sont d^8, plan-carré avec un total de 16 électrons. Ils possèdent la capacité d'accepter facilement un ligand ou un substrat car il reste des sites de coordination libres sur le métal et que l'ajout de deux électrons donne un composé à 18 électrons.

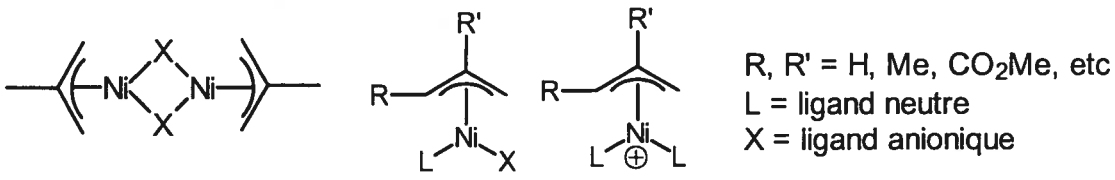

Figure 1.5. Composés de nickel-allyle

Les espèces cationiques allyles de nickel ont été utilisées avec succès comme catalyseurs homogènes dans la polymérisation de certaines oléfines (norbornène,[16] éthylène[17]), l'oligomérisation du norbornadiène[18] et du méthylacrylate[19] ainsi que la copolymérisation éthylène/acrylate.[20]

Dans ces cas, le ligand allyle n'est pas un ligand spectateur mais il est activement impliqué dans les réactions puisque son hapticité peut changer de η^3 (ligand anionique donneur de quatre électrons) à une coordination η^1 (ligand anionique donneur de deux électrons) libérant ainsi un site de coordination pour permettre la coordination d'un substrat. Le ligand η^1-allyle peut alors constituer un site d'insertion pour la polymérisation des oléfines (Schéma 1.5), ou subir plus facilement une élimination réductrice (Schéma 1.4).

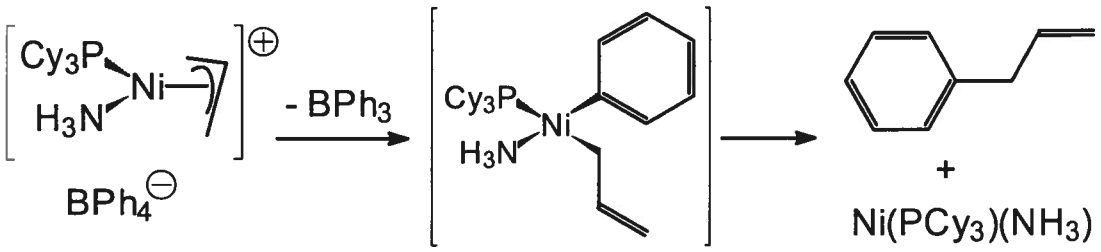

Schéma 1.4. Exemple de couplage impliquant l'allyle[19]

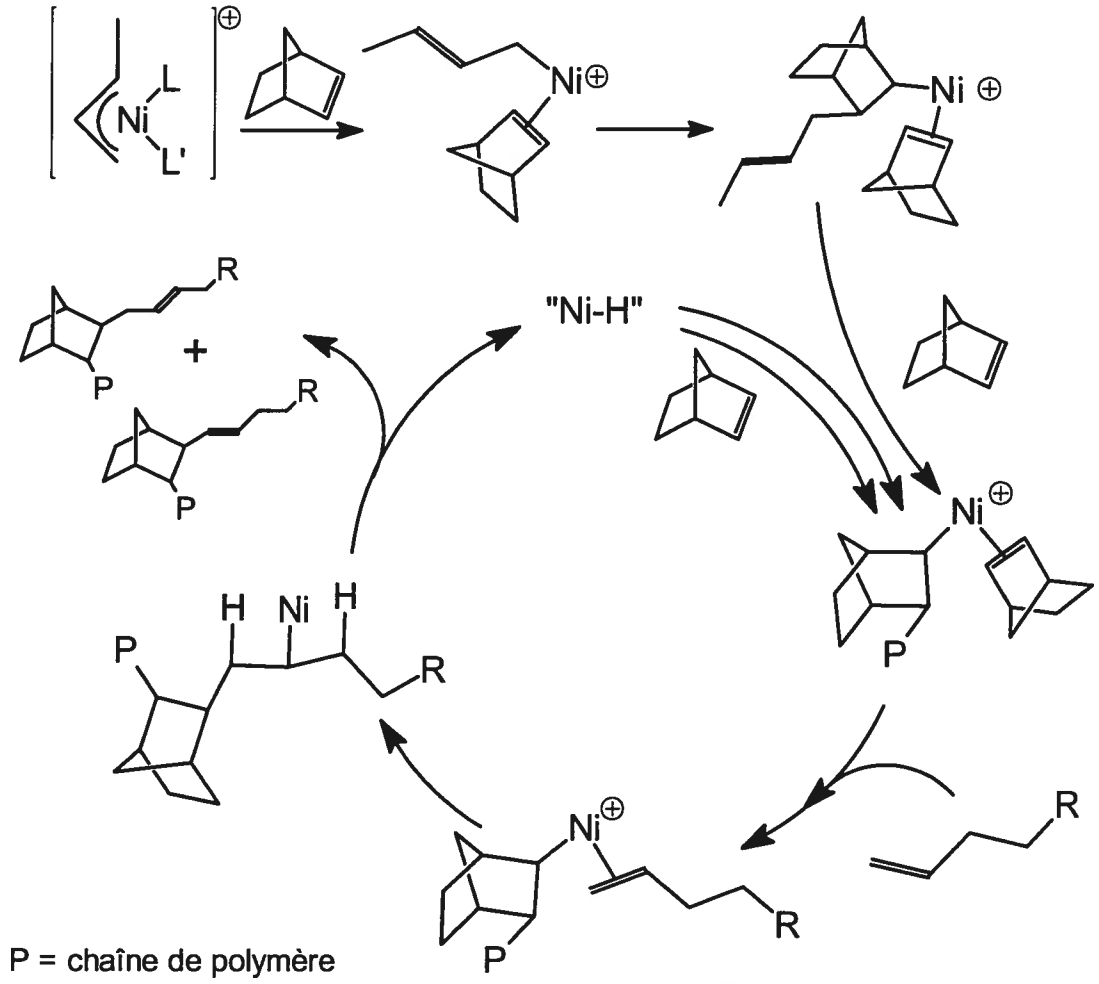

Schéma 1.5. Polymérisation du norbornène avec un nickel-allyle. Contrôle de la masse moléculaire par ajout d'une α-oléfine

1.2.2 Composés nickel-Cp

D'autre part, la chimie des composés nickel-Cp est également très développée. On y retrouve le nickelocène $Ni(Cp)_2$[21] qui est le seul métallocène avec 20 électrons de valences. Ceci implique qu'il est facile de déplacer au moins un des Cp (Schéma 1.6).[22] Comme on peut le constater, les composés Cp du nickel peuvent prendre des formes différentes : « two legged piano-stool », dimère et cluster (Schéma 1.6). On retrouve également une variété de degrés d'oxydation parmi les composés Cp du nickel :

$[(C_5Me_5)_2Ni]^{2+}$ est un rare exemple de Ni(IV) pouvant être isolé,[23] les nickel(III) sont représentés par un groupe important de nickelocéniums[24] et quelques autres composés comme le $CpNiBr_2$.[25] Les nickel(II) comptent pour la majorité des complexes[26] bien qu'il existe également plusieurs composés Cp de nickel(I) comme le (Cp)Ni(Bipy).[27]

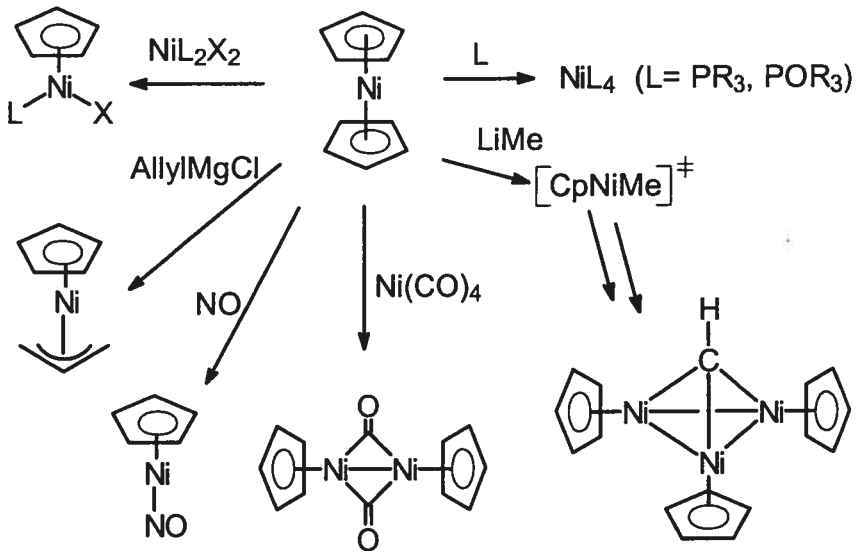

Schéma 1.6. Réactivité du nickelocène

La plupart des composés cyclopentadiényle de nickel(II) monométalliques stables sont de type « two legged piano-stool » : CpNiXL ou $[CpNiLL']^+$ et ont un total de 18 électrons. Certains de ces composés sont disponibles commercialement. Parmi ceux-ci, on retrouve le $(Cp)Ni(PPh_3)Cl$[28] (Aldrich, 1 g, 39 $ en 2003), qu'on peut facilement synthétiser[29] à partir du nickelocène et de $Ni(PPh_3)_2Cl_2$. C'est un précurseur pour la polymérisation des alcènes,[30] des isocyanides[31] et du méthylmétacrylate.[32] Il a permis la préparation de nombreux autres composés par échange de ligand (X ou L) afin de donner des composés possédant des liens Ni-alkyle,[33] Ni-Si,[34] Ni-Sn,[35] Ni-CCR,[36] Ni-In,[37] Ni-S,[38] Ni-Ge,[30c] Ni-Pb,[35b] Ni-CN, [35b] Ni-SCN, [35b] Ni-NO, [30c] Ni-NCO[35b] et $Ni-NO_2$. [35b et 39]

La majeure partie de ces composés est bien caractérisée par spectroscopie RMN (étude des spectres ^{31}P)[40] et de nombreuses structures par diffraction des rayons X ont été résolues. Ceci a permis, entre autre, à Bergman[41] de faire une étude approfondie des effets

trans des ligands dans les composés Cp* du nickel en comparant les déformations du ligand Cp* en fonction des autres ligands.

1.2.3 Composés nickel-indényle[42]

Très peu d'exemples de composés nickel-indényle ont été rapportés avant 1995. On peut citer le $Ni(ind)_2$,[43] qui avait été préparé et caractérisé.[44] La littérature des brevets montre que deux autres composés ont également été préparés, soit le $(Ind)Ni(P(C_{10}H_{21})_3)Br$ et le $(Ind)Ni(PBu_3)I$.[45] Toutefois, ce brevet relativement ancien ne donne que très peu de détails sur leur préparation et à peu près aucune caractérisation.

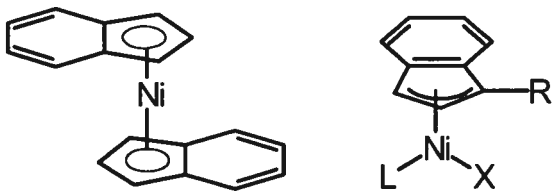

L = phosphine, carbène
X = halogénures, alkyles, alcényle, imides, thiols, triflate, et thiophène
R = alkyles

Figure 1.6. $Ni(Ind)_2$ et composés typiques nickel-indényle

À partir de 1995, le groupe du professeur Zargarian a ouvert la voie à une étude complète de ce type de composés. Ses succès ont permis la préparation et la caractérisation de composés de type $(Ind)Ni(PR_3)X$ (Ind = ligand indényle et ses analogues substitués en position 1, 2 et 3; R = Ph, Cy, Me, Bu; et X = halogénures, alkyles, alcényles, imides, thiols, triflate, et thiophène). Le choix de l'indényle se justifie, entre autre, par ses propriétés intéressantes parmi lesquelles on peut citer « l'effet indényle » qui fait référence à la réactivité supérieure des composés Ind par rapport au ligand Cp: dans plusieurs réactions de substitution, les composés indényles de métaux de transition sont beaucoup plus réactifs que leurs analogues avec le Cp. En 1969, Hart-Davis et Mawby[46] ont presenté le premier exemple de ce phénomène : $(Cp/Ind)Mo(CO)_3Me$ réagissait avec PR_3 pour donner $(Cp/Ind)Mo(PR_3)(CO)_2(COMe)$. Ainsi, la réaction avec le composé indényle était plus rapide de plusieurs ordres de grandeur que celle avec les dérivés Cp.

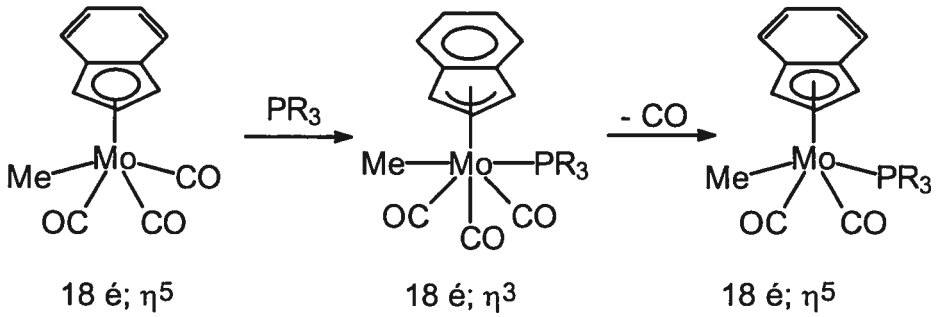

Schéma 1.7. Glissement de l'Indényle pour faciliter des réactions de substitution

L'effet indényle s'explique par la stabilisation du cycle benzénique de l'indényle lorsque ce dernier est sous sa forme η^3 (Schéma 1.7). Ainsi, le ligand va pouvoir varier sa contribution électronique et libérer un site de coordination en changeant son mode de coordination par glissement sans passer par un état de haute énergie. Par ailleurs, il est intéressant de remarquer que dans certains cas, l'utilisation de l'indényle ralentit la réaction pour des raisons stériques ou électroniques; il s'agit alors de l'effet indényle inverse.[47]

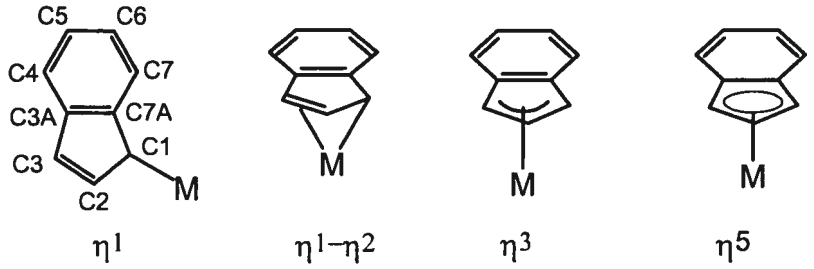

Figure 1.7. Modes de coordination du ligand indényle

D'un autre côté, l'indényle est capable de se lier au métal de plusieurs façons : on retrouve les modes η^5 et η^3 mais il existe également un bon nombre d'exemples de coordination η^1,[48] ainsi que des modes intermédiaires entre η^1-η^2 ou η^5-η^3. En fait, ces modes intermédiaires sont proposés pour expliquer les différences observées dans les études structurales des complexes comme dans le cas des composés indényle de nickel.

Le mode η^1-η^2 est proposé lorsque la distance M-C1 << M-C2 ≈ M-C3 << M-C3A ≈ M-C7A et que la distance C2-C3 < C1-C2.

On peut évaluer le degré de coordination en utilisant le paramètre Δ(M-C) qui se calcule à partir des distances métal-carbone: Δ(M-C) = ½ [(M-C3A + M-C7A)-(M-C3 + M-C1)].[49] Un mode η^5 aura donc un paramètre Δ(M-C) proche de zéro (toutes les distances M-C sont équivalentes) alors que le Δ(M-C) du mode η^3 sera positif. A titre d'exemple, les Δ(M-C) des composés $(\eta^5\text{-Ind})_2Fe$ [49b] et $[(\eta^3\text{-Ind})Fe(CO)_3]^-$ [50] sont de 0.043 et 0.689 Å, respectivement. Dans certains cas, le type de coordination peut également être déterminé par spectroscopie RMN ^{13}C.[49 et 51] Pour se faire, on calcule le paramètre $\Delta\delta^{13}C$ = δ [C(3A /7A) de M-Ind] - δ [C(3A /7A) de Na-Ind]. Il a pu être déterminé qu'un $\Delta\delta^{13}C$ négatif correspondait à un mode η^5 (-43.7 pour $(\eta^5\text{-Ind})_2Fe$))[52] alors qu'il est proche de 20-30 pour un mode η^3 (+27 pour $[(\eta^3\text{-Ind})Fe(CO)_3]^-$).[50]

Les composés préparés par Zargarian *et al.* adoptent différentes variations de structures plan-carré déformées avec l'indényle occupant deux sites de coordination et placé perpendiculairement au plan formé par Ni, L et X.[42] L'indényle est coordonné de façon η^5-η^3. Il est donc un ligand anionique donneur de 4-6 électrons pour former des composés de 16-18 électrons. Cette situation ambigüe mérite donc une attention particulière puisqu'elle se situe, dans un certain sens, entre le cas des composés allyles (coordination η^3, charge négative, donneur de 4 électrons) et des composés Cp (coordination η^5, charge négative, donneur de 6 électrons). On peut donc espérer que l'indényle soit spectateur dans certains cas comme le Cp ou alors bien impliqué dans les réactions en tant que site d'insertion similairement à l'allyle.

On a démontré que ces composés nickel-ind catalysent la polymérisation et l'oligomérisation des oléfines (styrène, norbornène, éthylène),[53] des alcynes (Phénylacétylène)[54] et de $PhSiH_3$ [55] ainsi que l'hydrosilylation des oléfines.[56]

Pour se faire, il était nécessaire de les activer en enlevant le chlorure (avec $AgBF_4$, $AlCl_3$ ou $NaBPh_4$) pour donner l'espèce cationique $[(Ind)Ni(PPh_3)]^+$ identifiée comme le cation « nu ». Ce catalyseur, quoique très efficace, souffrait d'un problème important : sa faible stabilité. En effet, lors des tentatives d'isolation de ce composé en absence de ligands donneurs (CH_3CN, PPh_3, PMe_3, etc.) ou de monomère, le composé

$[(Ind)Ni(PPh_3)_2]^+$ était obtenu par redistribution de phosphine. Ce composé bis-phosphine était inactif en catalyse et les autres produits de cette redistribution étaient perdus.

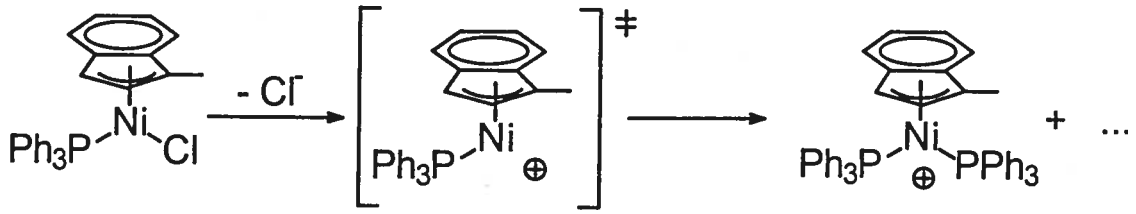

Schéma 1.8. Génération du cation nu

1.3 Objectifs

On propose donc d'utiliser les capacités hémilabiles des ligands indényles fonctionnalisés pour isoler de nouveaux catalyseurs de nickel cationiques stables mais actifs pour la polymérisation des oléfines. Idéalement, ils seront actifs sans nécessiter d'activateur. Cet objectif principal de la thèse sera atteint en passant par un certain nombre d'étapes intermédiaires :

a) Préparer des ligands indényles fonctionnalisés (Ind^L avec L = ligand donneur, typiquement NRR', PRR' et C=C; alors que ^ = chaîne aliphatique de longueur variable).
b) Isoler des composés de nickel comportant ces ligands.
c) Caractériser ces composés en solution (RMN, électrochimie) et à l'état solide (Structure par diffraction des rayons X).
d) Déterminer la bonne longueur de chaîne pour que la chélation ait lieu.
e) Classifier les substituants NRR' selon leur influence sur les interactions Ni-L.
f) Tester les complexes dans des réactions catalytiques (polymérisation et autre).
g) Comparer les résultats obtenus avec ceux des catalyseurs ne comportant pas de bras fonctionnalisé.
h) Conclure sur les effets et l'utilité des ligands indényles fonctionnalisés dans la chimie du nickel.

1.4 Description des travaux

Le premier chapitre de cette thèse présentée sous forme d'articles porte sur l'utilisation de ligands indényles fonctionnalisés dans la chimie du nickel et présente une mise en situation, une description des objectifs et une vue d'ensemble des travaux accomplis.

Le deuxième chapitre (Article 1) rapporte nos premières tentatives d'utilisation des ligands indényles fonctionnalisés comportant une amine en bout de chaîne. On y retrouve la synthèse de nouveaux ligands de type Ind^NRR' (^ représente une chaîne aliphatique de 2 à 4 carbones). Ces études ont montré la décomposition rapide des complexes lorsque le bras moléculaire greffé sur l'indène comportait une amine avec un atome d'hydrogène qui pouvait se coordonner au métal, empêchant l'isolation de composé stable. Par contre, en absence d'atome d'hydrogène sur l'amine ou lorsque celle-ci ne peut atteindre le métal, des composés stables ont pu être isolés et caractérisés. On retrouve notamment les premières structures cristallographiques de composés de nickel avec un ligand de type Ind^NRR'.

D'autre part, ces études ont permis de faire un choix quant à la longueur de la chaîne en montrant que deux carbones entre l'indène et l'amine donnaient une chance à l'amine de pouvoir se coordonner au nickel. Ce chapitre démontre la coordination-décoordination dynamique du bras $(CH_2)_2NMe_2$ en solution ainsi que la possibilité d'isoler un composé cationique avec le bras chélaté.

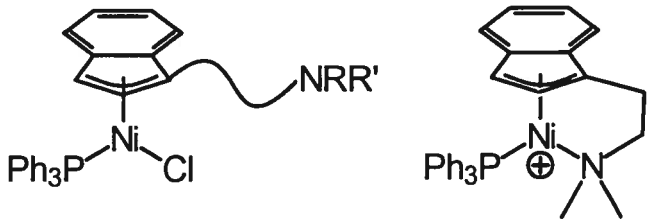

Figure 1.8. Composés de nickel avec un indényle fonctionnalisé

L'étude du composé cationique chélaté, $[(\eta^3{:}\eta^1\text{-Ind}(CH_2)_2NMe_2)Ni(PPh_3)][BPh_4]$, constitue la base du chapitre 3 (Article 2). Sa structure obtenue par diffraction des rayons X a permis de confirmer la coordination du bras et fournit les données structurales

relatives aux changements apportés par la chélation. De plus, l'opportunité de vérifier la force de la liaison Ni-N a motivé les études de réactions avec des bases de Lewis neutres (PR_3, dppe, pyridine et analogue). Elles ont permis de déterminer que le lien Ni-N était relativement fort et que pour le briser, il fallait de très bons ligands coordonnants et un excès de ligands monodentates ou un ligand bidentate. Les réactions avec des ligands anioniques (Ph_2P^-, Me_2N^-, Me^-, Cl^-, Br^- et I^-) n'ont pas été fructueuses puisque c'est seulement par la réaction avec LiI qu'un composé a pu être isolé : (η^3:η^0-$Ind(CH_2)_2NMe_2)Ni(PPh_3)I$. Finalement, le chapitre 3 présente l'utilisation de ce précurseur cationique dans la polymérisation du styrène, du norbornène et leur copolymérisation ainsi que la comparaison des résultats obtenus avec ceux du cation généré *in situ*.

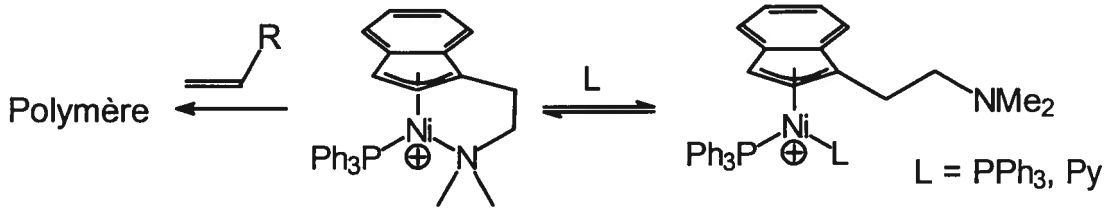

Schéma 1.9. Réactivité du cation chélaté

$(Ind(CH_2)_2NMe_2)Ni(PPh_3)Cl$ et $[\eta^3;\eta^1$-$(Ind(CH_2)_2NMe_2)Ni(PPh_3)]^+$ sont alors testés comme catalyseur dans la polymérisation de l'éthylène. Ces résultats, présentés dans le chapitre 4 (Article 3), montrent que le composé neutre peut être activé par le MAO (méthylaluminoxane) pour produire du polyéthylène linéaire alors que le complexe cationique ne peut que dimériser celui-ci. Des études mécanistiques montrant la réaction des catalyseurs avec les activateurs en présence et en absence de monomères apportent des éclaircissements sur la réactivité observée.

Le chapitre 5 (Article 4) décrit la préparation d'une série de nouveaux composés similaires avec, pour seule différence, un bras comportant d'autres amines choisies pour leurs capacités en tant qu'électrodonneur et pour leurs encombrements stériques variés. L'isolation de ces nouveaux composés a permis d'éclaircir les phénomènes de coordination dynamique des composés neutres (Ni-Cl). À ce stade, des études électrochimiques ainsi que de polymérisation ont montré l'importance de la densité

électronique sur le métal qui variait en fonction du bras utilisé. L'étude des réactivités des composés possédant des bras plus coordonnants et d'autres moins coordonnants a permis de déterminer l'influence du bras sur la polymérisation du styrène, qui dépend en partie de leur capacité à libérer un site pour la coordination du monomère.

Une deuxième façon de varier la densité électronique sur le métal est l'utilisation de phosphines autres que PPh_3, soit PMe_3 (meilleur donneur, moins encombrant) et PCy_3 (meilleur donneur, plus encombrant) ou de remplacer le ligand Cl par un méthyle ou un alcynyle. Cette stratégie a permis d'isoler de nouveaux composés stables : $(Ind(CH_2)_2NMe_2)Ni(PR_3)X$ et $[\eta^3;\eta^1\text{-}(Ind(CH_2)_2NMe_2)Ni(PR_3)]^+$ (R = Me ou Cy; X = Cl, Me ou CCPh). Leur caractérisation (rayons X, RMN et électrochimie) a permis d'observer un phénomène remarquable. En effet, la coordination des ligands phosphine et Ind avec le nickel dépend directement du ligand X. Plus le ligand X est donneur, plus les autres ligands sont liés fortement alors qu'un ligand X faible provoque un affaiblissement des autres liens tel que montré dans le chapitre 6 (Article 5).

Le chapitre 7 présente les difficultés à synthétiser des composés comportant un ligand Ind^PR_2 et les débuts d'un projet montrant de très belles perspectives : la chimie du nickel avec des ligands indényles comportant une oléfine en bout de chaîne.

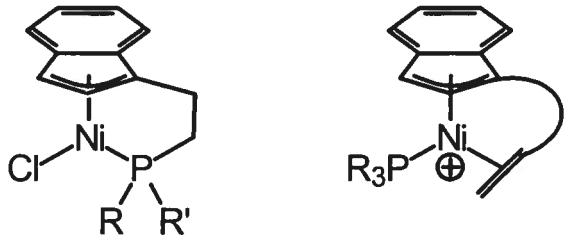

Figure 1.9. Composés ciblés possédant un bras phosphine ou oléfine

Finalement, la revue des résultats, une discussion de l'ensemble du projet et quelques perspectives constituent la conclusion (chapitre 8).

Chapitre 2 : Preparation and Characterization of Nickel Complexes with η-Indenyl Ligands Bearing a Pendant Aminoalkyl Chain

Article 1

Laurent F. Groux, Francine Bélanger-Gariépy, Davit Zargarian, et Rainer Vollmerhaus

Organometallics **2000**, *19*, 1507.

Abstract

The aminoindenyl complexes {Ind-$(CH_2)_{3,4}$N(*t*-Bu)H}Ni(PPh_3)Cl (**7**, **8**) and {Ind-$(CH_2)_{2,3}NMe_2$}Ni(PPh_3)Cl (**9**, **10**) have been prepared and characterized by spectroscopy and, in the case of **7** and **9**, by X-ray structural studies. Although there is no interaction between the Ni center and the amine moiety of these complexes in the solid state, solution spectra point to a temperature-dependent, intramolecular N→Ni coordination in complex **9** and a more facile, intermolecular interaction in **10**. Abstraction of Cl^- from these complexes led to the formation of the cations [{η^3:η^0-Ind-$(CH_2)_{3,4}$N(*t*-Bu)H}Ni$(PPh_3)_2]^+$ and [{η^3:η^1-Ind-$(CH_2)_{2,3}NMe_2$}Ni-$(PPh_3)]^+$ (**11**, **12**). The origin of the observed differences in the reactivities of these complexes is discussed in terms of the lengths of the tether and the nature of the N-substituents.

Introduction

There has been a growing interest over the recent years in the reactivities of complexes containing Cp-type ligands bearing amine- or amide-functionalized side chains, Cp^NR_n (^ = tethering side chains). A few of these compounds are excellent catalysts for the polymerization of olefins,[1] while others catalyze the dehydropolymerization of silanes[2] and show other intriguing properties.[3] A survey of the literature reveals that most of the reported studies on Cp^NR_n systems have focused on the complexes of early transition metals (groups 3-6) and relatively few complexes of this type are known for later metals. This is especially true in the case of group 10 metals, for which only a few examples have been reported by Fischer (e.g., (η^5:η^0-Cp^NMe_2)Ni(CO)($SnMe_3$), (η^5:η^0-Cp^NMe_2)Ni(PPh_3) ($Si(SiMe_3)_3$), and (η^5:η^1-Cp^NMe_2)NiI)[4] and Jutzi (e.g., (η^5:η^0-Cp^NMe_2) Ni(PMe_3)I, (η^5:η^0-Cp^NMe_2)Pd(η^3-allyl), and (η^5:η^0-Cp^NH_2)$PtMe_3$).[5]

Our interest in the structural properties and catalytic activities of the nickel indenyl complexes Ind$Ni(PR_3)X$[6] prompted us to explore the chemistry of analogous compounds bearing amino- and amidoalkyl side chains tethered to the Ind ligand. Thus, we set out to prepare the first examples of neutral and cationic Ind^NR_2 complexes of nickel with both dangling (η^0) and coordinating (η^1) N-functionalities, as illustrated in

Chart 2.1. The present paper reports the preparation of the complexes (η^3:η^0-Ind^NRR')Ni(PPh_3)X (^ = $(CH_2)_{2\text{-}4}$; R, R' = H, Me, *t*-Bu; X = Cl, Me, Bu) and [(η^3:η^1-Ind$(CH_2)_2NMe_2$)Ni(PPh_3)]$^+$.

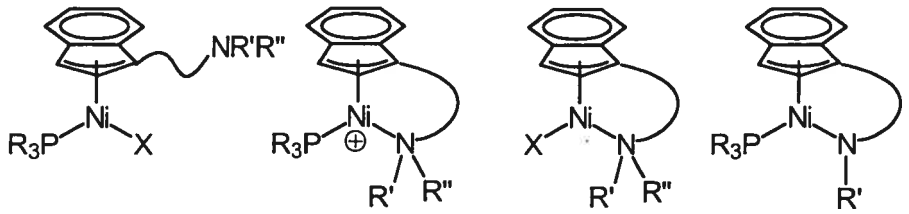

Chart 2.1.

Results and Discussion

Preparation of the ligands. The syntheses of the aminoindenyl ligands **1-6** are outlined in Scheme 2.1. The reaction of IndLi with an excess of 1,3-dibromopropane in Et_2O produced the desired (3-bromopropyl)indene in addition to the undesired by-product 1,3-diindenylpropane. The former was isolated in *ca.* 60% yield after vacuum distillation and subsequently reacted with *t*-BuNH_2 to give the HBr salt of Ind-$(CH_2)_3$N(*t*-Bu)H (**1**) as an air stable, white powder in *ca.* 85% yield. Using 1,4-dibromobutane in this synthesis yields the desired aminoindenyl ligand with a butyl side chain (**2**), whereas 1,2-dibromopropane leads to a known[7] spirocyclic byproduct. Using $BzNH_2$ (Bz = $PhCH_2$) instead of *t*-BuNH_2 gave Ind-$(CH_2)_3$N(Bz)H (**3**). The NMe_2 and NH_2 ligands (**4-6**) were prepared by reacting IndLi with X$(CH_2)_n$NR'$_2$ (n = 2, 3; X = Cl, Br; R' = Me, H;).

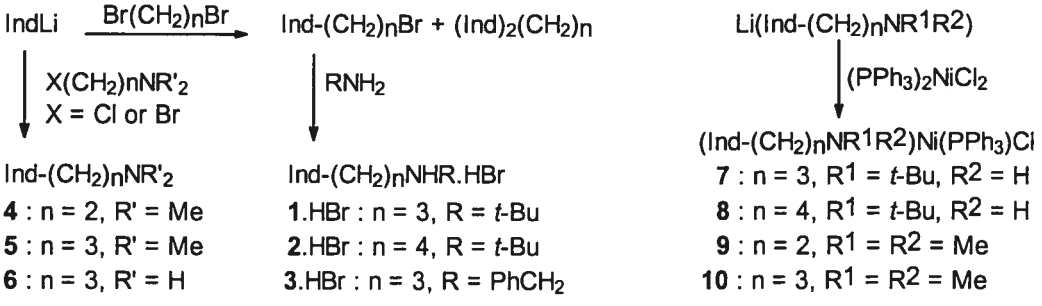

Scheme 2.1.

Type I complexes. The preparation of (η^3:η^0-aminoindenyl)nickel complexes was carried out by reacting $(PPh_3)_2NiCl_2$ with the singly deprotonated aminoindenes. Thus, reacting [Ind-$(CH_2)_3$N(*t*-Bu)H]$^-$ with $(PPh_3)_2NiCl_2$ in Et_2O gave a dark red solution from which the complex **7** could be isolated in 63% yield; similar protocols with the ligands **2**, **4** and **5** allowed the formation of the Ni complexes **8**, **9**, and **10**, respectively (Scheme 2.1). These compounds have been characterized by spectroscopy and, in the case of **7** and **9**, by X-ray diffraction studies (vide infra).

In contrast to the syntheses of **7-10**, the preparation of the analogous derivatives with the aminoindenyl ligands Ind$(CH_2)_3$NHR (R = Bz, **3**, and H, **6**) did not result in the isolation of stable compounds. For instance, addition of an Et_2O solution of singly deprotonated **3** (i.e., [Ind-$(CH_2)_3$N(CH_2Ph)H]$^-$) to the dark green Et_2O suspension of $(PPh_3)_2NiCl_2$ resulted, at first, in the appearance of the red color characteristic of the compounds (Ind)Ni(PR_3)X; however, the reaction mixture turned brown and then beige over a few minutes and no tractable compound could be isolated in the end. Lowering the temperature of the reaction did not prevent the decomposition of this material. A similar observation was made in the reaction of ligand **6**. The ^{1}H NMR spectra of the reaction mixtures in both reactions showed broad, featureless signals characteristic of paramagnetic or polymeric species, while the $^{31}P\{^1H\}$ spectra contained only the signal attributed to uncoordinated PPh_3.

It is conceivable that the complexes (η^3:η^0-Ind$(CH_2)_3$NRH)Ni(PPh_3)Cl (R = Bz, H) form at first but decompose afterward as a result of the interaction of the amine moieties with the Ni center (either intra- or intermolecularly). To test the validity of this supposition, we reacted the otherwise stable complex (1-Me-Ind)Ni(PPh_3)Cl with a number of amines and found that it decomposed readily upon contact with $BzNH_2$ and pyridine; BzN(Me)H also caused the decomposition of this complex but at a slower rate, while *t*-$BuNH_2$ and Et_3N did not react at all. We conclude, therefore, that the stabilities of complexes (Ind^NRR')Ni(PPh_3)Cl depend on the nature of the substituents on the amine moiety: the NH(*t*-Bu) and NMe_2 groups give the relatively stable species **7-10**, whereas NHBz and NH_2 groups allow side reactions which eventually lead to the decomposition of the complexes.

Characterization and dynamic behavior of (Ind^NRR')Ni(PPh_3)Cl. The general features of the NMR spectra obtained for compounds **7** and **8** are similar to those of the analogous complexes (1-Me-Ind)Ni(PPh_3)Cl. For instance, the ^1H NMR resonances for the H2 and H3 protons appear at ca. 6.5 and 3.5 ppm, respectively, while the $^{31}P\{^1H\}$ NMR spectra consist of a singlet resonance at *ca.* 33 ppm; these are very close to the corresponding resonances for (1-Me-Ind)Ni(PPh_3)Cl,[6c] indicating that the geometry around the Ni atom and the hapticity of the Ind ligand in **7** and **8** is very similar to that found in (1-Me-Ind)Ni(PPh_3)Cl. The solid state structure of **7** (Figure 2.1, vide infra) and variable-temperature ^1H and $^{13}C\{^1H\}$ NMR experiments showed that the N(*t*-Bu)H moiety in these complexes is not coordinated to Ni. Similarly, the X-ray structure of complex **9** (Figure 2.2, vide infra) showed that the NMe_2 moiety in this compound is not coordinated to the Ni atom *in the solid state*; in this case, however, the solution spectra indicated the presence of relatively fast equilibria which convert **9** and **10** into species involving N→ Ni interactions, as described below.

The first indication of a dynamic process involving complex **9** was the observation that some of the ^1H and $^{13}C\{^1H\}$ NMR signals were either broadened or missing from the ambient and higher temperature spectra (up to +50 °C) of this complex; at lower temperatures, the broad peaks sharpened and the missing peaks emerged. Significantly, the peaks corresponding to the nuclei on the side chain were the most affected during this process. In addition, the variable temperature $^{31}P\{^1H\}$ NMR spectra showed that the singlet resonance for **9** moved from ca. 31 ppm at 22 °C to ca. 38 ppm at +50 °C; cooling the sample to room temperature resulted in the reappearance of the signals for **9**. These observations imply that in solution the $\eta^3:\eta^0$-aminoindenyl complex **9** is in equilibrium with a species in which the NMe_2 moiety reversibly coordinates to the Ni center (Scheme 2.2). Given that the spectral features of this new complex are very different from those of the cationic complex which would arise from the displacement of Cl by the amine moiety (vide infra), we believe that the species in question is a *neutral* compound in which the Cl ligand remains coordinated to Ni. It is not certain, however,

whether the Ind moiety remains η^3-coordinated (giving an 18-electron species) or slips into an η^1-mode (giving a 16-electron species).

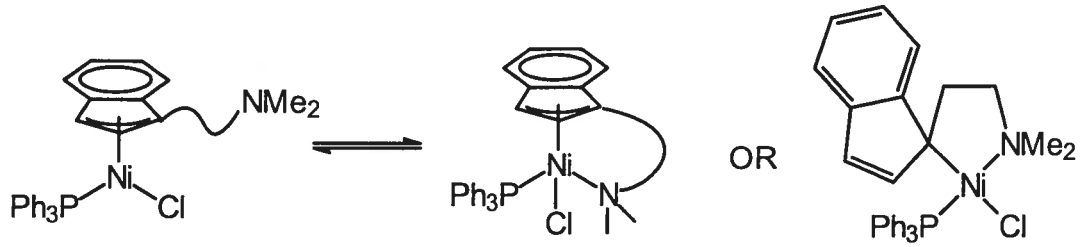

Scheme 2.2.

In contrast to the above described dynamic behavior displayed by complex **9**, complex **10** was found to undergo a gradual and irreversible transformation in solution, one which ultimately prevented the purification and complete characterization of this compound. Thus, repeated recrystallizations of complex **10** precipitate solid samples which are increasingly insoluble and give poorly resolved NMR spectra. For example, whereas **9** and freshly prepared samples of **10** were soluble in Et_2O, C_6H_6, toluene, etc., the solids obtained after recrystallizing **10** were soluble only in DMSO. Moreover, whereas the ^1H and $^{13}\{^1H\}$ NMR spectra of pre-recrystallization samples of **10** contained well-resolved signals quite similar to those of complex **9**, the aged solutions and recrystallized samples of **10** showed broad, featureless peaks. We believe that this "decomposition" of complex **10** is caused by the interaction between the NMe_2 moiety and the Ni center, and suggest that the longer side chain in this compound allows an *inter*molecular coordination which results in the formation of a sparingly soluble polymeric species.

Solid state structures of 7 and 9. As seen in Figures 2.1 and 2.2, the nickel centre in both **7** and **9** is within reasonable bonding distance from the P (ca. 2.18 Å), Cl (ca. 2.19 Å), C1 (ca. 2.14 Å), C2 (ca. 2.06 Å), and C3 (ca. 2.03 Å) atoms, but considerably farther away from C3a (av. 2.29 Å) and C7a (av. 2.35 Å). The geometry around the Ni is irregular but may be described as distorted square planar with C1=C2 occupying a single coordination site. The planes formed by P, Ni, and Cl on the one hand, and C1, C2, and

C3 on the other, are nearly perpendicular to each other. In both structures, the aminoalkyl side chain is oriented away from the Ni centre.

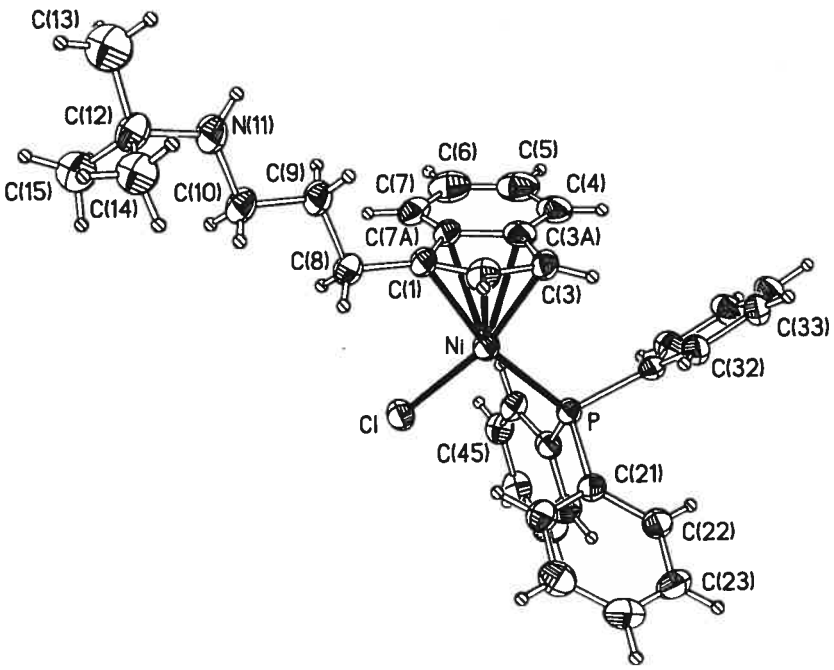

Figure 2.1. ORTEP plot of complex 7 with atom-numbering scheme.

Selected bond lengths (Å) and angles (deg): Ni-P = 2.181(3), Ni-Cl = 2.187(2), Ni-C1 = 2.135(6), Ni-C2 = 2.057(6), Ni-C3 = 2.028(6), Ni-C3a = 2.296(7), Ni-C7a = 2.357(8), C1-C2 = 1.409(10), C2-C3 = 1.423(9), C3-C3a = 1.456(10), C3a-C7a = 1.422(9), C7a-C1 = 1.452(9), C1-C8 = 1.497(9); Cl-Ni-P = 96.75(12), Cl-Ni-C3 = 162.4(2), Cl-Ni-C2 = 122.7(2), Cl-Ni-C1 = 95.8(2), P-Ni-C1 = 166.0(2), P-Ni-C2 = 130.6(2), P-Ni-C3 = 99.2(2), C1-Ni-C2 = 39.2(3), C1-Ni-C3 = 67.0(3), C2-Ni-C3 = 40.8(3).

The main features of **7** and **9** are very similar to those present in the solid state structure of (1-Me-Ind)Ni(PPh_3)Cl.[6c] For instance, all three structures exhibit virtually identical (i.e., within $\pm 3\sigma$) Ni-P (2.181(3), 2.1838(15), and 2.1782(11) Å) and Ni-Cl (2.187(2), 2.1763(14), and 2.1865(10) Å) bond lengths. Moreover, in all three structures the distortion of the Ind hapticity away from an η^5 mode and toward a fairly nonsymmetric η^3 coordination is reflected in the unequal Ni-C and C-C bond lengths: Ni-C7a > Ni-C3a >> Ni-C1 > Ni-C2 > Ni-C3 and C1-C7a (1.452(9) Å) $\approx$ C3-C3a (1.456(10) Å) > C3-C2

(1.423(9) Å) > C2-C1 (1.409(10) Å). These distortions are attributed to the tendency of the d^8 Ni center to form 16-electron complexes ($\eta^5 \rightarrow \eta^3$ slippage of Ind) and the unequal trans influences of the PPh_3 and Cl groups (unsymmetrical coordination of Ind).[6c]

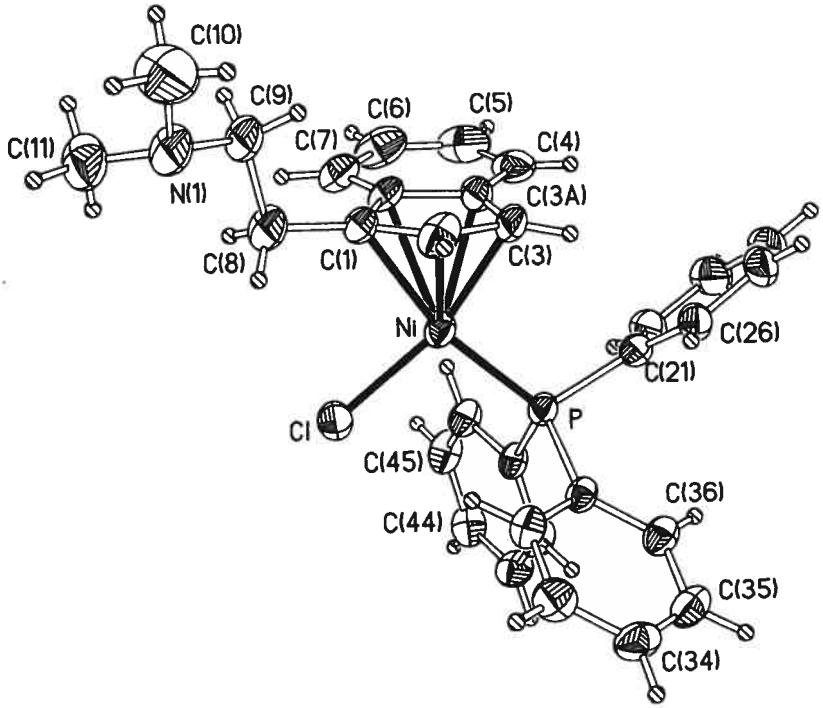

Figure 2.2. ORTEP plot of complex 9 with atom numbering scheme.

Selected bond lengths (Å) and angles (deg): Ni-P = 2.1838(15), Ni-Cl = 2.1763(14), Ni-C1 = 2.137(4), Ni-C2 = 2.060(4), Ni-C3 = 2.028(5), Ni-C3a = 2.283(5), Ni-C7a = 2.341(4), C1-C2 = 1.405(6), C2-C3 = 1.440(6), C3-C3a = 1.419(6), C3a-C7a = 1.424(6), C7a-C1 = 1.464(6), C1-C8 = 1.487(5); Cl-Ni-P = 98.01(6), Cl-Ni-C3 = 162.44(13), Cl-Ni-C2 = 122.61(15), Cl-Ni-C1 = 96.09(13), P-Ni-C1 = 165.87(13), P-Ni-C2 = 130.41(14), P-Ni-C3 = 99.32(13), C1-Ni-C2 = 39.07(15), C1-Ni-C3 = 66.65(17), C2-Ni-C3 = 41.25(18).

Type II complexes. We reacted the complexes **7-10** with $AgBF_4$, $NaBPh_4$, or $AlCl_3$ in order to abstract the Cl^- ligand from these complexes and facilitate the formation of the target $\eta^3:\eta^1$ cationic species. Abstraction of Cl^- from **7** resulted in the formation of a major species displaying an AB set of resonances in the $^{31}P\{^1H\}$ NMR spectrum of the

reaction mixture (ca. 34 and 32 ppm, d, $^2J_{P-P}$ = 26 Hz); the spectrum also contained a singlet resonance at ca. 24 ppm corresponding to a minor product. The major product was readily identified as $[\{\eta^3{:}\eta^0\text{-Ind}(CH_2)_3NH(t\text{-Bu})\}Ni(PPh_3)_2]^+$ on the basis of comparison to the $^{31}P\{^1H\}$ NMR spectrum of the fully characterized[6d] compound $[(1\text{-Me-Ind})Ni(PPh_3)_2]^+$, which displays a similar AB signal. The inequivalence of the PPh_3 ligands in these compounds is consistent with the hindered rotation of the unsymmetrically substituted Ind ligands. When the Cl^- abstraction from **7** is carried out in the presence of an excess of PPh_3, only the bis(phosphine) cation is obtained, suggesting that the minor product observed in the original reaction might be the desired $[\{\eta^3{:}\eta^1\text{-Ind}(CH_2)_3NH(t\text{-Bu})\}Ni(PPh_3)]^+$. Abstraction of the Cl^- ligand from complex **8** *with or without added PPh3* gave only the bis-PPh_3 cation $[\{\eta^3{:}\eta^0\text{-Ind}(CH_2)_4NH(t\text{-Bu})\}Ni(PPh_3)_2]^+$. These results indicate that N→ Ni coordination is fairly unfavorable in the $\eta^3{:}\eta^0$-aminoindenyl complexes bearing the N(*t*-Bu)H moiety. Consequently, the electronically and coordinatively unsaturated species $[\{\eta^3{:}\eta^0\text{-Ind}(CH_2)_nNH(t\text{-Bu})\}Ni(PPh_3)]^+$ resulting from the abstraction of Cl^- from **7** and **8** undergo a phosphine redistribution reaction to form the observed bis-PPh_3 cations (Scheme 2.3).

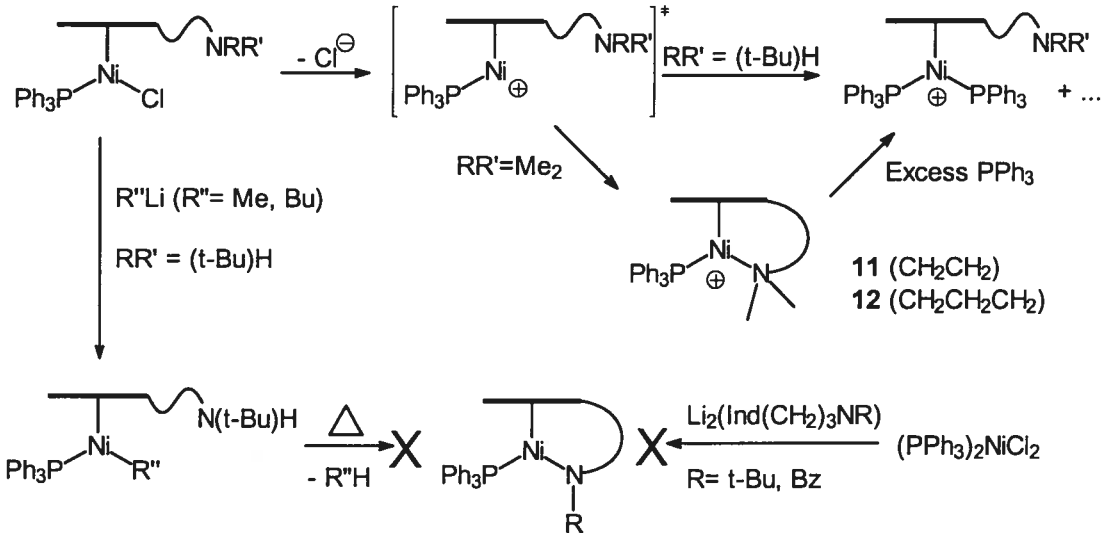

Scheme 2.3.

In contrast to the case for complexes **7** and **8**, Cl^- abstraction from **9** gave a new species which showed a singlet resonance at ca. 29 ppm in its $^{31}P\{^1H\}$ NMR spectrum instead of the AB pattern characteristic of the above-discussed bis-PPh_3 cations. Though we have not succeeded in our attempts to obtain suitable single crystals of this new compound for X-ray diffraction studies, the spectral and analytical data collected strongly support its formulation as $[\{\eta^3:\eta^1\text{-Ind}(CH_2)_2NMe_2\}Ni(PPh_3)]^+$ (**11**) (Scheme 2.3). Monitoring the reaction of complex **11** with ca. 30-fold excess of PPh_3 by $^{31}P\{^1H\}$ NMR ($CDCl_3$) showed the gradual emergence of the characteristic signals for the bis(phosphine) cation (two doublets at 36.4 and 32.5 ppm, $^2J_{P\text{-}P} = 20$ Hz); the conversion was complete within 60 minutes. In the case of complex **10**, Cl^- abstraction also leads to a new complex which shows a singlet at 26 ppm in its $^{31}P\{^1H\}$ NMR spectrum (Scheme 2.3). We conclude, therefore, that the ease of formation of $\eta^3:\eta^1$ cationic complexes of the type **II** is strongly influenced by the coordinating ability of the amine moiety, with the NMe_2 moiety being more suitable for this purpose than N(*t*-Bu)H.

Type III and IV complexes. All our attempts to prepare phosphine-free $\eta^3:\eta^1$ complexes of the type **III** have resulted in the decomposition of these materials. It appears that strong trans-influence ligands such as phosphines are needed to stabilize the coordination of the Ind moiety. We have also explored the deprotonation of the N(*t*-Bu)H moiety in complexes **7** and **8** as a route to neutral $\{\eta^3:\eta^1$-Ind^N(*t*-Bu)$\}Ni(PPh_3)$ complexes of the type **IV**. Reacting these complexes with $LiN(i\text{-Pr})_2$ led to side reactions which produced a complex mixture of intractable products. Attempts at deprotonation with BuLi at both low and high temperatures led instead to the formation of the Ni-Bu complex; analogous reactions with MeLi gave the Ni-Me analogue (Scheme 2.3). The identities of these compounds were established by comparing their ^1H and $^{31}P\{^1H\}$ NMR spectra to those of the analogous methyl complex (1-Me-Ind)(PPh_3)Ni-Me.[6c] For example, the downfield shifts in the $^{31}P\{^1H\}$ NMR resonances of these compounds (ca. 33 ppm in the Ni-Cl compound vs. 46-48 ppm in the Ni-Me and Ni-Bu analogues) are characteristic for Ni-C bond formation in these compounds. Additional evidence for this assignment include the characteristically upfield ^1H NMR resonances for the Ni-CH_n

protons (ca. -0.7 ppm for Ni-Me) and the downfield shift of the H3 signal (ca. 3.4 ppm for **7** and ca. 4.2 ppm for its Ni-Me derivative); the latter results from the change in the hapticity of the Ind ring brought about by the stronger trans influences of alkyl ligands compared to Cl.

The formation of these Ni-alkyl complexes raised the possibility that the target amidoindenyl complexes might be accessible via the intramolecular deprotonation of the dangling N-H bonds with the Ni-R moiety; this type of alkane elimination reaction has precedents in early metal complexes[8] but did not take place with our Ni-Me and Ni-Bu compounds even upon extended heating (Scheme 2.3). We also attempted the preparation of type **IV** complexes via direct metathetic reactions between $(PPh_3)_2NiCl_2$ and the dianionic ligands $[\mathbf{1}]^{2-}$ and $[\mathbf{3}]^{2-}$. These reactions gave deep green-blue solutions whose ^1H NMR spectra consisted of broad, featureless resonances while the $^{31}P\{^1H\}$ NMR spectra showed no signals; no tractable solids could be isolated from the reaction mixtures. These observations are reminiscent of the results from our previous studies on the preparation of the (nonchelating) amido compounds $IndNi(PPh_3)(NRR')$; these studies revealed that the Ni-NR_2 moiety in these compounds is very labile, precluding the isolation of thermally stable complexes except when the R substituents are strongly electron withdrawing.[6f]

Conclusion.

New complexes of the type $\{\eta^3{:}\eta^0\text{-Ind}\hat{}NRR'\}Ni(PPh_3)Cl$ (**7-10**) can be synthesized with NMe_2 and N(*t*-Bu)H moieties, but the NH_2 and N(Bz)H analogues decompose during synthesis. The N(*t*-Bu)H and NMe_2 moieties in these compounds are oriented away from the Ni atom in the solid state. The interaction of the N(*t*-Bu)H functionality with the Ni centre in complexes **7** and **8** is also weak in the solution, whereas the coordination of the NMe_2 moiety to Ni in the solutions of complexes **9** and **10** can be detected. The N→ Ni interaction appears to be intramolecular and reversible in the case of **9** but irreversible and intermolecular in the case of **10**. Therefore, the stability of these $\eta^3{:}\eta^0$-aminoindenyl compounds is modulated by the nature of the N-substituents as well as the length of the tethering chain. The cationic species $[\{\eta^3{:}\eta^0\text{-Ind}\hat{}N(t\text{-}$

Bu)H}Ni(PPh_3)$_2$]$^+$, [{η^3:η^1-Ind^NMe_2}Ni(PPh_3)]$^+$, and [{η^3:η^0-Ind^NMe_2}Ni(PPh_3)$_2$]$^+$ were prepared by abstracting the Cl$^-$ ligand from the neutral precursors. Experiments aimed at evaluating the catalytic reactivities of the η^3:η^0- and η^3:η^1-aminoindenyl compounds are in progress.

Experimental section

General Comments. All manipulations and experiments were performed under an inert atmosphere of nitrogen using standard Schlenk techniques and/or in an argon-filled glovebox. Dry, oxygen-free solvents were employed throughout. The elemental analyses were performed by Laboratoire d'analyse élémentaire (Université de Montréal). An AMXR400 spectrometer was used for recording the ambient-temperature ^{1}H (400 MHz), ^{13}C{^{1}H} (100.56 MHz), and ^{31}P{^{1}H} (161.92 MHz) NMR spectra; the variable temperature NMR studies were carried out on a Varian VXR4000 spectrometer. The ligand Ind-$CH_2CH_2NMe_2$, **4**, has been reported previously.[1e] The remaining aminoalkyl indenes were prepared either by the reaction of IndLi with the appropriate alkyl halides X$(CH_2)_n$NR_2 (n = 2, 3; X= Cl, Br; R= Me, H) which were purchased from Aldrich and used as received, or by reacting the appropriate amine with Ind-$(CH_2)_n$X (n = 3, 4; X = Br, I),[9] as described below.

IndH-$(CH_2)_3$N(*t*-Bu)H.HBr (**1**.HBr). IndH$(CH_2)_3$Br (7.04 g, 29.7 mmol) and *t*-BuNH_2 (ca. 15 mL) were stirred in CH_3CN (ca. 30 mL) at room temperature and then refluxed for 24 h, during which a white precipitate appeared. The final reaction mixture was evaporated to dryness and the resulting white solid was recrystallized from MeOH/Et_2O (2:1), yielding a white powder (8.10 g, 87%). The acid-free ligand was obtained by deprotonation with KOH or BuLi. ^{1}H NMR of the acid-free ligand (CD_3CN): 7.44 and 7.38 (d, $^3J_{H\text{-}H}$ = ca. 7.3, H4 and H7), 7.27 and 7.18 (t, $^3J_{H\text{-}H}$ = 7.2, H5 and H6), 6.24 (br s, H2), 3.31 (br s, H1), 2.60 (m, $CH_2CH_2CH_2$), 1.72 (quint, $^3J_{H\text{-}H}$ = 7.4, $CH_2CH_2CH_2$), 1.03 (s, C(CH_3)$_3$). ^{1}H NMR of the HBr salt ($CDCl_3$): 8.91 (br, NH_2), 7.38 and 7.31 (d, $^3J_{H\text{-}H}$ = ca. 7.7, H4 and H7), 7.28 and 7.17 (t, $^3J_{H\text{-}H}$ = ca. 6, H5 and H6), 6.30 (s, H2),

3.23 (s, H1), 3.00 (m, CH_2N), 2.6-2.4 (m, Ind-CH_2CH_2), 1.48 (s, $C(CH_3)_3$). $^{13}C\{^1H\}$ of the HBr salt ($CDCl_3$): 144.7 and 144.2 and 141.9 (C3a, C7a, C3), 128.5 and 126.0 and 124.6 and 123.6 (C4-7), 118.8 (C2), 57.7 (CMe_3), 41.7 (CH_2N), 37.6 (C1), 25.9 (Ind-CH_2), 24.8 ($CH_2CH_2CH_2$), 24.4 (Me). HRMS of acid-free ligand: 230.19170 (calc. 230.19087). Anal. Calcd for $C_{16}H_{23}N.HBr$: C, 61.94; H, 7.80; N, 4.51. Found: C, 61.67; H, 7.81; N, 4.51.

IndH-$(CH_2)_4$N(*t*-Bu)H.HBr (**2**.HBr). The above procedure for the preparation of IndH-$(CH_2)_3$NH(*t*-Bu) was repeated with IndH-$(CH_2)_4$Br to give a white powder (1.47 g, 28%). ^1H NMR of the HBr salt ($CDCl_3$): 8.88 (br, NH_2), 7.43 and 7.30 (d, $^3J_{H\text{-}H}$ = 7.3, H4 and H7), 7.24 and 7.17 (ps t, $^3J_{H\text{-}H}$ = 7.4, H5 and H6), 6.21 (s, H2), 3.32 (d, $^3J_{H\text{-}H}$ = 1.7, H1), 2.96 (br, CH_2N), 2.57 (t, $^3J_{H\text{-}H}$ = 7.3, IndCH_2), 2.25 (quint, $^3J_{H\text{-}H}$ = 8.1, NCH_2CH_2), 1.77 (quint, $^3J_{H\text{-}H}$ = 7.8, IndCH_2CH_2), 1.50 (s, *t*-Bu). $^{13}C\{^1H\}$ of the HBr salt ($CDCl_3$): 145.0 and 144.3 and 143.2 (C3a, C7a, C3), 128.2 and 125.9 and 124.4 and 123.6 (C4-7), 118.7 (C2), 57.6 ($NCMe_3$), 41.9 (CH_2N), 37.6 (C1), 27.1 (Ind-CH_2), 26.4 and 25.9 ($CH_2CH_2CH_2N$), 25.5 (Me). Anal. Calcd. for $C_{17}H_{25}N.HBr$: C, 62.96; H, 8.08; N, 4.32. Found: C, 62.57; H, 8.13; N, 4.29.

IndH-$(CH_2)_3$N(CH_2Ph)H.HCl (**3**.HCl). IndH-$(CH_2)_3Cl$ (932 mg, 4.84 mmol) and NaI (725 mg, 4.84 mmol) were stirred in CH_3CN (20 mL) for 10 min at room temperature followed by the addition of $PhCH_2NH_2$ (2.5 g, 24 mmol) and heating to reflux for 16 h. The reaction mixture containing a white precipitate was evaporated to dryness and extracted with Et_2O (ca. 50 mL) and a 10% solution of HCl (ca. 75 mL). The solid suspended between the two phases was isolated by filtration and recrystallized from MeOH/Et_2O (2:1) to yield 890 mg of a white solid. Two further recrystallizations were necessary to produce analytically pure product (766 mg, 52%). The acid-free product was obtained by deprotonation with NaOH or BuLi. ^1H NMR of acid-free ligand (C_6D_6): 7.3-7.0 (m), 5.92 (br t, H2), 3.55 (s, CH_2Ph), 3.02 (br d, $^3J_{H\text{-}H}$ = 2, H1), 2.45 (t, $^3J_{H\text{-}H}$ = 7.2, $CH_2CH_2CH_2$), 1.68 (quint, $^3J_{H\text{-}H}$ = 7.2, $CH_2CH_2CH_2$), 0.68 (br, NH).

$^{13}C\{^1H\}$ of HCl salt ($CDCl_3$): 143.8 and 142.3 (C3a, C7a), 128.6 and 128.1 (*o*- and *m*-C), 127.8, 127.5, 125.4, 123.9, 123.1, 118.3 (C2), 51.6 (Ph*C*H_2N), 46.7 (N*C*H_2CH_2), 37.0 (C1), 25.5 (Ind-*C*H_2), 24.4 (CH_2*C*H_2CH_2). Anal. Calcd for $C_{19}H_{21}N$.HCl: C, 76.11; H, 7.40; N, 4.67. Found: C, 76.03; H, 7.50; N 4.69. The solid state structure of the HBr salt of this ligand has been reported.[10]

IndH-$(CH_2)_3NMe_2$ (5). The mixture of BuLi (6.9 mL of a 2.5 M solution) and IndH (1.74 g, 15 mmol) in Et_2O was stirred for 3 h and added dropwise to an Et_2O mixture (ca. 100 mL) of $Cl(CH_2)_3NMe_2$.HCl (1.90 g, 12 mmol) and BuLi (6.0 mL of a 2.5 M solution). The resultant mixture was stirred for 4 days at room temperature and extracted with a 10% HBr solution. The aqueous portion was neutralized (KOH) and extracted with hexane; the hexane portion was dried ($MgSO_4$) and evaporated to give 1.15 g of a pale yellow oil (47% yield). ^1H NMR (C_6D_6): 7.38 and 7.29 (d, $^3J_{H\text{-}H}$ = 9, H4 and H7), 7.21 and 7.11 (t, $^3J_{H\text{-}H}$ = 8, H5 and H6), 6.02 (s, H2), 3.07 (s, H1), 2.55 (t, $^3J_{H\text{-}H}$ = 8, CH_2N), 2.22 (t, $^3J_{H\text{-}H}$ = 8, IndCH_2), 2.14 (s, NMe_2), 2.10 (quint, $^3J_{H\text{-}H}$ = 8, CH_2CH_2N). ^1H NMR ($CDCl_3$): 7.48 and 7.37 (d, $^3J_{H\text{-}H}$ = 8, H4 and H7), 7.29 and 7.20 (t, $^3J_{H\text{-}H}$ = 8, H5 and H6), 6.22 (s, H2), 3.33 (s, H1), 2.58 (t, $^3J_{H\text{-}H}$ = 8, CH_2N), 2.40 (t, $^3J_{H\text{-}H}$ = 8, IndCH_2), 2.27 (s, NMe_2), 1.88 (quint, $^3J_{H\text{-}H}$ = 8, CH_2CH_2N). $^{13}C\{^1H\}$ ($CDCl_3$): 145.3 and 144.4 and 144.0 (C3a, C7a, C3), 127.7 and 125.6 and 124.4 and 123.6 (C4,-7), 118.8 (C2), 59.7 (*C*H_2N), 45.4 (NMe), 37.6 (C1), 25.9 and 25.4 (Ind-*C*H_2*C*H_2). Anal. Calcd for $C_{14}H_{19}N$: C, 83.53; H, 9.51; N, 6.96. Found: C, 83.58; H, 9.63; N 6.85.

IndH-$(CH_2)_3NH_2$.HBr (6.HBr). Using the above procedure for the preparation of IndH-$(CH_2)_3NMe_2$, **5**, with Br-$(CH_2)_3NH_2$.HBr gave a white solid which remained suspended between the organic and aqueous layers during the extraction step. Filtration gave the desired IndH-$(CH_2)_3NH_2$.HBr (2.48 g, 88%). ^1H NMR of the acid-free ligand ($CDCl_3$): 7.45 and 7.36 (d, $^3J_{H\text{-}H}$ = 7.4, H4 and H7), 7.30 and 7.20 (t, $^3J_{H\text{-}H}$ = 7.3, H5 and H6), 6.22 (s, H2), 4.83 (s, NH_2), 3.33 (s, H1), 2.80 (t, $^3J_{H\text{-}H}$ = 7.0, CH_2N), 2.60 (t, $^3J_{H\text{-}H}$ = 7.0, Ind-CH_2), 1.85 (quint, $^3J_{H\text{-}H}$ = 7.3, Ind-CH_2CH_2). $^{13}C\{^1H\}$ ($CDCl_3$): 145.3 and

144.4 and 143.9 (C3a, C7a, C3), 127.8, 125.9, 124.4, 123.7 (C4-7), 118.8 (C2), 42.0 (CH_2NH_2), 37.6 (C1), 31.9 (Ind-CH_2), 25.0 ($CH_2CH_2CH_2$). Anal. Calcd for $C_{12}H_{15}N.HBr$: C, 56.71; H, 6.34; N, 5.51. Found: C, 56.64; H, 6.40; N 5.47.

(η^3:η^0-Ind-$(CH_2)_3$N(*t*-Bu)H)Ni(PPh_3)Cl (7). The mixture of **1**.HBr (1.07 g, 3.45 mmol) and BuLi (2.76 mL of a 2.5 M solution in hexane, 6.90 mmol) in Et_2O (200 mL) was stirred for 16 h at room temperature and then transferred (dropwise over 2h) to the stirring suspension of $(PPh_3)_2NiCl_2$ (2.93 g, 4.49 mmol) in Et_2O (50 mL). The final mixture was stirred for a further 30 min after the addition was complete, then filtered and evaporated. The solid residue was then dissolved in CH_2Cl_2 (ca. 15 mL), diluted with hexane (ca. 200 mL), and cooled to give the desired product as a dark red solid (1.27 g, 63%). ^{1}H NMR (C_6D_6): 7.64 and 6.97 (m, PPh_3), 7.24 (d, $^3J_{H\text{-}H}$ = 7.7, H7), 7.10 (t, $^3J_{H\text{-}H}$ = 7.4, H6), 6.84 (t, $^3J_{H\text{-}H}$ = 7.4, H5), 6.54 (s, H2), 6.18 (d, $^3J_{H\text{-}H}$ = 7.7, H4), 3.47 (s, H3), 2.70 and 2.35-2.13 (br m, Ind$CH_2CH_2CH_2$) 1.10 (s, *t*-Bu). $^{13}C\{^1H\}$ ($CDCl_3$): 134.2 (d, $^2J_{P\text{-}C}$ = 11.4, *o*-C), 134.0 (C3a/C7a), 132.0 (d, $J_{P\text{-}C}$ = 43.9, *i*-C), 130.2 (*p*-C), 128.1 (d, $^3J_{P\text{-}C}$ = 10.1, *m*-C), 125.6 and 126.1 (C5 and C6), 118.2 and 116.7 (C4 and C7), 105.9 (C1), 102.1 (s, C2), 69.3 (s, C3), 53.3 ($NCMe_3$), 42.6 (CH_2N), 28.9 (Me), 28.5 (Ind-CH_2), 23.2 (s, $CH_2CH_2CH_2$). $^{31}P\{^1H\}$ (C_6D_6): 33.6. The missing signal for C3a/C7a is presumably obscured by the other aromatic signals. Anal. Calcd. for $C_{34}H_{37}ClNNiP.CH_2Cl_2$: C, 62.77; H, 5.87; N, 2.09. Found: C, 62.84; H, 5.44; N, 1.62.

(η^3:η^0-Ind-$(CH_2)_4$N(*t*-Bu)H)Ni(PPh_3)Cl (8). The above procedure for **7** was repeated using **2**.HBr to yield 419 mg of the crude product (46%). ^{1}H NMR (C_6D_6): 7.62 and 6.98 (m, PPh_3 and H6), 7.22 (d, $^3J_{H\text{-}H}$ = ca. 7, H7), 6.85 (t, $^3J_{H\text{-}H}$ = ca. 7, H5), 6.37 (s, H2), 6.12 (d, $^3J_{H\text{-}H}$ = 7.2, H4), 3.58 (s, H3), 2.54 (br, CH_2N), 2.43 and 2.19 (br, IndCH_2), 1.96 and 1.86 (br, IndCH_2CH_2), 1.62 (br, Ind$CH_2CH_2CH_2$), 1.05 (s, *t*-Bu), 0.41 (br, N*H*). $^{13}C\{^1H\}$ (C_6D_6): 134.7 (d, $^2J_{P\text{-}C}$ = 10.8, *o*-C), 133.0 (C3a/C7a), 133.0 (d, $J_{P\text{-}C}$ = 43.8, *i*-C), 130.2 (*p*-C), 128.1 (d, $^3J_{P\text{-}C}$ = 10.1, *m*-C), 126.6 and 126.1 (s, C5 and C6), 119.0 and 116.9 (s, C4 and C7), 106.8 (s, C1), 102.4 (s, C2), 69.5 (s, C3), 50.0 ($NCMe_3$), 42.6

(CH_2N), 29.3 (Me), 27.5 (Ind-CH_2), 25.2 and 23.0 (s, Ind-$CH_2CH_2CH_2$). The signal for the *m*-C of PPh_3 is obscured by the solvent peak at 128 ppm. $^{31}P\{^1H\}$ (C_6D_6): 33.5 (s). Anal. Calcd. for $C_{35}H_{39}ClNNiP$: C, 70.20; H, 6.56; N, 2.34. Found: C, 70.02; H, 6.78; N, 2.22.

(η^3:η^0-Ind-$(CH_2)_2NMe_2$)Ni(PPh_3)Cl (9). An Et_2O solution (200 mL) containing **4** (500 mg, 2.67 mmol) and BuLi (1.08 mL of a 2.5 M solution in hexane) was stirred for 30 min and then transferred (dropwise over 4 h) to a stirring slurry of $(PPh_3)_2NiCl_2$ (2.62 g, 4.0 mmol) in Et_2O (20 mL). Evaporation of the resulting red mixture gave a reddish solid which was extracted with hexane (3 x 50 mL), concentrated, and cooled. Filtration of the cold mixture gave a first crop of the desired product (ca. 800 mg of a reddish solid) which was found to contain some PPh_3 and Ph_3P=O. Addition of hexane to the filtrate and cooling gave ca. 300 mg of a red solid. Micro crystals suitable for X-ray analysis were obtained by repeated recrystallization of the combined solids in Et_2O/hexane and cyclohexane/ hexane. ^1H NMR (C_6D_6): 7.63 and 6.99 (m, PPh_3), 7.22 (d, $^3J_{H\text{-}H}$ = 7.3, H7), 7.10 (t, $^3J_{H\text{-}H}$ = 7.4, H6), 6.84 (t, $^3J_{H\text{-}H}$ = 7.4, H5), 6.70 (s, H2), 6.11 (d, $^3J_{H\text{-}H}$ = 7.3, H4), 3.42 (s, H3), 2.89 and 2.74 (br, CH_2N), 2.40 and 2.16 (br, IndCH_2), 2.23 (br, NMe_2). $^{13}C\{^1H\}$ (toluene-d_8, 208 K): 134.4 (d, $^2J_{P\text{-}C}$ = 11.5, *o*-C), 132.2 (d, $J_{P\text{-}C}$ = 43.2, *i*-C), 130.3 (*p*-C), 126.4 and 126.1 (C5 and C6), 118.3 and 116.4 (C4 and C7), 105.3 (d, $^2J_{P\text{-}C}$= ca. 10, C1), 103.7 (C2), 66.9 (C3), 56.8 (CH_2N), 45.6 (NCH_3), 24.6 (Ind-CH_2); the signals corresponding to *m*-C of PPh_3 and C3a and C7a of the Ind are obscured by the solvent resonances. $^{31}P\{^1H\}$ (C_6D_6): 30.8 (s). Anal. Calcd. for $C_{31}H_{31}ClNNiP$: C, 68.61; H, 5.76; N, 2.58. Found: C, 68.01; H, 5.72; N, 2.40.

(η^3:η^0-Ind-$(CH_2)_3NMe_2$)Ni(PPh_3)Cl (10). An Et_2O solution (70 mL) containing **5** (802 mg, 3.98 mmol) and BuLi (1.60 mL of a 2.5 M solution in hexane) was stirred for 16 h and then transferred (dropwise over 3 h) to a stirring slurry of $(PPh_3)_2NiCl_2$ (3.90 g, 6.0 mmol) in Et_2O (30 mL). Filtration of the resulting wine-red mixture followed by evaporation gave the desired product as a red solid (1.90 g, ca. 85% crude yield) which

also contained some PPh_3 and $Ph_3P{=}O$. Repeated recrystallizations with CH_2Cl_2/hexane failed to yield analytically pure samples because of the formation of what appears to be a polymeric material (see Discussion). ^1H NMR of crude solid (DMSO-d_6): 7.7-7.2 (m, aromatic protons of PPh_3 and Ind), 7.06 (s), 6.92 (t, J = 6.0), 6.74 (d, J = 7.2), 4.13 (s), 2.33 and 2.19 (s, NMe_2), 1.9-1.4 (m, $CH_2CH_2CH_2$). $^{31}P\{^1H\}$ NMR (DMSO-d_6): 30.9 (s).

Reaction of Li[IndCH$_2$CH$_2$NHCH$_2$Ph] with (PPh$_3$)$_2$NiCl$_2$. Slow addition of an Et_2O solution (30 mL) of Li[**3**] (152 mg, 0.57 mmol) to the stirring slurry of $(PPh_3)_2NiCl_2$ (373 mg, 0.57 mmol) in Et_2O (30 mL) led to the formation of a reddish color characteristic of the complexes $IndNi(PPh_3)Cl$. The red color turned brown over a few minutes and a brown powder precipitated. Both the filtrate and the solid were analyzed by NMR spectroscopy: the $^{31}P\{^1H\}$ spectra showed no peaks except for free PPh_3 and the ^1H spectra contained very broad, featureless peaks. Repeating the reaction at -50 °C did not yield a tractable product.

Reaction of Li[Ind-(CH$_2$)$_3$NH$_2$] with (PPh$_3$)$_2$NiCl$_2$. Stirring an Et_2O (100 mL) mixture containing **6**.HBr (500 mg, 1.97 mmol) and BuLi (1.57 mL of a 2.5 M solution in hexane) for 1 h, followed by slow addition to the stirring slurry of $(PPh_3)_2NiCl_2$ (1.93 g, 2.95 mmol) in Et_2O (30 mL) led to the formation of a dark-red color. Filtration and evaporation of the solvent gave a dark solid (1.05 g) which was analyzed by NMR spectroscopy: the ^{31}P $\{^1H\}$ NMR spectrum contained a signal attributable to free PPh_3, while the ^1H NMR spectrum contained only broad, featureless peaks.

Reaction of Li$_2$[IndCH$_2$CH$_2$NCH$_2$Ph] with (PPh$_3$)$_2$NiCl$_2$. The mixture of **3**.HCl (250 mg, 0.83 mmol) and 3 equiv of BuLi (1.0 mL of a 2.5 M solution in hexane) was stirred in Et_2O (30 mL) for 16 h and added dropwise to the suspension of $(PPh_3)_2NiCl_2$ (818 mg, 1.25 mmol) in Et_2O (30 mL). The resulting red-brown mixture was filtered to remove the residual solids, evaporated and analyzed by NMR spectroscopy. The

$^{31}P\{^{1}H\}$ NMR spectrum showed only a peak corresponding to free PPh_3 while the ^{1}H NMR spectrum contained broad, featureless peaks.

$[(\eta^3:\eta^1\text{-Ind}(CH_2)_2NMe_2)Ni(PPh_3)]^+$ (11). To a CH_2Cl_2 solution (ca. 30 mL) of complex **9** (110 mg, 0.20 mmol) at room temperature was added $NaBPh_4$ (478 mg, 1.40 mmol) and the mixture was stirred for 1 h. Filtration of the mixture followed by washings with CH_2Cl_2 allowed the removal of the excess $NaBPh_4$ (solid); evaporation of the filtrate gave a reddish solid (ca. 100 mg, 60%). ^{1}H NMR ($CDCl_3$): 7.7-7.1 (m, aromatic signals of PPh_3, $[BPh_4]^-$, and H5, H6, and H7 of Ind), 6.78 (s, H2), 5.54 (d, $^{3}J_{H-H}$ = 7.8, H4), 3.94 (s, H3), 2.62 (m, IndCH_2), 1.73 (m, CH_2NMe_2), 1.67 (s, N*Me*), 1.30 (s, N*Me*). $^{13}C\ \{^{1}H\}$ ($CDCl_3$): 164.5 (4-line multiplet, J_{B-C} = 50, *i*-C of BPh_4), 136.9 (*m*-C of BPh_4), 134.1 (d, $^{2}J_{P-C}$ = 11.9, *o*-C of PPh_3), 132.2 (*p*-C of PPh_3), 129.9 (d, $^{2}J_{P-C}$ = 9.9, *m*-C of PPh_3), 131.1 and 125.5 (C3a/C7a), 129.0 and 128.4 (C5/C6), 126.3 (*o*-C of BPh_4), 122.5 (*p*-C of BPh_4), 119.0 and 118.7 (C4/C7), 109.8 (d, $^{3}J_{P-C}$ = 11.8, C1), 108.2 (C2), 76.3 (CH_2N), 70.2 (C3), 51.5 (N-Me), 24.3 (Ind-CH_2). $^{31}P\{^{1}H\}$ NMR ($CDCl_3$): 29.1 (s). Anal. Calcd. for $C_{55}H_{51}BNNiP$: C, 79.93; H, 6.22; N, 1.69. Found: C, 79.64; H, 6.54; N, 1.56.

$[(\eta^3:\eta^1\text{-Ind}(CH_2)_3NMe_2)Ni(PPh_3)]^+$ (12). To a CH_2Cl_2 solution (ca. 30 mL) of complex **10** (112 mg, 0.20 mmol) at room temperature was added $NaBPh_4$ (342 mg, 1.00 mmol) and the mixture was stirred for 1 h. Filtration of the mixture followed by washings with CH_2Cl_2 allowed the removal of the excess $NaBPh_4$ (solid); evaporation of the filtrate gave a reddish solid (ca. 110 mg, 65 %). $^{31}P\{^{1}H\}$ NMR ($CDCl_3$): 26.9 (s).

Table 2.1. X-ray Crystallographic Data for 7 and 9

	7	9
formula	$C_{34}H_{37}NiPNCl.CH_2Cl_2$	$C_{31}H_{31}NiPNCl$
mol wt	669.73	542.72
crystal color	orange red	dark red
habit	thin plate	block
crystal dimens, mm	0.43 x 0.15 x 0.07	0.29 x 0.11 x 0.07
cell setting	Triclinic	Triclinic
space group	P-1	P-1
a, Å	9.910(3)	9.215(2)
b, Å	10.383(12)	10.228(4)
c, Å	19.556(9)	16.250(6)
α, deg	90.24(6)	76.60(3)
β, deg	92.10(3)	87.94(2)
γ, deg	115.72(4)	65.43(2)
V, Å^3	1680(2)	1351.8(8)
Z	2	2
D (calc), g cm^{-1}	1.3324	1.3333
λ (Cu Kα), cm^{-1}	1.54056	1.54056
temp, K	293(2)	293(2)
diffractometer	Nonius CAD-4	Nonius CAD-4
$2\theta_{max}$, deg	140.0	140.0
data coll method	ω/2θ scan	ω/2θ scan
No. of refl used ($I > 2\sigma(I)$)	6366	5137
R, R_w	0.0820, 0.2346	0.0509, 0.1007

X-ray Diffraction Studies of 7 and 9. Orange-red crystals of **7** were grown from CH_2Cl_2/hexane at -20 °C; complex **7** cocrystallizes with one molecule of CH_2Cl_2 in each unit cell. Dark red crystals of **9** were grown from Et_2O/hexane at room temperature.

Crystallographic data for **7** and **9** are collected in Table 1. The structures were solved by direct methods using SHELXS96 and difmap synthesis using SHELXL96; refinements were done on F^2 by full-matrix least squares. The disorder observed in the positions of the solvent molecule and the *t*-Bu group in **7** are responsible for the relatively high R value of 8.2%. The occupancy factors for these groups were refined and in the last cycle fixed at 60% (for C12, C13, C14, C15 of the *t*-Bu group and C50, Cl51, Cl52 of CH_2Cl_2) and 40% (for C16, C17, C18, C19 of the *t*-Bu group and C60, Cl61, Cl62 of CH_2Cl_2) over the two observed positions. The atoms C12 and C16 are 0.088 Å apart; their thermal parameters were kept identical and the carbon atoms C13-C15 and C17-C19 as well as all the solvent atoms were refined isotropically. No hydrogen bonding was found between N-H and Cl atoms in **7**. The CH_2NMe_2 moiety in **9** is also disordered over two positions but this does not have a significant impact over the overall quality of the data obtained for this structure. The ORTEP diagrams are shown in Figures 2.1 and 2.2, along with selected bond distances and angles. Complete crystallographic data for both structures are included in the supplementary materials.

Acknowledgments. We are grateful to NSERC (Canada), FCAR (Québec), and Université de Montréal for financial support.

Supporting Information Available: Complete details on the X-ray analyses of **7** and **9**, including tables of bond distances and angles, anisotropic thermal parameters, and hydrogen atom coordinates. This material is available free of charge via the Internet at http://pubs.acs.org.

References

(1) a) Shapiro, P. J.; Bunel, E.; Schaefer, W. P.; Bercaw, J. E. *Organometallics*, **1990**, *9*, 867. b) Piers, W. E.; Shapiro, P. J.; Bunel, E.; Bercaw, J. E. *Synlett*, **1990**, *1*, 74. c) Shapiro, P. J.; Cotter, W. D.; Schaefer, W. P.; Labinger, J. A.; Bercaw, J. E. *J. Am. Chem. Soc.* **1994**, *116*, 4623. d) Emrich, R.; Heinemann, O.; Jolly, P. W.; Krüger, C.; Verhovnik, G. P. J. *Organometallics*, **1997**, *16*, 1511. e) Blais, M. S.; Chien, J. C. W.; Rausch, M. D. *Organometallics*, **1998**, *17*, 3775.

(2) Choi, N.; Onozawa, S.; Sakakura, T.; Tanaka, M. *Organometallics*, **1997**, *16*, 2765.

(3) a) Jutzi, P. and Redeker, T. *Eur. J. Inorg. Chem.* **1998**, 663.

(4) a) Fischer, R. A.; Nlate, S.; Hoffmann, H.; Herdtweck, E.; Blümel, J. *Organometallics*, **1996**, *15*, 5746. b) Nlate, S.; Herdtweck, E.; Fischer, R. A. *Angew. Chem. Int. Ed. Engl.* **1996**, *35*, 1861. c) Weiss, J.; Herdtweck, E.; Nlate, S.; Mattner, M.; Fischer, R. A. *Chem. Ber.* **1996**, *129*, 297.

(5) Jutzi, P.; Redeker, T.; Stammler, H.-G.; Neumann, B. *J. Organomet. Chem.* **1995**, *498*, 127.

(6) a) Huber, T. A.; Bélanger-Gariépy, F.; Zargarian, D. *Organometallics*, **1995**, *14*, 4997. b) Bayrakdarian, M.; Davis, M. J.; Reber, C.; Zargarian, D. *Can. J. Chem.*, **1996**, *74*, 2115. c) Huber, T. A.; Bayrakdarian, M.; Dion, S.; Dubuc, I.; G.-Bélanger, F.; Zargarian, D. *Organometallics*, **1997**, *16*, 5811. d) Vollmerhaus, R.; Bélanger-Gariépy, F.; Zargarian, D. *Organometallics*, **1997**, *16*, 4762. e) Fontaine, F.-G.; Kadkhodazadeh, T.; Zargarian, D. *J. Chem. Soc., Chem. Commun.* **1998**, 1253. f) Dubuc, I.; Dubois, M.-A.; G.-Bélanger, F.; Zargarian, D. *Organometallics*, **1999**, *18*, 30.

(7) Lemieux, R. P.; Beak, P. *J. Org. Chem.* **1990**, *55*, 5454.

(8) Mu, Y.; Piers, W. E.; MacQuarrie, D. C.; Zaworotko, M. J.; Young, V. G. *Organometallics* **1996**, *15*, 2720.

(9) Makosza, M. *Tet. Lett.* **1966**, *38*, 4621.

(10) Groux, L. F.; Bélanger-Gariépy, F.; Zargarian, D. *Acta Cryst. C*, **1999**, *C55*, IUC9900130.

Chapitre 3: Structure and Reactivity of the Cationic Nickel Compound [(η^3:η^1-Ind$(CH_2)_2NMe_2$)Ni(PPh_3)] [BPh_4]

Article 2

Laurent F. Groux, Davit Zargarian

Organometallics **2001**, *20*, 3811.

Abstract

The solid state structure of the first nickel compound containing a chelating amino-indenyl ligand, $[(\eta^3:\eta^1\text{-Ind}(CH_2)_2NMe_2)Ni(PPh_3)][BPh_4]$ (**2**), has been resolved and confirms the chelation of the amine tether to the nickel center. Complex **2** acts as a precatalyst for the oligomerization of norbornene, dimerization of phenylsilane, and the polymerization of styrene. The results of these catalytic reactions are qualitatively different from those catalyzed by the cationic species generated in situ from the precursor complex $(\eta^3:\eta^0\text{-Ind}(CH_2)_2NMe_2)Ni(PPh_3)Cl$ (**1**). Phosphines displace the amine tether in **2** to give the bis(phosphine) cations $[(\eta^3:\eta^0\text{-Ind}(CH_2)_2NMe_2)Ni(Ph_2PCH_2CH_2PPh_2)]^+$ (**3**) and $[(\eta^3:\eta^0\text{-Ind}(CH_2)_2NMe_2)Ni(PPh_3)(PR_3)]^+$ (**4**, R = Ph; **5**, R = Me), whereas LiI reacts to form the neutral compound $[(\eta^3:\eta^0\text{-Ind}(CH_2)_2NMe_2)Ni(PPh_3)I].LiBPh_4$ (**7**). The displacement of the amine tether by pyridine and its methyl substituted derivatives leads to an equilibrium between **2** and $[(\eta^3:\eta^0\text{-Ind}(CH_2)_2NMe_2)Ni(PPh_3)L]^+$ (**6**) with K_{eq} values of 9 (**6a**, L = pyridine), 2.0 (**6b**, L = 2-picoline), 23 (**6c**, L = 3-picoline), 33 (**6d**, L = 4-picoline), and 16 (**6e**, L = 3,5-lutidine).

Introduction

During the course of our investigations[1] into the chemistry of the complexes $(Ind)(PPh_3)Ni\text{-}X$ (Ind = indenyl and its substituted derivatives; X = halide, alkyl, alkynyl, imidate, thiolate, etc.), it was found that the in situ generated cationic species $[(Ind)(PPh_3)Ni]^+$ can catalyze a number of reactions including the dimerization of ethylene to butenes,[1a,e] the dehydrogenative oligomerization of $PhSiH_3$ to $(PhSiH)_n$,[1d] the oligomerization of styrene, the polymerization of norbornene, and the co-polymerization of styrene and norbornene. In situ generated $[(Ind)(PPh_3)Ni]^+$ also reacts with phosphines or donor solvents such as MeCN to form the adducts $[(Ind)(PPh_3)NiL]^+$; indeed, the electrophilicity of the "naked" cation is such that in the absence of added ligand and donor solvents it undergoes a redistribution reaction to form $[(Ind)Ni(PPh_3)_2]^+$ which is catalytically inert (Scheme 3.1). The presence of this deactivation pathway has hindered further investigations into the structure and reactivities of these highly electrophilic cations.

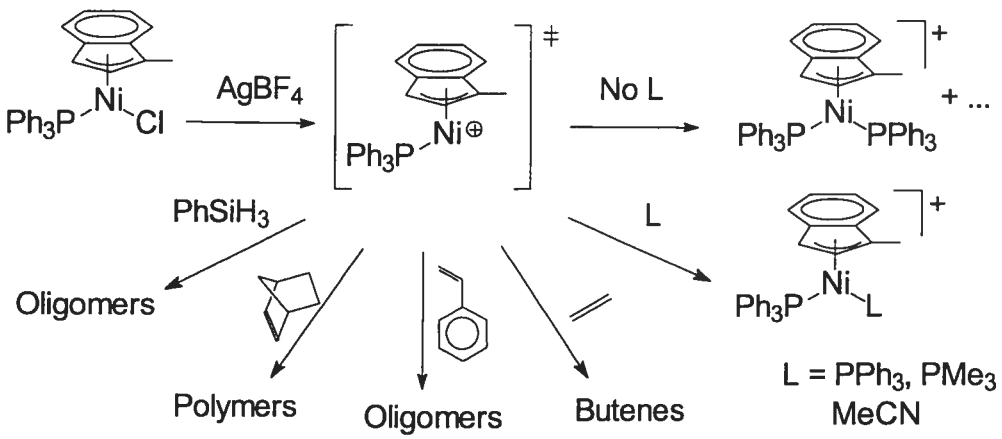

Scheme 3.1. Reactivity of $[(1\text{-MeInd})Ni(PPh_3)]^+$

In an effort to circumvent this deactivation of the unstable cations $[(Ind)(PR_3)Ni]^+$, we set out to prepare analogous complexes bearing hemilabile coordinating moieties[2] which might stabilize the cationic intermediates sufficiently to allow isolation and characterization while maintaining catalytic activity. Aminoindenyl ligands were chosen for this purpose because it was anticipated that (a) the proximity of the amine functionalized tether to the nickel center would facilitate N→Ni coordination and prevent the formation of the inert bis(phopshine) species and (b) the lower affinity of the amine moiety, relative to phosphines, for coordination to nickel[3] would not shut down the catalytic activity. In an earlier report,[4] we have described the preparation and complete characterization of the precursor complex $(\eta^3{:}\eta^0\text{-Ind}(CH_2)_2NMe_2)(PPh_3)Ni\text{-}Cl$ (**1**) and presented spectroscopic evidence for the formation of the cationic complex $[(\eta^3{:}\eta^1\text{-Ind}(CH_2)_2NMe_2)Ni(PPh_3)][BPh_4]$ (**2**). The present paper reports the structural characterization of **2** and describes the ligand substitution reactions and catalysis arising from the displacement of the amine tether by various ligands.

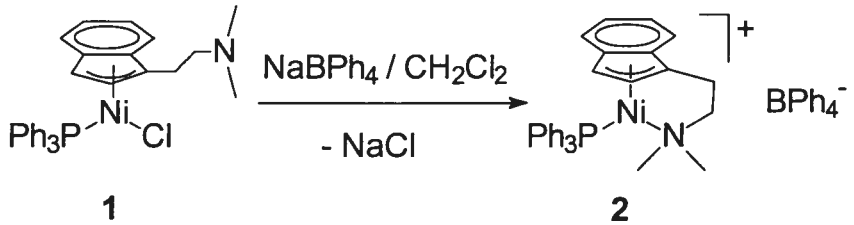

Scheme 3.2. Preparation of $[(\eta^3{:}\eta^1\text{-Ind}(CH_2)_2NMe_2)Ni(PPh_3)][BPh_4]$

Results and discussion

Complex **2** can be prepared in ca. 60% yield by abstracting Cl^- from **1** in CH_2Cl_2 (Scheme 3.2).[4] The $^{31}P\{^1H\}$ NMR spectrum of the product showed that the signal for the precursor (ca. 31 ppm) was replaced by a new singlet resonance (ca. 29 ppm). The absence of an AB resonance which is characteristic of the inequivalent P nuclei in the bis(phosphine) cations $[(1\text{-R-Ind})Ni(PPh_3)_2]^+$ [1e] indicated that the formation of undesired byproducts of this type had been circumvented. In addition, the appearance of two different N-Me signals in the ^1H NMR spectrum of the product was consistent with the coordination of the NMe_2 moiety to the nickel center which is dissymmetric (**2** has C_1 symmetry) and so the $Me_2N\rightarrow Ni$ coordination renders the Me groups diastereotopic. The structural characterization of **2**, which is air stable in the solid state, was completed by an X-ray analysis carried out on a single crystal grown by the slow vapor diffusion of Et_2O into a CH_2Cl_2 solution of this compound. An ORTEP diagram of **2** is shown in Figure 3.1, along with selected structural parameters. The main features of the structure are described below.

The Ni-N distance of 2.005(2) Å in **2** is within the expected range for Ni(II)-NR_3 bonds,[5] whereas the Ni-P distance is somewhat longer (by ca. 12σ) than the corresponding distance in the neutral Ni-Cl precursor **1**;[4] this is likely the result of the steric hindrance caused by the amine moiety. The strain imposed by the chelation of the tether is reflected in the small C1-Ni-N angle of 84.81(10)° (compared to ca. 96° for the C1-Ni-Cl angle in **1**) and the large P-Ni-N angle of 107.52(7)° (compared to ca. 98° for the P-Ni-Cl angle in **1**). The chelation can also be invoked to explain why Ni-C1 is shorter than Ni-C3 in spite of the greater relative trans influence of PPh_3 which would otherwise be expected to result in a longer Ni-C1 bond.

The coordination of the indenyl moiety in **2** is intermediate between η^5 and η^3, as inferred from the significantly shorter Ni-C1, Ni-C2 and Ni-C3 distances compared to Ni-C3A and Ni-C7A. The degree of such "slippage" away from the idealized η^5 coordination is often measured by the parameter $\Delta(M\text{-}C) = 0.5[(M\text{-}C3A + M\text{-}C7A) - (M\text{-}C1 + M\text{-}C3)]$,[6] which is 0.26 Å for **2**. Interestingly, this degree of slippage is similar to those of the neutral compounds $(1\text{-Me-Ind})(PPh_3)Ni\text{-}X$ (0.25 Å for X= Cl[1f] and 0.27 Å for X= phthalimidate[1c]) but larger than the Δ(M-C) of the cationic analogues such as [(1-

Me-Ind)Ni(PPh_3)(PMe_3)]$^+$ (0.19 Å).[1e] Similar structural parameters have been found in the recently reported Cp analogue [(η^5:η^1-Cp(CH_2)$_2$$NMe_2$)Ni($PPh_3$)]$^+$,[7] although there is little distortion in the hapticity of the Cp ligand in this compound.[8]

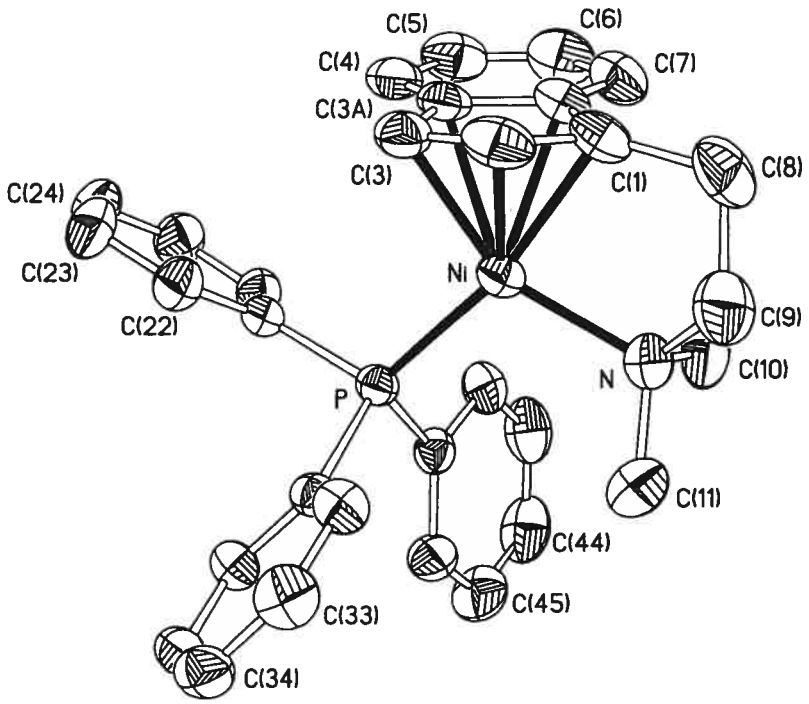

Figure 3.1. ORTEP view of complex 2.

The counterion and hydrogen atoms omitted for clarity. Thermal ellipsoids are shown at 40% probability. Selected bond distances (Å) and angles (deg): Ni-P = 2.1971(11), Ni-N = 2.005(2), Ni-C(1) = 2.040(2), Ni-C(2) = 2.056(3), Ni-C(3) = 2.078(3), Ni-C(3A) = 2.327(3), Ni-C(7A) = 2.314(2), C(1)-C(2) = 1.412(4), C(2)-C(3) = 1.399(4), C(3)-C(3A) = 1.455(3), C(3A)-C(7A) = 1.420(3), C(1)-C(7A) = 1.463(3), ΔM-C (ref. 6) = 0.26, P-Ni-N = 107.52(7), C(3)-Ni-N = 149.55(10), C(3)-Ni-P = 101.79(8), C(1)-Ni-N = 84.86(11), C(1)-Ni-P = 166.49(8), C(1)-Ni-C(3) = 66.97(11). C3A and C7A refer to the atoms shared by the 5- and 6- membered rings of the Ind.

Table 3.1. Crystal Data, Data Collection and Structure Refinement of 2

Formula, mol wt	$C_{55}H_{51}BNPNi$, 826.46
cryst color and habit	dark red block
cryst dimens, mm	0.36 × 0.28 × 0.16
symmetry	triclinic
space group	*P*-1
a, Å	11.161(6),
b, Å	14.119(5),
c, Å	15.115(9)
α, deg	82.69(4),
β, deg	79.86(6),
γ, deg	72.65(4)
Volume, $Å^3$	2231(2)
Z	2
D(calcd), g cm^{-1}	1.2303
diffractometer	Nonius CAD-4
temp, K	293(2)
λ (Cu Kα)	1.54056 Å
μ, mm^{-1}	1.240
scan type	$\omega/2\theta$ scan
θ_{max}	69.80°
h,k,l range	$-13 \le h \le 13$, $-17 \le k \le 17$, $-18 \le l \le 18$
Refl used ($I > 2\sigma(I)$)	6134
Absorption correction	Integration ABSORB[19]
T (min, max)	0.6601, 0.8336
R [$F^2>2\sigma(F^2)$], wR (F^2)	0.0386, 0.0942
GOF	0.898

Catalytic reactions. The availability of a pre-formed, stable cationic Ni compound in which one coordination site is occupied by a relatively labile amine moiety (vide infra) presented an opportunity to study the catalytic reactivities of **2**. Mindful of the catalytic activities of a number of cationic Ni(II) complexes in olefin oligomerization and

polymerization reactions,[9] we proceeded to examine the reactivities of complex **2** with alkenes. Our objective was to establish whether the proximity of the amine moiety to the Ni center would have a major influence on the course of the catalysis.

Table 3.2. Polymerization Experiments with (η^3:η^0-Ind$(CH_2)_2NMe_2$) Ni(PPh_3)Cl (1) and [(η^3:η^1-Ind$(CH_2)_2NMe_2$)Ni(PPh_3)][BPh_4] (2)

		Amt of monomer, equiv		T	Time			
run	Catalyst	styrene	norbornene	(°C)	(days)	M_w	M_w/M_n	TON
1	**2**	2000		20	7	-	-	0
2	**2**	2000		80	2	77338	3.2	364
3	**2**/$AgBF_4$[a]	2000		80	2	12726	1.9	980
4	**2**/AgCl[a]	2000		80	2	65980	1.2	860
5	**2**		1000	20	4	-	-	0
6	**2**		800	80	4	763	1.1	35
7	**2**	300	100	50	2	18320	12.0	19
8	**2**	200	200	50	2	3071	4.5	9
9	**2**	100	300	50	2	570	1.4	3
10	**1**/$AgBF_4$[a]	2000		20	2	1531	1.3	1650
11	**1**/$AgBF_4$[a]	2000		60	2	2066	1.5	1570
12	**1**/$AgBF_4$[a]		1000	20	2	Insol.[b]		270
13	**1**/$AgBF_4$[a]		1000	60	2	Insol.[c]		350
14	**1**/$AgBF_4$[a]	300	100	50	2	6935	1.4	400
15	**1**/$AgBF_4$[a]	200	200	50	2	7184[d]	1.5	200
16	**1**/$AgBF_4$[a]	100	300	50	2	7370[e]	1.5	300

[a] [Ag]/[Ni] = 10 [b] DSC analysis shows exothermic decomposition starting at 300 °C (before m.p.) [c] DSC analysis shows exothermic decomposition starting at ca. 290 °C (before m.p.) [d] Partially soluble in THF. DSC analysis shows exothermic decomposition starting at 270 °C (before m.p.) [e] Slightly soluble in THF. A DSC analysis shows exothermic decomposition starting at 300 °C (before m.p.)

Complex **2** reacted only very sluggishly with styrene at room temperature (run 1, Table 3.2), implying that the displacement of the amine moiety by styrene is not facile. However, heating the mixture to 80 °C accelerated the polymerization and gave a soluble polystyrene of M_w = 77338 and M_w/M_n = 3.15, and turnover numbers of ca. 300-400 (run 2, Table 3.2). The ^{1}H NMR spectra ($CDCl_3$) of these polymers show characteristically broad signals at 7.05, 6.59, 1.85 and 1.45 ppm, while the $^{13}C\{^1H\}$ NMR spectra show broad signals at 145.5 (ipso-C), 128.1 (o- and m-C), 125.5 (p-C) and 43.7 and 40.5 ppm. The analogous reaction with norbornene also requires heating to 80 °C but gives only oligomeric materials (M_w = 763; M_w/M_n = 1.1) with turnover numbers of 20-40 (runs 5 and 6, Table 3.2). Attempts at copolymerizing these two olefins were unsuccessful and gave instead polystyrenes only (runs 7-9, Table 3.2).

It is noteworthy that the outcomes of the reactions of styrene and norbornene with **2** are quite different from the analogous reactions catalyzed by the in situ generated species $[IndNi(PPh_3)]^+$. For instance, catalysis by $[IndNi(PPh_3)]^+$ proceeds at room temperature to give insoluble norbornene polymers and soluble styrene trimers and tertramers.[10] Moreover, the latter system can catalyze the formation of various copolymers of styrene-norbornene. To our surprise, the polymerization reactions catalyzed by the cationic species generated in situ by reacting the precursor complex (η^3:η^0-Ind(CH2)$_2$NMe$_2$)Ind) (PPh_3)Ni-Cl, **1**, with $AgBF_4$ gave results which were similar to those obtained from in situ generated $[IndNi(PPh_3)]^+$ but very different from the results of the polymerizations catalyzed by pre-formed **2** (compare runs 1 and 2 to 10 and 11, runs 5 and 6 to 12 and 13, and runs 7-9 to 14-16, Table 3.2). We suspect that the difference in the reactivities of **2** and the in situ generated $[IndNi(PPh_3)]^+$ results from the influence of the amine tether on the course of the reaction. Thus, when **2** is generated in situ (from **1** and $AgBF_4$) it is possible that the amine moiety remains coordinated to the unreacted $AgBF_4$ (or the in situ produced AgCl) and hence can not exert any influence on the course of the catalysis. This assertion is consistent with the results of experiments which showed that the catalysis with **2**/styrene in the presence of added $AgBF_4$ (run 3, Table 3.2) gave intermediate results between the catalysis with **2**/styrene and with **1**/$AgBF_4$/styrene (run 2 and 10, Table 3.2). Added AgCl had no influence in the catalysis, probably because of its poor solubility (run 4, Table 3.2). We believe that these

results indicate that the amine moiety in these complexes plays an important role in modulating these catalytic reactions. It should be noted, however, that the observed differences in the outcomes of the polymerizations catalyzed by **2** and **1**/$AgBF_4$ might also be due to the presence of some side products generated in the latter system.[11]

Another catalytic reaction which was studied briefly is the dehydrogenative oligomerization of $PhSiH_3$. Complex **2** was found to catalyze the dimerization of $PhSiH_3$ at room temperature to give PhH_2Si-$SiPhH_2$ in ca. 20 turnovers as well as small amounts of the trimer and tetramers.[12] As was the case for the reactions of styrene and norbornene, here too the outcome of the catalysis by **2** is qualitatively different from the analogous reaction catalyzed by the in situ generated cation which gives $(PhSiH)_n$ consisting of both cyclic (M_n ca. 600) and linear (M_n ca. 1500) oligomers.[1d] At this stage, we speculate that the dehydrogenative oligomerization of $PhSiH_3$ catalysed by **2** does not proceed beyond dimerization because the dimer produced in the initial Si-Si bond formation step can not compete effectively with the NMe_2 moiety for coordination to Ni. In contrast to the case with the olefin polymerizations, the combination of (η^3:η^0-Ind(CH2)$_2$NMe$_2$)Ind)(PPh_3)Ni-Cl/$AgBF_4$ did not catalyze the oligomerization of $PhSiH_3$.

The above results indicated that the strength of the coordination of the amine tether to the Ni center can determine the ease with which the catalytic reactions may be initiated (e.g., requirement for heating) and can affect the overall outcome of the reactions (e.g., oligomerization vs. polymerization). In order to evaluate the binding strength of the amine tether, we have studied the reaction of complex **2** with various neutral and anionic ligands, as follows.

Ligand substitution reactions with neutral Lewis bases. No reaction was observed between **2** and CO even with a 25 psi pressure of CO, but phosphines and some amines did react to displace the amine tether to varying degrees. Thus, only 1 equiv of bis(diphenylphosphino)ethane (dppe) was sufficient to displace both the amine tether and the PPh_3 ligand in **2**, giving an orange-red powder. Recrystallization of this material from Et_2O/CH_2Cl_2 gave, in ca. 64% yield, the complex [(η^3:η^0-Ind$(CH_2)_2NMe_2$)Ni(dppe)][BPh_4] (**3**) whose identity was confirmed by elemental analysis and NMR spectroscopy. The absence of a C_2 axis in **3** renders the two P nuclei of the

dppe ligand inequivalent, and so the $^{31}P\{^{1}H\}$ NMR spectrum displays two broad signals at 65.6 and 68.7 ppm at room temperature. At –40 °C, the two signals appear as sharp doublets at 66.4 and 70.8 ppm ($^{2}J_{P\text{-}P}$= 25.4 Hz), whereas warming to 35 °C brings about coalescence (broad signal at 66.6 ppm); an energy barrier of 14.3 Kcal.mol^{-1} was calculated for this process using the Holmes-Gutowski equation.[13] Similar dynamic exchange processes have been observed for other complexes of this family and are attributed to the hindered rotation of the indenyl moiety.[1e,h]

In contrast to the facile reaction with dppe, disruption of the N→Ni chelation in **2** by PPh_3 is much less favorable thermodynamically and requires a large excess of PPh_3. The reaction can be monitored by the emergence in the $^{31}P\{^{1}H\}$ NMR spectrum of a new set of AB resonances at 32.3 and 36.1 ppm ($^{2}J_{P\text{-}P}$ = 27 Hz). These signals are very similar to those reported[1d] for $[(1\text{-Me-Ind})Ni(PPh_3)_2]^+$ (cf. 32.5 and 35.8 ppm, $^{2}J_{P\text{-}P}$ = 25 Hz) and so the product of this reaction is proposed to be $[(\eta^3{:}\eta^0\text{-Ind}(CH2)_2NMe_2)Ni(PPh_3)_2][BPh_4]$ (**4**). Separation and isolation of pure **4** has not been possible because of the small K_{eq} of ca. 0.9 for this reaction (Scheme 3.3).

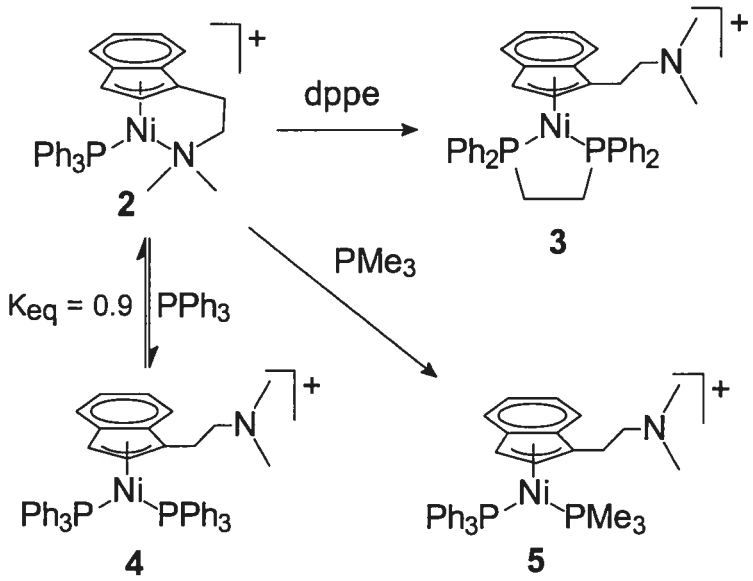

Scheme 3.3. Reactivity of 2 with phosphines.

The reaction of **2** with PMe_3 was less straightforward and its outcome depended on the relative amount of PMe_3 present in the reaction medium. For instance, reacting **2**

with an excess of PMe_3 gave free PPh_3 and $Ni(PMe_3)_4$[14] as the major products, whereas the reaction with 1 equiv of PMe_3 gave, in addition to free PPh_3 and small amounts of $Ni(PMe_3)_4$, two new species with the following spectral features (Table 3.4): the major species displayed an AX set of doublets at –10.9 ppm and 41.0 ppm for PMe_3 and PPh_3, respectively ($^2J_{P\text{-}P}$ = 42 Hz), while the minor product gave a singlet at –16.6 ppm in $^{31}P\{^1H\}$ NMR spectroscopy. The AX resonances are virtually identical to the signals displayed by the known[1e] bis(phosphine) compound $[(1\text{-Me-Ind})Ni(PPh_3)(PMe_3)]^+$ (cf. –10.1 and 41.2 ppm and $^2J_{P\text{-}P}$ = 42 Hz for one rotamer)[15] and so we propose that the major product of the reaction of one equivalent of PMe_3 with **2** is $[(\eta^3{:}\eta^0\text{-}Ind(CH_2)_2NMe_2)Ni(PPh_3)(PMe_3)][BPh_4]$ (**5**). The minor product is presumably the complex $[(\eta^3{:}\eta^1\text{-}Ind(CH_2)_2NMe_2)Ni(PMe_3)]^+$ arising from the displacement of the PPh_3 from **2** by PMe_3. These assignments are somewhat tentative, however, because all attempts at separation and isolation of these products have resulted in the formation of intractable materials, thus preventing their conclusive characterization.

The reaction of **2** with primary and secondary amines such as H_2NEt, $HNEt_2$, aniline, and $H_2N(t\text{-Bu})$ gave complex mixtures of products (by ^1H NMR) in which the only P-containing species was free PPh_3 (by $^{31}P\{^1H\}$ NMR) and from which no tractable compounds could be isolated. Tertiary amines such as NEt_3 do not react at all with **2** even in a large excess, but pyridine and its methyl substituted analogues showed reactivities similar to that observed with PPh_3 (Scheme 3.4). As was the case with PPh_3, we were unable to isolate the new compounds because removal of the excess ligand during isolation reformed **2**; nevertheless, the identity of the products can be ascertained from the following NMR data. The ^1H NMR spectra of the mixtures of **2** and the pyridines indicated the formation of a new compound in equilibrium with **2**. The signals arising from the Ind protons in the new compound were very similar to those of **2**, whereas the signals for the protons on the tether were broadened as a result of the exchange reaction. Significantly, a new singlet at ca. 2.1 ppm replaced the previously inequivalent N-Me resonances at 1.6 and 1.3 ppm. The $^{31}P\{^1H\}$ NMR spectra of the mixtures of **2** and the pyridines showed the conversion of **2** to new derivatives which displayed a singlet resonance at ca. 32 ppm for all but one case; the corresponding signal for the reaction with 2-picoline appeared at ca. 29 ppm. These observations are

consistent with the formation of the cations $[(\eta^3:\eta^0\text{-Ind}(CH_2)_2NMe_2)Ni(PPh_3)(L)][BPh_4]$ (**6**; Table 3.3) which arise from the displacement of the tether in **2**. The more upfield $^{31}P\{^1H\}$ signal in the 2-picoline derivative **6b** implies a less efficient $PPh_3 \rightarrow Ni$ donation due to larger steric interactions between PPh_3 and 2-picoline. The equilibrium constants for these exchange reactions were determined to be 33 (4-picoline), 23 (3-picoline), 16 (3,5-lutidine), 9 (pyridine), and 2.0 (2-picoline). The relative values of the K_{eq} reflect the sensitivity of this ligand substitution reaction to both steric (pyridine > 2-picoline) and electronic factors (4-picoline > 3-picoline > 3,5-lutidine > pyridine).

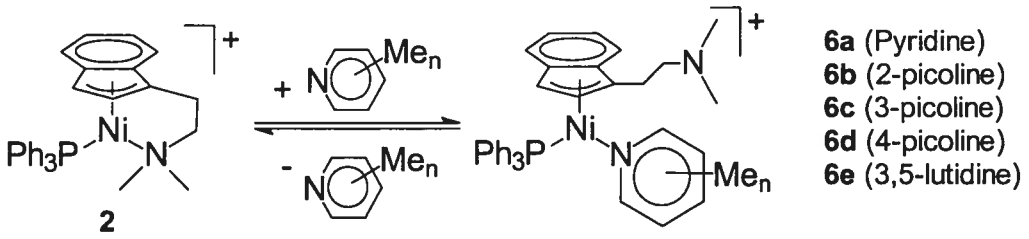

Scheme 3.4. Equilibrium reaction of 2 with pyridine and pyridine analogues

Table 3.3. Spectroscopic Data and Equilibrium Constants of $[(\eta^3:\eta^0\text{-Ind}(CH_2)_2NMe_2)Ni(PPh_3)(L)][BPh_4]$

		$^{31}P\{^1H\}$	^1H (ppm)			
	L	(ppm)	H2	H3	NMe_2	K_{eq}
6a	Pyridine	32.13	6.28	4.18	2.14	9 ± 1
6b	2-picoline	28.76	6.38	4.07	2.07	2.0 ± 0.2
6c	3-picoline	32.15	6.35	4.17	2.14	23 ± 2
6d	4-picoline	32.06	6.28	4.15	2.04	33 ± 3
6e	3,5-lutidine	32.03	6.39	4.15	2.11	16 ± 1

Reactivities of 2 with anionic ligands. The anionic nucleophiles Ph_2P^-, Me_2N^-, and Me^- did not show any reactivity with **2** in Et_2O and THF, presumably because of the limited solubility of **2** in these solvents. Even in CH_2Cl_2 in which it is soluble, **2** did not react with Cl^- or Br^- but reaction with a large excess of LiI resulted in the formation of a red powder which was crystallized from CH_2Cl_2/hexane/Et_2O to give $(\eta^3:\eta^0$-

Ind(CH2)$_2$NMe$_2$)(PPh$_3$)Ni-I.LiBPh$_4$ (**7**) in 84% yield.[16] Complex **7** has been characterized completely, including a single crystal X-ray analysis. The ^{1}H NMR spectrum of this compound was very similar to that of **1**, and the ^{31}P{^{1}H} NMR showed a singlet at 35.9 ppm (Table 3.4). The X-ray data we have obtained for complex **7** confirmed the connectivity, but the poor quality of the crystals, the significant absorption of the Cu kα radiation by iodine atoms, and the presence of LiBPh$_4$·H$_2$O in the crystal lattice prevented us from refining the structure to a satisfactory level.

Conclusion.

The results of the ligand substitution reactions described above show that the coordination of the tether in **2** is strong enough to stabilize this compound and prevent the formation of the catalytically inert complex [(η^3:η^0-Ind(CH2)$_2$NMe$_2$)Ind)Ni(PPh$_3$)$_2$]$^+$ yet labile enough to be displaced by relatively strong ligands. Thus, the amine tether in complex **1** can act as a hemilabile ligand which can stabilize cationic species such as **2** while allowing the coordination of some ligands and substrates. This property facilitates the use of complex **2** as a single-component precatalyst for the polymerization of styrene, oligomerization of norbornene, and dimerization of PhSiH$_3$. Comparisons with the analogous reactions catalyzed by cations generated in-situ from (1-Me-Ind)(PPh$_3$)Ni-Cl and (η^3:η^0-Ind(CH2)$_2$NMe$_2$)Ind)(PPh$_3$)Ni-Cl indicate that the presence of the amine tether has a marked influence on the course of the catalysis. Future studies will investigate the reactivity of **2** with ethylene and other olefins, and will focus on understanding the role of the amine tether in the catalysis.

Experimental section

General Comments. All manipulations, except for the GPC and DSC analyses, were performed under an inert atmosphere of N$_2$ or argon using standard schlenk techniques and a drybox. Dry, oxygen-free solvents were employed throughout. The syntheses of **1** and **2** have been reported previously.[4] LiPPh$_2$ and LiNMe$_2$ were prepared by deprotonation of HPPh$_2$ and HNMe$_2$, respectively; all other reagents used in the experiments were obtained from commercial sources and used as received. The elemental

analyses were performed by the Laboratoire d'analyse élémentaire (Université de Montréal). The spectrometers used for recording the NMR spectra are: Bruker AMXR400 (^{1}H (400 MHz), ^{13}C{^{1}H} (100.56 MHz), and ^{31}P{^{1}H} (161.92 MHz)), and Bruker AV300 (^{1}H (300 MHz), and ^{31}P{^{1}H} (121.49 MHz)).

Crystal Structure determinations. Dark red crystals of **2** were obtained at room temperature by the slow diffusion of Et_2O vapor into a CH_2Cl_2 solution of **2**. The crystal data for **2** was collected on a Nonius CAD-4 diffractometer with graphite-monochromatic Cu Kα radiation at 293(2) K using CAD-4 software. The refinement of the cell parameters was done with the CAD-4 software[18] and the data reduction used NRC-2 and NRC-2A.[19] The structure was solved by direct methods using SHELXS97[22] and difmap synthesis using SHELXL96;[23] the refinements were done on F^2 by full-matrix least squares. All non-hydrogen atoms were refined anisotropically, while the hydrogens (isotropic) were constrained to the parent atom using a riding model. Crystal data and experimental details for **2** are listed in Table 3.1 and selected bond distances and angles are listed under the ORTEP diagram.

Polymerization of styrene. Runs 1 and 2. 2 (18 mg) and styrene (4.5g, 2000 equiv) were stirred for 7 days in CH_2Cl_2 (8 mL) at room temperature (run 1) or for 2 days at 80 °C (run 2). For run 1, removal of the solvent and unreacted styrene gave a thin film which was washed with $CDCl_3$ and analyzed by ^{1}H NMR spectroscopy, showing broad peaks of polystyrene. For run 2, removal of solvent and unreacted styrene gave a light gray solid (829 mg, 18% yield) which was isolated and analyzed by GPC (THF; M_w = 77338; M_w/M_n = 3.15) and NMR spectroscopy. ^{1}H NMR ($CDCl_3$): 7.05 (br), 6.59 (br), 1.85 (br), 1.45 (br). ^{13}C{^{1}H} ($CDCl_3$): 145.5 (*ipso*-C), 128.1 (*o*- and *m*-C), 125.5 (*p*-C), 43.7 and 40.5 (alkyl chain).

Runs 3 and 4. 2 (15 mg), styrene (3.8 g, 2000 equiv) and AgCl (26 mg, run 4) or $AgBF_4$ (35 mg, run 3) were stirred for 2 days in CH_2Cl_2 (8 mL) at 80 °C. Removal of the solvent and unreacted styrene gave a thick gray oil which was isolated and analyzed by GPC (run 3: 1.7 g, 43% yield, GPC (THF): M_w = 65980; M_w/M_n = 1.2; run 4: 1.9 g, 49% yield, GPC (THF): M_w = 12726; M_w/M_n = 1.9).

Runs 10 and 11. Styrene (8.3 g, 2000 equiv.) and CH_2Cl_2 (8 mL) were syringed to a mixture of **1** (22 mg) and $AgBF_4$ (85 mg, 10 equiv). The solution was stirred for two days at room temperature (run 10) or at 60 °C (run 11). Removal of the solvent and the unreacted styrene under vacuum gave polystyrene (run 10: thick oil, 6.9 g, 83% yield; run 11: sticky solid, 9.0 g, 79% yield) which were analyzed by GPC (THF; run 10: M_w = 1531; M_w/M_n = 1.29; run 11: M_w = 2066; M_w/M_n = 1.48).

Polymerization of norbornene. Runs 5 and 6. 2 (ca. 19 mg) and norbornene (ca. 2.3 g, 1000 equiv) were stirred in CH_2Cl_2 (3 mL) for 4 days at room temperature (run 5) or at 80 °C (run 6). Removal of the solvent and unreacted norbornene left only unreacted **2** (run 5) or a gray solid (run 6, 101 mg, 4.4% yield) which was analyzed by GPC (THF; M_w = 763; M_w/M_n = 1.1).

Runs 12 and 13. CH_2Cl_2 (8 mL) is added to **1** (ca. 23 mg), $AgBF_4$ (ca. 80 mg, 10 equiv), and norbornene (ca. 4.0 g, 1000 equiv). A white solid precipitated immediately after the addition of the solvent. After two days at room temperature (run 12) or at 60 °C (run 13), a gray insoluble solid (run 12: 1.1 g, 27% yield, run 13: 1.2 g, 35% yield) was obtained. Thermal analysis (DSC) of the polymers showed an exothermic decomposition starting at 300 °C, giving a black powder after the analysis.

Copolymerization of styrene and norbornene. Runs 7-9. 2 (ca. 20 mg) was reacted with styrene and norbornene (with ratios of 300:100 (run 7), 200:200 (run 8), and 100:300 (run 9)) for 2 days in CH_2Cl_2 (2 mL) at 50 °C. The solvent and the unreacted monomers were then removed under vacuum to give a thick oil which was isolated (yields ca. 5% (run 7), 2% (run 8), and 1% (run 9)) and analyzed by ^1H NMR spectroscopy and GPC (THF). Integration of the alkane vs. aromatic protons in the ^1H NMR spectra showed that the product obtained was polystyrene.

Runs 14-16. Stirring **1** (ca. 18mg) and $AgBF_4$ (ca. 65mg) with mixtures of styrene and norbornene (with ratios of 300:100 (run 14), 200:200 (run 15), and 100:300 (run 16)) for 3 days in CH_2Cl_2 (3 mL) at 50 °C gave, after removal of solvent and unreacted monomers, a gray solid which was isolated (yields: run 14, >95 %; run 15, 75%; run 16, 56%) and analyzed by ^1H NMR spectroscopy, GPC, and DSC (runs 15 and 16). The results are presented in Table 2. Integration of alkane vs. aromatic protons in ^1H NMR

spectroscopy showed that copolymers were formed keeping the starting proportion of styrene and norbornene. The results of the GPC analyses (in THF) were as follows: run 14, totally soluble, $M_w = 6935$; $M_w/M_n = 1.4$; run 15, partially soluble, $M_w = 7184$; $M_w/M_n = 1.5$; run 16, slightly soluble, $M_w = 7370$; $M_w/M_n = 1.5$. Thermal analysis of the solids obtained from runs 15 and 16 showed exothermic degradations of the polymers (at ca. 300 °C), giving a black powder after the analysis.

Dehydropolymerization of Phenylsilane. Into a vessel containing **1** (ca. 15 mg) and $AgBF_4$ (ca. 55 mg, 10 equiv) was syringed a CH_2Cl_2 solution (3 mL) containing $PhSiH_3$ (ca. 600 mg, 200 equiv) and the mixture stirred for 3 days at room temperature or at 80 °C. Removal of the solvent and the remaining $PhSiH_3$ gave a black oil which was analyzed by ^1H NMR spectroscopy. None of the signals characteristic[12] of $(PhSiH_2)_2$ or the $(PhSiH)_n$ oligomers was detected. **2** (25.8 mg, 0,031 mmol) and $PhSiH_3$ (676 mg, 6.25 mmol) were stirred for 3 days in CH_2Cl_2 (2mL) at room temperature. Removal of the volatiles gave a colorless oil which was analyzed by ^1H NMR spectroscopy. Signals characteristic[12] of the dimer (the major product, 4.45 ppm) and the trimer and tetramer (broad signals at 4.56 ppm) were detected while the signals for linear or cyclic polymers were absent.

[Ind(CH$_2$)$_2$NMe$_2$)Ni(dppe)][BPh$_4$] (3). Overnight stirring of a CH_2Cl_2 (15 mL) mixture of **2** (415 mg, 0.503 mmol) and dppe (201 mg, 0.505 mmol), followed by removal of the solvent, gave a red-orange solid. Two recrystallizations from CH_2Cl_2 and Et_2O (1:10) gave an orange powder (309 mg, 0.32 mmol, 64% yield). $^{31}P\{^1H\}$ NMR ($CDCl_3$): 68.66 (br) and 65.65 (br.). ^1H NMR ($CDCl_3$): 7.15 and 6.96 (t, H5 and H6), 7.6 to 6.7 (m, -P*Ph*$_2$, B*Ph*$_4$), 6.53 (br. d, $J = 8.1$ Hz, H4 or H7), 6.02 (br, H2), 5.92 (d, $J = 8.2$ Hz, H4 or H7), 5.31 (d, $J = 2.8$ Hz, H3), 2.24 (m, Ind-C*H*$_2$-), 2.03 (s, NMe_2), 1.90 (m, -C*H*$_2$-N), 1.69 (m,-C*H*$_2$P). $^{13}C\{^1H\}$ NMR ($CDCl_3$): 163.5 (4-line multiplet, $J_{B\text{-}C} = 48$ Hz, *I*-C of BPH_4), 136.4 (*m*-C of BPH_4), 133.3 (d, $^2J_{P\text{-}C} = 8$ Hz, *o*-C of PPh_2), 132.2 (*p*-C of PPh_2), 129.6 (d, $^3J_{P\text{-}C} = 11$ Hz, *m*-C of PPh_2), 128.0 and 127.8 (C5/C6), 125.64 (*o*-C of BPH_4), 121.7 (*p*-C of BPH_4) 119.7 (d, $J_{P\text{-}C} = 9$ Hz, C1), 118.3 and 118.0 (C4/C7), 101.5 (C2), 79.8 (C3), 58.8 (*C*H$_2$N), 45.2 (NMe), 30.6 and 27.6 (br. m, P*C*H$_2$), 24.6 (Ind*C*H$_2$), Anal.

Calcd for $C_{63}H_{60}P_2Ni_1B_1N_1.CH_2Cl_2$: C, 73.38; H, 5.96; N, 1.34. Found: C, 73.05; H, 6.03; N, 1.23.

Table 3.4. $^{31}P\{^1H\}$-NMR data of complexes 1 - 7.

Compound	No.	δ (ppm)[a]	$^2J_{P-P}$ (Hz)	Ref
	1	30.8[b]		4
$(\eta^3:\eta^0$-Ind$(CH_2)_2NMe_2)Ni(PPh_3)Cl$				
$[(\eta^3:\eta^1$-Ind$(CH_2)_2NMe_2)Ni(PPh_3)][BPh_4]$	**2**	29.1		4
$[(\eta^3:\eta^0$-Ind$(CH_2)_2NMe_2)Ni(dppe)][BPh_4]$	**3**	70.8, 66.4[c]	25.4[c]	
$[(\eta^3:\eta^0$-Ind$(CH_2)_2NMe_2)Ni(PPh_3)(PMe_3)][BPh_4]$	**4**	41.0, -10.9	42	
$[(1$-Me-Ind$)Ni(PPh_3)(PMe_3)][BPh_4]$		41.2, -10.1	42	1e
$[(\eta^3:\eta^0$-Ind$(CH_2)_2NMe_2)Ni(PPh_3)_2][BPh_4]$	**5**	36.1, 32.3	27	
$[(1$-Me-Ind$)Ni(PPh_3)_2][BPh_4]$		32.5, 35.8	25	1e
$[(\eta^3:\eta^0$-Ind$(CH_2)_2NMe_2)Ni(PPh_3)(Py)][BPh_4]$	**6a**	32.1		
$(\eta^3:\eta^0$-Ind$(CH_2)_2NMe_2)Ni(PPh_3)I.LiBPh_4$	**7**	35.9		
$(1$-Me-Ind$)Ni(PPh_3)I$		38.6[b]		17

[a] Unless otherwise stated, all spectra are run in $CDCl_3$ at room temperature. [b] C_6D_6. [c] At –40 °C

Reaction of 2 with PPh_3. The ^1H and $^{31}P\{^1H\}$ NMR spectra of a $CDCl_3$ solution of **2** (18.5 mg, 0.022 mmol) and PPh_3 (95 mg, 0.36 mmol) showed the emergence of a new species: ^1H NMR : 7.0-7.9 (br m, aromatic signals of P*Ph*$_3$, B*Ph*$_4^-$ and Ind), 6.81 (H2), 6.37 (d, $^3J_{H-H}$ = 7.6 Hz, H4 or H7), 6.08 (d, $^3J_{H-H}$ = 7.0 Hz, H4 or H7), 4.94 (H3), 2.11 (NMe_2); broad signals for Ind-CH_2 and CH_2N protons of the new species and of **2** are overlapping. $^{31}P\{^1H\}$ NMR : 35.9 and 32.1 (d, $^2J_{P-P}$ = 27 Hz, PPh_3). The new signals are attributed to the complex $[(\eta^3:\eta^0$-Ind(CH2)$_2$NMe$_2$)Ni $(PPh_3)_2][BPh_4]$ (**4**). A 1:3 mixture of **4** and **2** was ascertained from the integration of the respective signals. Additional PPh_3 (0.37 mmol, 97 mg) was then added to the solution and the NMR spectra were recorded 15 min. later, showing a 1:1 ratio. Removal of the solvent and washing with Et_2O gave a

reddish solid of which the ^{31}P NMR spectrum shows only a small signal for **2** and traces of unknown compounds.

Reaction of 2 with PMe_3. PMe_3 (28.5 μL, 0.28 mmol) was transferred to a stirring solution of **2** (230 mg, 0.28 mmol) in 7 mL of CH_2Cl_2. Analysis of the resulting red solution by $^{31}P\{^1H\}$ NMR spectroscopy showed the presence of a few species ($CDCl_3$): 41.1 (d, $^2J_{P\text{-}P}$ = 42, PPh_3), -10.8 (d, $^2J_{P\text{-}P}$ = 42 Hz, PMe_3), 29.5 (s, unreacted **2**), 16.5 (s), -4.5 (s, free PPh_3), -21.5 (s, $Ni(PMe_3)_4$). The signals at 41.1 and –10.8 are attributed to $[(\eta^3{:}\eta^0$-Ind(CH2)$_2$NMe$_2$)Ni (PPh_3)(PMe_3)][BPh_4] (**5**). Removal of the solvent gave a red powder consisting mainly of **2** (187 mg, 20.1 mmol, 71% crude yield).

$[(\eta^3{:}\eta^0$Ind$(CH_2)_2NMe_2)Ni(PPh_3)(Py)][BPh_4]$ (6a) in equilibrium with 2. Compound **2** (19.3 mg, 0.023 mmol) and pyridine (13.8 μL, 0.17 mmol) were mixed together in $CDCl_3$ and the ^1H and $^{31}P\{^1H\}$ NMR spectra recorded 15 min. later, showing a 2:1 ratio of **6a** and **2** on the basis of the integration of the $^{31}P\{^1H\}$ NMR signals. ^1H NMR ($CDCl_3$): 8,6 to 6.8 (m, aromatic proton of P*Ph*$_3$, Ind and pyridine), 6.60 and 6.52 (H4/H7), 6.28 (br, H2), 4.18 (s, H3), 2.14 (s, NMe_2); the signals for Ind-CH_2 and CH_2N of **6a** and **2** are overlapping. $^{31}P\{^1H\}$ NMR ($CDCl_3$): 32.13 (s).

More pyridine (13.8 μL, 0.17 mmol) was then added to the above sample and the NMR spectra recorded 15 min. later, showing a 5:1 ratio of **6a** and **2**. Removal of volatiles under vacuum gave a red solid, which was identified as **2** by $^{31}P\{^1H\}$ and ^1H NMR spectroscopy. The equilibrium constants have been calculated using data obtained from these two sets of measurements at different concentrations; the integrals of the signals for **2** and **6a** in ^1H (signal for H3) and $^{31}P\{^1H\}$ NMR spectra were used for the calculations, and gave the same results within experimental error (See Annexe II).

$[(\eta^3{:}\eta^0$Ind$(CH_2)_2NMe_2)Ni(PPh_3)(L)][BPh_4]$ (6b-6e) in equilibrium with 2. General procedure: to a $CDCl_3$ (ca 0.75 mL) solution of **2** (ca. 20 mg) was added ca. 5 to 10 μL of L (2-picoline, 3-picoline, 4-picoline, 3,5-lutidine) and the NMR spectra were recorded 20 min later. This operation was repeated one or two times with additional aliquots of L.

Equilibrium constants were derived as explained for **6a** and are tabulated in Table 3.3, together with the spectroscopic data.

[(η^3:η^0-Ind(CH_2)$_2$$NMe_2$)Ni($PPh_3$)I]·$LiBPH_4$ 7. Compound **2** (508 mg, 0.615 mmol) and LiI (1.6 g, 12.3 mmol) were stirred for 2 h in CH_2Cl_2 (15 mL) and then filtered. Evaporation of the filtrate gave a red powder of crude **7** which was dissolved in 4 mL of CH_2Cl_2 and precipitated by addition of a 1:1 hexane/Et_2O solution to give pure product as a red powder (497 mg, 0.518 mmol, 84% yield). $^{31}P\{^1H\}$ NMR ($CDCl_3$): 35.94. ^1H NMR ($CDCl_3$): 7,6 to 6.7 (m, B*Ph*$_4$. P*Ph*$_3$, aromatic proton of Ind), 6.24 (d, $^3J_{H\text{-}H}$ = 5.2 Hz, H4), 6.11 (s, H2), 4.05 (m, H3), 2.50 (m, Ind-C*H*$_2$-), 2.17 (m, -C*H*$_2$-N), 2.03 (s, NMe_2). $^{13}C\{^1H\}$ NMR (C_6D_6): 164.2 (4-line multiplet, $J_{B\text{-}C}$ = 42 Hz, *I*-C of BPH_4), 136.1 (*m*-C of BPH_4), 135.4 (d, $^2J_{P\text{-}C}$ = 9 Hz, *o*-C of PPh_3), 132.9 and 132.1 (C3A/C7A), 130.7 (*p*-C of PPh_3), 128.4 (d, $^3J_{P\text{-}C}$ = 9 Hz, *m*-C of PPh_3), 128.8 and 127.4 (C5/C6), 126.3 64 (*o*-C of BPH_4), 122.4 (*p*-C of BPH_4), 118,4 and 117.5 (C4/C7), 101.1 (d, $^2J_{P\text{-}C}$ = 25 Hz, C1), 95.2 (C2), 75.1 (C3), 55.8 (*C*H_2N), 43.51 (N*Me*), 23.2 (Ind*C*H_2). Anal. Calcd for $C_{55}H_{51}LiBNPNiI$: C, 68.79; H, 5.35; N, 1.46. Found: C, 68.23; H, 4.90; N, 1.58.

Acknowledgment. Francine Bélanger-Gariépy and Ernesto Rivera-Garcia are gratefully acknowledged for their help with the crystallography and the GPC studies, respectively. The Natural Sciences and Engineering Research Council of Canada, le fond FCAR of Quebec, and the University of Montreal are gratefully acknowledged for financial support.

Supporting Information Available: Complete details on the X-ray analysis of **2**, including tables of crystal data, collection and refinement parameters, bond distances and angles, anisotropic thermal parameters, and hydrogen atom coordinates, VT NMR spectra of **3**, detailed calculations of the equilibrium constant for the reaction of **2** with pyridine, 2-picoline, 3-picoline, 4-picoline, 3,5-lutidine, and PPh_3. This material is available free of charge via the Internet at http://pubs.acs.org.

References

(1) a) Dubois, M.-A.; Wang, R.; Zargarian, D.; Tian, J.; Vollmerhaus, R.; Li, Z.; Collins, S. *Organometallics*, **2001**, *20*, 663. b) Wang, R.; Bélanger-Gariépy, F.; Zargarian, D. *Organometallics*, **1999**, *18*, 5548. c) Dubuc, I.; Dubois, M.-A.; Bélanger-Gariépy, F.; Zargarian, D. *Organometallics*, **1999**, *18*, 30. d) Fontaine, F.-G.; Kadkhodazadeh, T.; Zargarian, D. *J. Chem. Soc., Chem. Commun.*, **1998**, 1253. e) Vollmerhaus, R.; Bélanger-Gariépy, F.; Zargarian, D. *Organometallics*, **1997**, *16*, 4762. f) Huber, T. A.; Bayrakdarian, M.; Dion, S.; Dubuc, I.; Bélanger-Gariépy, F.; Zargarian, D. *Organometallics*, **1997**, *16*, 5811. g) Bayrakdarian, M.; Davis, M. J.; Reber, C.; Zargarian, D. *Can. J. Chem.* **1996**, *74*, 2194. h) Huber, T. A.; Bélanger-Gariépy, F.; Zargarian, D. *Organometallics*, **1995**, *14*, 4997.

(2) Recent reviews on side-chain-functionalized cyclopentadienyl compouds: a) Jutzi, P.; Redeker, T. *Eur. J. Inorg. Chem.* **1998**, 663. b) Müller, C.; Vos, D.; Jutzi, P. *J. Organomet. Chem.* **2000**, *600*, 127.

(3) The generally stronger binding of phosphines vs. amines to low valent late transition metals is well documented: a) Collman, J. P.; Hegedus, L. S.; Norton, J. R.; Finke, R. G. *Principles and Applications of Organotransition Metal Chemistry*; University Science Books: Mill Valley, CA, 1987, p.241 and references therein. b) Li, M. P.; Drago, R. S.; Pribula, A. J. *J. Am. Chem. Soc.* **1977**, *99*, 6900. c) de Graaf, W.; Boersma, J.; Smeets, W. J. J.; Spek, A. L.; van Koten, G. *Organometallics*, **1989**, *8*, 2907. d) Wang, L.; Wang, C.; Bau, R.; Flood, T. C. *Organometallics*, **1996**, *15*, 491. e) Widenhoefer, R. A.; Buchwald, S. L. *Organometallics*, **1996**, *15*, 2755. f) Widenhoefer, R. A.; Buchwald, S. L. *Organometallics*, **1996**, *15*, 3534. g) Pfeiffer, J.; Kickelbick, G.; Schubert, U. *Organometallics*, **2000**, *19*, 62.

(4) Groux, L. F.; Bélanger-Gariépy, F.; Zargarian, D.; Vollmerhaus, R. *Organometallics*, **2000**, *19*, 1507.

(5) On the basis of 1290 crystal structures of compounds containing a Ni-NR_3 bond (*Cambridge Structural Database,* version 5.18; Cambridge University: Cambridge, England; accessed Nov 2000), the average and median Ni-NR_3 bond lengths are 2.087 and 2.100 Å, respectively.

(6) a) Baker, R. T. ; Tulip, T. H. *Organometallics*, **1986**, *5*, 839. b) Westcott, S. A.; Kakkar, A.; Stringer, G.; Taylor, N. J.; Marder, T. B. *J. Organomet. Chem.* **1990**, 394, 777.

(7) Segnitz, O.; Winter, M.; Merz, K.; Fisher, R. *Eur, J. Inorg. Chem.* **2000**, 2077.

(8) For a detailed study on the hapticity in the analogous Ni(Cp) complexes see: Holland, P.L.; Smith, M.E.; Andersen, R.A.; Bergman, R.G. *J. Am. Chem. Soc.* **1997**, *119*, 12815.

(9) a) Johnson, L. K.; Killian, C. M.; Arthur, S. D.; Feldman, J.; McCord, E. F.; McLain, S. J.; Kreutzer, K. A.; Bennett, M. A.; Coughlin, E. B.; Ittel, S. D.; Parthasarathy, A.; Tempel, D. J.; Brookhart, M. S., DuPont, WO 96/23010, 1996. b) Johnson, L. K.; Killian, C. M.; Brookhart, M. S. *J. Am. Chem. Soc.* **1995**, *117*, 6414. c) Keim, W.; Appel, R.; Gruppe, S.; Knoch, F. *Angew. Chem.* **1987**, *99*, 1042. d) Ostoja-Starzewski, K. A.; Witte, J. *Angew. Chem.* **1985**, *97*, 610. e) Flid, V. R.; Kuznetsov, V. B.; Grigor'ev, A. A.; Belov, A. P. *Kinetics and Catalysis,* **2000**, *41*(5), 604. f) Flid, V. R.; Manulik, O. S.; Grigor'ev, A. A.; Belov, A. P. *Kinetics and Catalysis,* **2000**, *41*(5), 658. g) Goodall, B. L.; Benedikt, G. M.; McIntosh, L. H.; Barnes, D. A. US Patent-5468819, 1995. h) Goodall, B. L.; Benedikt, G. M.; McIntosh, L. H.; Barnes, D. A.; Rhodes, L. F. US Patent-5468819, 1995. i) Bonnet, M. C.; Dahan, F.; Ecke, A.; Keim, W.; Schulz, R. P.; Tkatchenko, I. *J. Chem. Soc., Chem. Commun.* **1994**, 615. j) Aresta, M.; Dibenedetto, A.; Quaranta, E.; Lanfanchi, M.; Tiripicchio, A. *Organometallics*, **2000**, *19*, 4199. k) Ihara, E.; Fujimura, T.; Yasuda, H.; Maruo, T.; Kanehisa, N.; Kai, Y. *J. Polym. Sci.: Part A: Polym. Chem.* **2000**, *38*, 4764.

(10) Fontaine, F.-G.; Dubois, M.-A.; Zargarian, D. Unpublished results.

(11) a) We thank one of the reviewers for pointing out this possibility. b) It should be noted that styrene can be polymerized by Ag^+ (Hermans, J.P.; Smets, G. *J. Poly. Sci., Part A*, **1965**, *3*, 3175), but this reaction is much slower than that catalyzed by the **1**/$AgBF_4$ and requires higher temperatures (above 70°C).

(12) These products were identified on the basis of their characteristic ^1H NMR signals as reported in: a) Gauvin, F. Ph.D. Thesis, McGill University, Montréal, Québec, Canada, 1992. b) Aitken, C.; Barry, J.-P.; Gauvin, F.; Harrod, J.F.; Malek, A.; Rousseau, D. *Organometallics*, **1989**, *8*, 1732.

(13) a) $\Delta G^{\ddagger} = R \cdot T_c \cdot [22.96 + \ln(T_c/\Delta v]$. b) Abraham, R.J.; Loftus, P. *Proton and Carbon-13 NMR Spectroscopy, an Integrated Approach,* Wiley, Toronto, 1985; pp 165-168.

(14) This compound is identified by its singlet resonance (at ca. -21.5 ppm) in the $^{31}P\{^{1}H\}$ NMR spectrum: Tolman, C. A.; Seidel, W. C.; Gosser, L. W. *J. Am. Chem. Soc.* **1974**, *96*, 53.

(15) It is interesting to note that the $^{31}P\{^{1}H\}$ spectrum of $[(1\text{-Me-Ind})Ni(PPh_3)(PMe_3)]^{+}$ shows two sets of signals (AX and A'X') attributed to the nonequivalent rotamers arising from the hindered rotation of the indenyl ring (ref. 1d), whereas compound **5** shows only one set of signals at room temperature, presumably because of a higher rotational barrier.

(16) The analogue Cp derivative has been reported without characterization data. Nlate, S.; Herdweck, E.; Fischer, R.A. *Angew. Chem. Int. Ed. Engl.* **1996**, *35*, 1861.

(17) Dubois, M.-A. M.Sc Thesis, Université de Montréal, Montréal, Québec, Canada, 1999.

(18) CAD-4 Software. Version 5.0. Enraf-Nonius, Delft, The Netherlands, 1989.

(19) Gabe, E. J.; Le Page, Y.; Charlant, J.-P.; Lee, F. L.; White, P. S. *J. Appl. Cryst.* **1989**, *22*, 384.

(22) Sheldrick, G.M. *SHELXS*. Program for the Solution of Crystal Structures. University of Goettingen, Germany, 1997.

(23) Sheldrick, G.M. *SHELXL*. Program for the Refinement of Crystal Structures. University of Goettingen, Germany, 1996.

Chapitre 4: Dimerization and polymerization of ethylene catalyzed by nickel complexes bearing multidentate amino-functionalized indenyl ligands

Article 3

Laurent F. Groux, Davit Zargarian, Leonardo C. Simon et Joao B. P. Soares

J. Molec. Cata. A, **2003,** *193*, 51.

Abstract

The combination of the neutral nickel compound (η^3:η^0-Ind$(CH_2)_2NMe_2$)Ni(PPh_3)Cl (**1**) and methylaluminoxane (MAO) produces catalysts for the dimerization and the polymerization of ethylene. On the other hand, activation of the cationic complex [(η^3:η^1-Ind$(CH_2)_2NMe_2$)Ni(PPh_3)][BPh_4] (**2**) by MAO or trimethylaluminum leads to a system which dimerizes ethylene with high turnover frequencies (2×10^3 s^{-1}), but does not promote its polymerization. The effects of parameters such as ethylene pressure, reaction temperature and time, solvent type, and the type and amount of activator used have been studied in order to optimize the conditions for the formation of polyethylene. In addition, a number of reactions have been studied by NMR and GC-MS analysis in an effort to identify the catalytically active species. The results of these studies point to the involvement cationic species in the dimerization of ethylene, whereas, the active catalyst for the polymerization of ethylene appears to be a non-cationic species.

Introduction

The recent success of late transition metal systems, especially those of Group 10 metals, in the polymerization of ethylene has opened new vistas in the development of the next generations of catalysts for olefin polymerization.[1] Unlike the catalysts based on early transition metals, late metal-based catalysts tolerate polar functional groups in the monomers. It is anticipated that this characteristic will expand the range of polyolefins accessible by catalysis. The key element for an efficient system is the choice of the ligand. For example, a family of bidentate α-diimine ligands has been used in the development of highly efficient Ni and Pd systems for the polymerization of ethylene and propylene. These catalysts operate through cationic intermediates formed by the action of MAO-type activators.[2,3] On the other hand, recent reports on the chemistry of nickel complexes containing salicylaldimine ligands have shown that neutral intermediates could also be active and effective for the polymerization of ethylene.[4]

We have shown[5,6] that the complexes (Ind)(PR_3)NiX (Ind = indenyl and its substituted derivatives; R = Ph, Me or Cy, X = Cl, Me, CCPh) react with MAO to generate both cationic and neutral intermediates which convert ethylene to mostly

butenes (>90%) as well as some polyethylene (M_w ca. 5 x 10^5). On the other hand, studies carried out on the polymerization of styrene and norbornene have shown that an amino alkyl substituent on the Ind ligand has a major influence on the course of the polymerization: polymers with high weight average molecular weight (M_w) were obtained with styrene, whereas only oligomers were formed with norbornene.[7] With these results in mind, we set out to study the polymerization of ethylene catalyzed by complexes bearing chelating aminoindenyl ligands.[8]

The present article reports the results of our investigation on the dimerization and polymerization of ethylene catalyzed by the neutral complex (η^3:η^0-Ind$(CH_2)_2NMe_2$)Ni(PPh_3)Cl (**1**) and the cationic complex [(η^3:η^1-Ind$(CH_2)_2NMe_2$) Ni(PPh_3)][BPh_4] (**2**), Fig. 4.1. The effects of ethylene pressure, reaction temperature, time, activator, and solvent on these reactions have been studied. The results of NMR studies on the reactivity of these complexes with the activators MAO and $AlMe_3$, both in the presence and absence of ethylene, are also presented. GC-MS analyses were performed on the resulting solutions in order to track the reaction and decomposition products, thus providing clues on the reaction mechanism.

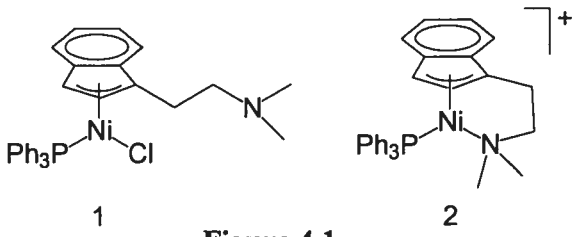

1 2

Figure 4.1.

Results and discussion

Polymerization of ethylene with the neutral complex 1. The outcome of the polymerization experiments with the neutral pre-catalyst **1** is summarized in Table 4.1. Most of these experiments resulted in the predominant formation of butenes, but various quantities of polyethylene (PE) representing ca. 1-4 % of the total mass of ethylene consumed were also produced. The PE thus obtained has high molecular weights and low polydispersity index ($M_w \approx 10^5$; M_w/M_n = 1.9-2.5), and is essentially linear with a small number of ethyl branches exclusively.

Runs 1-3 of Table 4.1 focused on the determination of the optimum amount of activator. Examination of the effect of pressure (run 3, 4a and 9) led us to select the conditions of run 4a (1000 equivalent of MAO, 300 mL toluene, 175 psi of ethylene, 40 °C for 30 min) as the standard run to which all the others would be compared. Next, we studied the effect of replacing MAO by $AlMe_3$ (runs 7 and 8), varying the reaction time (runs 4a-c), and temperature (runs 4a, 5 and 6 and 11 to 13), and finally the choice of solvent (polar and non-polar, aromatic and aliphatic). The results of these studies are described below.

Table 4.1. Reactivities[a] of (η^3:η^0-Ind$(CH_2)_2NMe_2$)Ni(PPh_3)Cl (1) with Ethylene.

	$AlMe_3$ (Eq.)	MAO (Eq.)	Solvent (300mL)	P (psi)	T (°C)	Total Activity (kg C2/ (mol Ni.h))	Activity (kg PE/ (mol Ni.h))	M_n (x 10^{-5} g/mol)	PDI (M_w/ M_n)
1	-	50	Toluene	75	40	84	0	-	-
2	-	200	Toluene	75	40	2270	0	-	-
3	-	1000	Toluene	75	40	2350	90	1.1	2.3
4a	-	1000	Toluene	175	40	8400	144	2.6	2.5
b						4790	360		
c						2920	695		
5	-	1000	Toluene	175	60	8190	89	1.3	2.1
6	-	1000	Toluene	175	80	3980	121	0.7	1.9
7	2000	-	Toluene	175	60	460	0	-	-
8	2000	200	Toluene	175	40	5090	25		
9	-	1000	Toluene	270	40	10950	108		
10	-	1000	Hexanes	175	40	8080	0	-	-
11	-	1000	DCE[b]	175	40	12970	23	1.7	2.1
12	-	1000	DCE[b]	175	60	11270	182	0.3	2.0
13	-	1000	DCE[b]	175	80	15330	516	C14-22	-
14	-	100	ClBz[b]	175	40	1820	0	-	-
15	-	1000	ClBz[b]	175	40	19810	77	1.6	2.0

[a] Reaction time, 30 min except for run 3 and 13 (60 min) and run 4b (10 min) and 4c (4 min);

[b] DCE = Dichloroethane, ClBz = Chlorobenzene.

Effect of activator. The dimerization of ethylene can be catalyzed by complex **1** in the presence of only a few equivalents of MAO or a large excess of $AlMe_3$, whereas only MAO (in large excess) is an effective co-catalyst for the production of PE (Runs 4-6, 9, 11-13 and 15). It is not clear why such a large excess of MAO is needed to activate the pro-catalyst but some of this excess is presumably used to eliminate all poisoning residues. This is illustrated by run 8 which shows that if $AlMe_3$, which doesn't activate the polymerization, is first used to clean the solvent, then a smaller amount of MAO can be used as activator (compare runs 2, 4, 7 and 8). A number of NMR experiments were carried out in order to shed light on the role of MAO in these reactions, as described next.

NMR studies with complex 1. The reactions of compound **1** with various amounts of MAO (2, 7, 14, 20, 30 and 100 equivalents; in the absence of ethylene) were monitored by ^{31}P and ^{1}H NMR (C_6D_6). Fig. 4.2 shows the conversion of complex **1** into various species as a function of MAO equivalents present in the reaction mixture. Some of the resulting species could be identified by comparison of their ^{31}P chemical shifts to those of known compounds[a] and the relative ratio of these products was calculated from the integration of signal intensities.

Thus, reacting **1** with 2 equivalents of MAO forms the Ni-Me analogue (η^3:η^0-Ind$(CH_2)_2NMe_2$)Ni(PPh_3)Me); this is evident from the characteristic ^{31}P NMR signal for the Ni-Me derivative (47.8 ppm)[b].[9] The same Ni-Me species is also obtained when **1** is reacted with $AlMe_3$ or MeLi. Experiments have shown that this Ni-Me species does not react with ethylene either on its own or when $AlMe_3$ is used as activator. On the other hand, MAO can activate the Ni-Me bond toward ethylene polymerization. We have proposed that the role of MAO is to weaken the Ni-Me bond, thereby promoting the insertion of ethylene.[c]

In order to determine the fate of the Ni-Me species, we monitored its reaction with increasing amounts of MAO. The ^{31}P $\{^{1}H\}$ NMR spectra showed that the relative concentration of the Ni-Me species decreases as the concentration of MAO increases, and

---

[a] The species were identified by correlation to completely characterized species : ref 7-9.

[b] The known (1-MeInd)(PPh_3)Ni-Me has a ^{31}P $\{^{1}H\}$ δ = 47.7 ppm.

a new species (28.6 ppm) is formed in the presence of 7 equivalents of MAO. The chemical shift of this new species is very close to that of the cationic **2**, but its ^{1}H NMR spectrum reveals some differences. In fact, this same compound is also obtained upon reacting **2** with MAO and leads to the dimerization of ethylene. Increasing the quantity of MAO beyond 20 equivalents leads to the formation of a number of unidentified species (46.1, 44.7, 41.0, 36.9, 30.4, and 27.5 ppm) one of which might well be the species producing polyethylene.

These results indicate that the Ni-Me species, which forms at the outset of the reaction between MAO and **1**, reacts further with MAO to produce a cationic species that is structurally very similar to **2**; the dimerization reaction is likely catalyzed by the homologue of **2**. The reaction of **1** with large excess of MAO also gives a number of unidentified species that show $^{31}P\{^{1}H\}$ NMR signals in a region associated with neutral Ni-Alkyl derivatives; we suspect that one or more of these species is involved in the polymerization reaction, but no firm conclusion can be drawn at this point.

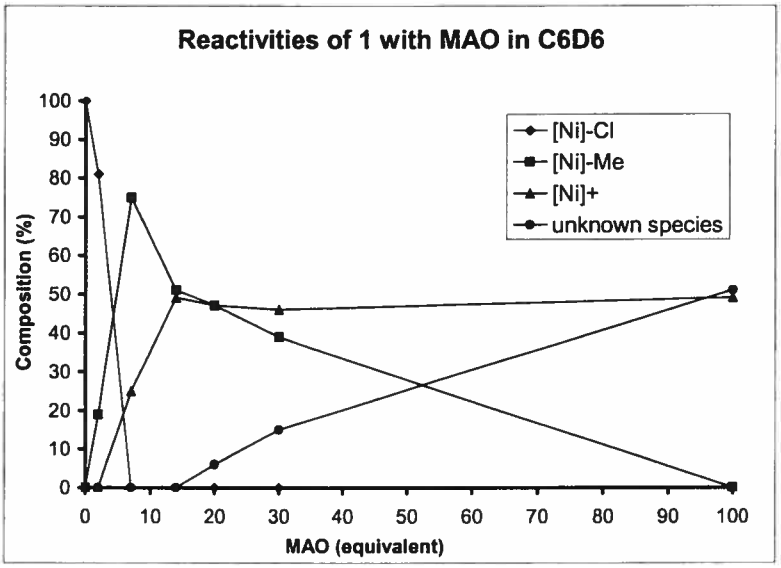

Figure 4.2. [Ni] = (Ind(CH$_2$)$_2$NMe$_2$)Ni(PPh$_3$). Reactivities of 1 with MAO in C$_6$D$_6$

[c] The complex (1-MeInd)(PPh$_3$)Ni-Me on its own is also inactive for the polymerization of ethylene, but can be activated with MAO. A weakening of the nickel-methyl bond in this complex by MAO has been proposed to explain the insertion of ethylene and chain growth.[5]

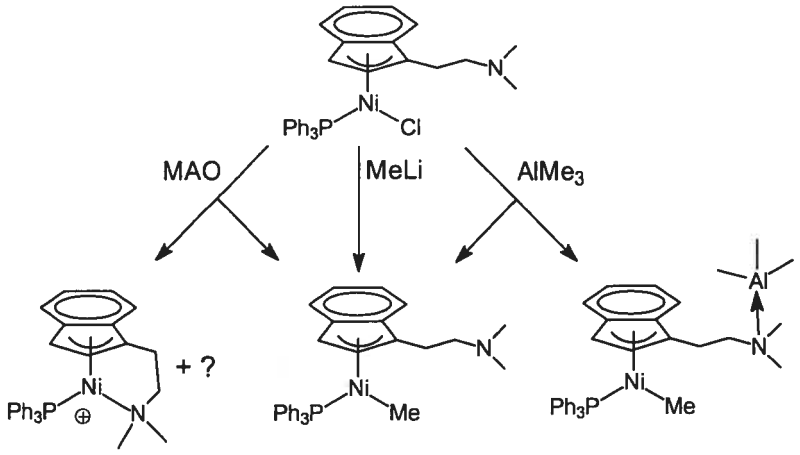

Scheme 4.1.

Effect of reaction time. In order to get more information on the active species producing polyethylene, three runs were conducted under otherwise identical conditions, changing only the reaction time (run 4a-c; 30, 10 and 4 min, respectively). The polymerization activity per unit of time increases drastically from run 4a to 4c, implying that the active species is unstable and desactivates over time. Thus, it appears that 65% of the PE is produced during the first 4 min, 20% in the next 6 min and 15% in the last 20 min. On the other hand, the consumption of ethylene increases during the first 15 min (TOF goes from 25 to 100 s^{-1}) and then stays constant over the last 15 min, during which the dimerization reaction is predominant.

Effects of pressure and reaction temperature. The total activity increases with pressure, but no significant increase has been observed on the formation of PE (run 3, 4a and 9). Higher temperatures lead to higher activities and shorter chain lengths (runs 4-6 and 11-13). The TOF curves for runs 4 and 6 show that higher temperatures increase the reaction rate initially followed by a rapid deactivation of the catalyst. The consumption of ethylene falls to nearly zero after 15 min at 80 °C in toluene (Fig. 4.3).

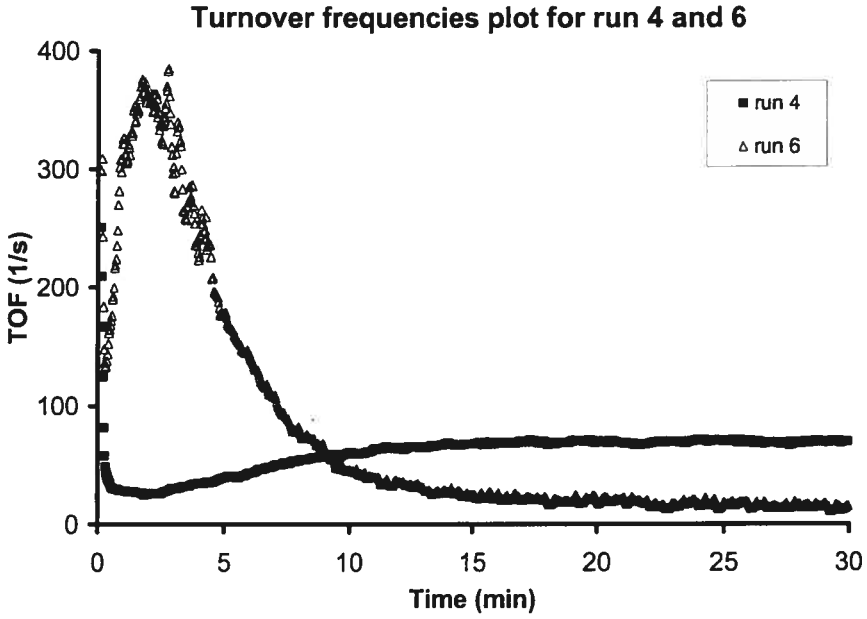

Figure 4.3. Turnover frequencies plot for runs 4 and 6.

Solvent effect. The total activity increases with the increasing polarity of the solvent (chlorobenzene > dichloroethane > toluene > hexanes), whereas aromatic solvents tend to favor the polymerization activity (runs 4a, 10, 11 and 15). Polymers with the highest number average molecular weight (M_n) were produced in toluene with modest activity. On the other hand, polymers of lower M_n or even oligomers were obtained in dichloroethane (DCE). These observations are consistent with the idea that the dimerization reaction is catalyzed by cationic species that are expected to be more stable in polar medium.

Dimerization of ethylene with the cationic complex 2.

The results of the attempted polymerization experiments with the cationic complex **2** are summarized in Table 4.2. Run 16 (40 °C) and run 7 (80 °C) were used to test the ability of complex **2** to react with ethylene without activator. The observed inertness of this complex is in contrast to its reactivity in the polymerization of norbornene and styrene at 80 °C.[7] As will be discussed later, this implies a different mechanism for the

polymerization of ethylene. The results of runs 19-21 show that a rather large amount of MAO is needed to induce the dimerization of ethylene; no polymers were obtained.

Table 4.2. Reactivities† of $[(\eta^3:\eta^1\text{-Ind}(CH_2)_2NMe_2)Ni(PPh_3)]^+$ (2) with Ethylene.

Run	MAO	Solvent (300 mL)	Total Activity (kg butenes§/(mol Ni.h))
16	0	Dichloroethane	0
17	0	Dichloroethane	0
18	25	Dichloroethane	0
19	400	Dichloroethane	51700
20	1000	Dichloroethane	74800
21	2000	Dichloroethane	76000
22	2000*	Dichloroethane	3000
23	1000	Chlorobenzene	54400
24	1000	Toluene	20000
25	1000	Hexanes	20600
26	400*	Hexanes	4900

† 175 psi, 40 °C except for run 17 (80 °C), reaction time 15-30 min; * $AlMe_3$ instead of MAO; § No solid isolated, only butenes are produced (^{13}C NMR, GC-MS analysis).

A large excess of activator (either MAO or $AlMe_3$) is crucial for both removing the contaminants present in the reaction medium and also for binding the chelating amino moiety in **2**; this binding frees a coordination site on the nickel center for ethylene. The cationic compound **2** in the presence of MAO (or $AlMe_3$) does not produce a Ni-Me species or catalyze the polymerization of ethylene. It is remarkable that no PPh_3-MAO adduct is formed even in the presence of a large excess of MAO (PPh_3-$AlMe_3$: δ -7.18 ppm (^{31}P {^1H} in C_6D_6));[10] evidently, the phosphine is strongly bonded to the nickel center and does not dissociate.

By analogy to previously reported studies, the efficient dimerization of ethylene in the present system points to a mechanism involving the insertion of ethylene into a

cationic Ni-H intermediate. The insertion of a second ethylene into the resulting Ni-ethyl bond, followed by β-H elimination would produce butene and regenerate the Ni-H species.[11,12] The initial formation of the cationic Ni-H species can occur by insertion of ethylene into the Ni-Ind bond followed by β-H elimination to give the corresponding vinyl indene 1,1- or 1,3-(CH_2=CH-Ind-$CH_2CH_2NMe_2$. The involvement of such mechanism has been supported by the results of studies carried out on the analogous complex (1-*i*Pr-ind)Ni(PPh_3)OTf.[13] In contrast, GC-MS analysis of the reaction mixtures using **2** as catalyst failed to detect the postulated vinyl indene intermediate in our studies (reaction of **2** plus MAO and ethylene (1 atm)); as a result, the validity of the above proposed mechanism in the present system can not be confirmed.

Conclusion

The combination of the neutral nickel compound (**1**) and MAO can convert ethylene to butenes and linear PE. The performance of the catalysts and the characteristics of the polymer were dependent upon the reaction parameters. It was observed that polar solvents favor the dimerization of ethylene versus its polymerization. On the other hand, activation of the cationic complex **2** by MAO or $AlMe_3$ leads to a system that only dimerizes ethylene with high activity. This result implies that a promising system for tandem production of linear low-density polyethylene (LLDPE) could be developed using a mixture of complex **2** and a selected catalyst for α-olefin polymerization.[14]

Experimental section

General Comments. All manipulations, except for the gel permeation chromatography (GPC), were performed under an inert atmosphere of N_2 or argon using standard Schlenk techniques and a drybox. The polymerization experiments were carried out in oxygen free solvents (dried using 3Å molecular sieves); $AlMe_3$ (2M in toluene, Aldrich) and MAO (10% wt in toluene, Aldrich) were used as received. Solid MAO was prepared by evaporating the toluene solution to dryness, was used for the NMR experiments. CP grade ethylene and ultra high purity nitrogen (Praxair) were purified by passing through 3 Å molecular sieves and de-oxygenation catalyst beds. Syntheses of (η^3:η^0-

Ind$(CH_2)_2NMe_2$) Ni$(PPh_3)Cl$, **1**, and [(η^3:η^1-Ind$(CH_2)_2NMe_2$)Ni(PPh_3)][BPh_4], **2**, have been reported previously.[8]

Polymerization of ethylene. Ethylene polymerization was done using a 500 mL Autoclave Engineering stainless steel reactor. The temperature was controlled within ± 0.5 °C of the set point by heating an electrical jacket and circulation of cooling fluid through an internal coil. A four-blade impeller rotating at 800 rpm was used for stirring. Prior to each reaction, the reactor was heated to 140 °C and purged 3 times with nitrogen (10 bar), then placed under vacuum for 30 min, and purged again with nitrogen three more times. Using transfer needles, 295 mL of solvent and the co-catalyst were transferred in the reactor under a nitrogen flux. The stirring was turned on, and the reactor was stabilized at the set point temperature and fed with ethylene. The ethylene flux was monitored using a mass flow sensor (Brooks 5860E) until diluent saturation was reached. When the set-point temperature and ethylene saturation were attained, 5 mL of a solution containing (2-10) x 10^{-6} mol of complex **1** or **2** was transferred into the reactor using a catalyst injection bomb. After the desired reaction time had expired, 25 mL of ethanol was pumped inside the reactor to quench the polymerization, and then the reactor was vented. The liquid was poured onto 500 mL of ethanol and kept there for 24 h to ensure complete precipitation. The polymer was filtered, washed twice with ethanol, and dried under vacuum at 50 °C. The results are presented in Table 4.1 and Table 4.2.

Polymer Characterization. The molecular weights (M_w) were determined by GPC using a Waters 150CV system equipped with three columns, differential viscometer, and refractive index detectors. The analyses were undertaken using 1,2,4-trichlorobenzene as solvent (with 0.5 g/L of Irganox 10/10 as antioxidant), at 140 °C, and M_w calculated using a universal calibration curve built with polystyrene standards. The results are reported in Table 4.1 and 4.2.

The polymers formed in our studies were shown to be linear PE with a small number of ethyl branches on the basis of ^{13}C {^1H} NMR spectroscopy (Bruker Avance 500 spectrometer, 125.75 MHz); the spectra were recorded at 120 °C in $C_2Cl_4D_2$. For example, the ^{13}C {^1H} NMR spectrum of the PE obtained from run 14 shows the

following signals (δ (integration, attribution[15,16])): 39.70 (1.0, brB_2), 34.07 (1.78, $^{\alpha}B_2$), 30.48 (2.71, $^{\gamma}B_2$), 30.00 (53.68, $^{\delta}B_2$), 27.32 (1.82, $^{\beta}B_2$), 26.74 (0.91, $^{2}B_2$), 11.20 (1.20, $^{1}B_2$). The branching is presumably due to the copolymerization of ethylene and the 1-butene formed in-situ.

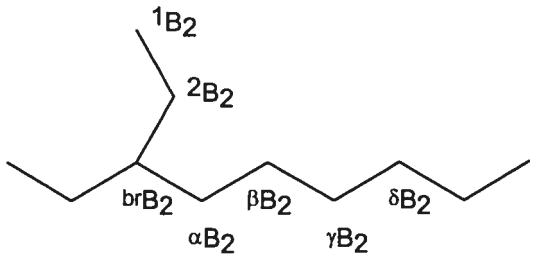

Figure 4.4.

Reactivities of 1 with MeLi. Compound **1** (13.0 mg, 0.024 mmol) and MeLi (0.038 mL of a 1.5M solution in Et_2O, 0.029 mmol, 2.4 equivalent) were mixed in C_6D_6. The ^{31}P $\{^1H\}$ spectrum was recorded 15 min later, showing only one phosphorus-containing species (47.8 ppm) characteristic of (η^3:η^0-Ind$(CH_2)_2NMe_2$)Ni(PPh_3)Me. The ^1H NMR spectrum confirms the formation of this species with the characteristic doublet at –0.67 ppm ($^3J_{P\text{-}H}$ = 5.5 Hz) due to the Ni-Me moiety.[9]

Reactivities of 1 with MAO. Compound **1** (20.1 mg, 0.037 mmol) and MAO (4.3 mg, 0.074 mmol assuming a M_W of 58) were mixed in C_6D_6. After 30 min, ^{31}P $\{^1H\}$ and ^1H NMR spectra were recorded on a Bruker AMXR400 spectrometer. The same procedure was repeated using 7, 14, 20, 30 and 100 equiv of MAO. The resulting species were identified by their chemical shifts (^{31}P $\{^1H\}$): 30.7 ppm (**1**), 47.8 ppm (η^3:η^0-Ind$(CH_2)_2NMe_2$)Ni(PPh_3)Me, 28.6 ppm (**2**), unidentified species: 46.1, 44.7, 41.0, 36.9, 30.4, 27.5 ppm.) and the ratios calculated from the integrations. The results are presented in Scheme 4.1 and Fig. 4.2.

Reactivities of 1 with $AlMe_3$. Compound **1** (13.0 mg, 0.024 mmol) and $AlMe_3$ (0.12 mL of a 2M solution in hexanes, 0.24 mmol, 10 equivalent) were mixed in C_6D_6. The ^{31}P $\{^1H\}$ spectrum was recorded after 15 min, showing two phosphorus-containing species

(47.2 and 47.0 ppm) characteristic of new Ni-Me complexes: (η^3:η^0-Ind$(CH_2)_2NMe_2$)Ni(PPh_3)Me and (η^3:η^0-Ind$(CH_2)_2NMe_2$-AlMe_3)Ni(PPh_3)Me.

Reactivities of 2 with MAO. Compound **2** (9.5 mg, 0.011 mmol) and MAO (67 mg, 1.1 mmol assuming a M_W of 58, 100 equivalent) were mixed in $CDCl_3$. The ^{31}P $\{^1H\}$ and ^1H NMR spectra were recorded 30 min later. Only one phosphorus-containing species was observed at 28.8 ppm.

Reactivities of 2 with MAO in the presence of ethylene (10 psi). Compound **2** (12.0 mg, 0.0145 mmol) and MAO (84 mg, 1.45 mmol assuming a M_W of 58, 100 equivalent) were mixed in $CDCl_3$ and the solution exposed to 10 psi of ethylene for a period of 10 min. The ^{31}P $\{^1H\}$, ^1H NMR and ^{13}C $\{^1H\}$ spectra were recorded on a Bruker AMXR400 spectrometer. One major phosphorus-containing species is observed at 28.8 ppm whereas traces of other phosphorus-containing species are observed at 37.9, 36.1, 26.7 and 24.0 ppm. The major products obtained were butenes (^{13}C $\{^1H\}$): Z-butene (12.5 and 124.7 ppm) and E-butene (18.0 and 126.0 ppm) in a 1:2 ratio[d].[17]

Acknowledgments. L. F. Groux and D. Zargarian thank Prof. S. Collins and R. Stapelton for valuable discussions and the Natural Sciences and Engineering Research Council of Canada (NSERC), le fond FCAR of Quebec, and the University of Montreal for financial support.

[d] The observation in the polymer of exclusively ethyl branches implies a 1-butene/ethylene co-polymerization. On the other hand, complexes such as (1-*I*-Pr-Ind)(PPh_3)NiOTf, which is a precursor to the cation [(1-*I*-Pr-Ind)(PPh_3)Ni]$^+$, isomerize 1-hexene to *Z*- and *E*-2-hexene.[13] Therefore, it is reasonable to assume that the initial product of the dimerization reaction is 1-butene, some of which is co-polimerized to give the polymer obtained. The unreacted 1-butene is then isomerized to *Z*- and *E*-2-butene.

References

(1) S. D. Ittel, L. K. Johnson, M. Brookhart, Chem. Rev. 100 (2000) 1169, and references therein.

(2) L. K. Johnson, C. M. Killian, M. Brookhart, J. Am. Chem. Soc. 117 (1995) 6414.

(3) L. K. Johnson, (DuPont) Int. Patent WO 96/23010 (1996).

(4) T. R. Younkin, E. F. Connor, J. L. Henderson, S. K. Friedrich, R. H. Grubbs, D. A. Bansleben, Science 287 (2000) 460, and references therein.

(5) M.-A. Dubois, R. Wang, D. Zargarian, J. Tian, R. Vollmerhaus, Z. Li, S. Collins, Organometallics, 20 (2001) 663.

(6) R. Vollmerhaus, F. Bélanger-Gariépy, D. Zargarian, Organometallics, 16 (1997) 4762.

(7) L. F. Groux, D. Zargarian, Organometallics, 20 (2001) 3811.

(8) L. F. Groux, F. Bélanger-Gariépy, D. Zargarian, R. Vollmerhaus, Organometallics, 19 (2000) 1507.

(9) T. A. Huber, M. Bayrakadarian, S. Dion, I. Dubuc, F. Bélanger-Gariépy, D. Zargarian, Organometallics 16 (1997) 5811.

(10) A.R. Barron, Organometallics, 14 (1995) 3581.

(11) W. Keim, Annals New York Academy Science (1989) 191.

(12) A. M. Al-Jarallah, J. A. Anabtawi, M. A. B. Siddiqui, A. M. Aitani, A. W. Al-Saâd-Doun, Cat. Today. 14 (1992) 1.

(13) R. Wang, L. F. Groux, D. Zargarian, Organometallics, 21 (2002) 5531.

(14) Z. J. A. Komon, G. C. Bazan, Macromolecular Rapid Com. 22 (2001) 467.

(15) W. Liu, D. G. Ray III, P. L. Rinaldi, Macromolecules, 32 (1999) 3817.

(16) G. B. Galland, R. F. de Souza, R. S. Mauler, F. F. Nunes, Macromolecules, 32 (1999) 1620.

(17) R. M. Silverstein, G. C. Basseler, T. C. Morill, Spectrometric Identification of Organic Compounds, John Willey and Sons, New York, 4th ed. 1981, p. 263.

Chapitre 5: Aminoalkyl - Substituted Indenyl - Nickel Compounds: Tuning Reactivities as a Function of the Pendant, Hemilabile Moiety

Article 4

Laurent F. Groux et Davit Zargarian

Organometallics **2003**, *22*, 3124.

Abstract

Indenyl ligands bearing three different aminoalkyl substituents have been used to prepare the complexes (Ind^NR_2)Ni(PPh_3)Cl (Ind^NR_2 = 2-(1-indenylmethyl) pyridine (**1**), *N*-(1-indenylethyl)pyrrolidine (**2**), and *N*-(1-indenylethyl) diisopropylamine (**3**)). The solution NMR spectra of complexes **1** and **2** point to the existence of a dynamic process involving the reversible coordination of the pendant amine moieties to the Ni center, but no N-Ni interaction is evident in complex **3**. Abstraction of Cl^- from the neutral precursors **1-3** yields the corresponding cationic derivatives $[(\eta^3:\eta^1\text{-Ind}\text{^}NR_2)Ni(PPh_3)]^+$ (**4-6**) wherein the amino tether is chelated to the nickel center. Complexes **1-5** have been isolated and fully characterized by multinuclear NMR spectroscopy and, in the case of **1** and **4**, by single crystal X-ray diffraction studies. The isolation of complex **6** is complicated by its partial conversion to the bis(phosphine) derivative $[\{\eta^3:\eta^0\text{-Ind}CH_2CH_2N(i\text{-}Pr)_2\}Ni(PPh_3)_2]^+$ (**7**). Studies on the displacement of the chelating amine moiety in **4** and **5** by dppe, PPh_3, and pyridine showed the pyridine moiety to be the least labile. Cyclic voltammetry studies have shown that the reduction potentials of the complexes vary as a function of the Ni-N interaction, the complexes bearing the NMe_2 moieties showing the strongest resistance to reduction. Olefin polymerization reactions also showed that the nature of the N-moiety has a considerable influence on the catalytic reactivity of the cationic complexes.

Introduction

The cyclopentadienyl ligand (Cp) and its congeners such as the indenyl (Ind) have played an important role in the development of organometallic chemistry. One attractive feature of these ligands is the ease with which their steric and electronic properties can be modified by the judicious introduction of diverse substituents. The versatility of Cp-type ligands can be further enhanced when their substituents bear coordinating moieties. For instance, the ligands Cp^NR_2 (^ denotes the tether that links the amine moiety to the Cp ring) are known to impart many interesting properties to their complexes, including superior catalytic reactivities, stabilization of otherwise unstable species, changing solubility properties, introducing chirality, and so on.[1] Although a wide variety of

complexes bearing Cp^NR_2 ligands are known for most transition metals, relatively few derivatives of group 10 metals have been reported[2] and little is known of their reactivities.

The above considerations and our long-standing interest in the chemistry of nickel indenyl complexes led us to study the reactivities of Ni complexes bearing the ligands Ind^NR_2. In earlier reports, we have described the structures and reactivities of the neutral complexes (Ind$(CH_2)_n$NRR')NiL(X) (n = 2-4; NRR' = NH(t-Bu), NH($PhCH_2$), NH_2, NMe_2; L = PPh_3, PCy_3, PMe_3; X = Cl, I, Me, Bu)[3] and the cationic complex $[(\eta^3:\eta^1\text{-Ind}(CH_2)_2NMe_2)Ni(PPh_3)]^+$.[4] These studies showed that using the ligand Ind$(CH_2)_2NMe_2$ offers an important advantage over the nonfunctionalized Ind ligands; namely, the presence of a hemilabile N→ Ni coordination in complexes incorporating this ligand prevents the formation of the catalytically inert bis(phosphine) derivatives $[IndNi(PR_3)_2]^+$, thereby improving the catalytic activities of the cationic complexes. Indeed, even when the amine moiety is not chelated, its proximity to the Ni center seems to have a marked influence over the course of the catalytic reactions and the nature of their products. These findings prompted us to prepare new complexes featuring Ind^NR_2 ligands with different coordinating properties in order to investigate further the role played by the amine moiety on the stability and reactivities of these complexes.

The present article describes the preparation and characterization of a new series of neutral and cationic nickel complexes bearing the ligands 2-(1-indenylmethyl)pyridine, *N*-(1-indenylethyl)pyrrolidine, and *N*-(1-indenylethyl) diisopropylamine. NMR studies were carried out to evaluate the interaction of the tethered amine moiety with the Ni center in the neutral compounds and study the reaction of nucleophiles with the cationic compounds. Reactivity studies have also shown that the cationic complexes can convert styrene into poly(styrenes); both the polymerization activities of the pre-catalysts and the molecular weights of the resulting polymers depend on the nature of Ni-N interaction.

Results and Discussion

The amino-functionalized Ind ligands were prepared according to literature procedures[5] by adding the appropriate Cl^NR_2 to an Et_2O solution of LiInd, followed by standard aqueous workup. Subsequent deprotonation of the resultant Ind^NR_2 and

reaction with $Ni(PPh_3)_2Cl_2$ gave the desired products (Scheme 5.1). In the process of isolating these complexes, we found that their solubilities varied greatly with the type of pendant amine moiety: whereas the complex $(IndCH_2\text{-}o\text{-}Py)Ni(PPh_3)Cl$ (**1**) readily precipitated from concentrated Et_2O solutions, the analogous complexes bearing the ligands *N*-(1-indenylethyl)pyrrolidine (**2**) and *N*-(1-indenylethyl)diisopropylamine (**3**) needed multiple re-crystallizations from less polar solutions.

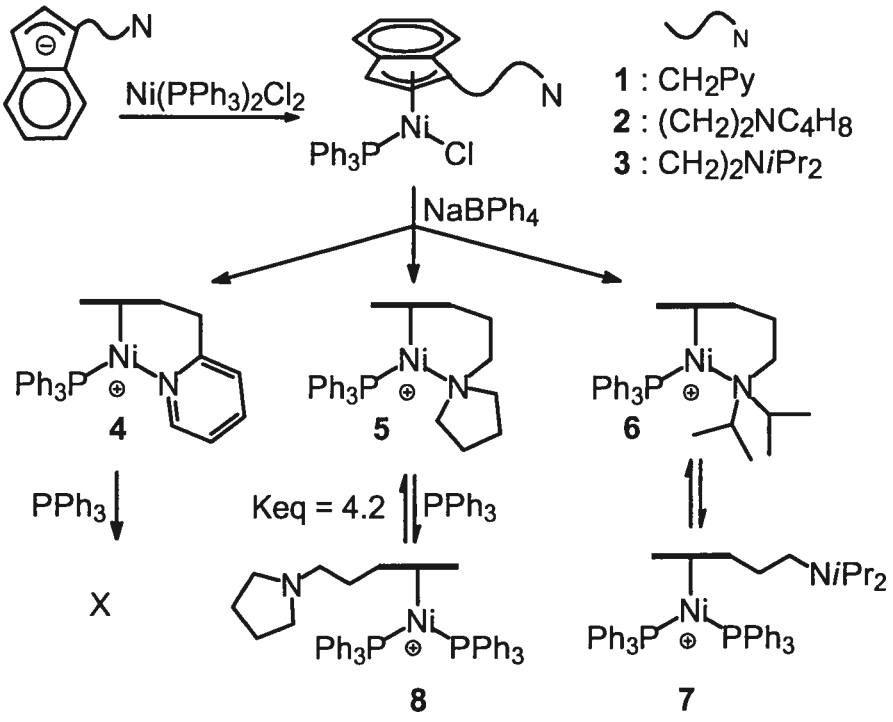

Scheme 5.1.

Solution NMR studies of the neutral complexes **1-3** revealed a dynamic process involving the reversible coordination of the amine moieties in complexes **1** and **2** to the Ni center (Scheme 5.2), but no such interaction was detected in complex **3**. As will be described in detail later, the Ni-N interaction in **1** and **2** is stronger at higher temperatures, while at lower temperatures the spectral features of these complexes resemble those of analogous complexes that do not bear functionalized substituents on Ind.

The solid state structure of complex **1** has been studied by X-ray crystallography. Table 5.1 lists the crystal data and the details of data collection and structure refinement, while Table 5.2 contains selected structural parameters. The ORTEP diagram of **1** (Figure 1) shows that the pyridine moiety is oriented away from the Ni center and does not coordinate to it; the same observation was made for the previously studied complex (Ind-$CH_2CH_2NMe_2$)Ni(PPh_3)Cl.[3] In this sense, the solid state structure of these complexes represents their low-temperature solution behavior. The plane containing P, Cl, and Ni is perpendicular to the Ind ligand, which adopts an intermediate hapticity (Δ(M-C) = 0.25 Å);[6] hence, the overall geometry around the Ni center can be described as intermediate between a two-legged piano stool (assuming η^5-Ind) and square planar (assuming η^3-Ind). As anticipated on the basis of the relative trans influences of PPh_3 and Cl ligands, the Ni-C3 bond length is significantly shorter (by > 20 σ) than the Ni-C1 distance; therefore, the Ind hapticity can be more accurately described as ($\eta^3 \leftrightarrow \eta^1 : \eta^2$).[7] The Ni-P, Ni-Cl, and C-C distances in complex **1** are similar to those found for the analogous complexes bearing nonfunctionalized Ind substituents.[8]

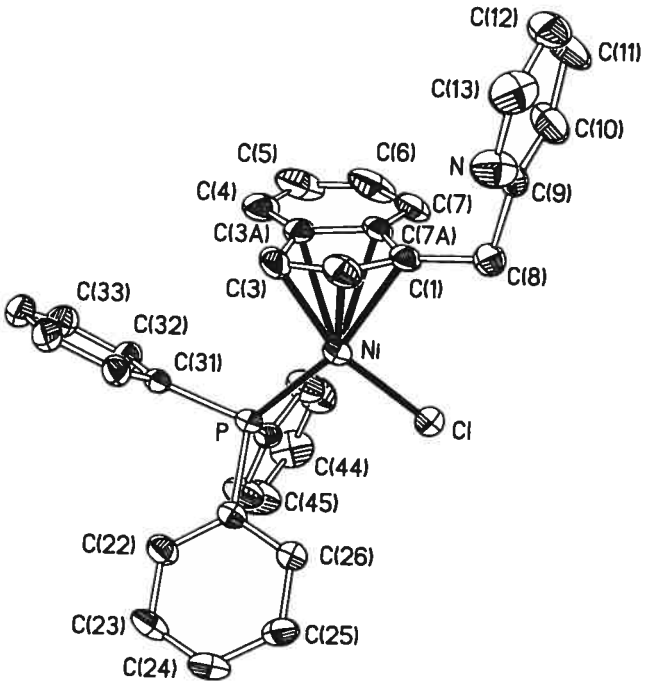

Figure 5.1. ORTEP view of complex 1.

Thermal ellipsoids are shown at 30% probability, and hydrogen atoms are omitted for clarity.

Reacting complexes **1** or **2** with excess $NaBPh_4$ in CH_2Cl_2 gave the corresponding cationic complexes **4** or **5**, respectively, in ca. 60% yield (Scheme 5.1). The $^{31}P\{^1H\}$ NMR spectra of the products showed new singlet resonances consistent with the coordination of only one PPh_3 to each Ni center, while the ^1H NMR spectra showed downfield shifts for the H3 signals (to ca. 4.0 ppm). Our previous studies showed that the conversion of $(Ind(CH_2)_2NMe_2)Ni(PPh_3)Cl$ to $[\eta^3:\eta^1(Ind(CH_2)_2NMe_2)Ni(PPh_3)]^+$ engendered similar changes in the NMR spectra;[3,4a] by analogy, we concluded that the amine moieties in **4** and **5** are chelated to the Ni center. This assertion was confirmed by the results of X-ray diffraction studies of complex **4** (vide infra).

In the case of complex **3**, abstraction of Cl^- gave both the anticipated N-chelated cation $[(\eta^3:\eta^1\text{-}IndCH_2CH_2N(i\text{-}Pr)_2Ni(PPh_3)]^+$ (**6**) and the bis(phosphine) cation $[(\eta^3:\eta^0\text{-}IndCH_2CH_2N(i\text{-}Pr)_2Ni(PPh_3)_2]^+$ (**7**) (Scheme 5.1). These species were identified on the basis of the $^{31}P\{^1H\}$ NMR spectrum of the reaction mixture, as follows. Complex **6** displayed a singlet resonance at 29.3 ppm, similar to the corresponding signal for complex **5** (30.3 ppm), whereas complex **7** gave rise to two AB doublets (36.5 and 32.1 ppm, $^2J_{P\text{-}P} = 25$ Hz), which are virtually identical to the corresponding signals for $[(1\text{-Me-Ind})Ni(PPh_3)_2]^+$ (35.8 and 32.5 ppm, $^2J_{P\text{-}P} = 25$ Hz),[9] suggesting that a second PPh_3 ligand is coordinated to the Ni center instead of the $N(i\text{-}Pr)_2$ moiety. This assignment was also corroborated by the fact that when excess PPh_3 was added to the mixture of **3** and $NaBPh_4$, the main product (>90%) was **7**. Complexes **6** and **7** interconvert in solution (Scheme 1), which prevented us from isolating pure **6** or **7**; this behavior is presumably caused by the large steric bulk of the $(i\text{-}Pr)_2N$ moiety in **3** that hinders the N→Ni coordination.

Suitable single crystals of **4** were obtained from a cold CH_2Cl_2/Et_2O solution of this complex and subjected to an X-ray diffraction analysis. Crystal data and details of data collection and structure refinement are presented in Table 5.1, selected structural parameters are listed in Table 5.2, and an ORTEP diagram is shown in Figure 5.2. The overall geometry in **4** is very similar to that of complex **1**, but chelation of the pyridine moiety alters some parameters. For instance, the Ni-C1 distance is reduced by more than

0.1 Å on going from **1** to **4** despite of the greater trans influence of PPh_3. The chelation also results in a smaller C1-Ni-N angle in **4** (ca. 84°) compared to the corresponding C1-Ni-Cl angle in **1** (ca. 96°). The Ind ligand also appears to be more tightly bound to the cationic center in **4**, as indicated by the generally shorter Ni-C distances. The Ni-N distance is 0.1 Å shorter than the average Ni-N distance found in the literature.[10] On the other hand, the Ni-P distance in **4** is longer by about 0.016 Å (ca. 20σ) compared to the neutral **1**; this is presumably because the Ni center becomes a harder Lewis acid upon ionization, thus being less compatible with the soft Lewis base PPh_3.

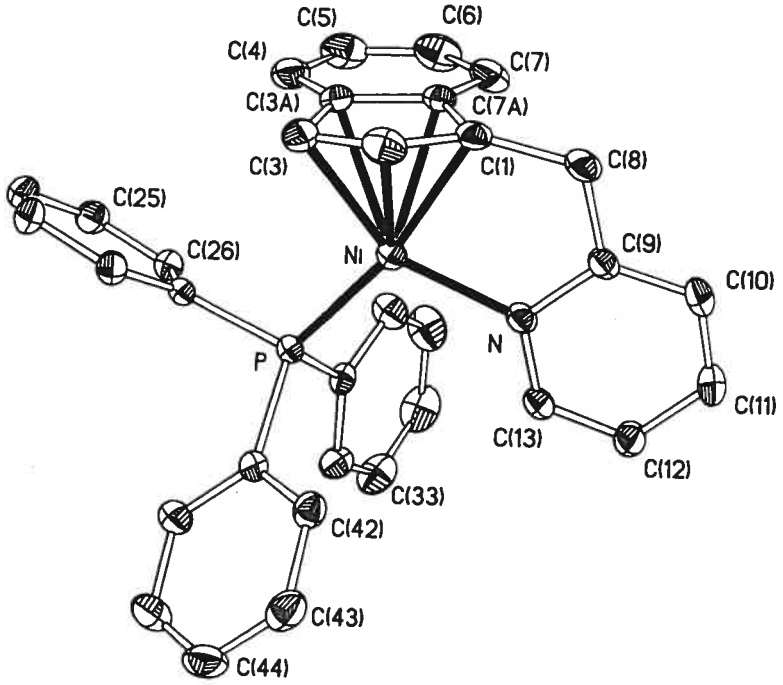

Figure 5.2. ORTEP view of complex 4.

Thermal ellipsoids are shown at 30% probability, and hydrogen atoms and the counterion (BPh_4) are omitted for clarity.

Table 5.1. Crystal Data, Data Collection and Structure Refinement of 1 and 4

	1	4
Formula, mol wt	$C_{33}H_{27}ClNPNi$, 562.69	$C_{57}H_{47}BNPNi.CH_2Cl_2$, 931.37
cryst color, habit	dark red, block	dark red, block
cryst dimens, mm	0.25 × 0.23 × 0.14	0.28 × 0.27 × 0.11
Symmetry	Triclinic	Monoclinic
space group	*P*-1	$P\,2_1/c$
a, Å	9.196(3)	10.4368(1)
b, Å	12.924(5)	21.0121(2)
c, Å	12.943(3)	21.7137(2)
α, deg	85.99(3)	90
β, deg	73.28(2)	96.340(1)
γ, deg	70.72(3)	90
volume, $Å^3$	1390.1(8)	4732.67(8)
Z	2	4
D(calcd), g cm^{-1}	1.3443	1.3072
Diffractometer	Nonius CAD-4	Bruker AXS SMART 2K
temp, K	293(2)	223(2)
λ (Cu Kα), Å	1.54178	1.54178
μ, mm^{-1}	2.595	2.247
scan type	$\omega/2\theta$ scan	ω scan
θ_{max}, deg	69.91	72.96
h,k,l range	$-11 \le h \le 11$	$-12 \le h \le 11$
	$-15 \le k \le 15$	$-25 \le k \le 25$
	$-15 \le l \le 15$	$-26 \le l \le 26$
No of Reflns used ($I > 2\sigma(I)$)	2892	6288
Abs corr	Integration ABSORB	multiscan SADABS
T (min, max)	0.4649, 0.7327	0.1816, 0.8306
$R[F^2>2\sigma(F^2)]$, $wR(F^2)$	0.0441, 0.0801	0.0508, 0.1221
GOF	0.979	1.041

Table 5.2. Selected Bond Distances (Å) and Angles (deg) for 1 and 4.

	1	4
Ni-P	2.1847(13)	2.2006(7)
Ni-(Cl or N)	2.1784(13)	1.949(2)
Ni-C1	2.132(3)	2.023(2)
Ni-C2	2.071(4)	2.063(3)
Ni-C3	2.037(4)	2.095(3)
Ni-C3A	2.308(4)	2.325(2)
Ni-C7A	2.352(2)	2.280(2)
C1-C2	1.400(4)	1.421(4)
C2-C3	1.413(5)	1.401(4)
C3-C3A	1.457(5)	1.457(4)
C3A-C7A	1.416(5)	1.417(3)
C7A-C1	1.450(4)	1.470(3)
C1-C8	1.504(4)	1.481(3)
Δ(M-C)[a]	0.25	0.24
C1-Ni-(Cl or N)	95.83(11)	83.61(9)
P- Ni-(Cl or N)	97.10(5)	106.51(6)
P- Ni-C3	101.16(12)	103.19(8)
C1-Ni-C3	65.98(14)	67.24(10)
C3-Ni-(Cl or N)	161.73(11)	150.29(10)
P- Ni-C1	165.54(10)	166.58(8)
N-C9-C8	116.4(4)	116.4(2)
C1-C8-C9	109.7(3)	109.8(2)
HA[a]	10.1(5)	11.48(14)
FA[a]	8.8(4)	8.10(13)

[a] Δ(M-C) = ½ {(M-C3a + M-C7a) - (M-C1 + M-C3)}; HA = angle between C1/C2/C3 plane and C1/C3/C3A/C7A plane; FA = angle between C1/C2/C3 plane and C3A/C4/C5/C6/C7/C7A plane.

Comparing the main structural features of **4** and its analogue $[(\eta^3:\eta^1\text{-IndCH}_2\text{CH}_2\text{NMe}_2)\text{Ni(PPh}_3)]^+$ shows that the Ni-N distance is shorter and the overall Ni-Ind interaction is somewhat stronger in complex **4**, while the Ni-P distances are quite similar (within 3σ). These observations seemed to suggest that the Ni-N bond in **4** might be less labile, which is supported by the results of ligand substitution reactions (vide infra). The stronger Ni-N and Ni-Ind interactions seemed to suggest also that the Ni center in **4** should be more electron rich, but this was not borne out by the results of our electrochemical measurements (vide infra); as will be described later, these apparently contradictory observations can be reconciled by invoking Ni→ N π-back-bonding in **4**.

Solution behavior of the neutral complexes. The solution NMR spectra of the neutral complexes **1-3** have been compared to those of other IndNi compounds in order to determine whether the amine moiety in **1-3** is involved in N→ Ni interactions (Table 5.3). Among the complexes examined, the most straightforward spectra were obtained for complex **3**, which displayed room temperature spectral features similar to those of the complexes bearing nonfunctionalized Ind ligands.[7] For example, the $^{31}P\{^1H\}$ NMR spectrum of this complex showed a singlet resonance at 30.8 ppm, and the ^1H NMR spectrum showed the anticipated signals at ca. 6.60 and 3.50 ppm for H2 and H3, respectively, of the Ind ligand (numbering scheme shown in the ORTEP diagram, Figure 1). According to these spectra, little or no N→ Ni interaction takes place in **3**, presumably because of the steric bulk of the $(i\text{-Pr})_2\text{N}$ moiety. In contrast, the amine moieties in complexes **1** and **2** reversibly coordinate to the Ni center, as inferred from their NMR spectral features described below.

The low temperature ^1H, $^{31}P\ \{^1H\}$, and $^{13}C\ \{^1H\}$ NMR spectra of complexes **1** and **2** displayed the requisite signals characteristic of the complexes bearing nonfunctionalized Ind ligands. Thus, the low-temperature $^{31}P\{^1H\}$ NMR spectra of these complexes (ca. – 40 °C, $CDCl_3$ or toluene-d_8) showed a singlet resonance at ca. 30-31 ppm, while the ^1H NMR spectra showed all the anticipated signals (e.g., 6.4-6.6 ppm for H2 and 3.2-3.4 ppm for H3). Warming the samples resulted in a gradual disappearance of all the signals, which occurred at around room temperature for complex **1** and at 40-50 °C for complex **2**. That this spectral bleaching is not caused by a thermal decomposition is

evident from the observation that subsequent cooling of the sample restored all the original signals. By analogy with the previously studied complex ($IndCH_2CH_2NMe_2$)Ni(PPh_3)Cl, which shows a similar spectral behavior,[3] we conclude that complexes **1** and **2** are also subject to a dynamic process involving the reversible coordination of the amine moiety to the Ni center. The compound dominant at the low-temperature regime can be represented by the solid state structure of this complex (Figure 1), in which no N→Ni interaction is evident. This was confirmed by the room-temperature CP-MAS NMR spectrum of a solid sample of complex **1**, which showed signals similar to those of complexes bearing nonfunctionalized susbtituents on Ind.

The high-temperature NMR spectra were studied next in search of clues on the identity of the species featuring N→Ni chelation. In the case of complex **2**, even the highest temperature accessible to us (ca. 100 °C) did not drive the dynamic process beyond the coalescence point; as a result, we were unable to directly observe the species formed by the coordination of the pyrrolidine moiety. On the other hand, the dynamic process involving complex **1** advanced beyond the coalescence point on the ^{1}H NMR frequency range (400 MHz); we could, thus, detect the species present at high temperature and compare some of its spectral features to those of the species dominant at low temperature. For example, the ^{1}H NMR signal for the H3 proton in **4** moved from 3.22 ppm at -40 °C to 4.46 ppm at 90 °C, while the signals for the methylene tether (IndCH_2py) moved from ca. 3.80 to 2.70 ppm. Most of the other signals also moved with the temperature, but these were partially or completely overlapped by other signals. Unfortunately, the high-temperature ^{31}P{^{1}H} and ^{13}C{^{1}H} NMR spectra of **1** did not show any signals and thus did not contribute to a reliable identification of the complex formed at the high-temperature regime.

We propose that the dynamic process observed for complexes **1** and **2** can be adequately described by the equilibria depicted in Scheme 5.2. According to this proposal, the amino tether can coordinate to the Ni center to form the 18-electron intermediate (or transition state) shown; the equilibrium is driven further forward at higher temperatures and with the more nucleophilic amine moiety (CH_2Py > $CH_2CH_2N(C_4H_8)$ ≈$CH_2CH_2NMe_2$). This chelation step serves as model for the initial step of the ligand substitution reaction for the complexes Ind$Ni(PR_3)Cl$, which has been

shown to proceed by an associative process.[11] The N→Ni coordination might be facilitated by either the slippage of the Ind ligand or the heterolytic dissociation of the Ni-Cl bond, which would form the chelating cations. Although the ionization of the Ni-Cl bond seemed unlikely on the basis of our earlier work,[12] we were prompted to see if it would occur more readily in polar media.[13] Examination of the NMR spectra of **1** and **4** in DMSO and acetone showed that the ionization does take place quite readily; on the other hand, the spectra of samples in acetonitrile or chloroform resemble those of samples in toluene. It appears, therefore, that the dissociated Cl^- is not sufficiently solvated in the latter media and tends to return to the coordination sphere of Ni; thus, the full ionization is difficult to attain. Therefore, the available data point to the presence of an equilibrium process leading up to the cations in polar solvant whereas slippage of the indenyl moiety is supported by some NMR evidences in non-polar solvent such as toluene, as shown in Scheme 5.2.

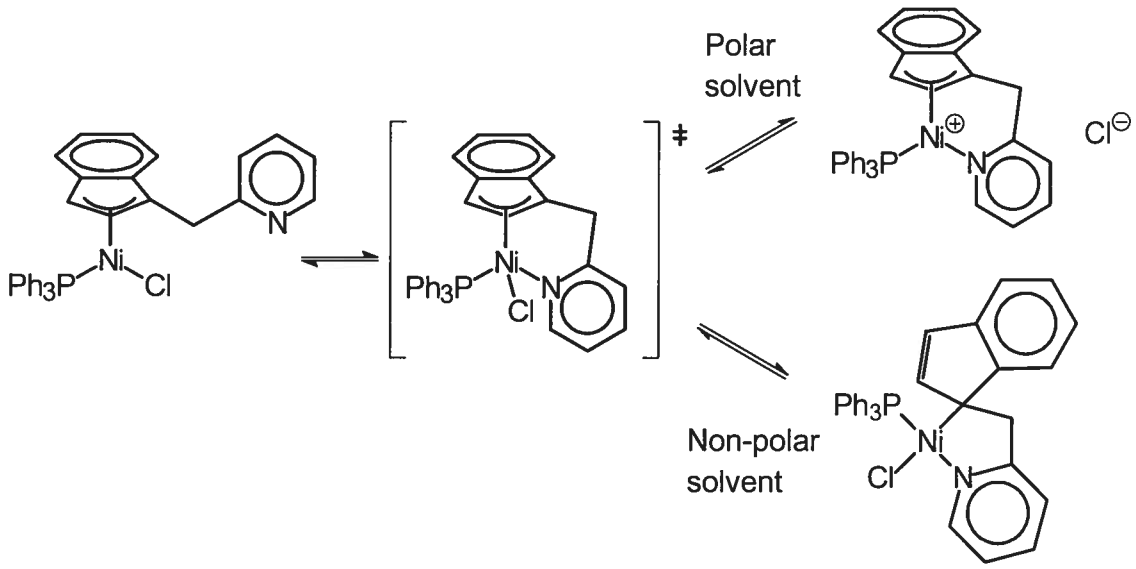

Scheme 5.2

Ligand Exchange Reactions of the Cationic Complexes. The previous section described the results of NMR studies aimed at evaluating the extent of Ni-N interaction in the neutral complexes under study. We have carried out a series of ligand substitution reactions on the cationic complexes **4** and **5** in order to measure the relative strength of

the N→ Ni binding. Comparing the results of these studies to those of the analogous studies carried out on $[(\eta^3:\eta^1\text{-IndCH}_2\text{CH}_2\text{NMe}_2)\text{Ni(PPh}_3)]^+$ has shown that the pyridine moiety in 4 binds more strongly to Ni than do the NMe_2 and the pyrrolidine moieties, as described below.

Reacting 1 equiv of dppe with **4** or **5** resulted in the displacement of both PPh_3 and the chelating amine. The resulting complexes $[(\eta^3:\eta^0\text{-IndCH}_2\text{Py})\text{Ni(dppe)}]^+$ (**9**) and $[\{\eta^3:\eta^0\text{-Ind(CH}_2)_2\text{N(C}_4\text{H}_8\}\text{Ni(dppe)}]^+$ (**10**) were identified on the basis of their characteristic $^{31}P\{^1H\}$ NMR spectra, which displayed two broad signals due to the inequivalent P nuclei in these complexes (67.7 and 70.8 ppm for **9**, 68.4 and 65.3 ppm for **10**). The broadness of these signals is attributed to the hindered rotation of the Ind ligand; a similar observation has been made for the complex $[\{\eta^3:\eta^0\text{-Ind(CH}_2)_2\text{NMe}_2\}\text{-Ni(dppe)}]^+$, which was found to have a rotational energy barrier of 14.3 kcal mol^{-1}.[4a]

In contrast to their similar reactivities with dppe, complexes **4** and **5** reacted differently with PPh_3 and pyridine. Thus, reaction of **5** with PPh_3 led to an equilibrium between **5** and $[\{\eta^3:\eta^0\text{-Ind(CH}_2)_2\text{N(C}_4\text{H}_8)\}\text{Ni(PPh}_3)_2]^+$ (**8**); as before, the bis(phosphine) species was identified readily on the basis of its characteristic AB pattern in the $^{31}P\{^1H\}$ NMR spectrum ($CDCl_3$; 36.1 ppm (d, $^2J_{P\text{-}P}$ = 26.8 Hz) and 31.9 (d, $^2J_{P\text{-}P}$ = 26.8 Hz)). The K_{eq} was found to be 4.2 (± 0.4), which is larger than the corresponding value of 0.9 for the equilibrium arising from the reaction of PPh_3 with $[\{\eta^3:\eta^1\text{-Ind(CH}_2)_2\text{NMe}_2\}\text{Ni(PPh}_3)]^+$.[4a] Similarly, the reaction of **5** with pyridine formed $[\{\eta^3:\eta^0\text{-Ind(CH}_2)_2\text{N(C}_4\text{H}_8)\}\text{-Ni(PPh}_3)(\text{Py})]^+$ (**11**), which showed a new signal at 32.1 ppm in the $^{31}P\{^1H\}$ NMR spectrum; the K_{eq} in this case was 33 (± 4), which is again larger than the corresponding value of 9 (±1) for the reaction of $[\{\eta^3:\eta^1\text{-Ind(CH}_2)_2\text{NMe}_2\}\text{Ni(PPh}_3)]^+$ with pyridine.[4a] We conclude, therefore, that the Ni-N bond is more labile in **5** relative to the NMe_2 analogue.

Contrary to the above reactivities, the reaction of complex **4** with excess PPh_3 (up to 45 equiv) resulted in the broadening of the original $^{31}P\{^1H\}$ NMR signal, but did not lead to the formation of the anticipated bis(PPh_3) cation. The reaction with pyridine also resulted in the broadening of the signal due to the coordinated PPh_3; in this case, however, the presence of > 20 equiv of pyridine led to the disappearance of the signal for coordinated PPh_3 and the appearance of the signal for free PPh_3. Thus, excess PPh_3 does

not displace the pyridine moiety, whereas excess pyridine displaces the coordinated PPh_3. It is significant that the presence of a chelating amine moiety should render the coordinated PPh_3 susceptible to displacement by an incoming amine ligand.[14]

Taken together, the above results suggest that the strength of the Ni-N bond in these complexes follows the order **6** < **5** < $[(\eta^3:\eta^1\text{-Ind}(CH_2)_2NMe_2)Ni(PPh_3)]^+$ < **4**. This order is further supported by the observation that the neutral complex **1** reacts with the cations **5** or $[(\eta^3:\eta^1\text{-Ind}(CH_2)_2NMe_2)Ni(PPh_3)]^+$ to form **4** and the corresponding neutral complex $(IndCH_2CH_2NR_2)Ni(PPh_3)Cl$ (R_2= Me_2 or $(CH_2)_4$) (Scheme 5.3).

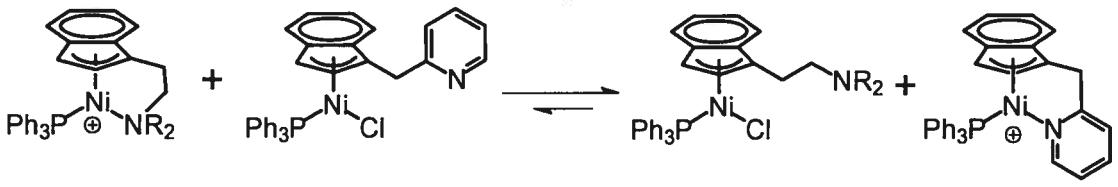

NR_2 = NMe_2 or Pyrrolidine

Scheme 5.3

Electrochemical Studies. It is reasonable to assume that, all other factors being equal, the electron density of the Ni center in the complexes $(Ind\text{^}NR_2)Ni(PPh_3)Cl$ and $[(\eta^3:\eta^1\text{-Ind}\text{^}NR_2)Ni(PPh_3)]^+$ should reflect the degree of the N→Ni interaction, stronger interactions leading to more electron-rich Ni centers. Thus, in principle, a direct correlation should exist between the strength of the Ni-N bond, as determined from NMR studies described in the preceding two sections, and the electron density at Ni, as inferred from the reduction potential of the complex. To determine the effect of N→Ni binding on the electron density at the Ni center, we have used cyclic voltammetry to measure the reduction potentials of complexes **1**-**5**, $(IndCH_2CH_2NMe_2)Ni(PPh_3)Cl$, and $[(\eta^3:\eta^1\text{-Ind}(CH_2)_2NMe_2)Ni(PPh_3)]^+$ $[BPh_4]^-$. The electrochemical measurements showed that these complexes undergo irreversible, one-electron reduction. The reduction potentials of these compounds and those of related complexes not having any Ni-N interaction were measured and corrected against the standard calomel electrode (SCE), and are listed in Table 5.3. These data allow the following observations:[15]

(a) The cationic species are easier to reduce than the neutral ones, as anticipated.

(b) For both the neutral and cationic complexes, the derivatives bearing the NMe_2 moiety were more difficult to reduce. For instance, the complexes **1-3** are reduced at -1.36 to -1.34 V, compared to -1.41 V for $(IndCH_2CH_2NMe_2)Ni(PPh_3)Cl$; the cations **4** (-1.05 V) and **5** (-1.08 V) were also easier to reduce than $[(\eta^3:\eta^1\text{-}Ind(CH_2)_2NMe_2)Ni(PPh_3)]^+$ (-1.16 V). Clearly, the nature of the tethered amine moiety modulates the level of electron density at the Ni center.

(c) The relatively easier reduction of the complexes not possessing a chelating moiety (e.g., (1-Me-Ind)$Ni(PPh_3)Cl$: E_{Red} = -1.26 V) shows that the N→ Ni interaction causes a net increase in the electron density at the Ni center in the neutral species. On the other hand, replacing the chelating amine donor in the cationic complexes by a second PPh_3 ligand results in a greater net transfer of electron density to Ni in the cationic species (e.g., $[(1\text{-Me-Ind})Ni(PPh_3)_2]^+$: E_{Red} = -1.24 V).

According to the data listed in Table 3.3, the electron density at the Ni center decreases in the order $(IndCH_2CH_2NMe_2)Ni(PPh_3)Cl$ > **1** ≈ **2** ≈ **3** and $[(IndCH_2CH_2NMe_2)Ni(PPh_3)]^+$ > **5** ≈**4**. On the other hand, the NMR studies indicated the following relative orders of N→ Ni interactions: **1** > $(IndCH_2CH_2NMe_2)Ni(PPh_3)Cl$ ≈**2** > **3** and **4** > $[(\eta^3:\eta^1\text{-}IndCH_2CH_2NMe_2)Ni(PPh_3)]^+$ > **5**. Comparison of these orders reveals that the complexes bearing the pyridine moiety (i.e., **1** and **4**) seem to defy the predicted correlation between Ni-N bond strength and the reduction potential. This anomaly might be rationalized in terms of the π-acidity of the pyridine moiety: Ni→ N π-back-bonding would be expected to reinforce the Ni-N interaction in **1** and **4**, which would be reflected in the NMR spectra, but it would also reduce the net electron density of the Ni center, which would be reflected in the reduction potentials of these complexes. The existence of some degree of Ni→ N π-back-bonding is also evident from the structural parameters of complex **4**. For example, the Ni-N bond is somewhat shorter and the Ni-Ind interaction is somewhat stronger in **4** than in $[(\eta^3:\eta^1\text{-}IndCH_2CH_2NMe_2)Ni(PPh_3)]^+$ (Ni-N = 1.95 vs 2.01 Å, Δ(M-C) = 0.24 vs 0.26 Å).

In conclusion, the electrochemical measurements are very sensitive to the net electrophilicity of the Ni center in these complexes, whereas the NMR studies can

evaluate the relative lability of the Ni-N chelation. There exists some correlation between these parameters, except in cases where there is Ni→ N π-back-bonding. While it might seem counterintuitive to suggest that the cationic Ni center is engaged in some back-bonding to the pyridine moiety, the above data support this possibility.

Table 5.3. Electrochemical and NMR Data for Complexes 1-5 and Related Derivatives

	$^{31}P\{^1H\}$ (ppm)	^1H (ppm) H2	H3	H4	E_{Red} (V obs.)	E_{Red} (V vs SCE)
1[a]	30.6	6.43	3.22	6.05	-1.65	-1.36
2[b]	30.7	6.60	3.50	6.04	-1.64	-1.34
3[c]	30.8	6.60	3.43	6.10	-1.64	-1.34
$(IndCH_2CH_2NMe_2)Ni(PPh_3)Cl$ [c]	30.8	6.70	3.42	6.11	-1.70	-1.41
$(1\text{-Me-Ind})Ni(PPh_3)Cl$ [b]	31.2	6.50	3.52	6.03		-1.26
4[d]	34.6	6.93	4.06	6.10	-1.34	-1.05
5[b]	30.3	6.80	3.97	5.50	-1.37	-1.08
$[(\eta^3,\eta^1\text{-Ind}(CH_2)_2NMe_2)Ni(PPh_3)]^+$ [b]	29.1	6.78	3.94	5.54	-1.45	-1.16
$(1\text{-Me-Ind})Ni(PPh_3)_2]^+$ [b]	36.5, 32.9	6.27	4.79	6.05		-1.24

All electrochemical studies were conducted in acetonitrile solutions and the NMR spectra are in the following solvents: [a] Toluene-d_8 –40°C; [b] $CDCl_3$; [c] C_6D_6; [d] CD_2Cl_2

Polymerization of Olefins. Many cationic Ni complexes are active in the catalytic polymerization and oligomerization of olefins.[16] We have reported recently that systems consisting of $IndNi(PR_3)X$ and methylaluminoxane (MAO) catalyze both the dimerization and polymerization of ethylene;[17] on the other hand, the dimerization of ethylene (but not its polymerization) is also promoted by the highly electrophilic cations generated in-situ from the complexes $(Ind)Ni(PR_3)(OTf)$.[18] The available mechanistic information indicates that the dimerization of ethylene in these systems proceeds by an initial insertion of ethylene into the Ni-Ind bond; subsequent β-H elimination from the

resulting alkyl ligand releases CH_2=CH-Ind (detected in some cases[18]) and generates, a postulated, cationic, and Ind-free Ni-H species that serves as the main catalyst. The mechanistic details of the ethylene polymerization reaction are not known with certainty, but the involvement of cationic species such as $[IndNi(PR_3)]^+$ in these reactions has been ruled out.[17]

Subsequent studies showed that cations bearing chelating amine moieties such as $[(\eta^3:\eta^1\text{-Ind}(CH_2)_2NMe_2)Ni(PPh_3)]^+$ are also active in the dimerization of ethylene (in the presence of MAO)[4b] and the polymerization of styrene (without cocatalysts).[4a] Although the dimerization of ethylene by these systems might operate by the insertion-type mechanisms discussed above, the polymerization of styrene can also proceed via carbocationic[19] or radical[20] pathways. It should be noted, however, that the complex $[(\eta^3:\eta^1\text{-Ind}(CH_2)_2NMe_2)Ni(PPh_3)]^+$ does not promote the polymerization of other monomers such as ethyl(vinyl)ether or methyl methacrylate, which are very prone to carbocationic[21] or radical[22] polymerizations, respectively.

As a follow-up to the latter studies,[4a] we have examined the polymerization activities of the cationic complexes **4**-**6** in order to assess the influence of the tether on these reactions. The bulk of our studies has concentrated on the polymerization of styrene, because it gave the most informative results among the monomers tested (e.g., norbornene gave < 5% yields of an intractable material). We have also studied briefly the reactivity of N-vinylcarbazole, which is prone to carbocationic[23] or radical[24] polymerizations, to address the mechanistic issues alluded to above. To compare the results of the present studies with those obtained from our previous studies with the $(CH_2)_2NMe_2$ analogue, we have performed most of the polymerization experiments under similar conditions, i.e., stirring the appropriate pre-catalyst and 1000-2000 equiv of monomer in CH_2Cl_2 or dichloroethane at 20-80 °C over 48 h. In experiments involving complex **6**, given the above-mentioned difficulty in isolating pure samples of this complex, we have used a combination of **3**/$NaBPh_4$ (1:5) to generate this species in-situ.

Initial tests showed that the reaction temperature had a very important influence on the course of the polymerization reaction, giving different results in terms of catalytic turnover numbers (TON), M_w of the products, and polydispersity index values (M_w/M_n). Thus, neither **4** nor **5** reacted with the monomers at room temperature (run 1, Table 5.4),

presumably because the relatively strong Ni-N bond does not break to facilitate the coordination of the monomer. On the other hand, the reaction of **4** with styrene at 40 °C resulted in low M_w oligomers (run 2); increasing the temperature to 60 °C gave a bimodal distribution of high M_w polymers and low M_w oligomers (run 3), whereas at 80 °C we obtained a fairly narrow distribution of high M_w species (run 4). Higher temperatures also led to higher activities (i.e., larger TON values). Similar observations were made for the polymeriztion of styrene catalyzed by **5** (runs 5-7).

In contrast to the reactivities of **4** and **5**, the polymerization of styrene in the presence of in-situ-generated **6** did proceed at room temperature, albeit with low yields and smaller M_w. Moreover, polymerization of styrene catalyzed by **6** at higher temperatures also gave much higher yields compared to the corresponding polymerizations catalyzed by **4** or **5**; on the other hand, the poly(styrene) obtained from the reaction of **6** displayed a unimodal distribution of fairly low M_w species (run 8).

The above results demonstrate that, among the complexes studied, in-situ generated **6** is the most active pre-catalyst for the polymerization of styrene, which is consistent with the weak Ni-N interaction in this complex. The pre-catalysts **4** and **5** possess similar activities, although **4** appears to give somewhat higher TON values. On the other hand, all of these pre-catalysts are more active than $[(\eta^3{:}\eta^1\text{-Ind}(CH_2)_2NMe_2)Ni(PPh_3)]^+$. On a first approximation, this order of reactivity seems to correlate with the electrochemical properties of these cationic complexes (Table 5.3): the most Lewis acidic cation (i.e., the one easiest to reduce) appears to be the most active catalyst for the polymerization of styrene. Thus, the nature of the amine moiety in Ind^NR_2 ligands modulates both the electrophilicity of the Ni center and its polymerization activity.

The importance of the nature of the tethered amine moiety on the reactivity of the complexes indicates that the Ind ligand remains coordinated to the Ni center, which implies, in turn, that the insertion-type mechanism described above for the dimerization of ethylene is not likely to be the polymerization pathway for styrene. To test the feasibility of a carbocationic propagation, we examined the reaction of N-vinylcarbazole; the reactions were carried out in the dark in order to avoid light-induced radical polymerization. This monomer does indeed react with complex **4** (1:100 ratio; 80°C) to

give a solid (95% yield) consisting of a broad mixture of oligomers (GPC in THF: M_w between 23725 and 367, maximum at 575); the reaction with **5** under the same conditions gave a solid with shorter oligomers (M_w between 2760 and 360, maximum at 433). For comparison, polymerization of this electron-rich olefin by the cationic complex $[L_2Pt(Me)(MeCN)]^+$ (L_2 = diaryldiazabutadienes) gives polymers with M_w values of ca. 23000 and M_w/M_n of ca. 3 (at room temperature),[23a] while initiation with the Lewis acid $B(C_6F_5)_3$ gives polymers with M_w values of ca. 100000 and M_w/M_n of ca. 3.6 (at –78 °C).[21a]

Table 5.4. Polymerization of Styrene Catalyzed by Complexes 4, 5, and 6[a]

Run	Catalyst	T (°C)	Time (h)	TON	High M_w Polymers M_w (x 10^3)	M_w/M_n	Low M_w Oligomers M_w (x 10^3)	M_w/M_n
1	**4** or **5**	20	48	0				
2	**4**	40	48	127			1.9	5.7
3	**4**	60	48	207	134	1.4	3.0	1.5
4	**4**	80	48	554	200	1.3		
5	**5**	40	48	35			2.3	1.2
6	**5**	60	48	180	153	1.6	3.0	1.4
7	**5**	80	48	486	145	1.7		
8	**6**[a]	80	48	1519	22.9	3.0		
9a	**4**	60	1	47			1.8	1.0
b			4.5	86			3.8	1.5
c			7	142			4.0	1.5
d			24	163	184	1.4	4.4	1.6
e			30	185	191	1.2	4.2	1.6
f			48	207	193	1.3	4.3	1.6

[a] Prepared in-situ by combining **3** with 5 equiv of $NaBPh_4$.

The above results seem to favor a carbocationic pathway for the polymerization of styrene and N-vinylcarbazole by the complexes **4/5**. To gain further insight on the course of the styrene polymerization reaction in these systems, we monitored the progress of a

typical polymerization experiment (reaction of **4** with styrene at 60°C, run 9) by performing GPC analyses on 1 mL samples of the reaction mixture after 1, 4.5, 7, 24, 30, and 48 h. The results of this experiment show that the reaction generated mainly oligomers (up to M_w of ca. 4000) during the initial stages. A steady increase was noted in M_w values as a function of time such that after a few hours the system seems to convert the oligomers into high M_w polymers, which constitute the dominant products after ca. 24 h. This reaction profile can be interpreted as implying that the polymerization reactions promoted by **4** proceed via two distinct pathways, one that is active throughout the experiment and generates oligomers, and another that is activated after a few hours and generates longer chain polymers.

To delineate the importance of continued heating for the polymerization process, two reactions were carried out under standard conditions (**4**/styrene/dichloroethane/80 °C/48 h) with the difference that one was heated only during the initial 2 h of the polymerization reaction, while the other was heated throughout the entire experiment. Analysis of the polymers showed that the partially heated reaction gave about a quarter of the yield of the poly(styrene) obtained from the other, indicating that higher temperatures are necessary not only for initiating the polymerization reaction but also for sustaining it.

Another experiment was carried out in order to answer the important question of whether PPh_3 remains coordinated to Ni during the polymerization reaction. Thus, we followed a polymerization experiment by monitoring the ^{31}P NMR spectrum of a 0.016 M solution of complex **4** containing 100 equivalents of styrene (0.5 mL $ClCH_2CH_2Cl$/0.1 mL C_6D_6) at 50°C. The NMR spectra did not show the presence of a free phosphine, implying that this ligand remains coordinated to Ni during the reaction; by inference, we believe that it is the amine moiety that detaches from the Ni center to open up a coordination site. As mentioned above, the displacement of the chelating amine ligand is slow at low temperatures, and so initiation of the catalysis requires higher temperatures. It is not clear, however, why the high temperatures must be sustained throughout the polymerization, because carbocationic propagation should not require high temperatures.[21b]

Conclusion

The preparation of the neutral and cationic complexes **1-6** has allowed us to study in more detail the effect of placing a hemilabile amino moiety adjacent to the Ni center in this family of complexes. Studying the reversible coordination of the amine moiety in the neutral complexes and measuring the impact of N→ Ni coordination on the reduction potentials of these complexes have allowed us to gauge the nucleophilicity of the hemilabile moiety. The correlation between the electrophilicity of the Ni center in the cationic complexes and their catalytic activities provides a convenient means of predicting catalytic activity on the basis of simple ligand kinetics and electrochemical measurements. Although our results do not provide strong support for the involvement of a carbocationic pathway in the polymerization reactions, this possibility is most consistent with the experimental observations.

Experimental Section

General Comments. All manipulations except the GPC analyses were performed under an inert atmosphere of N_2 using standard Schlenk techniques and a drybox. Dry, oxygen-free solvents were prepared by distillation from appropriate drying agents and employed throughout. The substituted indenyl ligands have been prepared by adding the appropriate Cl^NR_2 to a solution of LiInd, as described previously.[5] All other reagents used in the experiments were obtained from commercial sources and used as received. The elemental analyses were performed by the Laboratoire d'Analyse Élémentaire (Université de Montréal). The spectrometers used for recording the NMR spectra are: Bruker AMXR400 (^{1}H (400 MHz), ^{13}C{^{1}H} (100.56 MHz), and ^{31}P{^{1}H} (161.92 MHz)), and Bruker AV300 (^{1}H (300 MHz), and ^{31}P{^{1}H} (121.49 MHz)). ^{13}C{^{1}H}-CP-MAS (75.49 MHz) spectra were recorded on a Bruker DSX300 spectrometer.

Crystal Structure determinations. Dark red crystals of **1** were obtained from a -20 °C Et_2O solution of **1**. The crystal data for **1** were collected on a Nonius CAD-4 diffractometer with graphite-monochromated Cu Kα radiation at 293(2) K using CAD-4 software. The refinement of the cell parameters was done with the CAD-4 software,[25] and

the data reduction used NRC-2 and NRC-2A.[26] Dark red crystals of **4** were obtained from a -20 °C CH_2Cl_2/Et_2O solution of **4**. The crystal data for **4** were collected on a Bruker AXS SMART 2K diffractometer with graphite-monochromated Cu Kα radiation at 223(2) K using SMART.[27] Cell refinement and data reduction were done using SAINT.[28] Both structures were solved by direct methods using SHELXS97[29] and difmap synthesis using SHELXL96;[30] the refinements were done on F^2 by full-matrix least squares. All non-hydrogen atoms were refined anisotropically, while the hydrogens (isotropic) were constrained to the parent atom using a riding model. Crystal data and experimental details for **1** and **4** are listed in Table 5.1, and selected bond distances and angles are listed in Table 5.2.

(η^3:η^0-IndCH$_2$Py)Ni(PPh$_3$)Cl (1). An Et_2O solution (250 mL) containing $IndCH_2Py$ (300 mg, 1.45 mmol) and BuLi (0.58 mL of a 2.5 M solution in hexane) was stirred for 4 h at room temperature and then transferred (dropwise over 1.5 h) to a stirred slurry of $(PPh_3)_2NiCl_2$ (1.23 g, 1.89 mmol) in Et_2O (50 mL). The dark red solution was then filtered, and the solvent volume was reduced to ca. 75 mL. A dark red powder precipitated as fairly pure product (160 mg, 0.28 mmol, 20% yield), which was recrystallized from cold Et_2O to give crystals suitable for X-ray analysis. $^{31}P\{^1H\}$ NMR (Toluene-d_8, -40 °C): 30.6 ppm. ^1H NMR (Toluene-d_8, -40 °C): 7.50 and 7.00 (m, py and PPh_3), 7.33 (m, H7), 7.24 (m, H6), 6.60 (m, H5), 6.43 (H2), 6.05 (d, $^3J_{H\text{-}H}$ = 7.6 Hz, H4), 3.80 and 3.66 (m, Ind-CH_2), 3.22 (H3). ^{13}C $\{^1H\}$ CP-MAS: 157.9 (C9), 152.1 (C13), 134.9 (C11), 133.3 (*o*-C PPh_3), 130.0, 129.4 and 128.1 (C10/*p*-C and *m*-C PPh_3), 126.9 and 125.7 (C5/C6)), 121.6 and 120.7 (C7/C12), 115.9 (C4), 107.3 (C1), 104.3 (C2), 68.1 (C3), 35.7 (Ind*C*H_2). Anal. Calcd for $C_{33}H_{27}PNiNCl$: C, 70.44; H, 4.84; N, 2.49. Found: C, 70.56; H, 4.91; N, 2.11.

{η^3:η^0-Ind(CH$_2$)$_2$N(C$_4$H$_8$)}Ni(PPh$_3$)Cl (2). An Et_2O solution (200 mL) containing $Ind(CH_2)_2NC_4H_8$ (1.00 g, 4.69 mmol) and BuLi (1.88 mL of a 2.5 M solution in hexane) was stirred for 5 h and then transferred (dropwise over 2 h) to a stirred slurry of $(PPh_3)_2NiCl_2$ (3.7 g, 5.6 mmol) in Et_2O (30 mL). Half of the solvent was then evaporated and the solution filtered. The filtrate volume was further reduced to ca. 50 mL and the

resulting solution is cooled to -15 °C. A first crop of the desired product (ca. 1 g of a reddish solid) was isolated. Recrystallization from CH_2Cl_2/pentane gave 550 mg of pure product (0.97 mmol, 21% yield). ^{31}P $\{^1H\}$ NMR ($CDCl_3$): 30.7 ppm. ^1H NMR ($CDCl_3$, -40 °C): 7.7 to 7.0 (PPh_3, H6 and H7), 6.96 (H5), 6.60 (H2), 6.04 (H4), 3.50 (H3) 3.06 and 2.87 (CH_2N), 2.62 (NCH_2 cycle), 2.18 ($IndCH_2$), 1.82 (NCH_2CH_2 cycle). ^{13}C $\{^1H\}$ NMR ($CDCl_3$, -40°C): 133.9 (d, $^2J_{P-C}$ = 11 Hz, *o*-C of PPh_3), 132.1 and 131.9 (C3A/C7A), 131.1 (d, $^1J_{P-C}$ = 44.8 Hz, *i*-C of PPh_3), 130.4 (*p*-C of PPh_3), 128.3 (d, $^3J_{P-C}$ = 9 Hz, *m*-C of PPh_3), 126.7 and 126.3 (C5/C6), 117.9 and 116.4 (C4/C7), 104.9 (d, $^2J_{P-C}$ = 14 Hz, C1), 103.0 (C2), 67.1 (C3), 54.1 (NCH_2, cycle), 53.1 (CH_2N), 26.2 ($IndCH_2$), 23.2 (NCH_2CH_2, cycle). Anal. Calcd for $C_{33}H_{33}PNiNCl$: C, 69.69; H, 5.85; N, 2.46. Found: C, 69.33; H, 5.83; N, 2.44.

$\{\eta^3:\eta^0$-Ind$(CH_2)_2N(i\text{-}Pr)_2\}Ni(PPh_3)$Cl (3). An Et_2O solution (200 mL) containing $Ind(CH_2)_2N(i\text{-}Pr)_2$ (800 mg, 3.29 mmol) and BuLi (1.31 mL of a 2.5 M solution in hexane) was stirred for 16 h at room temperature and then transferred (dropwise over 2 h) to a stirred slurry of $(PPh_3)_2NiCl_2$ (2.8 g, 4.3 mmol) in Et_2O (50 mL). The mixture was then filtered and the filtrate volume was reduced to ca. 20 mL and cooled to -15 °C. The pure product was isolated as a dark red powder after multiple precipitation from cold ether and washings with hot hexanes (630 mg, 1.05 mmol, 32% yield). ^{31}P $\{^1H\}$ NMR (C_6D_6): 30.8 ppm. ^1H NMR (C_6D_6): 7.66 and 6.98 (PPh_3), 7.30 (d, $^3J_{H-H}$ = 7.8 Hz, H7), 7.10 (t, $^3J_{H-H}$ = 7.8 Hz, H6), 6.83 (t, $^3J_{H-H}$ = 7.6 Hz, H5), 6.60 (H2), 6.10 (d, $^3J_{H-H}$ = 7.6 Hz, H4), 3.43 (H3), 3.05 and 2.98 (m, Ind- CH_2CH_2N), 2.40 and 2.26 ($NCHMe_2$), 1.01 (m, $NCH(CH_3)_2$). ^{13}C $\{^1H\}$ NMR (C_6D_6): 134.6 (d, $^2J_{P-C}$ = 11 Hz, *o*-C of PPh_3), 132.8 (d, $^1J_{P-C}$ = 42.8 Hz, *i*-C of PPh_3), 130.3 (*p*-C of PPh_3), 128.5 (*m*-C of PPh_3), 126.5 and 126.2 (C5/C6), 118.7 and 116.9 (C4/C7), 106.8 (C1), 103.7 (C2), 66.9 (C3), 48.4 ($NCHMe_2$), 42.4 (CH_2N), 29.0 ($IndCH_2$), 21.1 ($NCH(CH_3)_2$). Anal. Calcd for $C_{35}H_{39}PNiClN$: C, 70.20; H, 6.56; N, 2.34. Found: C, 69.84; H, 6.81; N, 2.18.

$[(\eta^3:\eta^1$-IndCH$_2$Py)Ni$(PPh_3)][BPh_4]$ (4). A CH_2Cl_2 solution (10 mL) containing $(IndCH_2Py)Ni(PPh_3)Cl$ (200 mg, 0.36 mmol) and $NaBPh_4$ (730 mg, 2.2 mmol) was stirred for 24 h and then filtered. The filtrate volume was reduced to ca. 1 mL and Et_2O

(ca. 20 mL) was added to precipitate the product. Repeated precipitation gave the pure product as an orange powder (175 mg, 0.21 mmol, 58% yield). ^{31}P {^{1}H} NMR ($CDCl_3$): 33.1 ppm; (CD_2Cl_2): 34.6 ppm. ^{1}H NMR (CD_2Cl_2): 7.6 to 6.7 (PPh_3, BPh_4, H5 to H7, py), 6.93 (d, $^{3}J_{H-H}$ = 5.5 Hz, H2), 6.52 (t, $^{3}J_{H-H}$ = 6.6 Hz, H5), 6.10 (d, $^{3}J_{H-H}$ = 7.7 Hz, H4), 4.06 (H3), 3.87 and 3.57 (d, $^{2}J_{H-H}$ = 18.1 Hz, IndCH_2). ^{13}C {^{1}H} NMR (CD_2Cl_2): 175.7 (d, $^{2}J_{P-C}$ = 7 Hz, C9), 163.8 (4-lines multiplet, J_{B-C} = 49 Hz, *i*-C of BPH_4), 152.4 (d, $^{2}J_{P-C}$ = 4 Hz, C13), 139.1 (C11), 135.8 (*m*-C of BPH_4), 133.6 (d, $^{2}J_{P-C}$ = 12 Hz, *o*-C of PPh_2), 131.6 (*p*-C of PPh_2), 129.2 (d, $^{3}J_{P-C}$ = 10 Hz, *m*-C of PPh_2), 128.9, 128.6 and 128.5 (*i*-C of PPh_2/C5/C6), 125.5 (*o*-C of BPH_4), 124.7 (C10), 124.6 and 124.4 (C3A/C7A), 123.4 (C12), 121.6 (*p*-C of BPH_4), 118.3 and 117.9 (C4/C7), 108.7 (C2), 100.9 (d, $^{2}J_{P-C}$ = 8 Hz, C1), 72.3 (C3), 34.5 (IndCH_2). Anal. Calcd for $C_{57}H_{47}PNiNB$: C, 80.88; H, 5.60; N, 1.66. Found: C, 80.55; H, 5.86; N, 1.73.

[{η^3:η^1-Ind(CH_2)$_2$N(C_4H_8)}Ni(PPh_3)][BPh_4] (5). A CH_2Cl_2 solution (20 mL) containing {Ind(CH_2)$_2$N(C_4H_8)}Ni(PPh_3)Cl (300 mg, 0.53 mmol) and $NaBPh_4$ (1.08 g, 3.16 mmol) was stirred for 4 h and then filtered. The filtrate volume was reduced to ca. 6 mL and Et_2O (ca. 30 mL) was added to precipitate the product. Repeated precipitation gave the pure product as an orange powder (280 mg, 62% yield). ^{31}P {^{1}H} NMR ($CDCl_3$): 30.3 ppm. ^{1}H NMR ($CDCl_3$): 7.6 to 6.9 (PPh_3, BPh_4, H5 to H7), 6.80 (H2), 5.50 (d, $^{2}J_{H-H}$ = 7.4 Hz, H4), 3.97 (H3), 2.55 (m, IndCH_2), 2.4 to 1.4 (m, NCH_2), 1.2 to 0.6 (NCH_2CH_2). ^{13}C {^{1}H} NMR ($CDCl_3$): 163.5 (4-line multiplet, J_{B-C} = 49 Hz, *i*-C of BPH_4), 136.5 (*m*-C of BPH_4), 133.7 (d, $^{2}J_{P-C}$ = 12 Hz, *o*-C of PPh_2), 131.7 (*p*-C of PPh_2), 129.3 (d, $^{3}J_{P-C}$ = 10 Hz, *m*-C of PPh_2), 129.3 (d, $^{1}J_{P-C}$ = 36 Hz, *i*-C of PPh_2), 128.4 and 127.7 (C5/C6), 126.9 and123.9 (C3A/C7A), 125.7 (*o*-C of BPH_4), 121.9 (*p*-C of BPH_4), 118.4 and 118.3 (C4/C7), 109.8 (d, J_{P-C} = 10 Hz, C1), 106.8 (C2), 70.7 (C3), 70.1, 59.7 and 58.4 (CH_2N), 23.7 (IndCH_2), 21.3 and 21.1 (NCH_2CH_2). Anal. Calcd for $C_{57}H_{53}PNiNB$: C, 80.31; H, 6.27; N, 1.64. Found: C, 80.39; H, 6.54; N, 1.52.

Reaction of {Ind(CH_2)$_2$N(*i*-Pr)$_2$}Ni(PPh_3)Cl (3) with $NaBPh_4$. {Ind(CH_2)$_2$N(*i*-Pr)$_2$}Ni(PPh_3)Cl (31 mg, 0.05 mmol) and $NaBPh_4$ (106.3 mg, 0.31 mmol) were stirred in CH_2Cl_2 (80 mL) for 4 h, filtered, and evaporated. The resulting solid was dissolved in

CH_2Cl_2 (0.75 mL) and precipitated by adding hexanes (40 mL). The ^{31}P $\{^1H\}$ NMR ($CDCl_3$) spectrum showed four major signals, as follows: 29.3, attributed to [{η^3:η^1-Ind$(CH_2)_2N(i\text{-}Pr)_2$}Ni(PPh_3)][BPh_4] (**6**); 30.7, attributed to unreacted **3**; 32.1 and 36.5 (d, $^2J_{P\text{-}P}$= 25 Hz), attributed to [{η^3:η^0-Ind$(CH_2)_2N(i\text{-}Pr)_2$}Ni$(PPh_3)_2$][BPh_4] (**7**).

[{η^3:η^0-Ind$(CH_2)_2N(i\text{-}Pr)_2$}Ni$(PPh_3)_2$][BPh_4] (7). {Ind$(CH_2)_2N(i\text{-}Pr)_2$}Ni (PPh_3)Cl (95.4 mg, 0.16 mmol), PPh_3 (360 mg, 1.37 mmol), and $NaBPh_4$ (340 mg, 1.0 mmol) were stirred in CH_2Cl_2 (20 mL) for 4 h, then filtered and evaporated. The resulting solid was dissolved in CH_2Cl_2 (2 mL) and precipitated by adding hexanes (50 mL). Repeated recrystallizations did not give a pure product because the dissociation of one of the phosphines allowed the chelation of the tether to produce [{η^3:η^1-Ind$(CH_2)_2N(i\text{-}Pr)_2$}Ni(PPh_3)][BPh_4] (6-10%). ^{31}P $\{^1H\}$ NMR ($CDCl_3$): 36.8 (d, $^2J_{P\text{-}P}$= 25 Hz) and 32.5 (d, $^2J_{P\text{-}P}$= 25 Hz). ^1H NMR ($CDCl_3$): 7.6 to 6.9 (PPh_3, BPh_4, H5 to H7), 6.51 (H2), 6.25 (d, $^2J_{H\text{-}H}$ = 6.5 Hz, H4 or H7), and 6.02 (d, $^2J_{H\text{-}H}$ = 7.4 Hz, H4 or H7), 4.89 (d, $^2J_{H\text{-}H}$ = 3.2 Hz, H3), 2.75 (m, NCH_2), 2.35 and 2.28 (m, $IndCH_2$), 2.40 and 2.26 ($NCHMe_2$), 0.78 (m, $NCH(CH_3)_2$).

Polymerization of styrene. Runs 1-7: **4** and **5** (ca. 15 mg) and styrene (ca 3.7 g, 2000 equiv) were stirred for 2 days in CH_2Cl_2 (8 mL) at room temperature (runs 1 and 5), or in dichloroethane at 40 °C (runs 2 and 5), 60 °C (runs 3, 6, and 8), and 80 °C (runs 4 and 7). Evaporation of the solvent and unreacted styrene gave either a white solid, which was isolated (run 2: 0.23 g, 6.3 % yield; run 3: 0.37 g, 10 % yield; run 4: 1.02 g, 28% yield; run 5: 0.07 g, 1.8% yield; run 7: 0.33 g, 9% yield; run 8: 0.93 g, 24% yield) and analyzed by GPC (THF). A representative ^1H NMR ($CDCl_3$) spectrum: 7.07 (br), 6.57 (br), 1.88 (br), 1.46 (br). A representative ^{13}C $\{^1H\}$ ($CDCl_3$) spectrum: 145.3 (*ipso*-C), 128.1 (*o*- and *m*-C), 125.8 (*p*-C), 44.1 and 40.6 (alkyl chain).

Run 8: Neutral complex **3** (10.0 mg, 0.0167 mmol), $NaBPh_4$ (28.6 mg, 0.083 mmol, 5 equiv) and styrene (3.48 g, 33.4 mmol, 2000 equiv) were mixed together in dichloroethane (5 mL) and stirred for 48 h at 80 °C. Evaporation of the solvent and unreacted styrene gave a gray solid, which was isolated (2.642 g, 76% yield) and analyzed by GPC (THF).

Polymerization of *N*-vinylcarbazole. Complex **4** or **5** (ca. 11 mg) and *N*-vinylcarbazole (ca. 250 mg, 100 equiv.) were stirred for 4 days in dichloroethane (2 mL) at room temperature or at 80 °C. Evaporation of the solvent left a light red solid consisting of unreacted *N*-vinylcarbazole (room-temperature experiments) or poly(*N*-vinylcarbazole) at >95% yield (80 °C experiments). Analysis by GPC (THF) indicated that the molecular weight of the polymer ranges between 23725 and 367, with a maximum at 575 (reaction with **4**), or 2760 and 360, with a maximum at 433. These samples of poly(*N*-vinylcarbazole) were partially soluble in $CDCl_3$ and could be characterized by NMR spectroscopy (Chart 1).[31] ^1H NMR ($CDCl_3$): 8.1 (br, H5), 7.9 (br, H4), 7.6 (br), 7.3 (br, H7, H6), 6.6 (br, H3, H8, H2), 5.9 (br), 5.1 (br, H1), 3.7 (br), 2.4 (br), 2.0 (br), 1.8 (br), and 1.6 (br). ^{13}C {^1H} NMR ($CDCl_3$) 139.2 (C1a, C8a), 126.1 (C7, C2), 125.4 (C5a), 125.1 (C4a), 123.7 (C5), 123.4 (C4), 120.1 (C6), 118.9 (C3), 110.3 (C8), 110.1 (C1), 50.1, 48.1, 43.3.

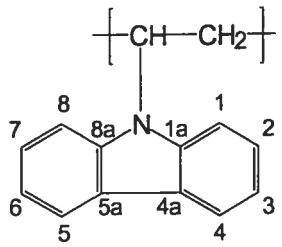

Chart 5.1

Cyclic voltammetry. Electrochemical measurements were performed on an Epsilon Electrochemical Analyzer using CH_3CN solutions of the nickel(II) complexes (0.002 M) and *n*-Bu_4NPF_6 (0.1 M). Cyclic voltammograms were obtained in a standard, one-compartment electrochemical cell using a graphite-disk electrode as working electrode, a platinum wire as the counter electrode, and an Ag-$AgNO_3$ (0.01 M in CH_3CN) reference electrode. The cyclic voltammetry was performed in the potential range of –2.8 to 0.8 V using scan rates of 50 –200 mV/s. Under these conditions, $E_{1/2}$ for the Fc^+-Fc couple is 90 mV.[32]

Reaction of [(η^3:η^1-IndCH$_2$Py)Ni(PPh$_3$)][BPh$_4$] (4) with PPh$_3$. Compound **4** (18 mg, 0.021 mmol) and PPh_3 (57 mg, 0.22 mmol, ca. 10 equiv) were dissolved in CD_2Cl_2 (0.75 mL) and ^1H and ^{31}P {^1H} NMR spectra were recorded 15 min later. The ^{31}P {^1H} NMR spectrum showed the signals of the starting material only (δ = 34.6 ppm); the signal due to free PPh_3 was not detected. In the ^1H NMR spectrum, the only difference noted was the increase of the intensities of the signals for PPh_3. A second portion of PPh_3 (76 mg, 0.29 mmol, total of ca. 24 equiv.) was added and the mixture analyzed by NMR. The $^{31}P\{^1H\}$ NMR spectrum showed the starting material (δ = 34.8 ppm) along with a new broad peak at 9.4 ppm. No new peaks were detected in the ^1H spectrum, which showed the signals for **4** and PPh_3 (increased intensity). A last portion of PPh_3 (116 mg, 0.44 mmol, for a total of ca. 45 equiv.) was added and the spectra were recorded. The ^{31}P {^1H} NMR spectrum showed the starting material (δ = 34.9 ppm) and a broad peak at –0.5 ppm. The ^1H NMR spectrum was as for the previous mixture. The anticipated AB signals (^{31}P) were not detected, implying that the complex [(η^3:η^0-IndCH$_2$Py)Ni(PPh$_3$)$_2$]$^+$ did not form.

[(η^3:η^0-Ind(CH$_2$)$_2$NC$_4$H$_8$)Ni(PPh$_3$)$_2$][BPh$_4$] (8) in equilibrium with 5. Compound **5** (12 mg, 0.015 mmol) and PPh_3 (14 mg, 0.054 mmol, ca. 3.7 equiv) were mixed together in $CDCl_3$ (0.65 mL) and analyzed by ^1H and $^{31}P\{^1H\}$ spectroscopy 15 min later. The emergence of the new product **8** was evident from the ^{31}P {^1H} NMR ($CDCl_3$) spectrum: 36.1 ppm (d, $^2J_{P\text{-}P}$ = 26.8 Hz) and 31.9 (d, $^2J_{P\text{-}P}$ = 26.8 Hz). ^1H NMR ($CDCl_3$): 7.6 to 6.9 (PPh_3, BPh_4, Ind), 6.46 (H2), 6.35 and 6.02 (H4/H7), 4.89 (br, H3), 2.6-1.1 (signals for the tether overlapping with those of **5**). A 0.34:1 ratio of **8**: **5** was determined on the basis of the integration of the $^{31}P\{^1H\}$ NMR signals. Additional PPh_3 (20 mg, 0.077 mmol) was added to the sample, and the NMR spectra were recorded 15 min later, showing a 0.71:1 ratio. A final portion of PPh_3 (25 mg, 0.095 mmol) was added and the mixture analyzed by NMR spectroscopy, which showed a 1.48:1 ratio. The equilibrium constant has been calculated: $K_{eq} = 4.2 \pm 0.4$.

[(η^3:η^0-IndCH$_2$Py)Ni(dppe)][BPh$_4$] (9). Compound **4** (13 mg, ca. 0.015 mmol) and bis(diphenylphosphino)ethane (dppe, 19 mg, ca. 0.048 mmol, 3 equiv) were dissolved in CD_2Cl_2 and the sample was analyzed by NMR after 2 h. The $^{31}P\{^1H\}$ NMR spectrum

showed free PPh_3 and free dppe along with two broad signals at 67.7 and 70.8 ppm. ^1H NMR (CD_2Cl_2): 7.6 to 6.7 (dppe, PPh_3, BPh_4, H5 to H7, py), 6.64 (d, $^3J_{H-H}$ = 7.3 Hz, H4 or H7), 6.34 (H2), 5.96 (d, $^3J_{H-H}$ = 7.8 Hz, H4 or H7), 5.47 (H3), 3.25 and 3.08 (d, $^2J_{H-H}$ = 14.2 Hz IndCH_2), 2.08 (CH_2P).

[(η^3:η^0-Ind$(CH_2)_2NC_4H_8$)Ni(dppe)][BPh_4] (10). Compound **5** (11 mg, ca. 0.013 mmol) and bis(diphenylphosphino)ethane (dppe; 15 mg, 0.039 mmol, ca. 3 equiv) were dissolved in CD_2Cl_2 and the sample was analyzed by NMR after 2 h. The $^{31}P\{^1H\}$ NMR spectrum showed free PPh_3 and free dppe along with two broad signals at 68.4 and 65.3 ppm. ^1H NMR (CD_2Cl_2): 7.6 to 6.7 (dppe, PPh_3, BPh_4, H5 to H7, py), 6.56 (d, $^3J_{H-H}$ = 7.8 Hz, H4 or H7), 6.03 (H2), 5.93 (d, $^3J_{H-H}$ = 8.2 Hz, H4 or H7), 5.31 (H3), 2.49, 2.38, and 2.29 (NCH_2CH_2), 2.11 (free dppe), 1.72 (CH_2P).

Reaction of [(η^3:η^1-IndCH_2Py)Ni(PPh_3)][BPh_4] (4) with pyridine. Compound **4** (29 mg, 0.034 mmol) and pyridine (10.9 μL, 0.14 mmol, ca. 4 equiv) were dissolved in CD_2Cl_2 (0.75 mL) and the sample was analyzed by NMR after 15 min. The $^{31}P\{^1H\}$ NMR spectrum showed the broadening of the signal of **4** (34.6 ppm). The addition of three portions of pyridine (for a total of 8, 16 and 24 equiv) led to further broadening of the signal of **4** until it disappeared and gave rise to the signal for free PPh_3. All the volatiles were then removed under vacuum and the ^{31}P $\{^1H\}$ NMR spectrum was recorded, which showed that the main phosphorus containing species is PPh_3 and implied the decomposition of **4**.

[{η^3:η^0-Ind$(CH_2)_2N(C_4H_8)$}Ni(PPh_3)(Py)][BPh_4] (11) in equilibrium with 5. Compound **5** (29 mg, 0.034 mmol) and pyridine (5.5 μL, 0.068 mmol, 2 equiv) were dissolved together in $CDCl_3$ (0.75 mL), and the ^1H and $^{31}P\{^1H\}$ NMR spectra were recorded 15 min later. New signals for **11**: ^{31}P $\{^1H\}$ NMR ($CDCl_3$): 32.1 ppm. ^1H NMR ($CDCl_3$): 7.6 to 6.9 (PPh_3, BPh_4, Ind), 6.60 and 6.52 (H4/H7), 6.28 (H2), 4.18 (br, H3), 2.79 and 2.55 (IndCH_2CH_2), 2.4 (m, NCH_2), 1.73 (NCH_2CH_2). On the basis of the integration of the ^{31}P $\{^1H\}$ NMR signals a 2.3:1 ratio was established for the complexes

11 and **5**. An additional equivalent of pyridine (2.3 μL, 0.034 mmol) was then added to the above sample and the NMR spectra were recorded 15 min later, which showed a 4.3:1 ratio of **11** and **5**. Repeated addition of 1 equiv of pyridine allowed the determination of the equilibrium constant: $K_{eq} = 33 \pm 4$. Evaporation of the solution to dryness re-formed the starting complex **5**.

Acknowledgment. The Natural Sciences and Engineering Research Council of Canada, le fond FCAR of Quebec, and the University of Montreal are gratefully acknowledged for financial support. W. Baille and Prof. J. Zhu are thanked for help with the GPC analyses, and F.-G. Fontaine is thanked for help with the electrochemistry experiments. Prof. M. C. Baird is thanked for valuable discussions on the relevance of carbocationic pathways in the polymerization reactions promoted by our complexes.

Supporting Information Available: Complete details on the X-ray analysis of **1** and **4**, including tables of crystal data, collection, and refinement parameters, bond distances and angles, anisotropic thermal parameters, and hydrogen atom coordinates. This material is available free of charge via the Internet at http://pubs.acs.org.

References

(1) For reviews of this topic see: a) Müller, C.; Vos, D.; Jutzi, P. *J. Organomet. Chem.* **2000** *600*, 127. b) Jutzi, P.; Redeker, T. *Eur. J. Inorg. Chem.* **1998**, 663. c) Jutzi, P.; Siemeling, U. *J. Organomet. Chem.* **1995**, *500*, 175. d) Jutzi, P.; Dahlaus, J. *Coord. Chem. Rev.* **1994**, *137*, 179.

(2) a) Oberbeckmann, N.; Merz, K.; Fischer, R. A. *Organometallics* **2001**, *20*, 3265. b) Segnitz, O.; Winter, M.; Merz, K.; Fischer, R. A. *Eur. J. Inorg. Chem.* **2000**, 2077. c) Hoffmann, H.; Fischer, R. A.; Antelmann, B.; Huttner, G. *J. Organomet. Chem.* **1999**, *584*, 131. d) Weiss, J.; Frank, A.; Herdweck, E.; Nlate, S.; Mattner, M.; Fischer, R. A. *Chem. Ber.* **1996**, *129*, 297. e) Fischer, R. A.; Nlate, S.; Hoffmann, H.; Herdweck, E.; Blumel, J. *Organometallics* **1996**, *15*, 5746. f) Nlate, S.; Herdweck, E.; Fischer, R. A. *Angew. Chem., Int. Ed. Eng.* **1996**, *35*, 1861. g) Jutzi, P.; Redeker, T.; Neumann, B.; Stammler, H.-G. *J. Organomet. Chem.* **1995**, *498*, 127.

(3) Groux, L.F.; Bélanger-Gariépy, F.; Zargarian, D.; Vollmerhaus, R. *Organometallics* **2000**, *19*, 1507.

(4) a) Groux, L. F.; Zargarian, D. *Organometallics* **2001**, *20*, 3811. b) Groux, L. F.; Zargarian, D.; Simon, L. C.; Soares, J. B. P. *J. Mol. Catal. A. Chem.* **2003**, *193*, 51.

(5) a) Döhring, A.; Göhre, J.; Jolly, P. W.; Kryger, B.; Rust, J.; Verhovnik, G. P. J. *Organometallics* **2000**, *19*, 388. b) Blais, M. S.; Chien, J. C. W.; Rausch, M. D. *Organometallics* **1998**, *17*, 3775. c) Ziniuk, Z.; Goldberg, I.; Moshe, K. *J. Organomet. Chem.* **1997**, *545-546*, 441

(6) For a definition of the slip parameter Δ(M-C) see the footnotes of Table 2; for a discussion of its values in various Ind complexes see these reports: a) Baker, R. T.; Tulip, T. H. *Organometallics* **1986**, *5*, 839. b) Westcott, S. A.; Kakkar, A.; Stringer, G.; Taylor, N. J.; Marder, T. B. *J. Organomet. Chem.* **1990**, 394, 777.

(7) Zargarian, D. *Coord. Chem. Rev.* **2002**, *233-234*, 157.

(8) a) Huber, T. A.; Bayrakdarian, M.; Dion, S.; Dubuc, I.; Bélanger-Gariépy, F.; Zargarian, D. *Organometallics* **1997**, *16*, 5811. b) Huber, T. A.; Bélanger-Gariépy, F.; Zargarian, D. *Organometallics* **1995**, *14*, 4997.

(9) Vollmerhaus, R.; Bélanger-Gariépy, F.; Zargarian, D.; *Organometallics* **1997**, *16*, 4762.

(10) A search using ConQuest (v 1.4, CCDC 2002) gave an average Ni-N distance of 2.054 Å when N = 2-(alkyl)pyridine.

(11) Fontaine, F.; Dubois, M.-A.; Zargarian, D. *Organometallics* **2001**, *20*, 5145.

(12) For instance, analogous Ni-Cl complexes bearing nonfunctionalized Ind substituents do not undergo ionization even in the presence of very strongly donating ligands such as phosphines.

(13) We would like to thank one of the reviewers of our manuscript for suggesting that we reexamine this issue.

(14) The generally stronger binding of phosphines vs amines to low-valent late transition metals is well documented: a) Collman, J. P.; Hegedus, L. S.; Norton, J. R.; finke, R. G. *Principles and Applications of Organotransition Metal Chemistry*; University Science Books: Mill Valley, CA, 1987; p 241, and references therein. b) Li, M. P.; Drago, R. S.; Pribula, A. J. *J. Am. Chem. Soc.* **1977**, *99*, 6900. c) de Graaf, W.; Boersma, J.; Smeets, W. J. J.; Spek, A. L.; van Koten, G. *Organometallics* **1989**, *8*, 2907. d) Wang, L.; Wang, C.; Bau, R.; Flood, T. C. *Organometallics* **1996**, *15*, 491. e) Widenhoefer, R. A.; Buchwald, S. L. *Organometallics*, **1996** *15*, 2755. f) Widenhoefer, R. A.; Buchwald, S. L. *Organometallics* **1996**, *15*, 3534. g) Pfeiffer, J.; Kickelbick, G.; Schubert, U. *Organometallics* **2000**, *19*, 62.

(15) One of the reviewers of our manuscript has asked for a justification for the use of reduction potentials in this context in light of the irreversibility of the reduction process. Strictly speaking, the reduction potential of an irreversible reduction (or oxidation) process might vary as a function of many different parameters such as electrolyte composition and nature of electrode. It is common practice, however, to consider that in situations where an analogous series of compounds are being studied under identical conditions, the values of reduction potential can be related, to a good approximation, to structural or electronic properties of the compounds. In the present case, since we are dealing with a family of complexes possessing very similar structural features and compositions, and since the electrochemical studies were performed under identical conditions, we believe that the reduction potential values represent fairly accurately the electron richness of the metal centers in this family of complexes.

(16) a) Johnson, L. K.; Killian, C. M.; Arthur, S. D.; Feldman, J.; McCord, E. F.; McLain, S. J.; Kreutzer, K. A.; Bennett, M. A.; Coughlin, E. B.; Ittel, S. D.; Parthasarathy, A.; Tempel, D. J.; Brookhart, M. S., DuPont, WO 96/23010, 1996. b) Johnson, L. K.; Killian, C. M.; Brookhart, M. S. *J. Am. Chem. Soc.* **1995**, *117*, 6414. c) Keim, W.; Appel, R.; Gruppe, S.; Knoch, F. *Angew. Chem.* **1987**, *99*, 1042. d) Ostoja-Starzewski, K. A.; Witte, J. *Angew. Chem.* **1985**, *97*, 610. e) Flid, V. R.; Kuznetsov, V. B.; Grigor'ev, A. A.; Belov, A. P. *Kinetics and Catalysis,* **2000**, *41*(5), 604. f) Flid, V. R.; Manulik, O. S.; Grigor'ev, A. A.; Belov, A. P. *Kinetics and Catalysis,* **2000**, *41*(5), 658. g) Goodall, B. L.; Benedikt, G. M.; McIntosh, L. H.; Barnes, D. A. US Patent-5468819, 1995. h) Goodall, B. L.; Benedikt, G. M.; McIntosh, L. H.; Barnes, D. A.; Rhodes, L. F. US Patent-5468819, 1995. i) Bonnet, M. C.; Dahan, F.; Ecke, A.; Keim, W.; Schulz, R. P.; Tkatchenko, I. *J. Chem. Soc., Chem. Commun.* **1994**, 615. j) Aresta, M.; Dibenedetto, A.; Quaranta, E.; Lanfanchi, M.; Tiripicchio, A. *Organometallics* **2000**, *19*, 4199. k) Ihara, E.; Fujimura, T.; Yasuda, H.; Maruo, T.; Kanehisa, N.; Kai, Y. *J. Polym. Sci.: Part A: Polym. Chem.* **2000**, *38*, 4764.

(17) Dubois, M.-A.; Wang, R.; Zargarian, D.; Tian, J.; Vollmerhaus, R.; Li, Z; Collins, S. *Organometallics* **2001**, *20*, 663.

(18) Wang, R.; Groux, L. F.; Zargarian, D. *Organometallics* **2002**, *21*, 5531.

(19) a) Yang, M.-L.; Li, K.; Stöver, H. H. *Macromol. Rapid Commun.* **1994**, *15*, 425. b) Satoh, K.; Nakashima, J.; Kamigaito, M.; Sawamoto, M. *Macromolecules* **2001**, *34*, 396.

(20) a) Li, P.; Qiu, K.-Y. *Polymer* **2002**, *43*, 5873. b) Grognec, E. L.; Claverie, J.; Poli, R. *J. Am. Chem. Soc.* **2001**, *123*, 9513.

(21) a) Wang, Q.; Baird, M. C. *Macromolecules* **1995**, *28*, 8021. b) Baird, M. C. *Chem. Rev.* **2000**, *100*, 1471.

(22) Xia, J.; Matyjaszewski, K. *Macromolecules* **1997**, *30*, 7692, and references therein.

(23) a) Albietz, P. J.; Kaiyuan, Y.; Eisenberg, R. *Organometallics* **1999**, *18*, 2747. b) Cho, H.-N.; Choi, S.-K. *J. Polymer Sci. A: Polymer Chem.* **1987**, *25*, 1769 and references 5-10 therein. c) Bowyer, P. M.; Ledwith, A.; Sherrington, D. C. *Polymer* **1971**, *12*, 509.

(24) a) Ellinger, L. P. *Polymer* **1964**, *5*, 559. b) Jones, R. G.; Khalid, N. *Makrom. Chem.* **1982**, *26*, 625.

(25) *CAD-4 Software.* Version 5.0; Enraf-Nonius: Delft, The Netherlands, 1989.

(26) Gabe, E. J.; Le Page, Y.; Charlant, J.-P.; Lee, F. L.; White, P. S. *J. Appl. Crystallogr.* **1989**, *22*, 384.

(27) *SMART*, Release 5.059; Bruker Molecular Analysis Research Tool, Bruker AXS Inc.: Madison, WI 53719-1173, 1999.

(28) *SAINT*, Release 6.06; Integration Software for Single Crystal Data, Bruker AXS Inc.: Madison, WI 53719-1173, 1999.

(29) Sheldrick, G. M. *SHELXS*. Program for the Solution of Crystal Structures; University of Goettingen: Germany, 1997.

(30) Sheldrick, G. M. *SHELXL*. Program for the Refinement of Crystal Structures; University of Goettingen: Germany, 1996.

(31) Karali, A.; Froudakis, G. E.; Dais. P. *Macromolecules* **2000**, *33*, 3180

(32) Pavlishchuk, V. V.; Addison, A. W. *Inorg. Chem. Acta*. **2000**, *298*, 97.

Chapitre 6 : Aminoalkyl-substituted indenylnickel(II) complexes (η^3:η^0-Ind$(CH_2)_2NMe_2$)Ni(PR_3)X and [(η^3:η^1-Ind$(CH_2)_2NMe_2$)Ni(PR_3)][BPh_4] : influence of the phosphine in ligand exchange and polymerization reactions

Article 5

Laurent F. Groux et Davit Zargarian

Organometallics **2003**, *accepted*

Abstract

Reaction of $LiInd(CH_2)_2NMe_2$ with $(PR_3)_2NiCl_2$ gave the neutral complexes $(\eta^3:\eta^0\text{-}Ind(CH_2)_2NMe_2)Ni(PR_3)Cl$ (R = Ph (**1**) or Me (**2**)), while the PCy_3 analogue, $(\eta^3:\eta^0\text{-}Ind(CH_2)_2NMe_2)Ni(PCy_3)Cl$ (**3**), was obtained by reacting **1** with PCy_3. These Ni-Cl species react with R'Li or $NaBPh_4$ to form, respectively, the corresponding Ni-R' derivatives $(\eta^3:\eta^0\text{-}Ind(CH_2)_2NMe_2)Ni(PR_3)R'$ (R = Ph: R' = Me (**4**) or CCPh (**5**); R = R' = Me (**6**)) or the cationic species $[(\eta^3:\eta^1\text{-}Ind(CH_2)_2NMe_2)Ni(PR_3)]^+$ (R = Ph (**7**), Me (**8**) or Cy (**9**)) in which the NMe_2 moiety is coordinated to the nickel centre. These complexes have been fully characterized, including solid state structure determinations by X-ray crystallography for complexes **2**, **4**, **5**, **6**, and **9**. Inspection of the structural data showed that replacing the Cl ligand by the more strongly donor ligands CCPh and Me reinforces the Ni-P and Ni-Ind interactions. On the other hand, electrochemical measurements showed that the reduction potentials of the Ni-Cl compounds are intermediate between the Ni-R' derivatives, which are more resistant to reduction, and the cationic species, which are the easiest to reduce. The cationic complexes are single component catalysts for the polymerization of styrene, giving poly(styrene) with M_w in the range of 10^4-10^5 Da, and the hydrosilylation of styrene and 1-hexene with $PhSiH_3$ and Ph_2SiH_2. The nature of the phosphine ligand has an important influence on the catalytic reactivities, the PMe_3 analogue **8** being the most active catalyst.

Introduction

An important class of hemilabile ligands consists of functionalized cyclopentadienyl ligands represented by Cp^L, with ^ denoting the side chain linking the Cp ligand to a functional group L such as NRR',[1] OR,[2] PRR',[3] SR,[3] AsRR',[3] C=C,[4] etc. The main role of the Cp moiety is to anchor these multidentate ligands to metal centres, while the reversible coordination of L modulates the reactivities of the metal centre. In principle, substrates can displace the hemilabile group L from the metal centre in order to initiate reactivity; on the other hand, since L is never far from the metal, it can re-coordinate readily in the absence of substrate to prevent the decomposition of the catalyst (Scheme 6.1). The potential of this class of compounds in catalysis has spurred research efforts in this area and resulted in the preparation of many transition metal complexes

bearing Cp^L type ligands or their indenyl analogues. Examination of the reactivities of some of these complexes has demonstrated the dramatic influence of the hemilabile ligands on catalytic reactivities, stabilization of otherwise unstable species, changing solubility properties, introducing chirality, and so on.[1,5]

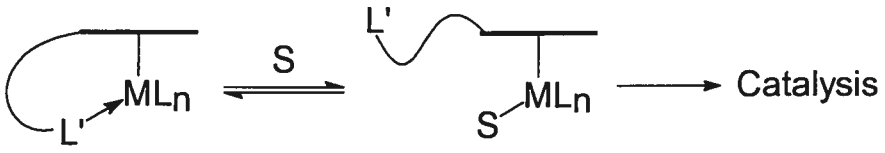

Scheme 6.1

We became interested in this area of research during our investigations on the catalytic reactivities of indenyl-nickel(II) complexes.[6] What inspired us to examine the influence of a hemilabile moiety in our complexes was the observation that the highly reactive, in situ generated cationic species $[IndNi(PR_3)]^+$ (Ind = indenyl and its substituted derivatives) are rapidly converted to the inactive compounds $[IndNi(PR_3)_2]^+$ in the absence of substrates. The presence of this deactivation pathway meant that these catalysts had to be generated in situ and in the presence of a large excess of substrate; otherwise, the formation of the bis(phosphine) derivatives would inhibit the catalysis. We reasoned that the incorporation of a hemilabile moiety in the vicinity of the Ni centre might circumvent catalyst deactivation, thereby improving catalyst lifetimes.

This assertion was borne out by the results of studies on the influence of an amino tether on the reactivity of the complexes.[7] Thus, we found that the cationic complexes $[(\eta^3:\eta^1\text{-Ind}\text{^}NR_2)Ni(PPh_3)]^+$ were active, single component catalysts (i.e., no activation or in situ generation needed) for polymerization of styrene and norbornene. Interestingly, the M_w and solubilities of the products obtained from these reactions were different from those of the products obtained from reactions promoted by the in situ generated $[(Ind)Ni(PPh_3)]^+$, implying that the hemilabile moiety might also influence the course of the catalysis.[7b] Isolation and complete characterization of the new complexes, as well as a study of their ligand exchange reactions, allowed an evaluation of the lability of N→ Ni binding as a function of incoming ligand's nucleophilicity[7b] and different amine substituents.[7d]

As a follow up to our previous studies, we have prepared analogous cationic compounds with PMe_3 and PCy_3 instead of PPh_3 in order to examine the influence of the phosphine ligand on the binding of the tether to the Ni centre and on the reactivities of these complexes. The present report describes the preparation and characterization of the chloro derivatives (η^3:η^0-Ind$(CH_2)_2NMe_2$)Ni(PR_3)Cl (R = Me (**2**) and Cy (**3**)), the cationic complexes [(η^3:η^1-Ind$(CH_2)_2NMe_2$)Ni(PR_3)]$^+$ (R = Me (**8**) and Cy (**9**)), and (η^3:η^0-Ind$(CH_2)_2NMe_2$)Ni(PR_3)R' (R = Ph: R' = Me (**4**) and CCPh (**5**); R = R' = Me (**6**)). The catalytic reactivities of these compounds in the polymerization of styrene and phenylacatylene, oligomerization of $PhSiH_3$, and the hydrosilylation of styrene and 1-hexene are also reported herein.

Results and discussion

Synthesis and spectroscopic characterization. The previously reported[7a] preparation of (η^3:η^0-Ind$(CH_2)_2NMe_2$)(PPh_3)NiCl, **1**, served as a model for the synthesis of (η^3:η^0-Ind$(CH_2)_2NMe_2$)(PMe_3)NiCl, **2**. Thus, slow addition of 1 equiv of LiInd$(CH_2)_2NMe_2$ to 1 equiv of Ni$(PMe_3)_2Cl_2$ in THF gave a dark red solution from which pure **2** precipitated gradually. On the other hand, the PCy_3 analogue (η^3:η^0-Ind$(CH_2)_2NMe_2$)(PCy_3)NiCl, **3**, was readily obtained by adding 1.5 equiv of PCy_3 to a solution of **1** in Et_2O (Scheme 6.2).

The new complexes have been fully characterized by NMR spectroscopy (^{1}H, ^{13}C, and ^{31}P), elemental analysis, and in the case of **2** by X-ray diffraction studies. The NMR spectra of complexes **2** and **3** display the characteristic signals observed for the analogous nonfunctionalized compounds (1-Me-Ind)Ni(PR_3)Cl (R = Ph, Me, Cy).[8] For instance, the ^{31}P{^{1}H} NMR spectra showed singlets for the phosphine ligands at -11 ppm for **2** (cf. –10.6 ppm for the 1-Me-Ind analogue) and 37.0 ppm for **3** (compared to 37.2 ppm for its 1-Me-Ind analogue).[8b] The ^{1}H and ^{13}C{^{1}H} NMR spectra also served to establish the degree of N→ Ni interaction in these complexes, as described below.

Previous studies had shown that the complexes (Ind^NR_2)PPh_3Ni(Cl) display variable degrees of dynamic N→ Ni binding: temperature-dependent ^{1}H and ^{13}C{^{1}H} NMR spectra were obtained, with the room temperature ^{1}H NMR spectra displaying very

broad signals, while the corresponding $^{13}C\{^1H\}$ NMR spectra contained few of the expected resonances. In the case of complexes **2** and **3**, however, no signal broadening was observed in the ^1H NMR spectra and all the anticipated ^{13}C NMR resonances were accounted for. Moreover, the $N(CH_3)_2$ groups in these complexes were found to be equivalent, which indicates that the amine moiety does not coordinate to the Ni centre. (Since these complexes have C_1 symmetry, i.e., they are chiral, N→Ni coordination would be expected to render the $N(CH_3)_2$ groups diastereotopic.) Therefore, we conclude that complexes **2** and **3** do not undergo a dynamic exchange process involving amine chelation, in contrast to their previously studied PPh_3 analogues. This difference is presumably related to the higher electron density of the Ni centre in **2** and **3**, which is in turn brought about by the more strongly donating phosphines PMe_3 and PCy_3. This issue will be addressed in the next section, along with the solid state structure of **2**.

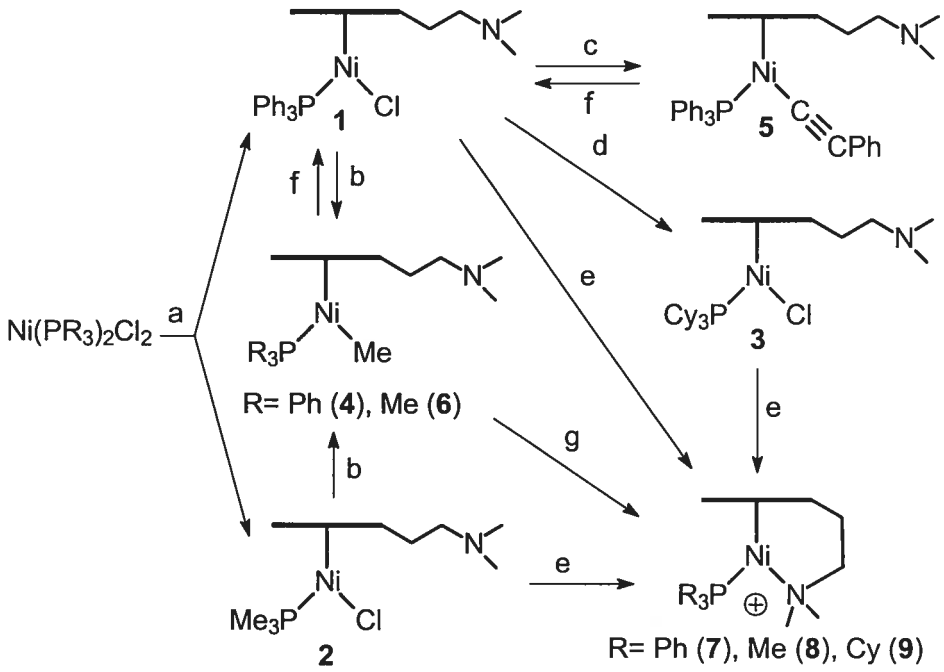

a = LiInd$(CH_2)_2NMe_2$; b = LiMe; c = LiCCPh; d = PCy_3; e = $NaBPh_4$; f = HCl; g = HBF_4

Scheme 6.2

The chloro complexes **1-3** have been used to prepare the new Ni-Me and Ni-CCPh derivatives (η^3:η^0-Ind$(CH_2)_2NMe_2$)Ni(PR_3)R' (R = Ph: R' = Me (**4**) and CCPh (**5**); R = R' = Me (**6**)) and the chelated cations [(η^3:η^1-Ind$(CH_2)_2NMe_2$)Ni(PR_3)]$^+$ (R = Me (**8**) and Cy (**9**)). The main motivation for preparing the neutral, non-chelating derivatives was an earlier observation that seemed to indicate that even when the amine moiety in the pre-catalysts is not chelated, its proximity to the Ni centre seems to have a marked influence over the course of the catalytic reactions and the nature of their products. Thus, the Ni-Me derivatives **4** and **6** were obtained by reacting MeLi with **1** or **2**, respectively, while the Ni-CCPh derivative **5** was prepared in a similar manner by the metathetic reaction between **1** and LiCCPh (Scheme 6.2); recrystallization of the crude products from hexanes gave pure compounds. Reacting compounds **4-6** with HCl gives back the Ni-Cl precursors.

The new complexes **4**, **5**, and **6** were characterized by NMR spectroscopy and their solid state structures were determined by X-ray crystallography.[9] For instance, the $^{31}P\{^1H\}$ NMR spectra showed singlets for the phosphine ligands at 46.9 ppm for **4** (cf. 47.7 ppm for its 1-Me-Ind analogue),[8a] 38.8 ppm for **5** (cf. 40.4 for its 1-Me-Ind analogue),[10] and –4.0 ppm for **6** (cf. –3.7 ppm for its 1-Me-Ind analogue).[11] In addition, the characteristic doublet resonances for the Ni-CH_3 moieties in **4** and **6** were observed at –0.65 ppm (**4**, $^3J_{P\text{-}H}$ = 5.6 Hz) and –0.73 ppm (**6**, $^3J_{P\text{-}H}$ = 6.3 Hz) in the ^1H NMR spectra, and at –18.3 ppm (**4**, $^2J_{P\text{-}C}$ = 24.8 Hz) and –21.7 ppm (**6**, $^2J_{P\text{-}C}$ = 25.2 Hz) in the $^{13}C\{^1H\}$ NMR spectra. As before, the equivalence of the N$(CH_3)_2$ groups confirmed the absence of any Ni-N interactions. On the other hand, the absorption signal for ν(CC) in the IR spectrum of **5** appeared at 2099 cm^{-1}, very close to the corresponding signals in the 1-Me-Ind analogue (2090 cm^{-1})[10] and free phenylacetylene (2110 cm^{-1}), implying little or no Ni-CCPh back-bonding in these complexes. The results of the X-ray diffraction studies will be discussed in the next section.

The cationic complexes **8** and **9** were prepared in analogy to their PPh_3 analogue, **7**,[7b] by reacting the chloro precursors with $NaBPh_4$ or the Ni-Me precursor **6** with HBF_4 (Scheme 1); these new complexes were purified by multiple recrystallizations from Et_2O/CH_2Cl_2 mixtures. The $^{31}P\{^1H\}$ NMR spectra of these compounds displayed one new singlet resonance at ca. –20.8 ppm for **8** and ca. 24.9 ppm for **9**; the absence of AA'

doublet resonances in these spectra indicated that formation of the corresponding bis-phosphine complexes had been circumvented by the chelation of the amine moiety. The N→Ni chelation was also supported by the observed inequivalence of Ind$CH_2CH_2N(CH_3)_2$ signals and confirmed by the solid structure of **9**, which is discussed below.

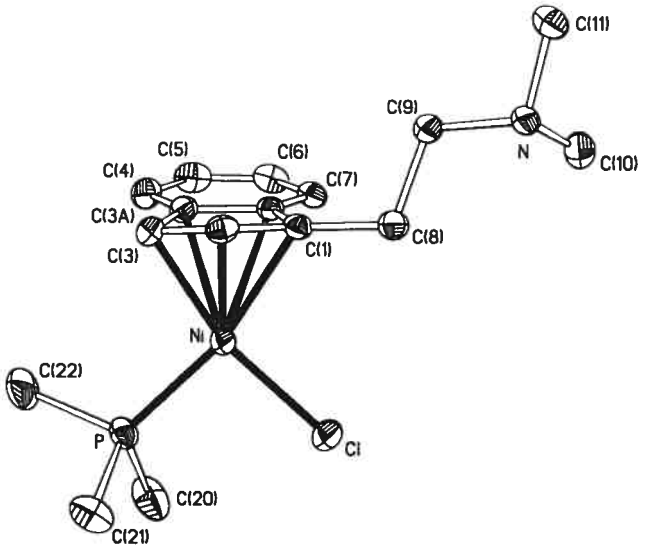

Figure 6.1. ORTEP plot of 2. Hydrogen atoms are omitted for clarity

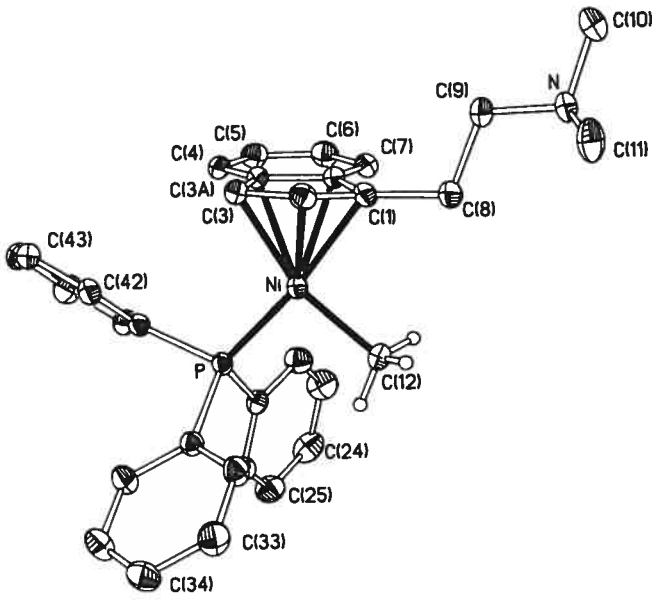

Figure 6.2. ORTEP plot of 4. Hydrogen (except on the Ni-Me) and solvent atoms are omitted for clarity

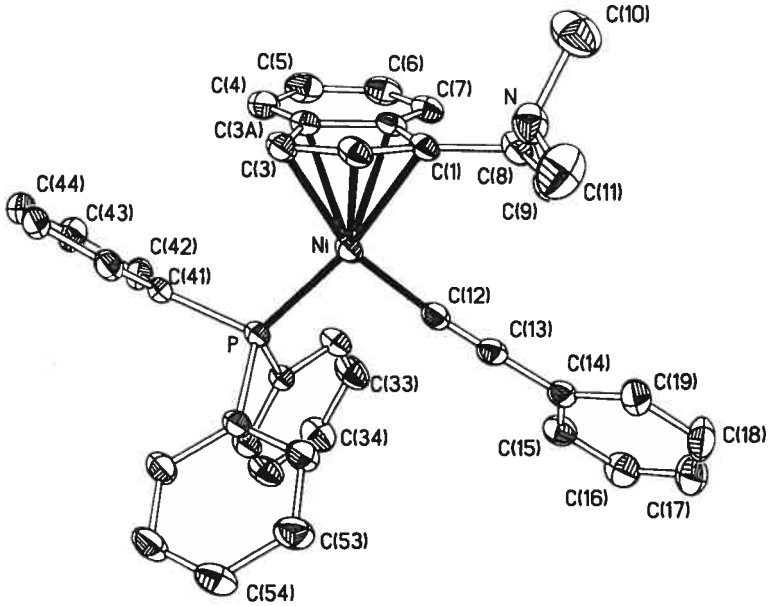

Figure 6.3. ORTEP plot of 5. Hydrogen and solvent atoms are omitted for clarity

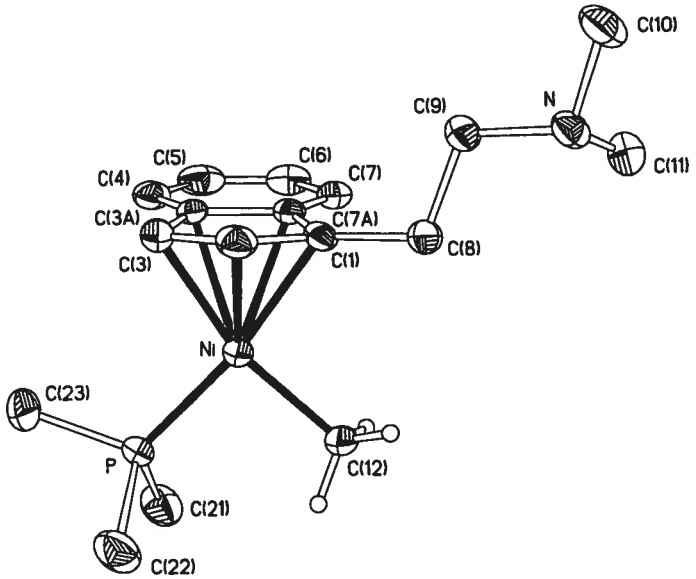

Figure 6.4. ORTEP plot of 6. Hydrogen atoms are omitted for clarity except on the Ni-Me

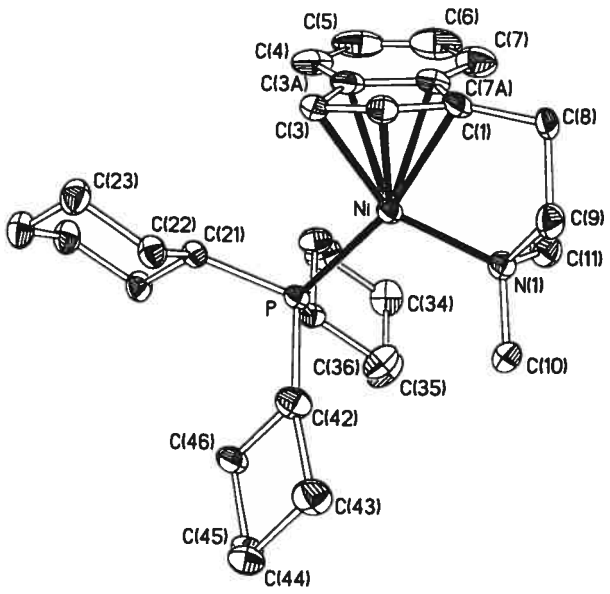

Figure 6.5. ORTEP plot of 9 with the major orientation of the tether. Hydrogen atoms, counterion, other orientation of the tether and disordered CH_2Cl_2 are omitted for clarity

Solid state structures and electrochemical studies. Suitable crystals for X-ray diffraction studies were obtained for **2**, **4**, **5**, **6**, and **9** as described in the Experimental section, and studied at 223 K. The details of data collection and the structure refinement parameters are listed in Table 6.1, while bond distances and angles are reported in Table 6.2. The overall geometry in all of the complexes studied can be described as distorted square planar, with the Ind moiety occupying two coordination sites and the largest distortion arising from the small C1-Ni-C3 angle of ca. 67°.[6] In complexes **2**, **4**, **5** and **6**, no Ni-N interaction is detected: the NMe_2 moiety is pointed away from the Ni, extending along the plane of coordination (as in **2**, **4**, and **6**) or almost perpendicular to it (as in **5**). The different orientation of the amine moiety is likely a result of packing interactions, and we have seen that complex **1** can adopt one or the other structure depending on crystallization conditions.[12]

Table 6.1. Crystal data, data collection and structure refinement parameters

	2	4	5	6	9
Formula	$C_{16}H_{25}NPNiCl$	$C_{32}H_{34}NPNi.$ Hex	$C_{39}H_{36}NPNi.$ THF	$C_{17}H_{28}NPNi$	$C_{55}H_{69}NBPNi.$ CH_2Cl_2
cryst color	dark red	dark red	dark red	dark red	dark red
cryst habit	needle	block	block	needle	Block
cryst dimens, mm	0.78 × 0.13 × 0.07	0.96 × 0.40 × 0.26	0.46 × 0.24 × 0.13	0.84 × 0.08 × 0.08	0.17 × 0.20 × 0.20
symmetry	monoclinic	triclinic	triclinic	triclinic	triclinic
space group	$P\,2_1/n$	P-1	P-1	P-1	P-1
a, Å	6.3037(2)	9.3419(3)	9.998(3)	6.4485(2)	10.9625(1)
b, Å	15.6826(5)	12.8669(5)	13.887(4)	8.5720(3)	13.4241(2)
c, Å	18.2702(6)	13.9322(5)	14.716(5)	16.7049(5)	17.6136(2)
α, deg	90	98.748(3)	111.58(3)	84.18(3)	83.939(1)
β, deg	96.106(2)	103.145(2)	99.68(3)	80.64(3)	87.023(1)
γ, deg	90	106.493(3)	99.55(3)	85.70(3)	78.308(1)
volume, $Å^3$	1795.92(10)	1521.01(10)	1814.2(10)	904.77(5)	2522.84(5)
Z	4	2	2	2	2
D(calcd),g cm^{-1}	1.3185	1.2345	1.2349	1.234	1.224
diffractometer	Bruker AXS SMART 2K	Bruker AXS SMART 2K	Nonius CAD-4	Bruker AXS SMART 2K	Bruker AXS SMART 2K
temp, K	223(2)	223(2)	223(2)	223(2)	223(2)
λ (Cu Kα)	1.54178 Å	1.54178 Å	1.54178 Å	1.54178 Å	1.54178 Å
μ, mm^{-1}	3.677	1.576	1.489	2.290	2.094
scan type	ω scan	ω scan	$\omega/2\theta$ scan	ω scan	ω scan
θ_{max}	72.75°	72.64°	69.93°	72.62°	72.95°
h,k,l range	$-6 \le h \le 7$	$-11 \le h \le 11$	$-12 \le h \le 12$	$-7 \le h \le 7$	$-13 \le h \le 13$
	$-19 \le k \le 19$	$-15 \le k \le 14$	$-16 \le k \le 16$	$-10 \le k \le 10$	$-16 \le k \le 16$
	$-22 \le l \le 22$	$-17 \le l \le 17$	$-17 \le l \le 17$	$-20 \le l \le 20$	$-21 \le l \le 21$
Refl used	2927	5440	4139	3405	7639
Absorption correction	multi-scan SADABS	multi-scan SADABS	Integration ABSORB	multi-scan SADABS	multi-scan SADABS
T (min, max)	0.398, 0.773	0.389, 0.662	0.5977, 0.8501	0.464, 0.833	0.620, 0.700
$R[F^2>2\sigma(F^2)]$, $wR(F^2)$	0.0363, 0.0967	0.0411, 0.1153	0.0428, 0.0948	0.0751, 0.1961	0.0441, 0.1268
GOF	1.003	1.086	1.014	1.005	1.011

Table 6.2. Selected bond distances (Å) and angles (deg) for 2, 4, 5, 6 and 9

	2	4	5	6	9
Ni-P	2.1608(6)	2.1277(5)	2.1573(11)	2.1290(12)	2.2424(5)
Ni-X[a]	2.1868(6)	1.9508(17)	1.852(4)	1.983(4)	2.022(5)
Ni-C1	2.1184(19)	2.0870(17)	2.092(2)	2.100(3)	2.0660(18)
Ni-C2	2.0389(19)	2.0810(17)	2.061(3)	2.090(4)	2.0466(19)
Ni-C3	2.0344(19)	2.1012(16)	2.051(3)	2.081(4)	2.096(2)
Ni-C3A	2.3817(19)	2.2659(15)	2.283(3)	2.285(3)	2.4172(19)
Ni-C7A	2.4035(18)	2.2811(16)	2.280(3)	2.294(3)	2.3932(19)
C1-C2	1.406(3)	1.421(2)	1.413(3)	1.418(5)	1.419(3)
C2-C3	1.419(3)	1.409(2)	1.395(4)	1.420(6)	1.408(3)
C3-C3A	1.468(3)	1.441(2)	1.454(4)	1.445(6)	1.463(3)
C3A-C7A	1.417(3)	1.429(2)	1.428(4)	1.430(5)	1.413(3)
C7A-C1	1.467(2)	1.456(2)	1.445(4)	1.467(5)	1.461(3)
C1-C8	1.495(3)	1.503(2)	1.493(3)	1.516(5)	1.503(5)
Δ(M-C)[b]	0.32	0.18	0.21	0.20	0.32
C1-Ni-X[a]	97.78(5)	94.39(7)	94.02(14)	96.90(15)	82.70(17)
P-Ni-X[a]	95.86(2)	93.23(6)	95.64(12)	93.18(11)	111.11(16)
P-Ni-C3	99.48(6)	107.25(5)	103.60(8)	103.05(12)	100.45(6)
C1-Ni-C3	66.92(8)	66.68(6)	66.88(11)	66.66(15)	66.42(8)
C3-Ni-X[a]	163.78(6)	157.91(8)	160.71(14)	162.69(16)	148.08(18)
P-Ni-C1	166.36(5)	168.83(5)	169.81(8)	169.59(11)	165.24(6)
N-C9-C8	113.42(15)	113.53(14)	115.4(3)	113.0(3)	109.8(4)
C1-C8-C9	110.75(16)	110.89(14)	116.5(2)	111.8(3)	107.4(4)
HA[c]	12.5(2)	8.2(2)	9.6(3)	9.4(2)	12.6(2)
FA[d]	13.2(2)	7.5(2)	9.2(3)	7.3(2)	13.2(2)

[a] X = Cl, C12 or N. [b] Δ(M-C) = {Ni-C_{av} (for C7a and C3a) – Ni-C_{av} (for C1 and C3} [c] HA = angle between C1/C2/C3 plane and C1/C3/C3A/C7A plane. [d] FA = angle between C1/C2/C3 plane and C3A/C4/C5/C6/C7/C7A plane.

The Ni-Ind interaction is fairly symmetrical (Ni-C1 ≈ Ni-C3; Ni-C3a ≈ Ni-C7a) in the Ni-Me complexes **4** and **6**, quite unsymmetrical in **2** (Ni-C1 > Ni-C3), and

somewhat unsymmetrical in **5** (Ni-C1 > Ni-C3 by greater than 13 e.s.d.) and **9** (Ni-C1 < Ni-C3 by about 15 e.s.d.). As described in detail elsewhere,[6] these observations can be attributed to the relative trans influences of the PR_3 and X ligands in the neutral complexes (X = Cl, Me, CCPh, etc.) or the geometrical constraints imposed by the chelation in the cationic species. The Ind hapticity, as measured by the slip parameter Δ(M-C),[13] seems to vary as a function of PR_3 basicity, showing a higher Ind hapticity (i.e., smaller Δ(M-C)) in **1** (0.23 Å)[7a] vs **2** (0.32 Å), **4** (0.18 Å) vs **6** (0.20 Å), and **7** (0.26 Å) vs **9** (0.32 Å). On the other hand, for complexes having the same phosphine ligand, the Ind hapticity increases (i.e., Δ(M-C) decreases) with the stronger basicity of the X ligand, as follows: **1** < **5** < **4**; **2** < **6**.

The Ni-alkynyl bond length in **5** (1.852(4) Å) is much shorter than the Ni-Me distances in **4** (1.9508(17) Å) and **6** (1.983(4) Å), presumably because of the greater sp character of the alkynyl carbon. On the other hand, the Ni-P distances are shortest in the Ni-Me complexes (ca. 2.13 Å) compared to the Ni-Cl and Ni-CCPh complexes (ca. 2.16 Å) or the cationic complex **9** (ca. 2.24 Å). This observation prompted us to compare the Ni-PPh_3 bond lengths as a function of the ligand X in the complexes $IndNi(PPh_3)X$, many of which have been characterized structurally.[6] This comparison confirmed a trend in the Ni-P bond distances that are shorter in the Ni-alkyl derivatives (ca. 2.12 – 2.13 Å), followed by derivatives of other anionic ligands such as chloro, alkynyl, phthalimidato, thienyl, etc. (ca. 2.16 - 2.19 Å),[6] and the cations featuring the chelating amino moieties (ca. 2.20 in **7**[7b] and ca. 2.22 Å in $[\{\eta^3:\eta^1\text{-}IndCH_2(2\text{-pyridine})\}Ni(PPh_3)]^+$).[7d] A similar trend is noted for the Ni-Ind interactions, which are stronger (i.e., the slip parameter Δ(M-C) is smaller) in the Ni-Me derivative **4**, followed by the Ni-Cl derivative **1** and the cationic **7**.

In the search for a relationship between the above noted structural trends and the relative electron richness of these complexes, we undertook electrochemical studies, with the following results. Cyclic voltammetry measurements of complexes **1** – **9** showed that they undergo irreversible reductions at potentials ranging from –1.16 and –2.33 V (vs SCE), as reported in Table 6.3. Inspection of the electrochemical data shows that:

a) As expected, the cationic species are more easily reduced than the neutral complexes.

b) The E_{red} values for the cationic species **8** (-1.22 V) and **7** (–1.16 V) follow the donor ability of the phosphine (PMe_3 > PPh_3), but the reduction potential of the PCy_3 analogue **9** is only slightly more negative (-1.17 V) than that of the PPh_3 analogue; this might be due to the greater steric volume of PCy_3 that results in a very long Ni-P bond and, presumably, a less effective electron donation.

c) The Ni-Me derivatives have more negative reduction potentials than their Ni-Cl counterparts: -2.33 V (**4**) vs –1.41 V (**1**); -2.12 V (**6**) vs –1.27 V (**2**). The E_{red} value for the Ni-CCPh derivative **5** (-1.72 V) is intermediate between those of its chloro and cationic analogues.

Table 6.3. Characterization of complexes 1 – 9

	$^{31}P\{^1H\}$	^1H (ppm)			E_{Red}[a]	E_{Red}
	(ppm)	H2	H3	H4	(V obs.)	(V vs SCE)
1[b]	30.8	6.70	3.42	6.11	-1.70	-1.41
2[b]	-11.0	6.57	3.66	6.59	-1.56	-1.27
3[b]	37.0	6.76	4.17		-1.96	-1.67
4[b]	46.9	6.39	4.22	6.54	-2.62	-2.33
5[c]	38.8	6.45	3.97	6.14	-2.01	-1.72
6[b]	-4.0	6.24	4.47	6.99	-2.41	-2.12
7[c]	29.1	6.78	3.94	5.54	-1.45	-1.16
8[d]	-20.8	6.79	4.29	6.78	-1.51	-1.22
9[d]	24.9	7.15	4.41	6.79	-1.46	-1.17

[a] CH_3CN. [b] C_6D_6. [c] $CDCl_3$. [d] CD_2Cl_2.

Therefore, the electrochemical measurements are in fairly good agreement with the solid state data and signal a correlation between the apparent electron-richness of the Ni centre and its interactions with the phosphine and Ind ligands.[14] On a first approximation, the above observations indicate that the most electron rich Ni centres (i.e., those with the strongly donor alkyl ligands) form the shortest Ni-P bonds and the strongest Ni-Ind interactions, whereas the longest Ni-P bonds and weakest Ni-Ind interactions occur with the least electron rich centres (i.e., the cationic species). This

correlation is evident from a graph of Δ(M-C) values and Ni-P distances against the E_{red} values (Figure 6.6). We have also noted an empirical correlation between the two structural parameters (Ni-P distances and Δ(M-C) values) and the reduction potentials of these complexes, on one hand, and their ^{31}P chemical shifts, on the other (Table 6.3). Thus, the Ni-Me derivatives and the cations show the most downfield and upfield shifts, respectively, whereas the Ni-Cl and Ni-CCPh deriviatves have intermediate shifts, as follows (δ values given in ppm): for PMe_3 complexes, **6** (-4.0) > **2** (-11.0) > **8** (-20.8); for PCy_3 complexes, **3** (37.0) > **9** (24.9); for PPh_3 complexes, **4** (46.9) > **5** (38.8) > **1** (30.8) > **7** (29.1).

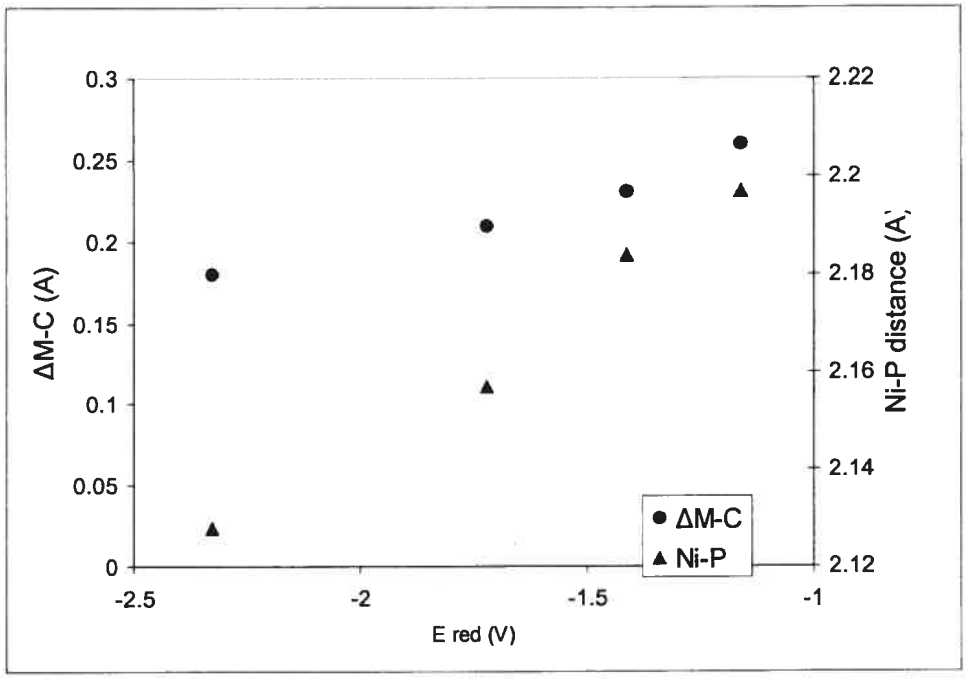

Figure 6.6. Correlation between electrodensity on the Ni and ligand donation

Although the above-noted correlation might appear counter-intuitive at first, they can be explained in terms of the hard-soft acid-base theory (or the E-C model), as proposed by Bergman and co-workers[15] for the analogous Cp^* complexes: when bonded to a soft ligand such as an alkyl group, the Ni centre becomes "softer" and binds more effectively with other soft ligands such as PR_3 and Ind; conversely, when bonded to a hard ligand such as Cl in the neutral compounds or an amine in the cationic species, the

"harder" Ni centre binds less effectively with soft ligands, resulting in weaker Ni-P and Ni-Ind interactions. Whereas this explanation applies fairly well to all of the complexes studied here, alternative explanations involving Ni→ P π-backbonding and Cl→ Ni π-donation account for the observed structural data in case of the PPh_3 and the chloro complexes only. Therefore, the conceptually simpler explanation based on the hard-soft acid-base theory is favored.

Ligand exchange reactions. The hemilabile chelation of the tethered amine in the cationic complexes $[(\eta^3:\eta^1\text{-Ind}\text{^}NR_2)Ni(PR_3)]^+$ is particularly important in view of using these compounds as pre-catalysts. In this sense, the ease with which the N-Ni binding can be displaced by incoming substrates should have a direct bearing on the catalytic activities of these complexes. In our previous studies,[7b,7d] we have measured the degree of Ni-N lability in some of these compounds using ligand exchange reactions. These studies showed that a number of strong ligands (e.g., pyridine, dppe, etc.) can displace the chelating amine moiety; this displacement is generally governed by an equilibrium process of which the K_{eq} depends on the relative nucleophilicities of the incoming ligand and the tethered amine. In addition, the activities of the cations in the polymerization of styrene were found to correlate with the lability of the N→ Ni bond, more labile cases showing higher catalytic activities. (One exception was the complex bearing a pyridine moiety wherein Ni→ N π backbonding gave stronger N→ Ni interaction while displaying higher catalytic activity.)[7d] In the present study, we have performed similar studies in order to evaluate the influence of different phosphines on the lability of the Ni-N bonds and the relative effectiveness of these complexes in catalysis.

Initial tests showed that even relatively weak ligands such as styrene and norbornene displace the chelating NMe_2 moiety in **8** and **9**. In order to compare the Ni-N bonding strength in these and the previously studied complexes, we reacted **8** and **9** with increasing portions of pyridine (py) and monitored the ensuing equilibria by NMR spectroscopy. A new species, $[(\eta^3:\eta^0\text{-Ind}(CH_2)_2NMe_2)Ni(PMe_3)(py)]^+$ (**10**), formed in the equilibrium between py and complex **8**; the K_{eq} was determined to be 41 ± 6, which is larger than the K_{eq} value of 9 ± 1 (at 20°C) found for the reaction of **7** with py. In the cases of complex **9**, only 1 equiv of py was sufficient for completely converting this

complex into $[(\eta^3:\eta^0\text{-Ind}(CH_2)_2NMe_2)Ni(PCy_3)(Py)]^+$ (**11**). On the basis of these observations, the Ni-N binding strength in the cationic compounds follows the order **7** (PPh_3) > **8** (PMe_3) > **9** (PCy_3). Therefore, both the greater steric bulk of PCy_3 and the greater basicity of PMe_3 increase the lability of the Ni-N bond. The next section describes how well the observed order of Ni-N bond lability is reflected in the relative catalytic activities of these complexes.

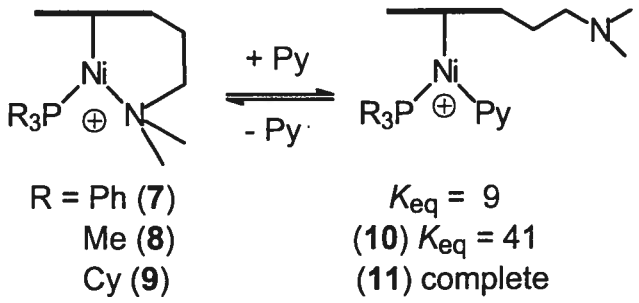

Scheme 6.3

Catalytic polymerization reactions. Previous studies[7b] had indicated that complex **7** is unreactive toward styrene at room temperature, but heating to 80 °C initiated the polymerization reaction; this requirement for heating was attributed to the difficulty of displacing the chelating NMe_2 moiety by styrene. Since **8** and **9** feature more labile Ni-N bonds, we set out to determine if the polymerization of styrene by these pre-catalysts would take place more readily. Indeed, complexes **8** and **9** do polymerize styrene at room temperature, but high levels of catalytic activity and large molecular weights are obtained only at higher temperatures (Table 6.4, runs 3-6). The level of catalytic activity in these reactions seems to be affected mainly by steric effects, the PMe_3 derivative **8** giving the highest activity while the PCy_3 derivative **9** and its PPh_3 analogue **7** displayed comparable activities. On the other hand, the M_w of the polymer appears to correlate with electronic effects: the pre-catalyst **8** featuring the most negative E_{red} value gives polymers with the longest chains, followed by **9** and **7**. That longer polymer chain length and/or higher catalytic activity arise from systems having the better

donating phosphines PCy_3 or PMe_3 suggests that the phosphine ligand remains coordinated to the Ni centre during the polymerization reaction.

We have also examined the reactivities of complexes **7**, **8**, and **9** with phenylacetylene for the following reason. Previous studies[10,16] have shown that combining the precursors (1-Me-indenyl)Ni(PR_3)X (R = Ph or Cy, X = Cl, Me, CCPh, thienyl) with methylaluminoxane (MAO) forms catalytically active species that polymerize phenylacetylene to *cis,transoidal*-poly(phenylacetylene) (PPA); this material is of interest for applications requiring nonlinear optical and magnetic susceptibilities, photoconductivity, and gas permeability.[17] Although the interaction of MAO with these precursors gives rise to cationic species, the role of the latter in the polymerization reaction has not been established with certainty. In an earlier attempt to address this issue, we studied the reaction of phenylacetylene with (1-*i*-Pr-indenyl)(PPh_3)Ni(OTf) (OTf = OSO_2CF_3), a compound that can generate the unsaturated cations by the in situ displacement of the triflate anion.[18] This reaction gave poor yields of a polymeric material possessing lower solubility and diminished M_w compared to the samples obtained from the MAO co-catalyzed reactions; these results did not allow an unambiguous conclusion on the role of the cationic species in the formation of PPA. Access to the cationic complexes **7**, **8**, and **9** provided a good opportunity to further probe this question, as described below.

As shown in Table 6.4, the cationic complexes do not promote the polymerization of phenylacetylene (run 7). Given the earlier discussed lability of the Ni-N bond in complexes **8** and **9**, it is reasonable to presume that excess phenylacetylene should compete effectively with the chelating NMe_2 moiety for coordination to the Ni centre; therefore, what hinders the polymerization in the absence of MAO is not the monomer's access to the Ni centre. A more likely reason is that unlike the polymerization of styrene, which can proceed by an electrophilic pathway, the polymerization of phenylacetylene proceeds by an insertion mechanism requiring a Ni-R moiety for initiation; thus, the cationic Ni centre must be converted into a neutral derivative possessing a moiety that can facilitate the initiation step. To test whether MAO could activate the cationic complexes, we carried out the polymerization of phenylacetylene in the presence of MAO (ca. 1:10 ratio of Ni: Al); these reactions gave PPA having similar properties as the

samples obtained from previous MAO co-catalyzed reactions (Table 6.4, runs 8-10). The M_w of the polymers obtained from these reactions are comparable to the values obtained with previously studied systems not bearing tethered amine moieties on the Ind ligand, but the activities of the present systems are inferior.

Table 6.4. Polymerization experiments

	Cat.	Monomer	equiv.	T (°C)	Time (d.)	M_w (10^{-3})	PDI	TON[c]
1	**7**	Styrene	2000	20	7			0
2	**7**[a]	Styrene	2000	80	2	77.3	3.2	364
3	**8**	Styrene	2000	20	2	38.1	2.9	23
4	**8**	Styrene	2000	80	2	243.4	4.0	630
5	**9**	Styrene	2000	20	2	11.6	1.8	57
6	**9**	Styrene	2000	80	2	147.9	4.2	350
7	**7, 8, or 9**	PhCCH	100	20	1	No reaction		
8	**7**/MAO[b]	PhCCH	100	20	1	34.5	3.2	<10
9	**8**/MAO[b]	PhCCH	100	20	1	57.7	1.8	<10
10	**9**/MAO[b]	PhCCH	100	20	1	41.5	1.8	<10
11	**5**/MAO[b]	PhCCH	100	20	1	3.4	1.5	<10

[a] see ref. 7b. [b] [Al]/[Ni] = 10. [c] based on isolated yield.

In an attempt to gain insight on how MAO activates the cationic complexes, we monitored the NMR spectra of a mixture consisting of **7** (ca 0.015M in CD_2Cl_2) and 10 equiv each of MAO and phenylacetylene. The $^{31}P\{^1H\}$ NMR spectrum showed the conversion of **7** to the analogous Ni-Me and Ni-CCPh derivatives, as evidenced by the singlet resonances at 45.5 and 39.9 ppm, respectively; evidently, MAO can bring about the formation of the requisite Ni-R moieties. We were intrigued to find, however, that polymerization reactions using combinations of MAO and independently prepared (as opposed to in situ formed) samples of the Ni-Me and Ni-CCPh derivatives **4** and **5**, respectively, yielded PPA samples with much lower M_w values (e.g., see run 11 for the reaction of **5** + MAO). Since the combination of MAO and the analogous neutral Ni-R

derivatives (R = Me or CCPh) bearing nonfunctionalized Ind ligands polymerize phenylacetylene,[10,18] it is clear that the amine moiety has a detrimental effect on these reactions.

We conclude, therefore, that the cationic species cannot polymerize phenylacetylene in the absence of activators. MAO can activate these precursors for the polymerization, but it is not clear whether the Ni-Me and Ni-CCPh species detected in the MAO reaction mixtures are active species or end-products of the reaction. Thus, the precise role of MAO in these reactions remains unknown.

Olefin hydrosilylation reactions. The complexes $Ind(PR_3)Ni(X)$, either used directly (X = alkyl) or generated in situ (X = H or positive charge), are known to catalyze the dehydrogenative oligomerization of $PhSiH_3$[11,19] and the hydrosilylation of olefins and ketones.[20] We have studied the influence of the tethered amine moiety on the course of these reactions, beginning with the reactivity of complexes **4-6** in the oligomerization of $PhSiH_3$. Thus, addition of neat $PhSiH_3$ (200 equiv) to solid samples of **4-6** caused an immediate evolution of gas (presumably H_2); ^1H NMR spectra of aliquots taken at various intervals showed the gradual conversion of the monomer to cyclic and linear $(PhSiH)_n$.[21] The viscous oil produced after 3 days was analyzed by NMR and GPC and found to consist primarily of cyclic and linear oligomers in ca. 3 : 1 ratio for **5** and 1 : 3 ratio for **4** and **6**. Qualitatively, the oligomers obtained from reactions promoted by complexes **4-6** and their nonfunctionalized counterparts are quite similar,[11] but the present pre-catalysts give higher conversions (monomer conversion was >90-95%).

Next, we examined the effectiveness of complexes **7-9** in the hydrosilylation of styrene and 1-hexene; most of the experiments were carried out at room temperature and on NMR scale in CD_2Cl_2 using 100 equiv each of olefin and silane (Table 6.5). Analysis of the reaction products[22] obtained from the hydrosilylation of styrene with $PhSiH_3$ confirmed the exclusive formation of $Ph(PhSiH_2)CHCH_3$ with a conversion of 45% (**9**), 70% (**7**), and 100% (**8**) (Table 6.5, runs 1-3); no evidence was found for the formation of poly(styrene) or $(PhSiH)_n$. The reaction of complex **8** was repeated on a larger scale and found to give a very good catalytic turnover number (run 4). Replacing $PhSiH_3$ by Ph_2SiH_2 gave the α-addition isomer $Ph(Ph_2SiH)CHCH_3$ as the major product (70%) plus

a small quantity (<10%) of the β-addition isomer $Ph(CH_2)_2SiHPh_2$ (run 5). Finally, reaction of 1-hexene with $PhSiH_3$ in the presence of **8** led to the formation of 1-($PhSiH_2$)hexane with only 20% conversion (run 6).

The above results demonstrate that the cationic complexes **7-9** can act as single-component pre-catalysts for the hydrosilylation reaction. It is noteworthy that the presence of hydrosilanes in the reaction mixture inhibits the polymerization of styrene, while the presence of styrene inhibits or minimizes the dehydrogenative oligomerization of $PhSiH_3$. That the most active pre-catalyst is the one bearing the most strongly donor phosphine ligand (PMe_3) suggests that the hydrosilylation reaction does not involve phosphine dissociation; by inference, we believe that the catalysis involves the dissociation of the chelating amine moiety. Although the mechanistic details of this reaction are not known with certainty, a number of observations from previous studies[20] have pointed to the following sequence of steps: a) the transfer of a hydride from the hydrosilane to the cationic Ni center forms a Ni-H intermediate; b) insertion of the olefin gives a Ni-alkyl species; c) a concerted, σ-bond metathesis reaction between the hydrosilane and the alkyl intermediate releases the hydrosilylation product and regenerates the Ni-H species. Precedent for the last step has been observed in our studies on the oligomerization of silanes.[11] In an attempt to extract mechanistic clues for the first two steps, we monitored near-stoicheometric reactions by NMR, with the following results.

No reaction took place between complex **8** (ca. 0.02 M in CD_2Cl_2) and styrene (5 equiv) over 2.5 h at room temperature, but addition of $PhSiH_3$ (5 equiv) to this sample resulted in the partial conversion of **8** to a new species displaying a $^{31}P\{^1H\}$ NMR signal at 32.7 ppm. Over time, two additional $^{31}P\{^1H\}$ NMR signals appeared (–5.8 and –8.3 ppm), but the starting material (ca. –20 ppm) was still the major P-containing species even after 24 h. The ^1H NMR spectrum contained the characteristic signals of the reaction product $Ph(PhSiH_2)CHCH_3$, but the putative Ni-H species was not detected. In a similar experiment, $PhSiH_3$ was added to **8** first and the sample was studied by $^{31}P\{^1H\}$ NMR; in this case, three other signals emerged over a few hours (43.9, -2.8, and -8.1 ppm) in addition to the one at 32.7 ppm that had been observed in the previous experiment. Addition of styrene to this sample caused the immediate disappearance of the signals at

43.9, –2.8, and –8.1 ppm, and gave rise to the same signals as in the previous experiment (32.7, -5.8 and -8.3 ppm) along with the signal for **8**. The ^{1}H NMR spectrum showed the formation of $Ph(PhSiH_2)CHCH_3$ as soon as the styrene was added.

Table 6.5. Hydrosilylation of olefins[a]

	Cat.	Olefin (equiv)	Silane (equiv)	Product (conversion, %)
1	7	Styrene (100)	$PhSiH_3$ (100)	$Ph(PhSiH_2)CHCH_3$ (70)
2	8	Styrene (100)	$PhSiH_3$ (100)	$Ph(PhSiH_2)CHCH_3$ (100)
3	9	Styrene (100)	$PhSiH_3$ (100)	$Ph(PhSiH_2)CHCH_3$ (45)
4	8	Styrene (1000)	$PhSiH_3$ (1000)	$Ph(PhSiH_2)CHCH_3$ (93)
5	8	Styrene (100)	Ph_2SiH_2 (100)	$Ph(Ph_2SiH)CHCH_3$ (70)
				$PhCH_2CH_2SiHPh_2$ (10)
6	8	1-Hexene (100)	$PhSiH_3$ (100)	1-$(PhSiH_2)$hexane (20)

[a] CD_2Cl_2, room temperature, 24 h.

The above results confirm that the first step in the hydrosilylation reaction takes place between the precursor and $PhSiH_3$, and generates at least 4 P-containing intermediate species. We believe that one of these intermediates is a Ni-H species formed via the transfer of H^- from $PhSiH_3$;[23] unfortunately, however, we were unable to detect the Ni-*H* signal in the ^{1}H NMR spectrum. This might be due to the weak intensity of this signal as a result of coupling to the P nucleus. To gain some indirect support for the conversion of complex **8** to a Ni-H species, we repeated the hydrosilylation reactions in $CDCl_3$; given the propensity of many metal hydrides to react with chloroform, we reasoned that the course of the hydrosilylation reaction should be affected in this medium. Indeed, these reaction mixtures turned dark blue immediately and the $^{31}P\{^1H\}$ NMR spectrum revealed two new signals at 40.7 and 38.9 ppm, but no trace of the hydrosilylation product was detected in the ^{1}H NMR spectrum. This observation is consistent with the postulated formation of Ni-H, though it does not validate it.

The postulated Ni-H intermediate would presumably promote the formation of Si-Si bonds in the absence of styrene, but insertion of styrene should form a Ni-alkyl species and drive the reaction toward hydrosilylation. Such Ni-alkyl intermediates should exhibit

a $^{31}P\{^{1}H\}$ NMR signal close to the corresponding signal for the Ni-Me complex **6** (–4.0 ppm); thus, of the $^{31}P\{^{1}H\}$ NMR signals detected at the end of the hydrosilylation reactions, those appearing at ca. –6 and –8 ppm might be due to the Ni-alkyl species.

To sum up, the cationic complexes **7-9** can catalyze the addition of $PhSiH_3$ to styrene and 1-hexene, our results indicate that the Si-H bond activation occurs first, followed by reaction with the olefin. The ^{31}P signals detected in the reaction mixtures are consistent with the presence of Ni-alkyl intermediates, but the postulated Ni-H signal has not been detected.

Conclusion

The results of the present study on the chemistry of the complexes $[(\eta^3:\eta^1\text{-}IndCH_2CH_2NMe_2)Ni(PR_3)]^+$ demonstrate the influence of phosphine ligands on the hemilabile nature of the Ni-N bond and the reactivities of these complexes. Although the lability of the N→ Ni binding, as measured by how easily the chelating amine moiety is displaced by pyridine, increases in the order $PPh_3 < PMe_3 < PCy_3$, the enhanced lability is not translated into superior catalytic activities in all cases. For instance, the significant steric bulk of the PCy_3 ligand seems to attenuate the impact of the hemilabile Ni-N moiety; as a result, the more labile Ni-N bond in the PCy_3 derivative does not confer a significant reactivity advantage to this complex relative to the PPh_3 derivative. On the other hand, the increased lability of the Ni-N bond is reflected in the superior catalytic activities of the complex bearing the strongly donor and relatively nonbulky phosphine PMe_3. Therefore, the more strongly donating PR_3 ligands result in better activities because they render the chelating amine moiety more labile, but the steric factors also exert an important influence. The results of the present study nicely complement those of our previous studies on the importance of the amine moiety for catalytic activities; the lessons learnt from these studies should lead to the development of highly active precatalysts bearing hemilabile amine moieties.

Experimental

General Comments. All manipulations were performed under an inert atmosphere of N_2 using standard schlenk techniques and a drybox. Dry, oxygen-free solvents were

employed throughout. Preparation of (η^3:η^0-Ind$(CH_2)_2NMe_2$)Ni(PPh_3)Cl (**1**),[7a] [(η^3-η^1-Ind$(CH_2)_2NMe_2$)Ni(PPh_3)][BPh_4] (**7**)[7a] and $(PMe_3)_2NiCl_2$[8b] have been reported previously. LiCCPh has been prepared by deprotonation of HCCPh with BuLi in hexanes. All other reagents used in the experiments were obtained from commercial sources and used as received. The elemental analyses were performed by the Laboratoire d'Analyse Élémentaire (Université de Montréal). The spectrometers used for recording the NMR spectra are: Bruker AMXR400 (^{1}H (400 MHz), $^{13}C\{^1H\}$ (100.56 MHz), and $^{31}P\{^1H\}$ (161.92 MHz)), and Bruker AV300 (^{1}H (300 MHz), and $^{31}P\{^1H\}$ (121.49 MHz)).

(η^3:η^0-Ind$(CH_2)_2NMe_2$)Ni(PMe_3)Cl (2). A THF solution of Ind$(CH_2)NMe_2$ (700 mg, 3.93 mmol) and BuLi (1.6 mL of a 2.5M solution in hexane) was stirred for 3 h and then transferred (dropwise over 2 h) to a stirred solution of $Ni(PMe_3)_2Cl_2$ (1.1 g, 3.93 mmol) in 30 mL of THF at 50 °C. The resulting solution is evaporated and extracted with 90 mL of hot Et_2O. The Et_2O solution is reduced to 40 mL and cooled (-20 °C). Dark red powder (365 mg, 26% yield) precipitated as pure **2**. Recrystallization from hot hexane/Et_2O gave crystals suitable for X-ray diffraction analysis. $^{31}P\{^1H\}$ NMR (C_6D_6): -11.01 ppm. ^{1}H NMR (C_6D_6): 7.11 (d, $^3J_{H\text{-}H}$ = 7.7 Hz, H7), 6.99 (t, $^3J_{H\text{-}H}$ = 7.3 Hz, H5 or H6), 6.91 (t, $^3J_{H\text{-}H}$ = 7.3 Hz, H5 or H6), 6.59 (d, $^3J_{H\text{-}H}$ = 7.3 Hz, H4), 6.57 (H2), 3.66 (H3), 2.80 and 2.65 (m, IndCH_2), 2.38 and 2.29 (CH_2N), 2.17 (NCH_3), 0.74 (d, $^3J_{H\text{-}P}$ = 9.4 Hz, PCH_3). $^{13}C\{^1H\}$ NMR (C_6D_6): 130.0 (C7A), 126.5 (C3A), 125.8 (C4), 125.6 (C5), 118.4 (C6) 116.1 (C7), 104.4 (C1), 102.8 (C2), 59.8 (C3), 57.3 (CH_2N), 45.6 (NCH_3), 24.7 (Ind-CH_2), 14.7 (d, $^2J_{C\text{-}P}$ = 29.1 Hz, PCH_3). Anal. Calcd for $C_{16}H_{25}NPNiCl$: C, 53.91; H, 7.07; N, 3.93. Found: C, 53.73; H, 7.24; N, 3.77.

(η^3:η^0-Ind$(CH_2)_2NMe_2$)Ni(PCy_3)Cl (3). Complex **1** (500 mg, 0.92 mmol) and PCy_3 (390 mg, 1.38 mmol) were mixed together in 80 mL of Et_2O and stirred for 3 h. The solution was then concentrated to 40 mL and cooled to -20 °C. After 24 h, a dark red solid precipitated as pure **3** (480 mg, 93% yield). $^{31}P\{^1H\}$ NMR (C_6D_6): 37.02 ppm. ^{1}H NMR (C_6D_6): 7.06 (m, H7/H6), 6.90 (m, H5/H6), 6.76 (H2), 4.17 (H3), 2.87 and 2.67 (m, IndCH_2), 2.33 (CH_2N), 2.21 (NCH_3), 1.95 to 1.09 (m, PCy_3). $^{13}C\{^1H\}$ NMR (C_6D_6):

130.2 (C7A), 128.9 (C3A), 126.3 and 125.4 (C4/C5), 118.6 (C6/C7), 103.5 (C2), 102.7 (C1), 59.0 (CH_2N), 57.4 (C3), 45.7 (NCH_3), 35.2 (d, $^1J_{P-C}$ = 19.4 Hz, *i*-C), 30.1 (d, $^2J_{P-C}$ = 6.2 Hz, *o*-C), 27.9 and 27.8 (d, $^3J_{P-C}$ = 4.5 Hz, *m*-C), 26.7 (s, *p*-C), 24.8 (ind-CH_2). Anal. Calcd for $C_{31}H_{49}NPNiCl.H_2O$: C, 64.32; H, 8.88; N, 2.42. Found: C, 64.24; H, 9.13; N, 2.07.

(η^3:η^0-Ind(CH_2)$_2$$NMe_2$)Ni($PPh_3$)Me (4). A solution of MeLi (0.374 mL of a 1.5 M solution in hexane) was added dropwise to a solution of **1** (203 mg, 0.374 mmol in 60 mL of Et_2O) and stirred for 1 h. The mixture was then filtered and evaporated to dryness. Recrystallization from hot hexane gave pure product (80 mg, 41% yield) as dark red crystals suitable for X-ray diffraction analysis. $^{31}P\{^1H\}$ NMR (C_6D_6): 46.9 ppm. ^1H NMR (C_6D_6): 7.7 to 7.0 (PPh_3, H5/H6/H7), 6.54 (d, $^3J_{H-H}$ = 7.7 Hz, H4), 6.39 (H2), 4.22 (H3), 2.8 to 2.5 (m, CH_2N and IndCH_2), 2.19 (NCH_3), -0.65 (d, $^3J_{H-P}$ = 5.6 Hz, Ni-CH_3). $^{13}C\{^1H\}$ NMR ($CDCl_3$): 134.2 (*i*-C of PPh_3), 133.7 (d, $^2J_{P-C}$ = 19.0 Hz, *o*-C of PPh_3), 129.7 (*p*-C of PPh_3), 128.5, 127.9 (d, $^3J_{P-C}$ = 14.5 Hz, *m*-C of PPh_3), 122.0 (C5/C6), 119.9 and 119.6 (C3A/C7A), 116.7 and 115.7 (C4/C7), 100.4 (C2), 91.1 (C1), 75.3 (C3), 59.1 (CH_2N), 45.7 (NCH_3), 24.0 (Ind-CH_2), -18.3 (d, $^2J_{C-P}$ = 24.8 Hz, Ni-Me). Anal. Calcd for $C_{32}H_{34}NPNi$: C, 73.59; H, 6.56; N, 2.28. Found: C, 73.62; H, 6.83; N, 2.67.

Reaction of 4 with HBF_4. $HBF_4.OEt_2$ (7 μL, 0.057 mmol) was added to a solution of **4** (27.8 mg, 0.053 mmol) in $CDCl_3$ (ca. 0.8 mL). The solution was then transferred to an NMR tube, shaken to ensure complete mixing, and the NMR spectra recorded 10 min later. The $^{31}P\{^1H\}$ and ^1H NMR spectra showed characteristic signals of **7**. Addition of more $HBF_4.OEt_2$ (14 μL, 0.114 mmol) provoked the decomposition of the product.

Reaction of 4 with HCl. HCl (17 μL of a 2M solution in Et_2O, 0.8 equiv) was added to a solution of **4** (22.7 mg, 0.043 mmol) in $CDCl_3$ (ca. 0.8 mL). The solution was then transferred to an NMR tube, shaken to ensure complete mixing, and the NMR spectra recorded 10 min later. The $^{31}P\{^1H\}$ and ^1H NMR spectra showed ca. 70% conversion of **4** into **1**.

(η^3:η^0-Ind(CH_2)$_2$NMe2)Ni(PPh_3)CCPh (5). A solution of LiCCPh (67 mg, 0.62 mmol in 15 mL of benzene) was added dropwise to a solution of **1** (270 mg, 0.50 mmol) in benzene (15 mL), and stirred for 2 h. The mixture was then concentrated to ca. 3 mL, hexanes (ca. 25 mL) added, and cooled to -20 °C to give a dark red solid. Repeated recrystallization gave pure product (152 mg, 50 % yield). $^{31}P\{^1H\}$ NMR ($CDCl_3$): 38.8 ppm. ^1H NMR (C_6D_6): 7.7 to 7.0 (PPh_3, CCPh, H6 and H7), 6.82 (H5), 6.45 (H2), 6.14 (H4), 3.97 (H3), 3.13 and 2.91 (CH_2N), 2.91 (IndCH_2), 2.25 (NCH_3). $^{13}C\{^1H\}$ NMR ($CDCl_3$): 134.1 (d, $^2J_{P\text{-}C}$ = 10.4 Hz, *o*-C of PPh_3), 133.2 (d, $^1J_{P\text{-}C}$ = 45.8 Hz, *i*-C of PPh_3), 132.2, 131.1 (CCPh, *o*-C), 130.1 (*p*-C of PPh_3), 128.8, 128.5, 128.1 (d, $^3J_{P\text{-}C}$ = 9.7 Hz, *m*-C of PPh_3), 127.4 (CCPh, *m*-C), 125.0 and 124.5 (C5/C6/CCPh, *p*-C), 123.0, 121.3, 117.9 and 116.7 (C4/C7), 101.8 (C2), 100.1, 99.0, 74.6 (C3), 58.4 (CH_2N), 45.7 (NCH_3), 25.6 (Ind-CH_2). IR (KBr, cm^{-1}) : 3050, 2924, 2099 (CC), 1591, 1477, 1431, 1383, 1095, 814, 745, 692, 530. Anal. Calcd for $C_{39}H_{36}NPNi.H_2O$: C, 74.78; H, 6.12; N, 2.24. Found: C, 74.66; H, 6.23; N, 2.25.

(η^3:η^0-Ind(CH_2)$_2$$NMe_2$)Ni($PMe_3$)Me (6). MeLi (0.7 mL of a 2M solution in Et_2O, 1.32 mmol) was added slowly to a solution of **2** (314 mg, 0.88 mmol) in Et_2O (40 mL) and stirred for 45 min. Desoxygenated water (0.7 mL) was then added, and the mixture was stirred for 10 min, filtered, dried ($MgSO_4$), and evaporated to give crude **6** as a sticky solid. Compound **6** is quite unstable in solution, decomposing to form a black insoluble powder; this prevented us from obtaining analytically pure samples. However, a small batch of crystals suitable for X-ray analysis was obtained after multiple recrystallizations from hexane solutions. $^{31}P\{^1H\}$ NMR (C_6D_6): -3.99 ppm. ^1H NMR (C_6D_6): 7.23 (d, $^3J_{H\text{-}H}$ = 7.8 Hz, H7), 7.07 (m, H5 or H6), 7.01 (m, H5 or H6), 6.99 (H4), 6.24 (H2), 4.47 (H3), 2.75 (m, IndCH_2), 2.61 (CH_2N), 2.19 (NCH_3), 0.64 (d, $^3J_{H\text{-}P}$ = 9.0 Hz, PCH_3), -0.73 (d, $^3J_{H\text{-}P}$ = 6.3 Hz, Ni-CH_3). $^{13}C\{^1H\}$ NMR (C_6D_6): 126.7 (C7A), 122.0 (C4/C5), 120.9 (C3A), 116.4 and 116.2 (C6/C7), 100.0 (C2), 91.4 (C1), 70.1 (C3), 59.5 (CH_2N), 45.8 (NCH_3), 24.9 (Ind-CH_2), 16.1 (d, $^2J_{C\text{-}P}$ = 44.5 Hz, PCH_3), -21.7 (d, $^2J_{C\text{-}P}$ = 25.2 Hz, Ni-Me). Anal. Calcd for $C_{17}H_{28}NPNi$: C, 60.76; H, 8.40; N, 4.17. Found: C, 55.67; H, 8.44; N, 3.88.

Reaction of 6 with HBF_4. $HBF_4.OEt_2$ (7 μL, 0.057 mmol) was added to a solution of **6** (20 mg, 0.060 mmol) in $CDCl_3$ (ca. 0.8 mL). The solution was then transferred to an NMR tube, shaken to ensure complete mixing, and the NMR spectra recorded 10 min later. The $^{31}P\{^1H\}$ and ^1H NMR spectra showed characteristic signals of **8**. Addition of more $HBF_4.OEt_2$ (14 μL, 0.114 mmol) provoked the decomposition of the product.

[(η^3:η^1-Ind$(CH_2)_2NMe_2$)Ni(PMe_3)][BPh_4] (8). A CH_2Cl_2 mixture of **2** (228 mg, 0.64 mmol) and $NaBPh_4$ (1.095 g, 3.2 mmol) was stirred at room temperature for 4 h and filtered. The orange filtrate was concentrated to ca. 1 mL and hexanes (40 mL) added to precipitate an orange-red solid, which was filtered, redissolved in ca. 1 mL of CH_2Cl_2, and precipitated by adding Et_2O (40 mL). Filtration and washing with Et_2O gave pure **8** (282 mg, 69% yield). $^{31}P\{^1H\}$ NMR (CD_2Cl_2): -20.77 ppm. ^1H NMR (CD_2Cl_2): 7.42 (d, $^3J_{H\text{-}H}$ = 7.2 Hz, H5), 7.34 (*o*-H, BPh_4), 7.24 (m, H6 and H7), 7.04 (m, *m*-H, BPh_4), 6.89 (m, *p*-H, BPh_4), 6.79 (s, H2), 6.78 (d, $^3J_{H\text{-}H}$ = 8.5 Hz, H4), 4.29 (m, H3), 3.19 and 2.80 (m, IndCH_2), 2.32 and 2.05 (s, NCH_3), 2.19 and 1.94 (m, CH_2N), 1.12 (d, $^3J_{H\text{-}P}$ = 8.8 Hz, PCH_3). $^{13}C\{^1H\}$ NMR (CD_2Cl_2) : 164,0 (4-line multiplet, $J_{B\text{-}C}$ = 49.2 Hz, *i*-C, BPh_4), 136.0 (*m*-C, BPh_4), 129.2 and 127.5 (C5 and C6), 126.0 and 124.8 (C3A and C7A), 125.7 (*o*-C, BPh_4), 121.8 (*p*-C, BPh_4), 117.9 (C4 and C7), 107.5 C2), 107.1 (d, $^2J_{C\text{-}P}$ = 8.3 Hz, C1), 75.2 (d, $^3J_{C\text{-}P}$ = 4.1 Hz, CH_2N), 65.4 (C3), 52.8 and 50.3 (NCH_3), 24.5 (Ind-CH_2), 14.7 (d, $^2J_{C\text{-}P}$ = 28.4 Hz, PCH_3). Anal. Calcd for $C_{40}H_{45}NPNiB.H_2O$: C, 72.98; H, 6.90; N, 2.13. Found: C, 72.93; H, 7.10; N, 2.14.

[(η^3:η^1-Ind$(CH_2)_2NMe_2$)Ni(PCy_3)][BPh_4] (9). The mixture of **3** (400 mg, 0.71 mmol) and $NaBPh_4$ (1.20 g, 3.57 mmol) in CH_2Cl_2 was stirred at room temperature for 4 h and then filtered. The red filtrate was concentrated to 1 mL and Et_2O (40 mL) added to precipitate a red solid, which was filtered and redissolved in ca. 1 mL of CH_2Cl_2 and precipitated by adding Et_2O (ca. 40 mL). Filtration and washing with Et_2O gave pure **9** (395 mg, 66% yield). Crystals suitable for X-ray analysis were obtained from a cold solution of **9** in CH_2Cl_2 / Et_2O. $^{31}P\{^1H\}$ NMR (CD_2Cl_2): 24.88 ppm. ^1H NMR (CD_2Cl_2): 7.39 (d, $^3J_{H\text{-}H}$ = 7.3 Hz, H5), 7.30 (*o*-H, BPh_4), 7.21-7.10 (m, H6, H7 and H2), 7.01 (m, *m*-H, BPh_4), 6.87 (m, *p*-H, BPh_4), 6.79 (d, $^3J_{H\text{-}H}$ = 7.5 Hz, H4), 4.41 (m, H3), 3.10 and

2.80 (m, IndCH_2), 2.22 and 2.13 (s, NCH_3), 2.1-1.1 (m, CH_2N and PCy_3). $^{13}C\{^1H\}$ NMR (CD_2Cl_2) : 164,0 (4-line multiplet, J_{B-C} = 49.5 Hz, *i*-C, BPh_4), 135.9 (*m*-C, BPh_4), 131.8 and 130.6 (C3A and C7A), 128.8 and 128.3 (C5 and C6), 125.6 (*o*-C, BPh_4), 121.8 (*p*-C, BPh_4), 119.3 and 118.2 (C4 and C7), 107.8 C2), 106.0 (d, $^2J_{C-P}$ = 8.3 Hz, C1), 75.5 (s, CH_2N), 65.4 (C3), 52.0 (NCH_3), 34.9 (d, $^1J_{P-C}$= 18.8 Hz, *i*-C), 30.4 and 29.8 (s , *o*-C), 27.6 (m, *m*-C), 26.2 (s, *p*-C), 23.0 (Ind-CH_2). Anal. Calcd for $C_{55}H_{69}NPNiB.CH_2Cl_2$: C, 72.36; H, 7.70; N, 1.51. Found: C, 72.05; H, 7.81; N, 1.55.

Polymerization of styrene. 8 (13.5 mg, 0.021 mmol) or **9** (15.5 mg, 0.018 mmol) and styrene (2000 equiv) were stirred at room temperature (Table 6.4, runs 3 and 5) or at 80 °C (runs 4 and 6) for 2 days in dichloroethane (6 mL). Removal of the solvent and unreacted styrene gave a white solid (run 3: 70 mg, 23 turnovers; run 4: 1.39 g, 630 turnovers; run 5: 128 mg, 57 turnovers; run 6: 670 mg, 350 turnovers), which was isolated and analyzed by GPC (THF). ^1H NMR ($CDCl_3$): 7.07 (br), 6.59 (br), 1.87 (br), 1.45 (br). $^{13}C\{^1H\}$ ($CDCl_3$): 145.4 (*ipso*-C), 128.0 (*o*- and *m*-C), 125.9 (*p*-C), 44.1 and 40.8 (alkyl chain).

Polymerization of Phenylacetylene. To a solution of the Ni pre-catalyst (ca. 0.0364 mmol) in 2 mL of THF was added phenylactylene (0.40 mL, 3.64 mmol, 100 equiv) and MAO (0.24 mL of a 10% ww solution in toluene, 10 equiv with respect to Ni) and stirred for 24 h at room temperature and under nitrogen. (No reaction is observed in the absence of MAO.) The reaction was quenched by adding a solution of ethanol/acetic acid; the resulting yellow precipitate (PPA, 5-10% yield) was filtered, washed with hexane, dried in vacuo, and analyzed by GPC (THF). ^1H NMR ($CDCl_3$): 6.94 (m, *m*- and *p*-H), 6.62 (d, $^3J_{H-H}$ = 6.8 Hz, *o*-H), 5.84 (s, vinylic H).

Dehydropolymerization of $PhSiH_3$. Addition of $PhSiH_3$ (2.0 mmol, 0.25 mL) to solid samples of **4**, **5** or **6** (0.01 mmol) led to the evolution of gas (H_2), which was most vigorous with the mixture of **6**. Stirring the mixtures for 3 days gave thick oils consisting of various mixtures of cyclic and linear polysilanes, as determined by the ^1H NMR spectra: broad peaks at 5.6-5.1 ppm (cyclic) and 4.8-4.4 ppm (linear). The cyclic : linear

ratio was determined for each case by integration of these peaks (25:75 for reaction with **4** and **6**; 78:22 for reaction with **5**), while the monomer conversion was determined relative to the PhSiH_3 signal at 4.22 ppm (ca. 90% for reactions of **4** and **5**; >95% for the reaction of **6**).

Hydrosilylation of styrene.

Preparation of PhCH(Me)(SiPhH$_2$). Styrene (140 μL, 1.2 mmol, 100 equiv) and $PhSiH_3$ (150 μL, 1.2 mmol, 100 equiv) were added to a solution of **7** (10.0 mg, 0.0121 mmol) in CD_2Cl_2 (ca. 0.8 mL). The sample was left to stand in an ultrasonic bath over 24 h during which the original orange colour changed to dark red. $^{31}P\{^1H\}$ NMR (CD_2Cl_2): 41.2 (br) and –4.9 (free PPh_3) ppm. The new signals in ^1H NMR (CD_2Cl_2): 4.59 (m, PhSiH_2), 2.82 (m, PhCH), 2.19 (d, $^3J_{H\text{-}H}$ = 7.56 Hz, PhCH(CH_3)). Monomer conversion: (determined by integration of the signals due to PhSiH_3 vs PhCH(Me)PhSiH_2) 70%.

The experiment was repeated in the same manner for the other precatalysts. For **8**: 100% conversion; $^{31}P\{^1H\}$ NMR (δ, CD_2Cl_2): -5.6 (br) and –19.7 (**8**). For **9**: 45% conversion; $^{31}P\{^1H\}$ NMR (δ, CD_2Cl_2): 58.9 (major) and 30.9 (trace). The reaction of **8** with 1000 equiv each of styrene and $PhSiH_3$ in CD_2Cl_2 led to similar results after 24 h (conversion 93%). No hydrosilylation was observed in $CDCl_3$.

Preparation of PhCH(Me)(SiPh$_2$H) and PhCH$_2$CH$_2$(SiPh$_2$H). Styrene (140 μL, 1.2 mmol, 100 equiv) and Ph_2SiH_2 (222 μL, 1.2 mmol, 100 equiv) were added to a solution of **8** (7.7 mg, 0.0121 mmol) in CD_2Cl_2 (ca. 0.75 mL). The sample was left to stand in an ultrasonic bath over 24 h during which the original orange colour changed to dark red. $^{31}P\{^1H\}$ NMR (δ, CD_2Cl_2): 28.3, 26.9, -5.5, -7.8, -19.6 (major). The new signals in ^1H NMR (δ, CD_2Cl_2): 5.27 (t, $PhCH_2CH_2SiHPh_2$), 5.21 (d, PhCH(Me)(SiHPh$_2$)), 3.14 (m, PhCH(Me)(SiHPh$_2$)), 3.05 (m, $PhCH_2CH_2SiHPh_2$), 1.82 (m, $PhCH_2CH_2SiHPh_2$), 1.77 (d, $^3J_{H\text{-}H}$ = 7.56 Hz, PhCH(*Me*)(SiHPh$_2$)). Total conversion 80%; ratio of PhCH(Me)(SiHPh$_2$)) : $PhCH_2CH_2SiHPh_2$ was 7:1.

Preparation of CH$_3$(CH$_2$)$_5$(SiPhH$_2$). The above protocol was carried out using 1-hexene (100 μL, 1.2 mmol, 100 equiv), $PhSiH_3$ (150 μL, 1.2 mmol, 100 equiv), and **8** (7.7 mg, 0.0121 mmol). $^{31}P\{^1H\}$ NMR (δ, CD_2Cl_2): weak, broad peaks at 87.3 and -4.9. ^1H NMR

(δ, CD_2Cl_2): 4.46 (t, Si*H*). (The weak conversion (ca. 20%) of the substrates results in a spectrum dominated by the signals of 1-hexene and $PhSiH_3$, such that the signal at 4.46 ppm is the only distinctly detected signal for the product.)

Cyclic voltammetry. Electrochemical measurements were performed on an Epsilon electrochemical analyzer using 0.002M solutions of the Ni(II) complexes in a 0.1M CH_3CN solution of *n*-Bu_4NPF_6. Cyclic voltammograms were obtained in a standard, one-compartment electrochemical cell using a graphite-disk electrode as working electrode, a platinum wire as the counter electrode, and an Ag-$AgNO_3$ (0.01M in CH_3CN) reference electrode. The experiments were performed in the potential range of –2.8 to 0.8 V (CH_3CN) using a scan rate of 100 mV/s. Under these conditions, $E_{1/2}$ for the Fc^+-Fc couple was 90 mV.[24]

[(η^3:η^0-Ind(CH_2)$_2$$NMe_2$)Ni($PMe_3$)(py)][$BPh_4$] (10) in equilibrium with 8. Pyridine (0.0371 mmol, 3.0 μL, 1.08 equiv) was added to a solution of **8** (22.0 mg, 0.0344 mmol) in CD_2Cl_2 (ca. 0.75 mL), allowed to stand for 15 min, and analyzed by ^1H and $^{31}P\{^1H\}$ NMR spectroscopy. By integrating the $^{31}P\{^1H\}$ NMR signals for **10** (-9.19 ppm) and **8** (-20 ppm) a 1:1 ratio was established. ^1H NMR (CD_2Cl_2): 7.6 to 6.9 (BPh_4, Ind and py), 6.43 (H2), 4.45 (br, H3), 2.55 and 2.28 (IndCH_2CH_2), 2.16 (s, NCH_3), 1.05 (d, $^3J_{H\text{-}P}$ = 8.8 Hz, PCH_3).

More pyridine (1.08 equiv, 3.0 μL, 0.0371 mmol) was then added to the above sample and the NMR spectra were recorded 15 min later, showing a 2.3:1 ratio of **10** and **8**. Repeated addition of pyridine allowed the determination of the equilibrium constant: $K_{eq} = 41 \pm 6$. Evaporation of the solution to dryness gave back the starting complex **8**.

[(η^3:η^0-Ind(CH_2)$_2$$NMe_2$)Ni($PCy_3$)(py)][$BPh_4$] (11). Pyridine (0.0309 mmol, 2.5 μL, 1.02 equiv.) was added to a solution of **9** (25.5 mg, 0.0302 mmol) in CD_2Cl_2 (ca. 0.75 mL), and the ^1H and $^{31}P\{^1H\}$ NMR spectra were recorded 15 min later. The $^{31}P\{^1H\}$ NMR spectrum showed the disappearance of the signal for **9** (24.88 ppm) and the emergence of a new signal at 33.20 ppm. ^1H NMR (CD_2Cl_2): 8.27, 7.75, 7.65, 7.40, 7.20 (m, py and Ind), 7.31 (*o*-H, BPh_4), 7.01 (m, *m*-H, BPh_4), 6.87 (m, *p*-H, BPh_4), 6.49 (d,

H4), 4.68 (m, H3), 2.48 (m, IndCH_2), 2.13 (s, NCH_3), 1.8-0.9 (m, CH_2N and PCy_3). Removing the volatiles under vacuum and recording the $^{31}P\{^1H\}$ NMR spectrum of the redissolved solid showed that **11** remained as the main product.

Crystal Structure determinations. Dark red crystals of **5** were obtained from a cold (-20 °C) THF/Hexanes solution. The crystal data for **5** were collected on a Nonius CAD-4 diffractometer with graphite-monochromated CuKα radiation at 223(2) K using the CAD-4 software.[25] Refinement of the cell parameters was done with the CAD-4 software, while the data reduction used NRC-2 and NRC-2A.[26]

Dark red crystals of **2**, **4**, **6** and **9** were obtained from cold solutions **2** in Et_2O/hexanes, **4** or **6** in hexanes, and **9** in CH_2Cl_2/Et_2O. The crystal data were collected on a Bruker AXS SMART 2K diffractometer with graphite-monochromated CuKα radiation at 223(2) K using SMART.[27] Cell refinement and data reduction used SAINT.[28] All five structures were solved by direct methods using SHELXS97[29] and difmap synthesis (SHELXL96).[30] The refinements were done on F^2 by full-matrix least squares. All non-hydrogen atoms were refined anisotropically, while the hydrogens (isotropic) were constrained to the parent atom using a riding model. Solving the structure of **5** entailed an interesting problem: the CC triple bond first obtained was much shorter than expected.[31] Careful inspection of the data revealed that the starting material **1** co-crystallized with **5** in a 9:91 ratio (also confirmed by NMR spectroscopy). Taking into account this ratio and solving for a THF molecule disordered over two positions (occupancy of 0.62 and 0.38) resulted in a good R factor (ca. 4.3%). Structure of **4** also contained a disordered solvent molecule of hexane, which was situated on the inversion point with two orientations (occupancy of 0.35 and 0.15). The relatively high R factor for the structure of **6** (ca. 7.5%) is due to poor quality of the crystals (small, twinned needles). Finally, the crystal structure of **9** presented a disorder on the chelated tether (two positions with occupancy of 0.72 and 0.28) and also contained a CH_2Cl_2 molecule disordered over three positions (occupancy of 0.20, 0.38 and 0.42). These disorders were solved and allowed an R factor of 4.41 %. Crystal data and experimental details for **2**, **4**, **5**, **6**, and **9** are listed in Table 6.1 and selected bond distances and angles are listed in Table 6.2.

Acknowledgment. The Natural Sciences and Engineering Research Council of Canada, le fond FCAR of Quebec, and the University of Montreal are gratefully acknowledged for financial support. H. Terrien is thanked for her help with the GPC.

Supporting Information Available: Complete details on the X-ray analysis of **2**, **4**, **5**, **6**, and **9**, including tables of crystal data, collection and refinement parameters, bond distances and angles, anisotropic thermal parameters, and hydrogen atom. This material is available free of charge via the Internet at http://pubs.acs.org.

References

(1) Review on Cp^NRR' ligands: Jutzi, P.; Redeker, T. *Eur. J. Inorg. Chem.* **1998**, 663.

(2) Review on Cp^OR ligands: Siemeling, U. *Chem. Rev.* **2000**, *100*, 1495.

(3) Review on Cp^L (L = PRR', AsRR' and SR) ligands: Butenschoen H. *Chem. Rev.* **2000**, *100*, 1527.

(4) General review on functionalized Cp ligands: Müller, C.; Vos, D.; Jutzi, P. *J. Organomet. Chem.* **2000**, *600*, 127.

(5) For reviews of this topic see: a) Müller, C.; Vos, D.; Jutzi, P. *J. Organomet. Chem.* **2000**, *600*, 127. b) Jutzi, P.; Siemeling, U. *J. Organomet. Chem.* **1995**, *500*, 175. c) Jutzi, P.; Dahlaus, J. *Coord. Chem. Rev.* **1994**, *137*, 179.

(6) Zargarian, D. *Coord. Chem. Rev.* **2002**, *233-234*, 157.

(7) a) Groux, L. F.; Bélanger-Gariépy, F.; Zargarian, D.; Vollmerhaus, R. *Organometallics*, **2000**, *19*, 1507. b) Groux, L. F.; Zargarian, D. *Organometallics*, **2001**, *20*, 3811. c) Groux, L. F.; Zargarian, D.; Simon, L. C.; Soares, J. B. P. *J. Molec. Cata. A: Chem.* **2003**, *193*, 51. d) Groux, L. F.; Zargarian, D. *Organometallics*, **2003**, *published on the web June 21st*.

(8) a) Huber, T. A.; Bayrakdarian, M.; Dion, S.; Dubuc, I.; Bélanger-Gariépy, F.; Zargarian, D. *Organometallics*, **1997**, *16*, 5811. b) Fontaine, F.-G.; Dubois, M.-A.; Zargarian, D. *Organometallics*, **2001**, *20*, 5156.

(9) It should be noted, however, that the results of combustion analysis for complex **6** were not acceptable, leading us to suspect that this compound is thermally unstable with respect to the reductive coupling of the Ind^NMe_2 and the methyl ligands.

(10) Wang, R.; Bélanger-Gariépy, F.; Zargarian, D. *Organometallics*, **1999**, *18*, 5548.

(11) Fontaine, F.-G.; Zargarian, D. *Organometallics*, **2002**, *21*, 401.

(12) Groux, L. F.; Zargarian, D. *Acta Cryst.* **2001**, *E57*, m547.

(13) The slip parameter, Δ(M-C), is determined according to the relationship (M-C3a + M-C7a)/2 - (M-C1 + M-C3)/2. Thus, a Δ(M-C) value of 0 would signal a perfectly η^5 coordination of Ind, whereas increasing degrees of slippage toward η^3 coordination would result in larger values: a) Baker, R. T.; Tulip, T. H. *Organometallics*, **1986**, *5*, 839. b) Westcott, S. A.; Kakkar, A.; Stringer, G.; Taylor, N. J.; Marder, T. B. *J. Organomet. Chem.* **1990**, 394, 777.

(14) Strictly speaking, the reduction potential of an irreversible reduction (or oxidation) process might vary as a function of many different parameters such as electrolyte composition, nature of electrode, etc. It is common practice, however, to consider that in situations where an analogous series of compounds are being studied under identical conditions, the values of reduction potential can be related, to a good approximation, to structural or electronic properties of the compounds. In the present case, since we are dealing with a family of complexes possessing very similar structural features and compositions, and since the electrochemical studies were performed under identical conditions, we believe that the reduction potential values represent fairly accurately the electron richness of the metal centers in this family of complexes.

(15) Holland, P. L.; Smith, M. E.; Andersen, R. A.; Bergmann, R. G. *J. Am. Chem. Soc.* **1997**, *119*, 12815.

(16) Wang, R.; Groux, L. F.; Zargarian, D. *J. Organomet. Chem*, **2002**, *660*, 98.

(17) a) Chien, J. C. W. *Polyacetylene Chemistry, Physics and Material Science*; Academic Press; NY, 1984. b) Bredas, J. L.; Street, G. B. *Acc. Chem. Res.* **1985**, *18*, 309. c) Masuda, T. Higashimura, T. *Adv. Polym. Sci.* **1986**, *81*, 121. d) Yoshimura, T.; Masuda, T.; Higashimura, T.; Ishihara, T. *J. Polym. Sci., Polym. Chem. Ed.* **1986**, *24*, 3569.

(18) Wang, R.; Groux, L. F.; Zargarian, D. *Organometallics*, **2002**, *21*, 5531.

(19) Fontaine, F.-G.; Kadkhodazadeh, T.; Zargarian, D. *J. Chem. Soc., Chem. Commun.* **1998**, 1253-1254.

(20) a) Fontaine, F.-G. Ph.D. Thesis, Université de Montréal, **2002**. b) Fontaine, F.-G.; Nguyen, R.-V.; Zargarian, D. *Can. J. Chem.* **2003**, *submitted.*

(21) For details on the analysis of these materials by NMR see reference 11.

(22) Analytical data for the hydrosilylation products discussed matched those given in: (a) Fu, P.-F.; Brard, L.; Li, F. C. ; Marks, T. J. *J. Am. Chem. Soc.* **1995**, *117*, 7157. (b) Rubin, M.; Schwier, T.; Gevorgyan, V. *J. Org.Chem.* **2002**, *67*, 1936.

(23) The fate of the resulting silylium cation is not known, but it might be stabilized by forming an adduct with the NMe_2 moiety.

(24) Pavlishchuk, V. V.; Addison, A. W. *Inorg. Chem. Acta*. **2000**, *298*, 97.

(25) CAD-4 Software. Version 5.0. Enraf-Nonius, Delft, The Netherlands.**1989**.

(26) Gabe, E. J.; Le Page, Y.; Charlant, J.-P.; Lee, F. L.; White, P. S. *J. Appl. Cryst.* **1989**, *22*, 384.

(27) *SMART*, Release 5.059; Bruker Molecular Analysis Research Tool, Bruker AXS Inc., Madison, WI 53719-1173, 1999.

(28) *SAINT*, Release 6.06; Integration Software for Single Crystal Data, Bruker AXS Inc., Madison, WI 53719-1173, 1999.

(28) Sheldrick, G. M. *SHELXS.*, Program for the Solution of Crystal Structures. University of Goettingen, Germany, 1997.

(30) Sheldrick, G. M. *SHELXL.*, Program for the Refinement of Crystal Structures. University of Goettingen, Germany, 1996.

(31) 24 structures containing a Ni-CCPh group have been found on the Cambridge Structural database with a mean CC (triple bond) distance of 1.204 Å.

Chapitre 7 : Ligands hémilabiles phosphine-indényle et oléfine-indényle.

7.1 Introduction

Dès le début des études de la réactivité des composés (Ind)Ni(PPh_3)Cl par notre groupe de recherche,[42] il a été démontré que ce type de composés agissait comme pré-catalyseur pour l'oligomérisation du styrène[57] et de l'éthylène,[53b, d] la polymérisation du norbornène et l'hydrosilylation des oléfines et des cétones.[56]

Pour se faire, il était nécessaire de les activer en enlevant le chlorure (avec $AgBF_4$, $AlCl_3$ ou $NaBPh_4$) pour donner l'espèce cationique $[(Ind)Ni(PPh_3)]^+$ identifiée comme le cation « nu ». Ce catalyseur, quoique très efficace, souffrait d'un problème important : sa faible stabilité. En effet, lors des tentatives d'isolation de ce composé en absence de ligands donneurs (CH_3CN, PPh_3, PMe_3, etc.) ou de monomère, le composé $[(Ind)Ni(PPh_3)_2]^+$ était obtenu par redistribution de phosphine. Ce composé bis-phosphine était inactif en catalyse et les autres produits de cette redistribution étaient perdus.

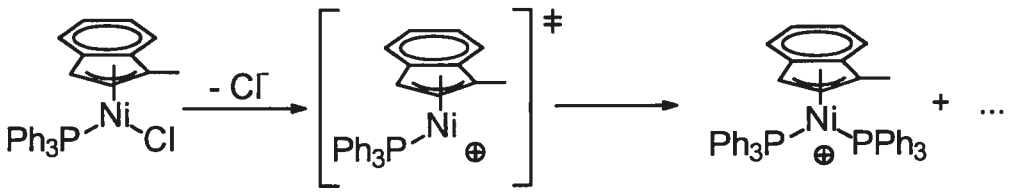

Schéma 7.1. Génération du cation nu

Nous avons pu montrer dans les chapitres précédents que l'utilisation de ligands amino-indényles hémilabiles apportait une réelle solution à ce problème en stabilisant des espèces cationiques tout en gardant leur activité catalytique. Cependant, deux autres voies ont aussi été envisagées pour palier au manque de stabilité des cations nus tout en aidant à résoudre certaines questions mécanistiques. La première voie consistait à lier la phosphine à l'indène ce qui doit augmenter la robustesse du composé, ralentir cette

redistribution de phosphines et donc augmenter la durée de vie du catalyseur. D'un autre côté, lors de nos études sur la polymérisation et l'hydrosilylation des oléfines catalysées par les composés Ni-Cl + MAO, il a été question de déterminer si la phosphine se dissocie du nickel pour permettre l'arrivée du substrat. Nous avons tenté de régler cette question en comparant les réactions des composés comportant des phosphines (PPh_3, PMe_3, PCy_3 principalement) de densité électronique différente donc ayant différentes capacités à donner de la densité électronique au métal. Ainsi, les composés avec PMe_3 et PCy_3 ont démontré une activité accrue dans la polymérisation de l'éthylène par rapport à ceux comportant la PPh_3. Par contre, dans les réaction d'hydrosilylation, le contraire est observé. En résumé, la comparaison des réactivités semble indiquer que ces systèmes suivent des mécanismes différents. La préparation de composés avec un ligand ind^P chélaté permettrait d'aborder ce point mécanistique de la dissociation des phosphines lors des réactions.

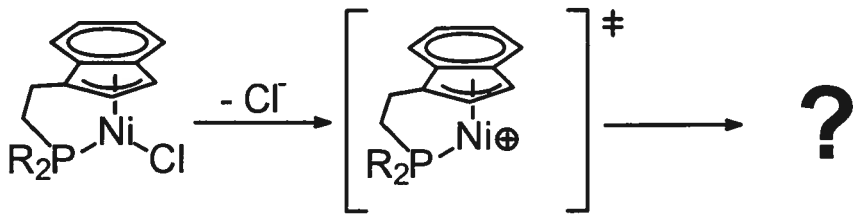

Schéma 7.2. Stabilisation du cation nu par chélation

La deuxième voie, quant à elle, utilisait des ligands bidentates indényle-oléfine pour agir comme l'amine en stabilisant le cation nu avec un ligand labile, avec l'avantage de pouvoir étudier les interactions entre le métal et l'oléfine. En effet, la coordination d'une oléfine constitue une étape importante de plusieurs des réactions étudiées au cours de cette thèse (polymérisation et hydrosilylation), il nous paraissait donc très pertinent de pouvoir isoler ce type de composés pour faire la lumière sur une des premières étapes de ces réactions. On a choisi d'utiliser une oléfine reliée à l'indène (ligand de type Ind^=) pour isoler un tel intermédiaire. L'effet chélate devrait favoriser une réaction intramoléculaire et permettre l'isolation du produit d'une réaction stœchiométrique entre le cation et une oléfine. De plus, si un composé cationique de ce type peut être isolé, il

devrait lui-même être un nouveau catalyseur car les alcènes ne sont pas de bons ligands et le bras moléculaire fonctionnalisé devrait donc être labile.

Ces deux approches reposent sur des informations déjà connues. En effet, une revue de la littérature montre que le premier ligand de type Cp^P, le $Cp(CH_2)_2PPh_2$, a été préparé selon deux voies différentes entre 1979 et 1980. La première implique une attaque nucléophile sur $Cl(CH_2)_2PPh_2$ par le CpNa.[58] La seconde implique l'ouverture d'un spirocycle sur le Cp par attaque nucléophile de $LiPPh_2$.[59] Ce ligand a tout d'abord été complexé sur le manganèse et le fer puis avec la plupart des métaux de transition, tel que décrit dans une revue de Butenschoen.[7] Par la suite, des dérivés ont été préparés en variant les longueurs de la chaîne de 1 à 4 carbones afin d'adapter celle-ci aux besoins stériques des métaux. Des centres chiraux ont été ajoutés dans la chaîne ou sur le Cp (et analogues) dans le but d'induire la chiralité dans les réactions catalysées. Finalement, le Cp a été remplacé par l'indène[60] afin de profiter de l'effet indényle et de sa chiralité planaire lorsque celui-ci est substitué en position 1 et/ou 3 (figure 7.1).

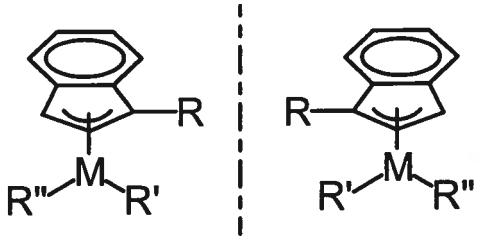

Figure 7.1. Chiralité des composés comprenant un indényle substitué

Parmi les produits préparés, on compte des composés avec le bras phosphine non-coordonné au centre métallique,[61] mais dans la plupart des cas, ils sont coordonnés. Cette coordination est intramoléculaire dans la majorité des exemples, dû à l'effet chélate, mais peut aussi être intermoléculaire; ainsi on a accès à des composés homo- et hétéro-bimétalliques. Finalement, on retrouve également des composés ayant deux bras phosphine qui se coordonnent au métal.[62] Des composés de presque tous les métaux de transition ont été préparés à partir de ces ligands bi-fonctionnels (Cp/Ind^P), dont certains

que très récemment. On peut cependant noter une lacune importante dans cette chimie : aucun composé du groupe 10 n'a été rapporté dans la littérature à ce jour.

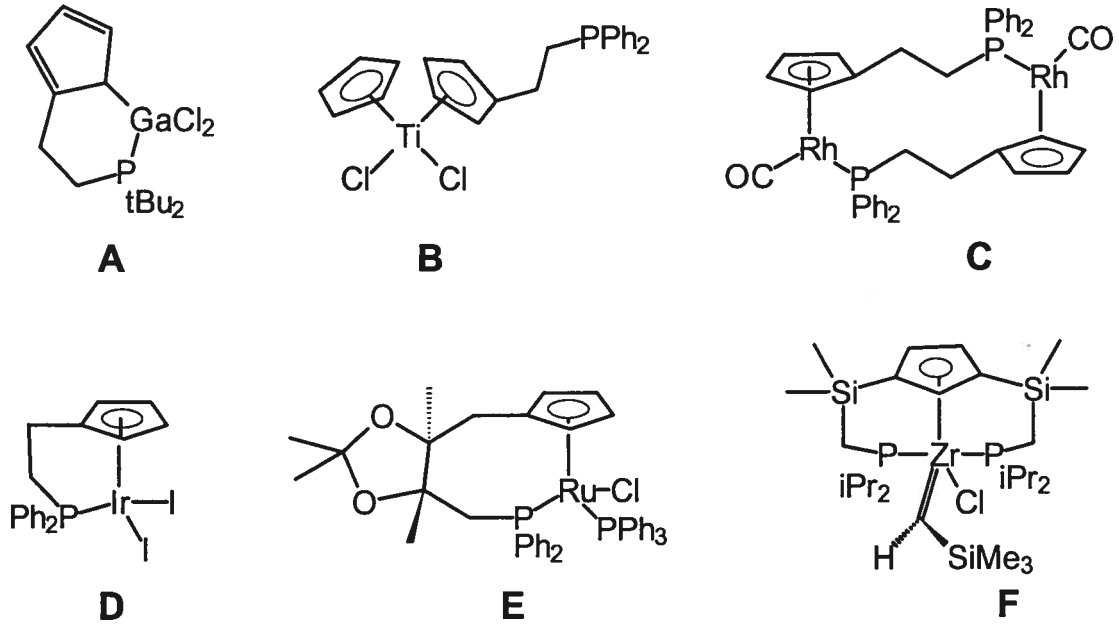

Figure 7.2. Exemples de composés possédant un ligand Cp^P (A,[63] B,[64] C et D,[65] E,[60h] F[62b])

De plus, bien que de nombreux avantages motivent l'étude de tels composés, il semble qu'on se soit arrêté au niveau de la préparation. En effet beaucoup de produits ont été synthétisés mais leurs réactivités ont été très peu étudiées. Parmi les réactions rapportées, on peut citer des substitutions de ligands qui n'impliquent pas le bras chélaté[66] et d'autres provoquant la décoordination du bras,[67] ainsi que des réactions d'insertion.[60c] On a également démontré que des composés de chrome pouvaient catalyser la polymérisation et l'oligomérisation de l'éthylène avec une activité 40 fois supérieure à leurs analogues où la phosphine n'est pas liée au Cp.[60a]

Le chemin est donc ouvert pour tenter de combler ces deux lacunes: préparer des composés de nickel et étudier leur réactivité.

D'un autre côté, une recherche dans la littérature montre que des ligands Cp^= [9] ont déjà été utilisé avec succès pour former des composés de cobalt,[68] de zirconium,[69] et de nickel.[70] Lehmkhul *et al*[70] ont pu d'une part isoler les composés neutres $(Cp/Cp^*(CH_2)_3CH{=}CH_2)Ni(PPh_3)Br$ ainsi que $(Cp^*(CH_2)_2CH{=}CH_2)Ni(PPh_3)Br$ et en former des cations avec le bras coordonné au nickel (Schéma 7.3). Bien que ces composés aient été caractérisés par spectroscopie RMN, analyse élémentaire et par diffraction des rayons X, leur réactivité n'a pas été étudiée. Ce défi reste donc à relever, en plus de vérifier s'ils peuvent être obtenus avec l'indène.

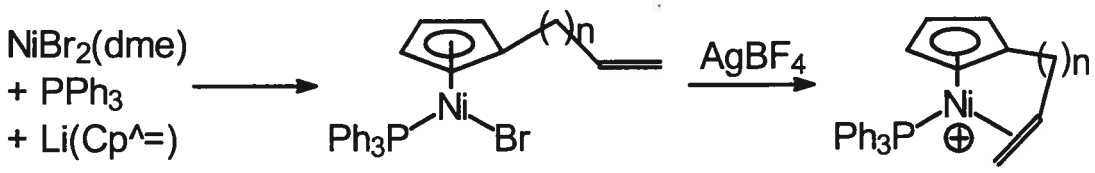

Schéma 7.3. Composés Ni-Cp^=

7.2 Résultats et discussion

7.2.1 Ligand Ind^P

Étant donné les succès obtenus dans la chimie des indényles amino-substitués, notre choix s'est porté sur une chaîne à deux ou trois carbones pour la synthèse des ligands avec une phosphine. Plusieurs voies de synthèse pour préparer un ligand indényle ayant une chaîne à deux carbones à laquelle est attaché le groupe PPh_2 ont été explorées. On peut soit commencer par préparer le $Cl(CH_2)_2PPh_2$ et ensuite le faire réagir avec l'IndLi selon l'approche **A** (Schéma 7.3) ou alors préparer un spirocycle sur l'indène et procéder à son ouverture par attaque nucléophile de $LiPPh_2$ (approche **B**). Dans les deux cas, le ligand désiré est isolé mais la seconde voie sera privilégiée car le rendement de la réaction et la pureté du produit sont meilleurs. Toutefois, il faut noter que cette approche limite à deux le nombre de carbones du bras tandis que la voie **A** peut être utilisée pour obtenir les analogues avec un ou trois carbones.

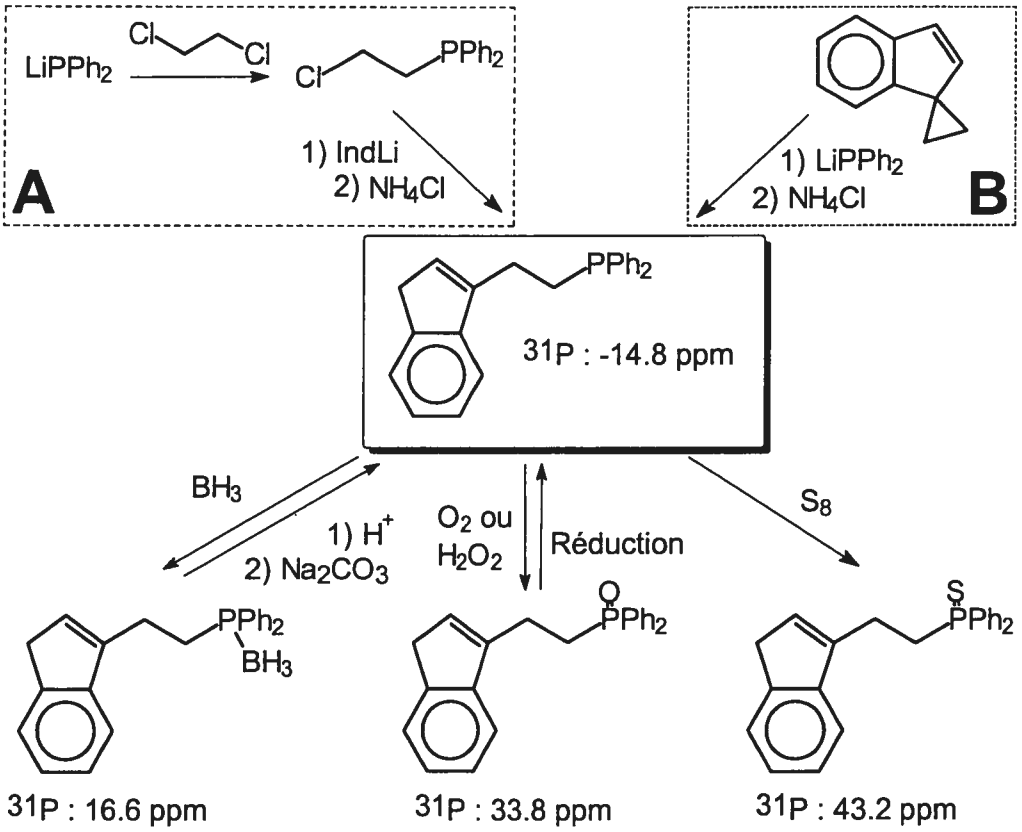

Schéma 7.4. Préparation et protection du ligand $Ind(CH_2)_2PPh_2$

Des ligands comprenant le groupe PMe_2 à l'extremité de la chaîne figuraient également parmi les ligands désirés car les phosphines aliphatiques sont de meilleurs donneurs[71] et devraient donc se lier plus fortement au métal. Pour les préparer, plusieurs voies ont été essayées (Schéma 7.5). La première tentative comprenait l'ouverture d'un spirocyle par attaque nucléophile de $LiCH_2PMe_2$ pour obtenir un bras de trois carbones. Il fut toutefois impossible d'isoler le ligand désiré car la protonation de $LiCH_2PMe_2$ (très basique) est favorisée par rapport à l'attaque nucléophile. On n'obtient donc que PMe_3 comme espèce contenant une phosphine. D'un autre côté, la seconde voie implique la formation d'un fulvène[72] qui subit alors une attaque nucléophile par le $LiCH_2PMe_2$. Le ligand désiré est obtenu dans un bon rendement et peut être utilisé tel quel, ou alors il peut être isolé sous sa forme protonée après addition de HCl, ce qui facilite sa purification.

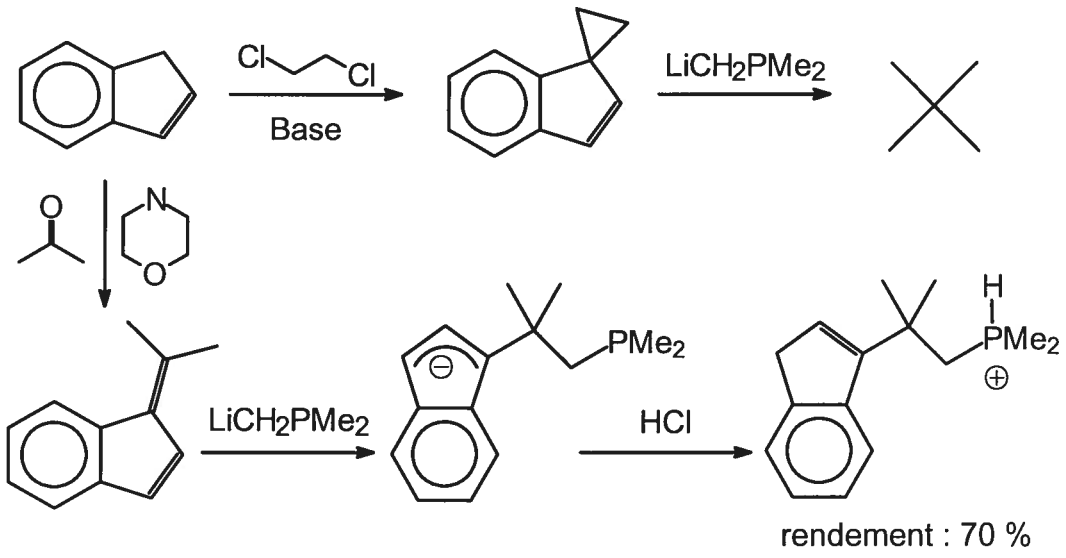

Schéma 7.5. Préparation de ligand Ind^PMe_2

Il faut noter que la purification de ces ligands est difficile car les phosphines s'oxydent très facilement. On ne peut pas chromatographier sur gel de silice ni même manipuler ces ligands à l'air libre sans que ceux-ci ne s'oxydent. Donc, comme il n'était pas toujours possible d'obtenir des ligands assez purs après réaction brute, nous avons testé plusieurs moyens de faciliter leur traitement.

Ainsi, la purification de $Ind(CH_2)_2PPh_2$ a été tentée. La première façon utilisée débutait par l'oxydation facile et complète de la phosphine simplement en mélangeant le ligand et l'oxydant (H_2O_2 ou S_8) dans THF pendant quelques heures. La purification ne posait plus de problèmes car le ligand était alors inerte. Par contre, il a ensuite été impossible de réduire complétement la phosphine malgré que plusieurs exemples de réduction avec $HSiCl_3$ aient été rapportés.[73] Ceci nous a mené a utiliser une deuxième voie qui, bien qu'elle ajoute plusieurs étapes, a permis de bien purifier $Ind(CH_2)_2PPh_2$. BH_3-THF est ajouté à une solution du ligand dans THF pour former un nouveau ligand $Ind(CH_2)_2PPh_2BH_3$, il a ensuite été purifié par chromatographie sur gel de silice et complètement caractérisé, y compris par diffraction des rayons X (Figure 7.3).[74] $Ind(CH_2)_2PPh_2$ peut alors être isolé par déplacement du BH_3 par un acide.

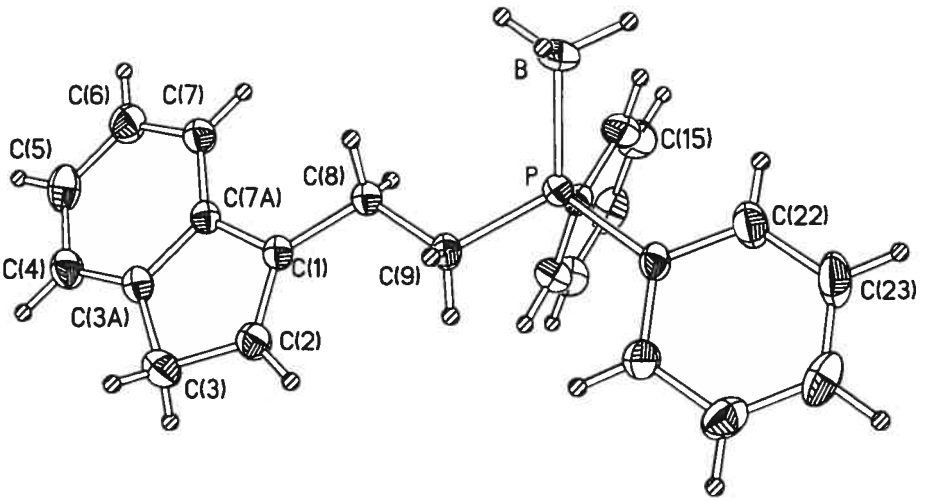

Figure 7.3. Dessin ORTEP de $Ind(CH_2)_2PPh_2BH_3$

Une troisième méthode, également la plus simple, consiste a protéger la phosphine par protonation car les phosphoniums sont insensibles et peuvent être purifié par recristallisation à l'air. Le ligand $Ind(CMe_2)CH_2PMe_2$ a été purifié ainsi puis isolé après déprotonation.

7.2.2 Composés de nickel avec un ligand Ind^P

Dès que le ligand $Ind(CH_2)_2PPh_2$ a pu être obtenu avec une relativement bonne pureté, sa complexation sur le nickel a été tentée. Le ligand a été déprotoné avec BuLi dans une grande quantité d'Et_2O, puis, après quelques heures d'agitation, il a été canulé goutte à goutte sur une suspension de $Ni(PPh_3)_2Cl_2$ dans un peu d'Et_2O (solution verte). Rapidement, la couleur de la solution devient rouge très foncée, indiquant certainement la coordination de l'indényle sur le métal. Mais, par la suite, un solide beige se forme et la solution devient trouble. Parmi le solide obtenu, un composé paramagnétique jaune a été isolé et identifié par diffraction des rayons X comme étant du $(PPh_3)_3Ni^{I}Cl$. Le nickel a donc été réduit, certainement par couplage de l'indène comme observé lors d'études préalables.[75] Malgré plusieurs tentatives, on n'a jamais pu isoler et identifier un composé avec le ligand coordonné parmi les nombreuses espèces obtenues en utilisant cette méthode.

Étant donné le peu de succès avec cette voie, la synthèse a été envisagée en utilisant le $NiCl_2(dme)$ comme source de nickel. En effet, notre groupe de recherche[76] a montré que les composés de type $(Ind)Ni(PPh_3)Cl$ pouvaient être obtenus en faisant réagir un équivalent de ligand indényle déprotoné avec un équivalent de PPh_3 et un léger excès de $NiCl_2(dme)$. Dans notre cas, le ligand déprotoné contient également la phosphine et donc la synthèse ne devait pas poser de problèmes. Hélas, là encore, des mélanges incompréhensibles et non-reproductibles d'espèces comprenant une phosphine ont été obtenus. Rien ne laissait croire à la formation d'un composé indényle avec la phosphine chélatée.

De même, aucun composé n'a pu être isolé en utilisant le ligand $Ind(CMe_2)CH_2PMe_2$ malgré que ce dernier devrait être un meilleur ligand. En effet, $RPMe_2$ est plus basique que $RPPh_2$ et devrait donc former un lien Ni-P plus fort. Lors de sa réaction sous forme déprotonée avec le nickel, on observe une espèce ayant un déplacement chimique à –22.0 ppm en spectroscopie RMN ^{31}P. Cette valeur est très similaire aux signaux de $Ni(PMe_3)_4$ (-21.3 ppm)[71 et 77] et $Ni(PMe_3)_2Cl_2$ (-22.2 ppm),[78] ce qui signifie que la phosphine se lie au métal. Par contre, rien ne montre la coordination de l'indényle (RMN ^1H).

Ces défaites sur le plan synthétique nous ont montré que la phosphine posait un problème. Une des raisons possibles est que la coordination au nickel de deux phosphines ait lieu avant que l'indényle ne puisse se lier au métal ce qui amène à une situation où deux indényles sont proches du centre métallique et peuvent être couplés ensemble. Pour palier à ce problème, on a décidé d'essayer les ligands protégés comme ligand pour le nickel. Les oxydes et thioxydes de phosphine n'ont pas donnés de résultats concluant, par contre le ligand $Ind(CH_2)_2PPh_2$ protégé par BH_3 a été coordonné au nickel par réaction du ligand déprotoné avec le $Ni(PPh_3)_2Cl_2$ (Schéma 7.6). Le bras étant non-coordonnant et agissant comme un simple groupement aliphatique encombrant, il n'a pas perturbé la réaction par une quelconque interaction avec le centre métallique. Le composé $(Ind(CH_2)_2PPh_2BH_3)Ni(PPh_3)Cl$ a donc pu être isolé et caractérisé, y compris par diffraction des rayons X. (Figure 7.4).

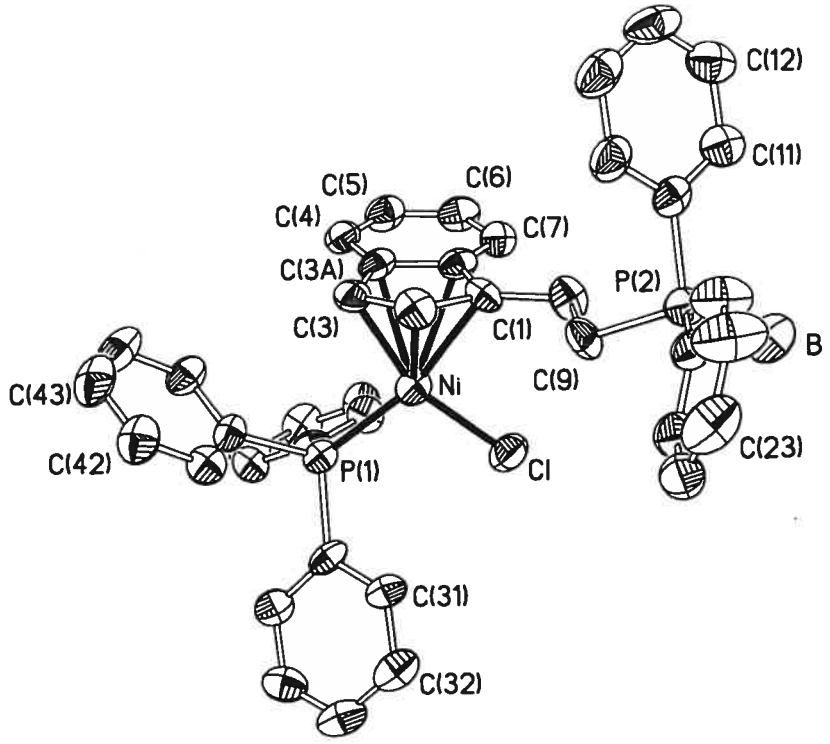

Figure 7.4. Dessin ORTEP de $(Ind(CH_2)_2PPh_2BH_3)Ni(PPh_3)Cl$. Les atomes d'hydrogène ont été omis afin d'améliorer la clarté du dessin.

Ce composé présente des paramètres structuraux similaires (angles et distances) aux autres composés nickel-Ind avec la PPh_3 déjà connus alors que la distance P-BH_3 reste identique à celle trouvée pour le ligand seul. Il adopte une coordination plan-carré déformée avec l'indényle placé perpendiculairement au plan formé par les atomes Ni, Cl, P, C1, C3 et occupant deux sites. Dans ce complexe, la chaîne fonctionnalisée se positionne sur le côté du chlore et pointe loin du centre métallique. Le spectre RMN $^{31}P\{^1H\}$ de $(Ind(CH_2)_2PPh_2BH_3)Ni(PPh_3)Cl$ présente deux signaux : un singulet à 29.9 ppm pour PPh_3 (le signal pour (1-MeInd)Ni(PPh_3)Cl se situe à 31.8 ppm) et un pic large à 17.5 ppm pour la phosphine protégée sur le bras (le signal du ligand libre se situe à 16.6 ppm).

Tableau 7.1. Distances (Å) sélectionnées de $Ind(CH_2)_2PPh_2BH_3$ et $(Ind(CH_2)_2PPh_2BH_3)Ni(PPh_3)Cl$

	Ligand	Complexe
C1-C2	1.338(3)	1.435(3)
C2-C3	1.502(3)	1.419(2)
P2-B	1.923(3)	1.912(3)
Ni-C1	-	2.143(2)
Ni-C2	-	2.054(3)
Ni-C3	-	2.031(2)
Ni-C3A	-	2.321(3)
Ni-C7A	-	2.365(2)
Ni-P1	-	2.1702(11)
Ni-Cl	-	2.797(2)

A partir de ce composé, on a espéré pouvoir parvenir à coordonner le bras phosphine en chauffant afin d'inciter un échange du BH_3 entre les deux phosphines pour libérer PPh_3BH_3 et obtenir $(\eta^3:\eta^1\text{-}Ind(CH_2)_2PPh_2)NiCl$; mais cette réaction ne s'est pas produite. D'un autre côté, le déplacement du BH_3 par une amine n'a pas non plus donné des résultats concluants. En effet, l'échange du BH_3 entre la phosphine et l'amine est une réaction d'équilibre, il faut donc ajouter un gros excès d'amines basiques pour promouvoir l'échange, mais le composé ne résiste pas à de telles conditions et se décompose.

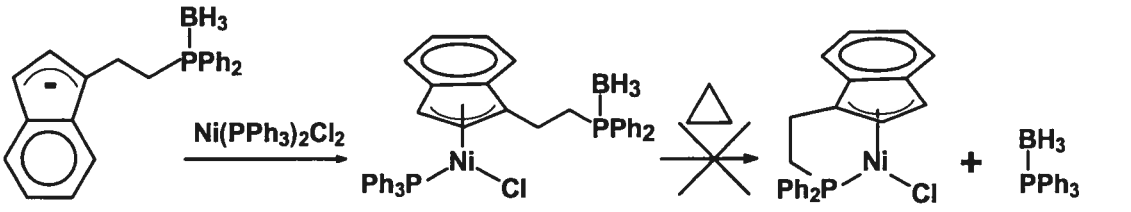

Schéma 7.6. Préparation du composé $(Ind(CH_2)_2PPh_2BH_3)Ni(PPh_3)Cl$

Nos recherches ont montré que des ligands Ind^PR_2 peuvent être préparés et protégés pour faciliter leur traitement. Par contre, nous n'avons pas été capable d'isoler un complexe avec une phosphine chélatée. Le seul composé préparé et complétement caractérisé ($(Ind(CH_2)_2PPh_2BH_3)Ni(PPh_3)Cl$) contient une phosphine protégée par BH_3 au bout de la chaîne.

7.2.3 Préparation et utilisation des ligands Ind^=

Suivant les mêmes stratégies qu'avec les amines, un bras oléfine a été ajouté à l'indène. Les ligands obtenus sont alors déprotonés et réagissent avec $Ni(PPh_3)_2Cl_2$ pour donner les composés nickel-indényle désirés tel qu'identifiés par RMN lors de tentatives préliminaires.

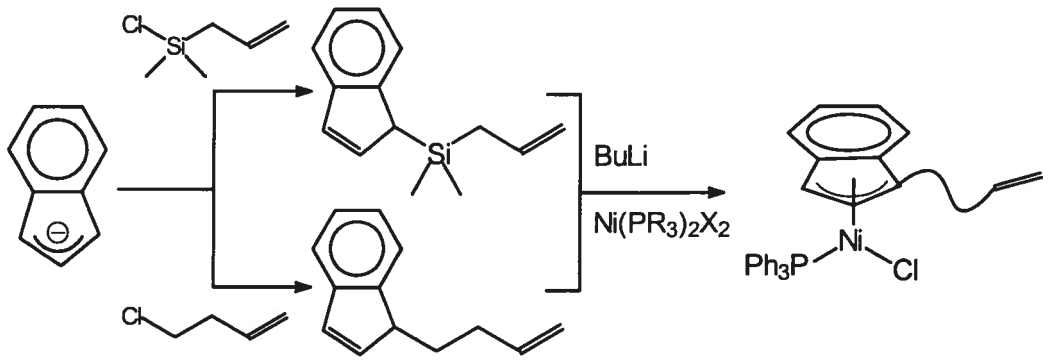

Schéma 7.7. Préparation et réactivité des ligands Ind^=

Cependant, par manque de temps et face au grand potentiel de cette partie du projet, il a été repris par un nouvel étudiant en maîtrise. Daniel Gareau a commencé l'étude de ces composés et a obtenu des résultats intéressants. Premièrement, il a obtenu les composés $(IndSiMe_2CH_2CH{=}CH_2)Ni(PPh_3)Cl$ et $(Ind(CH_2)_2CH{=}CH_2)Ni(PPh_3)Cl$ et les a caractérisé par spectroscopie et par diffraction des rayons X (Figure 7.5). Ses études démontrent que le bras n'interagit pas avec le centre métallique à l'état solide comme pour les composés ayant un bras amine. Par contre, il n'a pas observé de phénomène dynamique de coordination de l'oléfine en solution, ceci concorde avec le fait que les alcènes ne sont pas des ligands très forts.

Déjà, il a obtenu le composé cationique avec l'oléfine coordonnée au nickel et commencé l'étude de ce dernier. Il faut cependant que je m'arrête là pour lui laisser le privilège d'étoffer ses résultats et les présenter dans quelques temps lors du dépôt de son mémoire. On terminera donc cette partie en lui souhaitant bonne chance et en jettant un coup d'oeil aux structures.

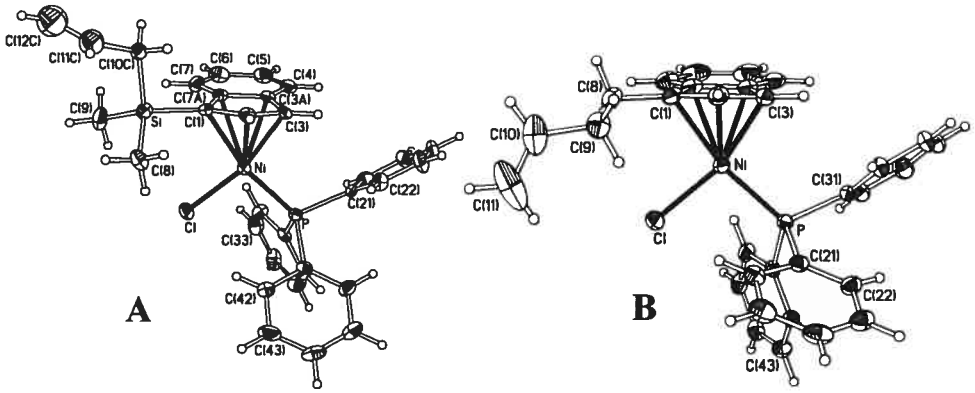

Figure 7.5. Dessins ORTEP de (Ind-$SiMe_2CH_2CH=CH_2$)Ni(PPh_3)Cl (A) et de (Ind-$(CH_2)_2CH=CH_2$)Ni(PPh_3)Cl (B)

7.3 Conclusion

Nos recherches ont montré que des ligands Ind^PR_2 peuvent être préparés mais que leur manipulation requière passablement d'attention pour éviter leur oxydation. Pour faciliter le travail et la purification, ces ligands peuvent être protégés en formant des complexes avec BH_3 (PPh_2) ou par protonation (PMe_2).

Tous nos efforts pour isoler un composé stable comprenant un ligand Ind^PR_2 se sont finalement soldés par des échecs. En effet, de nombreuses espèces se forment lors de la réaction, l'une d'elle étant probablement le produit désiré, mais nous n'avons pas été capable de l'isoler. De manière générale, il semble que, premièrement, il y ait complexation du ligand au métal, diagnostiqué par le changement de couleur de la solution (vert à rouge), puis décomposition (solide beige). Celle-ci semble se produire par élimination réductrice, puisque $(PPh_3)_3Ni^{I}Cl$ a pu être isolé (cristaux jaunes). Ainsi, l'absence de composé connu de nickel comprenant un ligand chélatant Cp^PRR' semble

ne pas être le fruit d'un manque d'attention à ce sujet mais plutôt à l'incapacité de pouvoir en isoler des exemples stables.

Heureusement, nous avons pu démontrer que le problème se situe au niveau de la phosphine puisque lorsqu'on la rend non disponible par protection avec BH_3, un composé stable a pu être isolé et complétement caractérisé. Ce dernier présente les mêmes caractéristiques générales que les composés nickel-indényle obtenus jusqu'à ce jour.

Un moyen eventuel pour réussir à préparer un composé ayant la phosphine chélatée avec le nickel serait d'ajouter le ligand déprotoné sur $Ni(PR_3)_2Cl_2$ (R = Me ou Cy). En effet, si des phosphines plus coordonnantes que PPh_3 sont liées au métal, elles ne devraient pas avoir tendance à partir rapidement du nickel. Ainsi, l'indényle devrait pouvoir se coordonner en premier, puis avec l'effet chélate, le bras phosphine pourrait déplacer PR_3 (spécialement avec PMe_3 qui peut être retirée du milieu par évaporation).

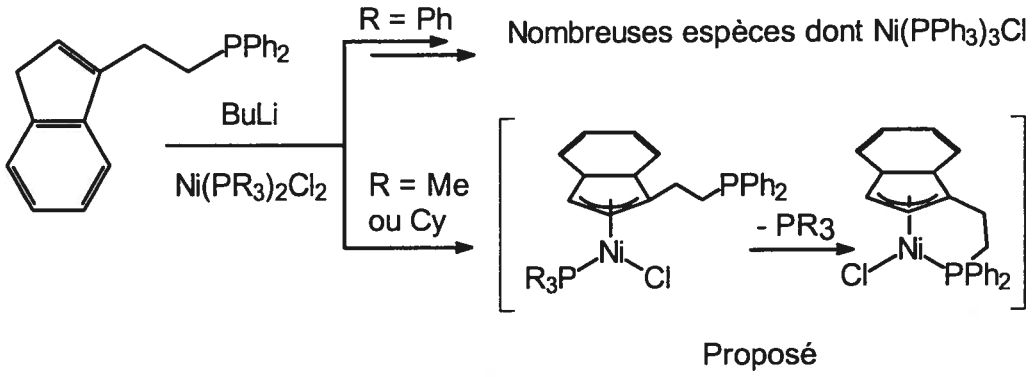

Schéma 7.8. Option pour la préparation de (η^3:η^1-Ind$(CH_2)_2PPh_2$)NiCl

Finalement, le projet avec les ligands indényle-oléfine a rencontré beaucoup de succès, au moins en ce qui a trait aux synthèses des composés ciblés. Il reste maintenant à voir quelles informations mécanistiques peuvent être tirées de leurs réactivités. De plus, il faudra encore tester leurs capacités à catalyser des réactions de polymérisation, d'oligomérisation et d'hydrosilylation des oléfines.

7.4 Partie expérimentale

Remarques générales.

Les manipulations ont été effectuées sous atmosphère inerte d'azote en utilisant les techniques standards de Schlenk[79] ainsi qu'une boîte à gants. Les solvants ont été séchés et dégazés avant utilisation. $Ni(PPh_3)_2Cl_2$,[80] $NiCl_2(dme)$,[81] 8,8-Diméthylebenzofulvène,[82] $Ind(CH_2)_2PPh_2$,[83] $Ind(CH_2)_2P(=O)Ph_2$[83] et $Ind(CH_2)_2P(=S)Ph_2$,[83] ont été préparés en suivant des procédures connues alors que $LiCH_2PMe_2$ et $LiPPh_2$ ont été obtenus par déprotonation de PMe_3 par le *t*-BuLi et déprotonation de $HPPh_2$ par BuLi dans l'hexane, respectivement. Les autres réactifs proviennent de sources commerciales (Aldrich) et ont été utilisés tel quel. Les analyses élémentaires ont été effectuées par le Laboratoire d'analyse élémentaire (Université de Montréal). Les spectres RMN ont été enregistrés sur un Bruker AMXR400 (^1H (400 MHz), $^{13}C\{^1H\}$ (100.56 MHz), et $^{31}P\{^1H\}$ (161.92 MHz)), et un Bruker AV300 (^1H (300 MHz), et $^{31}P\{^1H\}$ (121.49 MHz)).

$Ind(CH_2)_2PPh_2BH_3$[74]

BH_3.THF (6.1 mL d'une solution 1M dans THF, 6.1 mmol, 1.5 équivalent) est ajouté à une solution de $Ind(CH_2)_2PPh_2$ (1.33 g, 4.05 mmol) dans le THF (60 mL). Après une heure d'agitation à température de la pièce, le mélange contenant un précipité blanc est evaporé à sec. Le produit brut est alors purifié par chromatographie (gel de silice; 1:3 acétate d'éthyle/hexane). Le solide blanc (828 mg, rendement de 61%) est recristallisé d'une solution d'acétate d'éthyle/hexane (1:1). RMN $^{31}P\{^1H\}$ ($CDCl_3$): 16.6 ppm; ^1H ($CDCl_3$): 7.7, 7.5 et 7.2 (m, protons aromatiques de l'indène et PPh_2), 6.25 (s, H2), 3.29 (s, H3), 2.78 et 2.60 (m, C*H*$_2$), 1.15 (BH_3); $^{13}C\{^1H\}$ ($CDCl_3$): 144.5 et 143.6 (C3A et C7A), 132.3, 131.4, 129.0, 128.6, 124.5, 118.9 (C2), 24.6 (d, *C*H_2P), 21.5 (Ind-*C*H_2). Analyse élémentaire calculée pour $C_{23}H_{24}BP$: C, 80.72%; H, 7.07%. Mesurée : 80.62%; 7.31%.

$Ind(CMe_2)CH_2PMe_2$.HCl

8,8-Diméthylebenzofulvène (2.00 g, 12.8 mmol) en solution dans 150 mL d'Et_2O est canulé sur une solution de $LiCH_2PMe_2$ (1.15 g, 14.8 mmol) dans 150 mL d'Et_2O. Le

mélange est agité pendant trois jours à température de la pièce puis 50 mL d'Et_2O sont évaporés et 20 mL de HCl (2M dans Et_2O) sont ajoutés. Le ligand protoné précipite sous forme de solide beige (2.1 g, rendement de 70%). RMN $^{31}P\{^1H\}$ ($CDCl_3$): -3.06 ppm ; ^1H ($CDCl_3$): 7.53 (t, H5 et H6), 7.33 et 7.26 (m, H4 et H7), 6.45 (s, H2), 3.39 (s, H3), 3.05 (d, $^1J_{P-H}$ = 13.9 Hz, CH_2P), 1.87 (d, $^1J_{P-H}$ = 17.4 Hz, PCH_3), 1.63 (s, ind-C(CH_3).

Tableau 7.2. Réaction de LiInd$(CH_2)_2PPh_2$ avec Ni$(PPh_3)_2Cl_2$

L (éq.)	BuLi (éq.)	Ni (éq.)	T (°)	Traitement	$^{31}P\{^1H\}$ (ppm)
1	1	3	20	Évaporation complète	(C_6D_6) 44.6, 3.2 et –4.8.
1	1	1.3	20	Évaporation complète	(C_6D_6) 33.6, 33.0, 29.9, 29.4, 20.7, -4.9
				Ajout de PPh_3	(C_6D_6) 33.6, 33.3, 32.8, 32.5, 30.3, 30.1, 29.4, 29.1, 24.4, 20.7, -4.9
				Solution au congélateur	
				Un solide précipite	($CDCl_3$) 32.5, 29.5, -4.8
				Le filtrat est evaporé	($CDCl_3$) 57.9, 34.2, 32.8, 29.6, 24.6, 22..2, 21.2, -4.9
1	1	1.2	-55	Évaporation d'une portion	($CDCl_3$) 32.5, 29.5, -4.8, -15.0
				Filtration le lendemain:	
				solide	($CDCl_3$) 53.6, 34.2, 32.6, 29.7, -4.8, -14.0, -15.0
				filtrat	($CDCl_3$) 58.7, 55.9, 33.6, 32.5, 30.2, 24.8, 23.3, 21.6, 20.2, -3.5

Réaction de LiInd$(CH_2)_2PPh_2$ avec Ni$(PPh_3)_2Cl_2$

Ind$(CH_2)_2PPh_2$ est deprotoné avec BuLi dans 200 mL d'Et_2O. On agite quelques heures puis on canule lentement cette solution sur une suspension de Ni$(PPh_3)_2Cl_2$ dans 50 mL d'Et_2O. Rapidement la solution devient rouge foncée avec un solide brun qui précipite. Les conditions de réaction ainsi que le traitement des produits sont rapportés dans le tableau 7.2.

Lors des tentatives de purification, on finit toujours par obtenir des produits paramagnétiques et souvent peu solubles empêchant la caractérisation mais confirmant que le produit désiré n'est pas obtenu.

Les produits ayant été identifiés par spectroscopie RMN $^{31}P\{^{1}H\}$ sont : PPh_3 libre et $OPPh_3$, alors que $Ni(PPh_3)_3Cl$ a été cristallisé et identifié plusieurs fois par sa maille obtenue par diffraction des rayons X.[84]

Réaction de $LiInd(CH_2)_2PPh_2$ avec $NiCl_2(dme)$

BuLi est ajouté lentement sur $Ind(CH_2)_2PPh_2$ en solution dans l'Et_2O. On agite quelques heures puis on canule lentement sur une suspension de $NiCl_2(dme)$ dans l'Et_2O à température ambiante. Rapidement la solution devient plus foncée avec un solide brun-beige qui précipite. Les conditions de réaction ainsi que le traitement des produits sont rapportés dans le tableau 7.3.

Lors des tentatives de purification, on finit toujours par obtenir des produits paramagnétiques et souvent peu solubles empêchant la caractérisation mais confirmant que le produit désiré n'est pas obtenu.

Tableau 7.3. Réaction de $LiInd(CH_2)_2PPh_2$ avec $NiCl_2(dme)$

L (éq.)	BuLi (éq.)	Ni (éq.)	Traitement		$^{31}P\{^{1}H\}$ (ppm)
1	1	1.5	Filtration	Solide	Paramagnétique
				Filtrat	(C_6D_6) 35.1 (trace).
1	1	1.1	Filtration	Solide	Paramagnétique
				Filtrat	(C_6D_6) 34.2, 32.6, 27.8, 22.5, -14.9
			Le filtrat est dissous dans CH_2Cl_2 et ajout d'hexane.		
				Solide	(C_6D_6) 32.5, 29.3, -15.3
				Filtrat	(C_6D_6) 43.1, 29.7, 28.9, -15.2
1	1	2	Évaporation Complète		(C_6D_6) 29.9, 29.7, 29.2, 28.9, 26.0, 25.7, 24.9, 24.6, 20.7, -15.0, -20.2
1	1	5	Évaporation Complète		(C_6D_6) 34.8, 29.7, 24.9

Réaction de $Ind(CMe_2)CH_2PMe_2$ avec $NiCl_2(dme)$

BuLi (0.4 mL d'une solution 2.5 M dans l'hexane) est ajouté goutte à goutte sur une solution d'$Ind(CMe_2)CH_2PMe_2$.HCl (133 mg, 0.49 mmol) dans 40 mL d'Et_2O. Après 3 heures d'agitation, la solution est canulée lentement sur une suspension de $NiCl_2(dme)$

dans 20 mL d'Et_2O. Rapidement, la solution fonce un peu et un solide brun précipite. On évapore tout et on analyse par spectroscopie RMN. Le spectre RMN ^{31}P $\{^1H\}$ (C_6D_6) présente un seul pic à -22.6 ppm qui est très proche des déplacements chimiques de $Ni(PMe_3)_2Cl_2$ (-22.2 ppm) et de $Ni(PMe_3)_4$ (-21.3 ppm).[71 et 77] D'autres tentatives de synthèse ont mené aux mêmes résultats.

$(Ind(CH_2)_2PPh_2BH_3)Ni(PPh_3)Cl$

BuLi (0.47 mL d'une solution 2.5 M dans l'hexane) est ajouté lentement à une solution de $Ind(CH_2)_2PPh_2BH_3$ (400 mg, 1.17 mmol) dans l'Et_2O (200 mL). On agite deux heures puis cette solution est canulée lentement sur une suspension de $Ni(PPh_3)_2Cl_2$ (1.48 g, 2.27 mmol) dans l'Et_2O (50 mL). Rapidement la solution devient rouge très foncée. Le mélange est alors évaporé à sec puis le solide est dissous dans un minimum de CH_2Cl_2 (30 mL). 120 mL d'hexane sont ensuite ajoutés et la solution est mise au congélateur (-20 °C). Le lendemain, un solide rouge foncé a précipité et est récupéré (450 mg, rendement de 55%). RMN $^{31}P\{^1H\}$ ($CDCl_3$): 29.9 (Ni-PPh_3), 17.1 (PPh_2BH_3); ^1H ($CDCl_3$): 7.9-7.2 (PPh_3 et PPh_2), 7.16 (t, $^3J_{H-H}$ = 7.4 Hz, H6), 7.09 (d, $^3J_{H-H}$ = 8.0 Hz, H7), 6.91 (t, $^3J_{H-H}$ = 7.3 Hz, H5), 6.56 (d, $^3J_{H-H}$ = 3.0 Hz, H2), 6.08 (d, $^3J_{H-H}$ = 7.7 Hz, H4), 3.49 (m, H3), 3.01 et 2.56 (m, CH_2), 2.18 et 2.03 (m, CH_2) 1.26 (large, BH_3); $^{13}C\{^1H\}$ ($CDCl_3$): 139.7 (d), 138.6 (d), 137.6 (d), 137.6, 137.1, 136.9, 136.8 136.1, 134.6 134.5 134.0 (d), 132.4 et 132.3 (C5 et C6), 123.6 et 122.7 (C4 et C7), 115.0 (m, C1), 107.5 (C2), 68.2 (C3), 22.1 (d, $^1J_{C-P}$ = 45 Hz, CH_2P), 20.0 (ind-C). Analyse élémentaire calculée pour $C_{41}H_{38}BP_2NiCl$: C, 70.06 % ; H, 5.49 %. Mesurée : C, 69.81 % ; H, 5.47 %.

Études cristallographiques.

Les données cristallographiques pour $(Ind(CH_2)_2PPh_2BH_3)Ni(PPh_3)Cl$ et $Ind(CH_2)_2PPh_2BH_3$ ont été collectées à température ambiante à l'aide d'un diffractomètre CAD-4 de Nonius utilisant la radiation Cu Kα. L'affinement des paramètres de maille a été effectué avec le logiciel pour CAD-4,[85] alors que NRC-2 et NRC-2A[86] ont été utilisés pour la réduction des données. Les structures ont été résolues et affinées à l'aide des logiciels SHELXS97,[87] SHELXL96[88] et SHELXTL.[89] Les affinements ont été faits selon la méthode des moindres carrés en utilisant une matrice sur F^2. Tous les atomes, à

l'exception des hydrogènes, ont été affinés de façon anisotropique, alors que les hydrogènes (isotropiques) ont été contraints à un parent en utilisant un modèle de chevauchement.

Tableau 7.4. Données cristallographiques de $Ind(CH_2)_2PPh_2BH_3$ et $(Ind(CH_2)_2PPh_2BH_3)Ni(PPh_3)Cl$

	Ligand	**Composé**
Formule	$C_{23}H_{24}BP$	$C_{41}H_{38}BP_2ClNi$
Forme et Couleur	Plaquette blanche	Bloc rouge foncé
Dimensions, mm	0.88 × 0.12 × 0.02	0.31 × 0.19 × 0.04
Symétrie	Monoclinique	Triclinique
Groupe spacial	$P2_1/c$	P-1
a, Å	14.061(5)	8.952(5)
b, Å	6.644(3)	13.245(9)
c, Å	21.018(10)	15.670(8)
α, deg		84.66(4)
β, deg	96.82(3)	74.67(4)
γ, deg		81.02(5)
volume, Å^3	1949.6(15)	1767.3(18)
Z	4	2
Densité, g cm^{-1}	1.1658	1.3110
diffractomètre	Nonius CAD-4	Nonius CAD-4
temp, K	293(2)	293(2)
λ (Cu Kα)	1.54178 Å	1.54178 Å
μ, mm^{-1}	1.232	2.548
type de scan	$\omega/2\theta$ scan	$\omega/2\theta$ scan
θ_{max}	69.83°	70.00°
h,k,l	$-17 \le h \le 17$	$-10 \le h \le 10$
	$-8 \le k \le 8$	$-16 \le k \le 16$
	$-25 \le l \le 25$	$-19 \le l \le 19$
Réflexions utilisées ($I > 2\sigma(I)$)	3689	6688
R[$F^2>2\sigma(F^2)$], wR(F^2)	0.0367, 0.0674	0.0502, 0.1009
GOF	0.853	0.860

Chapitre 8 : Conclusion générale

L'utilisation de ligands hémilabiles ayant l'indényle comme ligand ancreur pour la préparation de composés de nickel a permis l'obtention d'une série de nouveaux catalyseurs neutres, qui, après activation, ont été utilisé efficacement pour polymériser le styrène, le norbornène, l'éthylène, le phénylacétylène et le phénylsilane. L'étude du comportement dynamique de ces composés en solution ainsi que de leurs réactions a permis de montrer le caractère hémilabile des ligands amino-indényles et leur influence sur le cours des réactions. En effet, les produits obtenus sont qualitativement et quantitativement différents de ceux obtenus par les catalyseurs utilisant le 1-méthyle-indényle.[53c]

D'un autre côté, après abstraction d'un ligand chlorure, des catalyseurs cationiques efficaces pour la polymérisation et l'hydrosilylation des oléfines ont été isolés. Dans ces derniers, le ligand amino-indényle est coordonné de façon bidentate au métal. Il est ancré sur le nickel par l'indényle alors que l'amine est plus ou moins fortement liée au métal. En fait, la labilité du lien Ni-N a été évaluée en fonction des substituants sur l'amine et de la phosphine utilisée dans le complexe. Il a pu ainsi être démontré que l'amine pouvait plus ou moins facilement se décoordonner pour libérer un site sur le métal et permettre une certaine activité catalytique.

Cette conclusion fera donc le point sur les ligands utilisés pour obtenir ces complexes neutres et cationiques. Les points saillants de ces deux groupes seront alors discutés en incluant leur caractérisation en solution et à l'état solide, leur comportement et leur réactivité. On terminera par quelques propositions pour la poursuite de ce projet.

8.1 Les ligands amino-indényles

Une série de ligands bidentates, potentiellement hémilabiles, ont été préparés, isolés et caractérisés. Ils sont formés à partir du ligand indényle sur lequel est greffé un bras moléculaire fonctionnalisé (Schéma 8.1).

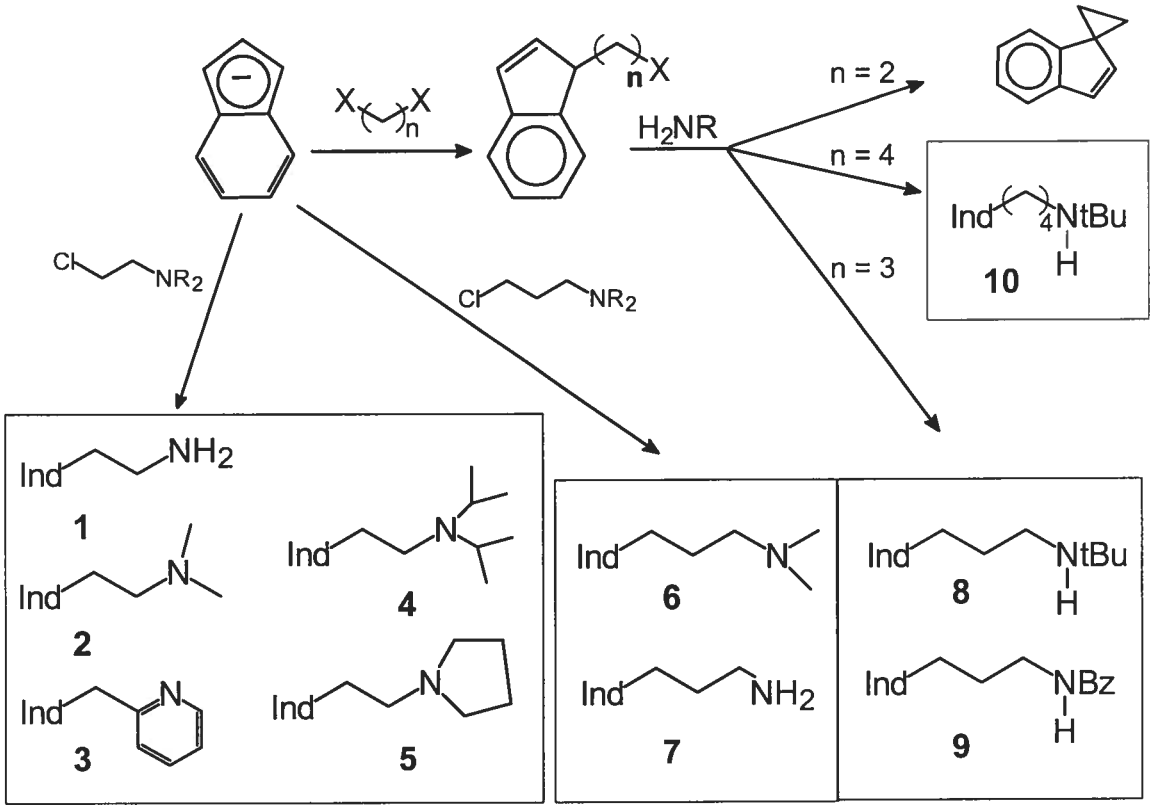

Schéma 8.1. Préparation de ligands amino-indényles

Ainsi, des ligands amino-indényles comportant une chaîne de deux à quatre carbones au bout de laquelle est fixée une amine ont été préparés. Un éventail de substituants, incluant des groupes alkyles encombrés ou non, cycliques, aromatiques et des hydrogènes, ont été rendus disponibles pour la synthèse de nouveaux composés de nickel.

Lors des tentatives de coordination de ces ligands sur le nickel par déprotonation de l'indène avec BuLi et réaction avec $Ni(PPh_3)_2Cl_2$, il a pu être constaté que les amines comportant un hydrogène accessible, c'est à dire pouvant s'approcher suffisamment du métal par une longueur de chaîne adéquate et un encombrement stérique faible (ligands **1**, **7** et **9**), ne permettaient pas l'isolation de composés stables. Par contre, tous les autres (ligands **2** – **6**, **8** et **10**) ont permis l'isolation de composés de type (η^3:η^0-Ind^N)$Ni(PPh_3)Cl$ avec le bras non-coordonné au nickel. Cette affirmation est soutenue

par la résolution de quatre structures par diffraction des rayons X. Ces dernières montrent clairement qu'à l'état solide, il n'y a pas d'interaction entre le métal et l'amine puisque celle-ci pointe loin de ce dernier. [53d, 90]

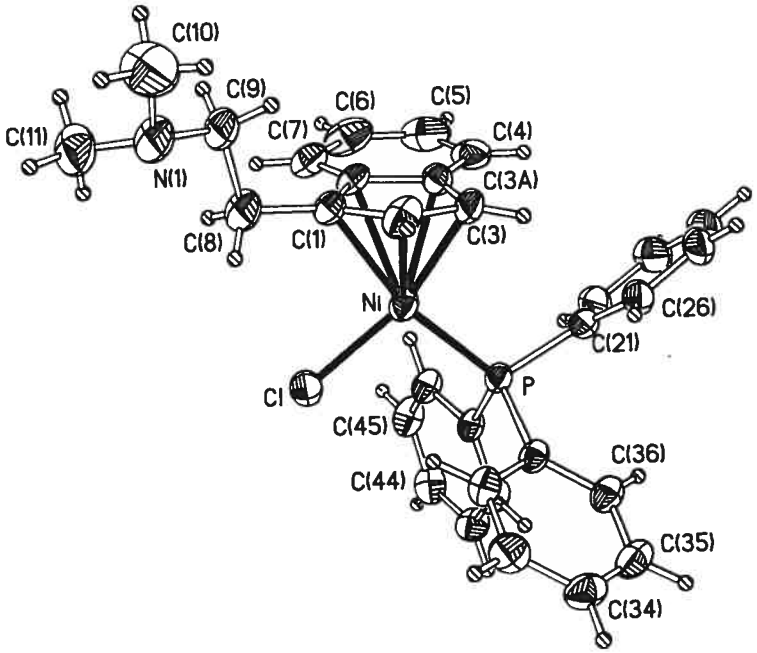

Figure 8.1. Dessin ORTEP de $(\eta^3:\eta^0$-Ind$(CH_2)_2NMe_2)$Ni(PPh_3)Cl

D'un autre côté, la situation en solution n'est pas aussi simple et un phénomène dynamique impliquant la coordination-décoordination du bras avec le centre métallique a été mis en évidence par des études spectroscopiques (RMN) à température variable pour les composés $(\eta^3:\eta^0$-Ind^N)Ni(PPh_3)Cl (^N = $(CH_2)_2NMe_2$, $(CH_2)_2N$-*cyclo*-C_4H_8 et CH_2Py). Ce comportement est influencé par quatre facteurs importants : la température (inactif à basse température), la longueur du bras (seulement pour deux carbones), les substituants sur l'amine (N-*i*Pr_2 bloque le phénomène) et la force des ligand X et PR_3 (seulement avec Cl et PPh_3 qui sont de faibles donneurs).

L'étude a montré qu'à basse température le composé se comportait comme à l'état solide (pas de coordination de l'amine) alors que l'état exact à haute température reste encore à démontrer. Cependant, l'utilisation de solvant ayant différentes polarités indique que l'ionisation du composé semble favorisée en milieu polaire (Schéma 8.2). Par contre, en milieu non-polaire, quelques évidences RMN (déplacements chimiques du proton H3 et du methylène) ont permis de proposer le glissement de l'Ind en mode η^1.

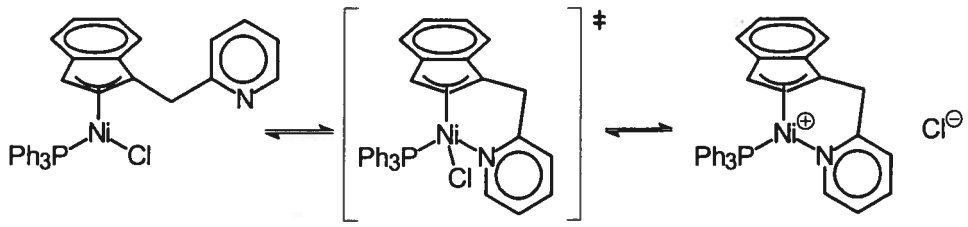

Schéma 8.2. Comportement hémilabile à haute température

Les études électrochimiques en solution (CH_3CN) ont également démontré une certaine contribution électronique des amines en bout de bras : ces composés sont plus difficiles à réduire que leurs analogues sans bras amine (E_{red} = -1.41 à -1.34 V pour les composés (η^3:η^0-Ind^N)Ni(PPh_3)Cl contre - 1.26 V pour (1-Me-Ind)Ni(PPh_3)Cl).

À partir de (η^3:η^0-Ind$(CH_2)_2NMe_2$)Ni(PPh_3)Cl, toute une gamme de composés neutres a pu être générée par échange de ligands comme décrit dans la Schéma 8.3, qui fournit également la valeur du déplacement chimique de la phosphine.

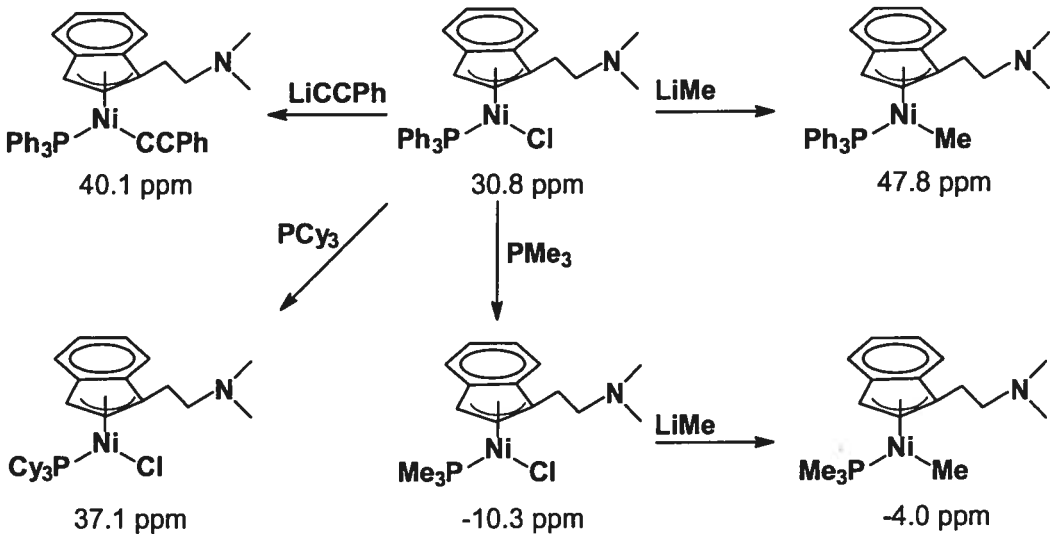

Schéma 8.3. Échange de ligands

On a donc pu obtenir des composés chlorés avec d'autres phosphines comme la PMe_3 qui est un meilleur ligand donneur avec un encombrement stérique faible et la PCy_3 qui est également un meilleur donneur que PPh_3 mais qui possède un encombrement

important. D'autre part, le chlore a pu être remplacé par un méthyle ou un alcynyle. Ces changements apportent une grande variété aux catalyseurs et offrent la possibilité de varier la densité électronique du métal tel que montré dans les analyses électrochimiques (chapitre 5 et 6), ainsi que l'encombrement stérique et la réactivité.

Le chlorure peut également être déplacé du nickel pour donner lieu à des composés cationiques avec ou sans la coordination de l'amine.

8.2 Les composés cationiques de nickel

Lorsque le chlorure était enlevé des composés de type (η^3:η^0-Ind^N)Ni(PPh_3)Cl, il a pu être constaté que deux types de produit en resultaient : [(η^3:η^1-Ind^N)Ni(PPh_3)]$^+$ et [(η^3:η^0-Ind^N)Ni(PPh_3)$_2$]$^+$. Le premier type implique une chélation de l'amine mais pas le deuxième. Ce phénomène est directement lié à deux facteurs : la longueur de la chaîne et les substituants sur l'azote. Pour ce qui est de la longueur, il semble qu'une chaîne de deux carbones soit idéale. La totalité des composés isolés de type chélaté comprennent un bras de deux carbones, mais en plus de cela, ils possèdent des substituants peu encombrants (par exemple, la coordination de N-iPr$_2$ est défavorisée).

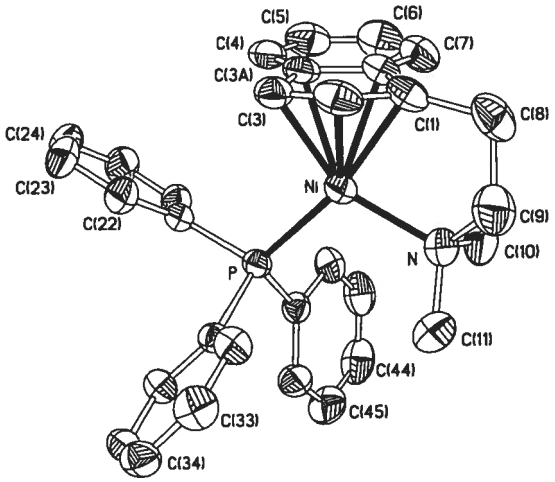

Figure 8.2. Dessin ORTEP de [(η^3:η^1-Ind(CH_2)$_2$$NMe_2$)Ni($PPh_3$)]$^+$

Lorsque les substituants sont trop encombrants ou lorsque la chaîne est trop longue, des composés avec le bras non-chélaté sont obtenus. Dans ces cas là, l'espèce

cationique de nickel formée est très électrophile et instable. Elle arrachera donc une phosphine à un de ses congénères pour former une espèce bis-phosphine cationique. On peut cependant noter que dans certains cas, les deux espèces, chélatée et bis-phosphine, cohabitent en équilibre en solution.

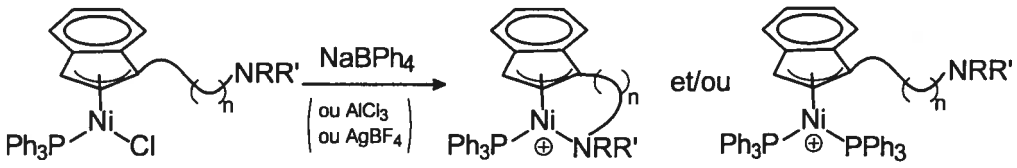

Schéma 8.4. Préparation des espèces cationiques

Le fait que les deux espèces peuvent se retrouvent en équilibre a permis d'evaluer la force du lien Ni-N. En fait, la réaction du cation chélaté avec divers ligands neutres a permis de classer les composés en fonction de la labilité du bras. Pour se faire, la réaction avec la pyridine a donné le plus d'information (Schéma 8.5) et a permis d'établir l'ordre suivant en commençant par le moins labile : $[(\eta^3:\eta^1\text{-IndCH}_2\text{Py})\text{Ni(PPh}_3)]^+$ (décomposition avant la décoordination) < $[(\eta^3:\eta^1\text{-Ind(CH}_2)_2\text{NMe}_2)\text{Ni(PPh}_3)]^+$ ($K_{eq} = 9$) < $[(\eta^3:\eta^1\text{-Ind(CH}_2)_2\text{Pyrrolidine)Ni(PPh}_3)]^+$ ($K_{eq} = 33$) < $[(\eta^3:\eta^1\text{-Ind(CH}_2)_2\text{NMe}_2)\text{Ni(PMe}_3)]^+$ ($K_{eq} = 41$) < $[(\eta^3:\eta^1\text{-Ind(CH}_2)_2\text{NMe}_2)\text{Ni(PCy}_3)]^+$ (réaction complète avec 1 équivalent de pyridine).

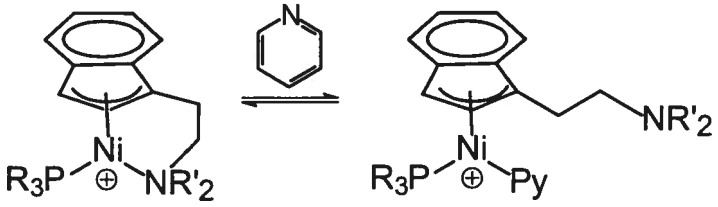

Schéma 8.5. Équilibre avec la pyridine

Comme on peut le constater, l'ordre dépend du bras, et donc de la capacité de l'amine à créer un lien fort avec le nickel, ainsi que de la phosphine impliquant alors la richesse électronique du métal et l'encombrement de ce dernier. Les deux phénomènes

jouent un rôle primordial dans les réactions catalytiques qui ont été testées, montrant la nécessité de la décoordination du bras pour libérer un site de coordination sur le métal.

Certains de ces composés ont également été étudiés à l'état solide afin de déterminer les implications structurales de la chélation du bras. Dans les trois structures obtenues, on peut constater que la coordination de l'indényle change. En effet, la coordination du bras diminue la distance Ni-C1 alors que Ni-C3 s'allonge. De plus, l'angle N-Ni-C1 est maintenant d'environ 84 ° alors que dans les composés neutres, il est plus grand et proche de 96 °. Ces observations impliquent réellement une contrainte non-négligeable lorsque le bras se coordonne et expliquent en partie sa capacité à se décoordonner.

En parallèle, les études électrochimiques montrent également la capacité de donner des amines avec une exception : la pyridine, qui semble la plus fortement liée, mais qui donne lieu au composé le moins riche en électrons. Dans ce cas, on a proposé qu'une rétrodonation du métal au ligand augmenterait la force du lien tout en diminuant la densité électronique du metal.

La donation des phosphines dans ces composés cationique suit la tendance établie, soit $PPh_3 < PCy_3 < PMe_3$.

8.3 Caractérisation

La série de composés obtenus a permis une meilleure compréhension des interactions métal-ligand (M-L). Le comportement global de ces composés nickel-indényle a provoqué une certaine surprise. En effet, si on considère les composés avec PPh_3 et le ligand $Ind(CH_2)_2NMe_2$, on remarque une concertation dans la force des liens M-L avec la capacité de donner de la densité électronique du troisième ligand ou ligand X (N, Cl, CCPh ou Me). Plus ce dernier est capable d'enrichir le métal plus la phosphine et l'indényle seront fortement liés au métal donnant accès à une plus grande richesse électronique tel que constaté par les mesures électrochimiques. Alors que si le ligand X est un moins bon donneur, les autres ligands seront eux aussi moins fortement liés.

Comme on peut le voir dans le Tableau 8.1, le méthyle, connu comme le meilleur donneur de la série, donne lieu au composé avec la plus grande richesse électronique, c'est à dire avec le potentiel de réduction le plus négatif. La phosphine, dans ce cas,

présente la plus petite distance Ni-P et le déplacement chimique le plus élevé représentatif de la plus forte interaction. De même, l'indényle possède la plus petite valeur de Δ(M-C), indiquant une coordination plus proche d'une hapticité de cinq, donc fortement donneur.

À l'inverse, le cation avec l'amine coordonnée possède la plus faible densité électronique avec également le lien Ni-P le plus faible (distance la plus longue et le déplacement chimique le plus faible) et l'indène possède un Δ(M-C) élevé indiquant une coordination plus proche d'une hapticité de trois. Les composés avec le chlore et l'alcynyle se situent entre ces deux extrêmes en gardant l'ordre selon leur capacité à donner de la densité électronique au métal, le chlorure étant moins bon que l'alcynyle.

Tableau 8.1. Influence du ligand X

	X	Δ(M-C) (Å)	Ni-P (Å)	δ (ppm)	E_{red} (V)
$[(\eta^3{:}\eta^1\text{-Ind}(CH_2)_2NMe_2)Ni(PPh_3)]^+$	N	0.26	2.197	29.1	-1.16
$(\eta^3{:}\eta^0\text{-Ind}(CH_2)_2NMe_2)Ni(PPh_3)X$	Cl	0.23	2.184	30.8	-1.41
$(\eta^3{:}\eta^0\text{-Ind}(CH_2)_2NMe_2)Ni(PPh_3)X$	CCPh	0.21	2.157	38.8	-1.72
$(\eta^3{:}\eta^0\text{-Ind}(CH_2)_2NMe_2)Ni(PPh_3)X$	Me	0.18	2.128	46.9	-2.33

Ce comportement quelque peu surprenant, peut être expliqué par la théorie des acides et des bases mous et durs qui dit que les métaux durs forment de bonnes liaisons avec les ligands durs et que les métaux mous ont une meilleure affinité avec les ligands mous. Ainsi, dans notre cas, lorsque le méthyle est coordonné au nickel, il lui donne beaucoup de densité électronique ce qui rend le métal plus mou. Comme la phosphine et l'indényle sont des ligands mous, leurs liens avec le centre métallique vont se renforcer tel qu'observé. Par contre, en présence du cation avec l'amine (ligand dur), le nickel est rendu plus dur à cause de la charge positive. Les liens qu'il fait avec la phosphine et l'indène sont ainsi affaiblis à cause de la diminution de leur compatibilité. Le comportement observé pour les composés avec le chlorure et l'alcynyle cadre parfaitement avec cette explication.

De plus, les mêmes observations peuvent être faites avec les composés comportant une autre phosphine mais la série est composée d'un plus petit nombre d'exemples.

8.4 Réactivité des composés

Cette série de composés neutres et cationiques forme un groupe intéressant de catalyseurs potentiels. En effet, les composés neutres permettent de poursuivre la chimie des composés nickel-indényle sans bras fonctionnalisé, et donnent la possibilité de déterminer l'influence de ces ligands hémilabiles.

On a ainsi pu voir que la présence d'un bras influençait grandement la réactivité : l'activité des catalyseurs et la qualité des produits obtenus changent lorsqu'un bras amino est greffé sur l'indényle, comme on peut le voir dans le chapitre 3 pour la polymérization du styrène et du norbornène ainsi que leur copolymérisation, et dans le chapitre 4 pour la polymérisation de l'éthylène. L'amine sur le bras interagit avec le centre métallique et les initiateurs (coordination N-Ag^+, N-$AlMe_3$ et N-MAO).

D'un autre côté, des résultats très similaires à ceux obtenus avec le 1-Me-Indényl pour la déhydropolymérisation du phénylsilane confirment une des propositions faites par Dr. F.-G. Fontaine qui envisageait une élimination de l'indène au début de la réaction.

Les composés cationiques, quant à eux, ont montré encore mieux la justesse de l'utilisation de ces ligands hémilabiles. En effet, comme démontré par des réactions non-catalytiques de substitution de ligands, le bras peut se décoordonner et libérer un site sur le nickel cationique, électrophile. Ainsi, ces cations ont permis de polymériser le styrène avec une très bonne activité. On a pu passer d'oligomères visqueux (2000 Da.) à du polystyrène solide (200 000 Da.) en ajoutant le bras amine. Une explication pour cela est justement la présence de ce bras fonctionnalisé qui augmente la densité électronique du métal et diminue le nombre d'élimination β-H du polymère. De plus, ces catalyseurs ont l'avantage de ne pas avoir besoin d'activateur et d'être modulable en fonction de l'amine utilisée, de la phosphine sur le nickel ainsi que de la température à laquelle ont lieu les réactions.

Par contre, contrairement à ces réactions de polymérisation, la polymérisation de l'éthylène n'a pas pu être observée qu'en présence de MAO ou $AlMe_3$. Le composé

$[(\eta^3{:}\eta^1\text{-Ind}(CH_2)_2NMe_2)Ni(PPh_3)]^+$ est très actif dans la dimérisation de l'éthylène en butène. Avec ce résultat, on a pu confirmer que le butène obtenu jusqu'alors avec les composés nickel indényle lors des expériences de polymérisation de l'éthylène était produit par un nickel cationique alors que le polyéthylène (environ 5% de l'éthylène consommé) était produit par une autre espèce.

Finalement, ces cations se sont montrés efficaces dans des réactions d'hydrosilylation des oléfines, le silane réagissant d'abord avec le composé pour ensuite s'ajouter sur l'oléfine. Par contre, leur utilisation comme acide de Lewis dans la réaction de Diels-Alder n'a pas été concluante. Il semble que les substrats utilisés aient provoqué la décomposition du catalyseur sans qu'il y ait eu de couplage.

8.5 Ligands phosphine-indényle et oléfine-indényle

Des ligands indényles comprenant un bras avec une phosphine ou une oléfine en bout de chaîne ont pu être synthétisés et complètement caractérisés. Lors du travail avec les ligands contenant une phosphine, une attention toute particulière doit être prise pour éviter l'oxydation de cette dernière. Cela peut se faire en n'exposant jamais ces ligands à l'air ou alors en les protégeant avec BH_3 ou H^+.

Bien qu'un composé comportant le ligand protégé ait pu être isolé par les voies de synthèse habituelles, cette partie du projet n'a pas eu grand succès car en aucun cas, nous n'avons été capable d'isoler un composé stable.

Par contre, l'utilisation des ligands ayant une oléfine a permis la préparation de composés stables. Leur étude fait maintenant partie du projet de maîtrise de Daniel Gareau, étudiant du professeur Davit Zargarian.

8.6 Perspectives futures

La plupart des objectifs proposés lors de l'établissement du projet ont été atteints. Ainsi, une étude approfondie de l'utilisation des ligands indényles hémilabiles a pu être menée à bien et a permis l'isolation de ligands fonctionnalisés (Ind^L avec L = ligand donneur, typiquement NRR', PRR' et C=C; alors que ^ = chaîne aliphatique de longueur variable). Les composés avec une amine ont été largement étudiés et divisés en deux types, les composés neutres avec le bras non-coordonné et les composés cationiques avec

le bras chélaté. Ils ont été complétement caractérisés en solution et à l'état solide et leur réactivité étudiée.

Par contre, le projet offre encore quelques bonnes possibilités pour compléter notre compréhension du sujet. Par exemple, on a vu que les différents bras ou phosphine changeaient de façon importante la réactivité lors de la polymérisation du styrène mais une étude complète de la polymérisation de l'éthylène n'a pas pu être achevée, en partie dû au fait que ces expériences ne peuvent pas être menées dans nos laboratoires par manque d'équipement.

Il serait également bon de pouvoir exploiter le potentiel de nos cations (**A**) à dimériser l'éthylène de façon très efficace. En effet, couplé avec un catalyseur (**B**) capable de co-polymériser des α-oléfines avec l'éthylène, du polyéthylène branché (LLDPE) pourrait être préparé sans avoir à ajouter du butène ou propène qui sont relativement plus chers que l'éthylène (Schéma 8.6).

Ce genre d'approche offre l'avantage de pouvoir produire à faible coût un polymère très utile car il est plus facilement façonnable que le polyéthylène linéaire (HDPE). En effet, les branches ainsi disposées le long de la chaîne principale diminuent la cristallinité du polymère. D'un autre côté, le LLDPE garde une plus grande résistance et robustesse que le polyéthylène de basse densité (LDPE) ce qui en motive la préparation.

Cependant, il est évident que si on veut pouvoir tout mettre dans le même réacteur, il faut que le second catalyseur (**B**) :

- Soit compatible chimiquement avec le premier (**A**)
- Fonctionne dans les mêmes conditions (T, P, activateur, solvant,...)
- Puisse insérer la majeur partie du butène produit dans le polymère.

Si ce n'est pas le cas, les deux réactions peuvent être faites dans des réacteurs séparés. Dans le réacteur **A**, le butène est produit pour ensuite être introduit dans le réacteur **B** où il sera copolymérisé avec l'éthylène par le catalyseur **B**. Ce type d'approche est étudié par Bazan *et al.*[91] qui en a démontré la puissance.

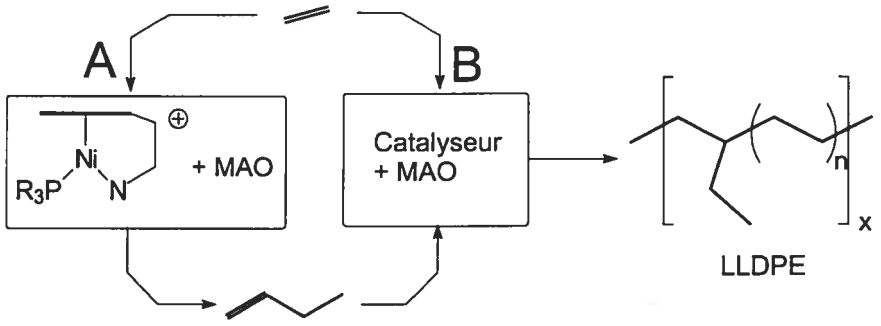

Schéma 8.6. Catalyse en tandem

D'un autre côté, on a pu constater que l'utilisation du ligand $IndCH_2Py$ donnait les meilleurs résultats dans la polymérisation du styrène et que le remplacement de la PPh_3 par la PMe_3 améliorait également la réactivité et la masse moléculaire du polymère. Il serait donc relativement facile de préparer le composé $[(\eta^3:\eta^1\text{-}IndCH_2Py)Ni(PMe_3)]^+$ afin de voir si ces deux améliorations sont compatibles et si leur combinaison forme un meilleur catalyseur.

Dans cette thèse, des études préliminaires ont montré que les composés cationiques permettaient la catalyse de réactions organiques comme l'hydrosilylation des oléfines (styrène et 1-hexène) avec une bonne régiosélectivité. Il serait donc très pertinent de voir jusqu'où on peut aller en matière d'oléfine (encombrement, effet électronique) ainsi que d'autres substrats tels que les cétones, les imines et les alcènes. Les produits de l'hydrosilylation des oléfines, cétones et imines peuvent alors donner accès à des alcools ou des amines chirales,[92] alors que pour les alcynes, une hydrosilylation simple donnerait accès à des vinyles silane, produits importants en chimie organique.[93] De plus, les études se sont limitées au phényle- et diphényle- silane, il serait bon de tester divers silanes.

Finalement, l'étude des composés avec des ligands comportant un bras oléfine a déjà trouvé preneur. Daniel tentera de démystifier la liaison Ni-oléfine en préparant des cations avec l'oléfine coordonnée. Il va alors pouvoir faire réagir des substrats avec cette oléfine pour étudier les mécanismes de l'hydrosilylation, de la polymérisation d'oléfine,etc.

Références

(1) Pearson, R. G. *J. Am. Chem. Soc.* **1963**, *85*, 3533.

(2) a) Eisenberg, A.H.; Ovchinnikov, M. V.; Mirkin, C. A. *J. Am. Chem. Soc.* **2003**, *125*, 2836. b) Holliday, B. J.; Jeon, Y.-M.; Mirkin, C. A.; Stren, C. L.; Incarvito, C. D.; Zakharov, L. N.; Sommer, R. D.; Rheingold, A. L. *Organometallics*, **2002**, *21*, 5713.

(3) Kuriyama, M.; Nagai, K.; Yamada, K.-I.; Miwa, Y.; Taga, T.; Tominoka, K. *J. Am. Chem. Soc.* **2002**, *124*, 8932.

(4) Rülke, R. E.; Kaasjager, V. E.; Wehman, P.; Elsevier, C. J.; van Leeuwen, P. W. N. M.; Vrieze, K.; Fraanje, J.; Goubitz, K.; Spek, A. L. *Organometallics*, **1996**, *15*, 3022.

(5) a) Jutzi, P.; Kristen, M. O.; Dahlhaus, J.; Neumann, B.; Stammler, H.-G. *Organometallics*, **1993**, *12*, 2980. b) Jutzi, P.; Kristen, M. O.; Neumann, B.; Stammler, H.-G. *Organometallics*, **1994**, *13*, 3854.

(6) Indényles fonctionnalisés: a) Doehring, A.; Goehre, J.; Jolly, P. W.; Kryger, B.; Rust, J.; Verhoovnik, G. P. J. *Organometallics*, **2000**, *19*, 388. b) Ziniuk, Z.; Goldberg, I.; Kol, M. *J. Organomet. Chem.* **1997**, *545-546*, 441. c) Blais, M. S.; Chien, J. C. W.; Rausch, M. D. *Organometallics*, **1998**, *17*, 3775.

(7) Revues sur les ligands de type Cp^NRR' : a) Jutzi, P.; Redeker, T. *Eur. J. Inorg. Chem.* **1998**, 663. b) Jutzi, P.; Siemeling, U. *J. Organomet. Chem.* **1995**, *500*, 175. c) Jutzi, P.; Dahlaus, J. *Coord. Chem. Rev.*, **1994**, *137*, 179.

(8) Revue sur les ligands de type Cp^PRR', Cp^AsRR' et Cp^SR : Butenschoen, H. *Chem. Rev.* **2000**, *100*, 1527.

(9) a) Revue sur les ligands de type Cp^OR : Siemeling, U. *Chem. Rev.* **2000**, *100*, 1495. b) Revue sur les ligands de type Cp fonctionnalisés : Müller, C.; Vos, D.; Jutzi, P. *J. Organomet. Chem.* **2000**, *600*, 127.

(10) Pour un récit historique de sa découverte voir Roberts, H. L. *J. Organomet. Chem.* **1999**, *372*, 1.

(11) a) Gibson, V. C.; Spitzmesser, S. K. *Chem. Rev.* **2003**, *103*, 283 et références incluses dans cette revue. b) Fontaine, F.-G. Thèse de doctorat, Université de Montréal, **2002**.

(12) Keim, W et al. (Shell Dev.) US patents 3 635 937, 3 686 159, 3 644 563 et 3 647 914, 1972.

(13) Johnson, L. K.; Killian, C. M.; Brookhart, M. *J. Am. Chem. Soc.* **1995**, *117*, 6414.

(14) a) Wang, C.; Friedrich, S.; Younkin, T. R.; Li, R. T.; Grubbs, R. H.; Bansleben, D. A.; Day, M. W. *Organometallics*, **1998**, *17*, 3149. b) Younkin, T. R.; Connor, E. F.; Henderson, J. I.; Friedrich, S.; Grubbs, R. H.; Bansleben, D. A. *Science*, **2000**, *287*, 460.

(15) Smith, A. K. dans Abel, E. W.; Stone, F. G. A.; Wilkinson, G.; Puddephatt, R. J. « Comprehensive Organometallic Chemistry II », vol 6, Pergamon, Oxford, **1995**, 29.

(16) a) Goodall, B. L.; Benedikt, G. M.; McIntosh, L. H.; Barnes, D. A. US Patent-5 468 819, 1995. b) Goodall, B. L.; Benedikt, G. M.; McIntosh, L. H.; Barnes, D. A.; Rhodes, L. F. US Patent-5 571 881, 1995. c) Lee, B. Y.; Kim, Y. H.; Shin, H. J.; Lee, C. H. *Organometallics*, **2002**, *21*, 3481. d) Janiak, C.; Lassahn, P. G. *J. Mol. Catal. A: Chem.* **2001**, *166*, 193.

(17) Bonnet, M. C.; Dahan, F.; Ecke, A.; Keim, W.; Schulz, R. P.; Tkatchenko, I. *J. Chem. Soc., Chem. Commun.*, **1994**, 615.

(18) Flid, V. R.; Kuznetsov, V. B.; Grigor'ev, A. A.; Belov, A. P. *Kinetics and Catalysis,* **2000**, *41*(5), 604.

(19) Aresta, M.; Dibenedetto, A.; Quaranta, E. *Organometallics*, **2000**, *19*, 4199.

(20) a) Johnson, L. K.; Wang, L.; McCord, E.F. (E.I. Du Pont De Nemours and Co., USA). PCT Int. Appl. Wo0192354, 2001; *Chem. Abstr.* **2002**, *136*, 20356. b) Johnson, L. K.; Bennett, A. M. A.; Dobbs, K. D.; Ionkin, A. S.; Ittel, S. D.; Wang, Y.; Radzewich, C. E.; Wang, L. (E.I. Du Pont De Nemours and Co., USA). PCT Int. Appl. Wo0192347, 2001; *Chem. Abstr.* **2002**, *136*, 20365. c) Wang, L.; Hauptman, E.; Johnson, L. K.; McCord, E. F.; Wang, Y.; Ittel, S. D. (E.I. Du Pont De Nemours and Co., USA). PCT Int. Appl. Wo0192342, 2001.; *Chem. Abstr.* **2002**, *136*, 20364.

(21) Pour une discussion sur les débuts du nickelocène voir: Werner, H *J. Organomet. Chem.* **1980**, *200*, 335.

(22) Pasynkiewicz, S.; Pietrzykowski, A. *Coord. Chem. Rev.* **2002**, *231*, 199.

(23) Robbins, J. L.; Robbins, N.; Spencer, B.; Smart, J. C. *J. Am. Chem. Soc.* **1982**, *104*, 1882.

(24) Chetcuti, M. J. dans Abel, E. W.; Stone, F. G. A.; Wilkinson, G.; Puddephatt, R. J. « Comprehensive Organometallic Chemistry II », vol 6, Pergamon, Oxford, **1995**, 107.

(25) Jutzi, P.; Schnittger, J.; Wieland, W.; Neumann, B.; Stammler, H.-G. *J. Organomet. Chem.* **1991**, *415*, 425.

(26) Sitzmann, H. *Coord. Chem. Rev.* **2001**, *214*, 287.

(27) Barefield, E. K.; Krost, D. A.; Edwards, D. S.; Van Derveer, D. G.; Trytko, R. L.; O'Rear, S. P. *J. Am. Chem. Soc.* **1986**, *108*, 6219.

(28) Yamazaki, H.; Nishido, T.; Matsumoto, Y.; Sumida, S.; Hagihara, M. *J. Organomet. Chem.* **1966**, 86.

(29) Barnett, K. W. *J. Chem. Edu.* **1974**, *51*, 422.

(30) a) Zhan, X.; Xu, S.; Yang, M.; Lei, Z. *Catal. Lett.* **2002**, *80*, 59. b) Douglas, W. E. *Applied Organomet. Chem.* **2001**, *15*, 23. c) Douglas, W. E. *J. Chem. Soc., Dalton.* **2000**, *1*, 57.

(31) Takei, F.; Tung, S.; Yanai, K.; Onitsuka, K.; Takahashi, S. *J. Organomet. Chem.* **1998**, *559*, 91.

(32) Ihara, E.; Fujimura, T.; Yasuda, H.; Maruo, T.; Kanehisa, N.; Kai, Y. *J. Poly. Sci., A: Poly. Chem.* **2000**, 39.

(33) Holland, P. J.; Andersen, R. A.; Bergman, R. G.; Huang, J.; Nolan, S. P. *J. Am. Chem. Soc.* **1997**, *119*, 12800.

(34) a) Kiso, Y.; Tamao, K.; Kumada, M. *J. Organomet. Chem.* **1974**, *76*, 95. b) Thomson, J.; Baird, M. C. *Inog. Chim. Acta* **1973**, *7*, 105.

(35) a) Van den Akker, M.; Jellinek, F. *J. Organomet. Chem.* **1967**, 10. b) Thomson, J.; Baird, M. C. *Inog. Chim. Acta*, **1973**, *7*, 105.

(36) a) Gallagher, J. F.; Butler, P.; Hudson, R. D. A.; Manning, A. *J. Chem. Soc., Dalton Trans.* **2002**, 75. b) Douglas, W. E. *Applied Organomet. Chem.* **2001**, *15*, 23. c) Takei, F.; Tung, S.; Yanai, K.; Onitsuka, K.; Takahashi, S. *J. Organomet. Chem.* **1998**, 559, 91.

(37) a) Weiss, J. Priermeier, T.; Fischer, R. A. *Inorg. Chem.* **1996**, *35*, 71. b) Weiss, J.; Frank, A.; Herdtweck, E.; Nlate, S.; Mattner, M.; Fischer, R. A. *Chem. Ber.* **1996**, *129*, 297.

(38) Nevondo, F. A.; Crouch, A. M.; Darkwa, J. *J. Chem. Soc., Dalton Trans.* **2000**, 43.

(39) Hernandez, E.; Royo, P. *J. Organomet. Chem.* **1985**, *291*, 387.

(40) Thomson, J.; Baird, M. C. *Can. J. Chem.* **1973**, 51.

(41) Holland, P. J.; Smith, M. E.; Andersen, R. A.; Bergman, R. G. *J. Am. Chem. Soc.* **1997**, *119*, 12815.

(42) Zargarian, D. *Coord. Chem. Rev.* **2002**, *233-234*, 157.

(43) Fritz, H. P.; Köhler, K. E.; Schwarzhans, K. E. *J. Organomet. Chem.* **1969**, 449.

(44) Westcoll, S. A.; Kakkar, A. K.; Stringer, G.; Taylor, N. J.; Marder, T. B. *J. Organomet. Chem.* **1990**, *394*, 777.

(45) Schroll, G. E. US patent-3 054 815, 1962.

(46) Hart-Davis, A. J.; Mawby, R. J. *J. Chem. Soc. A* **1969**, 2403.

(47) Pevear, K. A.; Banaszak Holl, M. M.; Carpenter, A. L.; Rieger, P. H.; Sweigart, D. A. *Organometallics*, **1995**, *14*, 212.

(48) Stradiotto, M.; McGlinchey, M. J. *Coord. Chem. Rev.* **2001**, *219-221*, 311.

(49) a) Baker, R. T.; Tulip, T. H. *Organometallics*, **1986**, *5*, 839. b) Westcott, S. A.; Kakkar, A.; Stringer, G.; Taylor, N. J.; Marder, T. B. *J. Organomet. Chem.* **1990**, *394*, 777.

(50) Forschner, T. C.; Cutler, A. R.; Kullnig, R. K. *Organometallics*, **1987**, *6*, 889.

(51) Köhler, F. H. *Chem. Ber.* **1974**, *107*, 570.

(52) Merola, J. S.; Kacmarcik, R. T.; Engen, D. V. *J. Am. Chem. Soc.* **1986**, *108*, 329.

(53) a) Groux, L. F.; Zargarian, D.; Simon, L. C.; Soares, J. B. P. *J. Mol. Catal. A: Chem.* **2003**, 51. b) Dubois, M.-A.; Wang, R.; Zargarian, D.; Tian, J.; Vollmerhaus, R.; Li, Z.; Collins, S. *Organometallics*, **2001**, *20*, 663. c) Groux, L. F.; Zargarian, D. *Organometallics*, **2001**, *20*, 3811. d) Vollmerhaus, R.; Bélanger-Gariépy, F.; Zargarian, D. *Organometallics*, **1997**, *16*, 4762.

(54) a) Wang, R.; Groux, L. F.; Zargarian, D. *J. Organomet. Chem.* **2002**, *660*, 98. b) Wang, R.; Groux, L. F.; Zargarian, D. *Organometallics*, **2002**, *21*, 5531. c) Wang, R.; Bélanger-Gariépy, F.; Zargarian, D. *Organometallics*, **1999**, *18*, 5548.

(55) a) Fontaine, F.-G.; Kadkhodazadeh, T.; Zargarian, D. *J. Chem. Soc., Chem. Commun.* **1998**, 1253. b) Fontaine, F.-G.; Zargarian, D. *Organometallics*, **2002**, *21*, 401.

(56) a) Fontaine, F.-G. Thèse de Doctorat, Université de Montréal, **2002**. b) Fontaine, F.-G.; Nguyen, R.-V.; Zargarian, D. *Can. J. Chem.* **2003**, *article soumis.*

(57) Fontaine, F.-G.; Dubois, M.-A.; Zargarian, D. *Résultats non publiés.*

(58) Charrier, C.; Mathey, F. *J. Organomet. Chem.* **1979**, *170*, C41.

(59) Kauffmann, T.; Ennen, J.; Lhotak, H.; Rensing, A.; Steinseifer, F.; Woltermann, A. *Angew. Chem. Int. Ed. Engl.* **1980**, *19*, 328.

(60) a) Doehring, A.; Jensen, V. R.; Jolly, P. W.; Thiel, W.; Weber, J. C. *Organometallics*, **2001**, *20*, 2234. b) Brookings, D. C.; Harrison, S. A.; Whitby, R. J. *Organometallics*, **2001**, *20*, 4574. c) Kataoka, Y.; Shibahara, A.; Yamagata, T.; Tani, K. *Organometallics*, **2001**, *20*, 2431. d) Kataoka, Y.; Iwato, Y.; Shibahara, A.; Yamagata, T.; Tani, K. *Chem. Commun.* **2000**, 841. e) Kataoka, Y.; Iwato, Y.; Yamagata, T.; Tani, K. *Organometallics*, **1999**, *18*, 5423. f) Kataoka, Y.; Shibahara, A.; Saito, Y.; Yamagata, T.; Tani, K. *Organometallics*, **1998**, *17*, 4338. g) Kataoka, Y.; Saito, Y.; Shibahara, A.; Tani, K. *Chem. Lett.* **1997**, 621. h) Kataoka, Y.; Saito, Y.; Nagata, K.; Kitamura, K.; Shibahara, A.; Tani, K. *Chem. Lett.* **1995**, 833.

(61) a) Bosch, B. E.; Erker, G.; Froelich, R; Meyer, O. *Organometallics*, **1997**, *16*, 5449. b) Krut'ko, D. P.; Borzov, M. V.; Veksler, E. N.; Churakov, A. V.; Howard, J. A. K. *Polyhedron* **1998**, *15*, 3889. c) Kettenbach, R. T.; Bonrath, W.; Butenschoen, H. *Chem. Ber.* **1993**, *126*, 1657.

(62) a) Fryzuk, M. D.; Mao, S. S.; Zaworotko, M. J.; MacGillivray, L. R. *J. Am. Chem. Soc.* **1993**, *115*, 5336. b) Fryzuk, M. D.; Duval, P. B.; Mao, S. S.; Rettig, S. J.; Zaworotko, M. J.; MacGillivray, L. R. *J. Am. Chem. Soc.* **1999**, *121*, 1707 et les références inclues dans cet article. c) Barthel-Rosa, L. P.; Catalano, V. J.; Maitra, K.; Nelson, J. H. *Organometallics*, **1996**, *15*, 3924.

(63) Cowley, A. H.; King, C. S.; Decken, A. *Organometallics*, **1995**, *14*, 20.

(64) Leblanc, J. C.; Moise, C.; Maisonnat, A.; Poilblanc, R.; Charrier, C.; Mathey, F. *J. Organomet. Chem.* **1982**, *231*, C43.

(65) Lee, I.; Dahan, F.; Maisonnat, A.; Poilblanc, R. *Organometallics*, **1994**, *13*, 2743.

(66) a) Foerstner, J.; Kettenbach, R.; Goddard, R.; Butenschoen, H. *Chem. Ber.* **1996**, *129*, 319. b) Wang, T.-F.; Juang, J.-P.; Wen, Y.-S. *J. Organomet. Chem.* **1995**, *503*, 117.

(67) Kettenbach, R.; Butenschoen, H. *New. J. Chem.* **1990**, *14*, 599.

(68) Matos, R. M.; Nixon, J. F.; Okuda, J. *Inorg. Chim. Acta* **1994**, *222*, 13.

(69) Galakhov, M. V.; Heinz, G.; Royo, P. *Chem. Commun.* **1998**, 17.

(70) Lehmkuhl, H.; Naeser, J.; Mehler, G.; Keil, T.; Danowski, F.; Benn, R.; Mynott, R.; Schroth, G.; Gabor, B.; Krueger, C.; Betz, P. *Chem. Ber.* **1991**, *124*, 441.

(71) Tolman, C. A. *J. Am. Chem. Soc.* **1970**, *92*, 2956.

(72) Wood, J. C.; Elofson, M.; Saunders, D. M. *Anal. Chem.* **1958**, *30*, 1339.

(73) a) Pye, P. J.; Rossen, K.; Reamer, A.; Tsou, N. N.; Volante, R. P.; Reider, P. J. *J. Am. Chem. Soc.* **1997**, *119*, 6207. b) Imamoto, T.; Kusumoto, T.; Suzuki, N.; Sato, K. *J. Am. Chem. Soc.* **1985**, *107*, 5301. c) Marsi, K. L. *J. Org. Chem.* **1974**, *39*, 265.

(74) Groux, L. F.; Zargarian, D. *Acta Cryst.* **2000**, *C56*, e366.

(75) Huber, T. A.; Bélanger-Gariépy, F.; Zargarian, D. *Organometallics*, **1995**, *14*, 4997.

(76) Zargarian, D. *Résultats non publiés.*

(77) Klein, H.-F.; Schmidbaur, H. *Angew. Chem. Int. Ed. Engl.* **1970**, *9*, 903.

(78) Dahl, O. *Acta Chem. Scand.* **1969**, *23*, 2342.

(79) Pour un récit historique sur Wilhelm Schlenk voir: Tidwell, T. T. *Angew. Chem. Int. Ed. Engl.* **2001**, *40*, 331.

(80) Barnett, K. W. *J. Chem. Edu.* **1974**, *51*, 422.

(81) Laird, G. L. *Inorg. Synth.* **1971**, *13*, 154.

(82) Wood, J. C.; Elofson, M.; Saunders, D. M. *Anal. Chem.* **1958**, *30*, 1339.

(83) Kauffmann, T.; Berghus, K.; Rensing, A.; Ennen, J. *Chem. Ber.* **1985**, *118*, 3747.

(84) Cassidy, J. M.; Whitmire, K. H. *Acta Cryst.* **1991**, *C47*, 2094.

(85) CAD-4 Software. Version 5.0. Enraf-Nonius, Delft, The Netherlands, 1989.

(86) Gabe, E. J.; Le Page, Y.; Charlant, J.-P.; Lee, F. L.; White, P. S. *J. Appl. Crystallogr.* **1989**, *22*, 384.

(87) Sheldrick, G.M. *SHELXS*. Program for the Solution of Crystal Structures. University of Goettingen, Germany, 1997.

(88) Sheldrick, G.M. *SHELXL*. Program for the Refinement of Crystal Structures. University of Goettingen, Germany, 1996

(89) Shelxtl Nt ver. 5.10; Program for the Solution of Crystal Structures, Bruker AXS Inc., Madison, WI 53719-1173, 1999.

(90) a) Groux, L. F.; Bélanger-Gariépy, F.; Zargarian, D. *Acta Cryst*, **2001**, *E57*, m547. b) Groux, L. F.; Zargarian, D. *Organometallics*, **2003**, *accepté*.

(91) Komon, Z. J. A.; Bazan, G. C. *Macromol. Rapid. Commun.* **2001**, *22*, 467.

(92) a) Reichl, J. A.; Berry, D. H. *Adv. Organomet. Chem.* **1999**, *43*, 197. b) Hayashi, T. *Comprehensive Asymmetric Catalysis,* Jacobsen, E. N.; Pfaltz, A.; Yamamoto, H. Eds. Berlin, 1999, chap. 7.

(93) Fleming, I.; Donogues, J.; Smithers, R. *Org. React.* **1989**, *37*, 57.

Annexes

Annexe I

Données cristallographiques supplémentaires, article 1

Table I.1. Crystal data and structure refinement for (η^3:η^0-Ind$(CH_2)_3$NH*t*Bu)$(PPh_3)NiCl.CH_2Cl_2$ **(7)**

Chemical formula	C35 H39 Cl3 N Ni P
Chemical formula weight	669.73
Temperature	293(2) (K)
Wavelength	1.54056 Å
Crystal system	Triclinic
Space group	P -1
Unit cell dimensions	a = 9.190(3) Å α = 90.24(6)° b = 10.383(12) Å β = 92.10(3)° c = 19.556(9) Å γ = 115.72(4)°
Volume	1680(2) $Å^3$
Z	2
Density calculated	1.324 Mg/m^3
Absorption coefficient	3.71 mm^{-1}
F(000)	700
Size	0.43 x 0.15 x 0.07 mm
Theta range for data collection	2.26 to 69.84°
Index ranges	$0 \le h \le 11$, $-12 \le k \le 11$, $-23 \le l \le 23$
Reflections collected	12523
Independent reflections	6366
Absorption correction	Integration
Max. and min. transmission	0.80 and 0.44
Refinement method	Full-matrix least-squares on F^2
Data / restraints / parameters	6366 / 54 / 374
Goodness-of-fit on F^2	0.880
Final R indices [I>2sigma(I)]	R_1 = 0.0820, wR_2 = 0.2037
R indices (all data)	R_1 = 0.1448, wR_2 = 0.2346
Extinction coefficient	0.0013(4)
Largest diff. peak and hole	0.538 and -0.619 e/$Å^3$

Table I.2. Atomic coordinates and equivalent isotropic displacement parameters ($Å^3 \times 10^2$) for $(\eta^3:\eta^0\text{-Ind}(CH_2)_3NHtBu)(PPh_3)NiCl.CH_2Cl_2$. (7)

	x	y	z	Ueq
Ni	0.25127(12)	0.49570(11)	0.71815(5)	5.03(4)
Cl	0.0214(2)	0.5049(2)	0.69495(9)	6.08(5)
P	0.1955(2)	0.2917(2)	0.66685(8)	4.47(4)
C(1)	0.3630(8)	0.6970(7)	0.7717(3)	5.6(2)
C(2)	0.3930(9)	0.5898(8)	0.8046(4)	6.6(2)
C(3)	0.4739(8)	0.5381(8)	0.7590(4)	6.4(2)
C(3A)	0.5205(8)	0.6352(8)	0.7019(4)	6.4(2)
C(4)	0.6151(9)	0.6446(10)	0.6462(5)	8.1(3)
C(5)	0.6367(11)	0.7477(12)	0.6009(5)	9.8(3)
C(6)	0.5656(11)	0.8425(11)	0.6056(4)	9.3(3)
C(7)	0.4690(9)	0.8309(8)	0.6607(4)	7.2(2)
C(7A)	0.4506(8)	0.7326(7)	0.7090(4)	5.4(2)
C(8)	0.2750(9)	0.7744(8)	0.8018(4)	6.8(2)
C(9)	0.3883(9)	0.9105(8)	0.8390(4)	7.0(2)
C(10)	0.2991(9)	0.9792(8)	0.8776(4)	7.5(2)
N(11)	0.4110(8)	1.1062(7)	0.9150(3)	9.4(2)
C(12)	0.343(2)	1.179(2)	0.9597(7)	7.3(2)
C(13)	0.481(2)	1.317(2)	0.9862(9)	11.7(7)
C(14)	0.268(2)	1.079(2)	1.0181(7)	8.7(5)
C(15)	0.216(2)	1.211(2)	0.9229(7)	9.1(5)
C(16)	0.353(3)	1.185(2)	0.9595(9)	7.3(2)
C(17)	0.310(2)	1.279(2)	0.9123(9)	7.8(6)
C(18)	0.490(2)	1.276(2)	1.0102(10)	8.4(7)
C(19)	0.209(3)	1.088(3)	0.9983(12)	12.4(11)
C(21)	0.0625(7)	0.1378(7)	0.7131(3)	4.8(2)
C(22)	0.0509(8)	0.0000(7)	0.7032(3)	5.6(2)
C(23)	-0.0537(9)	-0.1133(8)	0.7375(4)	6.7(2)
C(24)	-0.1502(9)	-0.0949(10)	0.7848(4)	7.5(2)
C(25)	-0.1417(9)	0.0389(10)	0.7957(4)	7.3(2)
C(26)	-0.0375(8)	0.1546(8)	0.7613(3)	6.0(2)
C(31)	0.3693(7)	0.2555(6)	0.6518(3)	5.1(2)
C(32)	0.4460(8)	0.2226(7)	0.7060(4)	6.3(2)
C(33)	0.5886(9)	0.2065(8)	0.6973(5)	7.5(2)
C(34)	0.6513(9)	0.2263(9)	0.6327(5)	8.1(3)
C(35)	0.5761(9)	0.2572(9)	0.5797(5)	8.0(3)
C(36)	0.4371(8)	0.2755(8)	0.5873(4)	6.7(2)
C(41)	0.0984(7)	0.2748(7)	0.5817(3)	4.9(2)
C(42)	-0.0242(8)	0.1449(7)	0.5562(3)	5.6(2)
C(43)	-0.0941(9)	0.1394(9)	0.4910(4)	7.0(2)
C(44)	-0.0449(9)	0.2585(9)	0.4528(4)	7.1(2)
C(45)	0.0759(9)	0.3857(8)	0.4772(3)	6.4(2)
C(46)	0.1454(9)	0.3938(8)	0.5422(3)	5.9(2)
C(50)	0.209(3)	0.592(2)	0.1379(11)	13.2(9)
Cl(51)	0.0449(10)	0.6003(9)	0.0914(4)	17.5(3)
Cl(52)	0.1828(8)	0.4116(7)	0.1200(3)	12.6(2)
C(60)	0.141(3)	0.544(2)	0.1409(11)	8.3(7)
Cl(61)	0.1331(12)	0.3935(10)	0.0961(5)	13.4(3)
Cl(62)	0.1318(11)	0.6751(10)	0.0860(4)	12.8(3)

Table I.3. Bond lengths (A) and angles (deg) for (η^3:η^0-Ind$(CH_2)_3$NHtBu)(PPh_3)NiCl.CH_2Cl_2. **(7)**

Ni-C(3)	2.028(6)	C(16)-C(19)	1.51(2)
Ni-C(2)	2.057(6)	C(16)-C(18)	1.53(2)
Ni-C(1)	2.135(6)	C(17)-H(17A)	0.960(4)
Ni-P	2.181(3)	C(17)-H(17B)	0.96
Ni-Cl	2.187(2)	C(17)-H(17C)	0.96
Ni-C(3A)	2.296(7)	C(18)-H(18A)	0.96
Ni-C(7A)	2.357(8)	C(18)-H(18B)	0.96
P-C(21)	1.806(7)	C(18)-H(18C)	0.96
P-C(31)	1.825(6)	C(19)-H(19A)	0.960(2)
P-C(41)	1.830(6)	C(19)-H(19B)	0.960(2)
C(1)-C(2)	1.409(10)	C(19)-H(19C)	0.96
C(1)-C(7A)	1.452(9)	C(21)-C(22)	1.399(9)
C(1)-C(8)	1.497(9)	C(21)-C(26)	1.403(9)
C(2)-C(3)	1.423(9)	C(22)-C(23)	1.353(9)
C(2)-H(2)	0.93	C(22)-H(22)	0.93
C(3)-C(3A)	1.456(10)	C(23)-C(24)	1.373(10)
C(3)-H(3)	0.93	C(23)-H(23)	0.93
C(3A)-C(4)	1.397(10)	C(24)-C(25)	1.373(11)
C(3A)-C(7A)	1.422(9)	C(24)-H(24)	0.93
C(4)-C(5)	1.344(13)	C(25)-C(26)	1.366(10)
C(4)-H(4)	0.93	C(25)-H(25)	0.93
C(5)-C(6)	1.402(13)	C(26)-H(26)	0.93
C(5)-H(5)	0.93	C(31)-C(32)	1.377(9)
C(6)-C(7)	1.393(11)	C(31)-C(36)	1.403(9)
C(6)-H(6)	0.93	C(32)-C(33)	1.408(9)
C(7)-C(7A)	1.353(10)	C(32)-H(32)	0.93
C(7)-H(7)	0.93	C(33)-C(34)	1.387(11)
C(8)-C(9)	1.506(9)	C(33)-H(33)	0.93
C(8)-H(8A)	0.97	C(34)-C(35)	1.342(11)
C(8)-H(8B)	0.97	C(34)-H(34)	0.93
C(9)-C(10)	1.516(9)	C(35)-C(36)	1.383(9)
C(9)-H(9A)	0.97	C(35)-H(35)	0.93
C(9)-H(9B)	0.97	C(36)-H(36)	0.93
C(10)-N(11)	1.447(9)	C(41)-C(46)	1.371(9)
C(10)-H(10A)	0.97	C(41)-C(42)	1.404(9)
C(10)-H(10B)	0.97	C(42)-C(43)	1.396(9)
N(11)-C(16)	1.45(2)	C(42)-H(42)	0.93
N(11)-C(12)	1.474(13)	C(43)-C(44)	1.356(10)
N(11)-H(111)	0.86	C(43)-H(43)	0.93
N(11)-H(112)	0.86	C(44)-C(45)	1.374(10)
C(12)-C(15)	1.50(2)	C(44)-H(44)	0.93
C(12)-C(14)	1.52(2)	C(45)-C(46)	1.387(9)
C(12)-C(13)	1.52(2)	C(45)-H(45)	0.93
C(13)-H(13A)	0.96	C(46)-H(46)	0.93
C(13)-H(13B)	0.96	C(50)-Cl(51)	1.77(2)
C(13)-H(13C)	0.96	C(50)-Cl(52)	1.81(2)
C(14)-H(14A)	0.960(2)	C(50)-H(50A)	0.97
C(14)-H(14B)	0.96	C(50)-H(50B)	0.97
C(14)-H(14C)	0.96	C(60)-Cl(61)	1.76(2)
C(15)-H(15A)	0.96	C(60)-Cl(62)	1.76(2)
C(15)-H(15B)	0.960(2)	C(60)-H(60A)	0.97
C(15)-H(15C)	0.96	C(60)-H(60B)	0.97
C(16)-C(17)	1.51(2)		
C(3)-Ni-C(2)	40.8(3)	C(2)-Ni-Cl	122.7(2)
C(3)-Ni-C(1)	67.0(3)	C(1)-Ni-Cl	95.8(2)
C(2)-Ni-C(1)	39.2(3)	P-Ni-Cl	98.13(9)
C(3)-Ni-P	99.2(2)	C(3)-Ni-C(3A)	38.7(3)
C(2)-Ni-P	130.6(2)	C(2)-Ni-C(3A)	63.8(3)
C(1)-Ni-P	166.0(2)	C(1)-Ni-C(3A)	62.6(2)
C(3)-Ni-Cl	162.4(2)	P-Ni-C(3A)	105.4(2)

Cl-Ni-C(3A)	137.4(2)
C(3)-Ni-C(7A)	63.9(3)
C(2)-Ni-C(7A)	63.1(3)
C(1)-Ni-C(7A)	37.3(2)
P-Ni-C(7A)	135.5(2)
Cl-Ni-C(7A)	105.2(2)
C(3A)-Ni-C(7A)	35.6(2)
C(21)-P-C(31)	103.6(3)
C(21)-P-C(41)	105.8(3)
C(31)-P-C(41)	104.0(3)
C(21)-P-Ni	114.0(2)
C(31)-P-Ni	115.4(2)
C(41)-P-Ni	113.0(2)
C(2)-C(1)-C(7A)	108.5(6)
C(2)-C(1)-C(8)	125.1(7)
C(7A)-C(1)-C(8)	125.9(7)
C(2)-C(1)-Ni	67.4(4)
C(7A)-C(1)-Ni	79.7(4)
C(8)-C(1)-Ni	125.2(5)
C(1)-C(2)-C(3)	108.7(7)
C(1)-C(2)-Ni	73.4(4)
C(3)-C(2)-Ni	68.6(4)
C(1)-C(2)-H(2)	125.7(4)
C(3)-C(2)-H(2)	125.7(5)
Ni-C(2)-H(2)	124.0(2)
C(2)-C(3)-C(3A)	106.6(6)
C(2)-C(3)-Ni	70.7(4)
C(3A)-C(3)-Ni	80.6(4)
C(2)-C(3)-H(3)	126.7(5)
C(3A)-C(3)-H(3)	126.7(4)
Ni-C(3)-H(3)	114.4(2)
C(4)-C(3A)-C(7A)	120.0(8)
C(4)-C(3A)-C(3)	131.5(8)
C(7A)-C(3A)-C(3)	108.6(6)
C(4)-C(3A)-Ni	131.0(5)
C(7A)-C(3A)-Ni	74.6(4)
C(3)-C(3A)-Ni	60.7(4)
C(5)-C(4)-C(3A)	117.6(9)
C(5)-C(4)-H(4)	121.2(6)
C(3A)-C(4)-H(4)	121.2(6)
C(4)-C(5)-C(6)	123.7(9)
C(4)-C(5)-H(5)	118.1(6)
C(6)-C(5)-H(5)	118.1(6)
C(7)-C(6)-C(5)	118.3(9)
C(7)-C(6)-H(6)	120.8(6)
C(5)-C(6)-H(6)	120.8(6)
C(7A)-C(7)-C(6)	119.6(9)
C(7A)-C(7)-H(7)	120.2(5)
C(6)-C(7)-H(7)	120.2(6)
C(7)-C(7A)-C(3A)	120.7(7)
C(7)-C(7A)-C(1)	132.7(7)
C(3A)-C(7A)-C(1)	106.6(7)
C(7)-C(7A)-Ni	130.6(5)
C(3A)-C(7A)-Ni	69.9(4)
C(1)-C(7A)-Ni	63.0(4)
C(1)-C(8)-C(9)	112.1(6)
C(1)-C(8)-H(8A)	109.2(4)
C(9)-C(8)-H(8A)	109.2(4)
C(1)-C(8)-H(8B)	109.2(4)
C(9)-C(8)-H(8B)	109.2(5)
H(8A)-C(8)-H(8B)	107.9
C(8)-C(9)-C(10)	112.4(6)
C(8)-C(9)-H(9A)	109.1(4)
C(10)-C(9)-H(9A)	109.1(5)
C(8)-C(9)-H(9B)	109.1(5)
C(10)-C(9)-H(9B)	109.1(4)
H(9A)-C(9)-H(9B)	107.9
N(11)-C(10)-C(9)	111.1(6)
N(11)-C(10)-H(10A)	109.4(5)
C(9)-C(10)-H(10A)	109.4(4)
N(11)-C(10)-H(10B)	109.4(5)
C(9)-C(10)-H(10B)	109.4(5)
H(10A)-C(10)-H(10B)	108.0
C(10)-N(11)-C(16)	121.0(10)
C(10)-N(11)-C(12)	117.7(8)
C(10)-N(11)-H(111)	121.2(4)
C(12)-N(11)-H(111)	121.2(6)
C(10)-N(11)-H(112)	119.5(4)
C(16)-N(11)-H(112)	119.5(8)
N(11)-C(12)-C(15)	112.5(10)
N(11)-C(12)-C(14)	106.5(10)
C(15)-C(12)-C(14)	109.6(12)
N(11)-C(12)-C(13)	107.6(11)
C(15)-C(12)-C(13)	109.8(12)
C(14)-C(12)-C(13)	110.9(11)
C(12)-C(13)-H(13A)	109.5(9)
C(12)-C(13)-H(13B)	109.5(8)
H(13A)-C(13)-H(13B)	109.5
C(12)-C(13)-H(13C)	109.5(9)
H(13A)-C(13)-H(13C)	109.47(10)
H(13B)-C(13)-H(13C)	109.5
C(12)-C(14)-H(14A)	109.5(8)
C(12)-C(14)-H(14B)	109.5(7)
H(14A)-C(14)-H(14B)	109.5(2)
C(12)-C(14)-H(14C)	109.5(7)
H(14A)-C(14)-H(14C)	109.47(10)
H(14B)-C(14)-H(14C)	109.5(3)
C(12)-C(15)-H(15A)	109.5(8)
C(12)-C(15)-H(15B)	109.5(8)
H(15A)-C(15)-H(15B)	109.5(2)
C(12)-C(15)-H(15C)	109.5(7)
H(15A)-C(15)-H(15C)	109.5(2)
H(15B)-C(15)-H(15C)	109.47(10)
N(11)-C(16)-C(17)	105.0(13)
N(11)-C(16)-C(19)	112.7(14)
C(17)-C(16)-C(19)	111(2)
N(11)-C(16)-C(18)	108.6(14)
C(17)-C(16)-C(18)	110.5(14)
C(19)-C(16)-C(18)	109.3(14)
C(16)-C(17)-H(17A)	109.5(10)
C(16)-C(17)-H(17B)	109.5(9)
H(17A)-C(17)-H(17B)	109.5(3)
C(16)-C(17)-H(17C)	109.5(9)
H(17A)-C(17)-H(17C)	109.5(2)
H(17B)-C(17)-H(17C)	109.5(2)
C(16)-C(18)-H(18A)	109.5(10)
C(16)-C(18)-H(18B)	109.5(10)
H(18A)-C(18)-H(18B)	109.5
C(16)-C(18)-H(18C)	109.5(10)
H(18A)-C(18)-H(18C)	109.5(2)
H(18B)-C(18)-H(18C)	109.47(13)
C(16)-C(19)-H(19A)	109.5(12)
C(16)-C(19)-H(19B)	109.5(11)
H(19A)-C(19)-H(19B)	109.47(12)
C(16)-C(19)-H(19C)	109.5(10)
H(19A)-C(19)-H(19C)	109.47(9)
H(19B)-C(19)-H(19C)	109.47(11)
C(22)-C(21)-C(26)	117.1(6)
C(22)-C(21)-P	123.9(5)
C(26)-C(21)-P	119.1(5)
C(23)-C(22)-C(21)	122.0(7)
C(23)-C(22)-H(22)	119.0(5)
C(21)-C(22)-H(22)	119.0(4)
C(22)-C(23)-C(24)	120.1(8)

C(22)-C(23)-H(23)	119.9(5)	C(46)-C(41)-P	118.7(5)
C(24)-C(23)-H(23)	119.9(5)	C(42)-C(41)-P	122.2(6)
C(23)-C(24)-C(25)	119.2(8)	C(43)-C(42)-C(41)	119.4(7)
C(23)-C(24)-H(24)	120.4(5)	C(43)-C(42)-H(42)	120.3(4)
C(25)-C(24)-H(24)	120.4(5)	C(41)-C(42)-H(42)	120.3(4)
C(26)-C(25)-C(24)	121.5(8)	C(44)-C(43)-C(42)	120.4(7)
C(26)-C(25)-H(25)	119.2(5)	C(44)-C(43)-H(43)	119.8(4)
C(24)-C(25)-H(25)	119.3(5)	C(42)-C(43)-H(43)	119.8(5)
C(25)-C(26)-C(21)	120.0(7)	C(43)-C(44)-C(45)	120.6(7)
C(25)-C(26)-H(26)	120.0(5)	C(43)-C(44)-H(44)	119.7(4)
C(21)-C(26)-H(26)	120.0(4)	C(45)-C(44)-H(44)	119.7(5)
C(32)-C(31)-C(36)	118.9(6)	C(44)-C(45)-C(46)	119.9(7)
C(32)-C(31)-P	119.6(5)	C(44)-C(45)-H(45)	120.0(5)
C(36)-C(31)-P	121.2(5)	C(46)-C(45)-H(45)	120.0(4)
C(31)-C(32)-C(33)	121.1(7)	C(41)-C(46)-C(45)	120.7(7)
C(31)-C(32)-H(32)	119.4(4)	C(41)-C(46)-H(46)	119.7(4)
C(33)-C(32)-H(32)	119.4(5)	C(45)-C(46)-H(46)	119.7(4)
C(34)-C(33)-C(32)	118.2(8)	Cl(51)-C(50)-Cl(52)	103.1(10)
C(34)-C(33)-H(33)	120.9(5)	Cl(51)-C(50)-H(50A)	111.1(8)
C(32)-C(33)-H(33)	120.9(5)	Cl(52)-C(50)-H(50A)	111.1(7)
C(35)-C(34)-C(33)	120.8(7)	Cl(51)-C(50)-H(50B)	111.1(8)
C(35)-C(34)-H(34)	119.6(5)	Cl(52)-C(50)-H(50B)	111.1(8)
C(33)-C(34)-H(34)	119.6(5)	H(50A)-C(50)-H(50B)	109.1
C(34)-C(35)-C(36)	121.9(8)	Cl(61)-C(60)-Cl(62)	112.8(12)
C(34)-C(35)-H(35)	119.1(5)	Cl(61)-C(60)-H(60A)	109.0(9)
C(36)-C(35)-H(35)	119.1(5)	Cl(62)-C(60)-H(60A)	109.0(9)
C(35)-C(36)-C(31)	119.0(8)	Cl(61)-C(60)-H(60B)	109.0(9)
C(35)-C(36)-H(36)	120.5(5)	Cl(62)-C(60)-H(60B)	109.0(9)
C(31)-C(36)-H(36)	120.5(4)	H(60A)-C(60)-H(60B)	107.8
C(46)-C(41)-C(42)	119.0(6)		

Table I.4. Torsion angles (deg) for (η^3:η^0-Ind$(CH_2)_3$NHtBu)(PPh_3)NiCl. **(7)**

C(3)-Ni-P-C(21)	100.8(3)	C(7A)-Ni-C(3)-C(2)	78.2(5)
C(2)-Ni-P-C(21)	71.5(4)	C(2)-Ni-C(3)-C(3A)	-111.4(6)
C(1)-Ni-P-C(21)	110.3(9)	C(1)-Ni-C(3)-C(3A)	-74.2(4)
Cl-Ni-P-C(21)	-75.8(2)	P-Ni-C(3)-C(3A)	103.3(4)
C(3A)-Ni-P-C(21)	140.0(3)	Cl-Ni-C(3)-C(3A)	-87.9(9)
C(7A)-Ni-P-C(21)	162.7(3)	C(3A)-Ni-C(3)-C(3A)	0.000(3)
C(3)-Ni-P-C(31)	-18.9(4)	C(7A)-Ni-C(3)-C(3A)	-33.2(4)
C(2)-Ni-P-C(31)	-48.2(4)	C(2)-C(3)-C(3A)-C(4)	173.0(7)
C(1)-Ni-P-C(31)	-9.4(9)	Ni-C(3)-C(3A)-C(4)	-120.5(7)
Cl-Ni-P-C(31)	164.5(3)	C(2)-C(3)-C(3A)-C(7A)	-7.2(7)
C(3A)-Ni-P-C(31)	20.3(3)	Ni-C(3)-C(3A)-C(7A)	59.3(4)
C(7A)-Ni-P-C(31)	42.9(4)	C(2)-C(3)-C(3A)-Ni	-66.5(4)
C(3)-Ni-P-C(41)	-138.4(3)	Ni-C(3)-C(3A)-Ni	0.000(2)
C(2)-Ni-P-C(41)	-167.7(4)	C(3)-Ni-C(3A)-C(4)	121.2(11)
C(1)-Ni-P-C(41)	-128.9(9)	C(2)-Ni-C(3A)-C(4)	163.9(10)
Cl-Ni-P-C(41)	45.0(2)	C(1)-Ni-C(3A)-C(4)	-151.9(10)
C(3A)-Ni-P-C(41)	-99.2(3)	P-Ni-C(3A)-C(4)	35.8(9)
C(7A)-Ni-P-C(41)	-76.5(3)	Cl-Ni-C(3A)-C(4)	-85.4(9)
C(3)-Ni-C(1)-C(2)	-38.6(5)	C(7A)-Ni-C(3A)-C(4)	-116.5(11)
C(2)-Ni-C(1)-C(2)	0.000(8)	C(3)-Ni-C(3A)-C(7A)	-122.3(6)
P-Ni-C(1)-C(2)	-48.8(11)	C(2)-Ni-C(3A)-C(7A)	-79.6(4)
Cl-Ni-C(1)-C(2)	137.3(4)	C(1)-Ni-C(3A)-C(7A)	-35.5(4)
C(3A)-Ni-C(1)-C(2)	-81.3(5)	P-Ni-C(3A)-C(7A)	152.3(4)
C(7A)-Ni-C(1)-C(2)	-115.1(6)	Cl-Ni-C(3A)-C(7A)	31.1(5)
C(3)-Ni-C(1)-C(7A)	76.5(4)	C(7A)-Ni-C(3A)-C(7A)	0.000(1)
C(2)-Ni-C(1)-C(7A)	115.1(6)	C(3)-Ni-C(3A)-C(3)	0.000(3)
P-Ni-C(1)-C(7A)	66.3(10)	C(2)-Ni-C(3A)-C(3)	42.7(4)
Cl-Ni-C(1)-C(7A)	-107.6(4)	C(1)-Ni-C(3A)-C(3)	86.8(4)
C(3A)-Ni-C(1)-C(7A)	33.8(4)	P-Ni-C(3A)-C(3)	-85.4(4)
C(7A)-Ni-C(1)-C(7A)	0.000(3)	Cl-Ni-C(3A)-C(3)	153.4(3)
C(3)-Ni-C(1)-C(8)	-156.5(7)	C(7A)-Ni-C(3A)-C(3)	122.3(6)
C(2)-Ni-C(1)-C(8)	-117.9(8)	C(7A)-C(3A)-C(4)-C(5)	0.2(10)
P-Ni-C(1)-C(8)	-166.7(6)	C(3)-C(3A)-C(4)-C(5)	180.0(7)
Cl-Ni-C(1)-C(8)	19.3(7)	Ni-C(3A)-C(4)-C(5)	95.6(10)
C(3A)-Ni-C(1)-C(8)	160.8(8)	C(3A)-C(4)-C(5)-C(6)	-2.1(13)
C(7A)-Ni-C(1)-C(8)	126.9(8)	C(4)-C(5)-C(6)-C(7)	1.1(13)
C(7A)-C(1)-C(2)-C(3	-10.1(7)	C(5)-C(6)-C(7)-C(7A)	2.0(11)
C(8)-C(1)-C(2)-C(3)	177.8(6)	C(6)-C(7)-C(7A)-C(3A)	-3.9(10)
Ni-C(1)-C(2)-C(3)	59.8(4)	C(6)-C(7)-C(7A)-C(1)	178.5(7)
C(7A)-C(1)-C(2)-Ni	-69.9(4)	C(6)-C(7)-C(7A)-Ni	-92.8(9)
C(8)-C(1)-C(2)-Ni	118.0(6)	C(4)-C(3A)-C(7A)-C(7)	2.8(9)
Ni-C(1)-C(2)-Ni	0.000(4)	C(3)-C(3A)-C(7A)-C(7)	-177.0(6)
C(3)-Ni-C(2)-C(1)	118.4(7)	Ni-C(3A)-C(7A)-C(7)	-126.0(6)
C(1)-Ni-C(2)-C(1)	0.000(8)	C(4)-C(3A)-C(7A)-C(1)	-179.1(6)
P-Ni-C(2)-C(1)	166.1(3)	C(3)-C(3A)-C(7A)-C(1)	1.2(7)
Cl-Ni-C(2)-C(1)	-53.3(5)	Ni-C(3A)-C(7A)-C(1)	52.2(4)
C(3A)-Ni-C(2)-C(1)	77.9(5)	C(4)-C(3A)-C(7A)-Ni	128.8(6)
C(7A)-Ni-C(2)-C(1)	38.0(4)	C(3)-C(3A)-C(7A)-Ni	-51.0(4)
C(3)-Ni-C(2)-C(3)	0.000(7)	Ni-C(3A)-C(7A)-Ni	0.0
C(1)-Ni-C(2)-C(3)	-118.4(7)	C(2)-C(1)-C(7A)-C(7)	-176.7(7)
P-Ni-C(2)-C(3)	47.7(6)	C(8)-C(1)-C(7A)-C(7)	-4.7(11)
Cl-Ni-C(2)-C(3)	-171.8(4)	Ni-C(1)-C(7A)-C(7)	121.5(7)
C(3A)-Ni-C(2)-C(3)	-40.5(4)	C(2)-C(1)-C(7A)-C(3A)	5.4(7)
C(7A)-Ni-C(2)-C(3)	-80.4(5)	C(8)-C(1)-C(7A)-C(3A)	177.5(6)
C(1)-C(2)-C(3)-C(3A)	10.6(7)	Ni-C(1)-C(7A)-C(3A)	-56.3(4)
Ni-C(2)-C(3)-C(3A)	73.4(4)	C(2)-C(1)-C(7A)-Ni	61.7(4)
C(1)-C(2)-C(3)-Ni	-62.8(5)	C(8)-C(1)-C(7A)-Ni	-126.2(7)
Ni-C(2)-C(3)-Ni	0.000(5)	Ni-C(1)-C(7A)-Ni	0.000(2)
C(2)-Ni-C(3)-C(2)	0.000(8)	C(3)-Ni-C(7A)-C(7)	149.8(8)
C(1)-Ni-C(3)-C(2)	37.2(4)	C(2)-Ni-C(7A)-C(7)	-164.4(8)
P-Ni-C(3)-C(2)	-145.3(4)	C(1)-Ni-C(7A)-C(7)	-124.4(9)
Cl-Ni-C(3)-C(2)	23.5(11)	P-Ni-C(7A)-C(7)	74.0(8)
C(3A)-Ni-C(3)-C(2)	111.4(6)	Cl-Ni-C(7A)-C(7)	-45.1(7)

C(3A)-Ni-C(7A)-C(7)	113.7(9)	C(26)-C(21)-C(22)-C(23)	1.1(9)
C(3)-Ni-C(7A)-C(3A)	36.1(4)	P-C(21)-C(22)-C(23)	-178.1(5)
C(2)-Ni-C(7A)-C(3A)	81.9(5)	C(21)-C(22)-C(23)-C(24)	-1.4(11)
C(1)-Ni-C(7A)-C(3A)	121.9(6)	C(22)-C(23)-C(24)-C(25)	1.4(11)
P-Ni-C(7A)-C(3A)	-39.7(5)	C(23)-C(24)-C(25)-C(26)	-1.1(12)
Cl-Ni-C(7A)-C(3A)	-158.8(4)	C(24)-C(25)-C(26)-C(21)	0.8(11)
C(3A)-Ni-C(7A)-C(3A)	0.000(1)	C(22)-C(21)-C(26)-C(25)	-0.8(10)
C(3)-Ni-C(7A)-C(1)	-85.8(5)	P-C(21)-C(26)-C(25)	178.5(5)
C(2)-Ni-C(7A)-C(1)	-40.0(4)	C(21)-P-C(31)-C(32)	-52.8(6)
C(1)-Ni-C(7A)-C(1)	0.000(4)	C(41)-P-C(31)-C(32)	-163.2(5)
P-Ni-C(7A)-C(1)	-161.6(3)	Ni-P-C(31)-C(32)	72.5(6)
Cl-Ni-C(7A)-C(1)	79.4(4)	C(21)-P-C(31)-C(36)	134.1(5)
C(3A)-Ni-C(7A)-C(1)	-121.9(6)	C(41)-P-C(31)-C(36)	23.7(6)
C(2)-C(1)-C(8)-C(9)	92.0(9)	Ni-P-C(31)-C(36)	-100.6(5)
C(7A)-C(1)-C(8)-C(9)	-78.7(9)	C(36)-C(31)-C(32)-C(33)	-1.1(10)
Ni-C(1)-C(8)-C(9)	177.4(5)	P-C(31)-C(32)-C(33)	-174.4(5)
C(1)-C(8)-C(9)-C(10)	-172.3(7)	C(31)-C(32)-C(33)-C(34)	0.7(11)
C(8)-C(9)-C(10)-N(11)	177.6(7)	C(32)-C(33)-C(34)-C(35)	-1.3(12)
C(9)-C(10)-N(11)-C(16)	-175.9(11)	C(33)-C(34)-C(35)-C(36)	2.2(13)
C(9)-C(10)-N(11)-C(12)	-175.2(9)	C(34)-C(35)-C(36)-C(31)	-2.6(12)
C(10)-N(11)-C(12)-C(15)	-52(2)	C(32)-C(31)-C(36)-C(35)	2.0(10)
C(16)-N(11)-C(12)-C(15)	117(22)	P-C(31)-C(36)-C(35)	175.1(5)
C(10)-N(11)-C(12)-C(14)	67.8(13)	C(21)-P-C(41)-C(46)	161.4(5)
C(16)-N(11)-C(12)-C(14)	-123(22)	C(31)-P-C(41)-C(46)	-89.8(5)
C(10)-N(11)-C(12)-C(13)	-173.3(10)	Ni-P-C(41)-C(46)	36.1(6)
C(16)-N(11)-C(12)-C(13)	-5(21)	C(21)-P-C(41)-C(42)	-17.5(6)
C(10)-N(11)-C(16)-C(17)	-82(2)	C(31)-P-C(41)-C(42)	91.3(6)
C(12)-N(11)-C(16)-C(17)	-94(22)	Ni-P-C(41)-C(42)	-142.9(5)
C(10)-N(11)-C(16)-C(19)	39(2)	C(46)-C(41)-C(42)-C(43)	0.7(10)
C(12)-N(11)-C(16)-C(19)	27(21)	P-C(41)-C(42)-C(43)	179.6(5)
C(10)-N(11)-C(16)-C(18)	159.6(12)	C(41)-C(42)-C(43)-C(44)	-0.3(11)
C(12)-N(11)-C(16)-C(18)	148(23)	C(42)-C(43)-C(44)-C(45)	0.8(12)
C(31)-P-C(21)-C(22)	-32.4(6)	C(43)-C(44)-C(45)-C(46)	-1.7(11)
C(41)-P-C(21)-C(22)	76.7(6)	C(42)-C(41)-C(46)-C(45)	-1.5(10)
Ni-P-C(21)-C(22)	-158.6(5)	P-C(41)-C(46)-C(45)	179.5(5)
C(31)-P-C(21)-C(26)	148.4(5)	C(44)-C(45)-C(46)-C(41)	2.0(10)
C(41)-P-C(21)-C(26)	-102.5(5)		
Ni-P-C(21)-C(26)	22.2(6)		

Table I.5. Hydrogen coordinates and isotropic displacement parameters ($Å^2$ x 10^2) for (η^3:η^0-Ind$(CH_2)_3$NHtBu)(PPh_3)NiCl.(7)

	x	y	z	Uiso
H(2)	0.3646(9)	0.5582(8)	0.8487(4)	7.9
H(3)	0.4932(8)	0.4579(8)	0.7647(4)	7.6
H(4)	0.6615(9)	0.5817(10)	0.6405(5)	9.7
H(5)	0.7025(11)	0.7568(12)	0.5645(5)	11.7
H(6)	0.5824(11)	0.9114(11)	0.5727(4)	11.1
H(7)	0.4176(9)	0.8904(8)	0.6643(4)	8.6
H(8A)	0.1975(9)	0.7125(8)	0.8333(4)	8.2
H(8B)	0.2157(9)	0.7970(8)	0.7654(4)	8.2
H(9A)	0.4563(9)	0.9775(8)	0.8062(4)	8.4
H(9B)	0.4580(9)	0.8897(8)	0.8710(4)	8.4
H(10A)	0.2331(9)	1.0043(8)	0.8454(4)	9.0
H(10B)	0.2279(9)	0.9113(8)	0.9092(4)	9.0
H(111)	0.5137(8)	1.1381(7)	0.9114(3)	11.3
H(112)	0.5133(8)	1.1355(7)	0.9109(3)	11.3
H(13A)	0.569(6)	1.298(3)	1.003(6)	17.5
H(13B)	0.445(5)	1.357(8)	1.023(5)	17.5
H(13C)	0.517(11)	1.384(5)	0.950(2)	17.5
H(14A)	0.350(3)	1.065(9)	1.044(3)	13.1
H(14B)	0.189(9)	0.988(4)	0.9998(7)	13.1
H(14C)	0.216(11)	1.119(5)	1.047(3)	13.1
H(15A)	0.116(4)	1.126(3)	0.919(5)	13.6
H(15B)	0.251(6)	1.245(11)	0.878(2)	13.6
H(15C)	0.200(10)	1.283(9)	0.948(3)	13.6
H(17A)	0.399(7)	1.331(12)	0.884(5)	11.7
H(17B)	0.29(2)	1.344(10)	0.9390(9)	11.7
H(17C)	0.217(11)	1.220(2)	0.884(5)	11.7
H(18A)	0.533(12)	1.217(4)	1.033(6)	12.5
H(18B)	0.450(5)	1.318(13)	1.044(4)	12.5
H(18C)	0.574(8)	1.350(10)	0.9862(14)	12.5
H(19A)	0.218(13)	1.002(10)	1.009(10)	18.6
H(19B)	0.112(3)	1.06(2)	0.971(4)	18.6
H(19C)	0.204(15)	1.136(9)	1.040(6)	18.6
H(22)	0.1171(8)	-0.0141(7)	0.6721(3)	6.7
H(23)	-0.0602(9)	-0.2039(8)	0.7290(4)	8.1
H(24)	-0.2205(9)	-0.1722(10)	0.8092(4)	9.0
H(25)	-0.2084(9)	0.0511(10)	0.8271(4)	8.7
H(26)	-0.0329(8)	0.2445(8)	0.7700(3)	7.2
H(32)	0.4028(8)	0.2109(7)	0.7490(4)	7.5
H(33)	0.6394(9)	0.1831(8)	0.7339(5)	9.0
H(34)	0.7466(9)	0.2180(9)	0.6261(5)	9.7
H(35)	0.6186(9)	0.2667(9)	0.5366(5)	9.6
H(36)	0.3893(8)	0.3007(8)	0.5502(4)	8.0
H(42)	-0.0585(8)	0.0633(7)	0.5824(3)	6.8
H(43)	-0.1750(9)	0.0536(9)	0.4736(4)	8.4
H(44)	-0.0932(9)	0.2540(9)	0.4096(4)	8.5
H(45)	0.1110(9)	0.4663(8)	0.4502(3)	7.7
H(46)	0.2246(9)	0.4807(8)	0.5591(3)	7.0
H(50A)	0.204(3)	0.608(2)	0.1865(11)	15.8
H(50B)	0.312(3)	0.662(2)	0.1221(11)	15.8
H(60A)	0.241(3)	0.586(2)	0.1689(11)	9.9
H(60B)	0.052(3)	0.514(2)	0.1712(11)	9.9

Table I.6. Anisotropic parameters ($Å^2 \times 10^2$) for (η^3:η^0-Ind$(CH_2)_3$NHtBu)(PPh_3)NiCl. **(7)**

	U11	U22	U33	U23	U13	U12
Ni	4.89(6)	5.02(7)	5.22(7)	-1.85(5)	-0.71(5)	2.29(5)
Cl	5.47(9)	6.83(12)	6.45(10)	-1.65(8)	-0.79(8)	3.24(9)
P	4.26(8)	4.49(10)	4.80(9)	-1.15(7)	-0.34(7)	2.08(7)
C(1)	5.5(4)	5.3(4)	6.0(4)	-2.5(3)	-0.9(3)	2.4(3)
C(2)	7.3(5)	6.8(5)	5.5(4)	-2.4(4)	-2.3(4)	3.0(4)
C(3)	6.0(4)	5.4(4)	8.1(5)	-2.8(4)	-2.6(4)	3.2(4)
C(3A)	4.5(4)	6.7(5)	6.7(5)	-3.2(4)	-1.2(3)	1.4(3)
C(4)	5.2(4)	8.1(6)	9.5(6)	-4.1(5)	0.3(4)	1.6(4)
C(5)	7.0(6)	9.9(8)	9.1(7)	-3.8(6)	1.8(5)	0.6(6)
C(6)	8.8(7)	9.1(7)	7.0(6)	-1.2(5)	-0.7(5)	1.2(6)
C(7)	7.1(5)	5.3(5)	8.1(6)	-1.8(4)	-0.4(4)	1.7(4)
C(7A)	5.3(4)	4.6(4)	6.0(4)	-2.1(3)	-1.3(3)	2.0(3)
C(8)	6.5(4)	6.2(5)	7.6(5)	-2.8(4)	0.1(4)	2.6(4)
C(9)	7.5(5)	6.9(5)	7.4(5)	-2.5(4)	-0.5(4)	3.8(4)
C(10)	8.2(5)	7.2(5)	7.4(5)	-3.9(4)	-1.1(4)	3.9(4)
N(11)	8.2(5)	9.8(5)	11.1(5)	-6.3(4)	-1.4(4)	4.9(4)
C(12)	9.0(6)	7.3(6)	5.9(4)	-2.3(4)	0.1(4)	3.7(5)
C(16)	9.0(6)	7.3(6)	5.9(4)	-2.3(4)	0.1(4)	3.7(5)
C(21)	4.5(3)	4.5(4)	5.2(4)	-0.7(3)	-0.6(3)	1.7(3)
C(22)	5.2(4)	5.4(4)	5.9(4)	-1.1(3)	-0.5(3)	2.2(3)
C(23)	6.5(5)	4.5(4)	7.9(5)	0.2(4)	-1.0(4)	1.2(4)
C(24)	6.0(5)	7.6(6)	7.2(5)	1.3(4)	-0.2(4)	1.4(4)
C(25)	6.8(5)	8.4(6)	6.5(5)	0.5(4)	0.7(4)	3.1(5)
C(26)	6.3(4)	5.7(4)	6.0(4)	-1.0(3)	0.2(3)	2.5(4)
C(31)	4.1(3)	3.9(4)	6.8(4)	-1.6(3)	-0.6(3)	1.3(3)
C(32)	5.3(4)	6.0(5)	7.9(5)	-1.6(4)	-0.5(4)	3.0(4)
C(33)	5.7(4)	6.0(5)	11.5(7)	-2.2(5)	-1.9(4)	3.4(4)
C(34)	4.5(4)	7.2(6)	12.6(8)	-3.5(5)	0.0(5)	2.6(4)
C(35)	5.3(4)	9.1(6)	9.8(6)	-3.3(5)	0.5(4)	3.2(4)
C(36)	5.9(4)	7.2(5)	6.9(5)	-2.1(4)	0.2(4)	2.9(4)
C(41)	4.5(3)	5.4(4)	4.9(4)	-1.3(3)	-0.3(3)	2.3(3)
C(42)	6.0(4)	5.2(4)	5.3(4)	-1.1(3)	-0.2(3)	2.1(3)
C(43)	7.2(5)	6.9(5)	5.5(4)	-1.5(4)	-1.5(4)	1.8(4)
C(44)	8.1(5)	9.2(6)	4.9(4)	-2.1(4)	-1.7(4)	5.0(5)
C(45)	7.8(5)	6.8(5)	5.3(4)	-0.4(4)	0.3(4)	3.7(4)
C(46)	6.9(4)	4.8(4)	6.0(4)	-0.5(3)	0.3(3)	2.7(4)

Table I.7. Crystal data and structure refinement for $(\eta^3:\eta^0$-$Ind(CH_2)_2NMe_2)(PPh_3)NiCl$. **(9)**

Chemical formula	C31 H31 Cl N Ni P
Chemical formula weight	542.72
Temperature	293(2) (K)
Wavelength	1.54056 Å
Crystal system	Triclinic
Space group	P -1
Unit cell dimensions	a = 9.215(2) Å α = 76.60(3)° b = 10.228(4) Å β = 87.94(2)° c = 16.250(6) Å γ = 65.43(2)°
Volume	1351.8(8) $Å^3$
Z	2
Density calculated	1.3333 Mg/m^3
Absorption coefficient	2.642 mm^{-1}
F(000)	568.0
Size	0.29 x 0.11 x 0.07 mm
Theta range for data collection	2.80 to 69.95°
Index ranges	$-11 \le h \le 11$, $-12 \le k \le 12$, $-19 \le l \le 19$
Reflections collected	19808
Independent reflections	5137
Absorption correction	Integration
Max. and min. transmission	0.84 and 0.60
Refinement method	Full-matrix least-squares on F^2
Data / restraints / parameters	5137 / 11 / 339
Goodness-of-fit on F^2	0.752
Final R indices [I>2sigma(I)]	R_1 = 0.0509, wR_2 = 0.1007
R indices (all data)	R_1 = 0.1107, wR_2 = 0.1152
Extinction coefficient	0.00055(14)
Largest diff. peak and hole	0.459 and -0.359 $e/Å^3$

Table I.8. Atomic coordinates and equivalent isotropic displacement parameters ($Å^2$ x 10^2) for (η^3:η^0-Ind$(CH_2)_2NMe_2$)(PPh_3)NiCl. **(9)**

	x	y	z	U_{eq}
Ni	0.18677(9)	0.13486(8)	0.72842(4)	4.78(2)
Cl	-0.02879(14)	0.10127(13)	0.75974(8)	6.37(4)
P	0.14184(14)	0.31232(12)	0.79248(7)	4.34(3)
C(1)	0.2850(5)	-0.0340(5)	0.6598(3)	5.29(12)
C(2)	0.2994(6)	0.0967(5)	0.6190(3)	6.89(15)
C(3)	0.3935(6)	0.1239(6)	0.6762(3)	6.57(15)
C(3A)	0.4573(6)	-0.0007(6)	0.7461(3)	5.67(13)
C(4)	0.5667(6)	-0.0380(7)	0.8131(4)	8.50(19)
C(5)	0.6049(7)	-0.1710(9)	0.8712(4)	10.2(2)
C(6)	0.5372(8)	-0.2656(7)	0.8646(4)	9.5(2)
C(7)	0.4274(6)	-0.2312(6)	0.7982(3)	7.08(15)
C(7A)	0.3918(6)	-0.1010(5)	0.7370(3)	5.42(12)
C(8)	0.2036(6)	-0.1085(6)	0.6233(3)	7.31(16)
C(9)	0.307(4)	-0.187(5)	0.560(2)	8.2(6)
N(1)	0.2107(15)	-0.1968(13)	0.4933(7)	8.9(4)
C(10)	0.2905(19)	-0.2183(19)	0.4185(8)	14.1(6)
C(11)	0.154(3)	-0.308(4)	0.527(2)	10.6(6)
C(19)	0.289(4)	-0.165(5)	0.548(2)	8.2(6)
N(11)	0.2812(12)	-0.2995(11)	0.5346(6)	6.7(3)
C(110)	0.3784(19)	-0.3515(18)	0.4668(9)	14.1(6)
C(111)	0.116(3)	-0.262(4)	0.512(2)	10.6(6)
C(21)	0.3181(5)	0.3415(5)	0.8123(3)	5.05(11)
C(22)	0.4031(6)	0.2845(5)	0.8896(3)	6.58(14)
C(23)	0.5487(7)	0.2917(6)	0.9002(4)	8.29(18)
C(24)	0.6067(7)	0.3592(7)	0.8325(5)	9.2(2)
C(25)	0.5224(7)	0.4195(6)	0.7556(4)	8.05(18)
C(26)	0.3764(6)	0.4147(5)	0.7452(3)	6.13(13)
C(31)	-0.0003(5)	0.4917(4)	0.7341(3)	4.59(11)
C(32)	-0.1080(6)	0.4992(5)	0.6730(3)	5.76(13)
C(33)	-0.2201(6)	0.6323(6)	0.6287(3)	6.99(15)
C(34)	-0.2312(6)	0.7626(6)	0.6456(3)	7.16(16)
C(35)	-0.1255(7)	0.7583(5)	0.7048(3)	6.80(15)
C(36)	-0.0130(6)	0.6247(5)	0.7492(3)	5.70(13)
C(41)	0.0657(5)	0.2806(5)	0.8971(3)	4.66(11)
C(42)	-0.0473(6)	0.3919(5)	0.9281(3)	5.71(13)
C(43)	-0.0991(6)	0.3596(6)	1.0090(3)	6.36(14)
C(44)	-0.0390(6)	0.2185(6)	1.0576(3)	6.49(14)
C(45)	0.0767(6)	0.1066(5)	1.0277(3)	6.73(14)
C(46)	0.1273(6)	0.1364(5)	0.9471(3)	5.66(13)

Table I.9. Bond lengths (Å) and angles (deg) for (η^3:η^0-Ind$(CH_2)_2NMe_2$)(PPh_3)NiCl. **(9)**

Ni-C(3)	2.028(5)	N(1)-C(10)	1.412(11)
Ni-C(2)	2.060(4)	N(1)-C(11)	1.432(17)
Ni-C(1)	2.137(4)	C(19)-N(11)	1.48(3)
Ni-Cl	2.1763(14)	N(11)-C(111)	1.441(17)
Ni-P	2.1838(15)	N(11)-C(110)	1.449(11)
Ni-C(3A)	2.283(5)	C(21)-C(22)	1.372(6)
Ni-C(7A)	2.341(4)	C(21)-C(26)	1.397(6)
P-C(31)	1.807(4)	C(22)-C(23)	1.393(6)
P-C(21)	1.821(5)	C(23)-C(24)	1.373(7)
P-C(41)	1.826(4)	C(24)-C(25)	1.364(7)
C(1)-C(2)	1.405(6)	C(25)-C(26)	1.384(6)
C(1)-C(7A)	1.464(6)	C(31)-C(36)	1.395(5)
C(1)-C(8)	1.487(5)	C(31)-C(32)	1.396(5)
C(2)-C(3)	1.440(6)	C(32)-C(33)	1.367(6)
C(3)-C(3A)	1.419(6)	C(33)-C(34)	1.383(6)
C(3A)-C(4)	1.384(7)	C(34)-C(35)	1.375(6)
C(3A)-C(7A)	1.424(6)	C(35)-C(36)	1.371(6)
C(4)-C(5)	1.377(8)	C(41)-C(42)	1.371(5)
C(5)-C(6)	1.375(8)	C(41)-C(46)	1.393(5)
C(6)-C(7)	1.385(7)	C(42)-C(43)	1.396(5)
C(7)-C(7A)	1.384(6)	C(43)-C(44)	1.361(6)
C(8)-C(9)	1.516(13)	C(44)-C(45)	1.375(6)
C(8)-C(19)	1.530(12)	C(45)-C(46)	1.383(5)
C(9)-N(1)	1.46(3)		

C(3)-Ni-C(2)	41.25(18)	C(3A)-C(3)-Ni	80.8(3)
C(3)-Ni-C(1)	66.65(17)	C(2)-C(3)-Ni	70.5(3)
C(2)-Ni-C(1)	39.07(15)	C(4)-C(3A)-C(3)	132.6(5)
C(3)-Ni-Cl	162.44(13)	C(4)-C(3A)-C(7A)	120.0(5)
C(2)-Ni-Cl	122.61(15)	C(3)-C(3A)-C(7A)	107.3(4)
C(1)-Ni-Cl	96.09(13)	C(4)-C(3A)-Ni	131.9(3)
C(3)-Ni-P	99.32(13)	C(3)-C(3A)-Ni	61.3(3)
C(2)-Ni-P	130.41(14)	C(7A)-C(3A)-Ni	74.3(3)
C(1)-Ni-P	165.87(13)	C(5)-C(4)-C(3A)	118.1(6)
Cl-Ni-P	98.01(6)	C(6)-C(5)-C(4)	122.1(6)
C(3)-Ni-C(3A)	37.87(17)	C(5)-C(6)-C(7)	121.1(6)
C(2)-Ni-C(3A)	64.68(19)	C(7A)-C(7)-C(6)	118.0(5)
C(1)-Ni-C(3A)	63.57(16)	C(7)-C(7A)-C(3A)	120.6(5)
Cl-Ni-C(3A)	138.15(14)	C(7)-C(7A)-C(1)	131.7(5)
P-Ni-C(3A)	104.58(12)	C(3A)-C(7A)-C(1)	107.6(4)
C(3)-Ni-C(7A)	62.74(18)	C(7)-C(7A)-Ni	129.6(3)
C(2)-Ni-C(7A)	63.23(18)	C(3A)-C(7A)-Ni	69.8(3)
C(1)-Ni-C(7A)	37.82(15)	C(1)-C(7A)-Ni	63.5(2)
Cl-Ni-C(7A)	105.97(13)	C(1)-C(8)-C(9)	109.9(8)
P-Ni-C(7A)	135.20(12)	C(1)-C(8)-C(19)	111.0(8)
C(3A)-Ni-C(7A)	35.84(14)	N(1)-C(9)-C(8)	112(2)
C(31)-P-C(21)	104.2(2)	C(10)-N(1)-C(11)	112.4(15)
C(31)-P-C(41)	105.96(19)	C(10)-N(1)-C(9)	113.6(11)
C(21)-P-C(41)	104.1(2)	C(11)-N(1)-C(9)	110(2)
C(31)-P-Ni	113.75(14)	N(11)-C(19)-C(8)	116(2)
C(21)-P-Ni	114.40(14)	C(111)-N(11)-C(110)	109.2(14)
C(41)-P-Ni	113.38(14)	C(111)-N(11)-C(19)	107(2)
C(2)-C(1)-C(7A)	107.9(4)	C(110)-N(11)-C(19)	111.3(12)
C(2)-C(1)-C(8)	126.2(5)	C(22)-C(21)-C(26)	118.5(5)
C(7A)-C(1)-C(8)	124.8(4)	C(22)-C(21)-P	122.2(4)
C(2)-C(1)-Ni	67.5(2)	C(26)-C(21)-P	119.1(4)
C(7A)-C(1)-Ni	78.7(2)	C(21)-C(22)-C(23)	121.1(5)
C(8)-C(1)-Ni	128.9(3)	C(24)-C(23)-C(22)	119.4(6)
C(1)-C(2)-C(3)	107.2(4)	C(25)-C(24)-C(23)	120.4(6)
C(1)-C(2)-Ni	73.4(3)	C(24)-C(25)-C(26)	120.3(6)
C(3)-C(2)-Ni	68.2(2)	C(25)-C(26)-C(21)	120.2(5)
C(3A)-C(3)-C(2)	109.2(4)	C(36)-C(31)-C(32)	117.6(4)

C(36)-C(31)-P	123.3(4)	C(42)-C(41)-P	123.0(3)
C(32)-C(31)-P	119.1(3)	C(46)-C(41)-P	117.8(3)
C(33)-C(32)-C(31)	121.1(4)	C(41)-C(42)-C(43)	119.8(4)
C(32)-C(33)-C(34)	120.2(5)	C(44)-C(43)-C(42)	120.9(5)
C(35)-C(34)-C(33)	119.8(5)	C(43)-C(44)-C(45)	119.7(4)
C(36)-C(35)-C(34)	120.0(5)	C(44)-C(45)-C(46)	120.1(5)
C(35)-C(36)-C(31)	121.3(5)	C(45)-C(46)-C(41)	120.3(4)
C(42)-C(41)-C(46)	119.2(4)		

Table I.10. Torsion angles (°) for (η^3:η^0-Ind$(CH_2)_2NMe_2$)(PPh_3)NiCl.(9)

C(3)-Ni-P-C(31)	98.8(2)	Ni-C(3)-C(3A)-C(4)	-122.1(5)
C(2)-Ni-P-C(31)	68.2(3)	C(2)-C(3)-C(3A)-C(7A)	-5.1(5)
C(1)-Ni-P-C(31)	105.5(6)	Ni-C(3)-C(3A)-C(7A)	60.4(3)
Cl-Ni-P-C(31)	-78.37(16)	C(2)-C(3)-C(3A)-Ni	-65.6(3)
C(3A)-Ni-P-C(31)	137.2(2)	C(3)-Ni-C(3A)-C(4)	123.0(7)
C(7A)-Ni-P-C(31)	159.2(2)	C(2)-Ni-C(3A)-C(4)	164.8(6)
C(3)-Ni-P-C(21)	-20.9(2)	C(1)-Ni-C(3A)-C(4)	-151.6(6)
C(2)-Ni-P-C(21)	-51.5(3)	Cl-Ni-C(3A)-C(4)	-83.8(6)
C(1)-Ni-P-C(21)	-14.1(6)	P-Ni-C(3A)-C(4)	36.6(6)
Cl-Ni-P-C(21)	161.98(17)	C(7A)-Ni-C(3A)-C(4)	-116.6(7)
C(3A)-Ni-P-C(21)	17.5(2)	C(2)-Ni-C(3A)-C(3)	41.7(3)
C(7A)-Ni-P-C(21)	39.6(2)	C(1)-Ni-C(3A)-C(3)	85.3(3)
C(3)-Ni-P-C(41)	-140.1(2)	Cl-Ni-C(3A)-C(3)	153.1(2)
C(2)-Ni-P-C(41)	-170.6(3)	P-Ni-C(3A)-C(3)	-86.5(3)
C(1)-Ni-P-C(41)	-133.3(6)	C(7A)-Ni-C(3A)-C(3)	120.4(4)
Cl-Ni-P-C(41)	42.79(17)	C(3)-Ni-C(3A)-C(7A)	-120.4(4)
C(3A)-Ni-P-C(41)	-101.7(2)	C(2)-Ni-C(3A)-C(7A)	-78.7(3)
C(7A)-Ni-P-C(41)	-79.6(2)	C(1)-Ni-C(3A)-C(7A)	-35.1(3)
C(3)-Ni-C(1)-C(2)	-39.9(3)	Cl-Ni-C(3A)-C(7A)	32.7(4)
Cl-Ni-C(1)-C(2)	136.8(3)	P-Ni-C(3A)-C(7A)	153.1(2)
P-Ni-C(1)-C(2)	-47.1(7)	C(3)-C(3A)-C(4)-C(5)	-179.3(5)
C(3A)-Ni-C(1)-C(2)	-81.6(3)	C(7A)-C(3A)-C(4)-C(5)	-2.2(7)
C(7A)-Ni-C(1)-C(2)	-114.9(4)	Ni-C(3A)-C(4)-C(5)	93.6(6)
C(3)-Ni-C(1)-C(7A)	75.1(3)	C(3A)-C(4)-C(5)-C(6)	-0.5(9)
C(2)-Ni-C(1)-C(7A)	114.9(4)	C(4)-C(5)-C(6)-C(7)	0.5(10)
Cl-Ni-C(1)-C(7A)	-108.3(3)	C(5)-C(6)-C(7)-C(7A)	2.1(8)
P-Ni-C(1)-C(7A)	67.8(7)	C(6)-C(7)-C(7A)-C(3A)	-4.7(7)
C(3A)-Ni-C(1)-C(7A)	33.3(3)	C(6)-C(7)-C(7A)-C(1)	179.2(5)
C(3)-Ni-C(1)-C(8)	-159.1(5)	C(6)-C(7)-C(7A)-Ni	-92.9(6)
C(2)-Ni-C(1)-C(8)	-119.2(6)	C(4)-C(3A)-C(7A)-C(7)	4.8(7)
Cl-Ni-C(1)-C(8)	17.6(4)	C(3)-C(3A)-C(7A)-C(7)	-177.3(4)
P-Ni-C(1)-C(8)	-166.3(4)	Ni-C(3A)-C(7A)-C(7)	-124.9(4)
C(3A)-Ni-C(1)-C(8)	159.2(5)	C(4)-C(3A)-C(7A)-C(1)	-178.2(4)
C(7A)-Ni-C(1)-C(8)	125.9(6)	C(3)-C(3A)-C(7A)-C(1)	-0.4(5)
C(7A)-C(1)-C(2)-C(3)	-8.9(5)	Ni-C(3A)-C(7A)-C(1)	52.0(3)
C(8)-C(1)-C(2)-C(3)	-177.2(4)	C(4)-C(3A)-C(7A)-Ni	129.8(4)
Ni-C(1)-C(2)-C(3)	60.2(3)	C(3)-C(3A)-C(7A)-Ni	-52.4(3)
C(7A)-C(1)-C(2)-Ni	-69.1(3)	C(2)-C(1)-C(7A)-C(7)	-177.6(5)
C(8)-C(1)-C(2)-Ni	122.7(5)	C(8)-C(1)-C(7A)-C(7)	-9.2(8)
C(3)-Ni-C(2)-C(1)	116.8(4)	Ni-C(1)-C(7A)-C(7)	120.7(5)
Cl-Ni-C(2)-C(1)	-54.0(3)	C(2)-C(1)-C(7A)-C(3A)	5.9(5)
P-Ni-C(2)-C(1)	166.4(2)	C(8)-C(1)-C(7A)-C(3A)	174.3(4)
C(3A)-Ni-C(2)-C(1)	78.5(3)	Ni-C(1)-C(7A)-C(3A)	-55.8(3)
C(7A)-Ni-C(2)-C(1)	38.5(3)	C(2)-C(1)-C(7A)-Ni	61.7(3)
C(1)-Ni-C(2)-C(3)	-116.8(4)	C(8)-C(1)-C(7A)-Ni	-129.9(5)
Cl-Ni-C(2)-C(3)	-170.8(2)	C(3)-Ni-C(7A)-C(7)	150.1(5)
P-Ni-C(2)-C(3)	49.6(4)	C(2)-Ni-C(7A)-C(7)	-163.3(5)
C(3A)-Ni-C(2)-C(3)	-38.3(3)	C(1)-Ni-C(7A)-C(7)	-123.5(6)
C(7A)-Ni-C(2)-C(3)	-78.3(3)	Cl-Ni-C(7A)-C(7)	-44.4(5)
C(1)-C(2)-C(3)-C(3A)	8.9(5)	P-Ni-C(7A)-C(7)	75.2(5)
Ni-C(2)-C(3)-C(3A)	72.4(3)	C(3A)-Ni-C(7A)-C(7)	113.5(6)
C(1)-C(2)-C(3)-Ni	-63.6(3)	C(3)-Ni-C(7A)-C(3A)	36.6(3)
C(2)-Ni-C(3)-C(3A)	-114.2(4)	C(2)-Ni-C(7A)-C(3A)	83.1(3)
C(1)-Ni-C(3)-C(3A)	-76.4(3)	C(1)-Ni-C(7A)-C(3A)	122.9(4)
Cl-Ni-C(3)-C(3A)	-87.6(6)	Cl-Ni-C(7A)-C(3A)	-158.0(3)
P-Ni-C(3)-C(3A)	101.8(2)	P-Ni-C(7A)-C(3A)	-38.4(3)
C(7A)-Ni-C(3)-C(3A)	-34.6(2)	C(3)-Ni-C(7A)-C(1)	-86.4(3)
C(1)-Ni-C(3)-C(2)	37.8(3)	C(2)-Ni-C(7A)-C(1)	-39.8(3)
Cl-Ni-C(3)-C(2)	26.6(7)	Cl-Ni-C(7A)-C(1)	79.1(3)
P-Ni-C(3)-C(2)	-144.0(3)	P-Ni-C(7A)-C(1)	-161.3(2)
C(3A)-Ni-C(3)-C(2)	114.2(4)	C(3A)-Ni-C(7A)-C(1)	-122.9(4)
C(7A)-Ni-C(3)-C(2)	79.6(3)	C(2)-C(1)-C(8)-C(9)	75(2)
C(2)-C(3)-C(3A)-C(4)	172.3(5)	C(7A)-C(1)-C(8)-C(9)	-91(2)

Ni-C(1)-C(8)-C(9)	164(2)	C(41)-P-C(31)-C(36)	74.0(4)
C(2)-C(1)-C(8)-C(19)	64(2)	Ni-P-C(31)-C(36)	-160.8(3)
C(7A)-C(1)-C(8)-C(19)	-102(2)	C(21)-P-C(31)-C(32)	147.1(3)
Ni-C(1)-C(8)-C(19)	153(2)	C(41)-P-C(31)-C(32)	-103.4(4)
C(1)-C(8)-C(9)-N(1)	-151(2)	Ni-P-C(31)-C(32)	21.8(4)
C(19)-C(8)-C(9)-N(1)	-53(7)	C(36)-C(31)-C(32)-C(33)	0.9(6)
C(8)-C(9)-N(1)-C(10)	158(2)	P-C(31)-C(32)-C(33)	178.4(4)
C(8)-C(9)-N(1)-C(11)	-75(4)	C(31)-C(32)-C(33)-C(34)	-1.6(7)
C(1)-C(8)-C(19)-N(11)	149(2)	C(32)-C(33)-C(34)-C(35)	2.3(8)
C(9)-C(8)-C(19)-N(11)	64(9)	C(33)-C(34)-C(35)-C(36)	-2.3(7)
C(8)-C(19)-N(11)-C(11)	66(4)	C(34)-C(35)-C(36)-C(31)	1.6(7)
C(8)-C(19)-N(11)-C(110)	-174(2)	C(32)-C(31)-C(36)-C(35)	-0.9(6)
C(31)-P-C(21)-C(22)	136.3(4)	P-C(31)-C(36)-C(35)	-178.3(3)
C(41)-P-C(21)-C(22)	25.5(4)	C(31)-P-C(41)-C(42)	-17.3(4)
Ni-P-C(21)-C(22)	-98.8(4)	C(21)-P-C(41)-C(42)	92.3(4)
C(31)-P-C(21)-C(26)	-48.6(4)	Ni-P-C(41)-C(42)	-142.8(3)
C(41)-P-C(21)-C(26)	-159.5(3)	C(31)-P-C(41)-C(46)	163.2(3)
Ni-P-C(21)-C(26)	76.2(4)	C(21)-P-C(41)-C(46)	-87.2(4)
C(26)-C(21)-C(22)-C(23)	-3.5(7)	Ni-P-C(41)-C(46)	37.8(4)
P-C(21)-C(22)-C(23)	171.6(4)	C(46)-C(41)-C(42)-C(43)	-0.1(7)
C(21)-C(22)-C(23)-C(24)	1.1(8)	P-C(41)-C(42)-C(43)	-179.5(3)
C(22)-C(23)-C(24)-C(25)	0.3(8)	C(41)-C(42)-C(43)-C(44)	-0.1(7)
C(23)-C(24)-C(25)-C(26)	0.8(8)	C(42)-C(43)-C(44)-C(45)	1.4(7)
C(24)-C(25)-C(26)-C(21)	-3.3(7)	C(43)-C(44)-C(45)-C(46)	-2.6(7)
C(22)-C(21)-C(26)-C(25)	4.6(7)	C(44)-C(45)-C(46)-C(41)	2.4(7)
P-C(21)-C(26)-C(25)	-170.7(4)	C(42)-C(41)-C(46)-C(45)	-1.0(7)
C(21)-P-C(31)-C(36)	-35.5(4)	P-C(41)-C(46)-C(45)	178.4(3)

Table I.11. Hydrogen coordinates and isotropic displacement parameters ($Å^2$ x 10^2) for (η^3:η^0-Ind$(CH_2)_2NMe_2$)(PPh_3)NiCl. **(9)**

	x	y	z	U_{eq}
H(2)	0.2561	0.1547	0.5652	8.3
H(3)	0.4100	0.2096	0.6686	7.9
H(4)	0.6131	0.0250	0.8188	10.2
H(5)	0.6789	-0.1978	0.9163	12.2
H(6)	0.5656	-0.3541	0.9054	11.4
H(7)	0.3791	-0.2937	0.7947	8.5
H(8A)	0.1011	-0.0358	0.5955	8.8
H(8B)	0.1846	-0.1794	0.6682	8.8
H(18A)	0.0938	-0.0394	0.6051	8.8
H(18B)	0.2021	-0.1912	0.6664	8.8
H(9A)	0.3698	-0.1349	0.5339	9.9
H(9B)	0.3800	-0.2865	0.5891	9.9
H(10A)	0.3187	-0.1373	0.3957	21.2
H(10B)	0.2213	-0.2231	0.3776	21.2
H(10C)	0.3856	-0.3092	0.4312	21.2
H(11A)	0.2416	-0.4037	0.5379	15.9
H(11B)	0.0769	-0.3029	0.4864	15.9
H(11C)	0.1038	-0.2908	0.5786	15.9
H(19A)	0.2439	-0.0864	0.4967	9.9
H(19B)	0.4010	-0.1840	0.5550	9.9
H(11D)	0.3314	-0.2828	0.4136	21.2
H(11E)	0.3841	-0.4468	0.4655	21.2
H(11F)	0.4842	-0.3593	0.4766	21.2
H(11G)	0.0509	-0.2231	0.5554	15.9
H(11H)	0.1059	-0.3495	0.5067	15.9
H(11I)	0.0829	-0.1895	0.4591	15.9
H(22)	0.3629	0.2402	0.9357	7.9
H(23)	0.6061	0.2511	0.9527	9.9
H(24)	0.7041	0.3639	0.8392	11.0
H(25)	0.5632	0.4639	0.7099	9.7
H(26)	0.3169	0.4603	0.6934	7.4
H(32)	-0.1033	0.4122	0.6622	6.9
H(33)	-0.2890	0.6353	0.5872	8.4
H(34)	-0.3100	0.8529	0.6168	8.6
H(35)	-0.1303	0.8459	0.7148	8.2
H(36)	0.0563	0.6228	0.7902	6.8
H(42)	-0.0894	0.4888	0.8955	6.8
H(43)	-0.1756	0.4354	1.0299	7.6
H(44)	-0.0761	0.1978	1.1109	7.8
H(45)	0.1211	0.0108	1.0616	8.1
H(46)	0.2027	0.0598	0.9262	6.8

Table I.12. Anisotropic parameters ($Å^2 \times 10^2$) for (η^3:η^0-Ind$(CH_2)_2NMe_2$)(PPh_3)NiCl. **(9)**

	U11	U22	U33	U23	U13	U12
Ni	5.88(6)	4.67(5)	4.76(5)	-2.13(4)	1.05(4)	-2.69(4)
Cl	6.38(9)	6.88(8)	7.27(8)	-2.83(7)	1.52(7)	-3.62(7)
P	4.78(8)	4.16(6)	4.63(7)	-1.63(5)	0.78(6)	-2.13(6)
C(1)	6.0(3)	5.6(3)	5.1(3)	-2.8(2)	0.8(2)	-2.6(3)
C(2)	10.5(5)	6.4(3)	4.7(3)	-2.4(3)	2.8(3)	-4.0(3)
C(3)	7.4(4)	6.5(3)	8.7(4)	-4.8(3)	3.3(3)	-4.2(3)
C(3A)	5.5(3)	6.8(3)	6.6(3)	-3.9(3)	1.5(3)	-3.4(3)
C(4)	5.0(4)	10.7(5)	11.4(5)	-7.7(4)	0.8(4)	-2.3(4)
C(5)	6.5(5)	13.5(6)	9.6(5)	-6.8(5)	-1.3(4)	-1.1(5)
C(6)	10.2(5)	7.4(4)	7.7(4)	-2.1(3)	-1.5(4)	-0.2(4)
C(7)	7.8(4)	5.8(3)	7.3(4)	-2.8(3)	0.2(3)	-1.8(3)
C(7A)	6.5(3)	4.6(3)	5.5(3)	-2.8(2)	0.8(3)	-1.8(3)
C(8)	8.9(4)	8.9(4)	6.4(3)	-4.6(3)	0.9(3)	-4.4(3)
C(9)	9.0(7)	10.0(11)	9.3(9)	-6.5(9)	2.6(7)	-5.4(8)
N(1)	10.6(11)	11.9(10)	8.0(8)	-6.9(8)	2.4(7)	-6.1(8)
C(10)	12.5(14)	22(2)	11.5(12)	-10.7(12)	3.2(9)	-8.0(12)
C(11)	12.7(11)	14.8(18)	9.6(10)	-7.3(11)	4.1(10)	-9.0(12)
C(19)	9.0(7)	10.0(11)	9.3(9)	-6.5(9)	2.6(7)	-5.4(8)
N(11)	6.3(7)	8.3(8)	6.9(7)	-4.3(6)	0.6(5)	-3.4(6)
C(110)	12.5(14)	22(2)	11.5(12)	-10.7(12)	3.2(9)	-8.0(12)
C(111)	12.7(11)	14.8(18)	9.6(10)	-7.3(11)	4.1(10)	-9.0(12)
C(21)	5.0(3)	5.1(3)	5.5(3)	-2.3(2)	0.8(2)	-2.2(2)
C(22)	5.8(4)	7.6(4)	7.5(4)	-3.7(3)	0.7(3)	-2.9(3)
C(23)	6.0(4)	10.1(5)	10.2(5)	-5.5(4)	-0.1(3)	-3.1(4)
C(24)	6.1(4)	10.4(5)	15.0(7)	-8.7(5)	2.4(4)	-4.5(4)
C(25)	7.2(4)	9.3(4)	11.6(5)	-6.3(4)	3.5(4)	-5.5(4)
C(26)	6.4(4)	6.5(3)	7.0(3)	-2.7(3)	1.5(3)	-3.7(3)
C(31)	5.8(3)	4.2(2)	4.2(2)	-1.4(2)	1.2(2)	-2.4(2)
C(32)	6.9(4)	5.1(3)	5.5(3)	-1.0(2)	0.1(3)	-2.9(3)
C(33)	6.8(4)	6.7(4)	6.5(3)	-0.2(3)	-0.5(3)	-2.4(3)
C(34)	7.1(4)	5.0(3)	7.2(4)	0.1(3)	1.8(3)	-1.3(3)
C(35)	8.7(4)	4.4(3)	6.9(4)	-1.4(3)	2.4(3)	-2.5(3)
C(36)	7.0(4)	5.0(3)	5.3(3)	-1.7(2)	1.1(3)	-2.6(3)
C(41)	6.1(3)	4.5(3)	4.2(2)	-1.6(2)	0.4(2)	-2.7(2)
C(42)	7.6(4)	5.3(3)	4.4(3)	-1.4(2)	0.8(3)	-2.8(3)
C(43)	7.4(4)	6.9(3)	5.3(3)	-2.7(3)	1.7(3)	-2.9(3)
C(44)	9.0(4)	8.5(4)	3.9(3)	-2.3(3)	1.7(3)	-5.2(3)
C(45)	9.9(4)	6.1(3)	4.9(3)	-0.7(3)	-0.2(3)	-4.2(3)
C(46)	7.4(4)	5.1(3)	5.0(3)	-1.6(2)	0.5(3)	-2.8(3)

Annexe 2

Données cristallographiques et matériel supplémentaires, article 2

Determination of the Equilibrium constants:

$a + b \Leftrightarrow c$ $\quad\quad$ $Keq = [c] / [a][b]$

Eq	Compound (a)	Ligand (b)	Product (c)	
A	**2**	Pyridine	$[(\eta^3\eta^0\text{-IndCH}_2\text{CH}_2\text{NMe}_2)\text{Ni(PPh}_3)\text{py}]^+$	**6a**
B	**2**	2-Picoline	$[(\eta^3\eta^0\text{-IndCH}_2\text{CH}_2\text{NMe}_2)\text{Ni(PPh}_3)\text{2-Pic}]^+$	**6b**
C	**2**	3-Picoline	$[(\eta^3\eta^0\text{-IndCH}_2\text{CH}_2\text{NMe}_2)\text{Ni(PPh}_3)\text{3-pic}]^+$	**6c**
D	**2**	4-Picoline	$[(\eta^3\eta^0\text{-IndCH}_2\text{CH}_2\text{NMe}_2)\text{Ni(PPh}_3)\text{4-pic}]^+$	**6d**
E	**2**	3,5-Lutidine	$[(\eta^3\eta^0\text{-IndCH}_2\text{CH}_2\text{NMe}_2)\text{Ni(PPh}_3)\text{3,5-lut}]^+$	**6e**
F	**2**	PPh_3	$[(\eta^3\eta^0\text{-IndCH}_2\text{CH}_2\text{NMe}_2)\text{Ni(PPh}_3)_2]^+$	**5**

A: **2** + pyridine $\Leftrightarrow$ **6a**

First measurement :

Starting point : vol = 0.63 mL

	2 (mmol)	**Py** (mmol)	[**2**] mol/L	[py^0]
1	0.0220	0.0668	0.0349	0.1060
2	0.0220	0.1113	0.0349	0.1767
3	0.0220	0.2225	0.0349	0.3531

At equilibrium (observed with ^{31}P NMR):

	2*	**6a***	**2** (eq)	**6a** (eq)	[**2**] mol/L	[**6a**] mol/L	[py] mol/L	Keq	Keq (mean)
1	1	0.698	0.589	0.411	0.0206	0.0143	0.9166	7.57	9 ± 2
2	1	1.479	0.403	0.597	0.0141	0.0208	0.1559	9.46	
3	1	3.449	0.225	0.775	0.0078	0.0270	0.3261	10.62	

*integration

Rem : **2** (eq) = **2** (integration)/ (**2**(integration)+ **3**(integration))
6a (eq) = **6a** (integration)/ (**2**(integration)+ **6a**(integration))
[py] = [py^0] - [**6a**]
Keq = [**6a**]/ ([**2**]*[Py])

At equilibrium (observed with ^1H NMR, H3):

	2*	**6a***	**2** (eq)	**6a** (eq)	[**2**] mol/L	[**6a**] mol/L	[py] mol/L	Keq	Keq (mean)
1	1	0.722	0.581	0.419	0.0203	0.0146	0.0914	7.87	9 ± 1
2	1	1.580	0.388	0.612	0.0135	0.0214	0.1553	10.20	
3	1	2.925	0.254	0.745	0.0089	0.0260	0.3271	8.93	

Second measurement

Starting point :Volume = 0.79 mL

	2 (mmol)	py(mmol)	[**2**] mol/L	[py^0]
1	0.0190	0.06182	0.0241	0.07825
2	0.0190	0.12364	0.0241	0.15651
3	0.0190	0.18546	0.0241	0.23476
4	0.0190	0.24728	0.0241	0.31301

At equilibrium (observed with ^{31}P NMR):

	2*	**6a***	**2** (eq)	**6a**(eq)	[**2**] mol/L	[**6a**] mol/L	[py] mol/L	Keq	Keq (mean)
1	1	0.6008	0.6247	0.3753	0.0151	0.0090	0.0693	8.60	8 ± 1
2	1	1.0467	0.4886	0.5114	0.0113	0.0124	0.1441	7.62	
3	1	2.0495	0.3279	0.6721	0.0080	0.0161	0.2186	9.21	
4	1	2.1790	0.3146	0.6854	0.0076	0.0165	0.2965	7.32	

B: **2** + 2-picoline ⇔ **6b**

Starting point :Volume = 0.76 mL

	2 (mmol)	2-picoline (mmol)	[**2**] mol/L	[2-pic^0] mol/L
1	0.0258	0.1823	0.0339	0.2399
2	0.0258	0.2835	0.0339	0.3730

At equilibrium (observed with ^{31}P NMR):

	2*	**6b***	**2** (eq)	**6b** (eq)	[**2**] mol/L	[**6b**] mol/L	[2-pic] mol/L	Keq	Keq (mean)
1	1	0.494	0.669	0.331	0.0227	0.0112	0.2287	2.16	2.0 ±
2	1	0.690	0.592	0.408	0.0201	0.0138	0.3592	1.92	0.2

C: **2** + 3-picoline ⇔ **6c**

Starting point :Volume = 0.77 mL

	2 (mmol)	3-picoline (mmol)	[**2**] mol/L	[3-pic^0] mol/L
1	0.0266	0.1439	0.0345	0.1869
2	0.0266	0.1952	0.0345	0.2535

At equilibrium (observed with ^{31}P NMR):

	2*	**6c***	**2** (eq)	**6c** (eq)	[**2**] mol/L	[**6c**] mol/L	[3-pic] mol/L	Keq	Keq (mean)
1	1	3.5461	0.220	0.780	0.0076	0.0269	0.16	22.1	23 ± 2
2	1	5.2411	0.160	0.840	0.0055	0.0299	0.2233	24.3	

D: **2** + 4-picoline ⇔ **6d**

First measurement

Starting point :Volume = 0.75 mL

	2 mmol	4-picoline mmol	[**2**] mol/L	[4-pic^0] mol/L
1	0.0180	0.1006	0.0240	0.1341
2	0.0180	0.1509	0.0240	0.2012
3	0.0180	0.2012	0.0240	0.2682

At equilibrium (observed with ^{31}P NMR):

	2*	**6d***	**2** (eq)	**6d** (eq)	[**2**] mol/L	[**6d**] mol/L	[4-pic] mol/L	Keq	Keq (mean)
1	1	4.0496	0.198	0.802	0.0048	0.0192	0.1149	34.8	34 ± 3
2	1	5.7113	0.149	0.851	0.0036	0.0204	0.1808	31.3	
3	1	9.0365	0.100	0.900	0.0024	0.0216	0.2466	36.5	

Second measurement

Starting point :Volume = 1.00 mL

	2 mmol	4-picoline mmol	[**2**] mol/L	[4-pic^0] mol/L
1	0.0203	0.0503	0.0203	0.0503
2	0.0203	0.1006	0.0203	0.1006

At equilibrium (observed with ^{31}P NMR):

	2 *	**6d***	**2** (eq)	**6d** (eq)	[**2**] mol/L	[**6d**] mol/L	[4-pic] mol/L	Keq	Keq (mean)
1	1	1.3114	0.433	0.567	0.0088	0.0115	0.0388	33.7	33.5 ± 0.3
2	1	2.8731	0.258	0.742	0.0053	0.0151	0.0855	33.3	

E: **2** + 3,5-lutidine ⇔ **6e**

Starting point :Volume = 0.66 mL

	2 (mmol)	3,5-lutidine (mmol)	[**2**] mol/L	[3,5-lut^0] mol/L
1	0.0244	0.1314	0.0370	0.1991
2	0.0244	0.1928	0.0370	0.2921
3	0.0244	0.2541	0.0370	0.3850

At equilibrium (observed with ^{31}P NMR):

	2 *	**6e***	**2** (eq)	**6e** (eq)	[**2**] mol/L	[**6e**] mol/L	[3,5-lut] mol/L	Keq	Keq (mean)
1	1	2.4969	0.286	0.714	0.0106	0.0264	0.1720	14.5	16 ± 1
2	1	4.4465	0.184	0.816	0.0068	0.0302	0.2619	16.9	
3	1	5.8207	0.147	0.853	0.0054	0.0316	0.3534	16.6	

F: **2** + PPh_3 ⇔ **5**

Starting point :Volume = 0.76 mL

	2 (mmol)	PPh_3 (mmol)	[**2**] mol/L	[PPh_3] mol/L
1	0.0224	0.362	0.0295	0.476
2	0.0224	0.732	0.0295	0.963

At equilibrium (^{31}P NMR: first doublet (1 and 2), second doublet (2 and 3):

	2 *	**5** *	**2** (eq)	**5** (eq)	[**2**] mol/L	[**5**] mol/L	[PPh_3] mol/L	Keq	Keq (mean)
1	1	0.3425	0.745	0.255	0.0220	0.0075	0.4675	0.73	0.9 ± 0.2
2	1	1.027	0.493	0.507	0.0145	0.0150	0.9480	1.09	
3	1	0.3818	0.724	0.276	0.0214	0.0081	0.4679	0.81	
4	1	1.014	0.496	0.504	0.0146	0.0149	0.9481	1.08	

VT NMR spectra of $[(\eta^3:\eta^0\text{-Ind}(CH_2)_2NMe_2)Ni(Ph_2PCH_2CH_2PPh_2)]^+$ (**3**)

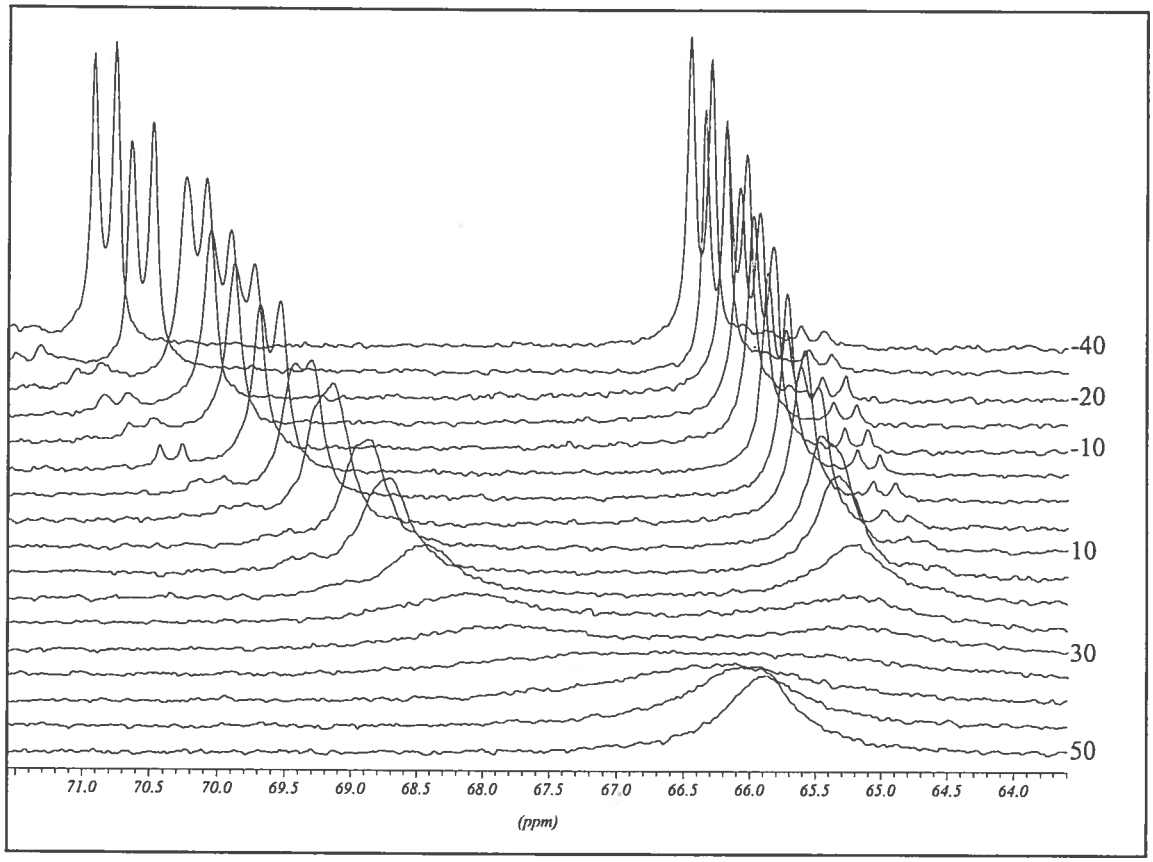

Table II.1. Crystal data and structure refinement for $[(\eta^3:\eta^1\text{-Ind}(CH_2)_2NMe_2)Ni(PPh_3)][BPh_4]$ (**2**)

Empirical formula	C55 H51 B N Ni P
Formula weight	826.458
Temperature	293(2)K
Wavelength	1.54056 Å
Crystal system	Triclinic
Space group	P-1
Unit cell dimensions	a = 11.161(6) Å α = 82.69(4)° b = 14.119(5) Å β = 79.86(6)° c = 15.115(9) Å γ = 72.65(4)°
Volume	2231(2)Å^3
Z	2
Density (calculated)	1.2303 Mg/m^3
Absorption coefficient	1.240 mm^{-1}
F(000)	872
Crystal size	0.36 x 0.28 x 0.16 mm
Theta range for data collection	2.98 to 69.80°
Index ranges	$-13 \le h \le 13$, $-17 \le k \le 17$, $-18 \le \ell \le 18$
Reflections collected	32773
Independent reflections	8462
Absorption correction	Integration
Max. and min. transmission	0.6601 and 0.8336
Refinement method	Full-matrix least-squares on F^2
Data / restraints / parameters	8462 / 0 / 535
Goodness-of-fit on F^2	0.898
Final R indices [I>2sigma(I)]	R_1 = 0.0386, wR_2 = 0.0942
R indices (all data)	R_1 = 0.0553, wR_2 = 0.1186
Extinction coefficient	0.00089(11)
Largest diff. peak and hole	0.485 and -0.272 e/Å^3

Table II.2. Atomic coordinates [x 10^4] and equivalent isotropic displacement parameters [$Å^2$ x 10^3] for [(η^3:η^1-Ind$(CH_2)_2NMe_2$)Ni(PPh_3)][BPh_4] (**2**)

U_{eq} is defined as one third of the trace of the orthogonalized Uij tensor.

	x	y	z	U(eq)
Ni	8509(1)	6467(1)	1937(1)	44(1)
P	7797(1)	8099(1)	1802(1)	37(1)
N	7712(2)	5995(1)	3140(1)	56(1)
C(1)	9236(2)	4990(2)	1739(2)	56(1)
C(2)	10215(2)	5461(2)	1524(2)	63(1)
C(3)	9906(2)	6191(2)	819(2)	57(1)
C(3A)	8853(2)	6053(2)	454(2)	51(1)
C(4)	8215(3)	6523(2)	-269(2)	62(1)
C(5)	7209(3)	6227(2)	-418(2)	74(1)
C(6)	6805(3)	5491(2)	138(2)	77(1)
C(7)	7407(3)	5020(2)	858(2)	66(1)
C(7A)	8440(2)	5295(2)	1022(2)	52(1)
C(8)	8983(3)	4356(2)	2583(2)	78(1)
C(9)	8609(3)	5018(2)	3384(2)	83(1)
C(10)	6441(3)	5862(2)	3111(2)	81(1)
C(11)	7527(4)	6653(2)	3877(2)	89(1)
C(21)	8009(2)	8677(1)	653(1)	41(1)
C(22)	9202(2)	8777(2)	289(2)	54(1)
C(23)	9429(3)	9170(2)	-590(2)	67(1)
C(24)	8469(3)	9453(2)	-1117(2)	68(1)
C(25)	7292(3)	9359(2)	-763(2)	62(1)
C(26)	7053(2)	8977(2)	117(2)	49(1)
C(31)	8537(2)	8758(1)	2405(1)	39(1)
C(32)	9501(2)	8212(2)	2884(2)	49(1)
C(33)	10101(2)	8693(2)	3330(2)	60(1)
C(34)	9756(2)	9710(2)	3297(2)	57(1)
C(35)	8808(2)	10264(2)	2814(2)	53(1)
C(36)	8205(2)	9795(2)	2360(1)	45(1)
C(41)	6097(2)	8502(1)	2180(1)	42(1)
C(42)	5344(2)	8062(2)	1822(2)	53(1)
C(43)	4051(2)	8304(2)	2110(2)	70(1)
C(44)	3509(2)	8970(2)	2753(2)	76(1)
C(45)	4233(2)	9406(2)	3114(2)	73(1)
C(46)	5530(2)	9180(2)	2830(2)	56(1)
C(51)	3686(2)	4068(2)	2903(1)	45(1)
C(52)	2652(2)	4580(2)	3500(2)	56(1)
C(53)	2092(2)	5602(2)	3381(2)	65(1)
C(54)	2533(2)	6147(2)	2652(2)	69(1)
C(55)	3514(3)	5675(2)	2036(2)	70(1)
C(56)	4075(2)	4650(2)	2166(2)	55(1)
C(61)	3361(2)	2300(2)	3582(2)	49(1)
C(62)	3366(2)	1741(2)	4412(2)	57(1)
C(63)	2425(3)	1287(2)	4784(2)	70(1)
C(64)	1433(3)	1376(2)	4328(2)	74(1)
C(65)	1383(3)	1909(2)	3504(2)	72(1)
C(66)	2327(2)	2366(2)	3145(2)	62(1)
C(71)	5302(2)	2403(1)	2220(1)	45(1)
C(72)	6435(2)	2635(2)	1876(2)	57(1)
C(73)	7166(3)	2325(2)	1066(2)	69(1)
C(74)	6802(3)	1732(2)	571(2)	73(1)
C(75)	5721(3)	1457(2)	897(2)	70(1)
C(76)	4991(2)	1782(2)	1702(2)	55(1)
C(81)	5398(2)	2821(2)	3866(1)	45(1)
C(82)	6271(2)	1916(2)	4090(2)	62(1)
C(83)	7115(3)	1824(2)	4687(2)	78(1)
C(84)	7110(3)	2647(2)	5095(2)	78(1)
C(85)	6279(3)	3544(2)	4899(2)	65(1)
C(86)	5437(2)	3625(2)	4299(2)	53(1)
B	4432(2)	2884(2)	3142(2)	44(1)

Table II.3. Bond lengths [Å] and angles [deg] for [(η^3:η^1-Ind$(CH_2)_2NMe_2$)Ni(PPh_3)][BPh_4] (**2**)

Ni-N	2.005(2)	C(35)-H(35)	0.9300
Ni-C(1)	2.040(2)	C(36)-H(36)	0.9300
Ni-C(2)	2.056(3)	C(41)-C(46)	1.393(3)
Ni-C(3)	2.078(3)	C(41)-C(42)	1.394(3)
Ni-P	2.1971(11)	C(42)-C(43)	1.382(4)
Ni-C(7A)	2.314(2)	C(42)-H(42)	0.9300
Ni-C(3A)	2.327(3)	C(43)-C(44)	1.372(4)
P-C(41)	1.819(2)	C(43)-H(43)	0.9300
P-C(31)	1.821(2)	C(44)-C(45)	1.366(4)
P-C(21)	1.829(2)	C(44)-H(44)	0.9300
N-C(11)	1.487(4)	C(45)-C(46)	1.386(3)
N-C(9)	1.489(3)	C(45)-H(45)	0.9300
N-C(10)	1.494(4)	C(46)-H(46)	0.9300
C(1)-C(2)	1.412(4)	C(51)-C(56)	1.383(3)
C(1)-C(7A)	1.463(3)	C(51)-C(52)	1.404(3)
C(1)-C(8)	1.497(4)	C(51)-B	1.656(3)
C(2)-C(3)	1.399(4)	C(52)-C(53)	1.394(3)
C(2)-H(2)	0.9300	C(52)-H(52)	0.9300
C(3)-C(3A)	1.455(3)	C(53)-C(54)	1.366(4)
C(3)-H(3)	0.9300	C(53)-H(53)	0.9300
C(3A)-C(4)	1.396(4)	C(54)-C(55)	1.370(4)
C(3A)-C(7A)	1.420(3)	C(54)-H(54)	0.9300
C(4)-C(5)	1.370(4)	C(55)-C(56)	1.398(3)
C(4)-H(4)	0.9300	C(55)-H(55)	0.9300
C(5)-C(6)	1.384(4)	C(56)-H(56)	0.9300
C(5)-H(5)	0.9300	C(61)-C(62)	1.395(3)
C(6)-C(7)	1.373(4)	C(61)-C(66)	1.402(3)
C(6)-H(6)	0.9300	C(61)-B	1.649(3)
C(7)-C(7A)	1.391(3)	C(62)-C(63)	1.390(4)
C(7)-H(7)	0.9300	C(62)-H(62)	0.9300
C(8)-C(9)	1.547(4)	C(63)-C(64)	1.371(4)
C(8)-H(8A)	0.9700	C(63)-H(63)	0.9300
C(8)-H(8B)	0.9700	C(64)-C(65)	1.371(4)
C(9)-H(9A)	0.9700	C(64)-H(64)	0.9300
C(9)-H(9B)	0.9700	C(65)-C(66)	1.391(4)
C(10)-H(10A)	0.9600	C(65)-H(65)	0.9300
C(10)-H(10B)	0.9600	C(66)-H(66)	0.9300
C(10)-H(10C)	0.9600	C(71)-C(72)	1.396(3)
C(11)-H(11A)	0.9600	C(71)-C(76)	1.398(3)
C(11)-H(11B)	0.9600	C(71)-B	1.649(3)
C(11)-H(11C)	0.9600	C(72)-C(73)	1.389(4)
C(21)-C(26)	1.386(3)	C(72)-H(72)	0.9300
C(21)-C(22)	1.389(3)	C(73)-C(74)	1.377(4)
C(22)-C(23)	1.384(3)	C(73)-H(73)	0.9300
C(22)-H(22)	0.9300	C(74)-C(75)	1.367(4)
C(23)-C(24)	1.381(4)	C(74)-H(74)	0.9300
C(23)-H(23)	0.9300	C(75)-C(76)	1.387(4)
C(24)-C(25)	1.367(4)	C(75)-H(75)	0.9300
C(24)-H(24)	0.9300	C(76)-H(76)	0.9300
C(25)-C(26)	1.382(3)	C(81)-C(86)	1.395(3)
C(25)-H(25)	0.9300	C(81)-C(82)	1.400(3)
C(26)-H(26)	0.9300	C(81)-B	1.643(3)
C(31)-C(32)	1.383(3)	C(82)-C(83)	1.384(4)
C(31)-C(36)	1.396(3)	C(82)-H(82)	0.9300
C(32)-C(33)	1.382(3)	C(83)-C(84)	1.380(4)
C(32)-H(32)	0.9300	C(83)-H(83)	0.9300
C(33)-C(34)	1.368(4)	C(84)-C(85)	1.362(4)
C(33)-H(33)	0.9300	C(84)-H(84)	0.9300
C(34)-C(35)	1.377(3)	C(85)-C(86)	1.389(3)
C(34)-H(34)	0.9300	C(85)-H(85)	0.9300
C(35)-C(36)	1.381(3)	C(86)-H(86)	0.93

N-Ni-C(1)	84.86(11)	C(6)-C(7)-H(7)	120.6
N-Ni-C(2)	110.61(11)	C(7A)-C(7)-H(7)	120.6
C(1)-Ni-C(2)	40.33(10)	C(7)-C(7A)-C(3A)	120.1(2)
N-Ni-C(3)	149.55(10)	C(7)-C(7A)-C(1)	132.7(2)
C(1)-Ni-C(3)	66.97(11)	C(3A)-C(7A)-C(1)	107.1(2)
C(2)-Ni-C(3)	39.56(11)	C(7)-C(7A)-Ni	129.71(17)
N-Ni-P	107.52(8)	C(3A)-C(7A)-Ni	72.67(12)
C(1)-Ni-P	166.49(8)	C(1)-C(7A)-Ni	60.49(11)
C(2)-Ni-P	134.09(9)	C(1)-C(8)-C(9)	108.0(2)
C(3)-Ni-P	101.79(8)	C(1)-C(8)-H(8A)	110.1
N-Ni-C(7A)	101.98(9)	C(9)-C(8)-H(8A)	110.1
C(1)-Ni-C(7A)	38.63(9)	C(1)-C(8)-H(8B)	110.1
C(2)-Ni-C(7A)	63.95(10)	C(9)-C(8)-H(8B)	110.1
C(3)-Ni-C(7A)	63.17(10)	H(8A)-C(8)-H(8B)	108.4
P-Ni-C(7A)	130.41(7)	N-C(9)-C(8)	110.1(2)
N-Ni-C(3A)	137.17(9)	N-C(9)-H(9A)	109.6
C(1)-Ni-C(3A)	63.75(10)	C(8)-C(9)-H(9A)	109.6
C(2)-Ni-C(3A)	63.62(11)	N-C(9)-H(9B)	109.6
C(3)-Ni-C(3A)	38.06(9)	C(8)-C(9)-H(9B)	109.6
P-Ni-C(3A)	102.82(7)	H(9A)-C(9)-H(9B)	108.2
C(7A)-Ni-C(3A)	35.62(8)	N-C(10)-H(10A)	109.5
C(41)-P-C(31)	107.41(10)	N-C(10)-H(10B)	109.5
C(41)-P-C(21)	105.02(11)	H(10A)-C(10)-H(10B)	109.5
C(31)-P-C(21)	101.89(10)	N-C(10)-H(10C)	109.5
C(41)-P-Ni	110.60(8)	H(10A)-C(10)-H(10C)	109.5
C(31)-P-Ni	115.63(8)	H(10B)-C(10)-H(10C)	109.5
C(21)-P-Ni	115.35(8)	N-C(11)-H(11A)	109.5
C(11)-N-C(9)	108.0(2)	N-C(11)-H(11B)	109.5
C(11)-N-C(10)	106.2(2)	H(11A)-C(11)-H(11B)	109.5
C(9)-N-C(10)	109.7(2)	N-C(11)-H(11C)	109.5
C(11)-N-Ni	115.08(17)	H(11A)-C(11)-H(11C)	109.5
C(9)-N-Ni	105.14(18)	H(11B)-C(11)-H(11C)	109.5
C(10)-N-Ni	112.60(17)	C(26)-C(21)-C(22)	118.6(2)
C(2)-C(1)-C(7A)	107.9(2)	C(26)-C(21)-P	123.09(16)
C(2)-C(1)-C(8)	126.6(2)	C(22)-C(21)-P	118.22(17)
C(7A)-C(1)-C(8)	125.4(2)	C(23)-C(22)-C(21)	120.6(2)
C(2)-C(1)-Ni	70.45(13)	C(23)-C(22)-H(22)	119.7
C(7A)-C(1)-Ni	80.88(13)	C(21)-C(22)-H(22)	119.7
C(8)-C(1)-Ni	111.29(18)	C(24)-C(23)-C(22)	119.9(2)
C(3)-C(2)-C(1)	107.9(2)	C(24)-C(23)-H(23)	120.1
C(3)-C(2)-Ni	71.09(14)	C(22)-C(23)-H(23)	120.1
C(1)-C(2)-Ni	69.23(13)	C(25)-C(24)-C(23)	119.8(2)
C(3)-C(2)-H(2)	126.1	C(25)-C(24)-H(24)	120.1
C(1)-C(2)-H(2)	126.1	C(23)-C(24)-H(24)	120.1
Ni-C(2)-H(2)	125.2	C(24)-C(25)-C(26)	120.6(2)
C(2)-C(3)-C(3A)	108.8(2)	C(24)-C(25)-H(25)	119.7
C(2)-C(3)-Ni	69.35(15)	C(26)-C(25)-H(25)	119.7
C(3A)-C(3)-Ni	80.26(14)	C(25)-C(26)-C(21)	120.4(2)
C(2)-C(3)-H(3)	125.6	C(25)-C(26)-H(26)	119.8
C(3A)-C(3)-H(3)	125.6	C(21)-C(26)-H(26)	119.8
Ni-C(3)-H(3)	116.6	C(32)-C(31)-C(36)	119.11(18)
C(4)-C(3A)-C(7A)	119.7(2)	C(32)-C(31)-P	118.87(15)
C(4)-C(3A)-C(3)	133.3(2)	C(36)-C(31)-P	121.94(15)
C(7A)-C(3A)-C(3)	106.9(2)	C(33)-C(32)-C(31)	120.1(2)
C(4)-C(3A)-Ni	129.98(15)	C(33)-C(32)-H(32)	119.9
C(7A)-C(3A)-Ni	71.71(13)	C(31)-C(32)-H(32)	119.9
C(3)-C(3A)-Ni	61.68(13)	C(34)-C(33)-C(32)	120.5(2)
C(5)-C(4)-C(3A)	118.7(3)	C(34)-C(33)-H(33)	119.8
C(5)-C(4)-H(4)	120.7	C(32)-C(33)-H(33)	119.8
C(3A)-C(4)-H(4)	120.7	C(33)-C(34)-C(35)	120.1(2)
C(4)-C(5)-C(6)	121.6(3)	C(33)-C(34)-H(34)	119.9
C(4)-C(5)-H(5)	119.2	C(35)-C(34)-H(34)	119.9
C(6)-C(5)-H(5)	119.2	C(34)-C(35)-C(36)	120.1(2)
C(7)-C(6)-C(5)	121.1(3)	C(34)-C(35)-H(35)	120.0
C(7)-C(6)-H(6)	119.4	C(36)-C(35)-H(35)	120.0
C(5)-C(6)-H(6)	119.4	C(35)-C(36)-C(31)	120.0(2)
C(6)-C(7)-C(7A)	118.8(3)	C(35)-C(36)-H(36)	120.0

C(31)-C(36)-H(36)	120.0	C(64)-C(65)-C(66)	119.8(3)
C(46)-C(41)-C(42)	119.1(2)	C(64)-C(65)-H(65)	120.1
C(46)-C(41)-P	123.76(17)	C(66)-C(65)-H(65)	120.1
C(42)-C(41)-P	117.06(16)	C(65)-C(66)-C(61)	123.0(3)
C(43)-C(42)-C(41)	120.0(2)	C(65)-C(66)-H(66)	118.5
C(43)-C(42)-H(42)	120.0	C(61)-C(66)-H(66)	118.5
C(41)-C(42)-H(42)	120.0	C(72)-C(71)-C(76)	114.2(2)
C(44)-C(43)-C(42)	120.1(3)	C(72)-C(71)-B	120.11(19)
C(44)-C(43)-H(43)	120.0	C(76)-C(71)-B	125.6(2)
C(42)-C(43)-H(43)	120.0	C(73)-C(72)-C(71)	123.5(2)
C(45)-C(44)-C(43)	120.7(2)	C(73)-C(72)-H(72)	118.2
C(45)-C(44)-H(44)	119.6	C(71)-C(72)-H(72)	118.2
C(43)-C(44)-H(44)	119.6	C(74)-C(73)-C(72)	119.8(3)
C(44)-C(45)-C(46)	120.1(3)	C(74)-C(73)-H(73)	120.1
C(44)-C(45)-H(45)	119.9	C(72)-C(73)-H(73)	120.1
C(46)-C(45)-H(45)	119.9	C(75)-C(74)-C(73)	118.7(3)
C(45)-C(46)-C(41)	119.9(2)	C(75)-C(74)-H(74)	120.7
C(45)-C(46)-H(46)	120.0	C(73)-C(74)-H(74)	120.7
C(41)-C(46)-H(46)	120.0	C(74)-C(75)-C(76)	120.9(3)
C(56)-C(51)-C(52)	114.8(2)	C(74)-C(75)-H(75)	119.6
C(56)-C(51)-B	124.23(19)	C(76)-C(75)-H(75)	119.6
C(52)-C(51)-B	120.7(2)	C(75)-C(76)-C(71)	122.8(2)
C(53)-C(52)-C(51)	122.7(2)	C(75)-C(76)-H(76)	118.6
C(53)-C(52)-H(52)	118.7	C(71)-C(76)-H(76)	118.6
C(51)-C(52)-H(52)	118.7	C(86)-C(81)-C(82)	114.7(2)
C(54)-C(53)-C(52)	120.2(2)	C(86)-C(81)-B	124.79(19)
C(54)-C(53)-H(53)	119.9	C(82)-C(81)-B	120.51(19)
C(52)-C(53)-H(53)	119.9	C(83)-C(82)-C(81)	122.9(2)
C(53)-C(54)-C(55)	119.2(2)	C(83)-C(82)-H(82)	118.6
C(53)-C(54)-H(54)	120.4	C(81)-C(82)-H(82)	118.6
C(55)-C(54)-H(54)	120.4	C(84)-C(83)-C(82)	119.9(2)
C(54)-C(55)-C(56)	120.1(3)	C(84)-C(83)-H(83)	120.1
C(54)-C(55)-H(55)	119.9	C(82)-C(83)-H(83)	120.1
C(56)-C(55)-H(55)	119.9	C(85)-C(84)-C(83)	119.5(2)
C(51)-C(56)-C(55)	122.9(2)	C(85)-C(84)-H(84)	120.3
C(51)-C(56)-H(56)	118.5	C(83)-C(84)-H(84)	120.3
C(55)-C(56)-H(56)	118.5	C(84)-C(85)-C(86)	120.0(2)
C(62)-C(61)-C(66)	114.5(2)	C(84)-C(85)-H(85)	120.0
C(62)-C(61)-B	124.3(2)	C(86)-C(85)-H(85)	120.0
C(66)-C(61)-B	121.2(2)	C(85)-C(86)-C(81)	123.1(2)
C(63)-C(62)-C(61)	123.2(2)	C(85)-C(86)-H(86)	118.5
C(63)-C(62)-H(62)	118.4	C(81)-C(86)-H(86)	118.5
C(61)-C(62)-H(62)	118.4	C(81)-B-C(71)	107.63(17)
C(64)-C(63)-C(62)	119.9(3)	C(81)-B-C(61)	110.47(18)
C(64)-C(63)-H(63)	120.1	C(71)-B-C(61)	112.22(17)
C(62)-C(63)-H(63)	120.1	C(81)-B-C(51)	108.77(16)
C(63)-C(64)-C(65)	119.6(3)	C(71)-B-C(51)	109.43(18)
C(63)-C(64)-H(64)	120.2	C(61)-B-C(51)	108.26(17)
C(65)-C(64)-H(64)	120.2		

Table II.4 Anisotropic displacement parameters [$Å^2$ x 10^3] for [(η^3:η^1-Ind$(CH_2)_2NMe_2$)Ni(PPh_3)][BPh_4] (**2**)

	U11	U22	U33	U23	U13	U12
Ni	47(1)	34(1)	48(1)	-8(1)	-3(1)	-8(1)
P	37(1)	34(1)	40(1)	-8(1)	-3(1)	-9(1)
N	66(1)	49(1)	53(1)	2(1)	-7(1)	-16(1)
C(1)	55(1)	35(1)	74(2)	-12(1)	-16(1)	0(1)
C(2)	47(1)	55(1)	83(2)	-27(1)	-12(1)	3(1)
C(3)	50(1)	53(1)	67(2)	-23(1)	8(1)	-13(1)
C(3A)	54(1)	43(1)	55(1)	-21(1)	1(1)	-8(1)
C(4)	81(2)	49(1)	51(1)	-17(1)	-3(1)	-8(1)
C(5)	82(2)	70(2)	67(2)	-20(1)	-25(2)	-3(1)
C(6)	71(2)	83(2)	86(2)	-22(2)	-26(2)	-23(2)
C(7)	70(2)	54(1)	81(2)	-16(1)	-12(1)	-22(1)
C(7A)	56(1)	37(1)	62(1)	-15(1)	-10(1)	-7(1)
C(8)	92(2)	41(1)	97(2)	6(1)	-35(2)	-5(1)
C(9)	99(2)	63(2)	78(2)	16(1)	-27(2)	-13(2)
C(10)	75(2)	76(2)	84(2)	21(2)	-2(2)	-28(2)
C(11)	35(3)	83(2)	49(2)	-5(1)	-1(2)	-36(2)
C(21)	45(1)	36(1)	42(1)	-8(1)	-2(1)	-12(1)
C(22)	50(1)	59(1)	53(1)	-3(1)	-4(1)	-19(1)
C(23)	57(1)	78(2)	62(2)	2(1)	8(1)	-26(1)
C(24)	81(2)	74(2)	46(1)	6(1)	0(1)	-27(1)
C(25)	72(2)	67(2)	50(1)	4(1)	-16(1)	-23(1)
C(26)	50(1)	51(1)	49(1)	-3(1)	-7(1)	-18(1)
C(31)	35(1)	40(1)	41(1)	-9(1)	-3(1)	-9(1)
C(32)	41(1)	46(1)	59(1)	-6(1)	-10(1)	-8(1)
C(33)	46(1)	74(2)	64(2)	-6(1)	-19(1)	-15(1)
C(34)	49(1)	76(2)	56(1)	-21(1)	-5(1)	-29(1)
C(35)	53(1)	49(1)	61(1)	-16(1)	-1(1)	-21(1)
C(36)	45(1)	41(1)	52(1)	-5(1)	-10(1)	-11(1)
C(41)	38(1)	40(1)	45(1)	-1(1)	-3(1)	-11(1)
C(42)	50(1)	50(1)	64(1)	-1(1)	-10(1)	-21(1)
C(43)	54(2)	72(2)	92(2)	15(2)	-22(1)	-31(1)
C(44)	40(1)	80(2)	95(2)	15(2)	2(1)	-14(1)
C(45)	54(2)	72(2)	78(2)	-12(1)	17(1)	-6(1)
C(46)	49(1)	57(1)	58(1)	-14(1)	5(1)	-14(1)
C(51)	46(1)	41(1)	52(1)	-10(1)	-15(1)	-9(1)
C(52)	53(1)	51(1)	59(1)	-11(1)	-12(1)	-5(1)
C(53)	51(1)	56(1)	87(2)	-26(1)	-17(1)	-1(1)
C(54)	57(2)	37(1)	113(2)	-11(1)	-20(2)	-5(1)
C(55)	69(2)	43(1)	96(2)	5(1)	-12(2)	-15(1)
C(56)	53(1)	39(1)	71(2)	-7(1)	-9(1)	-9(1)
C(61)	50(1)	41(1)	57(1)	-13(1)	-3(1)	-11(1)
C(62)	67(2)	58(1)	50(1)	-14(1)	-2(1)	-24(1)
C(63)	88(2)	71(2)	56(1)	-11(1)	3(1)	-37(2)
C(64)	77(2)	74(2)	79(2)	-21(2)	12(2)	-42(2)
C(65)	57(2)	69(2)	98(2)	-14(2)	-14(1)	-23(1)
C(66)	57(1)	56(1)	77(2)	-1(1)	-15(1)	-18(1)
C(71)	52(1)	32(1)	50(1)	-4(1)	-12(1)	-5(1)
C(72)	60(1)	44(1)	65(1)	-12(1)	-1(1)	-14(1)
C(73)	68(2)	55(1)	72(2)	-8(1)	9(1)	-10(1)
C(74)	77(2)	69(2)	56(2)	-16(1)	-5(1)	6(1)
C(75)	71(2)	66(2)	70(2)	-29(1)	-25(1)	2(1)
C(76)	53(1)	47(1)	64(1)	-14(1)	-18(1)	-3(1)
C(81)	46(1)	41(1)	47(1)	-4(1)	-5(1)	-10(1)
C(82)	69(2)	45(1)	66(2)	-11(1)	-19(1)	0(1)
C(83)	81(2)	64(2)	80(2)	-4(1)	-37(2)	7(1)
C(84)	84(2)	80(2)	76(2)	-6(2)	-43(2)	-13(2)
C(85)	75(2)	59(1)	70(2)	-11(1)	-27(1)	-20(1)
C(86)	57(1)	42(1)	63(1)	-7(1)	-16(1)	-12(1)
B	45(1)	38(1)	50(1)	-7(1)	-10(1)	-9(1)

Table II.5. Hydrogen coordinates (x 10^4) and isotropic displacement parameters [$Å^2$ x 10^3] for [(η^3:η^1-Ind$(CH_2)_2NMe_2$)Ni(PPh_3)] [BPh_4] (**2**)

	x	y	z	U(eq)
H(2)	10936	5312	1802	76
H(3)	10309	6685	616	69
H(4)	8468	7027	-642	75
H(5)	6788	6529	-904	89
H(6)	6114	5312	22	92
H(7)	7128	4527	1230	79
H(8A)	9735	3812	2669	93
H(8B)	8300	4078	2542	93
H(9A)	8213	4687	3905	99
H(9B)	9364	5123	3541	99
H(10A)	6503	5463	2627	121
H(10B)	5844	6501	3015	121
H(10C)	6161	5536	3672	121
H(11A)	7139	6373	4425	134
H(11B)	6988	7300	3718	134
H(11C)	8334	6710	3963	134
H(22)	9854	8578	640	65
H(23)	10228	9243	-825	80
H(24)	8623	9708	-1711	81
H(25)	6645	9554	-1118	75
H(26)	6247	8921	351	59
H(32)	9745	7521	2906	59
H(33)	10745	8322	3654	72
H(34)	10162	10027	3602	68
H(35)	8574	10956	2794	64
H(36)	7578	10171	2024	54
H(42)	5711	7606	1391	64
H(43)	3548	8014	1867	84
H(44)	2639	9127	2946	91
H(45)	3855	9855	3551	88
H(46)	6020	9481	3074	67
H(52)	2329	4222	3996	67
H(53)	1416	5914	3797	78
H(54)	2171	6831	2576	83
H(55)	3807	6036	1530	84
H(56)	4741	4346	1739	66
H(62)	4032	1668	4732	68
H(63)	2469	923	5341	84
H(64)	797	1078	4576	88
H(65)	720	1964	3187	87
H(66)	2269	2731	2589	75
H(72)	6716	3017	2208	68
H(73)	7900	2519	858	82
H(74)	7282	1522	26	87
H(75)	5472	1047	574	83
H(76)	4264	1577	1905	66
H(82)	6284	1352	3827	74
H(83)	7686	1210	4812	94
H(84)	7669	2588	5501	94
H(85)	6275	4103	5167	78
H(86)	4872	4244	4180	63

Table II.6. Torsion angles [deg] for [(η^3:η^1-Ind$(CH_2)_2NMe_2$)Ni(PPh_3)] [BPh_4] (**2**)

N-Ni-P-C(41)	-43.86(11)	C(3)-Ni-C(2)-C(1)	-118.5(2)
C(1)-Ni-P-C(41)	111.9(3)	P-Ni-C(2)-C(1)	-161.93(12)
C(2)-Ni-P-C(41)	171.08(13)	C(7A)-Ni-C(2)-C(1)	-39.84(15)
C(3)-Ni-P-C(41)	144.50(11)	C(3A)-Ni-C(2)-C(1)	-79.71(16)
C(7A)-Ni-P-C(41)	79.83(12)	C(1)-C(2)-C(3)-C(3A)	-11.7(3)
C(3A)-Ni-P-C(41)	105.52(11)	Ni-C(2)-C(3)-C(3A)	-71.37(16)
N-Ni-P-C(31)	78.48(11)	C(1)-C(2)-C(3)-Ni	59.71(16)
C(1)-Ni-P-C(31)	-125.8(3)	N-Ni-C(3)-C(2)	-14.4(3)
C(2)-Ni-P-C(31)	-66.59(14)	C(1)-Ni-C(3)-C(2)	-38.18(14)
C(3)-Ni-P-C(31)	-93.17(11)	P-Ni-C(3)-C(2)	149.69(13)
C(7A)-Ni-P-C(31)	-157.84(11)	C(7A)-Ni-C(3)-C(2)	-80.77(15)
C(3A)-Ni-P-C(31)	-132.14(10)	C(3A)-Ni-C(3)-C(2)	-114.5(2)
N-Ni-P-C(21)	-162.83(10)	N-Ni-C(3)-C(3A)	100.1(2)
C(1)-Ni-P-C(21)	-7.1(3)	C(1)-Ni-C(3)-C(3A)	76.32(15)
C(2)-Ni-P-C(21)	52.11(14)	C(2)-Ni-C(3)-C(3A)	114.5(2)
C(3)-Ni-P-C(21)	25.53(11)	P-Ni-C(3)-C(3A)	-95.81(13)
C(7A)-Ni-P-C(21)	-39.14(12)	C(7A)-Ni-C(3)-C(3A)	33.73(12)
C(3A)-Ni-P-C(21)	-13.45(10)	C(2)-C(3)-C(3A)-C(4)	-176.2(2)
C(1)-Ni-N-C(11)	149.6(2)	Ni-C(3)-C(3A)-C(4)	119.7(2)
C(2)-Ni-N-C(11)	118.0(2)	C(2)-C(3)-C(3A)-C(7A)	6.5(2)
C(3)-Ni-N-C(11)	127.8(2)	Ni-C(3)-C(3A)-C(7A)	-57.58(16)
P-Ni-N-C(11)	-35.9(2)	C(2)-C(3)-C(3A)-Ni	64.12(16)
C(7A)-Ni-N-C(11)	-175.6(2)	N-Ni-C(3A)-C(4)	102.8(2)
C(3A)-Ni-N-C(11)	-169.01(19)	C(1)-Ni-C(3A)-C(4)	150.0(3)
C(1)-Ni-N-C(9)	30.92(18)	C(2)-Ni-C(3A)-C(4)	-164.7(3)
C(2)-Ni-N-C(9)	-0.7(2)	C(3)-Ni-C(3A)-C(4)	-124.4(3)
C(3)-Ni-N-C(9)	9.1(3)	P-Ni-C(3A)-C(4)	-31.6(2)
P-Ni-N-C(9)	-154.62(16)	C(7A)-Ni-C(3A)-C(4)	113.9(3)
C(7A)-Ni-N-C(9)	65.75(19)	N-Ni-C(3A)-C(7A)	-11.07(19)
C(3A)-Ni-N-C(9)	72.3(2)	C(1)-Ni-C(3A)-C(7A)	36.18(14)
C(1)-Ni-N-C(10)	-88.48(19)	C(2)-Ni-C(3A)-C(7A)	81.40(16)
C(2)-Ni-N-C(10)	-120.09(18)	C(3)-Ni-C(3A)-C(7A)	121.7(2)
C(3)-Ni-N-C(10)	-110.3(2)	P-Ni-C(3A)-C(7A)	-145.47(12)
P-Ni-N-C(10)	85.98(17)	N-Ni-C(3A)-C(3)	-132.77(16)
C(7A)-Ni-N-C(10)	-53.66(18)	C(1)-Ni-C(3A)-C(3)	-85.53(16)
C(3A)-Ni-N-C(10)	-47.1(2)	C(2)-Ni-C(3A)-C(3)	-40.31(15)
N-Ni-C(1)-C(2)	-130.71(17)	P-Ni-C(3A)-C(3)	92.82(14)
C(3)-Ni-C(1)-C(2)	37.47(16)	C(7A)-Ni-C(3A)-C(3)	-121.7(2)
P-Ni-C(1)-C(2)	72.5(4)	C(7A)-C(3A)-C(4)-C(5)	-0.9(3)
C(7A)-Ni-C(1)-C(2)	112.8(2)	C(3)-C(3A)-C(4)-C(5)	-177.8(2)
C(3A)-Ni-C(1)-C(2)	79.37(17)	Ni-C(3A)-C(4)-C(5)	-91.3(3)
N-Ni-C(1)-C(7A)	116.51(16)	C(3A)-C(4)-C(5)-C(6)	1.1(4)
C(2)-Ni-C(1)-C(7A)	-112.8(2)	C(4)-C(5)-C(6)-C(7)	-0.6(4)
C(3)-Ni-C(1)-C(7A)	-75.31(16)	C(5)-C(6)-C(7)-C(7A)	-0.1(4)
P-Ni-C(1)-C(7A)	-40.3(4)	C(6)-C(7)-C(7A)-C(3A)	0.3(4)
C(3A)-Ni-C(1)-C(7A)	-33.41(14)	C(6)-C(7)-C(7A)-C(1)	176.3(2)
N-Ni-C(1)-C(8)	-8.00(19)	C(6)-C(7)-C(7A)-Ni	92.3(3)
C(2)-Ni-C(1)-C(8)	122.7(3)	C(4)-C(3A)-C(7A)-C(7)	0.2(3)
C(3)-Ni-C(1)-C(8)	160.2(2)	C(3)-C(3A)-C(7A)-C(7)	177.9(2)
P-Ni-C(1)-C(8)	-164.8(2)	Ni-C(3A)-C(7A)-C(7)	126.4(2)
C(7A)-Ni-C(1)-C(8)	-124.5(3)	C(4)-C(3A)-C(7A)-C(1)	-176.72(19)
C(3A)-Ni-C(1)-C(8)	-157.9(2)	C(3)-C(3A)-C(7A)-C(1)	1.0(2)
C(7A)-C(1)-C(2)-C(3)	12.2(2)	Ni-C(3A)-C(7A)-C(1)	-50.53(15)
C(8)-C(1)-C(2)-C(3)	-163.4(2)	C(4)-C(3A)-C(7A)-Ni	-126.2(2)
Ni-C(1)-C(2)-C(3)	-60.89(16)	C(3)-C(3A)-C(7A)-Ni	51.50(14)
C(7A)-C(1)-C(2)-Ni	73.06(15)	C(2)-C(1)-C(7A)-C(7)	175.6(2)
C(8)-C(1)-C(2)-Ni	-102.5(2)	C(8)-C(1)-C(7A)-C(7)	-8.8(4)
N-Ni-C(2)-C(3)	172.24(14)	Ni-C(1)-C(7A)-C(7)	-118.5(3)
C(1)-Ni-C(2)-C(3)	118.5(2)	C(2)-C(1)-C(7A)-C(3A)	-8.1(2)
P-Ni-C(2)-C(3)	-43.45(18)	C(8)-C(1)-C(7A)-C(3A)	167.6(2)
C(7A)-Ni-C(2)-C(3)	78.63(16)	Ni-C(1)-C(7A)-C(3A)	57.87(16)
C(3A)-Ni-C(2)-C(3)	38.76(14)	C(2)-C(1)-C(7A)-Ni	-65.92(15)
N-Ni-C(2)-C(1)	53.77(17)	C(8)-C(1)-C(7A)-Ni	109.7(2)

N-Ni-C(7A)-C(7)	57.2(2)	C(43)-C(44)-C(45)-C(46)	0.2(4)
C(1)-Ni-C(7A)-C(7)	122.9(3)	C(44)-C(45)-C(46)-C(41)	-0.4(4)
C(2)-Ni-C(7A)-C(7)	164.5(3)	C(42)-C(41)-C(46)-C(45)	0.1(3)
C(3)-Ni-C(7A)-C(7)	-151.1(3)	P-C(41)-C(46)-C(45)	-176.55(19)
P-Ni-C(7A)-C(7)	-68.6(3)	C(56)-C(51)-C(52)-C(53)	-2.4(3)
C(3A)-Ni-C(7A)-C(7)	-115.1(3)	B-C(51)-C(52)-C(53)	172.2(2)
N-Ni-C(7A)-C(3A)	172.34(13)	C(51)-C(52)-C(53)-C(54)	0.9(4)
C(1)-Ni-C(7A)-C(3A)	-122.0(2)	C(52)-C(53)-C(54)-C(55)	1.2(4)
C(2)-Ni-C(7A)-C(3A)	-80.39(17)	C(53)-C(54)-C(55)-C(56)	-1.6(4)
C(3)-Ni-C(7A)-C(3A)	-35.99(14)	C(52)-C(51)-C(56)-C(55)	1.9(3)
P-Ni-C(7A)-C(3A)	46.54(16)	B-C(51)-C(56)-C(55)	-172.5(2)
N-Ni-C(7A)-C(1)	-65.66(16)	C(54)-C(55)-C(56)-C(51)	0.1(4)
C(2)-Ni-C(7A)-C(1)	41.61(16)	C(66)-C(61)-C(62)-C(63)	-0.4(3)
C(3)-Ni-C(7A)-C(1)	86.02(17)	B-C(61)-C(62)-C(63)	177.5(2)
P-Ni-C(7A)-C(1)	168.55(13)	C(61)-C(62)-C(63)-C(64)	0.2(4)
C(3A)-Ni-C(7A)-C(1)	122.0(2)	C(62)-C(63)-C(64)-C(65)	0.5(4)
C(2)-C(1)-C(8)-C(9)	64.5(3)	C(63)-C(64)-C(65)-C(66)	-1.0(4)
C(7A)-C(1)-C(8)-C(9)	-110.3(3)	C(64)-C(65)-C(66)-C(61)	0.9(4)
Ni-C(1)-C(8)-C(9)	-16.4(3)	C(62)-C(61)-C(66)-C(65)	-0.2(3)
C(11)-N-C(9)-C(8)	-172.1(3)	B-C(61)-C(66)-C(65)	-178.1(2)
C(10)-N-C(9)-C(8)	72.6(3)	C(76)-C(71)-C(72)-C(73)	3.4(3)
Ni-N-C(9)-C(8)	-48.7(3)	B-C(71)-C(72)-C(73)	-174.6(2)
C(1)-C(8)-C(9)-N	43.3(3)	C(71)-C(72)-C(73)-C(74)	-2.1(4)
C(41)-P-C(21)-C(26)	-23.33(19)	C(72)-C(73)-C(74)-C(75)	-0.3(4)
C(31)-P-C(21)-C(26)	-135.23(17)	C(73)-C(74)-C(75)-C(76)	1.1(4)
Ni-P-C(21)-C(26)	98.69(17)	C(74)-C(75)-C(76)-C(71)	0.4(4)
C(41)-P-C(21)-C(22)	159.70(16)	C(72)-C(71)-C(76)-C(75)	-2.5(3)
C(31)-P-C(21)-C(22)	47.80(18)	B-C(71)-C(76)-C(75)	175.4(2)
Ni-P-C(21)-C(22)	-78.28(17)	C(86)-C(81)-C(82)-C(83)	-0.6(4)
C(26)-C(21)-C(22)-C(23)	0.1(3)	B-C(81)-C(82)-C(83)	179.2(3)
P-C(21)-C(22)-C(23)	177.25(19)	C(81)-C(82)-C(83)-C(84)	0.6(5)
C(21)-C(22)-C(23)-C(24)	-0.9(4)	C(82)-C(83)-C(84)-C(85)	-0.7(5)
C(22)-C(23)-C(24)-C(25)	1.0(4)	C(83)-C(84)-C(85)-C(86)	0.7(5)
C(23)-C(24)-C(25)-C(26)	-0.4(4)	C(84)-C(85)-C(86)-C(81)	-0.6(4)
C(24)-C(25)-C(26)-C(21)	-0.4(4)	C(82)-C(81)-C(86)-C(85)	0.6(4)
C(22)-C(21)-C(26)-C(25)	0.5(3)	B-C(81)-C(86)-C(85)	-179.2(2)
P-C(21)-C(26)-C(25)	-176.43(17)	C(86)-C(81)-B-C(71)	126.9(2)
C(41)-P-C(31)-C(32)	125.51(17)	C(82)-C(81)-B-C(71)	-52.8(3)
C(21)-P-C(31)-C(32)	-124.40(17)	C(86)-C(81)-B-C(61)	-110.3(2)
Ni-P-C(31)-C(32)	1.49(19)	C(82)-C(81)-B-C(61)	70.0(3)
C(41)-P-C(31)-C(36)	-57.79(19)	C(86)-C(81)-B-C(51)	8.4(3)
C(21)-P-C(31)-C(36)	52.30(19)	C(82)-C(81)-B-C(51)	-171.3(2)
Ni-P-C(31)-C(36)	178.20(14)	C(72)-C(71)-B-C(81)	-43.0(3)
C(36)-C(31)-C(32)-C(33)	1.6(3)	C(76)-C(71)-B-C(81)	139.2(2)
P-C(31)-C(32)-C(33)	178.42(18)	C(72)-C(71)-B-C(61)	-164.75(19)
C(31)-C(32)-C(33)-C(34)	-0.4(4)	C(76)-C(71)-B-C(61)	17.5(3)
C(32)-C(33)-C(34)-C(35)	-0.3(4)	C(72)-C(71)-B-C(51)	75.1(2)
C(33)-C(34)-C(35)-C(36)	-0.1(4)	C(76)-C(71)-B-C(51)	-102.7(2)
C(34)-C(35)-C(36)-C(31)	1.3(3)	C(62)-C(61)-B-C(81)	-6.6(3)
C(32)-C(31)-C(36)-C(35)	-2.1(3)	C(66)-C(61)-B-C(81)	171.13(19)
P-C(31)-C(36)-C(35)	-178.76(16)	C(62)-C(61)-B-C(71)	113.5(2)
C(31)-P-C(41)-C(46)	-1.2(2)	C(66)-C(61)-B-C(71)	-68.8(3)
C(21)-P-C(41)-C(46)	-109.12(19)	C(62)-C(61)-B-C(51)	-125.6(2)
Ni-P-C(41)-C(46)	125.83(18)	C(66)-C(61)-B-C(51)	52.1(3)
C(31)-P-C(41)-C(42)	-177.93(16)	C(56)-C(51)-B-C(81)	95.2(2)
C(21)-P-C(41)-C(42)	74.15(18)	C(52)-C(51)-B-C(81)	-78.9(2)
Ni-P-C(41)-C(42)	-50.90(18)	C(56)-C(51)-B-C(71)	-22.2(3)
C(46)-C(41)-C(42)-C(43)	0.4(3)	C(52)-C(51)-B-C(71)	163.79(19)
P-C(41)-C(42)-C(43)	177.26(18)	C(56)-C(51)-B-C(61)	-144.8(2)
C(41)-C(42)-C(43)-C(44)	-0.6(4)	C(52)-C(51)-B-C(61)	41.2(3)
C(42)-C(43)-C(44)-C(45)	0.3(4)		

Annexe 3

Données cristallographiques supplémentaires et voltammogrammes, article 4

Table III.1. Crystal data and structure refinement for $(\eta^3:\eta^0$-$IndCH_2Py)Ni(PPh_3)Cl$ **(1)**

Empirical formula	C33 H27 Cl N Ni P
Formula weight	562.69
Temperature	293(2) K
Wavelength	1.54178 Å
Crystal system	Triclinic
Space group	P-1
Unit cell dimensions	a = 9.196(3) Å α = 85.99(3)° b = 12.924(5) Å β = 73.28(2)° c = 12.943(3) Å γ = 70.72(3)°
Volume	1390.1(8) $Å^3$
Z	2
Density (calculated)	1.344 Mg/m^3
Absorption coefficient	2.595 mm^{-1}
F(000)	584
Crystal size	0.25 x 0.23 x 0.14 mm
Theta range for data collection	3.57 to 69.91°
Index ranges	$-11 \le h \le 11$, $-15 \le k \le 15$, $-15 \le \ell \le 15$
Reflections collected	19003
Independent reflections	5263
Absorption correction	Integration
Max. and min. transmission	0.7327 and 0.4649
Refinement method	Full-matrix least-squares on F^2
Data / restraints / parameters	5263 / 0 / 335
Goodness-of-fit on F^2	0.800
Final R indices [I>2sigma(I)]	R_1 = 0.0441, wR_2 = 0.0801
R indices (all data)	R_1 = 0.0912, wR_2 = 0.0906
Extinction coefficient	0.00086(11)
Largest diff. peak and hole	0.293 and -0.288 $e/Å^3$

Table III.2. Atomic coordinates (x 10^4) and equivalent isotropic displacement parameters ($Å^2$ x 10^3) for (η^3:η^0-IndCH$_2$Py)Ni(PPh$_3$)Cl (1)

U_{eq} is defined as one third of the trace of the orthogonalized Uij tensor.

	x	y	z	U_{eq}
Ni	2127(1)	6560(1)	7881(1)	46(1)
Cl	349(1)	7163(1)	9419(1)	60(1)
P	1271(1)	7984(1)	6939(1)	38(1)
N	5817(4)	3420(3)	9341(3)	78(1)
C(1)	3175(4)	4960(3)	8414(3)	48(1)
C(2)	4338(4)	5373(3)	7743(4)	64(1)
C(3)	4009(5)	5577(3)	6733(3)	71(1)
C(3A)	2792(5)	5090(3)	6723(3)	63(1)
C(4)	2085(6)	4958(3)	5928(4)	91(2)
C(5)	908(8)	4482(4)	6202(5)	117(2)
C(6)	374(6)	4166(3)	7233(5)	103(2)
C(7)	1025(5)	4278(3)	8033(3)	67(1)
C(7A)	2256(5)	4720(3)	7776(3)	51(1)
C(8)	3091(4)	4611(3)	9557(3)	62(1)
C(9)	4293(5)	3478(3)	9557(3)	53(1)
C(10)	3819(5)	2570(3)	9706(3)	84(2)
C(11)	4971(7)	1559(4)	9628(4)	110(2)
C(12)	6528(7)	1474(4)	9409(4)	95(2)
C(13)	6903(6)	2416(4)	9294(4)	88(2)
C(21)	1469(3)	9266(2)	7274(3)	39(1)
C(22)	1678(4)	10053(3)	6514(3)	54(1)
C(23)	1834(4)	11024(3)	6790(3)	64(1)
C(24)	1757(4)	11221(3)	7830(4)	64(1)
C(25)	1533(4)	10464(3)	8586(3)	63(1)
C(26)	1401(4)	9483(3)	8316(3)	51(1)
C(31)	2230(4)	7824(2)	5499(3)	40(1)
C(32)	1452(4)	7718(3)	4765(3)	54(1)
C(33)	2289(5)	7522(3)	3682(3)	70(1)
C(34)	3878(5)	7443(3)	3322(3)	67(1)
C(35)	4652(5)	7550(3)	4036(3)	60(1)
C(36)	3844(4)	7740(3)	5112(3)	50(1)
C(41)	-837(4)	8291(3)	7056(3)	41(1)
C(42)	-1485(5)	7455(3)	7244(3)	69(1)
C(43)	-3079(5)	7646(4)	7301(4)	87(2)
C(44)	-4044(5)	8681(4)	7163(4)	88(2)
C(45)	-3410(5)	9508(4)	6986(4)	94(2)
C(46)	-1836(4)	9324(3)	6926(3)	69(1)

Table III.3. Hydrogen coordinates (x 10^4) and isotropic displacement parameters ($Å^2$ x 10^3) for (η^3:η^0-IndCH_2Py)Ni(PPh_3)Cl **(1)**

	x	y	z	U_{eq}
H(2)	5177	5491	7928	76
H(3)	4486	5955	6173	85
H(4)	2416	5191	5230	109
H(5)	460	4371	5677	140
H(6)	-454	3866	7398	124
H(7)	645	4062	8732	80
H(8A)	2017	4601	9927	74
H(8B)	3325	5130	9936	74
H(10)	2741	2635	9856	101
H(11)	4674	929	9727	131
H(12)	7322	793	9338	114
H(13)	7972	2363	9177	105
H(22)	1716	9929	5806	65
H(23)	1990	11538	6267	77
H(24)	1858	11870	8019	77
H(25)	1467	10603	9297	75
H(26)	1266	8969	8844	62
H(32)	371	7778	4997	64
H(33)	1764	7442	3192	84
H(34)	4423	7317	2592	80
H(35)	5731	7494	3795	72
H(36)	4387	7815	5593	60
H(42)	-842	6749	7335	83
H(43)	-3497	7070	7433	105
H(44)	-5111	8812	7190	106
H(45)	-4059	10215	6904	113
H(46)	-1432	9906	6795	83

Table III.4. Anisotropic parameters ($Å^2$ x 10^3) for $(\eta^3:\eta^0\text{-IndCH}_2\text{Py})\text{Ni(PPh}_3\text{)Cl}$ **(1)**

The anisotropic displacement factor exponent takes the form:

$$-2\,\pi^2\,[\,h^2\,a^{*2}\,U_{11} + \ldots + 2\,h\,k\,a^*\,b^*\,U_{12}\,]$$

	U11	U22	U33	U23	U13	U12
Ni	51(1)	34(1)	49(1)	4(1)	-14(1)	-8(1)
Cl	70(1)	50(1)	50(1)	0(1)	-7(1)	-17(1)
P	39(1)	31(1)	45(1)	2(1)	-14(1)	-11(1)
N	77(3)	65(2)	99(3)	-4(2)	-54(2)	-7(2)
C(1)	53(2)	30(2)	56(3)	3(2)	-23(2)	-1(2)
C(2)	50(2)	46(2)	88(3)	10(2)	-23(2)	-5(2)
C(3)	65(3)	42(2)	70(3)	16(2)	6(2)	4(2)
C(3A)	88(3)	33(2)	47(3)	-1(2)	-21(2)	7(2)
C(4)	152(5)	41(3)	62(3)	1(2)	-52(3)	9(3)
C(5)	209(7)	47(3)	130(5)	7(3)	-127(5)	-22(3)
C(6)	154(5)	46(3)	154(5)	20(3)	-106(5)	-39(3)
C(7)	96(3)	35(2)	82(3)	12(2)	-46(3)	-22(2)
C(7A)	68(3)	28(2)	54(3)	6(2)	-25(2)	-7(2)
C(8)	77(3)	50(2)	53(3)	4(2)	-30(2)	-4(2)
C(9)	71(3)	44(2)	39(2)	5(2)	-26(2)	-6(2)
C(10)	76(3)	63(3)	97(4)	30(3)	-12(3)	-17(3)
C(11)	116(5)	50(3)	146(5)	42(3)	-32(4)	-17(3)
C(12)	116(5)	59(3)	89(4)	6(3)	-45(4)	14(3)
C(13)	75(3)	93(4)	92(4)	-12(3)	-54(3)	4(3)
C(21)	33(2)	34(2)	52(2)	5(2)	-15(2)	-10(1)
C(22)	71(3)	43(2)	57(3)	11(2)	-29(2)	-21(2)
C(23)	81(3)	37(2)	88(3)	17(2)	-38(3)	-28(2)
C(24)	72(3)	35(2)	94(4)	-6(2)	-36(3)	-16(2)
C(25)	81(3)	46(2)	61(3)	-11(2)	-21(2)	-18(2)
C(26)	61(2)	42(2)	50(2)	2(2)	-13(2)	-19(2)
C(31)	49(2)	30(2)	41(2)	3(2)	-14(2)	-12(2)
C(32)	58(2)	54(2)	47(2)	0(2)	-16(2)	-15(2)
C(33)	92(4)	69(3)	53(3)	-3(2)	-32(3)	-21(3)
C(34)	81(3)	57(3)	45(3)	2(2)	-7(2)	-9(2)
C(35)	63(3)	53(2)	54(3)	7(2)	-8(2)	-12(2)
C(36)	52(2)	48(2)	47(2)	8(2)	-14(2)	-14(2)
C(41)	40(2)	40(2)	46(2)	-3(2)	-12(2)	-15(2)
C(42)	54(3)	60(3)	104(4)	7(2)	-31(3)	-26(2)
C(43)	73(3)	88(4)	123(4)	12(3)	-35(3)	-51(3)
C(44)	46(3)	101(4)	122(4)	-15(3)	-32(3)	-19(3)
C(45)	53(3)	70(3)	159(5)	-4(3)	-46(3)	-5(2)
C(46)	49(3)	49(2)	113(4)	7(2)	-34(3)	-12(2)

Table III.5. Bond lengths [Å] and angles [°] for $(\eta^3:\eta^0\text{-IndCH}_2\text{Py})\text{Ni(PPh}_3\text{)Cl}$ **(1)**

Ni-C(3)	2.037(4)	C(12)-C(13)	1.359(6)
Ni-C(2)	2.071(4)	C(12)-H(12)	0.9300
Ni-C(1)	2.132(3)	C(13)-H(13)	0.9300
Ni-Cl	2.1784(13)	C(21)-C(26)	1.377(4)
Ni-P	2.1847(13)	C(21)-C(22)	1.385(4)
Ni-C(3A)	2.308(4)	C(22)-C(23)	1.391(4)
Ni-C(7A)	2.352(3)	C(22)-H(22)	0.9300
P-C(41)	1.808(3)	C(23)-C(24)	1.365(5)
P-C(31)	1.812(3)	C(23)-H(23)	0.9300
P-C(21)	1.819(3)	C(24)-C(25)	1.357(5)
N-C(9)	1.325(4)	C(24)-H(24)	0.9300
N-C(13)	1.344(5)	C(25)-C(26)	1.390(4)
C(1)-C(2)	1.400(4)	C(25)-H(25)	0.9300
C(1)-C(7A)	1.450(4)	C(26)-H(26)	0.9300
C(1)-C(8)	1.504(4)	C(31)-C(32)	1.381(4)
C(2)-C(3)	1.413(5)	C(31)-C(36)	1.393(4)
C(2)-H(2)	0.9300	C(32)-C(33)	1.386(5)
C(3)-C(3A)	1.457(5)	C(32)-H(32)	0.9300
C(3)-H(3)	0.9300	C(33)-C(34)	1.372(5)
C(3A)-C(4)	1.412(5)	C(33)-H(33)	0.9300
C(3A)-C(7A)	1.416(5)	C(34)-C(35)	1.356(5)
C(4)-C(5)	1.366(6)	C(34)-H(34)	0.9300
C(4)-H(4)	0.9300	C(35)-C(36)	1.373(4)
C(5)-C(6)	1.366(7)	C(35)-H(35)	0.9300
C(5)-H(5)	0.9300	C(36)-H(36)	0.9300
C(6)-C(7)	1.374(5)	C(41)-C(42)	1.373(4)
C(6)-H(6)	0.9300	C(41)-C(46)	1.379(4)
C(7)-C(7A)	1.380(5)	C(42)-C(43)	1.384(5)
C(7)-H(7)	0.9300	C(42)-H(42)	0.9300
C(8)-C(9)	1.516(4)	C(43)-C(44)	1.372(5)
C(8)-H(8A)	0.9700	C(43)-H(43)	0.9300
C(8)-H(8B)	0.9700	C(44)-C(45)	1.354(5)
C(9)-C(10)	1.365(5)	C(44)-H(44)	0.9300
C(10)-C(11)	1.372(5)	C(45)-C(46)	1.367(5)
C(10)-H(10)	0.9300	C(45)-H(45)	0.9300
C(11)-C(12)	1.345(6)	C(46)-H(46)	0.930
C(11)-H(11)	0.9300		

C(3)-Ni-C(2)	40.23(14)	C(41)-P-Ni	111.09(12)
C(3)-Ni-C(1)	65.98(14)	C(31)-P-Ni	115.07(11)
C(2)-Ni-C(1)	38.87(12)	C(21)-P-Ni	117.12(11)
C(3)-Ni-Cl	161.73(11)	C(9)-N-C(13)	117.0(4)
C(2)-Ni-Cl	123.62(13)	C(2)-C(1)-C(7A)	109.1(4)
C(1)-Ni-Cl	95.83(11)	C(2)-C(1)-C(8)	125.6(4)
C(3)-Ni-P	101.16(12)	C(7A)-C(1)-C(8)	124.3(3)
C(2)-Ni-P	133.89(12)	C(2)-C(1)-Ni	68.2(2)
C(1)-Ni-P	165.54(10)	C(7A)-C(1)-Ni	79.6(2)
Cl-Ni-P	97.10(5)	C(8)-C(1)-Ni	127.4(2)
C(3)-Ni-C(3A)	38.54(14)	C(1)-C(2)-C(3)	107.7(4)
C(2)-Ni-C(3A)	63.72(16)	C(1)-C(2)-Ni	72.9(2)
C(1)-Ni-C(3A)	62.26(14)	C(3)-C(2)-Ni	68.6(2)
Cl-Ni-C(3A)	135.24(12)	C(1)-C(2)-H(2)	126.2
P-Ni-C(3A)	103.69(10)	C(3)-C(2)-H(2)	126.2
C(3)-Ni-C(7A)	63.22(15)	Ni-C(2)-H(2)	124.0
C(2)-Ni-C(7A)	62.95(14)	C(2)-C(3)-C(3A)	107.9(3)
C(1)-Ni-C(7A)	37.32(12)	C(2)-C(3)-Ni	71.2(2)
Cl-Ni-C(7A)	103.65(10)	C(3A)-C(3)-Ni	80.8(2)
P-Ni-C(7A)	132.02(10)	C(2)-C(3)-H(3)	126.1
C(3A)-Ni-C(7A)	35.37(12)	C(3A)-C(3)-H(3)	126.1
C(41)-P-C(31)	104.15(16)	Ni-C(3)-H(3)	114.2
C(41)-P-C(21)	105.34(15)	C(4)-C(3A)-C(7A)	118.7(4)
C(31)-P-C(21)	102.76(15)	C(4)-C(3A)-C(3)	133.8(4)

C(7A)-C(3A)-C(3)	107.5(4)	C(24)-C(23)-C(22)	119.9(4)
C(4)-C(3A)-Ni	130.0(3)	C(24)-C(23)-H(23)	120.0
C(7A)-C(3A)-Ni	74.0(2)	C(22)-C(23)-H(23)	120.0
C(3)-C(3A)-Ni	60.6(2)	C(25)-C(24)-C(23)	119.6(4)
C(5)-C(4)-C(3A)	118.9(5)	C(25)-C(24)-H(24)	120.2
C(5)-C(4)-H(4)	120.6	C(23)-C(24)-H(24)	120.2
C(3A)-C(4)-H(4)	120.6	C(24)-C(25)-C(26)	121.0(4)
C(4)-C(5)-C(6)	121.3(5)	C(24)-C(25)-H(25)	119.5
C(4)-C(5)-H(5)	119.4	C(26)-C(25)-H(25)	119.5
C(6)-C(5)-H(5)	119.4	C(21)-C(26)-C(25)	120.5(3)
C(5)-C(6)-C(7)	121.9(5)	C(21)-C(26)-H(26)	119.7
C(5)-C(6)-H(6)	119.1	C(25)-C(26)-H(26)	119.7
C(7)-C(6)-H(6)	119.1	C(32)-C(31)-C(36)	118.0(3)
C(6)-C(7)-C(7A)	118.4(4)	C(32)-C(31)-P	122.7(3)
C(6)-C(7)-H(7)	120.8	C(36)-C(31)-P	119.2(3)
C(7A)-C(7)-H(7)	120.8	C(31)-C(32)-C(33)	119.8(4)
C(7)-C(7A)-C(3A)	120.8(4)	C(31)-C(32)-H(32)	120.1
C(7)-C(7A)-C(1)	132.4(4)	C(33)-C(32)-H(32)	120.1
C(3A)-C(7A)-C(1)	106.8(4)	C(34)-C(33)-C(32)	121.0(4)
C(7)-C(7A)-Ni	129.2(3)	C(34)-C(33)-H(33)	119.5
C(3A)-C(7A)-Ni	70.6(2)	C(32)-C(33)-H(33)	119.5
C(1)-C(7A)-Ni	63.08(18)	C(35)-C(34)-C(33)	119.7(4)
C(1)-C(8)-C(9)	109.7(3)	C(35)-C(34)-H(34)	120.2
C(1)-C(8)-H(8A)	109.7	C(33)-C(34)-H(34)	120.2
C(9)-C(8)-H(8A)	109.7	C(34)-C(35)-C(36)	120.1(4)
C(1)-C(8)-H(8B)	109.7	C(34)-C(35)-H(35)	120.0
C(9)-C(8)-H(8B)	109.7	C(36)-C(35)-H(35)	120.0
H(8A)-C(8)-H(8B)	108.2	C(35)-C(36)-C(31)	121.4(4)
N-C(9)-C(10)	122.6(4)	C(35)-C(36)-H(36)	119.3
N-C(9)-C(8)	116.4(4)	C(31)-C(36)-H(36)	119.3
C(10)-C(9)-C(8)	120.8(4)	C(42)-C(41)-C(46)	117.3(3)
C(9)-C(10)-C(11)	118.4(4)	C(42)-C(41)-P	119.2(3)
C(9)-C(10)-H(10)	120.8	C(46)-C(41)-P	123.4(3)
C(11)-C(10)-H(10)	120.8	C(41)-C(42)-C(43)	121.1(4)
C(12)-C(11)-C(10)	120.3(5)	C(41)-C(42)-H(42)	119.4
C(12)-C(11)-H(11)	119.8	C(43)-C(42)-H(42)	119.4
C(10)-C(11)-H(11)	119.8	C(44)-C(43)-C(42)	120.3(4)
C(11)-C(12)-C(13)	117.8(5)	C(44)-C(43)-H(43)	119.9
C(11)-C(12)-H(12)	121.1	C(42)-C(43)-H(43)	119.9
C(13)-C(12)-H(12)	121.1	C(45)-C(44)-C(43)	118.7(4)
N-C(13)-C(12)	123.7(5)	C(45)-C(44)-H(44)	120.7
N-C(13)-H(13)	118.1	C(43)-C(44)-H(44)	120.7
C(12)-C(13)-H(13)	118.1	C(44)-C(45)-C(46)	121.3(4)
C(26)-C(21)-C(22)	117.7(3)	C(44)-C(45)-H(45)	119.3
C(26)-C(21)-P	119.9(3)	C(46)-C(45)-H(45)	119.3
C(22)-C(21)-P	122.4(3)	C(45)-C(46)-C(41)	121.2(4)
C(21)-C(22)-C(23)	121.2(4)	C(45)-C(46)-H(46)	119.4
C(21)-C(22)-H(22)	119.4	C(41)-C(46)-H(46)	119.4
C(23)-C(22)-H(22)	119.4		

Table III.6. Torsion angles [°] for (η^3:η^0-IndCH$_2$Py)Ni(PPh$_3$)Cl **(1)**

C(3)-Ni-P-C(41)	125.10(18)	Ni-C(3)-C(3A)-C(4)	118.8(4)
C(2)-Ni-P-C(41)	152.22(19)	C(2)-C(3)-C(3A)-C(7A)	7.3(4)
C(1)-Ni-P-C(41)	98.8(4)	Ni-C(3)-C(3A)-C(7A)	-59.5(3)
Cl-Ni-P-C(41)	-54.39(12)	C(2)-C(3)-C(3A)-Ni	66.7(3)
C(3A)-Ni-P-C(41)	85.67(17)	C(3)-Ni-C(3A)-C(4)	-124.4(6)
C(7A)-Ni-P-C(41)	61.23(18)	C(2)-Ni-C(3A)-C(4)	-166.1(5)
C(3)-Ni-P-C(31)	7.08(19)	C(1)-Ni-C(3A)-C(4)	150.1(5)
C(2)-Ni-P-C(31)	34.2(2)	Cl-Ni-C(3A)-C(4)	81.6(5)
C(1)-Ni-P-C(31)	-19.2(5)	P-Ni-C(3A)-C(4)	-33.6(5)
Cl-Ni-P-C(31)	-172.41(12)	C(7A)-Ni-C(3A)-C(4)	114.3(6)
C(3A)-Ni-P-C(31)	-32.35(18)	C(3)-Ni-C(3A)-C(7A)	121.3(3)
C(7A)-Ni-P-C(31)	-56.79(18)	C(2)-Ni-C(3A)-C(7A)	79.6(2)
C(3)-Ni-P-C(21)	-113.83(18)	C(1)-Ni-C(3A)-C(7A)	35.8(2)
C(2)-Ni-P-C(21)	-86.7(2)	Cl-Ni-C(3A)-C(7A)	-32.7(3)
C(1)-Ni-P-C(21)	-140.1(4)	P-Ni-C(3A)-C(7A)	-147.9(2)
Cl-Ni-P-C(21)	66.68(13)	C(2)-Ni-C(3A)-C(3)	-41.7(2)
C(3A)-Ni-P-C(21)	-153.26(17)	C(1)-Ni-C(3A)-C(3)	-85.5(2)
C(7A)-Ni-P-C(21)	-177.70(17)	Cl-Ni-C(3A)-C(3)	-154.0(2)
C(3)-Ni-C(1)-C(2)	38.8(2)	P-Ni-C(3A)-C(3)	90.8(2)
Cl-Ni-C(1)-C(2)	-139.5(2)	C(7A)-Ni-C(3A)-C(3)	-121.3(3)
P-Ni-C(1)-C(2)	67.2(5)	C(7A)-C(3A)-C(4)-C(5)	0.2(6)
C(3A)-Ni-C(1)-C(2)	81.7(3)	C(3)-C(3A)-C(4)-C(5)	-177.9(4)
C(7A)-Ni-C(1)-C(2)	115.6(3)	Ni-C(3A)-C(4)-C(5)	-92.6(5)
C(3)-Ni-C(1)-C(7A)	-76.8(2)	C(3A)-C(4)-C(5)-C(6)	2.0(7)
C(2)-Ni-C(1)-C(7A)	-115.6(3)	C(4)-C(5)-C(6)-C(7)	-2.1(8)
Cl-Ni-C(1)-C(7A)	104.9(2)	C(5)-C(6)-C(7)-C(7A)	-0.3(7)
P-Ni-C(1)-C(7A)	-48.4(5)	C(6)-C(7)-C(7A)-C(3A)	2.5(5)
C(3A)-Ni-C(1)-C(7A)	-33.9(2)	C(6)-C(7)-C(7A)-C(1)	179.1(4)
C(3)-Ni-C(1)-C(8)	157.7(4)	C(6)-C(7)-C(7A)-Ni	91.8(5)
C(2)-Ni-C(1)-C(8)	118.9(4)	C(4)-C(3A)-C(7A)-C(7)	-2.5(5)
Cl-Ni-C(1)-C(8)	-20.6(3)	C(3)-C(3A)-C(7A)-C(7)	176.1(3)
P-Ni-C(1)-C(8)	-173.9(3)	Ni-C(3A)-C(7A)-C(7)	124.8(3)
C(3A)-Ni-C(1)-C(8)	-159.4(4)	C(4)-C(3A)-C(7A)-C(1)	-179.9(3)
C(7A)-Ni-C(1)-C(8)	-125.5(4)	C(3)-C(3A)-C(7A)-C(1)	-1.3(4)
C(7A)-C(1)-C(2)-C(3)	9.8(4)	Ni-C(3A)-C(7A)-C(1)	-52.6(2)
C(8)-C(1)-C(2)-C(3)	178.7(3)	C(4)-C(3A)-C(7A)-Ni	-127.3(3)
Ni-C(1)-C(2)-C(3)	-60.1(2)	C(3)-C(3A)-C(7A)-Ni	51.3(2)
C(7A)-C(1)-C(2)-Ni	69.9(2)	C(2)-C(1)-C(7A)-C(7)	177.8(4)
C(8)-C(1)-C(2)-Ni	-121.2(3)	C(8)-C(1)-C(7A)-C(7)	8.8(6)
C(3)-Ni-C(2)-C(1)	-117.5(3)	Ni-C(1)-C(7A)-C(7)	-119.7(4)
Cl-Ni-C(2)-C(1)	50.9(3)	C(2)-C(1)-C(7A)-C(3A)	-5.2(4)
P-Ni-C(2)-C(1)	-161.37(17)	C(8)-C(1)-C(7A)-C(3A)	-174.3(3)
C(3A)-Ni-C(2)-C(1)	-77.6(2)	Ni-C(1)-C(7A)-C(3A)	57.2(2)
C(7A)-Ni-C(2)-C(1)	-37.9(2)	C(2)-C(1)-C(7A)-Ni	-62.4(2)
C(1)-Ni-C(2)-C(3)	117.5(3)	C(8)-C(1)-C(7A)-Ni	128.5(3)
Cl-Ni-C(2)-C(3)	168.4(2)	C(3)-Ni-C(7A)-C(7)	-151.1(4)
P-Ni-C(2)-C(3)	-43.8(3)	C(2)-Ni-C(7A)-C(7)	163.6(4)
C(3A)-Ni-C(2)-C(3)	39.9(2)	C(1)-Ni-C(7A)-C(7)	124.1(5)
C(7A)-Ni-C(2)-C(3)	79.6(2)	Cl-Ni-C(7A)-C(7)	42.5(4)
C(1)-C(2)-C(3)-C(3A)	-10.5(4)	P-Ni-C(7A)-C(7)	-70.4(4)
Ni-C(2)-C(3)-C(3A)	-73.3(2)	C(3A)-Ni-C(7A)-C(7)	-114.4(5)
C(1)-C(2)-C(3)-Ni	62.8(3)	C(3)-Ni-C(7A)-C(3A)	-36.6(2)
C(1)-Ni-C(3)-C(2)	-37.5(2)	C(2)-Ni-C(7A)-C(3A)	-82.0(3)
Cl-Ni-C(3)-C(2)	-32.2(6)	C(1)-Ni-C(7A)-C(3A)	121.4(3)
P-Ni-C(3)-C(2)	149.4(2)	Cl-Ni-C(7A)-C(3A)	157.0(2)
C(3A)-Ni-C(3)-C(2)	-112.6(3)	P-Ni-C(7A)-C(3A)	44.0(3)
C(7A)-Ni-C(3)-C(2)	-78.9(2)	C(3)-Ni-C(7A)-C(1)	84.8(2)
C(2)-Ni-C(3)-C(3A)	112.6(3)	C(2)-Ni-C(7A)-C(1)	39.5(2)
C(1)-Ni-C(3)-C(3A)	75.0(2)	Cl-Ni-C(7A)-C(1)	-81.6(2)
Cl-Ni-C(3)-C(3A)	80.4(5)	P-Ni-C(7A)-C(1)	165.45(18)
P-Ni-C(3)-C(3A)	-98.0(2)	C(3A)-Ni-C(7A)-C(1)	121.4(3)
C(7A)-Ni-C(3)-C(3A)	33.6(2)	C(2)-C(1)-C(8)-C(9)	-79.1(4)
C(2)-C(3)-C(3A)-C(4)	-174.5(4)	C(7A)-C(1)-C(8)-C(9)	88.2(4)

Ni-C(1)-C(8)-C(9)	-167.5(3)	Ni-P-C(31)-C(32)	108.6(3)
C(13)-N-C(9)-C(10)	-1.5(6)	C(41)-P-C(31)-C(36)	170.6(2)
C(13)-N-C(9)-C(8)	-177.3(3)	C(21)-P-C(31)-C(36)	60.9(3)
C(1)-C(8)-C(9)-N	76.5(4)	Ni-P-C(31)-C(36)	-67.6(3)
C(1)-C(8)-C(9)-C(10)	-99.4(4)	C(36)-C(31)-C(32)-C(33)	0.7(5)
N-C(9)-C(10)-C(11)	0.1(7)	P-C(31)-C(32)-C(33)	-175.5(3)
C(8)-C(9)-C(10)-C(11)	175.7(4)	C(31)-C(32)-C(33)-C(34)	-0.8(6)
C(9)-C(10)-C(11)-C(12)	-0.1(8)	C(32)-C(33)-C(34)-C(35)	0.5(6)
C(10)-C(11)-C(12)-C(13)	1.4(8)	C(33)-C(34)-C(35)-C(36)	-0.3(6)
C(9)-N-C(13)-C(12)	3.0(7)	C(34)-C(35)-C(36)-C(31)	0.2(5)
C(11)-C(12)-C(13)-N	-3.0(8)	C(32)-C(31)-C(36)-C(35)	-0.5(5)
C(41)-P-C(21)-C(26)	93.8(3)	P-C(31)-C(36)-C(35)	175.9(3)
C(31)-P-C(21)-C(26)	-157.4(3)	C(31)-P-C(41)-C(42)	95.9(3)
Ni-P-C(21)-C(26)	-30.2(3)	C(21)-P-C(41)-C(42)	-156.3(3)
C(41)-P-C(21)-C(22)	-85.8(3)	Ni-P-C(41)-C(42)	-28.6(3)
C(31)-P-C(21)-C(22)	23.0(3)	C(31)-P-C(41)-C(46)	-81.6(3)
Ni-P-C(21)-C(22)	150.2(2)	C(21)-P-C(41)-C(46)	26.1(4)
C(26)-C(21)-C(22)-C(23)	0.7(5)	Ni-P-C(41)-C(46)	153.9(3)
P-C(21)-C(22)-C(23)	-179.7(3)	C(46)-C(41)-C(42)-C(43)	0.0(6)
C(21)-C(22)-C(23)-C(24)	-1.0(6)	P-C(41)-C(42)-C(43)	-177.7(3)
C(22)-C(23)-C(24)-C(25)	0.2(6)	C(41)-C(42)-C(43)-C(44)	0.4(7)
C(23)-C(24)-C(25)-C(26)	0.9(6)	C(42)-C(43)-C(44)-C(45)	-0.9(8)
C(22)-C(21)-C(26)-C(25)	0.3(5)	C(43)-C(44)-C(45)-C(46)	1.1(8)
P-C(21)-C(26)-C(25)	-179.3(3)	C(44)-C(45)-C(46)-C(41)	-0.8(7)
C(24)-C(25)-C(26)-C(21)	-1.1(6)	C(42)-C(41)-C(46)-C(45)	0.2(6)
C(41)-P-C(31)-C(32)	-13.2(3)	P-C(41)-C(46)-C(45)	177.8(3)
C(21)-P-C(31)-C(32)	-122.9(3)		

Table III.7. Crystal data and structure refinement for [(η^3:η^1-IndCH$_2$Py)Ni(PPh$_3$)][BPh$_4$] **(4)**

Empirical formula	C58 H49 B Cl2 N Ni P
Formula weight	931.37
Temperature	223(2)K
Wavelength	1.54178 Å
Crystal system	Monoclinic
Space group	P21/c
Unit cell dimensions	a = 10.4368(1) Å α = 90° b = 21.0121(2) Å β = 96.340(1)° c = 21.7137(2) Å γ = 90°
Volume	4732.67(8)Å^3
Z	4
Density (calculated)	1.307 Mg/m^3
Absorption coefficient	2.247 mm^{-1}
F(000)	1944
Crystal size	0.28 x 0.27 x 0.11 mm
Theta range for data collection	2.94 to 72.96°
Index ranges	$-12 \le h \le 11$, $-25 \le k \le 25$, $-26 \le \ell \le 26$
Reflections collected	57390
Independent reflections	9166 [R_{int} = 0.038]
Absorption correction	Semi-empirical from equivalents
Max. and min. transmission	0.8306 and 0.1816
Refinement method	Full-matrix least-squares on F^2
Data / restraints / parameters	9166 / 7 / 604
Goodness-of-fit on F^2	0.932
Final R indices [I>2sigma(I)]	R1 = 0.0508, wR_2 = 0.1221
R indices (all data)	R1 = 0.0738, wR_2 = 0.1338
Largest diff. peak and hole	0.530 and -0.364 e/Å^3

Table III.8. Atomic coordinates (x 10^4) and equivalent isotropic displacement parameters ($Å^2$ x 10^3) for [(η^3:η^1-IndCH$_2$Py)Ni(PPh$_3$)][BPh$_4$] **(4)**

U_{eq} is defined as one third of the trace of the orthogonalized Uij tensor.

	Occ.	x	y	z	U_{eq}
Ni	1	2161(1)	4058(1)	2164(1)	30(1)
P	1	3873(1)	4101(1)	1659(1)	27(1)
N	1	2692(2)	4381(1)	2995(1)	31(1)
C(1)	1	374(2)	4096(1)	2441(1)	35(1)
C(2)	1	504(2)	3516(1)	2116(1)	43(1)
C(3)	1	748(2)	3669(1)	1512(1)	42(1)
C(3A)	1	512(2)	4345(1)	1407(1)	36(1)
C(4)	1	546(3)	4733(2)	890(1)	50(1)
C(5)	1	350(3)	5373(2)	959(2)	61(1)
C(6)	1	146(3)	5638(2)	1524(2)	62(1)
C(7)	1	115(3)	5263(1)	2046(1)	47(1)
C(7A)	1	281(2)	4614(1)	1983(1)	33(1)
C(8)	1	433(2)	4191(1)	3119(1)	41(1)
C(9)	1	1726(2)	4455(1)	3364(1)	31(1)
C(10)	1	1959(3)	4727(1)	3947(1)	38(1)
C(11)	1	3171(3)	4909(1)	4172(1)	43(1)
C(12)	1	4163(3)	4816(1)	3809(1)	43(1)
C(13)	1	3881(2)	4561(1)	3229(1)	36(1)
C(21)	1	3531(2)	4052(1)	820(1)	29(1)
C(22)	1	3077(2)	3478(1)	563(1)	36(1)
C(23)	1	2690(3)	3427(1)	-68(1)	43(1)
C(24)	1	2770(3)	3952(2)	-445(1)	45(1)
C(25)	1	3230(3)	4524(1)	-197(1)	44(1)
C(26)	1	3609(2)	4573(1)	434(1)	36(1)
C(31)	1	4658(2)	4872(1)	1792(1)	31(1)
C(32)	1	5984(3)	4955(1)	1893(1)	41(1)
C(33)	1	6488(3)	5560(2)	2011(1)	59(1)
C(34)	1	5690(4)	6074(2)	2020(2)	67(1)
C(35)	1	4374(4)	6002(2)	1913(2)	66(1)
C(36)	1	3860(3)	5399(1)	1808(1)	48(1)
C(41)	1	5116(2)	3508(1)	1860(1)	32(1)
C(42)	1	5133(3)	3187(1)	2421(1)	37(1)
C(43)	1	6112(3)	2760(1)	2606(1)	51(1)
C(44)	1	7067(3)	2646(2)	2231(2)	60(1)
C(45)	1	7045(3)	2948(2)	1672(2)	56(1)
C(46)	1	6077(3)	3378(1)	1480(1)	45(1)
C(51)	1	10310(2)	2919(1)	4324(1)	30(1)
C(52)	1	10174(3)	2480(1)	3843(1)	37(1)
C(53)	1	11143(3)	2352(1)	3471(1)	44(1)
C(54)	1	12315(3)	2660(1)	3572(1)	46(1)
C(55)	1	12505(3)	3096(1)	4047(1)	44(1)
C(56)	1	11517(2)	3224(1)	4409(1)	35(1)
C(61)	1	8062(3)	2542(1)	4713(1)	34(1)
C(62)	1	6745(3)	2601(1)	4546(1)	45(1)
C(63)	1	5890(3)	2092(2)	4575(1)	54(1)
C(64)	1	6331(3)	1507(2)	4781(1)	55(1)
C(65)	1	7622(3)	1432(1)	4958(2)	54(1)
C(66)	1	8474(3)	1939(1)	4923(1)	45(1)
C(71)	1	8517(2)	3771(1)	4369(1)	29(1)
C(72)	1	7811(2)	3738(1)	3780(1)	35(1)
C(73)	1	7355(2)	4271(2)	3453(1)	43(1)
C(74)	1	7591(3)	4871(1)	3693(1)	46(1)
C(75)	1	8305(3)	4930(1)	4262(1)	43(1)
C(76)	1	8750(2)	4388(1)	4591(1)	35(1)
C(81)	1	9551(3)	3251(1)	5457(1)	36(1)

C(82)	1	8701(3)	3552(1)	5819(1)	47(1)
C(83)	1	8965(4)	3631(2)	6454(1)	68(1)
C(84)	1	10089(5)	3409(2)	6757(2)	84(1)
C(85)	1	10953(4)	3101(2)	6425(2)	74(1)
C(86)	1	10683(3)	3031(1)	5784(1)	51(1)
B	1	9121(3)	3127(1)	4718(1)	30(1)
C(99)	0.75	4909(12)	3254(5)	5742(4)	131(5)
Cl(1)	0.75	4719(3)	3860(1)	5217(1)	74(1)
Cl(2)	0.75	4739(3)	3463(1)	6478(1)	139(1)
C(99')	0.25	5130(19)	3179(9)	5776(9)	64(7)
Cl(1')	0.25	4739(15)	3767(7)	5248(6)	184(6)
Cl(2')	0.25	4082(8)	3188(4)	6329(4)	115(3)

Table III.9. Hydrogen coordinates (x 10^4) and isotropic displacement parameters ($Å^2$ x 10^3) for [(η^3:η^1-IndCH$_2$Py)Ni(PPh$_3$)][BPh$_4$] **(4)**

	Occ.	x	y	z	U_{eq}
H(2)	1	438	3104	2278	51
H(3)	1	1020	3381	1221	51
H(4)	1	699	4561	504	60
H(5)	1	353	5641	613	73
H(6)	1	28	6080	1554	74
H(7)	1	-14	5443	2431	56
H(8A)	1	292	3784	3322	49
H(8B)	1	-247	4486	3212	49
H(10)	1	1274	4786	4188	46
H(11)	1	3332	5095	4567	52
H(12)	1	5014	4925	3957	51
H(13)	1	4558	4509	2982	43
H(22)	1	3030	3120	819	43
H(23)	1	2376	3038	-238	52
H(24)	1	2510	3920	-872	54
H(25)	1	3287	4879	-455	52
H(26)	1	3921	4963	601	43
H(32)	1	6538	4604	1881	49
H(33)	1	7385	5616	2084	71
H(34)	1	6043	6481	2101	80
H(35)	1	3829	6358	1911	79
H(36)	1	2961	5346	1748	57
H(42)	1	4476	3261	2677	45
H(43)	1	6124	2548	2988	61
H(44)	1	7736	2360	2360	72
H(45)	1	7693	2863	1415	68
H(46)	1	6069	3583	1095	54
H(52)	1	9390	2258	3766	45
H(53)	1	11000	2054	3148	53
H(54)	1	12973	2573	3322	55
H(55)	1	13300	3307	4126	53
H(56)	1	11662	3529	4726	42
H(62)	1	6416	2998	4407	53
H(63)	1	5005	2152	4454	65
H(64)	1	5758	1163	4799	66
H(65)	1	7938	1034	5105	65
H(66)	1	9356	1873	5046	54
H(72)	1	7641	3335	3601	42
H(73)	1	6879	4223	3062	51
H(74)	1	7272	5234	3473	56
H(75)	1	8493	5336	4430	51
H(76)	1	9229	4441	4980	41
H(82)	1	7916	3708	5622	57
H(83)	1	8365	3838	6677	81
H(84)	1	10272	3466	7187	100
H(85)	1	11724	2938	6629	89
H(86)	1	11293	2826	5565	61
H(99A)	0.75	4278	2921	5613	158
H(99B)	0.75	5770	3070	5731	158
H(99C)	0.25	6012	3242	5971	77
H(99D)	0.25	5089	2765	5566	77

Table III.10. Anisotropic parameters ($Å^2$ x 10^3) for [(η^3:η^1-IndCH$_2$Py)Ni(PPh$_3$)][BPh$_4$] **(4)**

The anisotropic displacement factor exponent takes the form:

$$-2\,\pi^2\,[\,h^2\,a^{*2}\,U_{11} + \ldots + 2\,h\,k\,a^*\,b^*\,U_{12}\,]$$

	U11	U22	U33	U23	U13	U12
Ni	24(1)	36(1)	30(1)	-1(1)	5(1)	0(1)
P	25(1)	30(1)	26(1)	-1(1)	4(1)	1(1)
N	27(1)	38(1)	30(1)	3(1)	9(1)	4(1)
C(1)	20(1)	46(2)	39(1)	3(1)	5(1)	-3(1)
C(2)	32(2)	37(2)	60(2)	5(1)	8(1)	-8(1)
C(3)	30(1)	48(2)	47(2)	-11(1)	0(1)	-3(1)
C(3A)	25(1)	51(2)	33(1)	-1(1)	-2(1)	2(1)
C(4)	34(2)	78(2)	38(2)	12(2)	1(1)	8(1)
C(5)	50(2)	74(3)	58(2)	34(2)	3(2)	12(2)
C(6)	55(2)	49(2)	82(2)	17(2)	5(2)	17(2)
C(7)	37(2)	48(2)	56(2)	4(1)	9(1)	14(1)
C(7A)	22(1)	43(2)	36(1)	1(1)	2(1)	2(1)
C(8)	27(1)	61(2)	38(1)	7(1)	12(1)	2(1)
C(9)	29(1)	35(2)	32(1)	5(1)	9(1)	6(1)
C(10)	41(2)	40(2)	35(1)	0(1)	16(1)	4(1)
C(11)	53(2)	44(2)	34(1)	-9(1)	13(1)	-1(1)
C(12)	34(2)	58(2)	35(1)	-6(1)	6(1)	-7(1)
C(13)	28(1)	46(2)	35(1)	-3(1)	11(1)	1(1)
C(21)	24(1)	34(1)	28(1)	-2(1)	5(1)	3(1)
C(22)	38(2)	36(2)	33(1)	-4(1)	5(1)	0(1)
C(23)	43(2)	48(2)	38(2)	-15(1)	1(1)	-2(1)
C(24)	39(2)	67(2)	28(1)	-5(1)	-1(1)	5(1)
C(25)	44(2)	54(2)	33(1)	9(1)	5(1)	7(1)
C(26)	36(1)	38(2)	33(1)	-1(1)	4(1)	2(1)
C(31)	35(1)	35(2)	24(1)	-2(1)	4(1)	-5(1)
C(32)	35(2)	52(2)	36(1)	5(1)	4(1)	-7(1)
C(33)	53(2)	68(2)	55(2)	3(2)	2(2)	-29(2)
C(34)	85(3)	48(2)	68(2)	-5(2)	7(2)	-33(2)
C(35)	81(3)	38(2)	82(3)	-12(2)	17(2)	-6(2)
C(36)	43(2)	38(2)	63(2)	-5(1)	11(1)	-3(1)
C(41)	32(1)	33(1)	31(1)	-4(1)	2(1)	4(1)
C(42)	46(2)	32(2)	34(1)	-3(1)	2(1)	1(1)
C(43)	69(2)	36(2)	45(2)	-1(1)	-13(2)	7(1)
C(44)	53(2)	47(2)	75(2)	-10(2)	-17(2)	21(2)
C(45)	43(2)	60(2)	67(2)	-10(2)	7(2)	16(2)
C(46)	39(2)	57(2)	40(2)	-1(1)	8(1)	10(1)
C(51)	33(1)	26(1)	29(1)	4(1)	-1(1)	0(1)
C(52)	43(2)	34(2)	35(1)	-1(1)	5(1)	-9(1)
C(53)	64(2)	35(2)	36(1)	-2(1)	16(1)	-2(1)
C(54)	51(2)	39(2)	53(2)	7(1)	22(1)	8(1)
C(55)	33(2)	38(2)	61(2)	8(1)	7(1)	0(1)
C(56)	34(1)	29(1)	41(1)	-1(1)	-1(1)	1(1)
C(61)	41(2)	34(2)	27(1)	-4(1)	10(1)	-6(1)
C(62)	39(2)	48(2)	48(2)	2(1)	9(1)	-10(1)
C(63)	41(2)	63(2)	60(2)	2(2)	11(1)	-16(2)
C(64)	59(2)	53(2)	57(2)	-10(2)	28(2)	-28(2)
C(65)	66(2)	36(2)	65(2)	2(2)	28(2)	-8(1)
C(66)	43(2)	39(2)	53(2)	3(1)	12(1)	-6(1)
C(71)	23(1)	35(1)	29(1)	1(1)	5(1)	-2(1)
C(72)	27(1)	42(2)	35(1)	1(1)	2(1)	-4(1)
C(73)	27(1)	63(2)	38(1)	10(1)	2(1)	1(1)
C(74)	34(2)	45(2)	61(2)	20(2)	14(1)	13(1)
C(75)	40(2)	37(2)	54(2)	-1(1)	15(1)	3(1)
C(76)	33(1)	35(2)	37(1)	-1(1)	8(1)	0(1)

C(81)	53(2)	27(1)	28(1)	2(1)	2(1)	-6(1)
C(82)	67(2)	43(2)	33(1)	0(1)	10(1)	-2(1)
C(83)	127(3)	45(2)	35(2)	-1(2)	23(2)	4(2)
C(84)	175(5)	45(2)	27(2)	0(2)	-7(2)	6(2)
C(85)	113(3)	56(2)	45(2)	4(2)	-29(2)	14(2)
C(86)	73(2)	40(2)	38(2)	0(1)	-11(1)	4(2)
B	35(2)	28(2)	27(1)	-1(1)	1(1)	-4(1)
C(99)	180(11)	106(8)	116(9)	40(6)	52(7)	53(6)
Cl(1)	93(1)	58(1)	63(1)	-1(1)	-24(1)	-12(1)
Cl(2)	188(3)	143(2)	92(2)	41(2)	42(2)	71(2)
C(99')	42(9)	39(10)	120(20)	12(10)	25(10)	-15(7)
Cl(1')	236(13)	153(11)	149(10)	-12(8)	-33(9)	76(8)
Cl(2')	125(6)	111(5)	120(5)	-32(4)	54(4)	-22(4)

Table III.11. Bond lengths [Å] and angles [°] for [(η^3:η^1-IndCH$_2$Py)Ni(PPh$_3$)][BPh$_4$] **(4)**

Ni-N	1.949(2)	Ni-C(2)	2.063(3)
Ni-C(1)	2.023(2)	Ni-C(3)	2.095(3)
Ni-P	2.2006(7)	C(41)-C(46)	1.393(3)
Ni-C(7A)	2.280(2)	C(42)-C(43)	1.386(4)
Ni-C(3A)	2.325(2)	C(43)-C(44)	1.375(4)
P-C(41)	1.817(2)	C(44)-C(45)	1.369(4)
P-C(21)	1.820(2)	C(45)-C(46)	1.385(4)
P-C(31)	1.824(3)	C(51)-C(52)	1.391(3)
N-C(13)	1.343(3)	C(51)-C(56)	1.407(3)
N-C(9)	1.364(3)	C(51)-B	1.642(4)
C(1)-C(2)	1.421(4)	C(52)-C(53)	1.389(3)
C(1)-C(7A)	1.470(3)	C(53)-C(54)	1.380(4)
C(1)-C(8)	1.481(3)	C(54)-C(55)	1.377(4)
C(2)-C(3)	1.401(4)	C(55)-C(56)	1.390(3)
C(3)-C(3A)	1.457(4)	C(61)-C(62)	1.388(4)
C(3A)-C(4)	1.391(4)	C(61)-C(66)	1.398(4)
C(3A)-C(7A)	1.417(3)	C(61)-B	1.653(4)
C(4)-C(5)	1.373(4)	C(62)-C(63)	1.399(4)
C(5)-C(6)	1.385(5)	C(63)-C(64)	1.371(4)
C(6)-C(7)	1.384(4)	C(64)-C(65)	1.369(4)
C(7)-C(7A)	1.383(4)	C(65)-C(66)	1.395(4)
C(8)-C(9)	1.501(3)	C(71)-C(76)	1.395(3)
C(9)-C(10)	1.386(3)	C(71)-C(72)	1.406(3)
C(10)-C(11)	1.360(4)	C(71)-B	1.643(4)
C(11)-C(12)	1.382(3)	C(72)-C(73)	1.383(4)
C(12)-C(13)	1.370(3)	C(73)-C(74)	1.378(4)
C(21)-C(26)	1.388(3)	C(74)-C(75)	1.377(4)
C(21)-C(22)	1.390(3)	C(75)-C(76)	1.396(4)
C(22)-C(23)	1.389(3)	C(81)-C(86)	1.389(4)
C(23)-C(24)	1.380(4)	C(81)-C(82)	1.400(4)
C(24)-C(25)	1.381(4)	C(81)-B	1.638(3)
C(25)-C(26)	1.386(3)	C(82)-C(83)	1.386(4)
C(31)-C(32)	1.388(3)	C(83)-C(84)	1.362(5)
C(31)-C(36)	1.389(4)	C(84)-C(85)	1.378(5)
C(32)-C(33)	1.387(4)	C(85)-C(86)	1.397(4)
C(33)-C(34)	1.366(5)	C(99)-Cl(2)	1.686(8)
C(34)-C(35)	1.376(5)	C(99)-Cl(1)	1.706(8)
C(35)-C(36)	1.384(4)	C(99')-Cl(1')	1.704(14)
C(41)-C(42)	1.391(3)	C(99')-Cl(2')	1.712(14)
N-Ni-C(1)	83.61(9)	C(41)-P-C(21)	104.95(11)
N-Ni-C(2)	112.94(10)	C(41)-P-C(31)	105.95(12)
C(1)-Ni-C(2)	40.70(10)	C(21)-P-C(31)	104.14(11)
N-Ni-C(3)	150.29(10)	C(41)-P-Ni	116.71(8)
C(1)-Ni-C(3)	67.24(10)	C(21)-P-Ni	114.64(8)
C(2)-Ni-C(3)	39.38(10)	C(31)-P-Ni	109.40(8)
N-Ni-P	106.51(6)	C(13)-N-C(9)	117.2(2)
C(1)-Ni-P	166.58(8)	C(13)-N-Ni	127.21(16)
C(2)-Ni-P	136.04(8)	C(9)-N-Ni	115.48(16)
C(3)-Ni-P	103.19(8)	C(2)-C(1)-C(7A)	107.6(2)
N-Ni-C(7A)	97.60(9)	C(2)-C(1)-C(8)	127.8(2)
C(1)-Ni-C(7A)	39.37(9)	C(7A)-C(1)-C(8)	124.4(2)
C(2)-Ni-C(7A)	64.76(10)	C(2)-C(1)-Ni	71.17(14)
C(3)-Ni-C(7A)	63.61(10)	C(7A)-C(1)-Ni	79.80(14)
P-Ni-C(7A)	128.59(7)	C(8)-C(1)-Ni	111.22(17)
N-Ni-C(3A)	132.56(9)	C(3)-C(2)-C(1)	107.8(2)
C(1)-Ni-C(3A)	64.22(9)	C(3)-C(2)-Ni	71.53(15)
C(2)-Ni-C(3A)	63.70(10)	C(1)-C(2)-Ni	68.13(14)
C(3)-Ni-C(3A)	38.05(10)	C(2)-C(3)-C(3A)	108.9(2)
P-Ni-C(3A)	102.40(7)	C(2)-C(3)-Ni	69.09(15)
C(7A)-Ni-C(3A)	35.83(8)	C(3A)-C(3)-Ni	79.55(15)

C(4)-C(3A)-C(7A)	120.2(3)	C(45)-C(44)-C(43)	120.2(3)
C(4)-C(3A)-C(3)	132.7(3)	C(44)-C(45)-C(46)	120.6(3)
C(7A)-C(3A)-C(3)	107.0(2)	C(45)-C(46)-C(41)	119.9(3)
C(4)-C(3A)-Ni	129.84(19)	C(52)-C(51)-C(56)	114.6(2)
C(7A)-C(3A)-Ni	70.38(14)	C(52)-C(51)-B	123.2(2)
C(3)-C(3A)-Ni	62.40(13)	C(56)-C(51)-B	121.9(2)
C(5)-C(4)-C(3A)	117.8(3)	C(53)-C(52)-C(51)	123.1(2)
C(4)-C(5)-C(6)	122.1(3)	C(54)-C(53)-C(52)	120.4(3)
C(7)-C(6)-C(5)	121.1(3)	C(55)-C(54)-C(53)	118.9(3)
C(7A)-C(7)-C(6)	117.8(3)	C(54)-C(55)-C(56)	119.8(3)
C(7)-C(7A)-C(3A)	121.0(2)	C(55)-C(56)-C(51)	123.2(2)
C(7)-C(7A)-C(1)	131.5(2)	C(62)-C(61)-C(66)	115.2(2)
C(3A)-C(7A)-C(1)	107.3(2)	C(62)-C(61)-B	125.3(2)
C(7)-C(7A)-Ni	127.06(18)	C(66)-C(61)-B	119.4(2)
C(3A)-C(7A)-Ni	73.79(14)	C(61)-C(62)-C(63)	122.6(3)
C(1)-C(7A)-Ni	60.83(12)	C(64)-C(63)-C(62)	120.5(3)
C(1)-C(8)-C(9)	109.8(2)	C(65)-C(64)-C(63)	118.7(3)
N-C(9)-C(10)	121.1(2)	C(64)-C(65)-C(66)	120.7(3)
N-C(9)-C(8)	116.4(2)	C(65)-C(66)-C(61)	122.4(3)
C(10)-C(9)-C(8)	122.4(2)	C(76)-C(71)-C(72)	114.5(2)
C(11)-C(10)-C(9)	120.5(2)	C(76)-C(71)-B	124.3(2)
C(10)-C(11)-C(12)	118.7(3)	C(72)-C(71)-B	121.0(2)
C(13)-C(12)-C(11)	118.8(3)	C(73)-C(72)-C(71)	122.9(3)
N-C(13)-C(12)	123.6(2)	C(74)-C(73)-C(72)	120.7(3)
C(26)-C(21)-C(22)	118.9(2)	C(75)-C(74)-C(73)	118.6(3)
C(26)-C(21)-P	122.80(19)	C(74)-C(75)-C(76)	120.2(3)
C(22)-C(21)-P	118.12(18)	C(71)-C(76)-C(75)	123.1(2)
C(23)-C(22)-C(21)	120.7(2)	C(86)-C(81)-C(82)	114.8(3)
C(24)-C(23)-C(22)	119.6(3)	C(86)-C(81)-B	125.0(2)
C(23)-C(24)-C(25)	120.3(2)	C(82)-C(81)-B	120.0(2)
C(24)-C(25)-C(26)	120.0(3)	C(83)-C(82)-C(81)	122.9(3)
C(25)-C(26)-C(21)	120.5(3)	C(84)-C(83)-C(82)	120.4(3)
C(32)-C(31)-C(36)	119.0(3)	C(83)-C(84)-C(85)	119.1(3)
C(32)-C(31)-P	124.0(2)	C(84)-C(85)-C(86)	120.0(3)
C(36)-C(31)-P	116.9(2)	C(81)-C(86)-C(85)	122.7(3)
C(33)-C(32)-C(31)	119.7(3)	C(81)-B-C(51)	114.3(2)
C(34)-C(33)-C(32)	120.5(3)	C(81)-B-C(71)	111.7(2)
C(33)-C(34)-C(35)	120.6(3)	C(51)-B-C(71)	104.60(18)
C(34)-C(35)-C(36)	119.4(3)	C(81)-B-C(61)	103.68(19)
C(35)-C(36)-C(31)	120.8(3)	C(51)-B-C(61)	110.0(2)
C(42)-C(41)-C(46)	119.0(2)	C(71)-B-C(61)	112.8(2)
C(42)-C(41)-P	118.82(19)	Cl(2)-C(99)-Cl(1)	115.0(6)
C(46)-C(41)-P	122.2(2)	Cl(1')-C(99')-Cl(2')	109.9(12)
C(43)-C(42)-C(41)	120.3(3)		
C(44)-C(43)-C(42)	120.0(3)		

Table III.12. Torsion angles [°] for [(η^3:η^1-IndCH$_2$Py)Ni(PPh$_3$)][BPh$_4$] **(4)**

N-Ni-P-C(41)	74.15(11)	Ni-C(2)-C(3)-C(3A)	-70.35(18)
C(1)-Ni-P-C(41)	-148.0(4)	C(1)-C(2)-C(3)-Ni	58.69(18)
C(2)-Ni-P-C(41)	-79.08(15)	N-Ni-C(3)-C(2)	-26.5(3)
C(3)-Ni-P-C(41)	-104.85(12)	C(1)-Ni-C(3)-C(2)	-38.30(16)
C(7A)-Ni-P-C(41)	-171.46(12)	P-Ni-C(3)-C(2)	151.60(15)
C(3A)-Ni-P-C(41)	-143.90(11)	C(7A)-Ni-C(3)-C(2)	-81.61(17)
N-Ni-P-C(21)	-162.58(11)	C(3A)-Ni-C(3)-C(2)	-115.1(2)
C(1)-Ni-P-C(21)	-24.7(4)	N-Ni-C(3)-C(3A)	88.6(2)
C(2)-Ni-P-C(21)	44.18(15)	C(1)-Ni-C(3)-C(3A)	76.75(16)
C(3)-Ni-P-C(21)	18.42(12)	C(2)-Ni-C(3)-C(3A)	115.1(2)
C(7A)-Ni-P-C(21)	-48.19(13)	P-Ni-C(3)-C(3A)	-93.35(14)
C(3A)-Ni-P-C(21)	-20.64(12)	C(7A)-Ni-C(3)-C(3A)	33.44(14)
N-Ni-P-C(31)	-46.06(11)	C(2)-C(3)-C(3A)-C(4)	-176.5(3)
C(1)-Ni-P-C(31)	91.8(4)	Ni-C(3)-C(3A)-C(4)	120.1(3)
C(2)-Ni-P-C(31)	160.70(14)	C(2)-C(3)-C(3A)-C(7A)	7.3(3)
C(3)-Ni-P-C(31)	134.93(12)	Ni-C(3)-C(3A)-C(7A)	-56.18(18)
C(7A)-Ni-P-C(31)	68.32(12)	C(2)-C(3)-C(3A)-Ni	63.45(18)
C(3A)-Ni-P-C(31)	95.88(11)	N-Ni-C(3A)-C(4)	98.2(3)
C(1)-Ni-N-C(13)	-174.5(2)	C(1)-Ni-C(3A)-C(4)	150.5(3)
C(2)-Ni-N-C(13)	156.6(2)	C(2)-Ni-C(3A)-C(4)	-164.0(3)
C(3)-Ni-N-C(13)	174.5(2)	C(3)-Ni-C(3A)-C(4)	-124.1(3)
P-Ni-N-C(13)	-3.5(2)	P-Ni-C(3A)-C(4)	-28.5(3)
C(7A)-Ni-N-C(13)	-137.6(2)	C(7A)-Ni-C(3A)-C(4)	113.4(3)
C(3A)-Ni-N-C(13)	-128.7(2)	N-Ni-C(3A)-C(7A)	-15.2(2)
C(1)-Ni-N-C(9)	2.53(18)	C(1)-Ni-C(3A)-C(7A)	37.10(16)
C(2)-Ni-N-C(9)	-26.3(2)	C(2)-Ni-C(3A)-C(7A)	82.64(17)
C(3)-Ni-N-C(9)	-8.4(3)	C(3)-Ni-C(3A)-C(7A)	122.5(2)
P-Ni-N-C(9)	173.52(15)	P-Ni-C(3A)-C(7A)	-141.85(14)
C(7A)-Ni-N-C(9)	39.43(18)	N-Ni-C(3A)-C(3)	-137.72(16)
C(3A)-Ni-N-C(9)	48.3(2)	C(1)-Ni-C(3A)-C(3)	-85.41(17)
N-Ni-C(1)-C(2)	-137.03(17)	C(2)-Ni-C(3A)-C(3)	-39.88(15)
C(3)-Ni-C(1)-C(2)	37.10(16)	P-Ni-C(3A)-C(3)	95.64(14)
P-Ni-C(1)-C(2)	83.3(4)	C(7A)-Ni-C(3A)-C(3)	-122.5(2)
C(7A)-Ni-C(1)-C(2)	112.7(2)	C(7A)-C(3A)-C(4)-C(5)	0.0(4)
C(3A)-Ni-C(1)-C(2)	78.88(17)	C(3)-C(3A)-C(4)-C(5)	-175.9(3)
N-Ni-C(1)-C(7A)	110.26(15)	Ni-C(3A)-C(4)-C(5)	-88.8(3)
C(2)-Ni-C(1)-C(7A)	-112.7(2)	C(3A)-C(4)-C(5)-C(6)	1.2(5)
C(3)-Ni-C(1)-C(7A)	-75.61(16)	C(4)-C(5)-C(6)-C(7)	-0.9(5)
P-Ni-C(1)-C(7A)	-29.4(4)	C(5)-C(6)-C(7)-C(7A)	-0.6(5)
C(3A)-Ni-C(1)-C(7A)	-33.83(14)	C(6)-C(7)-C(7A)-C(3A)	1.8(4)
N-Ni-C(1)-C(8)	-12.85(19)	C(6)-C(7)-C(7A)-C(1)	176.0(3)
C(2)-Ni-C(1)-C(8)	124.2(3)	C(6)-C(7)-C(7A)-Ni	94.4(3)
C(3)-Ni-C(1)-C(8)	161.3(2)	C(4)-C(3A)-C(7A)-C(7)	-1.5(4)
P-Ni-C(1)-C(8)	-152.5(3)	C(3)-C(3A)-C(7A)-C(7)	175.3(2)
C(7A)-Ni-C(1)-C(8)	-123.1(3)	Ni-C(3A)-C(7A)-C(7)	123.9(2)
C(3A)-Ni-C(1)-C(8)	-156.9(2)	C(4)-C(3A)-C(7A)-C(1)	-176.9(2)
C(7A)-C(1)-C(2)-C(3)	11.4(3)	C(3)-C(3A)-C(7A)-C(1)	-0.1(3)
C(8)-C(1)-C(2)-C(3)	-163.5(2)	Ni-C(3A)-C(7A)-C(1)	-51.54(16)
Ni-C(1)-C(2)-C(3)	-60.83(18)	C(4)-C(3A)-C(7A)-Ni	-125.4(2)
C(7A)-C(1)-C(2)-Ni	72.28(16)	C(3)-C(3A)-C(7A)-Ni	51.41(17)
C(8)-C(1)-C(2)-Ni	-102.7(2)	C(2)-C(1)-C(7A)-C(7)	178.3(3)
N-Ni-C(2)-C(3)	166.12(16)	C(8)-C(1)-C(7A)-C(7)	-6.5(4)
C(1)-Ni-C(2)-C(3)	118.8(2)	Ni-C(1)-C(7A)-C(7)	-115.3(3)
P-Ni-C(2)-C(3)	-41.8(2)	C(2)-C(1)-C(7A)-C(3A)	-6.9(3)
C(7A)-Ni-C(2)-C(3)	78.46(17)	C(8)-C(1)-C(7A)-C(3A)	168.3(2)
C(3A)-Ni-C(2)-C(3)	38.53(16)	Ni-C(1)-C(7A)-C(3A)	59.44(18)
N-Ni-C(2)-C(1)	47.35(18)	C(2)-C(1)-C(7A)-Ni	-66.35(17)
C(3)-Ni-C(2)-C(1)	-118.8(2)	C(8)-C(1)-C(7A)-Ni	108.8(2)
P-Ni-C(2)-C(1)	-160.60(12)	N-Ni-C(7A)-C(7)	51.8(2)
C(7A)-Ni-C(2)-C(1)	-40.31(15)	C(1)-Ni-C(7A)-C(7)	122.0(3)
C(3A)-Ni-C(2)-C(1)	-80.24(16)	C(2)-Ni-C(7A)-C(7)	163.7(3)
C(1)-C(2)-C(3)-C(3A)	-11.7(3)	C(3)-Ni-C(7A)-C(7)	-152.4(3)

P-Ni-C(7A)-C(7)	-66.4(3)
C(3A)-Ni-C(7A)-C(7)	-116.9(3)
C(1)-Ni-C(7A)-C(3A)	-121.1(2)
C(2)-Ni-C(7A)-C(3A)	-79.41(17)
C(3)-Ni-C(7A)-C(3A)	-35.47(16)
P-Ni-C(7A)-C(3A)	50.52(18)
N-Ni-C(7A)-C(1)	-70.15(16)
C(2)-Ni-C(7A)-C(1)	41.68(15)
C(3)-Ni-C(7A)-C(1)	85.62(17)
P-Ni-C(7A)-C(1)	171.61(12)
C(3A)-Ni-C(7A)-C(1)	121.1(2)
C(2)-C(1)-C(8)-C(9)	101.9(3)
C(7A)-C(1)-C(8)-C(9)	-72.3(3)
Ni-C(1)-C(8)-C(9)	19.7(3)
C(13)-N-C(9)-C(10)	2.4(4)
Ni-N-C(9)-C(10)	-174.91(19)
C(13)-N-C(9)-C(8)	-174.0(2)
Ni-N-C(9)-C(8)	8.6(3)
C(1)-C(8)-C(9)-N	-18.8(3)
C(1)-C(8)-C(9)-C(10)	164.7(2)
N-C(9)-C(10)-C(11)	-2.1(4)
C(8)-C(9)-C(10)-C(11)	174.2(3)
C(9)-C(10)-C(11)-C(12)	-0.2(4)
C(10)-C(11)-C(12)-C(13)	1.9(4)
C(9)-N-C(13)-C(12)	-0.6(4)
Ni-N-C(13)-C(12)	176.4(2)
C(11)-C(12)-C(13)-N	-1.5(4)
C(41)-P-C(21)-C(26)	-124.5(2)
C(31)-P-C(21)-C(26)	-13.3(2)
Ni-P-C(21)-C(26)	106.2(2)
C(41)-P-C(21)-C(22)	60.7(2)
C(31)-P-C(21)-C(22)	171.84(19)
Ni-P-C(21)-C(22)	-68.7(2)
C(26)-C(21)-C(22)-C(23)	-0.8(4)
P-C(21)-C(22)-C(23)	174.2(2)
C(21)-C(22)-C(23)-C(24)	0.6(4)
C(22)-C(23)-C(24)-C(25)	0.0(4)
C(23)-C(24)-C(25)-C(26)	-0.3(4)
C(24)-C(25)-C(26)-C(21)	0.1(4)
C(22)-C(21)-C(26)-C(25)	0.5(4)
P-C(21)-C(26)-C(25)	-174.31(19)
C(41)-P-C(31)-C(32)	12.6(2)
C(21)-P-C(31)-C(32)	-97.9(2)
Ni-P-C(31)-C(32)	139.15(19)
C(41)-P-C(31)-C(36)	-165.7(2)
C(21)-P-C(31)-C(36)	83.9(2)
Ni-P-C(31)-C(36)	-39.1(2)
C(36)-C(31)-C(32)-C(33)	0.4(4)
P-C(31)-C(32)-C(33)	-177.8(2)
C(31)-C(32)-C(33)-C(34)	-0.9(4)
C(32)-C(33)-C(34)-C(35)	0.0(5)
C(33)-C(34)-C(35)-C(36)	1.4(6)
C(34)-C(35)-C(36)-C(31)	-2.0(5)
C(32)-C(31)-C(36)-C(35)	1.1(4)
P-C(31)-C(36)-C(35)	179.4(2)
C(21)-P-C(41)-C(42)	-146.7(2)
C(31)-P-C(41)-C(42)	103.5(2)
Ni-P-C(41)-C(42)	-18.6(2)
C(21)-P-C(41)-C(46)	35.5(3)
C(31)-P-C(41)-C(46)	-74.4(2)
Ni-P-C(41)-C(46)	163.6(2)
C(46)-C(41)-C(42)-C(43)	1.8(4)
P-C(41)-C(42)-C(43)	-176.1(2)
C(41)-C(42)-C(43)-C(44)	-0.7(4)
C(42)-C(43)-C(44)-C(45)	-0.8(5)
C(43)-C(44)-C(45)-C(46)	1.1(5)

N-Ni-C(7A)-C(3A)	168.76(16)
C(44)-C(45)-C(46)-C(41)	0.1(5)
C(42)-C(41)-C(46)-C(45)	-1.5(4)
P-C(41)-C(46)-C(45)	176.3(2)
C(56)-C(51)-C(52)-C(53)	-0.5(4)
B-C(51)-C(52)-C(53)	173.4(2)
C(51)-C(52)-C(53)-C(54)	0.8(4)
C(52)-C(53)-C(54)-C(55)	-0.2(4)
C(53)-C(54)-C(55)-C(56)	-0.7(4)
C(54)-C(55)-C(56)-C(51)	1.1(4)
C(52)-C(51)-C(56)-C(55)	-0.5(4)
B-C(51)-C(56)-C(55)	-174.4(2)
C(66)-C(61)-C(62)-C(63)	-1.1(4)
B-C(61)-C(62)-C(63)	-177.2(2)
C(61)-C(62)-C(63)-C(64)	0.7(4)
C(62)-C(63)-C(64)-C(65)	0.3(5)
C(63)-C(64)-C(65)-C(66)	-0.8(5)
C(64)-C(65)-C(66)-C(61)	0.3(4)
C(62)-C(61)-C(66)-C(65)	0.6(4)
B-C(61)-C(66)-C(65)	177.0(2)
C(76)-C(71)-C(72)-C(73)	-1.5(3)
B-C(71)-C(72)-C(73)	-175.8(2)
C(71)-C(72)-C(73)-C(74)	0.7(4)
C(72)-C(73)-C(74)-C(75)	0.9(4)
C(73)-C(74)-C(75)-C(76)	-1.4(4)
C(72)-C(71)-C(76)-C(75)	0.9(3)
B-C(71)-C(76)-C(75)	174.9(2)
C(74)-C(75)-C(76)-C(71)	0.5(4)
C(86)-C(81)-C(82)-C(83)	0.5(4)
B-C(81)-C(82)-C(83)	175.2(3)
C(81)-C(82)-C(83)-C(84)	-0.3(5)
C(82)-C(83)-C(84)-C(85)	-0.6(6)
C(83)-C(84)-C(85)-C(86)	1.3(6)
C(82)-C(81)-C(86)-C(85)	0.3(4)
B-C(81)-C(86)-C(85)	-174.2(3)
C(84)-C(85)-C(86)-C(81)	-1.2(6)
C(86)-C(81)-B-C(51)	-18.8(4)
C(82)-C(81)-B-C(51)	167.0(2)
C(86)-C(81)-B-C(71)	-137.4(3)
C(82)-C(81)-B-C(71)	48.5(3)
C(86)-C(81)-B-C(61)	100.9(3)
C(82)-C(81)-B-C(61)	-73.3(3)
C(52)-C(51)-B-C(81)	143.2(2)
C(56)-C(51)-B-C(81)	-3.4(3)
C(52)-C(51)-B-C(71)	-94.3(3)
C(56)-C(51)-B-C(71)	79.1(3)
C(52)-C(51)-B-C(61)	27.0(3)
C(56)-C(51)-B-C(61)	-159.5(2)
C(76)-C(71)-B-C(81)	21.8(3)
C(72)-C(71)-B-C(81)	-164.6(2)
C(76)-C(71)-B-C(51)	-102.4(2)
C(72)-C(71)-B-C(51)	71.2(3)
C(76)-C(71)-B-C(61)	138.1(2)
C(72)-C(71)-B-C(61)	-48.3(3)
C(62)-C(61)-B-C(81)	109.2(3)
C(66)-C(61)-B-C(81)	-66.8(3)
C(62)-C(61)-B-C(51)	-128.1(3)
C(66)-C(61)-B-C(51)	55.9(3)
C(62)-C(61)-B-C(71)	-11.8(3)
C(66)-C(61)-B-C(71)	172.2(2)

Voltammogrammes des complexes **1**-**5**, du $FeCp_2$, $(\eta^3:\eta^0\text{-Ind}(CH_2)_2NMe_2)Ni(PPh_3)Cl$ et $[(\eta^3:\eta^1\text{-Ind}(CH_2)_2NMe_2)Ni(PPh_3)]^+$

$FeCp_2$

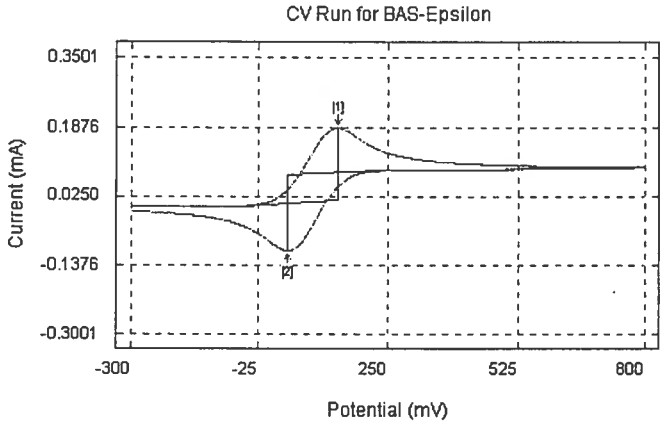

$(\eta^3:\eta^0\text{-IndCH}_2\text{Py})Ni(PPh_3)Cl$

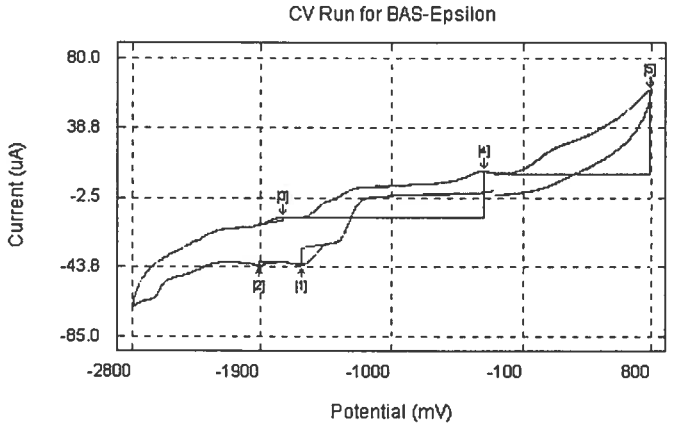

$(\eta^3:\eta^0\text{-Ind}(CH_2)_2NC_4H_8)Ni(PPh_3)Cl$

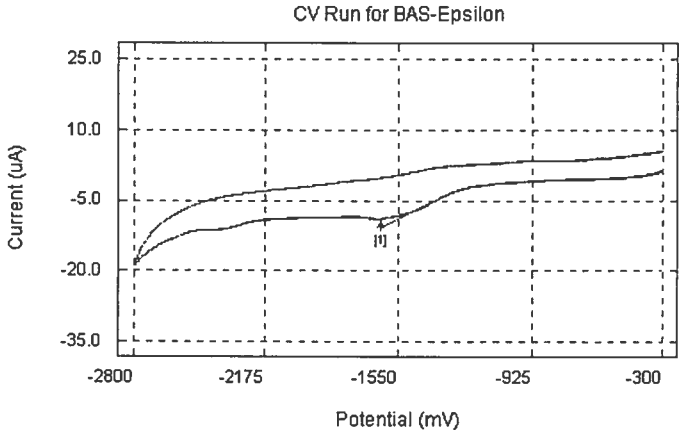

$(\eta^3:\eta^0\text{-Ind}(CH_2)\text{N-}i\text{Pr}_2)\text{Ni}(PPh_3)\text{Cl}$

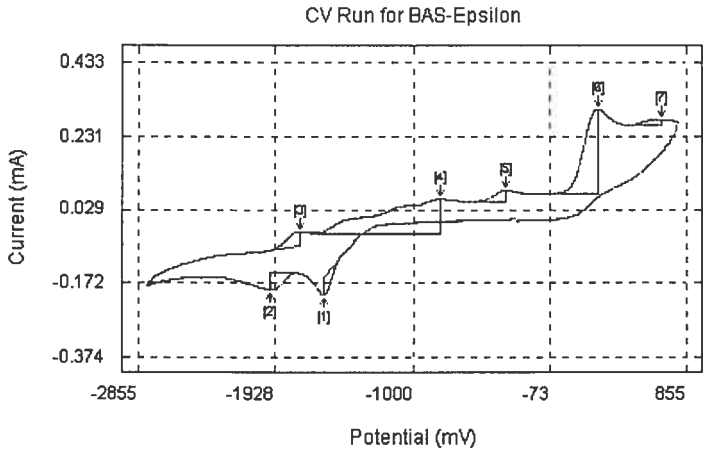

$(\eta^3:\eta^0\text{-Ind}(CH_2)_2NMe_2)\text{Ni}(PPh_3)\text{Cl}$

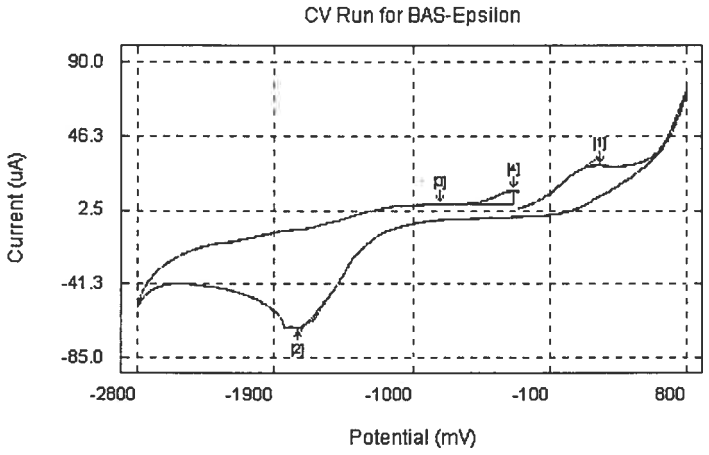

$[(\eta^3:\eta^1\text{-IndCH}_2\text{Py})\text{Ni}(PPh_3)]^+$

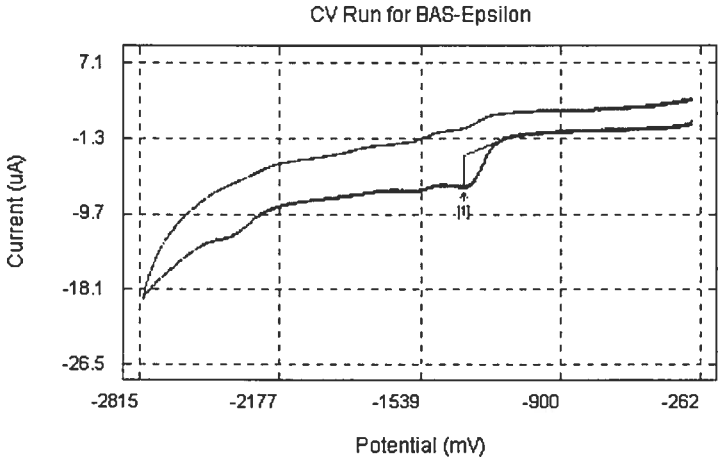

$[(\eta^3:\eta^1\text{-Ind}(CH_2)_2NC_4H_8)Ni(PPh_3)]^+$

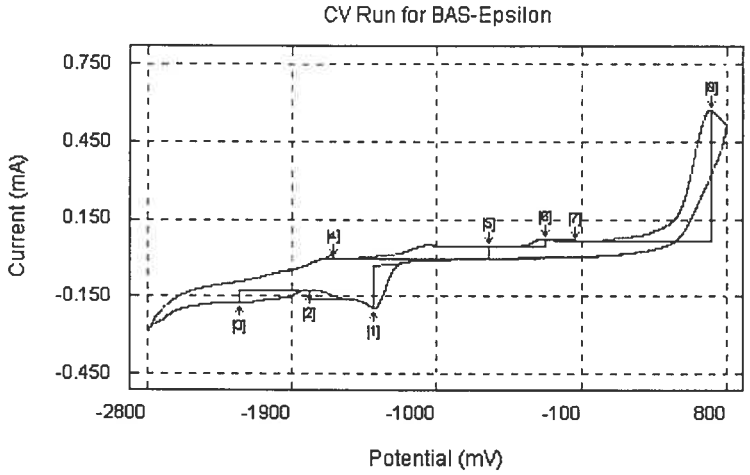

$[(\eta^3:\eta^1\text{-Ind}(CH_2)_2NMe_2)Ni(PPh_3)]^+$

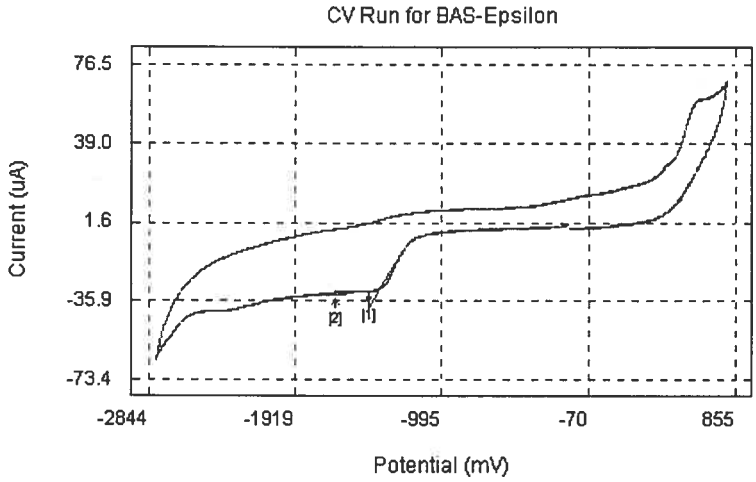

Annexe 4

Données cristallographiques supplémentaires et voltammogrammes, article 5

Table IV.1. Crystal data and structure refinement for $(\eta^3:\eta^0$-$Ind(CH_2)_2NMe_2)(PMe_3)NiCl$ **(2)**

Empirical formula	C16 H25 Cl N Ni P
Formula weight	356.50
Temperature	223(2)K
Wavelength	1.54178 Å
Crystal system	Monoclinic
Space group	P21/n
Unit cell dimensions	a = 6.3037(2) Å α = 90° b = 15.6826(5) Å β = 96.106(2)° c = 18.2702(6) Å γ = 90°
Volume	1795.92(10)Å^3
Z	4
Density (calculated)	1.319 Mg/m^3
Absorption coefficient	3.677 mm^{-1}
F(000)	752
Crystal size	0.78 x 0.13 x 0.07 mm
Theta range for data collection	3.72 to 72.75°
Index ranges	$-6 \le h \le 7$, $-19 \le k \le 19$, $-22 \le \ell \le 22$
Reflections collected	21727
Independent reflections	3542 [R_{int} = 0.052]
Absorption correction	Semi-empirical from equivalents
Max. and min. transmission	0.8300 and 0.4300
Refinement method	Full-matrix least-squares on F^2
Data / restraints / parameters	3542 / 0 / 186
Goodness-of-fit on F^2	1.003
Final R indices [I>2sigma(I)]	R1 = 0.0362, wR_2 = 0.0968
R indices (all data)	R1 = 0.0434, wR_2 = 0.1001
Largest diff. peak and hole	0.359 and -0.295 e/Å^3

Table IV.2. Atomic coordinates (x 10^4) and equivalent isotropic displacement parameters ($Å^2$ x 10^3) for (η^3:η^0-Ind$(CH_2)_2NMe_2$)(PMe_3)NiCl **(2)**

U_{eq} is defined as one third of the trace of the orthogonalized Uij tensor.

	Occ.	x	y	z	U_{eq}
Ni	1	595(1)	2683(1)	1295(1)	32(1)
Cl	1	-2507(1)	2377(1)	701(1)	44(1)
P	1	1761(1)	1387(1)	1362(1)	38(1)
N	1	-2796(3)	6000(1)	640(1)	36(1)
C(1)	1	177(3)	4020(1)	1361(1)	33(1)
C(2)	1	2191(3)	3793(1)	1157(1)	35(1)
C(3)	1	3268(3)	3302(1)	1735(1)	38(1)
C(3A)	1	2087(3)	3396(1)	2381(1)	36(1)
C(4)	1	2537(4)	3148(2)	3116(1)	48(1)
C(5)	1	1060(4)	3335(2)	3602(1)	54(1)
C(6)	1	-854(4)	3736(1)	3364(1)	49(1)
C(7)	1	-1342(3)	3970(1)	2636(1)	39(1)
C(7A)	1	155(3)	3823(1)	2145(1)	31(1)
C(8)	1	-1500(3)	4525(1)	911(1)	39(1)
C(9)	1	-1267(3)	5469(1)	1085(1)	36(1)
C(10)	1	-4934(4)	5916(2)	856(2)	53(1)
C(11)	1	-2138(4)	6890(1)	691(1)	50(1)
C(20)	1	-131(5)	608(2)	1633(2)	72(1)
C(21)	1	2465(4)	973(2)	499(1)	62(1)
C(22)	1	4121(4)	1177(2)	1994(2)	66(1)

Table IV.3. Hydrogen coordinates (x 10^4) and isotropic displacement parameters ($Å^2$ x 10^3) for (η^3:η^0-Ind$(CH_2)_2NMe_2$)(PMe_3)NiCl **(2)**

	Occ.	x	y	z	U_{eq}
H(2)	1	2789	3973	702	42
H(3)	1	4742	3082	1744	45
H(4)	1	3811	2860	3276	57
H(5)	1	1357	3189	4101	65
H(6)	1	-1837	3850	3704	59
H(7)	1	-2661	4224	2477	47
H(8A)	1	-2915	4330	1014	47
H(8B)	1	-1377	4432	387	47
H(9A)	1	-1447	5558	1606	43
H(9B)	1	179	5651	1008	43
H(10A)	1	-4928	6068	1370	80
H(10B)	1	-5411	5331	784	80
H(10C)	1	-5894	6292	557	80
H(11A)	1	-2060	7075	1199	76
H(11B)	1	-3167	7238	392	76
H(11C)	1	-746	6950	515	76
H(20A)	1	-1399	613	1281	109
H(20B)	1	-519	748	2118	109
H(20C)	1	511	45	1643	109
H(21A)	1	3706	1274	360	93
H(21B)	1	1279	1052	121	93
H(21C)	1	2788	370	551	93
H(22A)	1	4416	570	2005	99
H(22B)	1	3881	1369	2484	99
H(22C)	1	5328	1481	1833	99

Table IV.4. Anisotropic parameters ($Å^2$ x 10^3) for (η^3:η^0-$Ind(CH_2)_2NMe_2)(PMe_3)NiCl$ **(2)**

The anisotropic displacement factor exponent takes the form:

$$-2\pi^2 [h^2 a^{*2} U_{11} + ... + 2 h k a^* b^* U_{12}]$$

	U11	U22	U33	U23	U13	U12
Ni	30(1)	28(1)	36(1)	2(1)	0(1)	1(1)
Cl	37(1)	42(1)	51(1)	-1(1)	-6(1)	-4(1)
P	39(1)	30(1)	45(1)	5(1)	7(1)	4(1)
N	42(1)	27(1)	36(1)	3(1)	-5(1)	1(1)
C(1)	41(1)	24(1)	33(1)	1(1)	-2(1)	-2(1)
C(2)	38(1)	32(1)	36(1)	1(1)	5(1)	-9(1)
C(3)	28(1)	38(1)	47(1)	-2(1)	0(1)	-2(1)
C(3A)	38(1)	31(1)	36(1)	2(1)	-4(1)	-3(1)
C(4)	54(1)	42(1)	44(1)	9(1)	-13(1)	0(1)
C(5)	81(2)	49(1)	32(1)	6(1)	0(1)	-9(1)
C(6)	66(2)	41(1)	43(1)	-1(1)	18(1)	-6(1)
C(7)	44(1)	30(1)	44(1)	-2(1)	6(1)	-1(1)
C(7A)	35(1)	25(1)	32(1)	-1(1)	-1(1)	-3(1)
C(8)	47(1)	31(1)	36(1)	2(1)	-7(1)	1(1)
C(9)	39(1)	31(1)	37(1)	1(1)	-5(1)	-1(1)
C(10)	46(1)	47(1)	65(2)	8(1)	-4(1)	3(1)
C(11)	60(2)	31(1)	58(2)	2(1)	-2(1)	1(1)
C(20)	67(2)	40(1)	116(2)	22(2)	39(2)	1(1)
C(21)	81(2)	47(1)	60(2)	-9(1)	17(1)	5(1)
C(22)	69(2)	55(2)	71(2)	10(1)	-10(1)	26(1)

Table IV.5. Bond lengths [Å] and angles [°] for (η^3:η^0-Ind$(CH_2)_2NMe_2$)(PMe_3)NiCl **(2)**

Ni-C(3)	2.0344(19)	C(5)-H(5)	0.9400
Ni-C(2)	2.0389(19)	C(6)-C(7)	1.381(3)
Ni-C(1)	2.1184(19)	C(6)-H(6)	0.9400
Ni-P	2.1608(6)	C(7)-C(7A)	1.389(3)
Ni-Cl	2.1868(6)	C(7)-H(7)	0.9400
Ni-C(3A)	2.3817(19)	C(8)-C(9)	1.518(3)
Ni-C(7A)	2.4035(18)	C(8)-H(8A)	0.9800
P-C(21)	1.803(2)	C(8)-H(8B)	0.9800
P-C(20)	1.813(2)	C(9)-H(9A)	0.9800
P-C(22)	1.814(2)	C(9)-H(9B)	0.9800
N-C(10)	1.450(3)	C(10)-H(10A)	0.9700
N-C(11)	1.456(3)	C(10)-H(10B)	0.9700
N-C(9)	1.456(2)	C(10)-H(10C)	0.9700
C(1)-C(2)	1.406(3)	C(11)-H(11A)	0.9700
C(1)-C(7A)	1.467(2)	C(11)-H(11B)	0.9700
C(1)-C(8)	1.495(3)	C(11)-H(11C)	0.9700
C(2)-C(3)	1.419(3)	C(20)-H(20A)	0.9700
C(2)-H(2)	0.9900	C(20)-H(20B)	0.9700
C(3)-C(3A)	1.468(3)	C(20)-H(20C)	0.9700
C(3)-H(3)	0.9900	C(21)-H(21A)	0.9700
C(3A)-C(4)	1.398(3)	C(21)-H(21B)	0.9700
C(3A)-C(7A)	1.417(3)	C(21)-H(21C)	0.9700
C(4)-C(5)	1.386(3)	C(22)-H(22A)	0.9700
C(4)-H(4)	0.9400	C(22)-H(22B)	0.9700
C(5)-C(6)	1.389(3)	C(22)-H(22C)	0.9700
C(3)-Ni-C(2)	40.78(8)	C(1)-C(2)-C(3)	108.34(17)
C(3)-Ni-C(1)	66.92(8)	C(1)-C(2)-Ni	73.31(11)
C(2)-Ni-C(1)	39.48(7)	C(3)-C(2)-Ni	69.44(11)
C(3)-Ni-P	99.48(6)	C(1)-C(2)-H(2)	125.8
C(2)-Ni-P	129.85(6)	C(3)-C(2)-H(2)	125.8
C(1)-Ni-P	166.36(5)	Ni-C(2)-H(2)	125.8
C(3)-Ni-Cl	163.78(6)	C(2)-C(3)-C(3A)	107.47(18)
C(2)-Ni-Cl	123.58(6)	C(2)-C(3)-Ni	69.78(11)
C(1)-Ni-Cl	97.78(5)	C(3A)-C(3)-Ni	84.03(12)
P-Ni-Cl	95.86(2)	C(2)-C(3)-H(3)	125.2
C(3)-Ni-C(3A)	37.80(7)	C(3A)-C(3)-H(3)	125.2
C(2)-Ni-C(3A)	63.00(7)	Ni-C(3)-H(3)	125.2
C(1)-Ni-C(3A)	61.87(7)	C(4)-C(3A)-C(7A)	120.3(2)
P-Ni-C(3A)	107.05(5)	C(4)-C(3A)-C(3)	132.5(2)
Cl-Ni-C(3A)	140.31(6)	C(7A)-C(3A)-C(3)	107.22(16)
C(3)-Ni-C(7A)	62.45(7)	C(4)-C(3A)-Ni	133.69(15)
C(2)-Ni-C(7A)	62.44(7)	C(7A)-C(3A)-Ni	73.63(11)
C(1)-Ni-C(7A)	37.20(6)	C(3)-C(3A)-Ni	58.17(10)
P-Ni-C(7A)	136.52(5)	C(5)-C(4)-C(3A)	118.4(2)
Cl-Ni-C(7A)	108.98(5)	C(5)-C(4)-H(4)	120.8
C(3A)-Ni-C(7A)	34.43(6)	C(3A)-C(4)-H(4)	120.8
C(21)-P-C(20)	103.08(13)	C(4)-C(5)-C(6)	121.0(2)
C(21)-P-C(22)	103.34(13)	C(4)-C(5)-H(5)	119.5
C(20)-P-C(22)	102.86(14)	C(6)-C(5)-H(5)	119.5
C(21)-P-Ni	113.79(9)	C(7)-C(6)-C(5)	121.3(2)
C(20)-P-Ni	114.81(9)	C(7)-C(6)-H(6)	119.4
C(22)-P-Ni	117.20(9)	C(5)-C(6)-H(6)	119.4
C(10)-N-C(11)	109.71(18)	C(6)-C(7)-C(7A)	118.7(2)
C(10)-N-C(9)	112.00(16)	C(6)-C(7)-H(7)	120.6
C(11)-N-C(9)	110.21(15)	C(7A)-C(7)-H(7)	120.6
C(2)-C(1)-C(7A)	107.92(16)	C(7)-C(7A)-C(3A)	120.22(18)
C(2)-C(1)-C(8)	126.46(18)	C(7)-C(7A)-C(1)	132.37(18)
C(7A)-C(1)-C(8)	124.66(18)	C(3A)-C(7A)-C(1)	107.41(17)
C(2)-C(1)-Ni	67.21(11)	C(7)-C(7A)-Ni	132.40(14)
C(7A)-C(1)-Ni	82.02(11)	C(3A)-C(7A)-Ni	71.94(11)
C(8)-C(1)-Ni	125.32(13)	C(1)-C(7A)-Ni	60.79(10)

C(1)-C(8)-C(9)	110.75(16)	N-C(11)-H(11C)	109.5
C(1)-C(8)-H(8A)	109.5	H(11A)-C(11)-H(11C)	109.5
C(9)-C(8)-H(8A)	109.5	H(11B)-C(11)-H(11C)	109.5
C(1)-C(8)-H(8B)	109.5	P-C(20)-H(20A)	109.5
C(9)-C(8)-H(8B)	109.5	P-C(20)-H(20B)	109.5
H(8A)-C(8)-H(8B)	108.1	H(20A)-C(20)-H(20B)	109.5
N-C(9)-C(8)	113.42(15)	P-C(20)-H(20C)	109.5
N-C(9)-H(9A)	108.9	H(20A)-C(20)-H(20C)	109.5
C(8)-C(9)-H(9A)	108.9	H(20B)-C(20)-H(20C)	109.5
N-C(9)-H(9B)	108.9	P-C(21)-H(21A)	109.5
C(8)-C(9)-H(9B)	108.9	P-C(21)-H(21B)	109.5
H(9A)-C(9)-H(9B)	107.7	H(21A)-C(21)-H(21B)	109.5
N-C(10)-H(10A)	109.5	P-C(21)-H(21C)	109.5
N-C(10)-H(10B)	109.5	H(21A)-C(21)-H(21C)	109.5
H(10A)-C(10)-H(10B)	109.5	H(21B)-C(21)-H(21C)	109.5
N-C(10)-H(10C)	109.5	P-C(22)-H(22A)	109.5
H(10A)-C(10)-H(10C)	109.5	P-C(22)-H(22B)	109.5
H(10B)-C(10)-H(10C)	109.5	H(22A)-C(22)-H(22B)	109.5
N-C(11)-H(11A)	109.5	P-C(22)-H(22C)	109.5
N-C(11)-H(11B)	109.5	H(22A)-C(22)-H(22C)	109.5
H(11A)-C(11)-H(11B)	109.5	H(22B)-C(22)-H(22C)	109.5

Table IV.6. Torsion angles [°] for (η^3:η^0-Ind$(CH_2)_2NMe_2$)(PMe_3)NiCl(2)

C(3)-Ni-P-C(21)	-101.53(12)	Ni-C(3)-C(3A)-C(7A)	-57.33(14)
C(2)-Ni-P-C(21)	-70.92(13)	C(2)-C(3)-C(3A)-Ni	66.59(13)
C(1)-Ni-P-C(21)	-105.4(3)	C(3)-Ni-C(3A)-C(4)	-120.5(3)
Cl-Ni-P-C(21)	73.15(10)	C(2)-Ni-C(3A)-C(4)	-163.6(3)
C(3A)-Ni-P-C(21)	-139.65(12)	C(1)-Ni-C(3A)-C(4)	151.6(3)
C(7A)-Ni-P-C(21)	-161.16(12)	P-Ni-C(3A)-C(4)	-37.0(2)
C(3)-Ni-P-C(20)	140.02(13)	Cl-Ni-C(3A)-C(4)	85.4(2)
C(2)-Ni-P-C(20)	170.63(14)	C(7A)-Ni-C(3A)-C(4)	116.5(3)
C(1)-Ni-P-C(20)	136.1(3)	C(3)-Ni-C(3A)-C(7A)	123.07(17)
Cl-Ni-P-C(20)	-45.30(13)	C(2)-Ni-C(3A)-C(7A)	79.92(12)
C(3A)-Ni-P-C(20)	101.90(14)	C(1)-Ni-C(3A)-C(7A)	35.15(11)
C(7A)-Ni-P-C(20)	80.39(14)	P-Ni-C(3A)-C(7A)	-153.50(10)
C(3)-Ni-P-C(22)	19.14(12)	Cl-Ni-C(3A)-C(7A)	-31.05(15)
C(2)-Ni-P-C(22)	49.75(13)	C(2)-Ni-C(3A)-C(3)	-43.15(12)
C(1)-Ni-P-C(22)	15.2(3)	C(1)-Ni-C(3A)-C(3)	-87.92(13)
Cl-Ni-P-C(22)	-166.18(11)	P-Ni-C(3A)-C(3)	83.43(12)
C(3A)-Ni-P-C(22)	-18.99(12)	Cl-Ni-C(3A)-C(3)	-154.12(11)
C(7A)-Ni-P-C(22)	-40.50(13)	C(7A)-Ni-C(3A)-C(3)	-123.07(17)
C(3)-Ni-C(1)-C(2)	38.99(11)	C(7A)-C(3A)-C(4)-C(5)	-0.5(3)
P-Ni-C(1)-C(2)	43.2(3)	C(3)-C(3A)-C(4)-C(5)	180.0(2)
Cl-Ni-C(1)-C(2)	-135.40(10)	Ni-C(3A)-C(4)-C(5)	-96.6(3)
C(3A)-Ni-C(1)-C(2)	80.74(12)	C(3A)-C(4)-C(5)-C(6)	2.0(3)
C(7A)-Ni-C(1)-C(2)	113.32(15)	C(4)-C(5)-C(6)-C(7)	-0.8(4)
C(3)-Ni-C(1)-C(7A)	-74.33(11)	C(5)-C(6)-C(7)-C(7A)	-2.1(3)
C(2)-Ni-C(1)-C(7A)	-113.32(15)	C(6)-C(7)-C(7A)-C(3A)	3.6(3)
P-Ni-C(1)-C(7A)	-70.1(3)	C(6)-C(7)-C(7A)-C(1)	-177.30(19)
Cl-Ni-C(1)-C(7A)	111.28(10)	C(6)-C(7)-C(7A)-Ni	96.2(2)
C(3A)-Ni-C(1)-C(7A)	-32.58(10)	C(4)-C(3A)-C(7A)-C(7)	-2.3(3)
C(3)-Ni-C(1)-C(8)	158.5(2)	C(3)-C(3A)-C(7A)-C(7)	177.31(17)
C(2)-Ni-C(1)-C(8)	119.5(2)	Ni-C(3A)-C(7A)-C(7)	129.12(17)
P-Ni-C(1)-C(8)	162.69(17)	C(4)-C(3A)-C(7A)-C(1)	178.34(18)
Cl-Ni-C(1)-C(8)	-15.90(18)	C(3)-C(3A)-C(7A)-C(1)	-2.0(2)
C(3A)-Ni-C(1)-C(8)	-159.8(2)	Ni-C(3A)-C(7A)-C(1)	-50.19(12)
C(7A)-Ni-C(1)-C(8)	-127.2(2)	C(4)-C(3A)-C(7A)-Ni	-131.46(19)
C(7A)-C(1)-C(2)-C(3	11.9(2)	C(3)-C(3A)-C(7A)-Ni	48.19(13)
C(8)-C(1)-C(2)-C(3)	-178.94(18)	C(2)-C(1)-C(7A)-C(7)	174.8(2)
Ni-C(1)-C(2)-C(3)	-60.95(13)	C(8)-C(1)-C(7A)-C(7)	5.4(3)
C(7A)-C(1)-C(2)-Ni	72.89(13)	Ni-C(1)-C(7A)-C(7)	-122.4(2)
C(8)-C(1)-C(2)-Ni	-117.99(19)	C(2)-C(1)-C(7A)-C(3A)	-6.0(2)
C(3)-Ni-C(2)-C(1)	-117.60(16)	C(8)-C(1)-C(7A)-C(3A)	-175.41(17)
P-Ni-C(2)-C(1)	-167.86(8)	Ni-C(1)-C(7A)-C(3A)	56.80(13)
Cl-Ni-C(2)-C(1)	56.62(12)	C(2)-C(1)-C(7A)-Ni	-62.84(13)
C(3A)-Ni-C(2)-C(1)	-77.67(12)	C(8)-C(1)-C(7A)-Ni	127.79(19)
C(7A)-Ni-C(2)-C(1)	-38.77(10)	C(3)-Ni-C(7A)-C(7)	-150.2(2)
C(1)-Ni-C(2)-C(3)	117.60(16)	C(2)-Ni-C(7A)-C(7)	163.5(2)
P-Ni-C(2)-C(3)	-50.26(14)	C(1)-Ni-C(7A)-C(7)	122.3(2)
Cl-Ni-C(2)-C(3)	174.22(10)	P-Ni-C(7A)-C(7)	-76.5(2)
C(3A)-Ni-C(2)-C(3)	39.93(11)	Cl-Ni-C(7A)-C(7)	44.8(2)
C(7A)-Ni-C(2)-C(3)	78.83(12)	C(3A)-Ni-C(7A)-C(7)	-114.8(2)
C(1)-C(2)-C(3)-C(3A)	-13.2(2)	C(3)-Ni-C(7A)-C(3A)	-35.41(11)
Ni-C(2)-C(3)-C(3A)	-76.58(14)	C(2)-Ni-C(7A)-C(3A)	-81.69(12)
C(1)-C(2)-C(3)-Ni	63.42(13)	C(1)-Ni-C(7A)-C(3A)	-122.88(16)
C(1)-Ni-C(3)-C(2)	-37.77(11)	P-Ni-C(7A)-C(3A)	38.31(14)
P-Ni-C(3)-C(2)	143.23(11)	Cl-Ni-C(7A)-C(3A)	159.61(10)
Cl-Ni-C(3)-C(2)	-17.5(3)	C(3)-Ni-C(7A)-C(1)	87.47(12)
C(3A)-Ni-C(3)-C(2)	-111.11(17)	C(2)-Ni-C(7A)-C(1)	41.19(11)
C(7A)-Ni-C(3)-C(2)	-78.80(12)	P-Ni-C(7A)-C(1)	161.19(9)
C(2)-Ni-C(3)-C(3A)	111.11(17)	Cl-Ni-C(7A)-C(1)	-77.51(11)
C(1)-Ni-C(3)-C(3A)	73.35(12)	C(3A)-Ni-C(7A)-C(1)	122.88(16)
P-Ni-C(3)-C(3A)	-105.65(11)	C(2)-C(1)-C(8)-C(9)	-91.7(2)
Cl-Ni-C(3)-C(3A)	93.6(2)	C(7A)-C(1)-C(8)-C(9)	75.7(2)
C(7A)-Ni-C(3)-C(3A)	32.31(10)	Ni-C(1)-C(8)-C(9)	-177.89(14)
C(2)-C(3)-C(3A)-C(4)	-171.1(2)	C(10)-N-C(9)-C(8)	72.7(2)
Ni-C(3)-C(3A)-C(4)	122.3(2)	C(11)-N-C(9)-C(8)	-164.84(19)
C(2)-C(3)-C(3A)-C(7A)	9.3(2)	C(1)-C(8)-C(9)-N	177.33(17)

Table IV.7. Crystal data and structure refinement for $(\eta^3:\eta^0$-$Ind(CH_2)_2NMe_2)(PPh_3)NiMe$ **(3)**

Empirical formula	C35 H41 N Ni P
Formula weight	565.37
Temperature	223(2)K
Wavelength	1.54178 Å
Crystal system	Triclinic
Space group	P-1
Unit cell dimensions	a = 9.3419(3) Å α = 98.748(3)° b = 12.8669(5) Å β = 103.145(2)° c = 13.9322(5) Å γ = 106.493(3)°
Volume	1521.01(9)Å^3
Z	2
Density (calculated)	1.234 Mg/m^3
Absorption coefficient	1.576 mm^{-1}
F(000)	602
Crystal size	0.96 x 0.40 x 0.26 mm
Theta range for data collection	3.35 to 72.64°
Index ranges	$-11 \le h \le 11$, $-15 \le k \le 14$, $-17 \le \ell \le 17$
Reflections collected	18248
Independent reflections	5743 [R_{int} = 0.032]
Absorption correction	Semi-empirical from equivalents
Max. and min. transmission	0.6500 and 0.3800
Refinement method	Full-matrix least-squares on F^2
Data / restraints / parameters	5743 / 73 / 374
Goodness-of-fit on F^2	1.068
Final R indices [I>2sigma(I)]	R1 = 0.0411, wR_2 = 0.1153
R indices (all data)	R1 = 0.0426, wR_2 = 0.1166
Largest diff. peak and hole	0.425 and -0.305 e/Å^3

Table IV.8. Atomic coordinates (x 10^4) and equivalent isotropic displacement parameters ($Å^2$ x 10^3) for (η^3:η^0-Ind$(CH_2)_2NMe_2$)(PPh_3)NiMe(3) U_{eq} is defined as one third of the trace of the orthogonalized Uij tensor.

	Occ.	x	y	z	U_{eq}
Ni	1	1840(1)	7693(1)	7420(1)	31(1)
P	1	1231(1)	6567(1)	8347(1)	28(1)
N	1	2099(2)	10311(1)	4459(1)	36(1)
C(1)	1	2499(2)	9036(1)	6758(1)	34(1)
C(2)	1	3805(2)	8710(1)	7148(1)	37(1)
C(3)	1	4067(2)	8832(1)	8202(1)	35(1)
C(3A)	1	3046(2)	9381(1)	8513(1)	31(1)
C(4)	1	2829(2)	9730(1)	9463(1)	36(1)
C(5)	1	1747(2)	10254(2)	9511(1)	42(1)
C(6)	1	834(2)	10426(2)	8636(2)	44(1)
C(7)	1	980(2)	10054(1)	7693(1)	37(1)
C(7A)	1	2095(2)	9536(1)	7623(1)	32(1)
C(8)	1	1850(2)	9091(2)	5683(1)	41(1)
C(9)	1	2640(2)	10219(2)	5505(1)	38(1)
C(10)	1	2778(3)	11450(2)	4388(2)	59(1)
C(11)	1	2499(3)	9565(2)	3758(2)	56(1)
C(12)	1	41(2)	6831(2)	6267(1)	43(1)
C(21)	1	-812(2)	6254(1)	8338(1)	34(1)
C(22)	1	-1453(2)	7098(2)	8254(2)	48(1)
C(23)	1	-2992(3)	6914(2)	8249(2)	59(1)
C(24)	1	-3895(2)	5894(2)	8317(2)	58(1)
C(25)	1	-3271(2)	5056(2)	8404(2)	54(1)
C(26)	1	-1731(2)	5232(2)	8412(1)	42(1)
C(31)	1	1500(2)	5215(1)	8037(1)	32(1)
C(32)	1	1512(2)	4799(2)	7061(1)	42(1)
C(33)	1	1701(3)	3772(2)	6806(2)	55(1)
C(34)	1	1913(3)	3163(2)	7526(2)	54(1)
C(35)	1	1933(3)	3574(2)	8503(2)	51(1)
C(36)	1	1728(2)	4595(2)	8762(1)	42(1)
C(41)	1	2275(2)	7082(1)	9700(1)	32(1)
C(42)	1	3889(2)	7330(1)	10002(1)	38(1)
C(43)	1	4743(2)	7822(2)	11000(1)	45(1)
C(44)	1	3991(3)	8046(2)	11715(2)	53(1)
C(45)	1	2391(3)	7779(2)	11428(2)	53(1)
C(46)	1	1534(2)	7303(2)	10425(1)	41(1)
C(51)	0.35	7130(20)	3566(15)	5759(15)	83(1)
C(52)	0.35	6372(18)	4103(14)	4979(12)	71(1)
C(53)	0.35	5382(16)	4715(13)	5379(12)	64(1)
C(54)	0.35	4624(17)	5280(14)	4619(13)	64(1)
C(55)	0.35	3636(19)	5895(15)	5019(12)	71(1)
C(56)	0.35	2930(30)	6468(17)	4250(17)	83(1)
C(51')	0.15	6970(30)	3690(30)	5610(30)	83(1)
C(52')	0.15	5920(20)	4351(14)	5823(13)	71(1)
C(53')	0.15	5290(20)	4798(16)	4967(13)	64(1)
C(54')	0.15	4218(18)	5458(14)	5135(11)	64(1)
C(55')	0.15	3730(20)	5929(13)	4240(12)	71(1)
C(56')	0.15	2870(30)	6730(20)	4390(20)	83(1)

Table IV.9. Hydrogen coordinates (x 10^4) and isotropic displacement parameters ($Å^2$ x 10^3) for (η^3:η^0-Ind$(CH_2)_2NMe_2$)(PPh_3)NiMe **(3)**

	Occ.	x	y	z	U_{eq}
H(2)	1	4441	8453	6746	44
H(3)	1	4907	8665	8661	41
H(4)	1	3415	9607	10053	43
H(5)	1	1612	10504	10144	50
H(6)	1	115	10799	8695	52
H(7)	1	343	10147	7108	45
H(8A)	1	728	8956	5540	49
H(8B)	1	2005	8506	5219	49
H(9A)	1	2453	10795	5958	46
H(9B)	1	3766	10361	5681	46
H(10A)	1	3904	11653	4577	88
H(10B)	1	2482	11947	4842	88
H(10C)	1	2402	11513	3698	88
H(11A)	1	2285	9736	3096	84
H(11B)	1	1884	8801	3705	84
H(11C)	1	3597	9658	4002	84
H(12A)	1	-651	7262	6131	65
H(12B)	1	-509	6144	6420	65
H(12C)	1	389	6659	5675	65
H(22)	1	-844	7795	8200	57
H(23)	1	-3420	7490	8199	71
H(24)	1	-4941	5770	8305	70
H(25)	1	-3887	4362	8458	65
H(26)	1	-1311	4653	8467	50
H(32)	1	1390	5217	6569	51
H(33)	1	1685	3491	6139	66
H(34)	1	2044	2468	7351	64
H(35)	1	2086	3162	8996	61
H(36)	1	1742	4871	9430	50
H(42)	1	4400	7160	9521	45
H(43)	1	5832	8003	11193	54
H(44)	1	4568	8380	12394	63
H(45)	1	1880	7921	11916	64
H(46)	1	446	7128	10236	49
H(51A)	0.35	7787	3212	5485	125
H(51B)	0.35	6330	3012	5920	125
H(51C)	0.35	7761	4133	6369	125
H(52A)	0.35	7184	4628	4787	85
H(52B)	0.35	5718	3526	4370	85
H(53A)	0.35	6036	5282	5996	77
H(53B)	0.35	4564	4185	5563	77
H(54A)	0.35	5442	5808	4434	77
H(54B)	0.35	3968	4713	4003	77
H(55A)	0.35	4282	6454	5642	85
H(55B)	0.35	2798	5366	5187	85
H(56A)	0.35	2337	6870	4540	125
H(56B)	0.35	2250	5913	3645	125
H(56C)	0.35	3758	6986	4077	125
H(51D)	0.15	7268	3373	6179	125
H(51E)	0.15	7894	4181	5504	125
H(51F)	0.15	6415	3098	5004	125
H(52C)	0.15	5048	3869	6002	85
H(52D)	0.15	6508	4973	6411	85
H(53C)	0.15	4713	4172	4380	77
H(53D)	0.15	6164	5277	4793	77
H(54C)	0.15	3290	4973	5256	77
H(54D)	0.15	4756	6068	5739	77
H(55C)	0.15	4662	6307	4057	85
H(55D)	0.15	3068	5308	3665	85
H(56D)	0.15	2537	6939	3761	125
H(56E)	0.15	3550	7385	4909	125
H(56F)	0.15	1967	6376	4603	125

Table IV.10. Anisotropic parameters ($Å^2$ x 10^3) for $(\eta^3:\eta^0\text{-Ind}(CH_2)_2NMe_2)(PPh_3)NiMe$ **(3)**
The anisotropic displacement factor exponent takes the form:

$$-2\pi^2 [h^2 a^{*2} U_{11} + ... + 2 h k a^* b^* U_{12}]$$

	U11	U22	U33	U23	U13	U12
Ni	35(1)	31(1)	25(1)	9(1)	6(1)	10(1)
P	33(1)	29(1)	25(1)	7(1)	8(1)	11(1)
N	40(1)	43(1)	29(1)	15(1)	10(1)	17(1)
C(1)	40(1)	32(1)	29(1)	11(1)	10(1)	10(1)
C(2)	39(1)	38(1)	37(1)	11(1)	15(1)	12(1)
C(3)	32(1)	34(1)	35(1)	9(1)	5(1)	10(1)
C(3A)	32(1)	29(1)	29(1)	7(1)	5(1)	6(1)
C(4)	41(1)	34(1)	27(1)	6(1)	5(1)	6(1)
C(5)	50(1)	38(1)	35(1)	3(1)	16(1)	11(1)
C(6)	46(1)	38(1)	50(1)	9(1)	16(1)	18(1)
C(7)	39(1)	33(1)	39(1)	12(1)	6(1)	13(1)
C(7A)	35(1)	29(1)	27(1)	8(1)	5(1)	7(1)
C(8)	53(1)	39(1)	27(1)	10(1)	8(1)	11(1)
C(9)	42(1)	43(1)	28(1)	11(1)	7(1)	14(1)
C(10)	69(1)	58(1)	50(1)	29(1)	14(1)	16(1)
C(11)	69(1)	82(2)	35(1)	20(1)	22(1)	44(1)
C(12)	47(1)	40(1)	32(1)	7(1)	-2(1)	8(1)
C(21)	33(1)	38(1)	29(1)	5(1)	8(1)	12(1)
C(22)	44(1)	42(1)	59(1)	11(1)	17(1)	18(1)
C(23)	51(1)	60(1)	74(2)	8(1)	19(1)	32(1)
C(24)	36(1)	72(1)	61(1)	1(1)	17(1)	15(1)
C(25)	45(1)	53(1)	59(1)	12(1)	19(1)	6(1)
C(26)	41(1)	42(1)	44(1)	14(1)	14(1)	12(1)
C(31)	33(1)	32(1)	32(1)	7(1)	9(1)	13(1)
C(32)	57(1)	44(1)	32(1)	9(1)	13(1)	25(1)
C(33)	73(1)	54(1)	42(1)	1(1)	15(1)	34(1)
C(34)	65(1)	41(1)	62(1)	9(1)	18(1)	29(1)
C(35)	65(1)	46(1)	56(1)	23(1)	22(1)	30(1)
C(36)	55(1)	41(1)	38(1)	14(1)	18(1)	23(1)
C(41)	41(1)	29(1)	26(1)	8(1)	8(1)	11(1)
C(42)	43(1)	38(1)	33(1)	13(1)	8(1)	15(1)
C(43)	46(1)	41(1)	41(1)	13(1)	-2(1)	10(1)
C(44)	68(1)	45(1)	30(1)	2(1)	-1(1)	12(1)
C(45)	71(1)	53(1)	33(1)	1(1)	17(1)	19(1)
C(46)	47(1)	41(1)	32(1)	5(1)	13(1)	13(1)
C(51)	82(2)	62(3)	91(3)	-15(2)	12(2)	31(2)
C(52)	77(2)	61(2)	66(2)	-8(2)	28(2)	16(2)
C(53)	83(2)	65(2)	46(2)	13(2)	22(2)	23(2)
C(54)	83(2)	65(2)	46(2)	13(2)	22(2)	23(2)
C(55)	77(2)	61(2)	66(2)	-8(2)	28(2)	16(2)
C(56)	82(2)	62(3)	91(3)	-15(2)	12(2)	31(2)
C(51')	82(2)	62(3)	91(3)	-15(2)	12(2)	31(2)
C(52')	77(2)	61(2)	66(2)	-8(2)	28(2)	16(2)
C(53')	83(2)	65(2)	46(2)	13(2)	22(2)	23(2)
C(54')	83(2)	65(2)	46(2)	13(2)	22(2)	23(2)
C(55')	77(2)	61(2)	66(2)	-8(2)	28(2)	16(2)
C(56')	82(2)	62(3)	91(3)	-15(2)	12(2)	31(2)

Table IV.11. Bond lengths [Å] and angles [°] for $(\eta^3:\eta^0\text{-Ind}(CH_2)_2NMe_2)(PPh_3)NiMe$ **(3)**

Ni-C(12)	1.9508(17)	C(32)-H(32)	0.9400
Ni-C(2)	2.0810(17)	C(33)-C(34)	1.377(3)
Ni-C(1)	2.0870(17)	C(33)-H(33)	0.9400
Ni-C(3)	2.1012(16)	C(34)-C(35)	1.378(3)
Ni-P	2.1277(5)	C(34)-H(34)	0.9400
Ni-C(3A)	2.2659(15)	C(35)-C(36)	1.386(3)
Ni-C(7A)	2.2811(16)	C(35)-H(35)	0.9400
P-C(31)	1.8286(16)	C(36)-H(36)	0.9400
P-C(21)	1.8314(16)	C(41)-C(46)	1.387(2)
P-C(41)	1.8337(16)	C(41)-C(42)	1.396(2)
N-C(11)	1.450(2)	C(42)-C(43)	1.383(2)
N-C(10)	1.452(3)	C(42)-H(42)	0.9400
N-C(9)	1.463(2)	C(43)-C(44)	1.383(3)
C(1)-C(2)	1.421(2)	C(43)-H(43)	0.9400
C(1)-C(7A)	1.456(2)	C(44)-C(45)	1.381(3)
C(1)-C(8)	1.503(2)	C(44)-H(44)	0.9400
C(2)-C(3)	1.409(2)	C(45)-C(46)	1.386(3)
C(2)-H(2)	0.9900	C(45)-H(45)	0.9400
C(3)-C(3A)	1.441(2)	C(46)-H(46)	0.9400
C(3)-H(3)	0.9900	C(51)-C(52)	1.522(11)
C(3A)-C(4)	1.410(2)	C(51)-H(51A)	0.9700
C(3A)-C(7A)	1.429(2)	C(51)-H(51B)	0.9700
C(4)-C(5)	1.373(3)	C(51)-H(51C)	0.9700
C(4)-H(4)	0.9400	C(52)-C(53)	1.517(10)
C(5)-C(6)	1.407(3)	C(52)-H(52A)	0.9800
C(5)-H(5)	0.9400	C(52)-H(52B)	0.9800
C(6)-C(7)	1.378(3)	C(53)-C(54)	1.528(7)
C(6)-H(6)	0.9400	C(53)-H(53A)	0.9800
C(7)-C(7A)	1.400(2)	C(53)-H(53B)	0.9800
C(7)-H(7)	0.9400	C(54)-C(55)	1.517(10)
C(8)-C(9)	1.516(3)	C(54)-H(54A)	0.9800
C(8)-H(8A)	0.9800	C(54)-H(54B)	0.9800
C(8)-H(8B)	0.9800	C(55)-C(56)	1.523(12)
C(9)-H(9A)	0.9800	C(55)-H(55A)	0.9800
C(9)-H(9B)	0.9800	C(55)-H(55B)	0.9800
C(10)-H(10A)	0.9700	C(56)-H(56A)	0.9700
C(10)-H(10B)	0.9700	C(56)-H(56B)	0.9700
C(10)-H(10C)	0.9700	C(56)-H(56C)	0.9700
C(11)-H(11A)	0.9700	C(51')-C(52')	1.517(14)
C(11)-H(11B)	0.9700	C(51')-H(51D)	0.9700
C(11)-H(11C)	0.9700	C(51')-H(51E)	0.9700
C(12)-H(12A)	0.9700	C(51')-H(51F)	0.9700
C(12)-H(12B)	0.9700	C(52')-C(53')	1.477(12)
C(12)-H(12C)	0.9700	C(52')-H(52C)	0.9800
C(21)-C(26)	1.385(3)	C(52')-H(52D)	0.9800
C(21)-C(22)	1.389(3)	C(53')-C(54')	1.517(13)
C(22)-C(23)	1.388(3)	C(53')-H(53C)	0.9800
C(22)-H(22)	0.9400	C(53')-H(53D)	0.9800
C(23)-C(24)	1.375(3)	C(54')-C(55')	1.503(13)
C(23)-H(23)	0.9400	C(54')-H(54C)	0.9800
C(24)-C(25)	1.371(3)	C(54')-H(54D)	0.9800
C(24)-H(24)	0.9400	C(55')-C(56')	1.490(13)
C(25)-C(26)	1.389(3)	C(55')-H(55C)	0.9800
C(25)-H(25)	0.9400	C(55')-H(55D)	0.9800
C(26)-H(26)	0.9400	C(56')-H(56D)	0.9700
C(31)-C(32)	1.387(2)	C(56')-H(56E)	0.9700
C(31)-C(36)	1.395(2)	C(56')-H(56F)	0.9700
C(32)-C(33)	1.386(3)		

C(12)-Ni-C(2)	118.59(8)	C(2)-Ni-C(3)	39.37(7)
C(12)-Ni-C(1)	94.39(7)	C(1)-Ni-C(3)	66.68(6)
C(2)-Ni-C(1)	39.86(7)	C(12)-Ni-P	93.23(6)
C(12)-Ni-C(3)	157.91(8)	C(2)-Ni-P	140.02(5)

C(1)-Ni-P	168.83(5)	C(1)-C(8)-H(8B)	109.5
C(3)-Ni-P	107.25(5)	C(9)-C(8)-H(8B)	109.5
C(12)-Ni-C(3A)	144.03(7)	H(8A)-C(8)-H(8B)	108.0
C(2)-Ni-C(3A)	64.01(6)	N-C(9)-C(8)	113.53(14)
C(1)-Ni-C(3A)	64.47(6)	N-C(9)-H(9A)	108.9
C(3)-Ni-C(3A)	38.29(6)	C(8)-C(9)-H(9A)	108.9
P-Ni-C(3A)	104.80(4)	N-C(9)-H(9B)	108.9
C(12)-Ni-C(7A)	109.10(7)	C(8)-C(9)-H(9B)	108.9
C(2)-Ni-C(7A)	63.87(6)	H(9A)-C(9)-H(9B)	107.7
C(1)-Ni-C(7A)	38.61(6)	N-C(10)-H(10A)	109.5
C(3)-Ni-C(7A)	63.60(6)	N-C(10)-H(10B)	109.5
P-Ni-C(7A)	130.63(4)	H(10A)-C(10)-H(10B)	109.5
C(3A)-Ni-C(7A)	36.62(5)	N-C(10)-H(10C)	109.5
C(31)-P-C(21)	105.68(7)	H(10A)-C(10)-H(10C)	109.5
C(31)-P-C(41)	103.06(7)	H(10B)-C(10)-H(10C)	109.5
C(21)-P-C(41)	102.78(7)	N-C(11)-H(11A)	109.5
C(31)-P-Ni	116.88(5)	N-C(11)-H(11B)	109.5
C(21)-P-Ni	111.66(6)	H(11A)-C(11)-H(11B)	109.5
C(41)-P-Ni	115.33(5)	N-C(11)-H(11C)	109.5
C(11)-N-C(10)	109.50(17)	H(11A)-C(11)-H(11C)	109.5
C(11)-N-C(9)	111.78(14)	H(11B)-C(11)-H(11C)	109.5
C(10)-N-C(9)	109.57(15)	Ni-C(12)-H(12A)	109.5
C(2)-C(1)-C(7A)	107.07(14)	Ni-C(12)-H(12B)	109.5
C(2)-C(1)-C(8)	127.18(16)	H(12A)-C(12)-H(12B)	109.5
C(7A)-C(1)-C(8)	124.60(15)	Ni-C(12)-H(12C)	109.5
C(2)-C(1)-Ni	69.85(10)	H(12A)-C(12)-H(12C)	109.5
C(7A)-C(1)-Ni	77.92(9)	H(12B)-C(12)-H(12C)	109.5
C(8)-C(1)-Ni	127.30(12)	C(26)-C(21)-C(22)	119.06(16)
C(3)-C(2)-C(1)	108.89(15)	C(26)-C(21)-P	123.56(13)
C(3)-C(2)-Ni	71.09(10)	C(22)-C(21)-P	117.39(14)
C(1)-C(2)-Ni	70.30(10)	C(23)-C(22)-C(21)	120.10(19)
C(3)-C(2)-H(2)	125.6	C(23)-C(22)-H(22)	120.0
C(1)-C(2)-H(2)	125.6	C(21)-C(22)-H(22)	120.0
Ni-C(2)-H(2)	125.6	C(24)-C(23)-C(22)	120.3(2)
C(2)-C(3)-C(3A)	108.24(14)	C(24)-C(23)-H(23)	119.9
C(2)-C(3)-Ni	69.54(9)	C(22)-C(23)-H(23)	119.9
C(3A)-C(3)-Ni	77.05(9)	C(25)-C(24)-C(23)	120.08(19)
C(2)-C(3)-H(3)	125.6	C(25)-C(24)-H(24)	120.0
C(3A)-C(3)-H(3)	125.6	C(23)-C(24)-H(24)	120.0
Ni-C(3)-H(3)	125.6	C(24)-C(25)-C(26)	120.2(2)
C(4)-C(3A)-C(7A)	119.54(15)	C(24)-C(25)-H(25)	119.9
C(4)-C(3A)-C(3)	132.91(15)	C(26)-C(25)-H(25)	119.9
C(7A)-C(3A)-C(3)	107.53(14)	C(21)-C(26)-C(25)	120.35(18)
C(4)-C(3A)-Ni	127.29(12)	C(21)-C(26)-H(26)	119.8
C(7A)-C(3A)-Ni	72.27(9)	C(25)-C(26)-H(26)	119.8
C(3)-C(3A)-Ni	64.65(9)	C(32)-C(31)-C(36)	118.69(15)
C(5)-C(4)-C(3A)	118.71(16)	C(32)-C(31)-P	119.45(13)
C(5)-C(4)-H(4)	120.6	C(36)-C(31)-P	121.84(13)
C(3A)-C(4)-H(4)	120.6	C(33)-C(32)-C(31)	120.50(18)
C(4)-C(5)-C(6)	121.64(16)	C(33)-C(32)-H(32)	119.7
C(4)-C(5)-H(5)	119.2	C(31)-C(32)-H(32)	119.7
C(6)-C(5)-H(5)	119.2	C(34)-C(33)-C(32)	120.30(19)
C(7)-C(6)-C(5)	120.78(17)	C(34)-C(33)-H(33)	119.8
C(7)-C(6)-H(6)	119.6	C(32)-C(33)-H(33)	119.8
C(5)-C(6)-H(6)	119.6	C(33)-C(34)-C(35)	119.84(18)
C(6)-C(7)-C(7A)	118.85(16)	C(33)-C(34)-H(34)	120.1
C(6)-C(7)-H(7)	120.6	C(35)-C(34)-H(34)	120.1
C(7A)-C(7)-H(7)	120.6	C(34)-C(35)-C(36)	120.19(19)
C(7)-C(7A)-C(3A)	120.42(15)	C(34)-C(35)-H(35)	119.9
C(7)-C(7A)-C(1)	131.99(15)	C(36)-C(35)-H(35)	119.9
C(3A)-C(7A)-C(1)	107.54(14)	C(35)-C(36)-C(31)	120.45(17)
C(7)-C(7A)-Ni	129.13(12)	C(35)-C(36)-H(36)	119.8
C(3A)-C(7A)-Ni	71.11(9)	C(31)-C(36)-H(36)	119.8
C(1)-C(7A)-Ni	63.46(9)	C(46)-C(41)-C(42)	118.89(15)
C(1)-C(8)-C(9)	110.89(14)	C(46)-C(41)-P	122.29(13)
C(1)-C(8)-H(8A)	109.5	C(42)-C(41)-P	118.69(12)
C(9)-C(8)-H(8A)	109.5	C(43)-C(42)-C(41)	120.63(17)

C(43)-C(42)-H(42)	119.7	H(55A)-C(55)-H(55B)	107.9
C(41)-C(42)-H(42)	119.7	C(55)-C(56)-H(56A)	109.5
C(44)-C(43)-C(42)	119.90(18)	C(55)-C(56)-H(56B)	109.5
C(44)-C(43)-H(43)	120.1	H(56A)-C(56)-H(56B)	109.5
C(42)-C(43)-H(43)	120.1	C(55)-C(56)-H(56C)	109.5
C(45)-C(44)-C(43)	119.84(17)	H(56A)-C(56)-H(56C)	109.5
C(45)-C(44)-H(44)	120.1	H(56B)-C(56)-H(56C)	109.5
C(43)-C(44)-H(44)	120.1	C(52')-C(51')-H(51D)	109.5
C(44)-C(45)-C(46)	120.47(19)	C(52')-C(51')-H(51E)	109.5
C(44)-C(45)-H(45)	119.8	H(51D)-C(51')-H(51E)	109.5
C(46)-C(45)-H(45)	119.8	C(52')-C(51')-H(51F)	109.5
C(45)-C(46)-C(41)	120.23(18)	H(51D)-C(51')-H(51F)	109.5
C(45)-C(46)-H(46)	119.9	H(51E)-C(51')-H(51F)	109.5
C(41)-C(46)-H(46)	119.9	C(53')-C(52')-C(51')	114.1(14)
C(52)-C(51)-H(51A)	109.5	C(53')-C(52')-H(52C)	108.7
C(52)-C(51)-H(51B)	109.5	C(51')-C(52')-H(52C)	108.7
H(51A)-C(51)-H(51B)	109.5	C(53')-C(52')-H(52D)	108.7
C(52)-C(51)-H(51C)	109.5	C(51')-C(52')-H(52D)	108.7
H(51A)-C(51)-H(51C)	109.5	H(52C)-C(52')-H(52D)	107.6
H(51B)-C(51)-H(51C)	109.5	C(52')-C(53')-C(54')	116.4(11)
C(53)-C(52)-C(51)	112.0(10)	C(52')-C(53')-H(53C)	108.2
C(53)-C(52)-H(52A)	109.2	C(54')-C(53')-H(53C)	108.2
C(51)-C(52)-H(52A)	109.2	C(52')-C(53')-H(53D)	108.2
C(53)-C(52)-H(52B)	109.2	C(54')-C(53')-H(53D)	108.2
C(51)-C(52)-H(52B)	109.2	H(53C)-C(53')-H(53D)	107.3
H(52A)-C(52)-H(52B)	107.9	C(55')-C(54')-C(53')	111.6(12)
C(52)-C(53)-C(54)	113.3(7)	C(55')-C(54')-H(54C)	109.3
C(52)-C(53)-H(53A)	108.9	C(53')-C(54')-H(54C)	109.3
C(54)-C(53)-H(53A)	108.9	C(55')-C(54')-H(54D)	109.3
C(52)-C(53)-H(53B)	108.9	C(53')-C(54')-H(54D)	109.3
C(54)-C(53)-H(53B)	108.9	H(54C)-C(54')-H(54D)	108.0
H(53A)-C(53)-H(53B)	107.7	C(56')-C(55')-C(54')	115.5(14)
C(55)-C(54)-C(53)	113.4(8)	C(56')-C(55')-H(55C)	108.4
C(55)-C(54)-H(54A)	108.9	C(54')-C(55')-H(55C)	108.4
C(53)-C(54)-H(54A)	108.9	C(56')-C(55')-H(55D)	108.4
C(55)-C(54)-H(54B)	108.9	C(54')-C(55')-H(55D)	108.4
C(53)-C(54)-H(54B)	108.9	H(55C)-C(55')-H(55D)	107.5
H(54A)-C(54)-H(54B)	107.7	C(55')-C(56')-H(56D)	109.5
C(54)-C(55)-C(56)	111.9(10)	C(55')-C(56')-H(56E)	109.5
C(54)-C(55)-H(55A)	109.2	H(56D)-C(56')-H(56E)	109.5
C(56)-C(55)-H(55A)	109.2	C(55')-C(56')-H(56F)	109.5
C(54)-C(55)-H(55B)	109.2	H(56D)-C(56')-H(56F)	109.5
C(56)-C(55)-H(55B)	109.2	H(56E)-C(56')-H(56F)	109.5

Table IV.12. Torsion angles [°] for (η^3:η^0-Ind$(CH_2)_2NMe_2$)(PPh_3)NiMe (3)

C(12)-Ni-P-C(31)	72.25(8)	C(2)-C(3)-C(3A)-C(7A)	3.24(18)
C(2)-Ni-P-C(31)	-72.16(10)	Ni-C(3)-C(3A)-C(7A)	-59.80(11)
C(1)-Ni-P-C(31)	-154.8(3)	C(2)-C(3)-C(3A)-Ni	63.04(11)
C(3)-Ni-P-C(31)	-99.35(8)	C(12)-Ni-C(3A)-C(4)	90.92(19)
C(3A)-Ni-P-C(31)	-139.18(7)	C(2)-Ni-C(3A)-C(4)	-165.51(17)
C(7A)-Ni-P-C(31)	-169.05(8)	C(1)-Ni-C(3A)-C(4)	150.02(17)
C(12)-Ni-P-C(21)	-49.57(8)	C(3)-Ni-C(3A)-C(4)	-125.89(19)
C(2)-Ni-P-C(21)	166.02(9)	P-Ni-C(3A)-C(4)	-26.66(15)
C(1)-Ni-P-C(21)	83.4(3)	C(7A)-Ni-C(3A)-C(4)	114.02(18)
C(3)-Ni-P-C(21)	138.83(7)	C(12)-Ni-C(3A)-C(7A)	-23.09(17)
C(3A)-Ni-P-C(21)	99.00(7)	C(2)-Ni-C(3A)-C(7A)	80.47(10)
C(7A)-Ni-P-C(21)	69.13(8)	C(1)-Ni-C(3A)-C(7A)	36.00(10)
C(12)-Ni-P-C(41)	-166.40(9)	C(3)-Ni-C(3A)-C(7A)	120.09(14)
C(2)-Ni-P-C(41)	49.19(10)	P-Ni-C(3A)-C(7A)	-140.68(9)
C(1)-Ni-P-C(41)	-33.5(3)	C(12)-Ni-C(3A)-C(3)	-143.18(14)
C(3)-Ni-P-C(41)	22.00(8)	C(2)-Ni-C(3A)-C(3)	-39.62(10)
C(3A)-Ni-P-C(41)	-17.83(7)	C(1)-Ni-C(3A)-C(3)	-84.09(11)
C(7A)-Ni-P-C(41)	-47.70(8)	P-Ni-C(3A)-C(3)	99.23(9)
C(12)-Ni-C(1)-C(2)	-131.07(11)	C(7A)-Ni-C(3A)-C(3)	-120.09(14)
C(3)-Ni-C(1)-C(2)	37.13(10)	C(7A)-C(3A)-C(4)-C(5)	-2.7(2)
P-Ni-C(1)-C(2)	96.1(3)	C(3)-C(3A)-C(4)-C(5)	179.33(17)
C(3A)-Ni-C(1)-C(2)	79.29(10)	Ni-C(3A)-C(4)-C(5)	-92.19(19)
C(7A)-Ni-C(1)-C(2)	113.48(13)	C(3A)-C(4)-C(5)-C(6)	1.4(3)
C(12)-Ni-C(1)-C(7A)	115.45(10)	C(4)-C(5)-C(6)-C(7)	1.1(3)
C(2)-Ni-C(1)-C(7A)	-113.48(13)	C(5)-C(6)-C(7)-C(7A)	-2.3(3)
C(3)-Ni-C(1)-C(7A)	-76.34(10)	C(6)-C(7)-C(7A)-C(3A)	0.9(2)
P-Ni-C(1)-C(7A)	-17.4(3)	C(6)-C(7)-C(7A)-C(1)	178.11(17)
C(3A)-Ni-C(1)-C(7A)	-34.18(9)	C(6)-C(7)-C(7A)-Ni	90.55(19)
C(12)-Ni-C(1)-C(8)	-9.09(17)	C(4)-C(3A)-C(7A)-C(7)	1.6(2)
C(2)-Ni-C(1)-C(8)	122.0(2)	C(3)-C(3A)-C(7A)-C(7)	-179.98(14)
C(3)-Ni-C(1)-C(8)	159.12(18)	Ni-C(3A)-C(7A)-C(7)	124.93(15)
P-Ni-C(1)-C(8)	-141.9(2)	C(4)-C(3A)-C(7A)-C(1)	-176.25(14)
C(3A)-Ni-C(1)-C(8)	-158.72(18)	C(3)-C(3A)-C(7A)-C(1)	2.20(18)
C(7A)-Ni-C(1)-C(8)	-124.5(2)	Ni-C(3A)-C(7A)-C(1)	-52.89(11)
C(7A)-C(1)-C(2)-C(3)	8.86(19)	C(4)-C(3A)-C(7A)-Ni	-123.36(15)
C(8)-C(1)-C(2)-C(3)	176.97(16)	C(3)-C(3A)-C(7A)-Ni	55.09(11)
Ni-C(1)-C(2)-C(3)	-60.90(12)	C(2)-C(1)-C(7A)-C(7)	175.77(17)
C(7A)-C(1)-C(2)-Ni	69.76(11)	C(8)-C(1)-C(7A)-C(7)	7.3(3)
C(8)-C(1)-C(2)-Ni	-122.13(18)	Ni-C(1)-C(7A)-C(7)	-119.97(18)
C(12)-Ni-C(2)-C(3)	177.96(10)	C(2)-C(1)-C(7A)-C(3A)	-6.76(18)
C(1)-Ni-C(2)-C(3)	119.08(14)	C(8)-C(1)-C(7A)-C(3A)	-175.26(16)
P-Ni-C(2)-C(3)	-43.47(13)	Ni-C(1)-C(7A)-C(3A)	57.50(11)
C(3A)-Ni-C(2)-C(3)	38.53(10)	C(2)-C(1)-C(7A)-Ni	-64.26(11)
C(7A)-Ni-C(2)-C(3)	79.47(10)	C(8)-C(1)-C(7A)-Ni	127.25(17)
C(12)-Ni-C(2)-C(1)	58.88(12)	C(12)-Ni-C(7A)-C(7)	51.59(17)
C(3)-Ni-C(2)-C(1)	-119.08(14)	C(2)-Ni-C(7A)-C(7)	164.80(17)
P-Ni-C(2)-C(1)	-162.55(8)	C(1)-Ni-C(7A)-C(7)	123.90(19)
C(3A)-Ni-C(2)-C(1)	-80.56(10)	C(3)-Ni-C(7A)-C(7)	-151.07(17)
C(7A)-Ni-C(2)-C(1)	-39.61(9)	P-Ni-C(7A)-C(7)	-60.47(16)
C(1)-C(2)-C(3)-C(3A)	-7.59(19)	C(3A)-Ni-C(7A)-C(7)	-114.30(19)
Ni-C(2)-C(3)-C(3A)	-67.99(11)	C(12)-Ni-C(7A)-C(3A)	165.89(11)
C(1)-C(2)-C(3)-Ni	60.41(12)	C(2)-Ni-C(7A)-C(3A)	-80.90(10)
C(12)-Ni-C(3)-C(2)	-4.8(2)	C(1)-Ni-C(7A)-C(3A)	-121.80(14)
C(1)-Ni-C(3)-C(2)	-37.58(10)	C(3)-Ni-C(7A)-C(3A)	-36.77(10)
P-Ni-C(3)-C(2)	152.43(9)	P-Ni-C(7A)-C(3A)	53.83(11)
C(3A)-Ni-C(3)-C(2)	-115.38(14)	C(12)-Ni-C(7A)-C(1)	-72.31(11)
C(7A)-Ni-C(3)-C(2)	-80.19(11)	C(2)-Ni-C(7A)-C(1)	40.90(10)
C(12)-Ni-C(3)-C(3A)	110.6(2)	C(3)-Ni-C(7A)-C(1)	85.03(10)
C(2)-Ni-C(3)-C(3A)	115.38(14)	P-Ni-C(7A)-C(1)	175.62(8)
C(1)-Ni-C(3)-C(3A)	77.80(10)	C(3A)-Ni-C(7A)-C(1)	121.80(14)
P-Ni-C(3)-C(3A)	-92.19(9)	C(2)-C(1)-C(8)-C(9)	-88.3(2)
C(7A)-Ni-C(3)-C(3A)	35.19(9)	C(7A)-C(1)-C(8)-C(9)	77.9(2)
C(2)-C(3)-C(3A)-C(4)	-178.60(17)	Ni-C(1)-C(8)-C(9)	179.74(12)
Ni-C(3)-C(3A)-C(4)	118.36(18)	C(11)-N-C(9)-C(8)	-65.1(2)

C(10)-N-C(9)-C(8)	173.34(17)	C(32)-C(33)-C(34)-C(35)	0.2(3)
C(1)-C(8)-C(9)-N	177.84(15)	C(33)-C(34)-C(35)-C(36)	0.5(3)
C(31)-P-C(21)-C(26)	18.58(16)	C(34)-C(35)-C(36)-C(31)	0.0(3)
C(41)-P-C(21)-C(26)	-89.13(15)	C(32)-C(31)-C(36)-C(35)	-1.2(3)
Ni-P-C(21)-C(26)	146.66(13)	P-C(31)-C(36)-C(35)	-179.82(15)
C(31)-P-C(21)-C(22)	-161.48(14)	C(31)-P-C(41)-C(46)	-118.57(15)
C(41)-P-C(21)-C(22)	90.81(15)	C(21)-P-C(41)-C(46)	-8.88(16)
Ni-P-C(21)-C(22)	-33.40(15)	Ni-P-C(41)-C(46)	112.87(14)
C(26)-C(21)-C(22)-C(23)	0.3(3)	C(31)-P-C(41)-C(42)	65.65(14)
P-C(21)-C(22)-C(23)	-179.62(17)	C(21)-P-C(41)-C(42)	175.35(13)
C(21)-C(22)-C(23)-C(24)	-0.7(4)	Ni-P-C(41)-C(42)	-62.90(14)
C(22)-C(23)-C(24)-C(25)	0.9(4)	C(46)-C(41)-C(42)-C(43)	-2.2(3)
C(23)-C(24)-C(25)-C(26)	-0.7(3)	P-C(41)-C(42)-C(43)	173.69(13)
C(22)-C(21)-C(26)-C(25)	-0.2(3)	C(41)-C(42)-C(43)-C(44)	1.7(3)
P-C(21)-C(26)-C(25)	179.77(15)	C(42)-C(43)-C(44)-C(45)	0.0(3)
C(24)-C(25)-C(26)-C(21)	0.4(3)	C(43)-C(44)-C(45)-C(46)	-1.0(3)
C(21)-P-C(31)-C(32)	101.23(15)	C(44)-C(45)-C(46)-C(41)	0.4(3)
C(41)-P-C(31)-C(32)	-151.25(14)	C(42)-C(41)-C(46)-C(45)	1.2(3)
Ni-P-C(31)-C(32)	-23.66(16)	P-C(41)-C(46)-C(45)	-174.60(15)
C(21)-P-C(31)-C(36)	-80.12(15)	C(51)-C(52)-C(53)-C(54)	179.1(10)
C(41)-P-C(31)-C(36)	27.39(16)	C(52)-C(53)-C(54)-C(55)	-179.9(18)
Ni-P-C(31)-C(36)	154.98(13)	C(53)-C(54)-C(55)-C(56)	178.7(12)
C(36)-C(31)-C(32)-C(33)	1.8(3)	C(51')C(52')C(53')C(54')	180(2)
P-C(31)-C(32)-C(33)	-179.47(16)	C(52')C(53')C(54')C(55')	176.5(18)
C(31)-C(32)-C(33)-C(34)	-1.4(3)	C(53')C(54')C(55')C(56')	-171.4(19)

Table IV.13. Crystal data and structure refinement for (η^3:η^0-Ind$(CH_2)_2NMe_2$)(PPh_3)Ni-CCPh **(4)**

Empirical formula	C42.28 H43.55 Cl0.09 N Ni O P
Formula weight	674.56
Temperature	223(2)K
Wavelength	1.54178 Å
Crystal system	Triclinic
Space group	P-1
Unit cell dimensions	a = 9.998(3) Å α = 111.58(3)° b = 13.887(4) Å β = 99.68(3)° c = 14.716(5) Å γ = 99.55(3)°
Volume	1814.2(10)Å^3
Z	2
Density (calculated)	1.235 Mg/m^3
Absorption coefficient	1.489 mm^{-1}
F(000)	714
Crystal size	0.46 x 0.24 x 0.13 mm
Theta range for data collection	3.34 to 69.93°
Index ranges	$0 \le h \le 12$, $-16 \le k \le 16$, $-17 \le \ell \le 17$
Reflections collected	33837
Independent reflections	6864 [R_{int} = 0.054]
Absorption correction	Integration
Max. and min. transmission	0.8501 and 0.5977
Refinement method	Full-matrix least-squares on F^2
Data / restraints / parameters	6864 / 82 / 476
Goodness-of-fit on F^2	0.835
Final R indices [I>2sigma(I)]	R1 = 0.0428, wR_2 = 0.0949
R indices (all data)	R1 = 0.0810, wR_2 = 0.1028
Extinction coefficient	0.00099(13)
Largest diff. peak and hole	0.335 and -0.477 e/Å^3

Table IV.14. Atomic coordinates (x 10^4) and equivalent isotropic displacement parameters ($Å^2$ x 10^3) for (η^3:η^0-Ind$(CH_2)_2NMe_2$)(PPh_3)Ni-CCPh **(4)**

U_{eq} is defined as one third of the trace of the orthogonalized Uij tensor.

	Occ.	x	y	z	U_{eq}
Ni	1	3289(1)	8881(1)	1876(1)	37(1)
P	1	3742(1)	7361(1)	1122(1)	34(1)
N	1	702(3)	11362(2)	1802(2)	53(1)
C(2)	1	3251(3)	10201(2)	1553(2)	44(1)
C(3)	1	4491(3)	9892(2)	1436(2)	43(1)
C(1)	1	3185(3)	10470(2)	2566(2)	38(1)
C(3A)	1	5369(3)	10137(2)	2425(2)	40(1)
C(4)	1	6726(3)	10081(2)	2775(2)	52(1)
C(5)	1	7245(3)	10379(2)	3791(3)	60(1)
C(6)	1	6420(3)	10701(2)	4472(2)	57(1)
C(7)	1	5075(3)	10744(2)	4147(2)	47(1)
C(7A)	1	4534(3)	10490(2)	3120(2)	38(1)
C(8)	1	2091(3)	10861(2)	3076(2)	49(1)
C(9)	1	686(3)	10721(2)	2393(2)	54(1)
C(10)	1	1072(4)	12500(3)	2445(3)	86(1)
C(11)	1	-670(3)	11063(3)	1116(3)	83(1)
C(12)	0.91	2008(4)	8380(3)	2474(3)	40(1)
C(13)	0.91	1232(3)	8145(2)	2912(2)	40(1)
C(14)	0.91	304(3)	7870(2)	3502(2)	42(1)
C(15)	0.91	550(4)	7210(2)	3987(2)	51(1)
C(16)	0.91	-365(4)	6925(3)	4500(3)	64(1)
C(17)	0.91	-1513(4)	7310(3)	4564(3)	76(1)
C(18)	0.91	-1772(4)	7983(3)	4115(3)	72(1)
C(19)	0.91	-873(4)	8268(3)	3595(3)	57(1)
C(31)	1	4004(3)	6639(2)	1918(2)	35(1)
C(32)	1	4317(3)	7186(2)	2965(2)	47(1)
C(33)	1	4517(3)	6659(2)	3583(2)	61(1)
C(34)	1	4422(4)	5580(2)	3184(2)	63(1)
C(35)	1	4121(3)	5026(2)	2144(2)	59(1)
C(36)	1	3915(3)	5547(2)	1527(2)	46(1)
C(41)	1	5340(3)	7432(2)	676(2)	36(1)
C(42)	1	6563(3)	7330(2)	1187(2)	47(1)
C(43)	1	7800(3)	7501(2)	903(2)	58(1)
C(44)	1	7821(3)	7779(2)	104(3)	59(1)
C(45)	1	6624(4)	7872(2)	-430(2)	56(1)
C(46)	1	5375(3)	7704(2)	-144(2)	45(1)
C(51)	1	2372(3)	6426(2)	20(2)	38(1)
C(52)	1	998(3)	6487(2)	4(2)	46(1)
C(53)	1	-94(3)	5755(2)	-778(2)	57(1)
C(54)	1	168(3)	4949(2)	-1560(2)	60(1)
C(55)	1	1530(3)	4880(2)	-1567(2)	60(1)
C(56)	1	2629(3)	5612(2)	-788(2)	50(1)
O(1)	0.62	5839(5)	4011(4)	4309(3)	118(2)
C(62)	0.62	5502(5)	3203(5)	3303(4)	125(3)
C(63)	0.62	6861(6)	3088(6)	3086(6)	196(6)
C(64)	0.62	7847(6)	4113(7)	3740(5)	171(5)
C(65)	0.62	7299(5)	4534(6)	4633(5)	106(3)
O(2)	0.38	7854(7)	3468(11)	3290(7)	291(9)
C(66)	0.38	6356(7)	3192(11)	2967(5)	109(5)
C(67)	0.38	5964(9)	3305(10)	3913(7)	139(6)
C(68)	0.38	7067(8)	4175(13)	4707(7)	186(10)
C(69)	0.38	8289(8)	4292(9)	4292(7)	112(5)
Cl(1)	0.09	1523(12)	8279(10)	2476(10)	44(3)

Table IV.15. Hydrogen coordinates (x 10^4) and isotropic displacement parameters ($Å^2$ x 10^3) for (η^3:η^0-Ind$(CH_2)_2NMe_2$)(PPh_3)Ni-CCPh **(4)**

	Occ.	x	y	z	U_{eq}
H(2)	1	2579	10227	1048	53
H(3)	1	4719	9580	824	52
H(4)	1	7273	9844	2327	63
H(5)	1	8162	10367	4030	72
H(6)	1	6790	10887	5155	69
H(7)	1	4524	10940	4602	56
H(8A)	1	2461	11615	3507	58
H(8B)	1	1930	10493	3509	58
H(9A)	1	338	9974	1933	65
H(9B)	1	28	10896	2807	65
H(10A)	1	448	12648	2879	129
H(10B)	1	996	12897	2032	129
H(10C)	1	2017	12707	2846	129
H(11A)	1	-659	11468	710	124
H(11B)	1	-1358	11208	1498	124
H(11C)	1	-899	10314	687	124
H(15)	0.91	1350	6953	3967	61
H(16)	0.91	-189	6464	4805	77
H(17)	0.91	-2126	7117	4913	91
H(18)	0.91	-2563	8250	4160	87
H(19)	0.91	-1057	8737	3301	68
H(32)	1	4392	7918	3247	57
H(33)	1	4718	7035	4279	74
H(34)	1	4558	5225	3605	75
H(35)	1	4059	4296	1867	71
H(36)	1	3710	5165	832	55
H(42)	1	6554	7143	1732	56
H(43)	1	8614	7427	1253	69
H(44)	1	8658	7907	-79	71
H(45)	1	6644	8047	-981	67
H(46)	1	4563	7773	-501	54
H(52)	1	811	7030	528	55
H(53)	1	-1010	5805	-778	69
H(54)	1	-571	4452	-2084	72
H(55)	1	1706	4339	-2099	71
H(56)	1	3544	5565	-798	59
H(62A)	0.62	4970	3421	2831	150
H(62B)	0.62	4958	2534	3262	150
H(63A)	0.62	7137	2514	3235	235
H(63B)	0.62	6819	2936	2382	235
H(64A)	0.62	7894	4596	3404	205
H(64B)	0.62	8777	4016	3928	205
H(65A)	0.62	7765	4373	5174	127
H(65B)	0.62	7437	5302	4870	127
H(66A)	0.38	5996	2466	2458	131
H(66B)	0.38	6024	3679	2704	131
H(67A)	0.38	5062	3477	3906	167
H(67B)	0.38	5914	2648	4013	167
H(68A)	0.38	7300	4011	5291	223
H(68B)	0.38	6761	4833	4912	223
H(69A)	0.38	8529	4992	4279	134
H(69B)	0.38	9092	4193	4687	134

Table IV.16. Anisotropic parameters ($Å^2$ x 10^3) for $(\eta^3:\eta^0\text{-Ind}(CH_2)_2NMe_2)(PPh_3)Ni\text{-}CCPh$ **(4)**

	U11	U22	U33	U23	U13	U12
Ni	43(1)	28(1)	34(1)	8(1)	11(1)	10(1)
P	37(1)	27(1)	33(1)	7(1)	9(1)	8(1)
N	55(2)	56(2)	59(2)	29(1)	19(1)	25(1)
C(2)	60(2)	34(1)	37(2)	15(1)	9(1)	15(1)
C(3)	59(2)	33(1)	39(2)	13(1)	16(1)	13(1)
C(1)	49(2)	26(1)	41(2)	13(1)	12(1)	13(1)
C(3A)	43(2)	27(1)	46(2)	11(1)	10(1)	5(1)
C(4)	47(2)	39(2)	65(2)	16(2)	16(2)	8(1)
C(5)	43(2)	49(2)	72(2)	19(2)	-6(2)	6(2)
C(6)	57(2)	46(2)	50(2)	11(1)	-6(2)	3(2)
C(7)	56(2)	33(1)	38(2)	6(1)	3(1)	4(1)
C(7A)	43(2)	22(1)	42(2)	8(1)	7(1)	5(1)
C(8)	60(2)	39(2)	47(2)	13(1)	18(2)	21(1)
C(9)	54(2)	55(2)	63(2)	27(2)	23(2)	23(2)
C(10)	123(3)	58(2)	90(3)	38(2)	30(2)	38(2)
C(11)	61(2)	111(3)	93(3)	58(2)	14(2)	30(2)
C(12)	36(2)	32(2)	38(2)	3(1)	3(2)	9(2)
C(13)	38(2)	32(2)	38(2)	7(1)	0(1)	5(1)
C(14)	46(2)	35(2)	32(2)	5(1)	8(1)	3(1)
C(15)	61(2)	44(2)	41(2)	15(2)	6(2)	9(2)
C(16)	91(3)	58(2)	48(2)	25(2)	25(2)	14(2)
C(17)	93(3)	81(3)	64(2)	28(2)	48(2)	21(2)
C(18)	68(3)	87(3)	79(3)	34(2)	46(2)	35(2)
C(19)	58(2)	55(2)	62(2)	21(2)	25(2)	22(2)
C(31)	36(2)	30(1)	38(1)	10(1)	11(1)	9(1)
C(32)	61(2)	36(2)	40(2)	11(1)	8(1)	16(1)
C(33)	97(3)	50(2)	39(2)	17(1)	14(2)	27(2)
C(34)	91(3)	52(2)	57(2)	30(2)	18(2)	27(2)
C(35)	85(2)	33(2)	58(2)	17(1)	15(2)	19(2)
C(36)	58(2)	31(1)	42(2)	8(1)	12(1)	10(1)
C(41)	40(2)	28(1)	37(1)	8(1)	14(1)	9(1)
C(42)	43(2)	51(2)	46(2)	18(1)	15(1)	13(1)
C(43)	46(2)	63(2)	63(2)	20(2)	21(2)	15(2)
C(44)	57(2)	47(2)	73(2)	15(2)	35(2)	12(2)
C(45)	82(2)	38(2)	54(2)	16(1)	38(2)	16(2)
C(46)	58(2)	35(1)	42(2)	12(1)	19(1)	16(1)
C(51)	47(2)	27(1)	34(1)	8(1)	10(1)	7(1)
C(52)	45(2)	38(2)	44(2)	8(1)	6(1)	11(1)
C(53)	44(2)	48(2)	59(2)	6(2)	-2(2)	5(2)
C(54)	61(2)	45(2)	48(2)	3(1)	-5(2)	2(2)
C(55)	69(2)	43(2)	42(2)	-4(1)	6(2)	9(2)
C(56)	51(2)	42(2)	44(2)	3(1)	12(1)	12(1)
O(1)	130(4)	146(4)	99(4)	73(3)	27(3)	35(4)
C(62)	116(6)	78(5)	169(7)	59(5)	2(5)	6(4)
C(63)	183(8)	160(9)	217(9)	35(6)	91(7)	30(7)
C(64)	150(8)	184(8)	166(8)	61(6)	60(7)	16(6)
C(65)	116(6)	99(5)	91(5)	31(4)	32(5)	11(4)
O(2)	265(11)	296(12)	303(12)	91(8)	96(8)	92(9)
C(66)	125(8)	87(7)	93(8)	12(6)	27(7)	26(7)
C(67)	176(10)	112(9)	135(9)	63(7)	55(8)	4(7)
C(68)	195(13)	212(13)	166(12)	102(9)	55(9)	24(8)
C(69)	110(8)	113(7)	132(8)	72(6)	12(6)	43(6)

Table IV.17. Bond lengths [Å] and angles [°] for (η^3:η^0-Ind$(CH_2)_2NMe_2$)(PPh_3)Ni-CCPh **(4)**

Ni-C(12)	1.852(4)	C(32)-C(33)	1.372(4)
Ni-C(3)	2.051(3)	C(32)-H(32)	0.9300
Ni-C(2)	2.061(3)	C(33)-C(34)	1.372(4)
Ni-C(1)	2.092(2)	C(33)-H(33)	0.9300
Ni-P	2.1573(11)	C(34)-C(35)	1.388(4)
Ni-Cl(1)	2.275(13)	C(34)-H(34)	0.9300
Ni-C(7A)	2.280(3)	C(35)-C(36)	1.364(4)
Ni-C(3A)	2.283(3)	C(35)-H(35)	0.9300
P-C(31)	1.817(3)	C(36)-H(36)	0.9300
P-C(51)	1.818(3)	C(41)-C(42)	1.381(4)
P-C(41)	1.828(3)	C(41)-C(46)	1.394(3)
N-C(11)	1.452(4)	C(42)-C(43)	1.383(4)
N-C(10)	1.455(4)	C(42)-H(42)	0.9300
N-C(9)	1.456(3)	C(43)-C(44)	1.369(4)
C(2)-C(3)	1.394(4)	C(43)-H(43)	0.9300
C(2)-C(1)	1.413(3)	C(44)-C(45)	1.370(4)
C(2)-H(2)	0.9300	C(44)-H(44)	0.9300
C(3)-C(3A)	1.454(4)	C(45)-C(46)	1.394(4)
C(3)-H(3)	0.9300	C(45)-H(45)	0.9300
C(1)-C(7A)	1.445(4)	C(46)-H(46)	0.9300
C(1)-C(8)	1.493(3)	C(51)-C(52)	1.387(4)
C(3A)-C(4)	1.393(4)	C(51)-C(56)	1.403(3)
C(3A)-C(7A)	1.428(4)	C(52)-C(53)	1.377(4)
C(4)-C(5)	1.374(4)	C(52)-H(52)	0.9300
C(4)-H(4)	0.9300	C(53)-C(54)	1.377(4)
C(5)-C(6)	1.398(4)	C(53)-H(53)	0.9300
C(5)-H(5)	0.9300	C(54)-C(55)	1.382(4)
C(6)-C(7)	1.369(4)	C(54)-H(54)	0.9300
C(6)-H(6)	0.9300	C(55)-C(56)	1.380(4)
C(7)-C(7A)	1.403(4)	C(55)-H(55)	0.9300
C(7)-H(7)	0.9300	C(56)-H(56)	0.9300
C(8)-C(9)	1.521(4)	O(1)-C(65)	1.430(3)
C(8)-H(8A)	0.9700	O(1)-C(62)	1.431(3)
C(8)-H(8B)	0.9700	C(62)-C(63)	1.468(3)
C(9)-H(9A)	0.9700	C(62)-H(62A)	0.9700
C(9)-H(9B)	0.9700	C(62)-H(62B)	0.9700
C(10)-H(10A)	0.9600	C(63)-C(64)	1.460(3)
C(10)-H(10B)	0.9600	C(63)-H(63A)	0.9700
C(10)-H(10C)	0.9600	C(63)-H(63B)	0.9700
C(11)-H(11A)	0.9600	C(64)-C(65)	1.466(3)
C(11)-H(11B)	0.9600	C(64)-H(64A)	0.9700
C(11)-H(11C)	0.9600	C(64)-H(64B)	0.9700
C(12)-C(13)	1.168(5)	C(65)-H(65A)	0.9700
C(13)-Cl(1)	0.815(13)	C(65)-H(65B)	0.9700
C(13)-C(14)	1.469(4)	O(2)-C(69)	1.432(3)
C(14)-C(15)	1.381(4)	O(2)-C(66)	1.433(3)
C(14)-C(19)	1.388(4)	C(66)-C(67)	1.470(3)
C(15)-C(16)	1.376(4)	C(66)-H(66A)	0.9700
C(15)-H(15)	0.9300	C(66)-H(66B)	0.9700
C(16)-C(17)	1.347(5)	C(67)-C(68)	1.459(3)
C(16)-H(16)	0.9300	C(67)-H(67A)	0.9700
C(17)-C(18)	1.362(5)	C(67)-H(67B)	0.9700
C(17)-H(17)	0.9300	C(68)-C(69)	1.466(3)
C(18)-C(19)	1.373(4)	C(68)-H(68A)	0.9700
C(18)-H(18)	0.9300	C(68)-H(68B)	0.9700
C(19)-H(19)	0.9300	C(69)-H(69A)	0.9700
C(31)-C(36)	1.390(3)	C(69)-H(69B)	0.9700
C(31)-C(32)	1.394(3)		
C(12)-Ni-C(3)	160.70(14)	C(3)-Ni-C(2)	39.64(10)
C(12)-Ni-C(2)	122.86(15)	C(12)-Ni-C(1)	94.02(14)

C(3)-Ni-C(1)	66.86(11)	C(6)-C(7)-C(7A)	119.4(3)
C(2)-Ni-C(1)	39.77(10)	C(6)-C(7)-H(7)	120.3
C(12)-Ni-P	95.64(12)	C(7A)-C(7)-H(7)	120.3
C(3)-Ni-P	103.61(8)	C(7)-C(7A)-C(3A)	119.5(3)
C(2)-Ni-P	134.24(8)	C(7)-C(7A)-C(1)	131.9(3)
C(1)-Ni-P	169.81(8)	C(3A)-C(7A)-C(1)	108.6(2)
C(12)-Ni-Cl(1)	6.6(4)	C(7)-C(7A)-Ni	128.55(19)
C(3)-Ni-Cl(1)	157.7(4)	C(3A)-C(7A)-Ni	71.91(14)
C(2)-Ni-Cl(1)	118.4(4)	C(1)-C(7A)-Ni	63.80(13)
C(1)-Ni-Cl(1)	92.7(3)	C(1)-C(8)-C(9)	116.5(2)
P-Ni-Cl(1)	97.3(3)	C(1)-C(8)-H(8A)	108.2
C(12)-Ni-C(7A)	103.16(13)	C(9)-C(8)-H(8A)	108.2
C(3)-Ni-C(7A)	63.82(10)	C(1)-C(8)-H(8B)	108.2
C(2)-Ni-C(7A)	63.69(10)	C(9)-C(8)-H(8B)	108.2
C(1)-Ni-C(7A)	38.29(9)	H(8A)-C(8)-H(8B)	107.3
P-Ni-C(7A)	135.21(8)	N-C(9)-C(8)	115.4(3)
Cl(1)-Ni-C(7A)	106.0(3)	N-C(9)-H(9A)	108.4
C(12)-Ni-C(3A)	136.05(13)	C(8)-C(9)-H(9A)	108.4
C(3)-Ni-C(3A)	38.72(10)	N-C(9)-H(9B)	108.4
C(2)-Ni-C(3A)	64.23(11)	C(8)-C(9)-H(9B)	108.4
C(1)-Ni-C(3A)	64.27(10)	H(9A)-C(9)-H(9B)	107.5
P-Ni-C(3A)	106.18(8)	N-C(10)-H(10A)	109.5
Cl(1)-Ni-C(3A)	140.4(3)	N-C(10)-H(10B)	109.5
C(7A)-Ni-C(3A)	36.48(9)	H(10A)-C(10)-H(10B)	109.5
C(31)-P-C(51)	104.48(12)	N-C(10)-H(10C)	109.5
C(31)-P-C(41)	103.17(12)	H(10A)-C(10)-H(10C)	109.5
C(51)-P-C(41)	104.93(12)	H(10B)-C(10)-H(10C)	109.5
C(31)-P-Ni	113.49(9)	N-C(11)-H(11A)	109.5
C(51)-P-Ni	114.34(9)	N-C(11)-H(11B)	109.5
C(41)-P-Ni	115.16(8)	H(11A)-C(11)-H(11B)	109.5
C(11)-N-C(10)	110.0(3)	N-C(11)-H(11C)	109.5
C(11)-N-C(9)	109.0(3)	H(11A)-C(11)-H(11C)	109.5
C(10)-N-C(9)	111.6(2)	H(11B)-C(11)-H(11C)	109.5
C(3)-C(2)-C(1)	108.8(3)	C(13)-C(12)-Ni	174.6(3)
C(3)-C(2)-Ni	69.81(15)	Cl(1)-C(13)-C(12)	19.5(9)
C(1)-C(2)-Ni	71.30(15)	Cl(1)-C(13)-C(14)	162.7(10)
C(3)-C(2)-H(2)	125.6	C(12)-C(13)-C(14)	177.6(4)
C(1)-C(2)-H(2)	125.6	C(15)-C(14)-C(19)	116.7(3)
Ni-C(2)-H(2)	124.9	C(15)-C(14)-C(13)	122.3(3)
C(2)-C(3)-C(3A)	108.9(2)	C(19)-C(14)-C(13)	120.9(3)
C(2)-C(3)-Ni	70.55(16)	C(16)-C(15)-C(14)	121.4(3)
C(3A)-C(3)-Ni	79.31(16)	C(16)-C(15)-H(15)	119.3
C(2)-C(3)-H(3)	125.6	C(14)-C(15)-H(15)	119.3
C(3A)-C(3)-H(3)	125.6	C(17)-C(16)-C(15)	120.5(4)
Ni-C(3)-H(3)	116.5	C(17)-C(16)-H(16)	119.8
C(2)-C(1)-C(7A)	107.0(2)	C(15)-C(16)-H(16)	119.8
C(2)-C(1)-C(8)	129.8(3)	C(16)-C(17)-C(18)	119.7(4)
C(7A)-C(1)-C(8)	122.3(2)	C(16)-C(17)-H(17)	120.1
C(2)-C(1)-Ni	68.93(14)	C(18)-C(17)-H(17)	120.1
C(7A)-C(1)-Ni	77.91(15)	C(17)-C(18)-C(19)	120.4(4)
C(8)-C(1)-Ni	126.82(19)	C(17)-C(18)-H(18)	119.8
C(4)-C(3A)-C(7A)	119.8(3)	C(19)-C(18)-H(18)	119.8
C(4)-C(3A)-C(3)	134.5(3)	C(18)-C(19)-C(14)	121.1(3)
C(7A)-C(3A)-C(3)	105.7(2)	C(18)-C(19)-H(19)	119.4
C(4)-C(3A)-Ni	130.45(19)	C(14)-C(19)-H(19)	119.4
C(7A)-C(3A)-Ni	71.62(2)	C(36)-C(31)-C(32)	117.8(2)
C(3)-C(3A)-Ni	61.97(14)	C(36)-C(31)-P	122.5(2)
C(5)-C(4)-C(3A)	119.2(3)	C(32)-C(31)-P	119.69(19)
C(5)-C(4)-H(4)	120.4	C(33)-C(32)-C(31)	120.8(3)
C(3A)-C(4)-H(4)	120.4	C(33)-C(32)-H(32)	119.6
C(4)-C(5)-C(6)	121.2(3)	C(31)-C(32)-H(32)	119.6
C(4)-C(5)-H(5)	119.4	C(32)-C(33)-C(34)	120.6(3)
C(6)-C(5)-H(5)	119.4	C(32)-C(33)-H(33)	119.7
C(7)-C(6)-C(5)	120.9(3)	C(34)-C(33)-H(33)	119.7
C(7)-C(6)-H(6)	119.6	C(33)-C(34)-C(35)	119.2(3)
C(5)-C(6)-H(6)	119.6	C(33)-C(34)-H(34)	120.4

C(35)-C(34)-H(34)	120.4	O(1)-C(62)-H(62B)	110.8
C(36)-C(35)-C(34)	120.3(3)	C(63)-C(62)-H(62B)	110.8
C(36)-C(35)-H(35)	119.8	H(62A)-C(62)-H(62B)	108.9
C(34)-C(35)-H(35)	119.8	C(64)-C(63)-C(62)	105.4(3)
C(35)-C(36)-C(31)	121.2(3)	C(64)-C(63)-H(63A)	110.7
C(35)-C(36)-H(36)	119.4	C(62)-C(63)-H(63A)	110.7
C(31)-C(36)-H(36)	119.4	C(64)-C(63)-H(63B)	110.7
C(42)-C(41)-C(46)	118.5(3)	C(62)-C(63)-H(63B)	110.7
C(42)-C(41)-P	121.9(2)	H(63A)-C(63)-H(63B)	108.8
C(46)-C(41)-P	119.3(2)	C(63)-C(64)-C(65)	105.3(3)
C(41)-C(42)-C(43)	121.1(3)	C(63)-C(64)-H(64A)	110.7
C(41)-C(42)-H(42)	119.5	C(65)-C(64)-H(64A)	110.7
C(43)-C(42)-H(42)	119.5	C(63)-C(64)-H(64B)	110.7
C(44)-C(43)-C(42)	119.8(3)	C(65)-C(64)-H(64B)	110.7
C(44)-C(43)-H(43)	120.1	H(64A)-C(64)-H(64B)	108.8
C(42)-C(43)-H(43)	120.1	O(1)-C(65)-C(64)	105.4(4)
C(43)-C(44)-C(45)	120.7(3)	O(1)-C(65)-H(65A)	110.7
C(43)-C(44)-H(44)	119.6	C(64)-C(65)-H(65A)	110.7
C(45)-C(44)-H(44)	119.6	O(1)-C(65)-H(65B)	110.7
C(44)-C(45)-C(46)	119.7(3)	C(64)-C(65)-H(65B)	110.7
C(44)-C(45)-H(45)	120.2	H(65A)-C(65)-H(65B)	108.8
C(46)-C(45)-H(45)	120.2	C(69)-O(2)-C(66)	108.9(6)
C(45)-C(46)-C(41)	120.2(3)	O(2)-C(66)-C(67)	101.6(6)
C(45)-C(46)-H(46)	119.9	O(2)-C(66)-H(66A)	111.5
C(41)-C(46)-H(46)	119.9	C(67)-C(66)-H(66A)	111.5
C(52)-C(51)-C(56)	118.5(2)	O(2)-C(66)-H(66B)	111.5
C(52)-C(51)-P	118.23(19)	C(67)-C(66)-H(66B)	111.5
C(56)-C(51)-P	123.2(2)	H(66A)-C(66)-H(66B)	109.3
C(53)-C(52)-C(51)	120.9(3)	C(68)-C(67)-C(66)	105.3(5)
C(53)-C(52)-H(52)	119.6	C(68)-C(67)-H(67A)	110.7
C(51)-C(52)-H(52)	119.6	C(66)-C(67)-H(67A)	110.7
C(54)-C(53)-C(52)	120.2(3)	C(68)-C(67)-H(67B)	110.7
C(54)-C(53)-H(53)	119.9	C(66)-C(67)-H(67B)	110.7
C(52)-C(53)-H(53)	119.9	H(67A)-C(67)-H(67B)	108.8
C(53)-C(54)-C(55)	120.0(3)	C(67)-C(68)-C(69)	107.1(5)
C(53)-C(54)-H(54)	120.0	C(67)-C(68)-H(68A)	110.3
C(55)-C(54)-H(54)	120.0	C(69)-C(68)-H(68A)	110.3
C(56)-C(55)-C(54)	120.2(3)	C(67)-C(68)-H(68B)	110.3
C(56)-C(55)-H(55)	119.9	C(69)-C(68)-H(68B)	110.3
C(54)-C(55)-H(55)	119.9	H(68A)-C(68)-H(68B)	108.5
C(55)-C(56)-C(51)	120.2(3)	O(2)-C(69)-C(68)	104.3(5)
C(55)-C(56)-H(56)	119.9	O(2)-C(69)-H(69A)	110.9
C(51)-C(56)-H(56)	119.9	C(68)-C(69)-H(69A)	110.9
C(65)-O(1)-C(62)	110.5(4)	O(2)-C(69)-H(69B)	110.9
O(1)-C(62)-C(63)	104.9(4)	C(68)-C(69)-H(69B)	110.9
O(1)-C(62)-H(62A)	110.8	H(69A)-C(69)-H(69B)	108.9
C(63)-C(62)-H(62A)	110.8	C(13)-Cl(1)-Ni	151.7(12)

Table IV.18. Torsion angles [°] for (η^3:η^0-Ind$(CH_2)_2NMe_2$)(PPh_3)Ni-CCPh(4)

C(12)-Ni-P-C(31)	-44.75(15)	Cl(1)-Ni-C(1)-C(7A)	112.7(4)
C(3)-Ni-P-C(31)	136.73(12)	C(3A)-Ni-C(1)-C(7A)	-33.90(15)
C(2)-Ni-P-C(31)	166.25(14)	C(12)-Ni-C(1)-C(8)	-15.3(3)
C(1)-Ni-P-C(31)	116.5(5)	C(3)-Ni-C(1)-C(8)	161.9(3)
Cl(1)-Ni-P-C(31)	-51.1(3)	C(2)-Ni-C(1)-C(8)	124.7(3)
C(7A)-Ni-P-C(31)	70.34(14)	P-Ni-C(1)-C(8)	-176.6(3)
C(3A)-Ni-P-C(31)	96.69(12)	Cl(1)-Ni-C(1)-C(8)	-8.9(4)
C(12)-Ni-P-C(51)	74.98(16)	C(7A)-Ni-C(1)-C(8)	-121.5(3)
C(3)-Ni-P-C(51)	-103.53(13)	C(3A)-Ni-C(1)-C(8)	-155.4(3)
C(2)-Ni-P-C(51)	-74.02(15)	C(2)-C(3)-C(3A)-C(4)	-174.5(3)
C(1)-Ni-P-C(51)	-123.8(5)	Ni-C(3)-C(3A)-C(4)	120.5(3)
Cl(1)-Ni-P-C(51)	68.6(3)	C(2)-C(3)-C(3A)-C(7A)	6.4(3)
C(7A)-Ni-P-C(51)	-169.92(13)	Ni-C(3)-C(3A)-C(7A)	-58.60(17)
C(3A)-Ni-P-C(51)	-143.58(12)	C(2)-C(3)-C(3A)-Ni	64.99(18)
C(12)-Ni-P-C(41)	-163.35(16)	C(12)-Ni-C(3A)-C(4)	82.3(3)
C(3)-Ni-P-C(41)	18.13(13)	C(3)-Ni-C(3A)-C(4)	-126.1(3)
C(2)-Ni-P-C(41)	47.65(16)	C(2)-Ni-C(3A)-C(4)	-166.2(3)
C(1)-Ni-P-C(41)	-2.1(5)	C(1)-Ni-C(3A)-C(4)	149.4(3)
Cl(1)-Ni-P-C(41)	-169.7(3)	P-Ni-C(3A)-C(4)	-34.4(3)
C(7A)-Ni-P-C(41)	-48.26(15)	Cl(1)-Ni-C(3A)-C(4)	89.6(6)
C(3A)-Ni-P-C(41)	-21.91(12)	C(7A)-Ni-C(3A)-C(4)	113.9(3)
C(12)-Ni-C(2)-C(3)	168.96(18)	C(12)-Ni-C(3A)-C(7A)	-31.6(3)
C(1)-Ni-C(2)-C(3)	119.2(2)	C(3)-Ni-C(3A)-C(7A)	120.0(2)
P-Ni-C(2)-C(3)	-48.6(2)	C(2)-Ni-C(3A)-C(7A)	79.92(17)
Cl(1)-Ni-C(2)-C(3)	174.6(4)	C(1)-Ni-C(3A)-C(7A)	35.55(15)
C(7A)-Ni-C(2)-C(3)	79.94(17)	P-Ni-C(3A)-C(7A)	-148.27(14)
C(3A)-Ni-C(2)-C(3)	39.17(15)	Cl(1)-Ni-C(3A)-C(7A)	-24.3(6)
C(12)-Ni-C(2)-C(1)	49.8(2)	C(12)-Ni-C(3A)-C(3)	-151.7(2)
C(3)-Ni-C(2)-C(1)	-119.2(2)	C(2)-Ni-C(3A)-C(3)	-40.11(15)
P-Ni-C(2)-C(1)	-167.82(13)	C(1)-Ni-C(3A)-C(3)	-84.48(17)
Cl(1)-Ni-C(2)-C(1)	55.4(4)	P-Ni-C(3A)-C(3)	91.70(15)
C(7A)-Ni-C(2)-C(1)	-39.24(16)	Cl(1)-Ni-C(3A)-C(3)	-144.3(6)
C(3A)-Ni-C(2)-C(1)	-80.00(17)	C(7A)-Ni-C(3A)-C(3)	-120.0(2)
C(1)-C(2)-C(3)-C(3A)	-9.9(3)	C(7A)-C(3A)-C(4)-C(5)	-0.7(4)
Ni-C(2)-C(3)-C(3A)	-70.80(18)	C(3)-C(3A)-C(4)-C(5)	-179.7(3)
C(1)-C(2)-C(3)-Ni	60.90(18)	Ni-C(3A)-C(4)-C(5)	-91.3(3)
C(12)-Ni-C(3)-C(2)	-29.1(5)	C(3A)-C(4)-C(5)-C(6)	2.3(4)
C(1)-Ni-C(3)-C(2)	-37.40(15)	C(4)-C(5)-C(6)-C(7)	-1.1(5)
P-Ni-C(3)-C(2)	146.41(14)	C(5)-C(6)-C(7)-C(7A)	-1.7(4)
Cl(1)-Ni-C(3)-C(2)	-12.6(9)	C(6)-C(7)-C(7A)-C(3A)	3.3(4)
C(7A)-Ni-C(3)-C(2)	-79.59(17)	C(6)-C(7)-C(7A)-C(1)	-179.6(3)
C(3A)-Ni-C(3)-C(2)	-114.6(2)	C(6)-C(7)-C(7A)-Ni	92.9(3)
C(12)-Ni-C(3)-C(3A)	85.5(5)	C(4)-C(3A)-C(7A)-C(7)	-2.0(4)
C(2)-Ni-C(3)-C(3A)	114.6(2)	C(3)-C(3A)-C(7A)-C(7)	177.2(2)
C(1)-Ni-C(3)-C(3A)	77.18(16)	Ni-C(3A)-C(7A)-C(7)	124.6(2)
P-Ni-C(3)-C(3A)	-99.00(15)	C(4)-C(3A)-C(7A)-C(1)	-179.8(2)
Cl(1)-Ni-C(3)-C(3A)	102.0(9)	C(3)-C(3A)-C(7A)-C(1)	-0.6(3)
C(7A)-Ni-C(3)-C(3A)	35.00(14)	Ni-C(3A)-C(7A)-C(1)	-53.13(17)
C(3)-C(2)-C(1)-C(7A)	9.4(3)	C(4)-C(3A)-C(7A)-Ni	-126.7(2)
Ni-C(2)-C(1)-C(7A)	69.34(17)	C(3)-C(3A)-C(7A)-Ni	52.55(16)
C(3)-C(2)-C(1)-C(8)	179.0(3)	C(2)-C(1)-C(7A)-C(7)	177.3(3)
Ni-C(2)-C(1)-C(8)	-121.0(3)	C(8)-C(1)-C(7A)-C(7)	6.7(4)
C(3)-C(2)-C(1)-Ni	-59.98(18)	Ni-C(1)-C(7A)-C(7)	-119.5(3)
C(12)-Ni-C(1)-C(2)	-140.0(2)	C(2)-C(1)-C(7A)-C(3A)	-5.3(3)
C(3)-Ni-C(1)-C(2)	37.28(16)	C(8)-C(1)-C(7A)-C(3A)	-175.9(2)
P-Ni-C(1)-C(2)	58.7(5)	Ni-C(1)-C(7A)-C(3A)	57.95(18)
Cl(1)-Ni-C(1)-C(2)	-133.5(4)	C(2)-C(1)-C(7A)-Ni	-63.25(17)
C(7A)-Ni-C(1)-C(2)	113.8(2)	C(8)-C(1)-C(7A)-Ni	126.1(3)
C(3A)-Ni-C(1)-C(2)	79.90(18)	C(12)-Ni-C(7A)-C(7)	44.4(3)
C(12)-Ni-C(1)-C(7A)	106.22(19)	C(3)-Ni-C(7A)-C(7)	-150.8(3)
C(3)-Ni-C(1)-C(7A)	-76.52(17)	C(2)-Ni-C(7A)-C(7)	164.8(3)
C(2)-Ni-C(1)-C(7A)	-113.8(2)	C(1)-Ni-C(7A)-C(7)	124.0(3)
P-Ni-C(1)-C(7A)	-55.1(5)	P-Ni-C(7A)-C(7)	-67.9(3)

Cl(1)-Ni-C(7A)-C(7)	50.5(4)	C(33)-C(34)-C(35)-C(36)	-0.3(5)
C(3A)-Ni-C(7A)-C(7)	-113.7(3)	C(34)-C(35)-C(36)-C(31)	0.2(5)
C(12)-Ni-C(7A)-C(3A)	158.05(19)	C(32)-C(31)-C(36)-C(35)	0.2(4)
C(3)-Ni-C(7A)-C(3A)	-37.12(16)	P-C(31)-C(36)-C(35)	179.8(2)
C(2)-Ni-C(7A)-C(3A)	-81.55(17)	C(31)-P-C(41)-C(42)	-22.0(2)
C(1)-Ni-C(7A)-C(3A)	-122.3(2)	C(51)-P-C(41)-C(42)	-131.2(2)
P-Ni-C(7A)-C(3A)	45.80(19)	Ni-P-C(41)-C(42)	102.2(2)
Cl(1)-Ni-C(7A)-C(3A)	164.2(4)	C(31)-P-C(41)-C(46)	164.63(19)
C(12)-Ni-C(7A)-C(1)	-79.6(2)	C(51)-P-C(41)-C(46)	55.5(2)
C(3)-Ni-C(7A)-C(1)	85.19(18)	Ni-P-C(41)-C(46)	-71.2(2)
C(2)-Ni-C(7A)-C(1)	40.77(16)	C(46)-C(41)-C(42)-C(43)	0.5(4)
P-Ni-C(7A)-C(1)	168.11(13)	P-C(41)-C(42)-C(43)	-172.9(2)
Cl(1)-Ni-C(7A)-C(1)	-73.5(4)	C(41)-C(42)-C(43)-C(44)	0.2(4)
C(3A)-Ni-C(7A)-C(1)	122.3(2)	C(42)-C(43)-C(44)-C(45)	-1.1(4)
C(2)-C(1)-C(8)-C(9)	15.8(4)	C(43)-C(44)-C(45)-C(46)	1.3(4)
C(7A)-C(1)-C(8)-C(9)	-175.9(2)	C(44)-C(45)-C(46)-C(41)	-0.6(4)
Ni-C(1)-C(8)-C(9)	-76.5(3)	C(42)-C(41)-C(46)-C(45)	-0.3(4)
C(11)-N-C(9)-C(8)	174.1(2)	P-C(41)-C(46)-C(45)	173.23(19)
C(10)-N-C(9)-C(8)	-64.2(3)	C(31)-P-C(51)-C(52)	94.8(2)
C(1)-C(8)-C(9)-N	-67.2(3)	C(41)-P-C(51)-C(52)	-157.0(2)
C(3)-Ni-C(12)-C(13)	-34(4)	Ni-P-C(51)-C(52)	-29.8(2)
C(2)-Ni-C(12)-C(13)	-55(4)	C(31)-P-C(51)-C(56)	-81.6(2)
C(1)-Ni-C(12)-C(13)	-26(4)	C(41)-P-C(51)-C(56)	26.6(3)
P-Ni-C(12)-C(13)	151(4)	Ni-P-C(51)-C(56)	153.7(2)
Cl(1)-Ni-C(12)-C(13)	-104(6)	C(56)-C(51)-C(52)-C(53)	1.1(4)
C(7A)-Ni-C(12)-C(13)	12(4)	P-C(51)-C(52)-C(53)	-175.5(2)
C(3A)-Ni-C(12)-C(13)	30(4)	C(51)-C(52)-C(53)-C(54)	-0.2(5)
Ni-C(12)-C(13)-Cl(1)	112(6)	C(52)-C(53)-C(54)-C(55)	-0.6(5)
Ni-C(12)-C(13)-C(14)	-48(11)	C(53)-C(54)-C(55)-C(56)	0.5(5)
Cl(1)-C(13)-C(14)-C(15)	141(3)	C(54)-C(55)-C(56)-C(51)	0.4(5)
C(12)-C(13)-C(14)-C(15)	-61(8)	C(52)-C(51)-C(56)-C(55)	-1.2(4)
Cl(1)-C(13)-C(14)-C(19)	-39(4)	P-C(51)-C(56)-C(55)	175.3(2)
C(12)-C(13)-C(14)-C(19)	119(8)	C(65)-O(1)-C(62)-C(63)	11.4(10)
C(19)-C(14)-C(15)-C(16)	2.8(4)	O(1)-C(62)-C(63)-C(64)	-25.3(9)
C(13)-C(14)-C(15)-C(16)	-177.2(3)	C(62)-C(63)-C(64)-C(65)	29.7(10)
C(14)-C(15)-C(16)-C(17)	-1.8(5)	C(62)-O(1)-C(65)-C(64)	6.9(10)
C(15)-C(16)-C(17)-C(18)	0.2(6)	C(63)-C(64)-C(65)-O(1)	-22.6(10)
C(16)-C(17)-C(18)-C(19)	0.2(6)	C(69)-O(2)-C(66)-C(67)	-35.6(14)
C(17)-C(18)-C(19)-C(14)	1.0(6)	O(2)-C(66)-C(67)-C(68)	33.2(14)
C(15)-C(14)-C(19)-C(18)	-2.4(5)	C(66)-C(67)-C(68)-C(69)	-20.0(17)
C(13)-C(14)-C(19)-C(18)	177.6(3)	C(66)-O(2)-C(69)-C(68)	23.6(16)
C(51)-P-C(31)-C(36)	36.2(3)	C(67)-C(68)-C(69)-O(2)	-1.5(17)
C(41)-P-C(31)-C(36)	-73.3(2)	C(12)-C(13)-Cl(1)-Ni	-8.6(8)
Ni-P-C(31)-C(36)	161.4(2)	C(14)-C(13)-Cl(1)-Ni	168.7(11)
C(51)-P-C(31)-C(32)	-144.2(2)	C(12)-Ni-Cl(1)-C(13)	15.9(14)
C(41)-P-C(31)-C(32)	106.3(2)	C(3)-Ni-Cl(1)-C(13)	-109(3)
Ni-P-C(31)-C(32)	-19.0(2)	C(2)-Ni-Cl(1)-C(13)	-118(3)
C(36)-C(31)-C(32)-C(33)	-0.6(4)	C(1)-Ni-Cl(1)-C(13)	-86(3)
P-C(31)-C(32)-C(33)	179.8(2)	P-Ni-Cl(1)-C(13)	92(3)
C(31)-C(32)-C(33)-C(34)	0.5(5)	C(7A)-Ni-Cl(1)-C(13)	-50(3)
C(32)-C(33)-C(34)-C(35)	0.0(5)	C(3A)-Ni-Cl(1)-C(13)	-35(3)

Table IV.19. Crystal data and structure refinement for $(\eta^3:\eta^0$-$Ind(CH_2)_2NMe_2)(PMe_3)NiMe$ **(6)**

Empirical formula	C17 H28 N Ni P
Formula weight	336.08
Temperature	223(2)K
Wavelength	1.54178 Å
Crystal system	Triclinic
Space group	P-1
Unit cell dimensions	a = 6.4485(2) Å α = 84.18(3)° b = 8.5720(3) Å β = 80.64(3)° c = 16.7049(5) Å γ = 85.70(3)°
Volume	904.77(5)Å^3
Z	2
Density (calculated)	1.234 Mg/m^3
Absorption coefficient	2.290 mm^{-1}
F(000)	360
Crystal size	0.84 x 0.08 x 0.08 mm
Theta range for data collection	5.20 to 72.62°
Index ranges	$-7 \le h \le 7$, $-10 \le k \le 10$, $-20 \le \ell \le 20$
Reflections collected	6522
Independent reflections	3405 [R_{int} = 0.124]
Absorption correction	Semi-empirical from equivalents
Max. and min. transmission	0.833 and 0.464
Refinement method	Full-matrix least-squares on F^2
Data / restraints / parameters	3405 / 0 / 187
Goodness-of-fit on F^2	1.005
Final R indices [I>2sigma(I)]	R1 = 0.0751, wR_2 = 0.1961
R indices (all data)	R1 = 0.0867, wR_2 = 0.2059
Largest diff. peak and hole	0.709 and -0.453 e/Å^3

Table IV.20. Atomic coordinates (x 10^4) and equivalent isotropic displacement parameters ($Å^2$ x 10^3) for (η^3:η^0-Ind$(CH_2)_2NMe_2$)(PMe_3)NiMe **(6)**

U_{eq} is defined as one third of the trace of the orthogonalized Uij tensor.

	x	y	z	U_{eq}
Ni	3680(1)	6991(1)	7518(1)	37(1)
P	2316(2)	8916(1)	8174(1)	39(1)
N	7758(6)	2862(4)	5167(2)	46(1)
C(1)	4474(6)	4942(4)	6917(2)	39(1)
C(2)	2329(6)	5428(4)	6899(3)	47(1)
C(3)	1286(6)	5433(4)	7716(3)	49(1)
C(3A)	2691(6)	4701(4)	8255(2)	42(1)
C(4)	2476(8)	4336(4)	9113(3)	58(1)
C(5)	4172(10)	3672(5)	9448(3)	70(2)
C(6)	6118(8)	3358(5)	8963(3)	60(1)
C(7)	6377(6)	3718(4)	8123(3)	48(1)
C(7A)	4679(6)	4384(4)	7762(2)	39(1)
C(8)	6137(7)	4728(4)	6176(2)	49(1)
C(9)	6162(6)	3102(4)	5887(2)	45(1)
C(10)	7398(9)	1434(5)	4808(3)	64(1)
C(11)	9877(7)	2769(6)	5374(3)	62(1)
C(12)	6254(6)	8098(4)	7046(2)	43(1)
C(21)	3953(8)	9748(6)	8802(3)	69(1)
C(22)	1512(9)	10602(5)	7525(3)	73(1)
C(23)	-68(8)	8588(6)	8904(3)	67(1)

Table IV.21. Hydrogen coordinates (x 10^4) and isotropic displacement parameters ($Å^2$ x 10^3) for (η^3:η^0-Ind$(CH_2)_2NMe_2$)(PMe_3)NiMe **(6)**

	x	y	z	U_{eq}
H(2)	1707	5700	6429	56
H(3)	-92	5845	7880	59
H(4)	1185	4548	9446	69
H(5)	4029	3423	10015	84
H(6)	7258	2899	9207	72
H(7)	7689	3513	7801	57
H(8A)	7523	4891	6312	58
H(8B)	5861	5521	5735	58
H(9A)	6436	2313	6331	54
H(9B)	4770	2941	5757	54
H(10A)	8453	1296	4331	97
H(10B)	6008	1529	4650	97
H(10C)	7494	534	5204	97
H(11A)	10105	3724	5605	92
H(11B)	10898	2646	4887	92
H(11C)	10036	1874	5769	92
H(12A)	6679	7870	6484	65
H(12B)	7377	7744	7355	65
H(12C)	5964	9221	7068	65
H(21A)	3275	10724	8987	104
H(21B)	5318	9950	8482	104
H(21C)	4135	9011	9269	104
H(22A)	387	10330	7253	110
H(22B)	2701	10914	7121	110
H(22C)	1016	11466	7853	110
H(23A)	-568	9558	9143	101
H(23B)	236	7787	9329	101
H(23C)	-1142	8245	8627	101

Table IV.22. Anisotropic parameters ($Å^2$ x 10^3) for (η^3:η^0-Ind$(CH_2)_2NMe_2$)(PMe_3)NiMe **(6)**

The anisotropic displacement factor exponent takes the form:

$$-2\pi^2 [h^2 a^{*2} U_{11} + ... + 2 h k a^* b^* U_{12}]$$

	U11	U22	U33	U23	U13	U12
Ni	37(1)	30(1)	43(1)	-9(1)	1(1)	-5(1)
P	42(1)	30(1)	45(1)	-7(1)	-4(1)	1(1)
N	65(2)	38(2)	35(2)	-9(1)	-3(1)	3(1)
C(1)	50(2)	29(2)	37(2)	-10(1)	0(2)	-2(1)
C(2)	52(2)	37(2)	56(2)	-13(2)	-13(2)	-7(2)
C(3)	41(2)	41(2)	65(3)	-16(2)	2(2)	-7(2)
C(3A)	47(2)	27(2)	48(2)	-9(2)	9(2)	-12(1)
C(4)	86(3)	37(2)	44(2)	-11(2)	20(2)	-17(2)
C(5)	121(5)	44(2)	45(2)	0(2)	-7(3)	-23(3)
C(6)	79(3)	41(2)	64(3)	2(2)	-26(2)	-11(2)
C(7)	50(2)	33(2)	61(2)	-5(2)	-6(2)	-8(2)
C(7A)	48(2)	27(2)	40(2)	-8(1)	2(1)	-9(1)
C(8)	64(3)	39(2)	38(2)	-8(2)	10(2)	-8(2)
C(9)	52(2)	41(2)	40(2)	-9(2)	0(2)	-3(2)
C(10)	93(4)	46(2)	53(3)	-19(2)	-5(2)	5(2)
C(11)	59(3)	59(3)	61(3)	-11(2)	6(2)	1(2)
C(12)	47(2)	34(2)	49(2)	-8(2)	1(2)	-9(1)
C(21)	69(3)	65(3)	82(3)	-36(3)	-23(3)	-1(2)
C(22)	82(4)	54(3)	78(4)	7(2)	-15(3)	20(2)
C(23)	58(3)	66(3)	70(3)	-23(2)	19(2)	-2(2)

Table IV.23. Bond lengths [Å] and angles [°] for (η^3:η^0-Ind$(CH_2)_2NMe_2$)(PMe_3)NiMe **(6)**

Ni-C(12)	1.983(4)	C(1)-C(2)	1.418(5)
Ni-C(3)	2.081(4)	C(1)-C(7a)	1.467(5)
Ni-C(2)	2.090(4)	C(1)-C(8)	1.516(5)
Ni-C(1)	2.100(3)	C(2)-C(3)	1.420(6)
Ni-P	2.1290(12)	C(3)-C(3a)	1.445(6)
Ni-C(3a)	2.285(3)	C(3a)-C(4)	1.421(6)
Ni-C(7a)	2.294(3)	C(3a)-C(7a)	1.430(5)
P-C(22)	1.814(4)	C(4)-C(5)	1.369(7)
P-C(23)	1.820(4)	C(5)-C(6)	1.403(8)
P-C(21)	1.830(4)	C(6)-C(7)	1.391(6)
N-C(11)	1.457(6)	C(7)-C(7a)	1.393(5)
N-C(10)	1.466(5)	C(8)-C(9)	1.519(5)
N-C(9)	1.471(5)		
C(12)-NI-C(3)	162.69(16)	C(2)-C(1)-C(7A)	107.5(3)
C(12)-NI-C(2)	123.54(16)	C(2)-C(1)-C(8)	125.5(4)
C(3)-NI-C(2)	39.81(16)	C(7A)-C(1)-C(8)	125.9(3)
C(12)-NI-C(1)	96.90(15)	C(2)-C(1)-NI	69.9(2)
C(3)-NI-C(1)	66.66(15)	C(7A)-C(1)-NI	77.8(2)
C(2)-NI-C(1)	39.57(14)	C(8)-C(1)-NI	127.2(2)
C(12)-NI-P	93.18(11)	C(1)-C(2)-C(3)	108.1(4)
C(3)-NI-P	103.05(12)	C(1)-C(2)-NI	70.6(2)
C(2)-NI-P	131.09(12)	C(3)-C(2)-NI	69.7(2)
C(1)-NI-P	169.59(11)	C(2)-C(3)-C(3A)	108.9(4)
C(12)-NI-C(3A)	140.41(16)	C(2)-C(3)-NI	70.4(2)
C(3)-NI-C(3A)	38.31(15)	C(3A)-C(3)-NI	78.5(2)
C(2)-NI-C(3A)	64.22(15)	C(4)-C(3A)-C(7A)	119.3(4)
C(1)-NI-C(3A)	64.30(13)	C(4)-C(3A)-C(3)	133.6(4)
P-NI-C(3A)	108.93(10)	C(7A)-C(3A)-C(3)	107.0(3)
C(12)-NI-C(7A)	107.40(15)	C(4)-C(3A)-NI	128.0(3)
C(3)-NI-C(7A)	63.58(15)	C(7A)-C(3A)-NI	72.14(19)
C(2)-NI-C(7A)	63.93(14)	C(3)-C(3A)-NI	63.19(19)
C(1)-NI-C(7A)	38.70(13)	C(5)-C(4)-C(3A)	119.3(4)
P-NI-C(7A)	139.32(10)	C(4)-C(5)-C(6)	121.3(4)
C(3A)-NI-C(7A)	36.41(12)	C(7)-C(6)-C(5)	120.6(5)
C(22)-P-C(23)	102.4(3)	C(6)-C(7)-C(7A)	119.5(4)
C(22)-P-C(21)	103.3(3)	C(7)-C(7A)-C(3A)	120.0(3)
C(23)-P-C(21)	101.2(2)	C(7)-C(7A)-C(1)	132.4(3)
C(22)-P-NI	113.42(19)	C(3A)-C(7A)-C(1)	107.6(3)
C(23)-P-NI	117.32(16)	C(7)-C(7A)-NI	128.5(2)
C(21)-P-NI	117.10(16)	C(3A)-C(7A)-NI	71.5(2)
C(11)-N-C(10)	110.1(4)	C(1)-C(7A)-NI	63.49(18)
C(11)-N-C(9)	111.1(3)	C(1)-C(8)-C(9)	111.8(3)
C(10)-N-C(9)	110.4(3)	N-C(9)-C(8)	113.0(3)

Table IV.24. Torsion angles [°] for (η^3:η^0-Ind$(CH_2)_2NMe_2$)(PMe_3)NiMe **(6)**

C(12)-NI-P-C(22)	69.7(2)	NI-C(3)-C(3A)-C(7A)	-59.1(2)
C(3)-NI-P-C(22)	-104.2(2)	C(2)-C(3)-C(3A)-NI	64.5(3)
C(2)-NI-P-C(22)	-71.8(3)	C(12)-NI-C(3A)-C(4)	81.8(5)
C(1)-NI-P-C(22)	-95.8(6)	C(3)-NI-C(3A)-C(4)	-125.8(5)
C(3A)-NI-P-C(22)	-143.7(2)	C(2)-NI-C(3A)-C(4)	-166.0(5)
C(7A)-NI-P-C(22)	-168.7(2)	C(1)-NI-C(3A)-C(4)	149.9(4)
C(12)-NI-P-C(23)	-171.2(2)	P-NI-C(3A)-C(4)	-38.7(4)
C(3)-NI-P-C(23)	14.9(2)	C(7A)-NI-C(3A)-C(4)	113.7(5)
C(2)-NI-P-C(23)	47.3(3)	C(12)-NI-C(3A)-C(7A)	-31.9(3)
C(1)-NI-P-C(23)	23.4(6)	C(3)-NI-C(3A)-C(7A)	120.5(3)
C(3A)-NI-P-C(23)	-24.5(2)	C(2)-NI-C(3A)-C(7A)	80.4(2)
C(7A)-NI-P-C(23)	-49.5(3)	C(1)-NI-C(3A)-C(7A)	36.2(2)
C(12)-NI-P-C(21)	-50.5(2)	P-NI-C(3A)-C(7A)	-152.33(19)
C(3)-NI-P-C(21)	135.5(2)	C(12)-NI-C(3A)-C(3)	-152.4(3)
C(2)-NI-P-C(21)	167.9(3)	C(2)-NI-C(3A)-C(3)	-40.1(2)
C(1)-NI-P-C(21)	144.0(6)	C(1)-NI-C(3A)-C(3)	-84.3(2)
C(3A)-NI-P-C(21)	96.1(2)	P-NI-C(3A)-C(3)	87.2(2)
C(7A)-NI-P-C(21)	71.1(3)	C(7A)-NI-C(3A)-C(3)	-120.5(3)
C(12)-NI-C(1)-C(2)	-136.7(2)	C(7A)-C(3A)-C(4)-C(5)	-0.7(5)
C(3)-NI-C(1)-C(2)	37.7(2)	C(3)-C(3A)-C(4)-C(5)	-177.7(4)
P-NI-C(1)-C(2)	28.7(7)	NI-C(3A)-C(4)-C(5)	-90.3(5)
C(3A)-NI-C(1)-C(2)	79.9(2)	C(3A)-C(4)-C(5)-C(6)	0.5(6)
C(7A)-NI-C(1)-C(2)	114.0(3)	C(4)-C(5)-C(6)-C(7)	0.2(7)
C(12)-NI-C(1)-C(7A)	109.3(2)	C(5)-C(6)-C(7)-C(7A)	-0.6(6)
C(3)-NI-C(1)-C(7A)	-76.3(2)	C(6)-C(7)-C(7A)-C(3A)	0.4(5)
C(2)-NI-C(1)-C(7A)	-114.0(3)	C(6)-C(7)-C(7A)-C(1)	177.2(3)
P-NI-C(1)-C(7A)	-85.3(6)	C(6)-C(7)-C(7A)-NI	89.8(4)
C(3A)-NI-C(1)-C(7A)	-34.1(2)	C(4)-C(3A)-C(7A)-C(7)	0.2(5)
C(12)-NI-C(1)-C(8)	-16.8(4)	C(3)-C(3A)-C(7A)-C(7)	178.0(3)
C(3)-NI-C(1)-C(8)	157.6(4)	NI-C(3A)-C(7A)-C(7)	124.4(3)
C(2)-NI-C(1)-C(8)	119.9(4)	C(4)-C(3A)-C(7A)-C(1)	-177.3(3)
P-NI-C(1)-C(8)	148.6(4)	C(3)-C(3A)-C(7A)-C(1)	0.5(4)
C(3A)-NI-C(1)-C(8)	-160.2(4)	NI-C(3A)-C(7A)-C(1)	-53.1(2)
C(7A)-NI-C(1)-C(8)	-126.1(4)	C(4)-C(3A)-C(7A)-NI	-124.2(3)
C(7A)-C(1)-C(2)-C(3)	9.5(4)	C(3)-C(3A)-C(7A)-NI	53.5(2)
C(8)-C(1)-C(2)-C(3)	178.1(3)	C(2)-C(1)-C(7A)-C(7)	176.8(3)
NI-C(1)-C(2)-C(3)	-59.9(3)	C(8)-C(1)-C(7A)-C(7)	8.2(6)
C(7A)-C(1)-C(2)-NI	69.4(2)	NI-C(1)-C(7A)-C(7)	-119.2(4)
C(8)-C(1)-C(2)-NI	-122.0(3)	C(2)-C(1)-C(7A)-C(3A)	-6.1(4)
C(12)-NI-C(2)-C(1)	54.8(3)	C(8)-C(1)-C(7A)-C(3A)	-174.7(3)
C(3)-NI-C(2)-C(1)	-118.7(3)	NI-C(1)-C(7A)-C(3A)	57.9(2)
P-NI-C(2)-C(1)	-173.38(16)	C(2)-C(1)-C(7A)-NI	-64.1(2)
C(3A)-NI-C(2)-C(1)	-80.1(2)	C(8)-C(1)-C(7A)-NI	127.4(4)
C(7A)-NI-C(2)-C(1)	-39.5(2)	C(12)-NI-C(7A)-C(7)	45.4(4)
C(12)-NI-C(2)-C(3)	173.6(2)	C(3)-NI-C(7A)-C(7)	-150.6(4)
C(1)-NI-C(2)-C(3)	118.7(3)	C(2)-NI-C(7A)-C(7)	164.8(4)
P-NI-C(2)-C(3)	-54.7(3)	C(1)-NI-C(7A)-C(7)	124.4(4)
C(3A)-NI-C(2)-C(3)	38.6(2)	P-NI-C(7A)-C(7)	-71.6(4)
C(7A)-NI-C(2)-C(3)	79.2(3)	C(3A)-NI-C(7A)-C(7)	-114.0(4)
C(1)-C(2)-C(3)-C(3A)	-9.4(4)	C(12)-NI-C(7A)-C(3A)	159.3(2)
NI-C(2)-C(3)-C(3A)	-69.8(3)	C(3)-NI-C(7A)-C(3A)	-36.6(2)
C(1)-C(2)-C(3)-NI	60.4(2)	C(2)-NI-C(7A)-C(3A)	-81.2(2)
C(12)-NI-C(3)-C(2)	-18.3(7)	C(1)-NI-C(7A)-C(3A)	-121.6(3)
C(1)-NI-C(3)-C(2)	-37.5(2)	P-NI-C(7A)-C(3A)	42.4(3)
P-NI-C(3)-C(2)	140.9(2)	C(12)-NI-C(7A)-C(1)	-79.1(2)
C(3A)-NI-C(3)-C(2)	-115.0(3)	C(3)-NI-C(7A)-C(1)	85.0(2)
C(7A)-NI-C(3)-C(2)	-80.2(2)	C(2)-NI-C(7A)-C(1)	40.4(2)
C(12)-NI-C(3)-C(3A)	96.7(6)	P-NI-C(7A)-C(1)	163.96(17)
C(2)-NI-C(3)-C(3A)	115.0(3)	C(3A)-NI-C(7A)-C(1)	121.6(3)
C(1)-NI-C(3)-C(3A)	77.5(2)	C(2)-C(1)-C(8)-C(9)	-86.0(5)
P-NI-C(3)-C(3A)	-104.1(2)	C(7A)-C(1)-C(8)-C(9)	80.5(5)
C(7A)-NI-C(3)-C(3A)	34.8(2)	NI-C(1)-C(8)-C(9)	-176.6(3)
C(2)-C(3)-C(3A)-C(4)	-177.3(4)	C(11)-N-C(9)-C(8)	70.4(4)
NI-C(3)-C(3A)-C(4)	118.2(4)	C(10)-N-C(9)-C(8)	-167.2(4)
C(2)-C(3)-C(3A)-C(7A)	5.4(4)	C(1)-C(8)-C(9)-N	179.8(3)

Table IV.25. Crystal data and structure refinement for $[(\eta^3:\eta^1\text{-}Ind(CH_2)_2NMe_2)(PCy_3)Ni]^+ [BPh_4]^-$ **(9)**

Empirical formula	C56 H71 B Cl2 N Ni P
Formula weight	929.53
Temperature	223(2)K
Wavelength	1.54178 Å
Crystal system	Triclinic
Space group	P-1
Unit cell dimensions	a = 10.9625(1) Å α = 83.939(1)° b = 13.4241(2) Å β = 87.023(1)° c = 17.6136(2) Å γ = 78.308(1)°
Volume	2522.84(5)Å^3
Z	2
Density (calculated)	1.224 Mg/m^3
Absorption coefficient	2.094 mm^{-1}
F(000)	992
Crystal size	0.20 x 0.20 x 0.17 mm
Theta range for data collection	2.52 to 72.95°
Index ranges	$-13 \le h \le 13$, $-16 \le k \le 16$, $-21 \le \ell \le 21$
Reflections collected	30682
Independent reflections	9633 [R_{int} = 0.024]
Absorption correction	Semi-empirical from equivalents
Max. and min. transmission	0.7700 and 0.6700
Refinement method	Full-matrix least-squares on F^2
Data / restraints / parameters	9633 / 27 / 647
Goodness-of-fit on F^2	1.011
Final R indices [I>2sigma(I)]	R1 = 0.0441, wR_2 = 0.1211
R indices (all data)	R1 = 0.0544, wR_2 = 0.1268
Largest diff. peak and hole	0.345 and -0.288 e/Å^3

Table IV.26. Atomic coordinates (x 10^4) and equivalent isotropic displacement parameters ($Å^2$ x 10^3) for $[(\eta^3:\eta^1\text{-Ind}(CH_2)_2NMe_2)(PCy_3)Ni]^+ [BPh_4]^-$ **(9)**

U_{eq} is defined as one third of the trace of the orthogonalized Uij tensor.

	Occ.	x	y	z	U_{eq}
Ni	1	8666(1)	7315(1)	8216(1)	30(1)
P	1	8376(1)	6675(1)	7129(1)	29(1)
C(1)	1	9166(2)	7523(2)	9295(1)	39(1)
C(2)	1	10233(2)	7296(2)	8805(1)	39(1)
C(3)	1	10293(2)	6307(2)	8587(1)	42(1)
C(3A)	1	9423(2)	5819(2)	9079(1)	45(1)
C(4)	1	9223(3)	4820(2)	9182(2)	62(1)
C(5)	1	8321(3)	4600(2)	9703(2)	82(1)
C(6)	1	7614(3)	5340(3)	10118(2)	85(1)
C(7)	1	7800(3)	6342(2)	10035(1)	68(1)
C(7A)	1	8720(2)	6575(2)	9514(1)	45(1)
C(8)	0.72	8592(6)	8565(5)	9528(4)	42(2)
C(9)	0.72	8067(3)	9221(2)	8804(2)	49(1)
N(1)	0.72	7404(5)	8613(4)	8354(3)	38(1)
C(10)	0.72	6908(5)	9276(4)	7668(3)	57(1)
C(11)	0.72	6290(3)	8388(3)	8817(2)	55(1)
C(8B)	0.28	8510(20)	8492(15)	9533(14)	81(9)
C(9B)	0.28	7280(7)	8854(5)	9131(4)	37(2)
N(2)	0.28	7605(12)	8751(10)	8300(8)	37(3)
C(10B)	0.28	8401(8)	9499(5)	8023(5)	52(2)
C(11B)	0.28	6398(11)	9071(11)	7901(7)	64(3)
C(21)	1	9659(2)	5580(1)	6928(1)	35(1)
C(22)	1	10882(2)	5922(2)	6666(1)	41(1)
C(23)	1	11961(2)	4999(2)	6686(1)	51(1)
C(24)	1	11714(2)	4213(2)	6178(1)	53(1)
C(25)	1	10485(2)	3894(2)	6398(1)	50(1)
C(26)	1	9401(2)	4810(2)	6397(1)	42(1)
C(31)	1	6972(2)	6097(1)	7149(1)	34(1)
C(32)	1	7019(2)	5293(2)	7843(1)	46(1)
C(33)	1	5919(2)	4757(2)	7875(2)	58(1)
C(34)	1	4695(2)	5509(2)	7873(2)	59(1)
C(35)	1	4645(2)	6302(2)	7187(2)	63(1)
C(36)	1	5741(2)	6848(2)	7159(2)	54(1)
C(41)	1	8193(2)	7639(1)	6291(1)	35(1)
C(42)	1	9175(2)	8311(2)	6229(1)	45(1)
C(43)	1	8806(2)	9224(2)	5639(1)	54(1)
C(44)	1	8644(2)	8870(2)	4862(1)	57(1)
C(45)	1	7707(2)	8174(2)	4913(1)	51(1)
C(46)	1	8060(2)	7263(2)	5511(1)	44(1)
B	1	2303(2)	277(2)	7910(1)	34(1)
C(51)	1	888(2)	960(1)	7767(1)	36(1)
C(52)	1	133(2)	838(2)	7187(1)	55(1)
C(53)	1	-1073(2)	1407(2)	7094(2)	77(1)
C(54)	1	-1573(2)	2132(2)	7577(2)	68(1)
C(55)	1	-859(2)	2293(2)	8148(1)	51(1)
C(56)	1	344(2)	1724(2)	8240(1)	43(1)
C(61)	1	2291(2)	-648(1)	8603(1)	33(1)
C(62)	1	3173(2)	-1558(2)	8630(1)	41(1)
C(63)	1	3353(2)	-2245(2)	9280(1)	47(1)
C(64)	1	2634(2)	-2054(2)	9934(1)	43(1)
C(65)	1	1719(2)	-1189(2)	9923(1)	41(1)
C(66)	1	1549(2)	-510(1)	9271(1)	36(1)
C(71)	1	3169(2)	1030(1)	8194(1)	37(1)

C(72)	1	3242(2)	1967(2)	7778(1)	53(1)
C(73)	1	3992(2)	2602(2)	7977(2)	64(1)
C(74)	1	4716(2)	2332(2)	8609(2)	60(1)
C(75)	1	4673(2)	1419(2)	9044(1)	49(1)
C(76)	1	3909(2)	794(2)	8835(1)	38(1)
C(81)	1	2904(2)	-222(2)	7129(1)	38(1)
C(82)	1	3903(2)	71(2)	6698(1)	46(1)
C(83)	1	4386(2)	-367(2)	6038(1)	61(1)
C(84)	1	3886(3)	-1120(2)	5778(1)	66(1)
C(85)	1	2906(2)	-1440(2)	6181(1)	59(1)
C(86)	1	2440(2)	-1005(2)	6848(1)	46(1)
C(98)	0.20	4068(12)	6609(18)	4663(11)	129(8)
Cl(1)	0.20	4200(11)	7517(13)	3857(5)	145(5)
Cl(2)	0.20	2422(8)	6742(8)	4568(5)	123(3)
C(99)	0.38	3115(10)	7200(11)	4309(9)	153(6)
Cl(3)	0.38	3594(13)	5924(11)	4707(8)	362(9)
Cl(4)	0.38	4635(9)	7292(8)	3942(5)	210(5)
C(100)	0.42	3602(14)	6770(20)	4024(11)	353(19)
Cl(5)	0.42	2815(8)	6184(9)	4780(5)	217(5)
Cl(6)	0.42	5041(6)	6483(7)	4469(6)	303(5)

Table IV.27. Hydrogen coordinates (x 10^4) and isotropic displacement parameters ($Å^2$ x 10^3) for $[(\eta^3:\eta^1\text{-Ind}(CH_2)_2NMe_2)(PCy_3)Ni]^+ [BPh_4]^-$ **(9)**

	Occ.	x	y	z	U_{eq}
H(2)	1	10856	7732	8672	47
H(3)	1	10949	5949	8248	50
H(4)	1	9696	4311	8900	74
H(5)	1	8180	3929	9781	99
H(6)	1	6992	5163	10465	102
H(7)	1	7320	6843	10321	81
H(8A)	0.72	9221	8868	9744	51
H(8B)	0.72	7923	8518	9913	51
H(9A)	0.72	7487	9834	8946	59
H(9B)	0.72	8749	9438	8490	59
H(10A)	0.72	6382	9898	7822	86
H(10B)	0.72	6422	8918	7387	86
H(10C)	0.72	7595	9446	7344	86
H(11A)	0.72	5760	9024	8943	82
H(11B)	0.72	6562	7968	9284	82
H(11C)	0.72	5827	8025	8524	82
H(8B1)	0.28	9029	9004	9418	98
H(8B2)	0.28	8343	8421	10086	98
H(9A1)	0.28	6677	8430	9318	45
H(9A2)	0.28	6924	9567	9213	45
H(10D)	0.28	8422	9583	7469	79
H(10E)	0.28	9240	9249	8202	79
H(10F)	0.28	8060	10151	8217	79
H(11D)	0.28	6135	9808	7878	96
H(11E)	0.28	5769	8750	8178	96
H(11F)	0.28	6506	8863	7386	96
H(21)	1	9835	5179	7429	41
H(22A)	1	10803	6262	6146	49
H(22B)	1	11050	6412	7002	49
H(23A)	1	12733	5224	6510	61
H(23B)	1	12069	4684	7212	61
H(24A)	1	11699	4505	5644	64
H(24B)	1	12390	3611	6225	64
H(25A)	1	10540	3521	6908	60
H(25B)	1	10324	3431	6038	60
H(26A)	1	8633	4576	6570	51
H(26B)	1	9285	5144	5877	51
H(31)	1	7012	5736	6683	41
H(32A)	1	7796	4784	7814	56
H(32B)	1	7017	5626	8312	56
H(33A)	1	5974	4359	7435	69
H(33B)	1	5954	4282	8340	69
H(34A)	1	4592	5851	8344	71
H(34B)	1	4009	5145	7857	71
H(35A)	1	3863	6806	7213	76
H(35B)	1	4655	5968	6718	76
H(36A)	1	5697	7334	6701	65
H(36B)	1	5688	7234	7606	65
H(41)	1	7392	8109	6388	42
H(42A)	1	9253	8552	6727	54
H(42B)	1	9985	7909	6081	54
H(43A)	1	9451	9639	5596	65
H(43B)	1	8023	9650	5806	65
H(44A)	1	8362	9467	4499	68
H(44B)	1	9449	8505	4672	68
H(45A)	1	7662	7925	4414	61
H(45B)	1	6881	8563	5046	61

H(46A)	1	8849	6834	5356	53
H(46B)	1	7416	6847	5550	53
H(52)	1	449	351	6844	67
H(53)	1	-1549	1292	6695	92
H(54)	1	-2389	2509	7517	81
H(55)	1	-1182	2793	8480	61
H(56)	1	813	1854	8637	51
H(62)	1	3666	-1714	8189	49
H(63)	1	3970	-2843	9275	56
H(64)	1	2768	-2509	10379	52
H(65)	1	1205	-1057	10360	49
H(66)	1	905	71	9276	43
H(72)	1	2756	2173	7344	63
H(73)	1	4008	3222	7678	77
H(74)	1	5232	2762	8743	71
H(75)	1	5158	1224	9480	58
H(76)	1	3889	179	9140	46
H(82)	1	4263	587	6862	55
H(83)	1	5060	-146	5768	73
H(84)	1	4210	-1414	5330	80
H(85)	1	2549	-1951	6007	70
H(86)	1	1784	-1249	7122	55
H(98A)	0.20	4286	6827	5143	155
H(98B)	0.20	4535	5920	4591	155
H(99A)	0.38	2807	7675	4695	184
H(99B)	0.38	2507	7272	3909	184
H(10G)	0.42	3619	6450	3549	424
H(10H)	0.42	3277	7510	3935	424

Table IV.28. Anisotropic parameters ($Å^2$ x 10^3) for [(η^3:η^1-Ind$(CH_2)_2NMe_2$)$(PCy_3)Ni]^+$ $[BPh_4]^-$ **(9)**

The anisotropic displacement factor exponent takes the form:

$$-2\,\pi^2\,[\,h^2\,a^{*2}\,U_{11} + \ldots + 2\,h\,k\,a^*\,b^*\,U_{12}\,]$$

	U11	U22	U33	U23	U13	U12
Ni	34(1)	32(1)	27(1)	-5(1)	-3(1)	-7(1)
P	34(1)	31(1)	25(1)	-3(1)	-3(1)	-9(1)
C(1)	43(1)	47(1)	27(1)	-8(1)	-9(1)	-10(1)
C(2)	35(1)	46(1)	39(1)	-8(1)	-9(1)	-8(1)
C(3)	44(1)	47(1)	34(1)	-9(1)	-11(1)	0(1)
C(3A)	60(1)	40(1)	35(1)	3(1)	-21(1)	-10(1)
C(4)	91(2)	41(1)	57(2)	8(1)	-39(1)	-17(1)
C(5)	115(3)	67(2)	73(2)	34(2)	-49(2)	-47(2)
C(6)	89(2)	106(3)	65(2)	43(2)	-16(2)	-48(2)
C(7)	69(2)	87(2)	43(1)	16(1)	-2(1)	-18(2)
C(7A)	54(1)	52(1)	29(1)	5(1)	-10(1)	-12(1)
C(8)	42(2)	45(3)	39(4)	-23(2)	-7(2)	4(2)
C(9)	56(2)	40(2)	54(2)	-19(1)	-6(2)	-4(2)
N(1)	37(2)	41(2)	38(2)	-9(2)	-5(2)	-5(2)
C(10)	73(3)	42(2)	48(3)	-8(2)	-12(2)	13(2)
C(11)	39(2)	69(2)	55(2)	-14(2)	1(1)	-3(2)
C(8B)	121(16)	89(14)	53(14)	-16(10)	-16(11)	-58(12)
C(9B)	44(4)	35(3)	33(4)	-10(3)	6(3)	-7(3)
N(2)	40(6)	30(4)	39(5)	-13(4)	11(4)	-5(4)
C(10B)	74(5)	25(3)	59(5)	-1(3)	18(4)	-17(4)
C(11B)	72(8)	65(8)	46(7)	-23(6)	-10(5)	19(6)
B	37(1)	36(1)	29(1)	-1(1)	3(1)	-10(1)
C(21)	38(1)	35(1)	31(1)	-7(1)	-2(1)	-6(1)
C(22)	39(1)	45(1)	40(1)	-11(1)	1(1)	-11(1)
C(23)	38(1)	57(1)	58(1)	-14(1)	-1(1)	-4(1)
C(24)	49(1)	49(1)	60(2)	-17(1)	5(1)	-1(1)
C(25)	54(1)	41(1)	55(1)	-16(1)	2(1)	-4(1)
C(26)	45(1)	40(1)	44(1)	-15(1)	-4(1)	-7(1)
C(31)	37(1)	33(1)	33(1)	-3(1)	-5(1)	-10(1)
C(32)	46(1)	45(1)	49(1)	10(1)	-9(1)	-16(1)
C(33)	57(1)	49(1)	70(2)	14(1)	-7(1)	-26(1)
C(34)	48(1)	61(1)	76(2)	-10(1)	9(1)	-29(1)
C(35)	38(1)	50(1)	104(2)	1(1)	-11(1)	-14(1)
C(36)	39(1)	38(1)	85(2)	4(1)	-10(1)	-10(1)
C(41)	44(1)	33(1)	27(1)	-1(1)	-1(1)	-10(1)
C(42)	53(1)	45(1)	39(1)	3(1)	0(1)	-20(1)
C(43)	72(2)	43(1)	49(1)	6(1)	5(1)	-22(1)
C(44)	74(2)	51(1)	38(1)	13(1)	8(1)	-6(1)
C(45)	69(1)	51(1)	29(1)	-1(1)	-7(1)	-3(1)
C(46)	62(1)	41(1)	31(1)	-2(1)	-6(1)	-12(1)
C(51)	38(1)	38(1)	33(1)	0(1)	5(1)	-9(1)
C(52)	47(1)	65(2)	53(1)	-22(1)	-6(1)	1(1)
C(53)	50(1)	97(2)	83(2)	-36(2)	-22(1)	8(2)
C(54)	42(1)	75(2)	79(2)	-11(2)	-3(1)	8(1)
C(55)	55(1)	43(1)	48(1)	-3(1)	12(1)	0(1)
C(56)	50(1)	41(1)	36(1)	-4(1)	3(1)	-7(1)
C(61)	36(1)	37(1)	30(1)	-5(1)	1(1)	-15(1)
C(62)	42(1)	42(1)	37(1)	-4(1)	6(1)	-7(1)
C(63)	51(1)	41(1)	47(1)	2(1)	-1(1)	-6(1)
C(64)	53(1)	44(1)	36(1)	5(1)	-4(1)	-21(1)
C(65)	50(1)	47(1)	29(1)	-7(1)	6(1)	-20(1)
C(66)	41(1)	35(1)	33(1)	-8(1)	4(1)	-12(1)
C(71)	37(1)	37(1)	36(1)	-3(1)	4(1)	-8(1)

C(72)	58(1)	47(1)	54(1)	10(1)	-7(1)	-20(1)
C(73)	69(2)	46(1)	80(2)	13(1)	-3(1)	-27(1)
C(74)	61(1)	53(1)	74(2)	-8(1)	-4(1)	-30(1)
C(75)	46(1)	53(1)	50(1)	-9(1)	-2(1)	-16(1)
C(76)	38(1)	38(1)	39(1)	-6(1)	3(1)	-10(1)
C(81)	39(1)	43(1)	29(1)	2(1)	2(1)	0(1)
C(82)	42(1)	57(1)	33(1)	5(1)	3(1)	-2(1)
C(83)	52(1)	79(2)	38(1)	9(1)	12(1)	8(1)
C(84)	80(2)	70(2)	35(1)	-7(1)	11(1)	14(2)
C(85)	76(2)	52(1)	42(1)	-12(1)	-3(1)	4(1)
C(86)	53(1)	44(1)	37(1)	-4(1)	2(1)	-3(1)
Cl(1)	151(8)	243(12)	69(4)	15(6)	-17(5)	-121(9)
Cl(2)	114(4)	167(7)	105(6)	11(5)	-37(4)	-74(5)
Cl(3)	450(20)	345(14)	321(12)	92(10)	55(12)	-222(15)
Cl(4)	192(8)	279(11)	202(8)	-120(7)	127(6)	-129(7)
Cl(5)	267(9)	307(11)	133(4)	36(5)	-7(5)	-216(9)
Cl(6)	126(4)	306(9)	458(14)	-70(8)	61(6)	-3(5)

Table IV.29. Bond lengths [Å] and angles [°] for [(η^3:η^1-Ind$(CH_2)_2NMe_2$)$(PCy_3)Ni]^+$ $[BPh_4]^-$ **(9)**

Ni-N(1)	2.022(5)	C(21)-C(22)	1.536(3)
Ni-C(2)	2.0466(19)	C(21)-C(26)	1.540(2)
Ni-N(2)	2.055(12)	C(21)-H(21)	0.9900
Ni-C(1)	2.0660(18)	C(22)-C(23)	1.529(3)
Ni-C(3)	2.096(2)	C(22)-H(22A)	0.9800
Ni-P	2.2424(5)	C(22)-H(22B)	0.9800
Ni-C(7A)	2.3932(19)	C(23)-C(24)	1.524(3)
Ni-C(3A)	2.4172(19)	C(23)-H(23A)	0.9800
P-C(41)	1.8481(18)	C(23)-H(23B)	0.9800
P-C(31)	1.8562(18)	C(24)-C(25)	1.514(3)
P-C(21)	1.8675(19)	C(24)-H(24A)	0.9800
C(1)-C(2)	1.419(3)	C(24)-H(24B)	0.9800
C(1)-C(8B)	1.447(14)	C(25)-C(26)	1.526(3)
C(1)-C(7A)	1.461(3)	C(25)-H(25A)	0.9800
C(1)-C(8)	1.503(5)	C(25)-H(25B)	0.9800
C(2)-C(3)	1.408(3)	C(26)-H(26A)	0.9800
C(2)-H(2)	0.9900	C(26)-H(26B)	0.9800
C(3)-C(3A)	1.463(3)	C(31)-C(36)	1.513(3)
C(3)-H(3)	0.9900	C(31)-C(32)	1.538(3)
C(3A)-C(4)	1.394(3)	C(31)-H(31)	0.9900
C(3A)-C(7A)	1.413(3)	C(32)-C(33)	1.520(3)
C(4)-C(5)	1.370(4)	C(32)-H(32A)	0.9800
C(4)-H(4)	0.9400	C(32)-H(32B)	0.9800
C(5)-C(6)	1.379(5)	C(33)-C(34)	1.507(3)
C(5)-H(5)	0.9400	C(33)-H(33A)	0.9800
C(6)-C(7)	1.393(4)	C(33)-H(33B)	0.9800
C(6)-H(6)	0.9400	C(34)-C(35)	1.518(3)
C(7)-C(7A)	1.387(3)	C(34)-H(34A)	0.9800
C(7)-H(7)	0.9400	C(34)-H(34B)	0.9800
C(8)-C(9)	1.538(7)	C(35)-C(36)	1.525(3)
C(8)-H(8A)	0.9800	C(35)-H(35A)	0.9800
C(8)-H(8B)	0.9800	C(35)-H(35B)	0.9800
C(9)-N(1)	1.503(6)	C(36)-H(36A)	0.9800
C(9)-H(9A)	0.9800	C(36)-H(36B)	0.9800
C(9)-H(9B)	0.9800	C(41)-C(42)	1.533(3)
N(1)-C(10)	1.482(6)	C(41)-C(46)	1.536(3)
N(1)-C(11)	1.497(6)	C(41)-H(41)	0.9900
C(10)-H(10A)	0.9700	C(42)-C(43)	1.523(3)
C(10)-H(10B)	0.9700	C(42)-H(42A)	0.9800
C(10)-H(10C)	0.9700	C(42)-H(42B)	0.9800
C(11)-H(11A)	0.9700	C(43)-C(44)	1.525(3)
C(11)-H(11B)	0.9700	C(43)-H(43A)	0.9800
C(11)-H(11C)	0.9700	C(43)-H(43B)	0.9800
C(8B)-C(9B)	1.519(15)	C(44)-C(45)	1.516(3)
C(8B)-H(8B1)	0.9800	C(44)-H(44A)	0.9800
C(8B)-H(8B2)	0.9800	C(44)-H(44B)	0.9800
C(9B)-N(2)	1.502(12)	C(45)-C(46)	1.528(3)
C(9B)-H(9A1)	0.9800	C(45)-H(45A)	0.9800
C(9B)-H(9A2)	0.9800	C(45)-H(45B)	0.9800
N(2)-C(10B)	1.489(12)	C(46)-H(46A)	0.9800
N(2)-C(11B)	1.495(12)	C(46)-H(46B)	0.9800
C(10B)-H(10D)	0.9700	C(51)-C(52)	1.390(3)
C(10B)-H(10E)	0.9700	C(51)-C(56)	1.407(3)
C(10B)-H(10F)	0.9700	C(52)-C(53)	1.395(3)
C(11B)-H(11D)	0.9700	C(52)-H(52)	0.9400
C(11B)-H(11E)	0.9700	C(53)-C(54)	1.372(4)
C(11B)-H(11F)	0.9700	C(53)-H(53)	0.9400
B-C(81)	1.643(3)	C(54)-C(55)	1.366(3)
B-C(71)	1.647(3)	C(54)-H(54)	0.9400
B-C(61)	1.648(3)	C(55)-C(56)	1.391(3)
B-C(51)	1.652(3)	C(55)-H(55)	0.9400

C(56)-H(56)	0.9400	C(81)-C(82)	1.398(3)
C(61)-C(62)	1.394(3)	C(81)-C(86)	1.401(3)
C(61)-C(66)	1.401(2)	C(82)-C(83)	1.390(3)
C(62)-C(63)	1.388(3)	C(82)-H(82)	0.9400
C(62)-H(62)	0.9400	C(83)-C(84)	1.371(4)
C(63)-C(64)	1.379(3)	C(83)-H(83)	0.9400
C(63)-H(63)	0.9400	C(84)-C(85)	1.373(4)
C(64)-C(65)	1.371(3)	C(84)-H(84)	0.9400
C(64)-H(64)	0.9400	C(85)-C(86)	1.394(3)
C(65)-C(66)	1.385(3)	C(85)-H(85)	0.9400
C(65)-H(65)	0.9400	C(86)-H(86)	0.9400
C(66)-H(66)	0.9400	C(98)-Cl(1)	1.791(10)
C(71)-C(76)	1.396(3)	C(98)-Cl(2)	1.792(10)
C(71)-C(72)	1.402(3)	C(98)-H(98A)	0.9800
C(72)-C(73)	1.378(3)	C(98)-H(98B)	0.9800
C(72)-H(72)	0.9400	C(99)-Cl(3)	1.767(9)
C(73)-C(74)	1.375(4)	C(99)-Cl(4)	1.779(9)
C(73)-H(73)	0.9400	C(99)-H(99A)	0.9800
C(74)-C(75)	1.384(3)	C(99)-H(99B)	0.9800
C(74)-H(74)	0.9400	C(100)-Cl(6)	1.752(10)
C(75)-C(76)	1.387(3)	C(100)-Cl(5)	1.754(10)
C(75)-H(75)	0.9400	C(100)-H(10G)	0.9800
C(76)-H(76)	0.9400	C(100)-H(10H)	0.9800
N(1)-Ni-C(2)	110.07(18)	C(8)-C(1)-Ni	112.5(2)
N(1)-Ni-N(2)	9.0(5)	C(3)-C(2)-C(1)	107.49(18)
C(2)-Ni-N(2)	104.6(4)	C(3)-C(2)-Ni	72.03(11)
N(1)-Ni-C(1)	82.70(17)	C(1)-C(2)-Ni	70.55(10)
C(2)-Ni-C(1)	40.36(8)	C(3)-C(2)-H(2)	126.2
N(2)-Ni-C(1)	81.8(4)	C(1)-C(2)-H(2)	126.2
N(1)-Ni-C(3)	148.08(18)	Ni-C(2)-H(2)	126.2
C(2)-Ni-C(3)	39.72(8)	C(2)-C(3)-C(3A)	108.37(18)
N(2)-Ni-C(3)	144.0(4)	C(2)-C(3)-Ni	68.25(11)
C(1)-Ni-C(3)	66.42(8)	C(3A)-C(3)-Ni	83.54(12)
N(1)-Ni-P	111.11(16)	C(2)-C(3)-H(3)	125.1
C(2)-Ni-P	132.22(6)	C(3A)-C(3)-H(3)	125.1
N(2)-Ni-P	112.7(4)	Ni-C(3)-H(3)	125.1
C(1)-Ni-P	165.24(6)	C(4)-C(3A)-C(7A)	120.4(2)
C(3)-Ni-P	100.45(6)	C(4)-C(3A)-C(3)	132.5(2)
N(1)-Ni-C(7A)	98.64(16)	C(7A)-C(3A)-C(3)	107.10(18)
C(2)-Ni-C(7A)	62.75(8)	C(4)-C(3A)-Ni	135.07(14)
N(2)-Ni-C(7A)	102.6(4)	C(7A)-C(3A)-Ni	71.99(11)
C(1)-Ni-C(7A)	37.35(7)	C(3)-C(3A)-Ni	59.50(10)
C(3)-Ni-C(7A)	61.62(8)	C(5)-C(4)-C(3A)	118.3(3)
P-Ni-C(7A)	131.29(6)	C(5)-C(4)-H(4)	120.9
N(1)-Ni-C(3A)	132.37(17)	C(3A)-C(4)-H(4)	120.9
C(2)-Ni-C(3A)	62.22(8)	C(4)-C(5)-C(6)	121.7(3)
N(2)-Ni-C(3A)	136.8(4)	C(4)-C(5)-H(5)	119.2
C(1)-Ni-C(3A)	61.63(7)	C(6)-C(5)-H(5)	119.2
C(3)-Ni-C(3A)	36.96(8)	C(5)-C(6)-C(7)	121.4(3)
P-Ni-C(3A)	103.93(5)	C(5)-C(6)-H(6)	119.3
C(7A)-Ni-C(3A)	34.17(7)	C(7)-C(6)-H(6)	119.3
C(41)-P-C(31)	104.79(8)	C(7A)-C(7)-C(6)	117.7(3)
C(41)-P-C(21)	109.58(9)	C(7A)-C(7)-H(7)	121.2
C(31)-P-C(21)	102.40(8)	C(6)-C(7)-H(7)	121.2
C(41)-P-Ni	113.44(6)	C(7)-C(7A)-C(3A)	120.6(2)
C(31)-P-Ni	114.32(6)	C(7)-C(7A)-C(1)	132.0(2)
C(21)-P-Ni	111.55(6)	C(3A)-C(7A)-C(1)	107.37(18)
C(2)-C(1)-C(8B)	130.2(13)	C(7)-C(7A)-Ni	132.82(16)
C(2)-C(1)-C(7A)	108.01(18)	C(3A)-C(7A)-Ni	73.85(11)
C(8B)-C(1)-C(7A)	121.7(13)	C(1)-C(7A)-Ni	59.08(10)
C(2)-C(1)-C(8)	125.3(4)	C(1)-C(8)-C(9)	107.0(4)
C(8B)-C(1)-C(8)	5.3(14)	C(1)-C(8)-H(8A)	110.3
C(7A)-C(1)-C(8)	126.6(4)	C(9)-C(8)-H(8A)	110.3
C(2)-C(1)-Ni	69.08(11)	C(1)-C(8)-H(8B)	110.3
C(8B)-C(1)-Ni	111.2(8)	C(9)-C(8)-H(8B)	110.3
C(7A)-C(1)-Ni	83.57(11)	H(8A)-C(8)-H(8B)	108.6

N(1)-C(9)-C(8)	109.8(4)	C(25)-C(24)-C(23)	111.27(18)
N(1)-C(9)-H(9A)	109.7	C(25)-C(24)-H(24A)	109.4
C(8)-C(9)-H(9A)	109.7	C(23)-C(24)-H(24A)	109.4
N(1)-C(9)-H(9B)	109.7	C(25)-C(24)-H(24B)	109.4
C(8)-C(9)-H(9B)	109.7	C(23)-C(24)-H(24B)	109.4
H(9A)-C(9)-H(9B)	108.2	H(24A)-C(24)-H(24B)	108.0
C(10)-N(1)-C(11)	106.0(4)	C(24)-C(25)-C(26)	112.03(18)
C(10)-N(1)-C(9)	107.8(5)	C(24)-C(25)-H(25A)	109.2
C(11)-N(1)-C(9)	108.4(4)	C(26)-C(25)-H(25A)	109.2
C(10)-N(1)-Ni	118.9(4)	C(24)-C(25)-H(25B)	109.2
C(11)-N(1)-Ni	111.0(3)	C(26)-C(25)-H(25B)	109.2
C(9)-N(1)-Ni	104.4(3)	H(25A)-C(25)-H(25B)	107.9
C(1)-C(8B)-C(9B)	111.5(11)	C(25)-C(26)-C(21)	110.38(16)
C(1)-C(8B)-H(8B1)	109.3	C(25)-C(26)-H(26A)	109.6
C(9B)-C(8B)-H(8B1)	109.3	C(21)-C(26)-H(26A)	109.6
C(1)-C(8B)-H(8B2)	109.3	C(25)-C(26)-H(26B)	109.6
C(9B)-C(8B)-H(8B2)	109.3	C(21)-C(26)-H(26B)	109.6
H(8B1)-C(8B)-H(8B2)	108.0	H(26A)-C(26)-H(26B)	108.1
N(2)-C(9B)-C(8B)	104.9(12)	C(36)-C(31)-C(32)	109.79(17)
N(2)-C(9B)-H(9A1)	110.8	C(36)-C(31)-P	115.07(13)
C(8B)-C(9B)-H(9A1)	110.8	C(32)-C(31)-P	108.96(13)
N(2)-C(9B)-H(9A2)	110.8	C(36)-C(31)-H(31)	107.6
C(8B)-C(9B)-H(9A2)	110.8	C(32)-C(31)-H(31)	107.6
H(9A1)-C(9B)-H(9A2)	108.8	P-C(31)-H(31)	107.6
C(10B)-N(2)-C(11B)	107.5(11)	C(33)-C(32)-C(31)	111.70(17)
C(10B)-N(2)-C(9B)	108.5(10)	C(33)-C(32)-H(32A)	109.3
C(11B)-N(2)-C(9B)	105.4(9)	C(31)-C(32)-H(32A)	109.3
C(10B)-N(2)-Ni	107.2(7)	C(33)-C(32)-H(32B)	109.3
C(11B)-N(2)-Ni	120.1(10)	C(31)-C(32)-H(32B)	109.3
C(9B)-N(2)-Ni	107.7(8)	H(32A)-C(32)-H(32B)	107.9
N(2)-C(10B)-H(10D)	109.5	C(34)-C(33)-C(32)	111.61(19)
N(2)-C(10B)-H(10E)	109.5	C(34)-C(33)-H(33A)	109.3
H(10D)-C(10B)-H(10E)	109.5	C(32)-C(33)-H(33A)	109.3
N(2)-C(10B)-H(10F)	109.5	C(34)-C(33)-H(33B)	109.3
H(10D)-C(10B)-H(10F)	109.5	C(32)-C(33)-H(33B)	109.3
H(10E)-C(10B)-H(10F)	109.5	H(33A)-C(33)-H(33B)	108.0
N(2)-C(11B)-H(11D)	109.5	C(33)-C(34)-C(35)	110.7(2)
N(2)-C(11B)-H(11E)	109.5	C(33)-C(34)-H(34A)	109.5
H(11D)-C(11B)-H(11E)	109.5	C(35)-C(34)-H(34A)	109.5
N(2)-C(11B)-H(11F)	109.5	C(33)-C(34)-H(34B)	109.5
H(11D)-C(11B)-H(11F)	109.5	C(35)-C(34)-H(34B)	109.5
H(11E)-C(11B)-H(11F)	109.5	H(34A)-C(34)-H(34B)	108.1
C(81)-B-C(71)	110.92(15)	C(34)-C(35)-C(36)	111.5(2)
C(81)-B-C(61)	109.02(15)	C(34)-C(35)-H(35A)	109.3
C(71)-B-C(61)	106.60(15)	C(36)-C(35)-H(35A)	109.3
C(81)-B-C(51)	110.95(16)	C(34)-C(35)-H(35B)	109.3
C(71)-B-C(51)	108.07(15)	C(36)-C(35)-H(35B)	109.3
C(61)-B-C(51)	111.20(15)	H(35A)-C(35)-H(35B)	108.0
C(22)-C(21)-C(26)	109.32(15)	C(31)-C(36)-C(35)	111.31(18)
C(22)-C(21)-P	112.57(13)	C(31)-C(36)-H(36A)	109.4
C(26)-C(21)-P	118.28(13)	C(35)-C(36)-H(36A)	109.4
C(22)-C(21)-H(21)	105.2	C(31)-C(36)-H(36B)	109.4
C(26)-C(21)-H(21)	105.2	C(35)-C(36)-H(36B)	109.4
P-C(21)-H(21)	105.2	H(36A)-C(36)-H(36B)	108.0
C(23)-C(22)-C(21)	110.18(17)	C(42)-C(41)-C(46)	109.92(16)
C(23)-C(22)-H(22A)	109.6	C(42)-C(41)-P	113.31(13)
C(21)-C(22)-H(22A)	109.6	C(46)-C(41)-P	117.31(13)
C(23)-C(22)-H(22B)	109.6	C(42)-C(41)-H(41)	105.0
C(21)-C(22)-H(22B)	109.6	C(46)-C(41)-H(41)	105.0
H(22A)-C(22)-H(22B)	108.1	P-C(41)-H(41)	105.0
C(24)-C(23)-C(22)	110.80(18)	C(43)-C(42)-C(41)	110.24(18)
C(24)-C(23)-H(23A)	109.5	C(43)-C(42)-H(42A)	109.6
C(22)-C(23)-H(23A)	109.5	C(41)-C(42)-H(42A)	109.6
C(24)-C(23)-H(23B)	109.5	C(43)-C(42)-H(42B)	109.6
C(22)-C(23)-H(23B)	109.5	C(41)-C(42)-H(42B)	109.6
H(23A)-C(23)-H(23B)	108.1	H(42A)-C(42)-H(42B)	108.1

C(42)-C(43)-C(44)	110.71(18)	C(65)-C(66)-C(61)	123.07(18)
C(42)-C(43)-H(43A)	109.5	C(65)-C(66)-H(66)	118.5
C(44)-C(43)-H(43A)	109.5	C(61)-C(66)-H(66)	118.5
C(42)-C(43)-H(43B)	109.5	C(76)-C(71)-C(72)	114.40(19)
C(44)-C(43)-H(43B)	109.5	C(76)-C(71)-B	124.37(17)
H(43A)-C(43)-H(43B)	108.1	C(72)-C(71)-B	121.19(18)
C(45)-C(44)-C(43)	111.23(17)	C(73)-C(72)-C(71)	123.2(2)
C(45)-C(44)-H(44A)	109.4	C(73)-C(72)-H(72)	118.4
C(43)-C(44)-H(44A)	109.4	C(71)-C(72)-H(72)	118.4
C(45)-C(44)-H(44B)	109.4	C(74)-C(73)-C(72)	120.4(2)
C(43)-C(44)-H(44B)	109.4	C(74)-C(73)-H(73)	119.8
H(44A)-C(44)-H(44B)	108.0	C(72)-C(73)-H(73)	119.8
C(44)-C(45)-C(46)	111.59(19)	C(73)-C(74)-C(75)	119.0(2)
C(44)-C(45)-H(45A)	109.3	C(73)-C(74)-H(74)	120.5
C(46)-C(45)-H(45A)	109.3	C(75)-C(74)-H(74)	120.5
C(44)-C(45)-H(45B)	109.3	C(74)-C(75)-C(76)	119.6(2)
C(46)-C(45)-H(45B)	109.3	C(74)-C(75)-H(75)	120.2
H(45A)-C(45)-H(45B)	108.0	C(76)-C(75)-H(75)	120.2
C(45)-C(46)-C(41)	110.00(16)	C(75)-C(76)-C(71)	123.42(19)
C(45)-C(46)-H(46A)	109.7	C(75)-C(76)-H(76)	118.3
C(41)-C(46)-H(46A)	109.7	C(71)-C(76)-H(76)	118.3
C(45)-C(46)-H(46B)	109.7	C(82)-C(81)-C(86)	114.52(19)
C(41)-C(46)-H(46B)	109.7	C(82)-C(81)-B	124.41(19)
H(46A)-C(46)-H(46B)	108.2	C(86)-C(81)-B	121.06(17)
C(52)-C(51)-C(56)	114.39(19)	C(83)-C(82)-C(81)	122.9(2)
C(52)-C(51)-B	124.07(18)	C(83)-C(82)-H(82)	118.6
C(56)-C(51)-B	121.54(18)	C(81)-C(82)-H(82)	118.6
C(51)-C(52)-C(53)	122.7(2)	C(84)-C(83)-C(82)	120.5(2)
C(51)-C(52)-H(52)	118.6	C(84)-C(83)-H(83)	119.8
C(53)-C(52)-H(52)	118.6	C(82)-C(83)-H(83)	119.8
C(54)-C(53)-C(52)	120.9(2)	C(83)-C(84)-C(85)	119.1(2)
C(54)-C(53)-H(53)	119.6	C(83)-C(84)-H(84)	120.5
C(52)-C(53)-H(53)	119.6	C(85)-C(84)-H(84)	120.5
C(55)-C(54)-C(53)	118.5(2)	C(84)-C(85)-C(86)	120.0(2)
C(55)-C(54)-H(54)	120.7	C(84)-C(85)-H(85)	120.0
C(53)-C(54)-H(54)	120.7	C(86)-C(85)-H(85)	120.0
C(54)-C(55)-C(56)	120.5(2)	C(85)-C(86)-C(81)	123.1(2)
C(54)-C(55)-H(55)	119.7	C(85)-C(86)-H(86)	118.5
C(56)-C(55)-H(55)	119.7	C(81)-C(86)-H(86)	118.5
C(55)-C(56)-C(51)	122.9(2)	Cl(1)-C(98)-Cl(2)	92.9(6)
C(55)-C(56)-H(56)	118.5	Cl(1)-C(98)-H(98A)	113.1
C(51)-C(56)-H(56)	118.5	Cl(2)-C(98)-H(98A)	113.1
C(62)-C(61)-C(66)	114.63(17)	Cl(1)-C(98)-H(98B)	113.1
C(62)-C(61)-B	122.05(16)	Cl(2)-C(98)-H(98B)	113.1
C(66)-C(61)-B	122.39(16)	H(98A)-C(98)-H(98B)	110.5
C(63)-C(62)-C(61)	122.73(19)	Cl(3)-C(99)-Cl(4)	93.4(6)
C(63)-C(62)-H(62)	118.6	Cl(3)-C(99)-H(99A)	113.0
C(61)-C(62)-H(62)	118.6	Cl(4)-C(99)-H(99A)	113.0
C(64)-C(63)-C(62)	120.4(2)	Cl(3)-C(99)-H(99B)	113.0
C(64)-C(63)-H(63)	119.8	Cl(4)-C(99)-H(99B)	113.0
C(62)-C(63)-H(63)	119.8	H(99A)-C(99)-H(99B)	110.4
C(65)-C(64)-C(63)	118.73(19)	Cl(6)-C(100)-Cl(5)	94.5(6)
C(65)-C(64)-H(64)	120.6	Cl(6)-C(100)-H(10G)	112.8
C(63)-C(64)-H(64)	120.6	Cl(5)-C(100)-H(10G)	112.8
C(64)-C(65)-C(66)	120.26(18)	Cl(6)-C(100)-H(10H)	112.8
C(64)-C(65)-H(65)	119.9	Cl(5)-C(100)-H(10H)	112.8
C(66)-C(65)-H(65)	119.9	H(10G)-C(100)-H(10H)	110.3

Table IV.30. Torsion angles [°] for $[(\eta^3:\eta^1\text{-Ind}(CH_2)_2NMe_2)(PCy_3)Ni]^+ [BPh_4]^-$ **(9)**

N(1)-Ni-P-C(41)	47.98(19)	N(2)-Ni-C(2)-C(1)	57.7(4)
C(2)-Ni-P-C(41)	-99.91(11)	C(3)-Ni-C(2)-C(1)	-116.71(18)
N(2)-Ni-P-C(41)	38.5(4)	P-Ni-C(2)-C(1)	-161.56(9)
C(1)-Ni-P-C(41)	-153.5(2)	C(7A)-Ni-C(2)-C(1)	-39.22(12)
C(3)-Ni-P-C(41)	-127.19(9)	C(3A)-Ni-C(2)-C(1)	-77.90(13)
C(7A)-Ni-P-C(41)	171.58(10)	C(1)-C(2)-C(3)-C(3A)	-12.9(2)
C(3A)-Ni-P-C(41)	-164.87(9)	Ni-C(2)-C(3)-C(3A)	-74.92(14)
N(1)-Ni-P-C(31)	-72.10(19)	C(1)-C(2)-C(3)-Ni	62.02(13)
C(2)-Ni-P-C(31)	140.00(10)	N(1)-Ni-C(3)-C(2)	-23.5(4)
N(2)-Ni-P-C(31)	-81.6(4)	N(2)-Ni-C(3)-C(2)	-9.2(6)
C(1)-Ni-P-C(31)	86.5(2)	C(1)-Ni-C(3)-C(2)	-39.14(12)
C(3)-Ni-P-C(31)	112.73(9)	P-Ni-C(3)-C(2)	147.92(11)
C(7A)-Ni-P-C(31)	51.49(10)	C(7A)-Ni-C(3)-C(2)	-80.55(13)
C(3A)-Ni-P-C(31)	75.05(9)	C(3A)-Ni-C(3)-C(2)	-112.75(17)
N(1)-Ni-P-C(21)	172.31(19)	N(1)-Ni-C(3)-C(3A)	89.2(3)
C(2)-Ni-P-C(21)	24.42(11)	C(2)-Ni-C(3)-C(3A)	112.75(17)
N(2)-Ni-P-C(21)	162.8(4)	N(2)-Ni-C(3)-C(3A)	103.5(6)
C(1)-Ni-P-C(21)	-29.1(2)	C(1)-Ni-C(3)-C(3A)	73.61(12)
C(3)-Ni-P-C(21)	-2.85(9)	P-Ni-C(3)-C(3A)	-99.33(11)
C(7A)-Ni-P-C(21)	-64.09(10)	C(7A)-Ni-C(3)-C(3A)	32.20(11)
C(3A)-Ni-P-C(21)	-40.54(9)	C(2)-C(3)-C(3A)-C(4)	-170.4(2)
N(1)-Ni-C(1)-C(2)	-133.2(2)	Ni-C(3)-C(3A)-C(4)	125.1(2)
N(2)-Ni-C(1)-C(2)	-124.2(4)	C(2)-C(3)-C(3A)-C(7A)	8.3(2)
C(3)-Ni-C(1)-C(2)	38.52(12)	Ni-C(3)-C(3A)-C(7A)	-56.17(14)
P-Ni-C(1)-C(2)	66.9(3)	C(2)-C(3)-C(3A)-Ni	64.50(13)
C(7A)-Ni-C(1)-C(2)	112.10(17)	N(1)-Ni-C(3A)-C(4)	104.3(4)
C(3A)-Ni-C(1)-C(2)	79.48(13)	C(2)-Ni-C(3A)-C(4)	-163.1(3)
N(1)-Ni-C(1)-C(8B)	-6.9(13)	N(2)-Ni-C(3A)-C(4)	115.3(6)
C(2)-Ni-C(1)-C(8B)	126.4(13)	C(1)-Ni-C(3A)-C(4)	150.9(3)
N(2)-Ni-C(1)-C(8B)	2.1(14)	C(3)-Ni-C(3A)-C(4)	-121.3(3)
C(3)-Ni-C(1)-C(8B)	164.9(13)	P-Ni-C(3A)-C(4)	-32.4(3)
P-Ni-C(1)-C(8B)	-166.8(13)	C(7A)-Ni-C(3A)-C(4)	115.3(3)
C(7A)-Ni-C(1)-C(8B)	-121.5(13)	N(1)-Ni-C(3A)-C(7A)	-10.9(3)
C(3A)-Ni-C(1)-C(8B)	-154.2(13)	C(2)-Ni-C(3A)-C(7A)	81.64(13)
N(1)-Ni-C(1)-C(7A)	114.7(2)	N(2)-Ni-C(3A)-C(7A)	0.0(6)
C(2)-Ni-C(1)-C(7A)	-112.10(17)	C(1)-Ni-C(3A)-C(7A)	35.61(12)
N(2)-Ni-C(1)-C(7A)	123.7(4)	C(3)-Ni-C(3A)-C(7A)	123.40(17)
C(3)-Ni-C(1)-C(7A)	-73.57(13)	P-Ni-C(3A)-C(7A)	-147.68(11)
P-Ni-C(1)-C(7A)	-45.2(3)	N(1)-Ni-C(3A)-C(3)	-134.3(3)
C(3A)-Ni-C(1)-C(7A)	-32.61(12)	C(2)-Ni-C(3A)-C(3)	-41.76(12)
N(1)-Ni-C(1)-C(8)	-12.4(4)	N(2)-Ni-C(3A)-C(3)	-123.4(6)
C(2)-Ni-C(1)-C(8)	120.8(4)	C(1)-Ni-C(3A)-C(3)	-87.79(13)
N(2)-Ni-C(1)-C(8)	-3.4(5)	P-Ni-C(3A)-C(3)	88.92(11)
C(3)-Ni-C(1)-C(8)	159.3(4)	C(7A)-Ni-C(3A)-C(3)	-123.40(17)
P-Ni-C(1)-C(8)	-172.3(4)	C(7A)-C(3A)-C(4)-C(5)	0.9(3)
C(7A)-Ni-C(1)-C(8)	-127.1(4)	C(3)-C(3A)-C(4)-C(5)	179.5(2)
C(3A)-Ni-C(1)-C(8)	-159.7(4)	Ni-C(3A)-C(4)-C(5)	-93.7(3)
C(8B)-C(1)-C(2)-C(3)	-163.5(9)	C(3A)-C(4)-C(5)-C(6)	0.4(4)
C(7A)-C(1)-C(2)-C(3)	12.5(2)	C(4)-C(5)-C(6)-C(7)	-1.1(4)
C(8)-C(1)-C(2)-C(3)	-166.3(3)	C(5)-C(6)-C(7)-C(7A)	0.4(4)
Ni-C(1)-C(2)-C(3)	-62.99(13)	C(6)-C(7)-C(7A)-C(3A)	0.9(3)
C(8B)-C(1)-C(2)-Ni	-100.6(9)	C(6)-C(7)-C(7A)-C(1)	-179.1(2)
C(7A)-C(1)-C(2)-Ni	75.51(13)	C(6)-C(7)-C(7A)-Ni	97.1(3)
C(8)-C(1)-C(2)-Ni	-103.3(3)	C(4)-C(3A)-C(7A)-C(7)	-1.6(3)
N(1)-Ni-C(2)-C(3)	167.0(2)	C(3)-C(3A)-C(7A)-C(7)	179.4(2)
N(2)-Ni-C(2)-C(3)	174.4(4)	Ni-C(3A)-C(7A)-C(7)	130.6(2)
C(1)-Ni-C(2)-C(3)	116.71(18)	C(4)-C(3A)-C(7A)-C(1)	178.38(18)
P-Ni-C(2)-C(3)	-44.85(15)	C(3)-C(3A)-C(7A)-C(1)	-0.6(2)
C(7A)-Ni-C(2)-C(3)	77.49(13)	Ni-C(3A)-C(7A)-C(1)	-49.37(13)
C(3A)-Ni-C(2)-C(3)	38.81(12)	C(4)-C(3A)-C(7A)-Ni	-132.25(19)
N(1)-Ni-C(2)-C(1)	50.3(2)	C(3)-C(3A)-C(7A)-Ni	48.82(13)

C(2)-C(1)-C(7A)-C(7)	172.7(2)	C(8B)-C(9B)-N(2)-Ni	48.7(13)
C(8B)-C(1)-C(7A)-C(7)	-10.8(9)	N(1)-Ni-N(2)-C(10B)	-177(4)
C(8)-C(1)-C(7A)-C(7)	-8.5(4)	C(2)-Ni-N(2)-C(10B)	54.0(8)
Ni-C(1)-C(7A)-C(7)	-121.8(2)	C(1)-Ni-N(2)-C(10B)	87.6(8)
C(2)-C(1)-C(7A)-C(3A)	-7.3(2)	C(3)-Ni-N(2)-C(10B)	60.1(11)
C(8B)-C(1)-C(7A)-C(3A)	169.1(8)	P-Ni-N(2)-C(10B)	-95.4(8)
C(8)-C(1)-C(7A)-C(3A)	171.5(3)	C(7A)-Ni-N(2)-C(10B)	118.8(7)
Ni-C(1)-C(7A)-C(3A)	58.19(15)	C(3A)-Ni-N(2)-C(10B)	118.8(7)
C(2)-C(1)-C(7A)-Ni	-65.52(12)	N(1)-Ni-N(2)-C(11B)	-54(3)
C(8B)-C(1)-C(7A)-Ni	110.9(8)	C(2)-Ni-N(2)-C(11B)	176.9(9)
C(8)-C(1)-C(7A)-Ni	113.3(3)	C(1)-Ni-N(2)-C(11B)	-149.5(10)
N(1)-Ni-C(7A)-C(7)	54.8(3)	C(3)-Ni-N(2)-C(11B)	-177.0(6)
C(2)-Ni-C(7A)-C(7)	163.0(3)	P-Ni-N(2)-C(11B)	27.5(11)
N(2)-Ni-C(7A)-C(7)	63.0(5)	C(7A)-Ni-N(2)-C(11B)	-118.3(9)
C(1)-Ni-C(7A)-C(7)	120.6(3)	C(3A)-Ni-N(2)-C(11B)	-118.3(9)
C(3)-Ni-C(7A)-C(7)	-151.8(3)	N(1)-Ni-N(2)-C(9B)	66(3)
P-Ni-C(7A)-C(7)	-73.4(3)	C(2)-Ni-N(2)-C(9B)	-62.5(8)
C(3A)-Ni-C(7A)-C(7)	-117.0(3)	C(1)-Ni-N(2)-C(9B)	-29.0(7)
N(1)-Ni-C(7A)-C(3A)	171.9(2)	C(3)-Ni-N(2)-C(9B)	-56.5(11)
C(2)-Ni-C(7A)-C(3A)	-79.94(13)	P-Ni-N(2)-C(9B)	148.0(6)
N(2)-Ni-C(7A)-C(3A)	-180.0(4)	C(7A)-Ni-N(2)-C(9B)	2.2(8)
C(1)-Ni-C(7A)-C(3A)	-122.40(18)	C(3A)-Ni-N(2)-C(9B)	2.2(11)
C(3)-Ni-C(7A)-C(3A)	-34.79(12)	C(41)-P-C(21)-C(22)	53.43(15)
P-Ni-C(7A)-C(3A)	43.68(14)	C(31)-P-C(21)-C(22)	164.26(13)
N(1)-Ni-C(7A)-C(1)	-65.7(2)	Ni-P-C(21)-C(22)	-73.04(14)
C(2)-Ni-C(7A)-C(1)	42.45(12)	C(41)-P-C(21)-C(26)	-75.67(16)
N(2)-Ni-C(7A)-C(1)	-57.6(4)	C(31)-P-C(21)-C(26)	35.16(17)
C(3)-Ni-C(7A)-C(1)	87.61(13)	Ni-P-C(21)-C(26)	157.86(13)
P-Ni-C(7A)-C(1)	166.07(10)	C(26)-C(21)-C(22)-C(23)	-59.3(2)
C(3A)-Ni-C(7A)-C(1)	122.40(18)	P-C(21)-C(22)-C(23)	167.15(14)
C(2)-C(1)-C(8)-C(9)	66.4(5)	C(21)-C(22)-C(23)-C(24)	58.2(2)
C(8B)-C(1)-C(8)-C(9)	-90(12)	C(22)-C(23)-C(24)-C(25)	-55.5(3)
C(7A)-C(1)-C(8)-C(9)	-112.2(5)	C(23)-C(24)-C(25)-C(26)	54.6(3)
Ni-C(1)-C(8)-C(9)	-13.2(6)	C(24)-C(25)-C(26)-C(21)	-56.0(2)
C(1)-C(8)-C(9)-N(1)	43.5(6)	C(22)-C(21)-C(26)-C(25)	57.8(2)
C(8)-C(9)-N(1)-C(10)	179.6(4)	P-C(21)-C(26)-C(25)	-171.60(14)
C(8)-C(9)-N(1)-C(11)	65.3(5)	C(41)-P-C(31)-C(36)	-54.99(17)
C(8)-C(9)-N(1)-Ni	-53.0(4)	C(21)-P-C(31)-C(36)	-169.37(16)
C(2)-Ni-N(1)-C(10)	125.0(4)	Ni-P-C(31)-C(36)	69.82(16)
N(2)-Ni-N(1)-C(10)	72(3)	C(41)-P-C(31)-C(32)	-178.76(14)
C(1)-Ni-N(1)-C(10)	155.2(5)	C(21)-P-C(31)-C(32)	66.85(15)
C(3)-Ni-N(1)-C(10)	140.8(3)	Ni-P-C(31)-C(32)	-53.96(15)
P-Ni-N(1)-C(10)	-30.2(5)	C(36)-C(31)-C(32)-C(33)	55.4(2)
C(7A)-Ni-N(1)-C(10)	-170.9(4)	P-C(31)-C(32)-C(33)	-177.73(16)
C(3A)-Ni-N(1)-C(10)	-164.8(3)	C(31)-C(32)-C(33)-C(34)	-55.6(3)
C(2)-Ni-N(1)-C(11)	-111.7(3)	C(32)-C(33)-C(34)-C(35)	55.1(3)
N(2)-Ni-N(1)-C(11)	-165(4)	C(33)-C(34)-C(35)-C(36)	-55.7(3)
C(1)-Ni-N(1)-C(11)	-81.6(3)	C(32)-C(31)-C(36)-C(35)	-55.8(3)
C(3)-Ni-N(1)-C(11)	-96.0(4)	P-C(31)-C(36)-C(35)	-179.13(17)
P-Ni-N(1)-C(11)	93.0(3)	C(34)-C(35)-C(36)-C(31)	56.9(3)
C(7A)-Ni-N(1)-C(11)	-47.7(3)	C(31)-P-C(41)-C(42)	172.35(14)
C(3A)-Ni-N(1)-C(11)	-41.5(5)	C(21)-P-C(41)-C(42)	-78.41(15)
C(2)-Ni-N(1)-C(9)	4.8(4)	Ni-P-C(41)-C(42)	46.99(16)
N(2)-Ni-N(1)-C(9)	-48(3)	C(31)-P-C(41)-C(46)	-57.86(17)
C(1)-Ni-N(1)-C(9)	35.0(3)	C(21)-P-C(41)-C(46)	51.39(18)
C(3)-Ni-N(1)-C(9)	20.6(6)	Ni-P-C(41)-C(46)	176.78(13)
P-Ni-N(1)-C(9)	-150.4(3)	C(46)-C(41)-C(42)-C(43)	59.0(2)
C(7A)-Ni-N(1)-C(9)	68.8(3)	P-C(41)-C(42)-C(43)	-167.59(15)
C(3A)-Ni-N(1)-C(9)	75.0(4)	C(41)-C(42)-C(43)-C(44)	-57.8(3)
C(2)-C(1)-C(8B)-C(9B)	105.4(17)	C(42)-C(43)-C(44)-C(45)	55.9(3)
C(7A)-C(1)-C(8B)-C(9B)	-70(2)	C(43)-C(44)-C(45)-C(46)	-55.4(3)
C(8)-C(1)-C(8B)-C(9B)	131(13)	C(44)-C(45)-C(46)-C(41)	56.4(2)
Ni-C(1)-C(8B)-C(9B)	25(2)	C(42)-C(41)-C(46)-C(45)	-57.9(2)
C(1)-C(8B)-C(9B)-N(2)	-49(2)	P-C(41)-C(46)-C(45)	170.77(15)
C(8B)-C(9B)-N(2)-C(10B)	-67.0(13)	C(81)-B-C(51)-C(52)	21.9(3)
C(8B)-C(9B)-N(2)-C(11B)	178.1(13)	C(71)-B-C(51)-C(52)	143.7(2)

C(61)-B-C(51)-C(52)	-99.7(2)	C(61)-B-C(71)-C(76)	10.4(2)
C(81)-B-C(51)-C(56)	-158.59(17)	C(51)-B-C(71)-C(76)	130.07(19)
C(71)-B-C(51)-C(56)	-36.8(2)	C(81)-B-C(71)-C(72)	69.8(2)
C(61)-B-C(51)-C(56)	79.9(2)	C(61)-B-C(71)-C(72)	-171.66(18)
C(56)-C(51)-C(52)-C(53)	-1.5(4)	C(51)-B-C(71)-C(72)	-52.0(2)
B-C(51)-C(52)-C(53)	178.1(2)	C(76)-C(71)-C(72)-C(73)	0.8(3)
C(51)-C(52)-C(53)-C(54)	0.5(5)	B-C(71)-C(72)-C(73)	-177.3(2)
C(52)-C(53)-C(54)-C(55)	0.7(5)	C(71)-C(72)-C(73)-C(74)	-0.2(4)
C(53)-C(54)-C(55)-C(56)	-0.8(4)	C(72)-C(73)-C(74)-C(75)	-0.4(4)
C(54)-C(55)-C(56)-C(51)	-0.3(3)	C(73)-C(74)-C(75)-C(76)	0.3(4)
C(52)-C(51)-C(56)-C(55)	1.4(3)	C(74)-C(75)-C(76)-C(71)	0.4(3)
B-C(51)-C(56)-C(55)	-178.24(18)	C(72)-C(71)-C(76)-C(75)	-0.9(3)
C(81)-B-C(61)-C(62)	29.3(2)	B-C(71)-C(76)-C(75)	177.11(19)
C(71)-B-C(61)-C(62)	-90.5(2)	C(71)-B-C(81)-C(82)	-9.1(3)
C(51)-B-C(61)-C(62)	151.93(17)	C(61)-B-C(81)-C(82)	-126.21(19)
C(81)-B-C(61)-C(66)	-162.40(17)	C(51)-B-C(81)-C(82)	111.0(2)
C(71)-B-C(61)-C(66)	77.8(2)	C(71)-B-C(81)-C(86)	170.10(17)
C(51)-B-C(61)-C(66)	-39.8(2)	C(61)-B-C(81)-C(86)	53.0(2)
C(66)-C(61)-C(62)-C(63)	-3.8(3)	C(51)-B-C(81)-C(86)	-69.8(2)
B-C(61)-C(62)-C(63)	165.38(19)	C(86)-C(81)-C(82)-C(83)	0.9(3)
C(61)-C(62)-C(63)-C(64)	1.2(3)	B-C(81)-C(82)-C(83)	-179.84(19)
C(62)-C(63)-C(64)-C(65)	1.6(3)	C(81)-C(82)-C(83)-C(84)	0.2(3)
C(63)-C(64)-C(65)-C(66)	-1.7(3)	C(82)-C(83)-C(84)-C(85)	-0.4(4)
C(64)-C(65)-C(66)-C(61)	-1.1(3)	C(83)-C(84)-C(85)-C(86)	-0.5(4)
C(62)-C(61)-C(66)-C(65)	3.7(3)	C(84)-C(85)-C(86)-C(81)	1.7(4)
B-C(61)-C(66)-C(65)	-165.37(17)	C(82)-C(81)-C(86)-C(85)	-1.8(3)
C(81)-B-C(71)-C(76)	-108.1(2)	B-C(81)-C(86)-C(85)	178.9(2)

Voltammogrammes des complexes **1-9** et du $FeCp_2$,

$(\eta^3:\eta^0\text{-Ind}(CH_2)_2NMe_2)Ni(PPh_3)Cl$

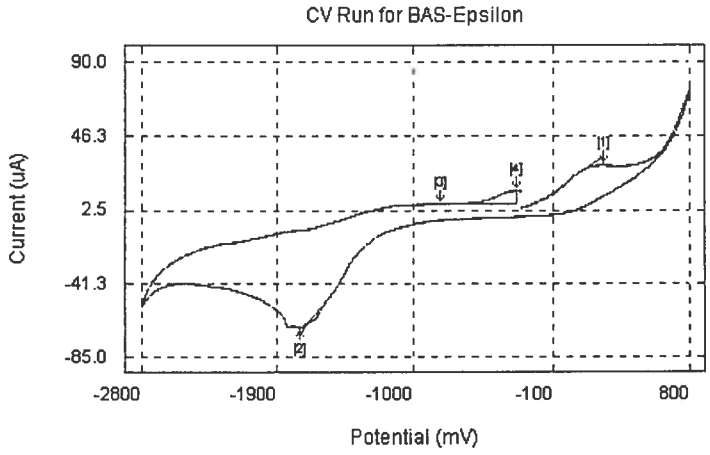

$(\eta^3:\eta^0\text{-Ind}(CH_2)_2NMe_2)Ni(PMe_3)Cl$

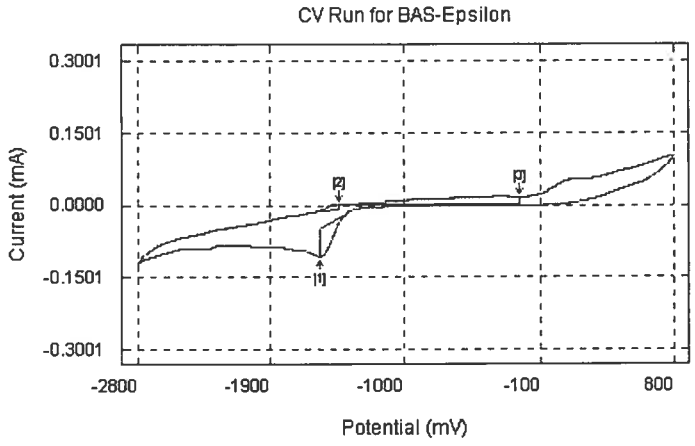

$(\eta^3:\eta^0\text{-Ind}(CH_2)_2NMe_2)Ni(PCy_3)Cl$

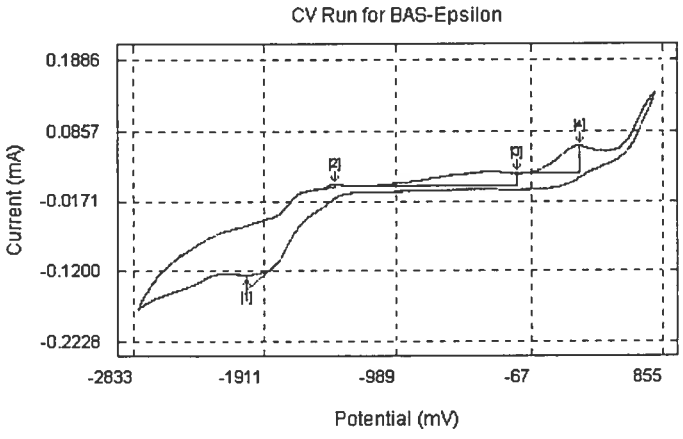

$(\eta^3:\eta^0\text{-Ind}(CH_2)_2NMe_2)Ni(PPh_3)Me$

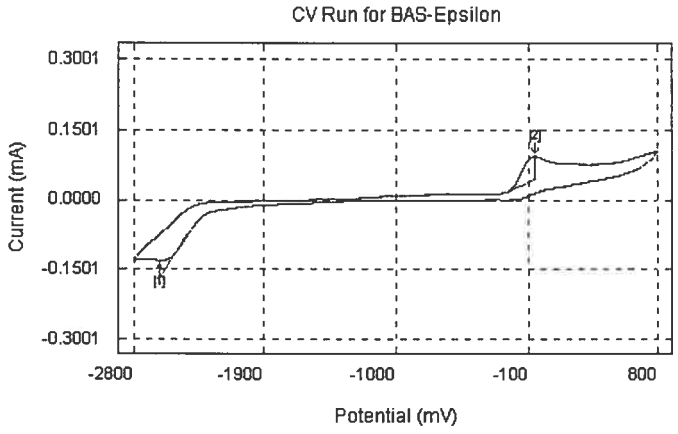

$(\eta^3:\eta^0\text{-Ind}(CH_2)_2NMe_2)Ni(PPh_3)CCPh$

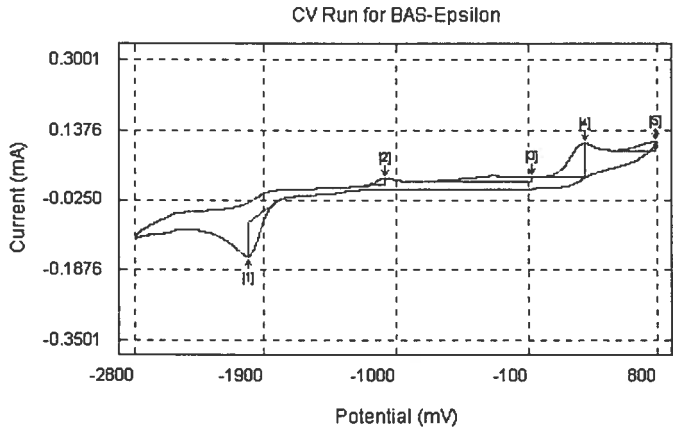

$(\eta^3:\eta^0\text{-Ind}(CH_2)_2NMe_2)Ni(PMe_3)Me$

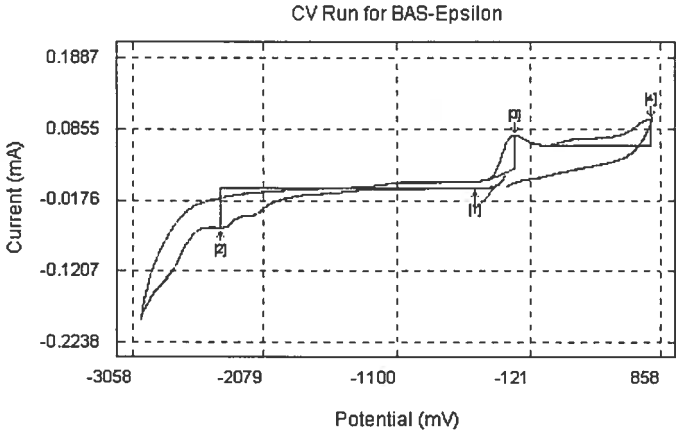

$[(\eta^3:\eta^1\text{-Ind}(CH_2)_2NMe_2)Ni(PPh_3)]^+$

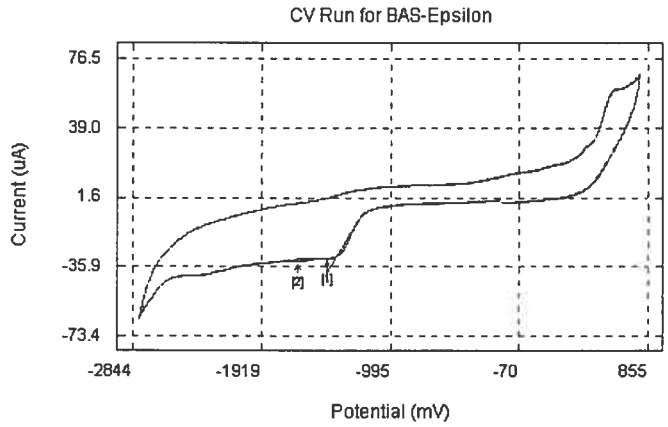

$[(\eta^3:\eta^1\text{-Ind}(CH_2)_2NMe_2)Ni(PMe_3)]^+$

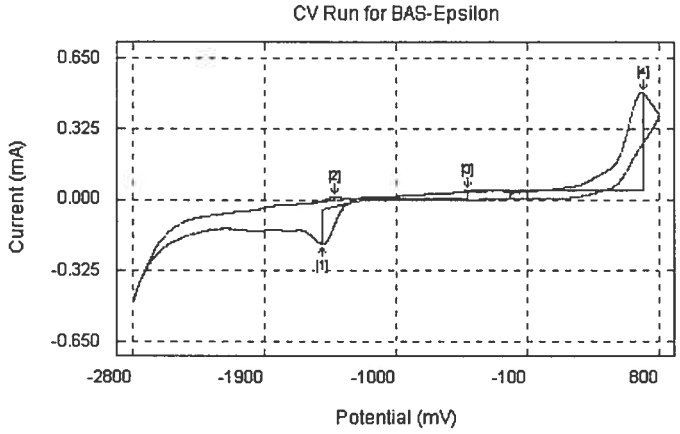

$[(\eta^3:\eta^1\text{-Ind}(CH_2)_2NMe_2)Ni(PCy_3)]^+$

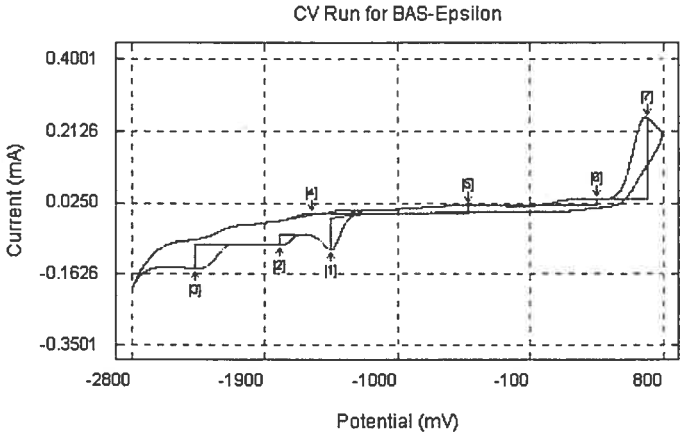

Annexe 5

Données cristallographiques supplémentaires, chapitre 7

Table V.1. Crystal data and structure refinement for $(\eta^3:\eta^0\text{-}Ind(CH_2)_2PPh_2BH_3)(PPh_3)NiCl$

Empirical formula	C41 H38 B Cl Ni P2
Formula weight	697.62
Temperature	293(2)K
Wavelength	1.54178 Å
Crystal system	Triclinic
Space group	P-1
Unit cell dimensions	a = 8.952(5) Å α = 84.66(5)° b = 13.245(9) Å β = 74.67(4)° c = 15.670(8) Å γ = 81.02(5)°
Volume	1767.3(18)Å^3
Z	2
Density (calculated)	1.311 Mg/m^3
Absorption coefficient	2.548 mm^{-1}
F(000)	728
Crystal size	0.31 x 0.19 x 0.04 mm
Theta range for data collection	2.93 to 70.12°
Index ranges	$0 \le h \le 10$, $-15 \le k \le 16$, $-18 \le \ell \le 19$
Reflections collected	6682
Independent reflections	6682
Absorption correction	None
Max. and min. transmission	0.9067 and 0.5889
Refinement method	Full-matrix least-squares on F^2
Data / restraints / parameters	6682 / 0 / 416
Goodness-of-fit on F^2	0.691
Final R indices [I>2sigma(I)]	R_1 = 0.0610, wR_2 = 0.1256
R indices (all data)	R_1 = 0.1851, wR_2 = 0.1638
Largest diff. peak and hole	0.340 and -0.651 e/Å^3

Table V.2. Atomic coordinates (x 10^4) and equivalent isotropic displacement parameters ($Å^2$ x 10^3) for $(\eta^3:\eta^0\text{-Ind}(CH_2)_2PPh_2BH_3)(PPh_3)NiCl$

U_{eq} is defined as one third of the trace of the orthogonalized Uij tensor.

	x	y	z	U_{eq}
Ni	6615(1)	2556(1)	5309(1)	65(1)
Cl	9068(2)	2742(2)	5024(1)	91(1)
P(1)	5682(2)	3318(1)	6551(1)	58(1)
P(2)	8990(2)	2407(2)	1574(1)	68(1)
C(1)	6897(8)	1680(5)	4180(5)	61(2)
C(2)	5432(8)	2340(6)	4397(5)	75(2)
C(3)	4646(9)	2005(6)	5263(5)	72(2)
C(3A)	5422(9)	1084(6)	5539(5)	66(2)
C(4)	5098(9)	403(6)	6263(5)	76(2)
C(5)	6189(11)	-437(7)	6317(5)	85(3)
C(6)	7582(10)	-642(6)	5687(6)	82(2)
C(7)	7942(9)	17(6)	4946(5)	69(2)
C(7A)	6868(9)	862(6)	4875(5)	63(2)
C(8)	8165(8)	1681(5)	3338(4)	75(2)
C(9)	7933(8)	2659(5)	2716(4)	75(2)
C(10)	8039(10)	1405(6)	1341(4)	65(2)
C(11)	8931(10)	468(7)	1099(4)	80(2)
C(12)	8215(12)	-327(7)	971(5)	95(3)
C(13)	6672(15)	-219(9)	1052(6)	112(4)
C(14)	5769(12)	701(9)	1294(6)	101(3)
C(15)	6463(10)	1495(7)	1424(5)	89(3)
C(20)	8401(8)	3530(6)	938(5)	71(2)
C(21)	8497(9)	4482(7)	1155(5)	82(2)
C(22)	8092(9)	5365(6)	672(6)	89(3)
C(23)	7611(10)	5253(8)	-78(7)	108(3)
C(24)	7528(12)	4337(8)	-312(6)	131(4)
C(25)	7938(10)	3448(6)	165(5)	103(3)
C(30)	6330(8)	4520(5)	6607(5)	61(2)
C(31)	7248(8)	4977(5)	5884(5)	69(2)
C(32)	7827(9)	5868(6)	5915(6)	84(3)
C(33)	7408(10)	6377(6)	6709(7)	89(3)
C(34)	6486(9)	5938(6)	7434(6)	84(3)
C(35)	5871(8)	5061(6)	7401(5)	75(2)
C(40)	3572(7)	3586(6)	6883(4)	60(2)
C(41)	2833(9)	4466(6)	6518(4)	72(2)
C(42)	1252(10)	4633(7)	6632(5)	90(3)
C(43)	360(10)	3926(8)	7107(6)	102(3)
C(44)	1026(10)	3051(8)	7482(6)	107(3)
C(45)	2640(9)	2873(6)	7366(5)	79(2)
C(50)	6267(8)	2505(5)	7467(5)	57(2)
C(51)	5475(8)	2695(5)	8352(5)	72(2)
C(52)	5980(10)	2043(6)	9016(5)	84(3)
C(53)	7148(10)	1277(7)	8803(6)	91(3)
C(54)	7916(9)	1082(6)	7937(6)	94(3)
C(55)	7420(8)	1728(5)	7273(5)	70(2)
B	11204(9)	2085(7)	1395(6)	100(3)

Table V.3. Hydrogen coordinates (x 10^4) and isotropic displacement parameters ($Å^2$ x 10^3) for (η^3:η^0-Ind$(CH_2)_2PPh_2BH_3$)(PPh_3)NiCl

	x	y	z	U_{eq}
H(2)	5072	2876	4043	90
H(3)	3732	2353	5603	86
H(4)	4167	509	6702	91
H(5)	5975	-894	6807	102
H(6)	8280	-1222	5759	98
H(7)	8875	-108	4512	82
H(8A)	8190	1077	3025	90
H(8B)	9164	1642	3480	90
H(9A)	8315	3222	2909	90
H(9B)	6829	2853	2752	90
H(11)	10008	382	1024	96
H(12)	8815	-956	824	114
H(13)	6213	-762	945	135
H(14)	4693	778	1369	121
H(15)	5850	2118	1573	107
H(21)	8851	4544	1653	98
H(22)	8143	6009	846	106
H(23)	7343	5829	-422	130
H(24)	7182	4284	-814	158
H(25)	7906	2810	-27	124
H(31)	7494	4669	5345	82
H(32)	8492	6135	5412	101
H(33)	7754	6997	6737	107
H(34)	6264	6243	7973	101
H(35)	5156	4820	7894	91
H(41)	3435	4949	6190	86
H(42)	786	5226	6387	108
H(43)	-717	4037	7178	123
H(44)	402	2579	7811	129
H(45)	3097	2277	7611	95
H(51)	4655	3226	8493	86
H(52)	5494	2149	9609	100
H(53)	7453	860	9255	109
H(54)	8728	545	7798	113
H(55)	7910	1611	6682	84
H(0A)	11683	1977	780	151
H(0B)	11438	1475	1744	151
H(0C)	11605	2642	1572	151

Table V.4. Anisotropic parameters ($Å^2$ x 10^3) for (η^3:η^0-$Ind(CH_2)_2PPh_2BH_3)(PPh_3)NiCl$

The anisotropic displacement factor exponent takes the form:

$-2\pi^2$ [h^2 a^{*2} U_{11} + ... + 2 h k a* b* U_{12}]

	U11	U22	U33	U23	U13	U12
Ni	67(1)	80(1)	53(1)	4(1)	-22(1)	-19(1)
Cl	75(1)	107(2)	94(2)	-7(1)	-15(1)	-37(1)
P(1)	59(1)	65(1)	54(1)	7(1)	-22(1)	-16(1)
P(2)	84(2)	73(1)	54(1)	4(1)	-26(1)	-17(1)
C(1)	69(5)	54(5)	62(5)	-17(4)	-27(4)	9(4)
C(2)	69(5)	96(6)	73(5)	-10(5)	-47(4)	1(5)
C(3)	83(6)	86(6)	55(5)	-18(4)	-19(4)	-31(5)
C(3A)	71(6)	80(6)	57(5)	5(4)	-23(4)	-34(5)
C(4)	80(6)	86(7)	65(5)	-9(5)	-8(5)	-37(5)
C(5)	101(7)	91(7)	68(6)	13(5)	-20(6)	-38(6)
C(6)	92(7)	74(6)	88(6)	8(5)	-38(5)	-20(5)
C(7)	76(6)	70(6)	62(5)	0(4)	-20(4)	-12(5)
C(7A)	74(6)	70(6)	58(5)	4(4)	-30(4)	-26(5)
C(8)	96(6)	85(6)	40(4)	6(4)	-20(4)	0(5)
C(9)	98(6)	73(5)	46(4)	-12(4)	-6(4)	0(5)
C(10)	74(6)	78(6)	44(4)	17(4)	-18(4)	-25(5)
C(11)	99(7)	88(7)	63(5)	8(5)	-36(5)	-23(6)
C(12)	135(9)	84(7)	76(6)	4(5)	-36(6)	-32(7)
C(13)	161(12)	129(10)	75(7)	28(7)	-47(8)	-96(9)
C(14)	98(8)	141(10)	73(6)	21(7)	-23(6)	-56(8)
C(15)	89(7)	115(8)	65(5)	7(5)	-11(5)	-41(6)
C(20)	80(6)	82(6)	57(5)	10(4)	-21(4)	-28(5)
C(21)	99(7)	93(7)	55(5)	5(5)	-17(5)	-29(6)
C(22)	102(7)	68(6)	86(6)	2(5)	-9(6)	-12(5)
C(23)	105(7)	110(9)	117(8)	51(7)	-52(6)	-29(7)
C(24)	209(12)	112(9)	116(8)	49(7)	-106(8)	-69(9)
C(25)	159(9)	86(7)	89(6)	25(5)	-70(6)	-41(6)
C(30)	58(5)	71(5)	64(5)	25(4)	-32(4)	-29(4)
C(31)	73(5)	61(5)	80(5)	11(4)	-31(4)	-21(4)
C(32)	79(6)	85(7)	97(7)	35(5)	-42(5)	-24(5)
C(33)	93(7)	74(6)	121(8)	28(6)	-64(6)	-30(5)
C(34)	104(7)	72(6)	94(7)	-7(5)	-56(6)	-9(5)
C(35)	83(6)	74(6)	74(6)	11(5)	-28(5)	-18(5)
C(40)	52(5)	91(6)	45(4)	-4(4)	-19(3)	-19(4)
C(41)	78(6)	87(6)	59(5)	-2(4)	-31(4)	-14(5)
C(42)	68(6)	126(8)	84(6)	-1(6)	-38(5)	-9(6)
C(43)	60(6)	169(11)	90(7)	-14(7)	-36(5)	-20(7)
C(44)	81(7)	162(10)	91(7)	11(7)	-25(6)	-58(7)
C(45)	72(6)	101(7)	73(5)	9(5)	-28(5)	-31(5)
C(50)	69(5)	45(4)	67(5)	11(4)	-35(4)	-17(4)
C(51)	82(6)	73(6)	66(5)	-6(4)	-33(5)	0(4)
C(52)	105(7)	99(7)	62(5)	12(5)	-42(5)	-33(6)
C(53)	89(7)	109(8)	83(7)	24(6)	-47(6)	-9(6)
C(54)	80(6)	102(7)	94(7)	16(6)	-32(6)	10(5)
C(55)	82(6)	66(5)	65(5)	13(4)	-33(4)	-2(5)
B	82(7)	116(9)	112(9)	18(7)	-47(7)	-15(7)

Table V.5. Bond lengths [Å] and angles [°] for $(\eta^3:\eta^0\text{-Ind}(CH_2)_2PPh_2BH_3)(PPh_3)NiCl$

Ni-C(3)	2.031(7)	C(20)-C(21)	1.357(9)
Ni-C(2)	2.054(6)	C(20)-C(25)	1.399(9)
Ni-C(1)	2.143(7)	C(21)-C(22)	1.387(9)
Ni-Cl	2.170(2)	C(21)-H(21)	0.9300
Ni-P(1)	2.179(3)	C(22)-C(23)	1.382(10)
Ni-C(3A)	2.321(7)	C(22)-H(22)	0.9300
Ni-C(7A)	2.365(8)	C(23)-C(24)	1.318(11)
P(1)-C(30)	1.793(7)	C(23)-H(23)	0.9300
P(1)-C(40)	1.808(7)	C(24)-C(25)	1.387(10)
P(1)-C(50)	1.851(6)	C(24)-H(24)	0.9300
P(2)-C(20)	1.800(7)	C(25)-H(25)	0.9300
P(2)-C(10)	1.796(7)	C(30)-C(31)	1.364(8)
P(2)-C(9)	1.824(6)	C(30)-C(35)	1.426(9)
P(2)-B	1.912(8)	C(31)-C(32)	1.370(9)
C(1)-C(2)	1.435(8)	C(31)-H(31)	0.9300
C(1)-C(7A)	1.462(8)	C(32)-C(33)	1.406(10)
C(1)-C(8)	1.495(8)	C(32)-H(32)	0.9300
C(2)-C(3)	1.419(8)	C(33)-C(34)	1.357(9)
C(2)-H(2)	0.9300	C(33)-H(33)	0.9300
C(3)-C(3A)	1.397(9)	C(34)-C(35)	1.373(8)
C(3)-H(3)	0.9300	C(34)-H(34)	0.9300
C(3A)-C(4)	1.379(9)	C(35)-H(35)	0.9300
C(3A)-C(7A)	1.439(9)	C(40)-C(41)	1.399(8)
C(4)-C(5)	1.373(9)	C(40)-C(45)	1.393(8)
C(4)-H(4)	0.9300	C(41)-C(42)	1.364(9)
C(5)-C(6)	1.377(9)	C(41)-H(41)	0.9300
C(5)-H(5)	0.9300	C(42)-C(43)	1.364(10)
C(6)-C(7)	1.383(9)	C(42)-H(42)	0.9300
C(6)-H(6)	0.9300	C(43)-C(44)	1.373(11)
C(7)-C(7A)	1.374(9)	C(43)-H(43)	0.9300
C(7)-H(7)	0.9300	C(44)-C(45)	1.393(9)
C(8)-C(9)	1.568(8)	C(44)-H(44)	0.9300
C(8)-H(8A)	0.9700	C(45)-H(45)	0.9300
C(8)-H(8B)	0.9700	C(50)-C(55)	1.334(8)
C(9)-H(9A)	0.9700	C(50)-C(51)	1.406(8)
C(9)-H(9B)	0.9700	C(51)-C(52)	1.412(9)
C(10)-C(11)	1.393(9)	C(51)-H(51)	0.9300
C(10)-C(15)	1.369(9)	C(52)-C(53)	1.334(10)
C(11)-C(12)	1.370(9)	C(52)-H(52)	0.9300
C(11)-H(11)	0.9300	C(53)-C(54)	1.377(10)
C(12)-C(13)	1.339(11)	C(53)-H(53)	0.9300
C(12)-H(12)	0.9300	C(54)-C(55)	1.404(9)
C(13)-C(14)	1.379(12)	C(54)-H(54)	0.9300
C(13)-H(13)	0.9300	C(55)-H(55)	0.9300
C(14)-C(15)	1.357(10)	B-H(0A)	0.9600
C(14)-H(14)	0.9300	B-H(0B)	0.9600
C(15)-H(15)	0.9300	B-H(0C)	0.9600
C(3)-Ni-C(2)	40.7(2)	P(1)-Ni-C(3A)	104.2(2)
C(3)-Ni-C(1)	66.0(3)	C(3)-Ni-C(7A)	62.0(3)
C(2)-Ni-C(1)	39.9(2)	C(2)-Ni-C(7A)	63.6(3)
C(3)-Ni-Cl	160.0(2)	C(1)-Ni-C(7A)	37.5(2)
C(2)-Ni-Cl	126.0(2)	Cl-Ni-C(7A)	99.6(2)
C(1)-Ni-Cl	94.7(2)	P(1)-Ni-C(7A)	135.14(19)
C(3)-Ni-P(1)	98.0(2)	C(3A)-Ni-C(7A)	35.7(2)
C(2)-Ni-P(1)	127.6(2)	C(30)-P(1)-C(40)	104.4(3)
C(1)-Ni-P(1)	164.0(2)	C(30)-P(1)-C(50)	104.3(3)
Cl-Ni-P(1)	101.09(9)	C(40)-P(1)-C(50)	106.1(3)
C(3)-Ni-C(3A)	36.7(2)	C(30)-P(1)-Ni	116.6(3)
C(2)-Ni-C(3A)	63.9(3)	C(40)-P(1)-Ni	114.5(2)
C(1)-Ni-C(3A)	62.8(3)	C(50)-P(1)-Ni	110.1(3)
Cl-Ni-C(3A)	130.5(2)	C(20)-P(2)-C(10)	106.2(3)

C(20)-P(2)-C(9)	104.4(3)	C(13)-C(12)-H(12)	119.3
C(10)-P(2)-C(9)	102.0(3)	C(11)-C(12)-H(12)	119.3
C(20)-P(2)-B	113.8(4)	C(12)-C(13)-C(14)	119.6(10)
C(10)-P(2)-B	115.0(4)	C(12)-C(13)-H(13)	120.2
C(9)-P(2)-B	114.1(4)	C(14)-C(13)-H(13)	120.2
C(2)-C(1)-C(7A)	108.0(7)	C(13)-C(14)-C(15)	119.5(10)
C(2)-C(1)-C(8)	128.3(7)	C(13)-C(14)-H(14)	120.3
C(7A)-C(1)-C(8)	123.0(6)	C(15)-C(14)-H(14)	120.3
C(2)-C(1)-Ni	66.7(4)	C(14)-C(15)-C(10)	122.0(9)
C(7A)-C(1)-Ni	79.5(4)	C(14)-C(15)-H(15)	119.0
C(8)-C(1)-Ni	127.2(5)	C(10)-C(15)-H(15)	119.0
C(3)-C(2)-C(1)	105.8(7)	C(21)-C(20)-C(25)	117.6(7)
C(3)-C(2)-Ni	68.8(4)	C(21)-C(20)-P(2)	121.2(6)
C(1)-C(2)-Ni	73.4(4)	C(25)-C(20)-P(2)	121.0(7)
C(3)-C(2)-H(2)	127.1	C(20)-C(21)-C(22)	123.1(8)
C(1)-C(2)-H(2)	127.1	C(20)-C(21)-H(21)	118.4
Ni-C(2)-H(2)	122.4	C(22)-C(21)-H(21)	118.4
C(2)-C(3)-C(3A)	111.4(7)	C(21)-C(22)-C(23)	117.4(8)
C(2)-C(3)-Ni	70.5(4)	C(21)-C(22)-H(22)	121.3
C(3A)-C(3)-Ni	83.0(5)	C(23)-C(22)-H(22)	121.3
C(2)-C(3)-H(3)	124.3	C(24)-C(23)-C(22)	120.7(9)
C(3A)-C(3)-H(3)	124.3	C(24)-C(23)-H(23)	119.7
Ni-C(3)-H(3)	113.8	C(22)-C(23)-H(23)	119.7
C(4)-C(3A)-C(7A)	118.1(8)	C(23)-C(24)-C(25)	122.3(9)
C(4)-C(3A)-C(3)	134.7(8)	C(23)-C(24)-H(24)	118.8
C(7A)-C(3A)-C(3)	107.2(7)	C(25)-C(24)-H(24)	118.8
C(4)-C(3A)-Ni	131.8(5)	C(24)-C(25)-C(20)	118.7(8)
C(7A)-C(3A)-Ni	73.8(4)	C(24)-C(25)-H(25)	120.6
C(3)-C(3A)-Ni	60.3(4)	C(20)-C(25)-H(25)	120.6
C(5)-C(4)-C(3A)	118.0(8)	C(31)-C(30)-C(35)	116.6(7)
C(5)-C(4)-H(4)	121.0	C(31)-C(30)-P(1)	121.7(6)
C(3A)-C(4)-H(4)	121.0	C(35)-C(30)-P(1)	121.7(5)
C(4)-C(5)-C(6)	123.8(8)	C(30)-C(31)-C(32)	123.1(8)
C(4)-C(5)-H(5)	118.1	C(30)-C(31)-H(31)	118.5
C(6)-C(5)-H(5)	118.1	C(32)-C(31)-H(31)	118.5
C(7)-C(6)-C(5)	119.9(8)	C(31)-C(32)-C(33)	119.6(8)
C(7)-C(6)-H(6)	120.0	C(31)-C(32)-H(32)	120.2
C(5)-C(6)-H(6)	120.0	C(33)-C(32)-H(32)	120.2
C(7A)-C(7)-C(6)	117.5(7)	C(34)-C(33)-C(32)	118.1(8)
C(7A)-C(7)-H(7)	121.3	C(34)-C(33)-H(33)	120.9
C(6)-C(7)-H(7)	121.3	C(32)-C(33)-H(33)	120.9
C(7)-C(7A)-C(3A)	122.7(7)	C(33)-C(34)-C(35)	122.3(8)
C(7)-C(7A)-C(1)	130.4(8)	C(33)-C(34)-H(34)	118.8
C(3A)-C(7A)-C(1)	106.9(7)	C(35)-C(34)-H(34)	118.8
C(7)-C(7A)-Ni	131.7(5)	C(34)-C(35)-C(30)	119.8(7)
C(3A)-C(7A)-Ni	70.5(4)	C(34)-C(35)-H(35)	120.1
C(1)-C(7A)-Ni	63.0(4)	C(30)-C(35)-H(35)	120.1
C(1)-C(8)-C(9)	112.6(6)	C(41)-C(40)-C(45)	117.8(7)
C(1)-C(8)-H(8A)	109.1	C(41)-C(40)-P(1)	118.8(6)
C(9)-C(8)-H(8A)	109.1	C(45)-C(40)-P(1)	122.5(6)
C(1)-C(8)-H(8B)	109.1	C(42)-C(41)-C(40)	121.7(7)
C(9)-C(8)-H(8B)	109.1	C(42)-C(41)-H(41)	119.1
H(8A)-C(8)-H(8B)	107.8	C(40)-C(41)-H(41)	119.1
C(8)-C(9)-P(2)	110.2(5)	C(41)-C(42)-C(43)	119.6(9)
C(8)-C(9)-H(9A)	109.6	C(41)-C(42)-H(42)	120.2
P(2)-C(9)-H(9A)	109.6	C(43)-C(42)-H(42)	120.2
C(8)-C(9)-H(9B)	109.6	C(44)-C(43)-C(42)	121.0(9)
P(2)-C(9)-H(9B)	109.6	C(44)-C(43)-H(43)	119.5
H(9A)-C(9)-H(9B)	108.1	C(42)-C(43)-H(43)	119.5
C(11)-C(10)-C(15)	117.7(8)	C(43)-C(44)-C(45)	119.7(8)
C(11)-C(10)-P(2)	118.7(7)	C(43)-C(44)-H(44)	120.2
C(15)-C(10)-P(2)	123.5(7)	C(45)-C(44)-H(44)	120.2
C(12)-C(11)-C(10)	119.7(8)	C(44)-C(45)-C(40)	120.2(8)
C(12)-C(11)-H(11)	120.1	C(44)-C(45)-H(45)	119.9
C(10)-C(11)-H(11)	120.1	C(40)-C(45)-H(45)	119.9
C(13)-C(12)-C(11)	121.5(10)	C(55)-C(50)-C(51)	120.9(7)

C(55)-C(50)-P(1)	119.0(6)	C(53)-C(54)-H(54)	121.4
C(51)-C(50)-P(1)	120.1(6)	C(55)-C(54)-H(54)	121.4
C(50)-C(51)-C(52)	117.1(7)	C(50)-C(55)-C(54)	121.8(7)
C(50)-C(51)-H(51)	121.5	C(50)-C(55)-H(55)	119.1
C(52)-C(51)-H(51)	121.5	C(54)-C(55)-H(55)	119.1
C(53)-C(52)-C(51)	120.8(8)	P(2)-B-H(0A)	109.5
C(53)-C(52)-H(52)	119.6	P(2)-B-H(0B)	109.5
C(51)-C(52)-H(52)	119.6	H(0A)-B-H(0B)	109.5
C(52)-C(53)-C(54)	122.4(8)	P(2)-B-H(0C)	109.5
C(52)-C(53)-H(53)	118.8	H(0A)-B-H(0C)	109.5
C(54)-C(53)-H(53)	118.8	H(0B)-B-H(0C)	109.5
C(53)-C(54)-C(55)	117.1(8)		

Table V.6. Torsion angles [°] for (η^3:η^0-Ind$(CH_2)_2PPh_2BH_3$)(PPh_3)NiCl

C(3)-Ni-P(1)-C(30)	-141.8(3)	Ni-C(3)-C(3A)-C(4)	121.0(8)
C(2)-Ni-P(1)-C(30)	-111.0(4)	C(2)-C(3)-C(3A)-C(7A)	6.7(8)
C(1)-Ni-P(1)-C(30)	-145.2(8)	Ni-C(3)-C(3A)-C(7A)	-59.2(5)
Cl-Ni-P(1)-C(30)	44.2(2)	C(2)-C(3)-C(3A)-Ni	65.9(5)
C(3A)-Ni-P(1)-C(30)	-178.7(3)	C(3)-Ni-C(3A)-C(4)	-125.2(11)
C(7A)-Ni-P(1)-C(30)	160.2(3)	C(2)-Ni-C(3A)-C(4)	-166.1(10)
C(3)-Ni-P(1)-C(40)	-19.6(4)	C(1)-Ni-C(3A)-C(4)	149.0(10)
C(2)-Ni-P(1)-C(40)	11.2(4)	Cl-Ni-C(3A)-C(4)	77.6(9)
C(1)-Ni-P(1)-C(40)	-23.0(8)	P(1)-Ni-C(3A)-C(4)	-40.8(9)
Cl-Ni-P(1)-C(40)	166.4(3)	C(7A)-Ni-C(3A)-C(4)	113.5(10)
C(3A)-Ni-P(1)-C(40)	-56.5(3)	C(3)-Ni-C(3A)-C(7A)	121.3(6)
C(7A)-Ni-P(1)-C(40)	-77.6(4)	C(2)-Ni-C(3A)-C(7A)	80.4(4)
C(3)-Ni-P(1)-C(50)	99.7(3)	C(1)-Ni-C(3A)-C(7A)	35.5(4)
C(2)-Ni-P(1)-C(50)	130.6(3)	Cl-Ni-C(3A)-C(7A)	-35.9(5)
C(1)-Ni-P(1)-C(50)	96.4(8)	P(1)-Ni-C(3A)-C(7A)	-154.3(4)
Cl-Ni-P(1)-C(50)	-74.2(2)	C(2)-Ni-C(3A)-C(3)	-40.9(4)
C(3A)-Ni-P(1)-C(50)	62.8(3)	C(1)-Ni-C(3A)-C(3)	-85.7(5)
C(7A)-Ni-P(1)-C(50)	41.8(3)	Cl-Ni-C(3A)-C(3)	-157.1(4)
C(3)-Ni-C(1)-C(2)	40.3(4)	P(1)-Ni-C(3A)-C(3)	84.4(4)
Cl-Ni-C(1)-C(2)	-145.3(4)	C(7A)-Ni-C(3A)-C(3)	-121.3(6)
P(1)-Ni-C(1)-C(2)	44.0(10)	C(7A)-C(3A)-C(4)-C(5)	1.4(10)
C(3A)-Ni-C(1)-C(2)	81.0(5)	C(3)-C(3A)-C(4)-C(5)	-178.8(7)
C(7A)-Ni-C(1)-C(2)	115.0(6)	Ni-C(3A)-C(4)-C(5)	-91.7(9)
C(3)-Ni-C(1)-C(7A)	-74.7(4)	C(3A)-C(4)-C(5)-C(6)	-0.5(12)
C(2)-Ni-C(1)-C(7A)	-115.0(6)	C(4)-C(5)-C(6)-C(7)	-0.2(12)
Cl-Ni-C(1)-C(7A)	99.7(4)	C(5)-C(6)-C(7)-C(7A)	0.1(10)
P(1)-Ni-C(1)-C(7A)	-71.0(9)	C(6)-C(7)-C(7A)-C(3A)	0.8(10)
C(3A)-Ni-C(1)-C(7A)	-34.0(4)	C(6)-C(7)-C(7A)-C(1)	-179.2(6)
C(3)-Ni-C(1)-C(8)	161.7(7)	C(6)-C(7)-C(7A)-Ni	93.0(8)
C(2)-Ni-C(1)-C(8)	121.3(8)	C(4)-C(3A)-C(7A)-C(7)	-1.6(10)
Cl-Ni-C(1)-C(8)	-24.0(6)	C(3)-C(3A)-C(7A)-C(7)	178.6(6)
P(1)-Ni-C(1)-C(8)	165.3(5)	Ni-C(3A)-C(7A)-C(7)	127.6(6)
C(3A)-Ni-C(1)-C(8)	-157.6(7)	C(4)-C(3A)-C(7A)-C(1)	178.5(6)
C(7A)-Ni-C(1)-C(8)	-123.7(8)	C(3)-C(3A)-C(7A)-C(1)	-1.4(7)
C(7A)-C(1)-C(2)-C(3)	8.0(7)	Ni-C(3A)-C(7A)-C(1)	-52.4(4)
C(8)-C(1)-C(2)-C(3)	178.6(6)	C(4)-C(3A)-C(7A)-Ni	-129.2(6)
Ni-C(1)-C(2)-C(3)	-61.6(4)	C(3)-C(3A)-C(7A)-Ni	51.0(4)
C(7A)-C(1)-C(2)-Ni	69.6(5)	C(2)-C(1)-C(7A)-C(7)	175.8(7)
C(8)-C(1)-C(2)-Ni	-119.9(7)	C(8)-C(1)-C(7A)-C(7)	4.7(11)
C(1)-Ni-C(2)-C(3)	114.8(7)	Ni-C(1)-C(7A)-C(7)	-123.1(7)
Cl-Ni-C(2)-C(3)	159.4(4)	C(2)-C(1)-C(7A)-C(3A)	-4.2(7)
P(1)-Ni-C(2)-C(3)	-51.2(5)	C(8)-C(1)-C(7A)-C(3A)	-175.3(6)
C(3A)-Ni-C(2)-C(3)	36.9(4)	Ni-C(1)-C(7A)-C(3A)	56.9(5)
C(7A)-Ni-C(2)-C(3)	76.9(5)	C(2)-C(1)-C(7A)-Ni	-61.1(4)
C(3)-Ni-C(2)-C(1)	-114.8(7)	C(8)-C(1)-C(7A)-Ni	127.8(7)
Cl-Ni-C(2)-C(1)	44.5(5)	C(3)-Ni-C(7A)-C(7)	-152.2(8)
P(1)-Ni-C(2)-C(1)	-166.0(3)	C(2)-Ni-C(7A)-C(7)	161.9(9)
C(3A)-Ni-C(2)-C(1)	-78.0(5)	C(1)-Ni-C(7A)-C(7)	121.4(9)
C(7A)-Ni-C(2)-C(1)	-38.0(4)	Cl-Ni-C(7A)-C(7)	36.3(8)
C(1)-C(2)-C(3)-C(3A)	-9.3(8)	P(1)-Ni-C(7A)-C(7)	-80.2(8)
Ni-C(2)-C(3)-C(3A)	-73.9(5)	C(3A)-Ni-C(7A)-C(7)	-116.8(9)
C(1)-C(2)-C(3)-Ni	64.7(4)	C(3)-Ni-C(7A)-C(3A)	-35.3(4)
C(1)-Ni-C(3)-C(2)	-39.6(4)	C(2)-Ni-C(7A)-C(3A)	-81.3(4)
Cl-Ni-C(3)-C(2)	-56.1(10)	C(1)-Ni-C(7A)-C(3A)	-121.8(6)
P(1)-Ni-C(3)-C(2)	141.4(4)	Cl-Ni-C(7A)-C(3A)	153.1(4)
C(3A)-Ni-C(3)-C(2)	-115.6(7)	P(1)-Ni-C(7A)-C(3A)	36.6(5)
C(7A)-Ni-C(3)-C(2)	-81.2(5)	C(3)-Ni-C(7A)-C(1)	86.4(4)
C(2)-Ni-C(3)-C(3A)	115.6(7)	C(2)-Ni-C(7A)-C(1)	40.5(4)
C(1)-Ni-C(3)-C(3A)	76.0(5)	Cl-Ni-C(7A)-C(1)	-85.1(4)
Cl-Ni-C(3)-C(3A)	59.5(9)	P(1)-Ni-C(7A)-C(1)	158.4(3)
P(1)-Ni-C(3)-C(3A)	-102.9(4)	C(3A)-Ni-C(7A)-C(1)	121.8(6)
C(7A)-Ni-C(3)-C(3A)	34.4(4)	C(2)-C(1)-C(8)-C(9)	12.0(10)
C(2)-C(3)-C(3A)-C(4)	-173.1(7)	C(7A)-C(1)-C(8)-C(9)	-178.7(6)

Ni-C(1)-C(8)-C(9)	-76.0(7)	Ni-P(1)-C(30)-C(35)	-176.3(5)
C(1)-C(8)-C(9)-P(2)	-157.7(5)	C(35)-C(30)-C(31)-C(32)	5.2(10)
C(20)-P(2)-C(9)-C(8)	172.7(5)	P(1)-C(30)-C(31)-C(32)	-176.7(5)
C(10)-P(2)-C(9)-C(8)	62.3(6)	C(30)-C(31)-C(32)-C(33)	-3.3(11)
B-P(2)-C(9)-C(8)	-62.4(6)	C(31)-C(32)-C(33)-C(34)	2.6(11)
C(20)-P(2)-C(10)-C(11)	130.1(6)	C(32)-C(33)-C(34)-C(35)	-4.5(12)
C(9)-P(2)-C(10)-C(11)	-120.8(6)	C(33)-C(34)-C(35)-C(30)	6.7(12)
B-P(2)-C(10)-C(11)	3.3(7)	C(31)-C(30)-C(35)-C(34)	-6.8(10)
C(20)-P(2)-C(10)-C(15)	-52.7(7)	P(1)-C(30)-C(35)-C(34)	175.1(5)
C(9)-P(2)-C(10)-C(15)	56.4(6)	C(30)-P(1)-C(40)-C(41)	45.9(6)
B-P(2)-C(10)-C(15)	-179.5(6)	C(50)-P(1)-C(40)-C(41)	155.7(5)
C(15)-C(10)-C(11)-C(12)	-1.3(10)	Ni-P(1)-C(40)-C(41)	-82.8(6)
P(2)-C(10)-C(11)-C(12)	176.0(5)	C(30)-P(1)-C(40)-C(45)	-145.4(6)
C(10)-C(11)-C(12)-C(13)	1.7(12)	C(50)-P(1)-C(40)-C(45)	-35.6(6)
C(11)-C(12)-C(13)-C(14)	-1.9(14)	Ni-P(1)-C(40)-C(45)	86.0(6)
C(12)-C(13)-C(14)-C(15)	1.9(14)	C(45)-C(40)-C(41)-C(42)	0.5(10)
C(13)-C(14)-C(15)-C(10)	-1.6(13)	P(1)-C(40)-C(41)-C(42)	169.8(6)
C(11)-C(10)-C(15)-C(14)	1.3(11)	C(40)-C(41)-C(42)-C(43)	-0.5(12)
P(2)-C(10)-C(15)-C(14)	-175.9(6)	C(41)-C(42)-C(43)-C(44)	0.7(13)
C(10)-P(2)-C(20)-C(21)	159.3(6)	C(42)-C(43)-C(44)-C(45)	-0.9(14)
C(9)-P(2)-C(20)-C(21)	51.9(7)	C(43)-C(44)-C(45)-C(40)	0.9(12)
B-P(2)-C(20)-C(21)	-73.1(8)	C(41)-C(40)-C(45)-C(44)	-0.7(10)
C(10)-P(2)-C(20)-C(25)	-25.4(8)	P(1)-C(40)-C(45)-C(44)	-169.6(6)
C(9)-P(2)-C(20)-C(25)	-132.9(7)	C(30)-P(1)-C(50)-C(55)	-110.0(6)
B-P(2)-C(20)-C(25)	102.1(7)	C(40)-P(1)-C(50)-C(55)	140.2(6)
C(25)-C(20)-C(21)-C(22)	3.0(12)	Ni-P(1)-C(50)-C(55)	15.8(6)
P(2)-C(20)-C(21)-C(22)	178.4(6)	C(30)-P(1)-C(50)-C(51)	71.5(6)
C(20)-C(21)-C(22)-C(23)	-1.8(13)	C(40)-P(1)-C(50)-C(51)	-38.4(6)
C(21)-C(22)-C(23)-C(24)	0.8(14)	Ni-P(1)-C(50)-C(51)	-162.7(5)
C(22)-C(23)-C(24)-C(25)	-1.2(17)	C(55)-C(50)-C(51)-C(52)	1.3(10)
C(23)-C(24)-C(25)-C(20)	2.4(16)	P(1)-C(50)-C(51)-C(52)	179.8(5)
C(21)-C(20)-C(25)-C(24)	-3.2(13)	C(50)-C(51)-C(52)-C(53)	-0.7(11)
P(2)-C(20)-C(25)-C(24)	-178.6(7)	C(51)-C(52)-C(53)-C(54)	0.1(13)
C(40)-P(1)-C(30)-C(31)	-121.7(6)	C(52)-C(53)-C(54)-C(55)	0.0(13)
C(50)-P(1)-C(30)-C(31)	127.2(6)	C(51)-C(50)-C(55)-C(54)	-1.3(11)
Ni-P(1)-C(30)-C(31)	5.7(6)	P(1)-C(50)-C(55)-C(54)	-179.8(5)
C(40)-P(1)-C(30)-C(35)	56.3(6)	C(53)-C(54)-C(55)-C(50)	0.6(12)
C(50)-P(1)-C(30)-C(35)	-54.8(6)		